

**TRANSPORT, TRANSFORMATION, AND EFFECTS
OF SELENIUM AND CARBON IN THE DELTA
OF THE SACRAMENTO-SAN JOAQUIN RIVERS:
IMPLICATIONS FOR ECOSYSTEM RESTORATION**

Ecosystem Restoration Program
Agreement No. 4600001955
Project No. ERP-01-C07

Prepared by:

Lisa Lucas and Robin Stewart
U.S. Geological Survey, Menlo Park, CA

ACKNOWLEDGEMENTS

This project was made possible in accordance with the funds appropriated through Proposition 204 for the Ecosystem Restoration Program activities beginning with Division 24 of the California Water Code beginning with Section 78684, entitled CALFED Bay-Delta Ecosystem Restoration Program.

The proposal for this project “Transport, transformation and effects of Se and C in the Delta: Implications for ERP” was submitted in May 2000 for the CALFED Ecosystem Restoration Program 2001 Proposal Solicitation Process (PSP) and approved for funding by the Resources Agency.

COST SHARE PARTNERS

U.S. Geological Survey (Menlo Park and Sacramento District office) and U.S. Geological Survey Place-Based Program (Suisun Bay), UC Berkeley, Old Dominion University, Stanford, and State University of New York (Stony Brook) provided funds, staffing resources and equipment as its cost share contribution towards the completion of this project.

TABLE OF CONTENTS

ACKNOWLEDGEMENTS 2

COST SHARE PARTNERS 2

PRINCIPAL INVESTIGATORS & RESEARCH SECTIONS 5

ACRONYMS AND ABBREVIATIONS 6

I. EXECUTIVE SUMMARY 8

 Hydrodynamic conceptual model 8

 Phytoplankton carbon conceptual model 9

 Selenium conceptual model 9

 Timescales 10

II. PROJECT BACKGROUND INFORMATION 11

 The Physical System 11

 Organic Carbon 11

 Status of Se Issues in San Francisco Bay Case Study 13

III. PROJECT OBJECTIVES/GOALS 16

 Hydrodynamic Measurements in Shallow Water Habitats (HS) 16

 Regional Hydrodynamic Field Investigations (HR) 17

 Bivalve distribution and grazing rates (B) 18

 Carbon field studies (C) 18

 Field studies of selenium distributions and transformations (SED) 19

 Se transformations by phytoplankton and bacteria (SET) 20

 Se in Bay-Delta Food Webs (SEF) 21

 Local scale modeling (ML) 21

 Delta scale modeling (MD) 22

IV. APPROACH/METHODOLOGY 23

 Hydrodynamic Measurements in Shallow Water Habitats (HS) 23

 Regional Hydrodynamic Field Investigations (HR) 24

 Bivalve distribution and grazing rates (B) 28

 Carbon field studies (C) 30

 Field studies of selenium distributions and transformations (SED) 32

 Se transformations by phytoplankton and bacteria (SET) 33

 Se in Bay-Delta Food Webs (SEF) 36

 Local scale modeling (ML) 39

 Delta scale modeling (MD) 42

V. FINDINGS 44

 Hydrodynamic Measurements in Shallow Water Habitats (HS) 44

 Regional Hydrodynamic Field Investigations (HR) 44

 Bivalve distribution and grazing rates (B) 45

 Carbon field studies (C) 47

 Field studies of selenium distributions and transformations (SED) 48

 Se transformations by phytoplankton and bacteria (SET) 49

 Se in Bay-Delta Food Webs (SEF) 54

 Local scale modeling (ML) 55

 Delta scale modeling (MD) 56

VI. NARRATIVE 58

 Hydrodynamic Measurements in Shallow Water Habitats (HS) 58

Regional Hydrodynamic Field Investigations (HR)	64
Bivalve distribution and grazing rates (B)	77
Carbon field studies (C)	78
Field studies of selenium distributions and transformations (SED)	84
Se transformations by phytoplankton and bacteria (SET)	88
Se in Bay-Delta Food Webs (SEF)	89
Local scale modeling (ML).....	92
Delta scale modeling (MD).....	95
VII. RECOMMENDATIONS	97
Hydrodynamic Measurements in Shallow Water Habitats (HS)	97
Regional Hydrodynamic Field Investigations (HR)	98
Bivalve distribution and grazing rates (B)	99
Carbon field studies (C)	100
Se transformations by phytoplankton and bacteria (SET)	101
Se in Bay-Delta Food Webs (SEF)	101
Local scale modeling (ML).....	102
Delta scale modeling (MD).....	102
VIII. CONCLUSIONS	103
Hydrodynamic Measurements in Shallow Water Habitats (HS)	103
Regional Hydrodynamic Field Investigations (HR)	103
Bivalve distribution and grazing rates (B)	104
Carbon field studies (C)	104
Field studies of selenium distributions and transformations (SED)	105
Se transformations by phytoplankton and bacteria (SET)	105
Se in Bay-Delta Food Webs (SEF)	106
Local scale modeling (ML).....	106
Delta scale modeling (MD).....	107
IX. REFERENCES	109
A. List of products	109
B. Service to Calfed and Bay-Delta Community	119
C. Bibliography.....	121
X. EXHIBITS	130
A. Tables	131
B. Figures.....	200
XI. ATTACHMENTS	407
A. Selenium Monitoring Proposal	
B. Monsen et al. (in prep.)	

PRINCIPAL INVESTIGATORS & RESEARCH SECTIONS

Hydrodynamic Measurements in Shallow Water Habitats (Section HS)

Mark Stacey, Deanna Sereno and Seungjin Baek
University of California, Berkeley, CA

Regional Hydrodynamic Field Investigations (Section HR)

Jon Burau
U.S. Geological Survey, Sacramento, CA

Bivalve distribution and grazing rates (Section B)

Janet Thompson and Francis Parchaso
U.S. Geological Survey, Menlo Park, CA

Carbon field studies (Section C)

Lisa Lucas, Jim Cloern, Tara Schraga and Cary Lopez
U.S. Geological Survey, Menlo Park, CA

Field studies of selenium distributions and transformations (Section SED)

Greg Cutter, Lynda Cutter and Martina Doblin
Old Dominion University, Norfolk, VA

Se transformations by phytoplankton and bacteria (Section SET)

Stephen Baines and Nick Fisher
State University of New York, Stony Brook

Se in Bay-Delta Food Webs (Section SEF)

Robin Stewart
U.S. Geological Survey, Menlo Park, CA

Local scale modeling (Section ML)

Lisa Lucas, Nancy Monsen,
U.S. Geological Survey, Sacramento, CA
Deanna Sereno, Seungjin Baek, Mark Stacey
University of California, Berkeley, CA

Delta scale modeling (Section MD)

Nancy Monsen and Lisa Lucas
U.S. Geological Survey, Menlo Park, CA

ACRONYMS AND ABBREVIATIONS

AAS	Atomic absorption spectroscopy
ADV	Acoustic Doppler Velocimeters
AFDW	Ash-free-dry-weight
BDOC	bioavailable dissolved organic carbon
BPOC	bioavailable particulate organic carbon
C	Carbon
CBL	Concentration boundary layer
CDFG	California Department of Fish and Game
CDWR	California Department of Water Resources
chl <i>a</i>	chlorophyll <i>a</i>
CTD	Conductivity, temperature and depth
DCC	Delta Cross Channel
DIC	Dissolved inorganic carbon
DO	Dissolved oxygen
DOC	Dissolved organic carbon
FR	Filtration rate
FT	Frank's Tract
GOTM	General Ocean Turbulence Model
GR	Grazing rate
HORB	Head of Old River Barrier
IEP	Interagency Ecological Program
MI	Mildred's Island
MILS	sampling station in the southeast corner of Mildred Island
NIST	National Institute of Standards and Technology
NOPN	sampling station at the north opening of Mildred Island
OC	organic carbon
PB	phytoplankton biomass
POC	particulate organic carbon
PP	phytoplankton primary productivity
PP _{res}	residual primary productivity
P _μ	phytoplankton specific growth rate
SAV	Submerged Aquatic Vegetation
SC	specific conductivity
SCUFA	Self-contained underwater fluorescence apparatuses
Se	Selenium
SFB	San Francisco Bay
SJR	San Joaquin River
SL	Shell length
SPM	Suspended particulate matter
SWP	State Water Project
T	water temperature
THM	trihalomethane
USBR	U.S. Bureau of Reclamation
USEPA	U.S. Environmental Protection Agency

USFWS	U.S. Fish and Wildlife Service
VCF	
ZB	zooplankton biomass
ZG	zooplankton grazing rate

I. EXECUTIVE SUMMARY

Hydrodynamic conceptual model

Our Delta hydrodynamic conceptual model addresses hydrodynamics and transport on four different scales: 1) the Delta-scale, 2) the regional scale (i.e. encompassing more than one shallow water habitat or channel), 3) shallow water habitat-channel exchange locations, and 4) the scale of/within one shallow water habitat.

Figure E1 describes the predominant forcings underlying hydrodynamics on the Delta scale. River hydrology and operations (e.g. pumps, gates, Delta Cross channel, barriers, reservoir releases) primarily govern residual (net) hydrodynamics and transport in the northern and southern Delta. The central Delta is a region of intense mixing, with tides---and their interaction with the complex, interconnected Delta geometry---playing a significant role.

Figure E2 describes the north-south freshwater corridor (FWC) through the Delta. This phenomenon is regulated by the interplay between the fresh Sacramento and salty San Joaquin river flows and the situation of the Delta to the east of the oceanic source of salt. This FWC fluctuates in dimension on both seasonal and spring-neap timescales. Due to the large wintertime Sacramento contributions of freshwater, the Delta is typically all or largely fresh during January-March. In the Spring, Summer, and early Fall, Sacramento flows decrease, allowing the contributions of saltwater from the SJR and SFB to contract the FWC. The FWC is at its narrowest around November-December, due to further decreased Sacramento River flows and, consequently, a large ratio of SJR to Sacramento flows. The dimension of the FWC fluctuates also on the spring/neap cycle, narrowing during spring tide due to increased tidal excursion, tidal prism, and import of oceanic salt, and widening during neap.

Regional scale hydrodynamics and transport (see Figure E3) depend on the relative lengths of channels/habitats (L_c), advective length scales (L_u , e.g. tidal excursion), and the tidal propagation length scale (L_t). If the channel or habitat length is longer than the advective and tidal propagation length scales, then the regional system acts like a river. If the advective length scale is greater than the channel/habitat length, then tidal excursions exceed the habitat dimension, mixing generally occurs once a water parcel has exited the far end of the habitat, and material that returns on the succeeding tidal phase is different in character from that which previously passed. This is a highly dispersive situation. Phasing of currents and stage can become complicated when interconnected channels and habitats of different lengths and depths thus result in the tidal wave splitting and taking different lengths of time to reach the same point via different routes.

Exchange between broad shallow habitats and deeper channels to some degree follows the classic tidal pumping paradigm, with water entering the shallow habitat as a jet and leaving as a radial potential flow (see Figure E4). In Delta habitats, this classic exchange paradigm is altered by the details of the environment: 1) geometry (i.e. exact location, size of levee breaches), 2) vegetation (SAV can constrain a jet), and 3) meteorology (wind and heating driven baroclinic flows can cause dispersion and redirection of jet and radial flows).

At the within-habitat scale (Fig. E5), physical environments like Mildred Island and Franks Tract are affected by a combination of tides (dominant at the levee breaches and, to some degree, in the interior), atmospheric forcing (wind and baroclinic flows can be significant players in basin scale transport, as well as export from quiescent corners and coves), geometry, and SAV. SAV reduces velocities, bed stresses and horizontal exchange.

Phytoplankton carbon conceptual model

Our conceptual model for phytoplankton addresses hydrodynamics and transport on three different scales: 1) the Delta-scale, 2) the regional scale (i.e. encompassing more than one shallow water habitat or channel), and 3) the scale of/within one shallow water habitat.

Jassby and Cloern (2000) showed that the balance between within-Delta autochthonous production of phytoplankton and river import shifts seasonally (see Figure E6). During Spring, Summer, and Fall, sources of Delta phytoplankton biomass are dominated by within-Delta production; whereas, in the Winter, riverine import dominates the sources of biomass. Through our Delta-scale measurements of benthic biomass and phytoplankton biomass, we have learned that Delta scale variations in phytoplankton biomass are somewhat inversely related to the presence of invasive clams (e.g. chl *a* is high but clam biomass low in the San Joaquin River upstream of Stockton, but generally lower phytoplankton biomass in the central Delta where clam biomass is overall higher, see Figure E7).

Phytoplankton variability at the regional scale (i.e. that encompassing more than one adjacent habitat) contains sharp gradients in growth-consumption conditions, biomass, and transport. For example, the interior of Mildred Island contains very few benthic grazers and is thus a local net source of phytoplankton biomass; the adjacent river channels are associated with large abundances of clams and lower depth averaged light, resulting in negative effective phytoplankton growth rates in the channels (see Figure E8). Tidally driven dispersive exchange between the shallow and deep environments, as well as residual flows driven by operations and hydrology, can cause the phytoplankton produced within MI to be shared with the less productive channels, supporting zooplankton secondary production in the channels. Without this hydrodynamic connection, consumers in the channels may be more severely food limited.

The opposite configuration between donor and recipient habitats appears to be present in the Franks Tract region, with the interior lake being heavily colonized with clams but most of the outside channels uncolonized (Figure E9). Our calculations suggest that Franks Tract is a net phytoplankton sink while most of its adjacent channels are net phytoplankton sources. These channels may serve as donor habitats to the interior of Franks Tract. Ongoing work will quantitatively test this hypothesis.

At the within-habitat scale, atmospheric forcing is critical in governing transport, especially between quiescent coves and the open water. Tides are dominant at the levee openings. The relationships between phytoplankton and SAV is not yet well understood, but we have learned that horizontal exchange is diminished significantly by SAV.

Selenium conceptual model

The selenium conceptual models shown in Figures E10-E12 illustrate the differences in Se concentrations and bioavailability that occur in the San Francisco Bay/Delta as well as within-habitat transformations. A more detailed conceptual model of Se transformations and cycling is described in Section SED (Figure SED1).

At the Delta-scale total dissolved Se concentrations ($\mu\text{g L}^{-1}$) are highest in the inflowing San Joaquin River near Stockton (Figure E10). Concentrations of dissolved Se are approximately 8 times lower in the Sacramento River (at Rio Vista) and at Antioch, near the confluence of the Sacramento and San Joaquin Rivers. These distributions suggest the elevated dissolved Se

concentrations are progressively diluted by the Sacramento River and possibly Bay water. Our research has shown that Se is predominantly accumulated by organisms via the diet and furthermore that Se bioavailability can vary by orders of magnitude between sediment and phytoplankton. Consequently, total particulate Se concentrations critical in understanding uptake by organisms can be misleading since phytoplankton and bacteria contribute a relatively small amount of mass to the total particulates (Figure E11). As a result we illustrate differences in bioavailable particulate Se by normalizing the Se content of the suspended particulate material by carbon content on a molar basis. Figure E11 shows that bioavailable Se varies both seasonally and spatially. In early summer (June) bioavailable Se is slightly higher in the San Joaquin River than the Sacramento River or Antioch. Alternatively, in the fall we observe the highest bioavailable Se particulate concentrations nearest the estuary (Antioch). The higher bioavailable Se concentrations correspond to the elevated Se concentrations observed in *Potamocorbula amurensis* in the fall at Carquinez St.

At the within-habitat scale in the Delta Se shows marked cycling and transformations. Figure E12 shows a conceptual model for Se uptake and regeneration in the southwestern Mildred's Island during the 2001 process study. The southwestern corner of Mildred's Island is characterized by high phytoplankton concentrations and limited transport (although transport does occur), which allowed us to examine *in situ* Se transformation processes. Under these relatively quiescent conditions dissolved Se is taken up by phytoplankton late in the day and by bacteria at night and released by phytoplankton during the day. Laboratory uptake experiments (see Section SET) and cycling during field study (see SED4-8) suggest that dissolved organo-selenide is utilized by the phytoplankton and rapidly exchanges with the Selenite pool.

Timescales

Important timescales governing within-Delta selenium distributions, transformations, and export to San Francisco Bay are shown in the graphic in Figure E13. Mosen has shown with hydrodynamic modeling that cross-Delta transport from Vernalis to the confluence takes on the order of a few weeks. Within the Delta, selenium is undergoing transformations, including those which package dissolved Se into edible particulate form and those which pass Se through the food web. Dissolved Se is "stripped" or taken up by phytoplankton, which repackages Se into a form which can be consumed by upper trophic levels. The timescale associated with this uptake process depends on how much phytoplankton biomass is present: this timescale is a few days in high-phytoplankton biomass environments like southern Mildred Island but more like weeks where phytoplankton biomass and productivity are low, as in less productive Delta channels. Where the uptake timescales are short, residence times may be comparable (e.g. southern Mildred Island), rendering uptake and transport of comparable importance. Phytoplankton growth timescales are on the order of days. Phytoplankton is then consumed by benthic grazers (clams) and pelagic grazers (zooplankton), passing incorporated Se as well as carbon and other elements on to the consumers. Where clam grazing rates are rapid (e.g. Franks Tract), the water column turnover time by the clams can be on the order of hours; where clams are absent, that turnover time is infinity (southern Mildred Island). Zooplankton consumption timescales are on the order of days. The time scales for Se consumed to be reflected in the tissues of the consumers is on the order of a month.

II. PROJECT BACKGROUND INFORMATION

The Physical System

The Sacramento-San Joaquin River Delta (hereafter “Delta”) is a complex physical system that transitions from a strictly riverine regime at its landward margin to a tidally oscillating interconnected network of channels and open water areas. Situated at the head of San Francisco Bay and encompassing the confluence of California’s two largest rivers (the Sacramento and the San Joaquin), this freshwater ecosystem is subject to numerous physical influences. Operating over timescales ranging from hours to months, these influences are both natural and anthropogenic. Natural influences include: primarily semidiurnal tides (the tidal wave propagates from the Pacific Ocean upstream through San Francisco Bay), river and stream inflow, wind stress, solar radiation, density variations due to salinity and temperature gradients, and fluctuations in atmospheric pressure. The complex interconnected and channelized geometry of the Delta, coupled with the oscillatory nature of the tidal currents, result in a large degree of dispersion of water and transported particles and substances. This interconnectedness also results in a system with relatively limited numbers of locations with long residence times.

The Delta drains a 153,000 km² watershed that captures runoff from winter-spring rainfall in the Central Valley and coastal range and spring snowmelt in the Sierra Nevada mountains (Monsen *et al.* In prep.). The Delta was a 1,400-km² wetland (Atwater and others (1979)) that has been transformed into a patchwork of agricultural tracts surrounded by leveed channels, tidal lakes and remnant patches of marsh. The Delta is also the hub of a water-development infrastructure that captures 7.1 km³ of runoff during the wet season and transfers water from the water-rich north to the arid south and coast, for use during the dry summer-autumn (CDWR 1998). Reservoir releases are routed across the Delta to provide drinking water for 22 million people in coastal cities, and supply water to over 18,000 km² of irrigated farmland producing crops valued at over \$13 billion annually (CALFED 2000; CDFA 2002). These interbasin transfers are made as pumped exports from the south Delta by the State Water Project (SWP) and the Central Valley Project (CVP) whose combined capacity is 360 m³ s⁻¹.

Over 2200 diversions from Delta channels also supply water for local municipalities and irrigation of local farmland (Herren and Kawasaki 2001). Multiple demands for water transiting the Delta are satisfied through the operation of several man-made structures using a complex suite of flow manipulations and diversions both upstream and within the Delta. A large fraction of the freshwater inflow to the Delta (up to 65% during the dry season in some years) is exported via the SWP and CVP pumps to meet agricultural and municipal demands. The Delta Cross Channel (DCC), a man-made channel and gates, connects the SAC with natural channels east of the SAC to transfer high-quality fresh water into the central Delta mixing zone for export by the SWP and CVP. A rock barrier is constructed at the head of Old River during spring and autumn to improve conditions for Chinook salmon migrating through the Delta via the SJR. Three other temporary barriers are constructed each spring and removed each autumn to increase water depth for irrigation intakes within south Delta channels. Each hydraulic manipulation directly alters the regional flow paths or rates and indirectly changes the source mixture and quality of water across the Delta landscape.

Organic Carbon

Previous work on sources, quantity and quality of organic carbon (OC) in the Delta helped shape the work described in this report.

Jassby and Cloern (2000) performed a budget of sources and quantities of OC, showing that tributary-borne load of detritus is the largest OC source on an average annual Delta-wide basis. Dissolved organic carbon (DOC) is the largest OC pool in the Delta, and its bioavailable component (BDOC) is important in supporting ecosystem metabolism (i.e. bacterial production, Sobczak *et al.* (2002; 2005)). DOC, however, contributes little to production of forage biota for fish (e.g. copepods, rotifers, cladocerans, insect larvae) because even the bioavailable portion needs to be repackaged in particulate form---with significant losses to heterotroph growth inefficiency---before it becomes available to the metazoan food web (Jassby and Cloern 2000, Sobczak *et al.* (2002; 2005)). The bulk particulate organic carbon (POC) pool is small relative to the DOC pool and is dominated by low-value detritus, rendering the bioavailable portion (BPOC) a third or less of the total POC (Sobczak *et al.* (2002; 2005)).

A typically small component of the POC pool in the Delta is phytoplankton biomass; this is the component that has been shown to support production of forage biota for fish. Phytoplankton derived organic matter was shown by Sobczak *et al.* (2002; 2005) to be a large and important component of the BPOC. Detrital POC is a large component of POC but a small component of BPOC. Sobczak *et al.* (2002) concluded that the Delta's planktonic food web may be highly reliant on phytoplankton production although this organic matter source represents a small amount of the ecosystem's potential energy to higher trophic levels. Detrital linkages to the planktonic food web are relatively weak even under the best-case scenarios.

Zooplankton growth experiments by Mueller-Solger *et al.* (2003) supported the hypothesized trophic linkage between the Delta's planktonic food web and phytoplankton production. Assays with the cladoceran *Daphnia magna* showed that zooplankton growth and fecundity were strongly related to phytoplankton biomass and unrelated to the amount of detrital matter. This relationship is strongest for chl *a* concentrations from 0-10 ug/L, suggesting that Delta zooplankton may be food-limited when chl *a* < 10 ug/L. Concentrations rarely exceed 10 ug chl *a*/L through most of the Delta (San Joaquin River is an exception). This suggests that the Delta's zooplankton may be routinely food limited. This also suggests that the Delta's phytoplankton, although routinely low in biomass, is generally of high nutritional quality.

This collective previous work indicates that planktonic food webs in low-productivity estuarine and riverine ecosystems may be especially sensitive to changes in phytoplankton production, although phytoplankton biomass represents a small fraction of the flux of organic matter through many rivers and estuaries.

Although phytoplankton primary production (PP) represents an important energy supply to pelagic and benthic food webs, other ecologically important food webs are supported by other sources (e.g. epiphytes→amphipods).

Jassby *et al.* (2002) showed that, although the Delta is generally very high in nutrient concentrations, PP is low. Moreover, PP has decreased 43% over the past 3 decades. These findings further indicate chronic food limitation of pelagic and benthic consumers. A concomitant decline in Delta zooplankton stocks has also been observed over the past three decades. Long-term declines in Delta phytoplankton, native zooplankton, and native fish suggest a potential trophic linkage (Bennett and Moyle 1996).

The Delta is a turbid system, so phytoplankton growth rates are light-limited; however, water clarity has increased over time while phytoplankton biomass has decreased, so turbidity

cannot explain the downward decadal trend in phytoplankton biomass and productivity. Invasion by the clam *Potamocorbula amurensis* in 1986 is implicated as one factor contributing to the decline in phytoplankton biomass and productivity (Jassby *et al.* 2002).

Lucas *et al.* (2002) showed that effective phytoplankton growth and delivery to pelagic consumers can vary dramatically between similar shallow Delta environments, depending on benthic consumption and hydrodynamics. For example, Mildred Island (mostly uncolonized by clams) acts as a net producer of phytoplankton biomass and Franks Tract (heavily colonized by clams) functions as a net consumer. In this way, similar habitats may function in opposite ways and generic functionalities should not be assigned to or expected of all habitats within a habitat category. Residence time (or flushing time) is an important habitat or sub-habitat characteristic that can govern net phytoplankton biomass accumulation; residence time is determined by the local geometry, tides, meteorology, hydrology, and operations.

Other previous numerical modeling work highlighted the importance of considering phytoplankton as Lagrangian particles that react to a range of growth-consumption environments along their tidal trajectories (Lucas *et al.* (1999b)). This fluctuating exposure of phytoplankters to different conditions---and not necessarily the average condition---can determine whether phytoplankton biomass grows or declines in the long-term.

In summary, phytoplankton do not only represent a potential nuisance, as in systems such as the Chesapeake, where excessive amounts of phytoplankton biomass result in hypoxic conditions; in low-productivity systems such as the Delta, phytoplankton represent a scarce but ecologically critical food resource for the pelagic and benthic food webs. They also represent a critical entry point for contaminants such as selenium and mercury into those food webs.

Status of Se Issues in San Francisco Bay Case Study

Selenium contamination in the Bay-Delta is a complex, but serious, threat to CALFED's proposals to restore important populations of species of concern. That threat could grow under some of the scenarios for both restoration and water management. Selenium is hazardous because it is biomagnified through food webs (Stewart *et al.* 2004) and it is strongly toxic to reproduction in upper trophic level organisms.

Concern about Se contamination in the Bay-Delta watershed started in the mid-1980's with an episode of overt toxicity to birds and fish at Kesterson Reservoir (adjacent to Kesterson National Wildlife Refuge). Water from the San Luis Drain was discharged to the reservoir and the high concentrations of Se in that water caused widespread deformities and reproductive failure in birds and the extirpation of most fish species. Concern about San Francisco Bay followed shortly thereafter, when high Se concentrations were found in some predators. Selenium contamination in the tissues of some species was sufficient to threaten reproduction (> 10 µg Se/g in tissue). The most threatened species appear to include, but may not be restricted to, white sturgeon (*Acipenser transmontanus*), Sacramento splittail (*Pogonichthys macrolepidotas*), starry flounder (*Platichthys stellatus*), Dungeness crab (*Cancer magister*), surf scoter (*Melanitta perspicillata*), and greater and lesser scaup (*Aythya marilla* and *Aythya affinis*) (Ohlendorf *et al.* 1986; Urquhart and Regalado 1991; Ohlendorf *et al.* 1989). In 1990, Se concentrations in scoter tissues were 10 times the threshold level for avian reproductive toxicity (Skorupa 1998). Sturgeon flesh exceeded the threshold for reproductive threat by fivefold (CDFG, Mary Dunne, personal communication, December, 1996). Portions of the Bay-Delta are listed by regulatory agencies as known toxic hotspots of high priority due to Se. Portions of the

San Joaquin River (SJR) are designated as water quality limited due to Se. A biological opinion (USFWS and National Marine Fisheries Service, 1998; amended, 2000) on USEPA's proposed California Toxics Rule (*Proposed Rule for the Promulgation of Water Quality Standards: Establishment of Numeric Criteria for Priority Toxic Pollutants for the State of California*) found that the USEPA standard for Se jeopardizes several Bay-Delta or SJR fish, birds and amphibians/reptiles.

The sources of selenium contamination in the Bay-Delta are well-known. The main watershed source is agricultural drainage from the San Joaquin Valley (SJV). The USBR is obligated to sustain agriculture by draining salts and Se from saline soils in the valley and dispose of the collected subsurface drainage. However, the reservoir of Se on the west side of the Central Valley is immense, and the original plans for a drain to San Francisco Bay raise a high likelihood of severe risk to wildlife (Luoma and Presser 2000). Water-quality in the San Joaquin River has degraded significantly since the 1940's, partly because of de-watering and partly because of disposal of agricultural wastewater in the river. So it is not clear how to resolve the drainage issue, without further degrading the SJR and/or transferring that degradation to the Delta or the Bay. A second selenium source is oil refiners who discharge waste to the Suisun Bay from processing Se-enriched crude oil that originates from the SJV and adjacent Coast Ranges (Linville and Luoma In press). This was the primary source of Se to the Bay until studies identifying that source (Cutter 1989; Johns *et al.* 1988; Luoma *et al.* 1992) led to regulation of that discharge in the mid- to late-1990's.

Concentrations of Se in the various water bodies differ depending upon their proximity to these sources. A sixteen year record of concentrations in the uncontaminated Sacramento River shows a remarkably constant concentration: $0.071 \pm 0.021 \mu\text{g Se/L}$ (Cutter and Cutter 2004). Selenium concentrations in the San Joaquin River are 18 times higher than this at Vernalis: $1.25 \pm 0.83 \mu\text{g Se/L}$, reflecting inputs from the SJV that vary in intensity from year-to-year. Water from the SJR historically was recycled back to the San Joaquin Valley before it reached the Bay; so, in the 1980's this was not an important source to the Delta or the Bay. The Delta also traps Se before it gets to the Bay (Meseck 2002). Concentrations of Se in the Delta are highly variable. In 8 transects they varied from $0.08 - 0.91 \mu\text{g Se/L}$, depending upon flow conditions and the time of year (dilution of SJR water by Sacramento River water is probably a major factor in the Delta). Particulate concentrations in the Delta are also highly variable in space and time. Some places such concentration are low during all flow regimes ($< 1 \mu\text{g Se/g SPM}$; Mildred's Island). But in areas near the main channel of the San Joaquin River (e.g. Venice Cut) very high particulate concentrations are observed during some low flow regimes ($5 - 8 \mu\text{g Se/g SPM}$).

Concentrations of Se in Bay waters are lower than in the San Joaquin River: $0.2 - 0.5 \mu\text{g Se/L}$. Refinery inputs of Se to the Bay were reduced by half after 1998. Disappearance of a peak in selenite concentrations, once typical of Carquinez Straits area, occurred after the reductions. Suspended particulate concentrations in the Bay are also variable ($0.3 - 2.5 \mu\text{g Se/g SPM}$), but usually relatively low. Selenium in sediments is typically $< 1 \mu\text{g Se g}^{-1}$ wherever it has been determined. Particulate Se is the most important source of bioavailable Se to the food web. There is a general consensus that particulate concentrations from $2 - 4 \mu\text{g Se/g}$ could be problematic, but concentrations $> 4 \mu\text{g Se g}^{-1}$ are likely a source of risk for Se toxicity in the food web. Despite the low Se concentrations in solution in the system, periodic high particulate concentrations in both the Bay and Delta raise the likelihood that at least some species could be threatened.

The specific bioaccumulation pathway from sediment and suspended biomass to consumer organisms to predators (bottom feeding fish, diving ducks, and Dungeness crab) is the most important route of Se transfer to the upper trophic levels in the estuary. The reason for the problems in the Bay-Delta, despite relatively low Se concentrations in water, is that some food webs are particularly vulnerable to moderate Se contamination. Analyses in 1982-1996 showed that the animals with the highest Se concentrations from the North Bay (i.e., Suisun Bay, Carquinez Strait, and San Pablo Bay) all eat bivalves (*Corbicula fluminea* prior to 1986 and *Potamocorbula amurensis* in subsequent samplings) as a major component of their diet. Bivalves accumulate 5 times more Se than zooplankton in the Bay (Schlekat *et al.* 2004), because physiological loss rates from bivalves are much slower than loss rates from crustacean zooplankton. So bivalve predators, like sturgeon and splittail, are much more at risk than water column predators, like striped bass or Chinook salmon (Stewart *et al.* 2004).

Selenium concentrations in the predominant bivalve in the Bay-Delta were higher in the mid-1990's (Linville and Luoma In press) than in 1977 through 1990 (Cutter 1989; Johns *et al.* 1988). One contributing factor might be that a new species (*Potamocorbula amurensis*) became predominant in the Bay (Linville *et al.* 2002) after 1986. *P. amurensis* is somewhat more effective at bioaccumulating Se than was the previously dominant species, *Corbicula fluminea*. Levels in *P. amurensis* reached 20 $\mu\text{g Se g}^{-1}$ dry weight in the North Bay in October, 1996, exceeding by twofold the threshold in food for predators ($> 10 \mu\text{g Se g}^{-1}$ dry weight) that result in adverse effects.

Se concentrations in the liver of white sturgeon appear to have declined modestly since the refinery inputs declined. But it is not clear that Se concentrations in bivalves declined in the Bay after the reduction of inputs from the refineries. Limited data exists for *P. amurensis* from the period before the refineries reduced their inputs; there was a 10 year hiatus when no support was available for study of the element in the Bay. Direct comparisons with the same species before and after refinery reductions should, therefore, be made cautiously. Se in *P. amurensis* can be compared to Se in *C. fluminea*. Selenium concentrations in *P. amurensis* living in Grizzly Bay are now lower than concentrations were in *C. fluminea*, but only during periods of high Sacramento River inflows. In fall, Se concentrations in *P. amurensis* reach the high levels described above; much higher than the maximum of $\sim 6 \mu\text{g Se/g}$ dry weight observed in *C. fluminea*. Thus predators that occupy the Bay during spring and summer are probably less at risk from Se contamination as a result of the treatment of the refinery discharges. But predators that are present during fall and winter (\sim Nov. – March) are more at risk. Many of the predator species described as threatened above are migratory, and, unfortunately spend fall and early winter in the Bay. The strong seasonal cycle in *Potamocorbula* Se content requires more analysis before drawing conclusions about long term trends.

Several explanations for the temporal trends in bivalve Se concentrations (which did not exist in the 1980's) are possible. One possibility is that refinery inputs of selenium have been replaced by San Joaquin River inputs. Models indicate that if SJR inflows to the Bay increase, as they may have in recent years with barrier management, particulate Se concentrations in the Bay could double, even with no increase in irrigation drainage inputs to the SJR (Fig. 1; Meseck (2002)). The fall increase in Se in *P. amurensis* also occurs during the time period when the ratio of SJR/Sac River inflow is highest. Further changes in water management could exacerbate these trends. Other explanations for the bivalve Se concentrations are also possible, however (see attached Calfed *Potamocorbula* Monitoring Proposal 2005).

Experimental studies conducted in the last few years have verified the threat suggested by high tissue concentrations in some of the native fishes. White sturgeon produce a high proportion of damaged embryos, when Se concentrations in their reproductive tissues are similar to those found in the Bay (Linville In prep). Teratogenic (deformed) Sacramento splittail were recently discovered in Suisun Marsh (cause unknown). Experiments show that a diet of Se-contaminated yeast can cause deformities in juvenile splittail, at about the Se concentration found in bivalves (the food of older splittail living in Suisun Marsh; (Stewart *et al.* 2004; Ohlendorf *et al.* 1989; Teh 2004). Currently, populations and catches per unit effort (where applicable) of all the predator species mentioned above are either in decline, or periodically reach very low numbers. A number of causative factors could contribute to the latter observation, but the weight of evidence suggests that Se is likely to be one of the important causes of stress.

Major restoration is planned for shallow water habitats and wetlands in the Delta and upper Bay (e.g. Suisun Marsh, North Delta and Dutch Slough). Studies clearly demonstrate that Delta and Central Valley wetlands, and some kinds of shallow water habitats, can trap and recycle selenium (Cutter *et al* In prep; (Presser and Ohlendorf 1987)), ultimately releasing it in forms that can threaten food webs. Recent work conclusively shows that existing levels of selenium contamination already threaten some native fishes that spend time in or near such habitats, notably Green and White Sturgeon, and Sacramento splittail (Stewart *et al.* 2004; Teh 2004; Linville In prep.), along with a number of migratory bird species. Greater recycling of Se in restored wetlands could accentuate effects of greater inputs. If so, the gains made by creation of restored habitat and reduction of refinery inputs would be reversed. One location of these cumulative impacts is likely to be Suisun Bay, a key habitat for many native species at the head of the estuary (Luoma and Presser 2000) and a key focus for CALFED restoration efforts.

Studies through the last 8 years show that Se is not a hypothetical, but a real threat to the Bay-Delta. We understand what species are threatened and why. Monitoring the fate of Se in the Bay and Delta seems an important adaptive management need as water management changes and restoration of the Bay-Delta proceed. Management of the Delta, the Bay and the Westside of the San Joaquin Valley will all be changing in the years ahead as a result of changes in water management plans. These programs must consider the fate of Se. It is especially important to understand whether San Joaquin inputs of Se are now important in the Bay, and whether or not those inputs are increasing. An on-going monitoring program will require a cost-effective approach to be sustainable. That will require resolving some of the questions remaining from the previous years of work on Se; and persistently tracking the fate and effects of this contaminant. Continued funding of Se studies seems essential. We have attached a proposal for follow-on funding, from our earlier work. The appropriate route to take for such funding is unclear, given the focused nature of ERP solicitations. So we attach the proposal to this final report in hopes the need will be appreciated (Calfed Potamocorbula Monitoring Proposal 2005).

III. PROJECT OBJECTIVES/GOALS

Hydrodynamic Measurements in Shallow Water Habitats (HS)

In this section of the report, we present results from our detailed observational program that focused on the hydrodynamics in the interiors of shallow water habitats in the Delta. Further, we

consider the implications of these interior dynamics on channel-shallow exchange and scalar transport. Specific questions that we addressed included:

- (1) *What are the dominant dynamics in the interior of shallow water habitats? How important is atmospheric (wind and heating/cooling) forcing to the internal dynamics of shallow habitats in the Delta?*
- (2) *What is the nature of shallow-channel exchange? What are the dominant processes in establishing this exchange?*
- (3) *What is the role of submerged aquatic vegetation (SAV) in the hydrodynamics of these shallow habitats? What are the implications for flow and transport throughout the annual cycle of vegetation development?*

Regional Hydrodynamic Field Investigations (HR)

The purpose of regional hydrodynamic field investigations were to 1) identify and understand crucial Delta transport/export processes; 2) provide the data necessary to verify DELTA-TRIM's ability to capture the dominant transport processes (see Sections ML and MD); 3) provide hydrodynamic information for interpreting measured temporal and spatial variability of selenium and carbon (see Sections C, SED, and SET).

The regional scale hydrodynamic field investigations were designed to provide the regional context for the detailed studies of Mildred Island and Franks Tract because Delta-scale natural and anthropogenic variability strongly influences transport into and within these Island habitats. And, to a somewhat lesser degree, these investigations were aimed at gaining an understanding of how Island/channel exchange processes and internal dynamics influence Delta-scale variability. Franks Tract, in particular, plays a crucial role in governing salinity intrusion into the central Delta from the bay (Figure HR1). From a strictly water management perspective, the influence that Mildred Island and Franks Tract have on water supply, water quality and ecosystem function in the Delta as a whole is of greatest interest. Therefore, the *Regional Hydrodynamic Field Investigations* component of this overall effort was aimed at placing Mildred Island and Franks Tract within the Delta-scale landscape. The hydrodynamics internal to these environments is discussed in Section HS. In so far as we are aware, the data sets described in this report represents the first comprehensive field assessment of transport in the Mildred Island and Franks Tract regions.

Mildred Island and Franks Tract were chosen as study sites because they represent two hydrodynamically distinct flooded island habitats. Franks Tract is a large flooded Island (12.65 km²) located in the central Delta, it is relatively shallow with mean tide depths on the order of 2 m (and thus a mean tide volume of 28.74 km³), its geometry is characterized by numerous levee breaches, it is strongly tidally forced and is susceptible to landward salinity intrusion from the bay on its western boundary. Moreover, Franks Tracts eastern shore provides the critical connection between the fresh Sacramento River water supplies that enter the central Delta through the Mokelumne River and the pumping facilities in the southern Delta; the so called "fresh water corridor" (Figure HR2). Mildred Island, on the other hand, is much smaller (3.82 km²), is relatively deep with a mean tide water depth of roughly 6 m (a mean tide volume of 22.9x10⁶ m³), it has two major openings instead of many, is less strongly tidally forced, and has higher salinities on its southern boundary from the San Joaquin River and agricultural sources in the southern Delta. Mildred Island is located within the central core of the Fresh

water corridor along Middle River, and because of its size, may mediate transport of San Joaquin River derived salinity through the central Delta to the export facilities.

Bivalve distribution and grazing rates (B)

The clam *Corbicula fluminea* was hypothesized to represent a dominant sink for phytoplankton and thus to be a recipient of particulate Se in the delta. Therefore for the Delta-scale physical-biogeochemical model to accurately reflect sources and sinks of carbon and particulate Se, we needed to measure the grazing rate of this bivalve. The benthic grazing rate of a second bivalve, the euryhaline *Corbicula amurensis* (previously known as *Potamocorbula amurensis*), was also estimated at the estuarine boundary. Assessment of benthic grazing rates was performed at the Delta scale, regional scale (i.e. Mildred Island and Franks Tract regions), and the within-channel scale. Both spatial and temporal variability were examined.

Carbon field studies (C)

The “Carbon Field Study” portion of the project focuses primarily on phytoplankton biomass because it is the most important source of fuel to the Delta’s pelagic food web and a major route for Se transfer to upper trophic levels. This work consists of three primary parts: 1) a component of the larger multidisciplinary 2001 process study at Mildred Island (with surrounding channels); 2) a component of the larger multidisciplinary 2002 process study at Franks Tract (with surrounding channels); and 3) a component of the 2003 Delta-scale “Benthic Boogie” effort. This carbon work at MI and FT was conducted in an intricately coordinated fashion with the simultaneous hydrodynamic and selenium related measurements in those environments. As such, the goals of the carbon work were to 1) understand the physical-biological processes governing variability in phytoplankton biomass in a range of environments in the Delta (i.e. the various components of the mass balance); 2) provide biological context and process information for the concurrent selenium work; 3) provide a comparison between conservative transported water quality constituents (specific conductivity, temperature) and a reactive constituent (phytoplankton biomass, as represented by the proxy chlorophyll *a*) to better understand transport processes in the Delta and how transport interfaces with reactions; 4) provide detailed spatial-temporal information to assist the development and refinement of a coupled hydrodynamic-biological model. The goal of the 2003 Delta-scale carbon related measurements was to 1) provide spatially detailed coverage of phytoplankton biomass measurements for a snapshot in time at locations coincident with benthic biomass measurements; 2) obtain turbidity and nutrient information on a Delta scale for better understanding and modeling Delta-scale phytoplankton dynamics; 3) comparing USGS and DWR chlorophyll *a* analysis methods for identifying potential discrepancies and providing context for the future use of DWR fluorescence and chlorophyll measurements for modeling.

Field studies of selenium distributions and transformations (SED)

Selenium is an essential, but also toxic, trace element whose chemical speciation (form) and concentration affect this dual role (e.g., (Harrison *et al.* 1988; Ohlendorf *et al.* 1989). The biogeochemical cycle of selenium and its chemical forms have been examined in the oceans (e.g., Cutter and Bruland (1984)), estuaries including the San Francisco Bay (Cutter 1989; Cutter and Cutter 2004), and freshwaters (see review by Cutter (1989)). However, the work described here was the first to examine selenium biogeochemistry in the highly dynamic interface between freshwater ecosystems and estuaries – tidal freshwaters that are the Sacramento-San Joaquin River Delta.

Dissolved selenium exists as the oxyanions selenate (Se+6 as SeO_4^{2-}) and selenite (Se+4 as $\text{SeO}_3^{2-} + \text{HSeO}_3^-$), and as organic selenides (Se-2), primarily in the form of dissolved free amino acids and soluble peptides (Cutter 1982). In the particulate state, Se can be found as adsorbed selenate and selenite, particulate organic selenide, and as insoluble elemental selenium (Se0). Based on marine and estuarine studies, a conceptual model for Se biogeochemical cycling (i.e., fate and transport) in the Delta is depicted in Figure SED1. This cycle includes the multistep regeneration of particulate organic selenide to dissolved selenate (via dissolved organic selenide and selenite) that is analogous to nitrification in the nitrogen cycle, and the selective uptake of dissolved Se species (organic selenide = selenite > selenate) by autotrophs (phytoplankton) and perhaps heterotrophic bacteria. In the process of uptake, selenite and selenate are reduced to particulate organic selenides. This organic selenide can be recycled as above, transferred to grazers such as zooplankton or benthic invertebrates, or deposited in the underlying sediments. Dissolved Se can also exchange with the sediments via diffusion (depending on the concentration gradient), with reducing sediments producing elemental Se via the dissimilatory reduction of selenate and selenite (Figure SED1; (Oremland *et al.* 1989). Of course all of this cycling is superimposed upon physical transport processes driven by river and tidal flows, and dispersion that are major features of the Delta ecosystem (Monsen 2001).

The findings discussed here are particularly relevant to the San Francisco Bay system since any effects of San Joaquin River selenium inputs to the Bay depend critically on transformations and removal in the Delta. This Delta effect is amply demonstrated in a simulation model of selenium biogeochemistry and transport in the SF Bay by Meseck (2002). These simulations show that increasing the San Joaquin flow will increase both dissolved and particulate selenium in the mid estuary (Suisun Bay and Carquinez Strait); the amount of these increases is a function of the relative input to, and removal rates in, the Delta. Once dissolved selenium is taken up by phytoplankton or bacteria, it can move through the food web (trophic transfer from phytoplankton and bacteria eventually to higher organisms such as fish or waterfowl). Thus, biogeochemical processes in the Delta affect selenium transport to the San Francisco Bay estuary where its cycling affects trophic transfer and adverse ecological effects. Although refinery effluents were a major source of dissolved selenium (largely as selenite) to the estuary prior to 1998, these discharges have dropped by 66%, making river inputs the largest fluxes of selenium to the Bay except during very low flow periods (Cutter and Cutter 2004). Because the San Joaquin River has selenium concentrations at least 10 times those of the Sacramento (Cutter and Cutter 2004), future CALFED restoration efforts that increase San Joaquin flows into the Delta may cause the dissolved selenium concentrations in the estuary to rise again (Cutter and Cutter 2004). Hence, it is critically important to fully and quantitatively

describe the processes affecting selenium cycling in these tidal freshwaters. In consideration of the above, the major objectives of the selenium field studies were to:

- 1) *Investigate the Delta-wide distributions and speciation of dissolved and suspended particulate selenium by sampling seasonally (and different river flow conditions) from Carquinez Strait to Stockton and Rio Vista.*
- 2) *Collect monthly dissolved and particulate selenium samples at bivalve monitoring stations in the Suisun Bay to evaluate the relationship between selenium dynamics in the water column and that in bivalve consumers.*
- 3) *Conduct detailed process studies at Mildred Island to: identify critical biogeochemical processes affecting Se in the Delta; measure in situ rates of transformations between dissolved and particulate selenium forms; and measure sediment-water fluxes of dissolved and particulate Se.*
- 4) *Obtain representative sediment cores (box and gravity) at multiple sites in the Delta to derive a historical record of Se inputs and cycling in the Delta*

Se transformations by phytoplankton and bacteria (SET)

Our general goal was to develop and parameterize models describing the bioaccumulation of dissolved selenium by phytoplankton of the San Joaquin/Sacramento River Delta (the Delta) and San Francisco Bay (SFB). Our efforts were focused on the uptake of two forms, inorganic selenite and dissolved organic selenide. Our efforts can be divided into four components.

- 1) *Estimating selenite uptake by algae in the Delta and SFB.* Marine algal species differ dramatically in their ability to bioaccumulate selenite (Baines and Fisher 2001). We were interested in determining whether similar variability occurs among freshwater algal species that are typical of those in the Bay-Delta ecosystem. Such information is important for assessing uncertainty in models of uptake and possibly in designing appropriate monitoring schemes. We were also interested in comparing algae from the two environments to determine if uptake differed systematically between the two groups. Moreover, we wanted to describe the dependence of selenite uptake on ambient selenite concentrations in the two environments so that uptake could be modeled more appropriately.
- 2) *Estimating the uptake of organic selenides by phytoplankton.* Organic selenides are readily produced by phytoplankton through excretion, or as a result of cell lysis. Where algal productivity is high, this labile dissolved organic Se can be an alternate source of Se to phytoplankton. We assessed uptake of mixed DOSe by a range of phytoplankton in the lab to determine its bioavailability. We also interpreted field data in this respect.
- 3) *Evaluating effects of ambient chemistry on selenite uptake by a range of freshwater and marine algae.* Ambient conditions such as ionic strength of the media, pH, phosphate concentration and sulfate concentration have been implicated in Se bioaccumulation (Riedel *et al.* 1991; Riedel and Sanders 1996; Riedel *et al.* 1996). Because many of the variables vary spatially across the Delta and SFB ecosystem and temporally due to variation in water sources and movements, we studied the effect of each of these on the uptake of selenite from solution by both marine and freshwater algae.

- 4) *Measurement of selenium concentrations in phytoplankton in situ.* As is generally the case with rivers and estuaries, most of the suspended particulate material within the Delta and SFB is non-living. This non-living material can be inorganic particles or organic detritus derived from terrestrial plants or algae. Se associated with such non-living material may not be as bioavailable to consumers as Se associated with living particles (Schlekat *et al.* 2000). Moreover, living organisms selectively ingest living particles over non-living particles. If the Se concentrations in this living material are different than those in non-living particles, standard chemistry may not reflect the true exposure of consumer organisms to dietary Se. Methods are needed to assess the Se content of live phytoplankton cells to address this issue.
- 5) *Uptake of selenite and organic selenide by bacteria.* During the course of the study it became clear that bacteria could potentially be an important source of Se to organisms in the SJR/SR-Delta and SFB. So a fourth line of research developed looking at the uptake of selenite and organic selenide by bacteria. We did this under both laboratory and field conditions.

Results from these experiments were designed to better parameterize models of Se transformations in the Delta for the purposes of predicting Se availability to different parts of the Bay/Delta food web.

Se in Bay-Delta Food Webs (SEF)

The goal of the food web group was to conduct studies to better understand mechanisms of Se transfers within the food webs of the Bay-Delta and examine the importance of trophic dynamics. Our specific objectives were to:

- 1) *Quantify Se concentrations in food webs of the Delta and identify species at risk for Se toxicity.*
- 2) *Identify pathways of Se exposure in Delta food webs.*
- 3) *Identify linkages between Se exposure and carbon source to food webs.*
- 4) *Identify Se hotspots in Delta and suggest possible mechanisms that explain hotspots (hydrodynamics, Se cycle).*

During the course of this study we observed Se concentrations in *Corbicula fluminea* to vary throughout the Delta as a function of growth and not significant changes in Se bioavailability. As a result we use this opportunity (constant Se bioavailability) to develop and refine a *Corbicula* Se model for the Delta.

Local scale modeling (ML)

Residence time in shallow water habitats. We wanted to understand the mechanisms by which San Joaquin River water exchanged between Delta channels and shallow water habitats, without considering chemical reactions. Toward this goal, we used a hydrodynamic model to characterize the residence times and exposure times of non-reactive particles within the shallow water habitats.

A literature search revealed several different approaches to parameterize “residence time.” Several different approaches were applied to Mildred Island and we published the results in *Limnology and Oceanography*. The goals of this paper were to: (1) compare three transport time scales commonly used to measure the retention of water or scalar quantities transported with water, (2) identify the underlying assumptions associated with each time scale, (3) describe procedures for computing these time scales in idealized cases, and (4) identify pitfalls when real-world systems deviate from these idealizations. Our purpose was to stimulate critical thinking in the application of transport time concepts and in the computation of these time scales where hydrodynamics are more complex than idealized cases. (Please see Monsen (2002) for more information.)

Franks Tract---The effect of SAV on hydrodynamics. The objective of this modeling effort was to develop a numerical model of the vertical structure of flow in the presence of submerged aquatic vegetation (SAV) using the Franks Tract observations described in the Section HS.

Franks Tract---Regional hydrodynamics. The goal of this modeling component was to develop a hydrodynamic base model for the Franks Tract region at a regional scale (i.e. including neighboring channel environments). The time period for this base model is April 2002, the same as for the Franks Tract Process Study discussed elsewhere in this report.

Mildred Island—Modeling with reactions. The goals of this modeling component were to 1) develop a numerical tool that links hydrodynamics, biology, and geochemistry for the Mildred Island region; 2) build on and synthesize multidisciplinary measurements from the 2001 Mildred Island field experiment; 3) develop and test methodologies to be implemented at the Delta scale; 4) understand process interactions governing the spatial and temporal variability of phytoplankton biomass and selenium relevant to upper trophic levels.

Delta scale modeling (MD)

Hydrodynamic modeling. This task was designed to understand what influences the transport of San Joaquin derived water as it traverses the Delta beginning at Vernalis through the Delta towards Suisun Bay without considering any chemical reactions. We wanted to understand the mechanisms by which San Joaquin River water was distributed through the various Delta channels and exchanged with the shallow water habitats of the Delta.

There were two major efforts within this task: First, based on modeling and observations we developed an understanding (and conceptual model) of the influence of barriers, gate, and pump operations on circulation at a Delta scale. Second, we developed simulations in conjunction with field data that showed the influence of gate, barrier and pump operations on the distribution of different water sources in the Delta.

Understanding the influence of barriers, gate, and pump operations on source distribution.

Multiple demands for water transiting the Delta are satisfied through the operation of several man-made structures using a complex suite of flow manipulations and diversions both upstream

and within the Delta. Local-scale water diversions are designed to modify the routings of water from the different fresh water sources. In the process, regional-scale flow paths are transformed to an extent that they alter system wide fluxes of water, salt, nutrients and contaminants, migration routes of anadromous fish, and quality of water delivered to municipalities. We use a simplified schematic of water sources and transport paths linked to the central Delta mixing zone (Figure MD1, inset) to illustrate hydraulic alterations of individual diversions and their significance to the Delta ecosystem. Our purpose was to encourage a broader framework for water-resource management that explicitly recognizes the interconnections between hydrologic manipulations, water quality, and life-support functions provided by aquatic ecosystems. These findings are in a manuscript that will be re-submitted to *Water Resources Research* after revision. Please see Monsen (In prep.) for more information.

Source distribution through the Delta. The goal of the source distribution simulations was to understand how changes in the operations affect the distribution of individual water sources throughout the Delta. For example, the purpose of operating the Delta Cross Channel is to direct Sacramento water into the central Delta. Our simulations demonstrate how this gate operation changes the mixture of Sacramento and San Joaquin throughout the Delta landscape.

Modeling with reactions. The goals of this modeling component were to 1) develop a numerical tool that links hydrodynamics, biology, and geochemistry at the Delta scale; 2) build on and synthesize multidisciplinary measurements from various field campaigns; 3) understand process interactions governing the spatial and temporal variability of phytoplankton biomass and selenium relevant to upper trophic levels.

IV. APPROACH/METHODOLOGY

Hydrodynamic Measurements in Shallow Water Habitats (HS)

The work we describe here was carried out in two contrasting shallow water habitats: Franks Tract (FT), which is characterized by dense SAV development and numerous levee breaches between the shallows and the channel, and Mildred Island (MI), which is relatively clear of SAV and has 1 primary channel-shallow opening.

The Mildred Island experiment was carried out in August-September of 2001 and consisted of a combination of moored instrumentation and boat-mounted surveys of the northern end of the basin. The moored instrumentation we discuss here is primarily from the south island station (MILS, Figure HS1), and consisted of two conductivity-temperature-depth sensors (one near-bed and one mid-column) and an acoustic Doppler current profiler to measure velocity profiles.

In Franks Tract, a series of five experiments near one of the northern levee breaches (see Figure HS2) spanning the period of vegetation development, from March through September, were carried out. In each experiment, a set of acoustic Doppler velocimeters (ADV) were deployed in a vertical array on a sawhorse frame (see Figure HS3). In each case, the instruments were deployed inside a bed of SAV, and we attempted to return to the same site for each experiment. In one of the experiments, a second frame was deployed in the open water adjacent to the vegetated site. Each experiment lasted for at least one spring-neap cycle (2 weeks), and

boat-mounted surveys captured the spatial variation in the flows several times within each study period (an example appears in Figure HS12, discussed below). See Table HS1 for a summary of these experiments.

In order to evaluate the important forcing mechanisms for the hydrodynamics of Delta shallow water habitats, a field-based observation program was required. In the development of field studies to evaluate processes, there is always a tradeoff between spatial and temporal resolution. Due to the large horizontal scales in these habitats, and the expectation of a local, vertical balance dominating the hydrodynamics, we focused our activity on the collection of time series data at carefully chosen points within the habitats. Further, instruments were arrayed in the vertical in order to capture the vertical structure. In Mildred Island, sites were chosen to be representative of the two extremes of the system: the strongly tidal north island, and the more isolated south island. In Franks Tract, we selected study sites that were along a well-known area of SAV development so that we could track the seasonal flow changes in response to SAV growth.

In each case, the instrumentation deployed was state-of-the-art, including as many as 6 acoustic Doppler velocimeters. This provided us with the most accurate measurements possible of flows in these low-energy environment. With this approach, we have successfully resolved currents as small as just a few centimeters per second – and have reliably estimated vertical shears in these environments.

Regional Hydrodynamic Field Investigations (HR)

General Experimental Design. A combination of Eulerian (fixed site) and Lagrangian measurements were used in Mildred Island and Franks Tract to study the regional hydrodynamics.

The Eulerian measurements were used in to monitor the exchange of water, temperature, salt (and sometimes Chl-a) past key locations within the islands, in levee breaches and in the surrounding channels (Figure HR3 and HR4, respectively). Each Eulerian sampling station consisted of an upward-looking Acoustic Doppler Current Profiler (ADCP), a conductivity-temperature-depth (CTD) probe, and, sometimes, a SCUFA (which monitors Cl-a and turbidity) (Figure HR5). Specifically, at each sampling location, six distinct time series were collected on three separate pieces of equipment: (1) sea level measured with a pressure sensor at depth, (2) velocity consisting of a depth-averaged magnitude and direction (at some stations, a velocity profile was collected), (3) water temperature, (4) conductivity, (5) fluorescence, and (6) turbidity. At each of the channel stations, and within the breaches, a sequence of discharge measurements were made over a twelve hour flood-ebb tidal cycle, so that the ADCP measurements could be used as an index to compute the mass flux, or discharge, at each station. These mass fluxes are then used to compute conductivity, temperature, chl-a, and turbidity fluxes at each station location (see *Fluxes – Uses, Computation* below). We achieved a perfect data return rate in both of these studies: every single sensor on every single piece of equipment gave viable data (See Cuetara and others, in prep.).

Finally, a meteorological station was deployed during each study that measured atmospheric pressure, wind speed and direction, air temperature, and visible light. These data were used to understand phytoplankton dynamics, thermal stratification and atmospheric pressure and wind induced transports.

Eulerian Measurements.

Mildred Island study design. ADCP's were deployed in the major breaches (station NOPN, SOPN), within the interior of the Island (stations MILN, MILS) and within the key connecting channels (Stations CON, MIDCON, MIDCOL, LATH) for a ~ 3 month period from 8/23/2001 to 11/13/2001 (Figure HR3). Velocity profilers were specifically used in the interior to measure the effects of temperature stratification and wind shear (Section HS). A low-profile depth-average velocity meters (SONTEK Argonaut) was deployed in the southern breach. The breaches along Mildred Island's southeast levee were not monitored. All of the velocity meters, with the exception of those in the Islands interior, were flow calibrated using moving boat discharge measurements (see *Calculation of Discharge* section below). Near-bed CTD's were deployed adjacent to each velocity sensor to monitor sea-level variations and to measure specific conductance. Two high precision pressure sensors were deployed across Mildred Island to examine the barotropic pressure gradient.

Franks Tract study design. The Franks Tract levee system has a large number of significant levee breaches on its north-western flank and the north-east levee is virtually non-existent (Figure HR4). This physical configuration made it impractical to directly monitor the exchange between Franks Tract and its surrounding channels. Instead, we decided to monitor exchanges between Franks Tract and the Delta by instrumenting the major channels that exchange with the Franks Tract as a whole (Stations FALSE, FISH, OLDR, MAN, HOL, SMS). Within the interior of Franks Tract, low-profile depth-average velocity meters (Argonauts) were deployed (FRW, FRW). All of the velocity meters, with the exception of those in the Islands interior, were flow calibrated using moving boat discharge measurements (see calculation of discharge section below). Near-bed CTD's and SCUFA's were deployed adjacent to each velocity sensor to monitor sea-level variations, temperature, specific conductance, turbidity and chl-a. Data were collected from April 10, 2002 through August 27, 2002 in Franks Tract; > 4.5 months of data (See Cuetara and others, in prep.).

Flow station network. The Mildred Island and Franks Tract instruments were placed in the context of a USGS-run permanent flow station network (Figure HR6). The data from the flow station network were combined with the roughly 3-month detailed studies in Mildred Island and Franks Tract to address Delta-scale interactions. Specifically, the data from stations JPT, TMS, DCH, OLD and MID were used as part of the Franks Tract study.

Data collection/processing - Calculation of Discharge. At each station in the flow network (Figure HR6) and at most of the data collection locations in the Mildred and Franks Tract experiments, the index velocity, discharge, and stage data were measured at 15-minute intervals. Discharge, flow, or mass flux, Q , is a computed quantity involving the product of the cross-sectional area, A , and mean velocity, V : $Q=VA$. Unfortunately, the area and mean velocity cannot be easily measured directly; particularly in the tidally affected channels common in the Delta (Ruhl and Simpson, 2005). Therefore, stage and an index velocity are used as surrogates on which the discharge is computed. Calibration relations for the area and the mean velocity must be developed for each station based on stage and index velocity, respectively, in what is referred to as the "rating process".

Over the last several decades, many advances have been made in the field of hydroacoustic technology and a wide range of instruments are commercially available that can measure index velocities (Rantz, 1982; Morlock and others, 2002). Examples of equipment used in the Sacramento-San Joaquin Delta permanent flow monitoring network (Figure HR6) for measuring index velocities include Ultrasonic Velocity Measurement (UVMs) and sideward-looking ADCPs (both single-bin and profiling). Upward-looking ADCP's were used in both the Mildred Island and Franks Tract field investigations. Index velocities are related to discharge through the "rating" process where actual discharge measurements are made using a boat-mounted downward-looking ADCP at each station location. The procedures used to collect the calibration discharge measurements are described in detail in Simpson and Oltmann (1993), Morlock (1994), and Simpson (2001). In tidally affected environments, it is important to collect discharge measurements that adequately characterize the high frequency variability of the tides as well as the seasonal variability associated with the annual variations in the hydrologic cycle (Simpson and Bland, 1999), and in the case of the south Delta, annual variations in export rates. Tidal variability in the calibration data sets is captured by collecting 50 to 120 discharge measurements over a 12- to 13-hour period and seasonal variability by collecting data (10 to 20 measurements) during periods that cover the full range of hydrologic cycle variability (such as extreme high or low flow events) at a given site. The final relationship for discharge is based on a least-squares regression between the index velocity collected at the gage station and mean velocity based on the boat-mounted downward-looking ADCP discharge measurement system. A wide range of relationships have been developed in the Bay and Delta region. Most relationships are linear; however, more complex ratings also are possible. In the Delta, we have documented several higher-order polynomial ratings; loop ratings that are indicative of ebb-flood asymmetries in the current structures at the measurement location causing a different relationship between the flood-to-ebb transition versus the ebb-to-flood transition; and occasionally we have found a bimodal relationship.

Computation of tidally averaged flow – the need for high accuracy tidal timescale

measurements. Based on the frequency content (power spectral density estimates) of historical sea level, flow, and salinity data collected in the Delta it is clear that transport in the Delta occurs at two distinct timescales: the tidal and tidally averaged, or residual timescales (Dyer, 1974; Fischer et.al., 1979; Walters and Gartner, 1984)(Figure HR7A). Because of this, sea level, flow, and salinity data can be separated into tidal and tidally averaged components. This separation is useful because the influence of the rivers and water project operations on *water movements* in the Delta occurs primarily at the tidally averaged, residual or net timescale. This time separation suggests a linearity that somewhat oversimplifies the dynamics and mixing that occurs within this system; particularly when one considers the reduction in the tidal current magnitudes and concomitant reduction in tidal timescale mixing of constituents that can accompany periods of high net flows. Nonetheless, the net flows are a useful construct that have helped us understand and manage the Delta for several decades and are therefore computed as a routine procedure for each station in the network.

The net flows for this report were computed using a digital tidal filter after Walters and Heston, 1982; and Wang and Cheng, 1993. Digital filters have been widely used in this estuary (Lacy et.al., 1996, Ruhl et.al. 1999, Warner et.al., 1997) and in estuaries around the world (Dronkers and Van De Kreeke, 1996; Geyer and Nepf, 1996). The tidally averaged flow is often

less than 5% of the tidal flows (Figure HR7B), which places extremely rigorous demands on the accuracy of the measured flows. The net flow is essentially the difference between the ebb and flood tidal flows. Therefore, small inaccuracies in the often very large measured tidal flows can easily dominate the calculated net flow. High frequency random measurement errors are of little concern in the computation of the net flows since the tidal filter effectively removes these errors, however, ebb/flood bias errors in the measured flows can be problematic. Many of the standard operating procedures and quality assurance measures used in the collection and processing of discharge data are in place specifically to minimize bias errors (Ruhl and Simpson, 2005). Simpson and Bland (1999) discuss bias errors and their implications in the computation of net discharge in tidally affected environments.

Fluxes – Uses, Computation. Fluxes are Eulerian measures that integrate, and thus simplify, in a local regional sense, processes that fundamentally occur in a Lagrangian reference frame. The flux of a constituent measured past a given point encapsulates a combination of advective and dispersive mixing processes that occur within a tidal excursion of the measurement location. Fluxes therefore help us get at mechanisms in a way that simply looking at time-series of constituent variations cannot.

One of the key variables used to manage transport in the Delta is the mass flux (or discharge or flow), $Q(t)$, typically computed as the total amount of water passing a given cross section. From a management perspective, the *tidally averaged* discharges are generally considered – tidal timescale discharges are virtually ignored as a management tool. Although less used for management purposes, but potentially of greater use, is the flux of constituents of interest through a given cross section, such as salinity, temperature, chlorophyll, organic carbon, etc. If one assumes that the cross-channel variation in a generic constituent, $C(t)$, is negligible, which is mostly true in the predominantly narrow channels in the Delta, then the constituent flux, $\dot{C}(t)$, is simply the product of the mass flux and concentration, $\dot{C}(t) = Q(t)C(t)$.

Flux Decomposition. Constituent flux decompositions, which allow us to separate advective from dispersive transport mechanisms, have been used extensively to understand the processes that control transport in estuaries throughout the world (Geyer and Nepf (1996), Jay et.al. (1997), Dyer (1974), Dronkers and Van De Kreeke, (1986), Fischer, (1979)) and in the San Francisco Bay and Delta (Lacy et.al. (1996), Ruhl et.al. (1999), McKee et.al. (2002), Warner et.al. (1997)).

In both field and modeling studies, mass and constituent fluxes are typically computed at key cross sections within the Delta. As an example, Figure HR4 shows the locations where mass and salt fluxes were measured in Franks Tract in summer/fall 2002 and in Mildred Island in Figure HR3. Constituent fluxes can be decomposed into advective and dispersive components to understand transport mechanisms, at least in a bulk, or regional sense. Flux decompositions are accomplished by first separating the concentration and mass fluxes into tidal (primed terms) and tidally averaged components (bracketed, $\langle \rangle$), $C(t) = C'(t) + \langle C(t) \rangle$, $Q(t) = Q'(t) + \langle Q(t) \rangle$, respectively (theory section justifies this time separation). These relations are used to decompose the total tidally averaged constituent flux into advective and dispersive components through a number of simplifying assumptions as

$$\begin{aligned} \langle \dot{C}(t) \rangle &= \langle Q(t)C(t) \rangle = \langle Q(t) \rangle \langle C(t) \rangle + \langle Q'(t)C'(t) \rangle \\ \langle \dot{C}(t) \rangle &= \langle \dot{C}(t) \rangle_{Adv} + \langle \dot{C}(t) \rangle_{Disp} \end{aligned}$$

where $\langle \dot{C}(t) \rangle_{Adv} = \langle Q(t) \rangle \langle C(t) \rangle$ and $\langle \dot{C}(t) \rangle_{Disp} = \langle Q'(t)C'(t) \rangle$ are the advective and dispersive flux components, respectively.

The advective flux represents the transport of the tidally-averaged concentration of a constituent through a given cross-section (or point). The dispersive flux, on the other hand, represents the transport of a constituent that occurs when and where the tidal discharge and tidal concentrations are correlated. For example, the dispersive flux will be large and in the flood direction in situations where higher concentrations occur on (are correlated with) flood tides over ebbs. Similarly, in situations where higher concentrations occur on ebbs over floods, the dispersive flux will be in the ebb direction. Mechanistically, flood/ebb concentration differences occur whenever the concentration within a tidal excursion of a sampling location is mixed as it travels along its tidal excursion trajectory. Mixing, in tidally forced systems, is primarily due to velocity shears created by bathymetric variability. Generally, then, the greater the bathymetric variability within a tidal excursion of a given sampling location, the greater the mixing and concomitant dispersive flux. The dispersive flux can therefore be thought of as a bulk measure of the amount of mixing (dispersion) that occurs within a tidal excursion of a given sampling location, for a given spatial concentration gradient.

Lagrangian Measurements. Lagrangian measurements were also made in both Mildred Island and in Franks Tract. Transport of constituents and non-motile or feeble-swimming biota in the tidally forced regions of the Delta is a fundamentally Lagrangian process, yet unfortunately Lagrangian measures are man-power intensive and difficult to obtain in the field. Nonetheless, we conducted several drifter studies using underwater sails fitted with differential GPS receivers (Figure HR8) to measure tidal excursions within channels and mixing characteristics within the Islands. Drifters are generally placed in the water at key locations during slack water and measure water movements for a complete tidal cycle (~ 12 hour period).

Bivalve distribution and grazing rates (B)

Delta Scale Benthic Grazing Rates for Use in Models. The study was designed to assess bivalve grazing within the Delta-scale model domain during late spring after spring recruitment of bivalves, but before the exponential growth phase of the *Egeria densa* beds began, which can make sampling in some shallower system difficult. We had hoped that careful location of samples would allow us to assign a regional/habitat average that could be used in future field and model investigations. To this end stations were located within strata (Figure B1) that were based on average temperature and electrical conductivity of each region; data collected by the California Department of Water Resources, California Fish and Game, and the Bureau of Reclamation since 1977 and furnished to us by Alan Jassby (UC Davis) and Wim Kimmerer (Romberg Tiburon Center) were used to establish these strata. Stations were assigned to a habitat type within each stratum based on the type of river or enclosure and the designation of the habitat as natural or man-made. Types of river and slough were assigned a degree classification relative to their connections to Suisun Bay and the San Joaquin and Sacramento Rivers which were assigned degree 4 to make the designations consistent between the bay and rivers (Figure B2).

Modeling and scaling exercises prior to the Mildred Island and Franks Tract process studies revealed the importance of the channels surrounding the flooded island habitat. Therefore we chose to sample that habitat in great detail during those process studies and our conclusions on the delta-scale distribution of *C. fluminea* will reflect a combination of those studies and the delta-scale study (summary of stations shown in Table B1).

Our first delta-wide sampling in May 2003 (Figure B3, Table B2) revealed a predominance of young clams (see below). For that reason we sampled about a third of the stations again in October 2003 (Table B3) to determine if the pattern that we observed was consistent through the year or if those young clams grew sufficiently through the summer and fall to change their grazing rates.

Samples were collected with a 0.05 m² van Veen grab in all of our studies. Samples were sieved on a 0.5mm screen, preserved in 10% formalin, and transferred to 70% ethyl alcohol stained with Rose Bengal at 1-2 weeks. All *C. fluminea* and *C. amurensis* were removed from the samples and the longest dimension of the shell (SL) measured to the nearest 0.1 mm using Vernier calipers. Animals from the full size range of bivalves available in as many samples as possible (based on availability of clams in the sample) were removed live and frozen for conversion to dry tissue weight. Bivalves in the frozen subsample were sorted into 1-mm SL size groups. The clams were weighed then ashed in a 500°C muffle furnace to determine the average ash-free-dry tissue weight (AFDW) of the clams in each 1-mm size group, ie the dry weight of the tissue. These data were used to calculate a regression equation relating SL to AFDW for each site. Both SL and AFDW were log-transformed for the regressions ($p < 0.05$, $r^2 > 0.9$ for all regressions). AFDW of bivalves in the preserved samples was estimated using the SL to AFDW regressions. A summation of the AFDW in each sample represents the biomass of *C. fluminea* in each sample (/0.05m²).

Dry weight was used to estimate temperature corrected pumping rates. Pumping rate per unit weight (PR_{wt}) was derived from data published by Foe and Knight (1985) for *C. fluminea* from the Delta: $PR_{wt} \text{ (ml (mg AFDW)}^{-1} \text{ hr}^{-1}) = 0.4307 e^{0.1113(\text{temp})}$. This equation is valid for temperatures between 16° and 30°C. Pumping rates for *C. amurensis* were based on the conversion of 400L/g AFDW/day (Cole *et al.* 1992) that was adjusted for seasonal changes in water temperature using coefficients (Q₁₀) from studies of *M. edulis*: Q₁₀ of 2.2 at 5°C, 1.2 at 10°C, 1 at 15°-20°C (Winters 1978). Pumping rate for each individual clam was then calculated as PR (L/d) = (PR_{wt})(AFDW). The population filtration rate at each site was based on summed individual pumping rates.

Grazing rate (GR) at each site was estimated assuming a maximum effect of a concentration boundary layer (CBL) by decreasing filtration rate (FR) using two refiltration relationships: (1) *C. fluminea*: $n_{max} = 3/(s/d_o)$, derived by O'Riordan *et al.* (1995) for *Venerupis japonica*, a bivalve with a pumping rate ($\approx 8 \text{ ml mg}^{-1} \text{ hr}^{-1}$) similar to *C. fluminea*, and (2) *C. amurensis*: $n_{max} = 2.5/(s/d_o)$, derived by O'Riordan *et al.* (1995) for this species. The refiltration proportion n_{max} is that proportion of water previously filtered by a square meter of bivalves (GR = FR (1 - n_{max})). The parameter s is the distance between siphon pairs (decreases with clam density) and d_o is the average diameter of the excurrent siphon of the animals collected at each site (a measure of animal size). Benthic grazing rates calculated in this manner represent the minimum grazing rates because they assume that the near bottom boundary layer is depleted of suspended algae and mixing of the water column is inadequate to replenish that lower layer with biomass from above. The final assumption is that the animals are feeding all of the time.

Temperatures used in the benthic grazing estimates were based on measured temperatures during the studies: 17°C in May and 26°C in October in the Delta and 17°C in May and 20°C in October in Suisun Bay.

Regional Scale Benthic Grazing Rates for Process Studies – Mildred Island Process Studies.

C. fluminea was sampled at 36 locations within the island and at 26 stations in the external channels (Figure B11, Table B4) using the techniques described above. Biomass and grazing rate was calculated as described in the previous section. Pumping rate estimates were based on temperatures (23-24°C) measured in the bottom water during the process study.

Channel Scale Benthic Grazing Rates – Is There a Distribution Pattern? Based on our findings on the importance of channel processes in and around flooded islands and our interest in the habitat quality of fast-moving river channels, we designed a study to determine if *C. fluminea* are an important sink for particulate Se and phytoplankton in these habitats, and if it was possible to predict where the largest populations might occur. We hypothesized that based on their ability to be transport as bedload, small *C. fluminea* were likely to accumulate in hydrodynamic “dead zones” or at the least in areas with relatively low current velocities. Based on our knowledge of hydrodynamics, we would expect the largest numbers of small animals, and potentially of adults, to occur on the inside of bends and on the banks of the deep channels in the straight sections of the rivers. Our sample locations were therefore oriented as transects running perpendicular to the axial flow (Figures B16a, B16b, and B17a, Table B6).

Spatial Variability in Benthic Grazing Rates – Franks Tract Processes. Stations were located within a tidal excursion of Franks Tract (Figure B20) for this process study due to the hypothesized importance of the surrounding channels to the production of phytoplankton inside the island. We sampled 24 stations inside the island, 6 in False River, 14 in the San Joaquin River, 5 in Middle River, 30 in Old River and 29 in the connecting sloughs and flooded islands around the Tract (Table B8) for a total of 108 stations. Grazing rates were calculated using temperatures that were recorded inside and around the island by *in situ* thermometers.

Temporal Variability in Benthic Grazing Rates – Franks Tract Processes. Two stations within the island (FTI09 and FTI17, Figure B23) were sampled for a year to examine the temporal variability in grazing rates within the island. We also sampled monthly at stations coincident with *in situ* fluorometers at False River, Taylor Slough, Sandmound Slough, Holand Tract, Mandeville Tract, Old River and Fishermans Cut to determine changes in grazing rates in those locations during the time that the meters were in place. An additional 7 stations were sampled between the internal island stations, along a transect, to determine phytoplankton loss along this mid-island advective channel.

Carbon field studies (C)

Mildred Island. Several methodologies were employed to gather data relevant to phytoplankton carbon in the Mildred Island region. Spatial mapping of phytoplankton biomass was performed during a 30-hour field study inside MI and in its surrounding channels using two research vessels with continuous water flow-through systems that measured chlorophyll *a* fluorescence, water

temperature, specific conductivity, turbidity, and dissolved oxygen. Five such spatial maps were performed, temporally centered on five consecutive slack tides. In order to calibrate instruments, discrete water samples (chlorophyll *a*, suspended particulate matter [SPM], dissolved oxygen [DO]) were taken within and outside MI. Sampling for nutrients (nitrate, nitrite, phosphate, silicate), zooplankton, phytoplankton community, and the underwater light field was also conducted throughout the 30-hour study at locations within and outside MI. Several vertical profiles of conductivity, temperature, chlorophyll fluorescence, and dissolved oxygen were obtained in different locations and on different tidal phases. Measurements of primary productivity were performed in a lab van using samples gathered during the 30-hour study. Weekly discrete sampling was conducted four times on dates surrounding the 30-hour study; during these sampling expeditions, chlorophyll, zooplankton, SPM, and irradiance were measured at locations within MI and its adjacent channels (see Fig. C1). High frequency time series of chlorophyll fluorescence were obtained with two pair of SCUFA's (self-contained underwater fluorescence apparatuses) which were deployed for approximately one month during the period of the weekly sampling and 30-hour study; SCUFA's were collocated with ADCPs (for velocity) and CTDs (for conductivity, temperature, depth) at the main northern entrance (see NOPN, Fig. HS1) and in the southeast interior near the location of maximum chlorophyll (see MILS, Fig. HS1). At the chlorophyll max, a bottom DO sensor was deployed to assess the potential for DO limitation of benthic herbivores. Much of this work was in addition to what was originally proposed, e.g. expansion of mapping from MI interior into the channels, deployment of SCUFA's and DO sensor, weekly sampling, sampling of nutrients, zooplankton, phytoplankton community, SPM, and irradiance.

Irradiance and turbidity were measured to aid the assessment and modeling of light-limited phytoplankton growth, as the Delta is a turbid environment; nutrients were measured to confirm conclusions from past studies that suggested that phytoplankton in the Delta are rarely if ever nutrient-limited. Zooplankton taxa, abundances, and biomass were assessed to illuminate a potentially significant sink for phytoplankton in the water column (zooplankton grazing). Temperature was measured because it can regulate phytoplankton growth as well. Measurement of these various quantities over space and time, and across gradients in bathymetry and flow, together with measured benthic biomass, allow for a thorough assessment of the local sources and sinks for phytoplankton biomass, both *in situ* and for future use in models. Phytoplankton community provides information relevant to species succession, selenium uptake rates (i.e. different phytoplankton species take up selenium at different rates, see Baines and Fisher (2001)), sinking/floating/swimming, and food quality for upper trophic levels. Detailed measurements in several peripheral channels allowed for assessment of not only isolated channel dynamics but also of flooded island-channel connectivity; such assessment is enhanced by the coordinated hydrodynamic and fluorescence time series (SCUFA) measurements at the main northern levee opening. Given the relatively "open" nature of the Delta's flooded islands with their many levee breaks and connections to tidal channels, as well as the ultra-connectedness of the Delta in general, a study that spanned the interface between habitats was critical to better understanding the Delta overall. The temporal design of our sampling captured hourly (diel/tidal) variability, weekly variability (e.g. spring/neap), and the summer-fall transition.

Franks Tract. As in the case of Mildred Island, our study of carbon in the Franks Tract region involved a multi-pronged measurement strategy. In this case, we deployed 9 SCUFA's to characterize variability in phytoplankton biomass within FT and in each of the 7 primary

channels connecting to it (see Fig. C2). These instruments were collocated with ADCPs and CTDs described under Section HF and were in the water between April and August. Four expeditions occurred at 2-3 week intervals between May and July to conduct discrete sampling, instrument servicing, and chlorophyll mapping. Discrete samples included chlorophyll *a*, SPM, phytoplankton community, irradiance, zooplankton, and dissolved inorganic carbon (DIC). Water samples were taken near surface and at depth, at stations coinciding with instruments inside and outside FT, and at additional stations further up the adjoining channels. As in the case of Mildred Island, the additional discrete samples allowed for assessment of local sources and sinks for phytoplankton biomass. Chlorophyll mapping was conducted across FT (as far as *Egeria densa* beds would allow) and along and across adjoining channels for assessing spatial gradients in phytoplankton biomass. The SCUFA, zooplankton, light, phytoplankton community, SPM, DIC and zooplankton measurements transcended the measurements originally proposed, as did the inclusion of multiple connected channels and the weekly-scale sampling work. As at MI, the concurrent study of shallow water habitat and adjacent channels---including relevant physical and biological processes in each---allows for a more thorough understanding of this specific region and also of the Delta in general due to the pervasiveness of interhabitat connectivity in the system. The temporal design of our sampling captured hourly (diel/tidal) variability, weekly-monthly variability (e.g. spring/neap), environmental shifts due to the annual development of dense *Egeria densa* beds, and the spring-summer transition, when zooplankton are most food limited and larval fish are most dependent on zooplankton for forage.

Delta scale. 2003 measurements of Delta-scale phytoplankton biomass involved discrete chlorophyll measurements at 75 stations throughout the Delta, Suisun Bay, the Sacramento River, and the San Joaquin. Additional point measurements included 75 nutrient samples and 132 Secchi disk readings, for conversion to light extinction coefficient. This sampling was not originally proposed but was deemed crucial for obtaining a detailed snapshot of chlorophyll spatial variability coinciding with the detailed variability in benthic grazers, and for potentially using CDWR/IEP's monitoring data for driving models. Nutrients and Secchi readings were necessary for estimating the growth rates of phytoplankton in the Delta-scale coupled model.

Field studies of selenium distributions and transformations (SED)

Water samples were acquired with 5 L Go-Flo bottles deployed on a Kevlar cable and triggered with a plastic messenger 1 m below the surface. After recovery, the bottle was pressurized with 8 psi nitrogen and water directed through a precleaned and tared 142 mm diameter, 0.4 μm polycarbonate membrane held in a Teflon filter holder (filters frozen for particulate analyses). Filtered water was placed in 1 L borosilicate bottles (Teflon-lined caps), acidified to pH 1.6 with HCl, and stored in the dark until analysis for Se speciation. Filtered water was also placed in 125 mL borosilicate bottles for salinity/chlorinity determinations, and 125 mL polyethylene bottles that were immediately frozen for nutrients. Sediment and pore water samples were collected using box and gravity corers off the RV David Johnson. From each box core, one sub-core was taken for sediment sectioning and two sub-cores were taken to obtain pore water samples. Sediment sub-cores (20 cm deep) were obtained with an acrylic core tube (o.d. of 5.7 cm). Within an hour of collection, the sediment sub-core was sectioned in 1 cm intervals up to 5 cm,

and below this depth, in 2 cm intervals. All sediment samples were placed in polyethylene bags and immediately frozen until processing.

High-resolution pore water samples were collected using the whole-core squeezer method described by Bender *et al.* (1987). The acrylic sub-core tube (o.d. of 7.7 cm) was inserted into the box core sediments, and the top piston, fitted with a 3.5 cm porous polyethylene disk on the bottom, and three-way valve to extract pore water was placed in the top of the sub-core tube before removal. Once removed, the bottom piston was quickly inserted into the bottom of the core. The sub-core was placed in a rack that held the core tube and top piston in place, while a hydraulic jack pushed the bottom piston up, causing the sediment to move to the upper piston of the squeezer. Water was pre-filtered through the porous polyethylene disk and glass fibre filter paper (nominal pore size 0.7 μm) before it was transferred through a three-way valve into a gas-tight glass syringe (Zhang *et al.* 1998). After 10 mL of pore water were taken, the three-way valve was closed, another syringe attached, and the extraction process continued. The sample was directly filtered through a 0.4 μm membrane filter into pre-cleaned glass vials. Due to low concentrations of dissolved selenium, pore waters from two sub-cores were combined. Pore water samples were immediately acidified to pH of 1.5 and refrigerated. Sub-cores were also taken to determine sediment porosity in order to convert the volume of pore water collected to depth intervals (Bender *et al.* 1987).

The speciation of dissolved Se was determined using the selective hydride generation/atomic absorption detection method described by Cutter (1978; 1982; 1983). The standard additions method of calibration was used to ensure accuracy, and all samples are analyzed in triplicate to quantify precision (typically < 4% for concentrations above 0.4 nmol l^{-1}). Detection limits were 0.02 nmol l^{-1} for all dissolved forms of Se. The concentration of total particulate Se on filters or sediments was determined using wet oxidative digestion followed by selective hydride generation atomic absorption spectroscopy (Cutter 1985). Selective leaches on filters or sediments were conducted for determination of particulate Se speciation (elemental Se, (Velinsky and Cutter 1990); SeIV + SeVI, (Cutter 1985)). Accuracy was evaluated using the digestion and analysis of standard reference material (NIST 1566 or 1566b oyster tissue. The detection limit for particulate Se was 0.005 nmol L^{-1} , with precision (relative standard deviation) of <5%.

Nutrients were determined using the standard colorimetric procedures of Parsons *et al.* (1984) adapted for use on an Alpkem Rapid Flow Analyzer. Chloride concentrations were determined using ion chromatography with a detection limit of 0.03 $\mu\text{mol l}^{-1}$ and a precision better than 3% (relative standard deviation). Filters for organic C and N analyses were dried at 40°C and processed using a Carlo Erba 1500 Elemental Analyzer (Cutter and Radford-Knoery 1991). The concentrations of chlorophyll and phaeophytin on a glass fiber filter were determined using solvent extraction and fluorometric analysis (Parsons *et al.* 1984).

Se transformations by phytoplankton and bacteria (SET)

Culture studies of dissolved selenium uptake by phytoplankton. To measure uptake of selenium by phytoplankton, we have conducted experiments measuring uptake of radiolabeled selenite by algae in laboratory cultures. The use of a radiotracer allows us to easily measure the movement of Se between water and particles at concentration approximating natural background levels. Radioisotope was added only as ^{75}Se labeled dissolved selenite, the most bioavailable form of

selenium. While we intended to study the uptake of selenate as well, our source for radiolabeled selenite (Los Alamos National Laboratory) discontinued production in 2001 and we have not yet been successful in synthesizing pure selenate from our selenite stocks. Pure selenate is essential for these experiments because the algae could take up any remaining selenite much more efficiently, possibly causing our uptake measurements to be badly biased. Despite lacking data on selenate, we believe that our results are very relevant to the Bay-Delta ecosystem. Based on current concentrations of selenate in the Bay-Delta ecosystem, this form of inorganic Se is unlikely to be the major source of Se to algae, although this situation may not hold under future scenarios for drainage of contaminated waters of the central valley since they may increase selenate concentrations significantly. In comparison, we have found that algae are able to accumulate selenite very effectively at the concentrations typically observed in the Bay-Delta ecosystem. Radioisotope based estimates of Se:C ratios in a region dominated by phytoplankton agreed well with standard chemical measurements, suggesting that selenite was the predominant source of Se to algae in the delta (Baines *et al.* 2004)

The algal cultures used include both marine species and freshwater species, including a species isolated by us from the Delta and several genera representative of those in the Bay-Delta ecosystem. Marine species can vary a great deal in their ability to concentrate selenite from solution. We selected algae that varied widely in their ability to accumulate selenite. Purely synthetic media were used for both freshwater (WCL-1, Guillard (1975)) and marine (Aquil, Price (1988)) experiments to attain complete control over chemistry. Selenite concentrations in experiments ranged between 0.05 nM and 10 nM, or 4 times lower and >5 times higher than has been observed in the Bay-Delta ecosystem over the last 20 years (Cutter 1989; Cutter and Cutter 2004). Uptake as a function of added selenite concentration was measured over 1-4 h periods to estimate gross uptake rates. The accumulation of selenite was also followed until the cells attained a stable concentration of Se, allowing us to estimate the equilibrium Se concentrations attained by the cells at that concentration of ambient selenite. These experiments were stopped before selenite was depleted by >20% so that changing concentration of selenite did not affect uptake during the experiments. The media used for the standard uptake experiments were amended with f/40 nutrients since this approximated the concentrations of phosphate, nitrate and ammonia present in the Bay-Delta. The pH was corrected to 7.5 and 8.1 in the freshwater and marine cultures respectively, as these values are typical of the Delta and Bay respectively.

The effect of water chemistry was only assayed for short term selenite uptake under the assumption that equilibrium cellular selenium concentrations would reflect the same trends. In experiments assessing the role of phosphate, nitrate and silicate on uptake of selenite, we compared uptake of selenite by species that differ in their ability to concentrate selenite. Uptake in a nutrient poor treatment (F/200 nutrient levels) was compared to uptake in media containing F/2 levels of each of the nutrients in turn. The effect of these nutrients in controlled adsorption onto dead particles was also assessed. Each nutrient was varied independently and uptake was monitored. The effect of pH on uptake of selenite was only assessed for freshwater algae since only in freshwater does pH vary significantly. The media pH was adjusted between 6.5 and 9.0 by adding NaOH to the media and letting it come to equilibrium with the atmosphere at the experimental temperature.

Culture studies of dissolved selenium uptake by bacteria. We also conducted studies on the accumulation of both selenite and dissolved organic selenium by marine bacteria. Natural bacteria were used in these experiments so as to evaluate the response of an intact community to

the experimental conditions. This also avoided biases associated with using a small subset of bacteria that can be cultured. Water collected from Stony Brook harbor was filtered through 0.8 μm pore size filter. This pore size allows some bacteria through while removing all eukaryotes, including small flagellates that feed on the bacteria. To this solution we then added glucose as a carbon source for bacteria. To determine the effect of nutrient levels on uptake, nitrate and phosphate were added in a factorial design. Selenium was added as either radiolabeled selenite, or lysates of algae grown up in the presence of radiolabeled selenite. Incorporation into particles $> 0.2\mu\text{m}$ in size was then followed over time. Killed controls consisted of a microwaved treatment and a treatment with formalin added at 0.25%.

Estimation of selenium uptake and Se:C ratios in native phytoplankton and bacteria using radioisotopes. To estimate the Se:C ratio in newly produced living material in the field, we developed a new method that involved measuring the simultaneous uptake of radiolabeled selenite and bicarbonate into particles. By simultaneously measuring the uptake of selenite and C into particles and corrected for non-biological uptake using killed controls, this method provides a way of measuring the Se content of newly produced living material. Consumers preferentially ingest this living material over the non-living material and Se associated with living material is frequently more bioavailable to consumers. Thus, it is important to know if this living material has a different signature than the bulk material, and what that signature is. We were also interested in whether algae and bacteria concentrated Se to different degrees. Our measurements were made within the framework of a large intensive study of Se transformation and bioaccumulation in Mildred Island on Sept 6-9, 2001. Data on stable Se and C content of particles was therefore available on the same samples for comparison. This allowed us to compare our measurements with those determined using standard chemistry. Also, because particles at one of the sites were predominately living, we could assess whether measurements of Se:C ratios based on selenite uptake alone could yield reasonable estimates of Se:C ratios in situ.

In the morning and afternoon water was collected from the main river channel 1 mile N of Mildred Island where algal biomass was low ($2\text{-}3 \mu\text{g Chl } a \text{ L}^{-1}$) and from the Southwest corner where algal biomass was highest ($13\text{-}30 \mu\text{g Chl } a \text{ L}^{-1}$). Radiolabeled selenite and bicarbonate were added to water samples at tracer concentrations. Samples were exposed to seven light levels and uptake into particles followed over 6-8 hours in a custom made incubator kept at constant temperature. We measured uptake into both the $>0.2\text{-}\mu\text{m}$ and the $>1.0\text{-}\mu\text{m}$ size fractions in an attempt to determine if there was a bacterial ($0.2\text{-}1.0 \mu\text{m}$ size class) component to selenite uptake. We also measured uptake in the dark and onto particles killed using a microwave treatment to assess adsorption. As a cross-check, our C uptake measurements were compared to others conducted by Brian Cole using standard methods and a photosynthetron. Filtered samples were then prepared for radioanalysis and assayed for beta and gamma emissions at USGS in Menlo Park. Daily depth integrated Se uptake was normalized to daily depth integrated C-fixation and bacterial production, estimated to be 28% of primary production (Sobczak *et al.* 2002).

Development of a method for estimating cellular Se concentration in individual protist cells. We have also developed a means of measuring Se content of individual phytoplankton cells using synchrotron based x-ray fluorescence microscopy (SXRF). This method allows one to measure elemental content of specific particle types and, thus, it can be used to estimate the Se content of living cells as opposed to non-living material (Twining *et al.* 2003; Twining *et al.*

2004a; Twining *et al.* 2004b). It also allows one to measure Se concentrations in different types of living cells, which is important since different species of algae can concentrate selenite to very different degrees. Use of this method in the future may provide a means of testing models of Se incorporation developed using lab experiments more directly in the field. It also will allow us to distinguish the Se content of living, non-living and inorganic material (see attached proposal CalFed Potamocorbula Monitoring Proposal 2005).

In SXRF a focused excitation x-ray beam (in this case with a spatial resolution of about 1 μm) is moved across a specimen and the fluorescent x-rays that are then emanated by excited atoms are collected, producing a spectrum of such x-rays (Fig. SET1). At an excitation wavelength of 13 keV, the concentration of elements ranging in atomic number from Si to Se can be determined by modeling the spectra of fluorescent x-rays summed over the entire region of the cell. To test this method, we grew cells of several marine and freshwater species in culture media containing selenite and prepared them for analysis according to (Twining *et al.* 2003). Cells were analyzed at the 2-ID-E beamline at Argonne National Laboratory's Advanced Photon Source. Measurements of Se content in cells were compared to measurements made using radioisotopes. Measurements of particulate Se measurements of filters collected during the experiment have not been completed but are planned to provide further verification of the method.

Se in Bay-Delta Food Webs (SEF)

Analytical methodology

Stable Isotope Analysis. Individual fish muscle, soft tissues of clams, and pooled whole invertebrates (e.g. zooplankton, amphipods) were analysed for $\delta^{13}\text{C}$ and $\delta^{15}\text{N}$ at the Stable Isotope Facility, University of California, Davis using a Europa Scientific Hydra 20/20 continuous flow isotope ratio mass spectrometer and Europa ANCA-SL elemental analyzer to convert organic C and N into CO_2 and N_2 gas. Results are presented as deviations from standards, expressed as $\delta^{13}\text{C}$ and $\delta^{15}\text{N}$:

$$\delta X = [R_{\text{sample}}/R_{\text{standard}} - 1] \times 10^3$$

where X is ^{13}C or ^{15}N and R is $^{13}\text{C}/^{12}\text{C}$ or $^{15}\text{N}/^{14}\text{N}$. The standard for C is Peedee Belemnite, and for N it is atmospheric diatomic nitrogen. Instrument precision was 0.1‰ for carbon and 0.3‰ for nitrogen based on replicate analyses of standard reference materials.

Selenium Analyses. Analyses were conducted on individual fish muscle and pooled livers due to insufficient sample mass for Se analysis, except for striped bass. Invertebrates were analyzed whole. Samples of large mass (fish, clams) were analyzed using oxidative digest and selective hydride generation atomic absorption spectroscopy (AAS). Samples (stored at -30°C for < 6 months) were dried at 40°C , weighed, and subsequently digested in concentrated nitric and perchloric acids at 200°C , reconstituted in hydrochloric acid, and then stored until analysis. Quality control was maintained by frequent analysis of blanks, analysis of NIST standard reference materials with each analytical run, and internal comparisons with prepared quality control standards. Samples of small mass (zooplankton, amphipod) were also determined using

oxidative digest and selective hydride generation atomic absorption spectroscopy (AAS), but with a three-step nitric-perchloric acid reflux procedure (Cutter 1985). After evaporation of the nitric acid, the residue was redissolved in 4M HCl and stored until final Se analysis. To determine Se concentrations, 1-2 ml aliquots of digest solution were diluted to 40 ml with distilled water in a 400 ml glass beaker to which Teflon boiling stones, 0.5 ml of 2% (w/v) persulfate solution and 22 ml concentrated HCl were added. The beaker was covered with a watch glass, and the solution brought to a boil for 30 min, with the heat being reduced to the minimum capable of sustaining boiling. After cooling overnight, the samples were analyzed using hydride generation. The standard additions method of calibration was used to ensure accuracy, and all determinations were made in triplicate to establish precision. In addition to the standard addition method, accuracy was verified using the digestion and determination of Se in NIST Oyster Tissue with each group of ten samples. All sample weights were corrected for salt content by measuring Na concentrations using flame AAS.

Monthly sampling of *Potamocorbula* at Carquinez Strait. Monthly sampling of Se in *Potamocorbula amurensis* (n = 3 composite of ~20-50 individuals) at Carquinez Strait was conducted according to methods described in (Linville *et al.* 2002). This is an extension of Se monitoring in bivalves in Suisun Bay since 1995. In addition to Se concentrations, clam soft tissues were analyzed for stable isotopes of carbon and nitrogen to examine changes in food sources for the clams.

Field studies of Se in *Corbicula* in the Delta. In order to evaluate the relationships between selenium dynamics and phytoplankton dynamics and their relationship to Se uptake by herbivores at the consumer level we conducted a series of spatially intensive field studies of Se in *Corbicula* in the Delta. Clam collections were done in conjunction with measurements of Se distributions (see Section SED), benthic community status (see Section B) and phytoplankton dynamics (see Section C). The field studies were

1. Mildred Island Process Study – August 28-29, 2001, 22 sites
2. Frank's Tract Process Study – April 1-4, 2002, 8 sites
3. Delta Boogie – May 12-15, 2003, 7 sites
4. Overlap – September 11 & October 9, 2002, 1 site, *Corbicula fluminea* and *Potamocorbula amurensis*.

Locations of the sampling sites are shown in Figure SEF1. Replicate samples of *Corbicula* (n = 3 composites of 5 individuals) were collected at each site and analyzed for Se and stable isotopes of carbon and nitrogen. Additional clams were collected monthly at stations FT17 and FT09 in Frank's Tract from April 2002 through May 2003 in conjunction with benthic community measurements.

Se distributions in Delta food webs. Selenium concentrations and stable isotopes of carbon and nitrogen were measured in biota from Mildred's Island (November 1999 and September 2001) and Frank's Tract (2002) (Figure SEF1). A wide variety of invertebrates and fish were collected according to the methods described in Croteau *et al.* (2005). Using stable isotopes of carbon and nitrogen trophic relationships were determined and food webs identified. Selenium concentrations in biota were related to food web dynamics and carbon source.

Kinetics of Se bioaccumulation.

Kinetic model constants. Biodynamic constants for Se bioaccumulation in a large variety of consumer organisms and predators that inhabit the Bay-Delta determined using a dynamic multipathway bioaccumulation model (DYMBAM) were compiled (Luoma and Fisher 1997; Schlekot *et al.* 2001). Model parameters were obtained through laboratory experiments and through a search of the literature.

Clam Se model. Using the biodynamic constants determined by Lee *et al.* (In prep.), ingestion rates estimated from *Corbicula* community grazing rates and biomass measured in this study (see Section B), estimated site specific *Corbicula* growth rates (Foe 2002), and a Se phytoplankton food factor determined through field and laboratory studies by Baines (see Section SET) we developed a clam Se model for *Corbicula* in the Delta. The model predicts Se accumulation from dietborne uptake (waterborne uptake is assumed to be negligible (Luoma *et al.* 1992)), and is expressed as

$$\begin{aligned}
 [\text{Se}_{\text{clam}}]^{\text{SF}} &= (\text{food}) - (\text{efflux} + \text{growth}) \\
 &= (\text{AE} \times (\text{IR}_{\text{PHYTOC/COM}} \times \text{F}_{\text{SF}})) / (\text{k}_e + \text{k}_g)
 \end{aligned}$$

where, AE is the assimilation efficiency (%), $\text{IR}_{\text{PHYTOC/COM}}$ is the ingestion rate estimated from community consumption of chlorophyll and community biomass ((Pumping Rate ($\text{m}^3 \text{m}^{-2} \text{d}^{-1}$) x Chlorophyll *a* ($\mu\text{g L}^{-1}$))/ Bed biomass (Tissue Ash-free Dry weight g m^{-2})) adjusted for a phytoplankton C to chlorophyll ratio of 32 (Lopez *et al.* In press) ($\text{g C g}^{-1} \text{d}^{-1}$), F_{SF} combines the bioavailable particulate Se per unit phytoplankton carbon (constant of 4.6) and Se per unit bacterial carbon (constant of 56 multiplied by a factor accounting for bacterial: phytoplankton biomass ratios (Sobczak *et al.* 2002)) developed by Baines ($\mu\text{g g C}^{-1}$), k_e is the efflux rate from dietborne Se (d^{-1}) and k_g is the loss due to growth (d^{-1}). We also ran the model using IR_{SPM} which is the ingestion rate estimated from site specific SPM ($0.137[\text{SPM mg L}^{-1}]^{0.421}$ x Filtration Rate (temperature specific (Foe and Knight 1986; Reinfelder *et al.* 1998) ($\text{g g}^{-1} \text{d}^{-1}$)).

Corbicula Se concentrations were predicted at 24 sites in the Delta where chlorophyll (discrete and SCUFA, see Lucas) and benthic community data had also been collected. Sensitivity of the model was tested by varying the model parameters including IR (IR_{SPM} and $\text{IR}_{\text{PHYTOC/COM}}$) AE (30 and 70 %), F_{SF} (4.6 – assumes Se from phytoplankton alone and 9.08 – assumes Se from phytoplankton and bacteria and a bacterial: phytoplankton biomass ratio of 8%). The purpose of this model was to test: 1) how well the laboratory based model parameters fit field measured Se concentrations in clams, 2) the assumption that Se: phytoplankton + bacteria C ratios are constant throughout the Delta, 3) the accuracy of the Se: phytoplankton + bacteria C ratios measured by Greg Cutter and Stephen Baines in the south eastern corner of Mildred’s Island in predicting clam Se concentrations throughout the Delta.

We compared the results of the clam Se food factor model to a similar biodynamic model that uses bulk particulate Se concentrations measured in the field (see Section SED) and IR_{SPM} . The model is expressed as

$$[Se_{clam}]^{SPM} = (\text{food}) - (\text{efflux} + \text{growth})$$
$$= (AE \times (IR_{SPM} \times C_F)) / (k_e + k_g)$$

where C_F is the Se concentration in bulk food (e.g. phytoplankton, suspended particulate matter, sediment) ($\mu\text{g g}^{-1}$). This model assumes that all of the bulk particulate Se is equally assimilated by the clams.

Local scale modeling (ML)

Residence time in shallow water habitats. To illustrate the concepts of flushing time, age, and residence time for Mildred Island, the trajectories of neutrally-buoyant conservative particles were calculated from the velocity field produced by the hydrodynamic model. (Although these particular studies were focused on particular Delta sub-regions, they were conducted using the Delta-scale hydrodynamic model described below under Section MD). We focused on low-flow conditions of June 1999, a period for which results of drifter experiments and water-quality mapping are available for model validation.

Flows and particle trajectories from these simulations were used to calculate of flushing time, age and residence time (and exposure time) for Mildred Island. Our intent was not a direct comparison of the calculated values but rather to illustrate and compare various approaches used to estimate transport times and to select the most appropriate transport timescale for the application to Mildred Island. Please see Mosen et al. (2002) for more information.

Franks Tract---The effect of SAV on hydrodynamics. The model used to explore relationships between SAV and hydrodynamics is GOTM (the General Ocean Turbulence Model, www.gotm.org). GOTM simulates a vertical water column under the assumption of horizontal homogeneity. We drive the model with a specified barotropic pressure gradient and adjust the frictional coefficients to calibrate the model. GOTM resolves both bed stresses and allows for the inclusion of distributed drag elements to approximate the effects of vegetation.

Two modeling approaches are presented here. The first is the traditional approach to modeling vegetation, which involves specifying an elevated bed drag coefficient. The second approach to modeling the effects of SAV involves the use of a distributed drag parameterization, with the resistance to flow being applied throughout the portion of the water column filled with SAV.

This exploration of modeling approaches was considered a critical step toward accurately modeling scalar transport in Delta environments that are riddled with SAV (e.g. Franks Tract). SAV appears to increase heterogeneities in mixing and scalar concentrations in all three dimensions, turning a relatively two-dimensional (e.g. vertically well-mixed) environment into a very much three-dimensional environment. Such complexities and heterogeneities can have

significant consequences for production and vertical and horizontal transport of phytoplankton and associated particulate Se, as well as the delivery of those items to grazers.

Franks Tract---Regional hydrodynamics. Although this particular component was focused on a particular Delta sub-region, it was conducted using the Delta-scale hydrodynamic model described below in Section MD. This work used hydrologic, tidal, and operational input data from the April 2002 (i.e. Franks Tract Process Study) time period to drive the hydrodynamics. The approach involves using detailed time series measurements of velocity and stage to calculate flow rate at high frequency at several locations in the channels surrounding Franks Tract and refine the model such that it performs well in capturing phase and amplitude. The data compared to are described in the Section HF.

Mildred Island—Modeling with reactions. TRIM3D forms the hydrodynamic basis of this model, “TRIM-MILLIE,” which in this case is applied to the physical domain of Mildred Island and its surrounding channels (Latham Slough, Connection Slough, northern and southern Middle River, and Empire Cut). The version of TRIM3D used in this case is that adapted by colleagues at UC Berkeley (Baek, Stacey), who added atmospheric forcing to the tidally and river driven version previously adapted by E. Gross. This model uses the same base model implemented by Mosen at the Delta-scale. The newly included atmospheric forcing includes wind and its effects on advection and vertical turbulent mixing, as well as diurnal heating and resultant baroclinic flows, vertical density stratification, and its effects on turbulent mixing. (The addition of atmospheric forcing to TRIM3D has been conducted as part of a companion project funded under a separate CALFED grant.) Because hydrodynamic field experiments at Mildred Island revealed the significance of wind and heating influences on hydrodynamics there (see Section HS), we then decided to use UC Berkeley’s TRIM adaptation for the coupled modeling of phytoplankton, physics, and selenium in that region.

The domain of TRIM-MILLIE is shown in Figure ML1. There are approximately 53,000 wet grid cells in the horizontal dimension (i.e. if run in depth-averaged mode); however, the Mildred-scale simulations discussed here were fully three-dimensional, with vertical grid spacing of 0.5 m and total wet cells in 3D numbering about 510,000. Measured time series of wind speed at Mildred Island (this study), solar radiation and other atmospheric variables (CIMIS), and velocity for the September 2001 process study period were used to drive the physics of this model. Colleagues at UC Berkeley carefully calibrated and validated the model against measured spatial and temporal patterns of water temperature during the process study; this model performs extremely well in replicating observations of the physics.

Phytoplankton dynamics were added to this model in a manner similar to the approaches used in (Lucas and Cloern 2002; Lucas *et al.* 1999a; Lucas *et al.* 1999b), except for the fact that those implementations were for a depth-averaged water column; TRIM-MILLIE is fully 3D, with a fine vertical discretization of the domain, necessitating a modified approach that calculates vertically variable biological processes. Phytoplankton growth is a function primarily of water column irradiance, zooplankton grazing, benthic grazing, and respiration loss. Photosynthesis follows the expression of Verity (1981) and requires photosynthesis-irradiance parameters that were measured using C14 incubations during the process study. Calculation of water column irradiance necessitates a time varying surface irradiance (converted from measured solar radiation, CIMIS) and a light extinction coefficient, which is derived from measured irradiance profiles, SPM, and chlorophyll *a*. Zooplankton grazing rate was calculated using

measured abundance, taxa, individual size, phytoplankton biomass, and water temperature (Lopez *et al.* In press); although horizontally variable, zooplankton grazing is assumed to be uniform over the depth. Benthic grazing rates were calculated by Thompson, based on 2001 measurements of bivalve abundance and biomass (see Section B); benthic grazing rate within the model may be non-zero only at the bottom cell of a local water column. Conversion from photosynthetic rate to growth rate requires a cellular carbon-to-chlorophyll ratio, taken as 32 based on measured nutrients, light, and temperature in the Mildred Island environment (Lopez *et al.* In press; Cloern *et al.* 1995). Ten sub-areas of the model domain were defined based on environmental characteristics; each sub-area was assigned a typical zooplankton grazing rate, benthic grazing rate, and light attenuation coefficient based on process study and weekly measurements in the region (see Fig. ML1 for area definitions and associated values).

Modeled phytoplankton are treated as a continuous (dissolved) concentration field, not as individual particles. As such, photosynthesis, growth, respiration, and grazing are all functions of local conditions in space, including in some cases the local instantaneous phytoplankton biomass (e.g. augmentation of the light attenuation coefficient by biomass itself, or “self shading”). Irradiance, photosynthesis, growth, and respiration are calculated at computational cell centers (horizontal and vertical) so that within each cell, and during each time step, the biomass change within the cell is a function of simultaneous three dimensional transport (advection and mixing), growth, respiration, and grazing. The currency used for calculating phytoplankton biomass in the model is carbon, which is converted to chlorophyll *a* for comparison with measurements using the C:Chl of 32.

Modeling of edible particulate selenium is based on relationships developed by Baines (see Section SET) derived from measurements of selenium uptake during the Mildred Island process experiment. Selenium and carbon were observed to be taken up by phytoplankton in a ratio of 4.6 ug/g and by bacteria in a ratio of 56 ug/g. If we assume that the loss functions for C and Se from cells are similar or minimal, we then can make the assumption that the phytoplankton and bacterial cellular Se:C ratios matched the uptake ratios. This assumption is also bolstered by the strong relationship between Se measured in clams and the percent nitrogen in the clam tissue, i.e. the implication that Se exposure is relatively invariant (see Section SEF). Furthermore, as shown in Baines *et al.* (2004), the Se:C ratio derived from uptake rates matched the ratio of measured particulate Se to particulate organic carbon for the MI environment. The order-of-magnitude difference in bacteria and phytoplankton cellular ratios suggests that bacterial uptake of Se may be very important for delivery of edible particulate Se to upper trophic levels, even if the standing stock of bacteria is much smaller than the standing stock of phytoplankton. Measurements by Sobczak *et al.* (2002) showed that bacterial biomass in the water column can range from about 8% (e.g. upper San Joaquin River) to about 30% (e.g. Franks Tract, the Sacramento River). Therefore, although the potential importance of bacterial uptake of Se was surprising and the assessment of bacterial biomass and production not part of this proposal, we can use those previous measurements, coupled with Baines’ cellular ratios, to bound the total edible particulate Se available to primary consumers at our study sites and within our modeling domains. Minimum total edible particulate Se (“ Se_p^{ed} ” in pg/L) may be estimated as phytoplankton carbon (ug/L) multiplied by 4.6 (assuming only phytoplankton are consumed); maximum Se_p^{ed} may be estimated as phytoplankton carbon multiplied by 21.4 (i.e. 4.6 + 0.30*56). This is the method implemented with TRIM-MILLIE.

The initial condition for phytoplankton biomass is a north-to-south linear increase in concentration from 128 ug C/L to 384 ug C/L, based on observed overall north-south gradients during the 2001 process study (see Fig. C3 for these measurements). Inflowing boundary conditions were set at 96 ug C/L for Connection Slough and Northern Middle River, 224 ug C/L for Empire Cut, and 128 ug C/L for Southern Middle River. These values were based on average observed chlorophyll *a* in the five mapping transects performed during the 2001 process study.

Additional modeling that occurred: Understanding the circulation and mixing of Mildred Island and Franks Tract. Simulations were also created to support the field experiments in this project in addition to the modeling done in support of the efforts outlined above. Particle tracking simulations using June 1999 hydrology were used to assist in the development of the Mildred Island and Franks Tract field studies. These simulations were a tool used to determine the location of field instruments and to determine when certain sampling efforts should occur. For instance, the model was used as a tool by the field scientists to help visualize the circulation patterns around Franks Tract prior to the experiment.

Simulations of the Fall 2001 and Spring/Summer 2002 hydrology have been developed to assist in the analysis of data. Observations from these simulations will also be incorporated in the next version of the paper to be resubmitted to *Water Resources Research* Mosen *et al.* (In prep.) to support findings from field and monitoring data.

Delta scale modeling (MD)

Hydrodynamic modeling. The numerical modeling tool used for all simulations in this task was Delta TRIM3D, a multi-dimensional hydrodynamic and scalar transport model. The core of the hydrodynamic model was developed by Casulli and Cattani (1994), and the associated scalar transport routines were incorporated by Gross *et al.* (1999). The model has been applied to the bathymetry of the Delta and then calibrated and compared against measured stage, flow and salinity (Mosen 2001). The numerical model is driven at the western boundary with measured tides at the western side of Suisun Bay (Martinez) (Figure MD1), and the river boundaries are specified with measured flows on the Sacramento and San Joaquin Rivers. Results presented here were calculated using the model in two-dimensional depth-averaged mode, with a grid resolution of 50 m and a 40 second time step.

Understanding the influence of barriers, gate, and pump operations on source distribution. Model simulations from many different simulation periods created for the purpose of this research and previous modeling efforts allowed us to make hypotheses about how diversion operations affected source distributions. We used field monitoring data to support the model-based hypotheses.

We developed a simplified schematic of water sources and transport paths linked to the central Delta mixing zone (Figure MD1, inset) to illustrate hydraulic alterations of individual diversions and their significance to the Delta ecosystem. The dark blue arrows on the schematic perimeter represent the outer boundaries of the Delta (north: Sacramento @ Freeport, south: San Joaquin @ Vernalis) and export pump operations in the southwest corner of the Delta. The bi-directional

arrow on the left hand side of the diagram represents tidal exchange between the Delta (at the junction of the SAC and SJR) and SFB. Without exports from the system, all freshwater would tidally exchange with SFB at this boundary. The network of channels and open-water regions within the Delta are represented as a central mixing zone with a series of channels that transport water to and from that region.

We developed schematics illustrating how each diversion in our examples alters flow routing through the Delta (Figure MD2). Red denotes the significant flow change caused by each diversion. (a) Keeping the DCC gates open enhances the transfer of SAC water to the central Delta mixing zone. (b) Closing the gates at the DCC redirects flow down the SAC towards SFB rather than flowing into the central Delta mixing zone. (c) Placement of the HORB directs SJR flow towards the central Delta mixing zone rather than flowing through the south Delta towards the export pumps. (d) Placement of all four temporary barriers creates a temporary storage region in the south Delta. (Please see Monsen (In prep.) for more information.)

Source distribution through the Delta. To identify how Delta Cross Channel operations change source water distribution throughout the Delta, the numerical model was run for September 2001 with three separate passive scalars introduced in the Sacramento at Freeport, in the San Joaquin downstream of Vernalis near Mossdale Landing, and at the agricultural return points within the Delta. Each passive scalar tracks the distribution of water that originates at the three source boundaries. Concentrations of each of the passive scalars were recorded throughout the Delta throughout the two month simulation. In one simulation, the DCC gates were opened and closed with the same timing as had actually occurred in September, 2001. In a second simulation, the model kept the gates closed for the entire period.

Modeling with reactions. Very similar phytoplankton and selenium relationships were incorporated into Monsen's Delta-scale hydrodynamic model (Delta TRIM3D) as in TRIM-MILLIE, with some slight modifications due to the depth-averaged nature of Delta TRIM3D in its current state of use. (Since photosynthesis and irradiance are highly non-linear functions of elevation in the water column, numerical depth-averaging of photosynthesis was performed in the Delta-scale model, as opposed to simple computation of photosynthesis in the vertical center of the computational cell/water column.)

Monsen's April 2002 simulation was used as the hydrodynamic basis of the coupled Delta scale model. Primary input parameters (benthic grazing rate, light attenuation coefficient) for the biological part of the model were based on May 2003 measurements during the "Benthic Boogie" effort. Light attenuation coefficient was calculated using an algebraic conversion from the Secchi measurements. Individual point measurements were clustered into regions with similar parameter values, and one model input parameter value was used to represent each region (see Figure MD3 for input parameter regions and values). Zooplankton grazing rate, photosynthesis-irradiance parameters, and C:Chl ratio were all specified based on 2001 and 2002 measurements in the Mildred Island and Franks Tract regions. Boundary conditions were specified according to discrete chlorophyll *a* measurements on the Sacramento River, San Joaquin River, near Clifton Court and Martinez. The initial condition for phytoplankton biomass used an east-to-west gradient that accommodated the boundary conditions, to avoid numerical instabilities at the boundaries due to sharp spatial gradients. Time series of chl *a*, minimum Se_p^{ed} ,

and maximum Se_p^{ed} were saved at several locations throughout the Delta, corresponding to locations where measurements of chl *a* and Se in clams were taken (see Figure MD4).

V. FINDINGS

Hydrodynamic Measurements in Shallow Water Habitats (HS)

Detailed discussion of the analysis and scientific conclusions are included under “Narrative,” but here we summarize the key findings:

- The dynamics in southern Mildred Island are dominated by wind and atmospheric heating/cooling
- In northern Mildred Island, the hydrodynamics are produced by mixture of tidal and atmospheric forcing
- The importance of atmospheric forcing in MI is particularly pronounced when considering flushing times for sub-habitats along the perimeter of the island.
- Franks Tract circulation is set by a combination of local forcing (from local openings) and larger-scale forcing (the background tidal pressure gradient)
- The circulation in Franks Tract is strongly influenced by the seasonal development of SAV, which ‘channelizes’ the basin
- The vertical structure of flows in the presence of SAV is characterized by a strong shear layer at the top of the SAV canopy
- Channel-shallow exchange is strongly tidal, but the traditional tidal pumping structure is modified by:
 - The orientation of the ambient tidal gradient relative to the opening (MI and FT)
 - The presence of multiple opening (FT)
 - The presence of SAV (FT)
 - Atmospheric forcing (MI)

Regional Hydrodynamic Field Investigations (HR)

Our major findings include:

- The concept of the fresh water corridor, a region defined by the salt field, extending from the Mokelumne River system to the South delta export facilities, is introduced and discussed as a useful conceptual paradigm for understanding salinity time series and as a potential management tool.
- Dispersive processes are not as spatially ubiquitous as was once thought; transport of constituents through dispersive mechanisms occur primarily in the tidally influenced regions of the Delta and can be significant in regions that have the following three geometric features: (1) junctions, (2) locations where the channel length < tidal excursion, and (3) where shallow/channel exchange processes occur.
- Franks Tract plays a significant role in intrusion of salinity into the central Delta. Specifically, tidal timescale exchange and mixing of high saline water from False River into Franks Tract greatly increases the rate of intrusion of salinity into the fresh water corridor and ultimately elevates salinities at the south Delta pumps. Modeling studies,

conducted following our field investigations, clearly show that changes in Franks Tracts geometry can significantly change the salt field, and, in some cases, reduce salinities at the export facilities in the southern Delta ((Resource Management Associates, 2005b)).

- The Mildred Island levee system is extremely porous.
- Mildred Island is not an isolated flooded island habitat, but is an important conveyance pathway within the fresh water corridor.
- Northern Mildred Island is very efficient at mixing constituents.
- The net flow through Connection Slough is toward Franks Tract which reduces salinity from mixing into the fresh water corridor through interactions with Mildred Island.
- Salinity time series suggest that the location of Mildred Island's northern opening on the northeast side of the Island likely keeps Mildred Island fresher than it would have been had the opening been on the Connection Slough (west) side of the island. Moreover, had the opening been on the west side of the Island, Mildred Island would likely contribute to increases in salinity at the export facilities to a greater extent than it does now. Therefore, breach location and geometry are critical to the exchange and long-term transport of constituents such as salinity within the Island and regionally.
- Residual circulation, in particular, and transport of constituents in general in the Mildred Island region would be very different in the absence of pumping in the south Delta.

Bivalve distribution and grazing rates (B)

Delta Scale Benthic Grazing Rates for Use in Models.

- *C. fluminea* abundance did not show a consistent pattern in May 2003 that could be related to habitat or strata (Table B2, Figure B4).
- *C. fluminea* biomass in May 2003 was low everywhere except inside and around Franks Tract and in the Middle River north of and along side Mildred Island.
- Patterns changed in October 2003 with *C. fluminea* density being uniformly high in most places sampled and biomass increasing substantially except in the San Joaquin River south of Empire Tract, Middle River south of Bacon Island, and the Mokelumne River (Table B3, Figures B5, B6, and B7)
- Largest populations and biomass of *C. fluminea* were found in the central delta strata with 20.5 to 22°C water temperatures and <2500 µS (EC) in spring. This distribution pattern persisted into fall when those temperatures and EC were much different.
- Grazing rates followed the biomass patterns and were thus higher over a large area in October than May. The grazing rates were elevated in October due to the much higher pumping rates resulting from the increased temperature (Figure B8).
- A comparison of grazing rates and chlorophyll *a* concentration (Figure B9 and B10) shows phytoplankton biomass to be low in the central delta where grazing rates are highest, low in the Sacramento River where grazing rates were low in May but elevated in October, and higher in the southern San Joaquin where grazing rates were consistently low.

Regional Scale Benthic Grazing Rates for Process Studies – Mildred Island Process Studies.

- *C. fluminea* occupy few locations within the island and the largest numbers and biomass occurs near the northern opening (Figure B12, Table B5)
- All individuals found within the lake were large (SL>10mm)
- Boundary channels had larger populations than within the lake with the eastern boundary (Latham Slough) having larger populations than the western slough.
- Largest populations and grazing rates (Figure B13a) were seen in Middle River north and south of the Island (some in excess of 30 m/d)
- *C. fluminea* population structure can be used as an indicator of the relative food availability if we compare populations with similar densities and biomass (ie similar crowding or competition for food) and assume that predation is similar within the environments examined. If we examine the size of the oldest year class (Figure B13b) or the size frequency distributions of the clams in the boundary channels (Figure B14) or in the connecting channels (Figure B15), we see that:
 - (1) although the biomass is similar along the eastern boundary channel, the clams show a southerly increase in size within each population,
 - (2) the locations within the lake with reasonable sized populations, which are still an order of magnitude smaller than populations in the boundary channels, have very large clams,
 - (3) Connection Slough, with relatively small populations and thus presumably little competition for food between clams, when compared to the other connecting rivers and sloughs (Figure B15), has some of the smallest animals,
 - (4) animal size increases with closer proximity to Mildred Island in Middle River north of the island,
 - (5) animal size increases in the Middle River south of Mildred Island with increasing distance from Mildred Island although animal crowding increases coincidentally with the apparent increase in animal size
 - (6) Empire Cut, a highly channelized man-made canal had very low numbers of *C. fluminea* but those that lived there were some of the largest individuals seen.

Channel Scale Benthic Grazing Rates – Is There a Distribution Pattern?

- The largest abundance of clams frequently occurred in the deep channels in the San Joaquin River (Figure B17b, Tables B6 and B7).
- The largest abundance of clams occurred on the edges of the deep channels in the Sacramento River.
- The largest abundance of clams occurred on the edges and within the sharp curve of Threemile Slough, on the external edge of the curve. Large accumulations were also seen at the entrance of Threemile Slough into the Sacramento River.
- The abundance distribution patterns described above for all systems were determined by bivalves less than 10mm in shell length (Figure B18).
- Biomass and grazing rate were low in all environments with maximum grazing rates (2 m/d) occurring in the Sacramento River and on the external edge of the sharpest bend in Threemile Slough (Figure B19).

Spatial Variability in Benthic Grazing Rates – Franks Tract Processes.

- Abundance of *C. fluminea* was rarely less than 50/m² with highest densities occurring within the island and in the areas south and southeast of the Tract (Figure B21, Table B9).
- Biomass and grazing rate were highest in southern Old River, Middle River north of Mildred Island as seen in the previous year, on the San Joaquin River north-northeast of the Tract and within the island (Figure B21 and B22).

Temporal Variability in Benthic Grazing Rates – Franks Tract Processes.

- Grazing Rates at the two stations sampled for the year showed some seasonal patterns but changes were on the order of doubling of grazing rates at the most (Figure B24). Maximum grazing rates were seen in summer at both locations.
- Annual average grazing rates at the western end of the transect (FTI09 : 2.7 ±.4 m/d) were not significantly different ($p>0.17$) than those at the eastern end of the transect (FTI17 : 3.5 ±.4 m/d).
- Grazing rates were consistently >0.5 m/d at stations on the eastern and southern meter stations (Figure B25 and B26) with peaks in grazing of the same order as those seen at the stations within the island. Grazing rates at Mandeville Island and Sandmound Slough increased through the spring into summer, peaking at 8-10 m/d.
- Grazing rates in False River were lower and much more variable than the stations mentioned above (Figure B27).
- Grazing rates mostly increased from spring into summer in Old River with a peak occurring in July (>1 m/d, Figure B28)
- Lowest grazing rates were seen at locations that were “one slough removed” from Franks Tract. Fishermans Cut, connected to False River and the San Joaquin River is a man-made canal with very low clam densities (Figure B28). Taylor Slough, conjoined with a southern arm of False river and running outside the southwestern levee of Franks Tract had similarly low grazing rates (Figure B28)

Carbon field studies (C)

Our major findings include:

- Phytoplankton biomass and production are only weakly related to phytoplankton specific growth rate and habitat depth. Other processes such as transport and consumption are important, sometimes dominant, controls on biomass and production. Therefore, shallow habitats do not necessarily sustain high algal biomass, despite fast phytoplankton population growth.
- Colonization by the invasive clam *Corbicula fluminea* will determine a habitat’s value to the pelagic foodweb. In this way, invasive species can act as over-riding controls of habitat function.
- Habitats colonized by *Corbicula fluminea* function as food (phytoplankton) sinks (e.g. deep channels outside Mildred Island); surplus primary production in uncolonized shallow habitats (e.g. Mildred Island interior) provides potential subsidies to neighboring consumer habitats. Thus, zooplankton in deeper habitats may be supported by the food exported from donor habitats.

- The benefits of some ecosystem functions are displaced by water movements. Specifically, transport of phytoplankton biomass by advection and tidal dispersion is important in providing communication between donor and recipient habitats. In the absence of transport, biomass would accumulate in the producing habitats and become depleted in the consuming habitats.
- Measurements of dynamics at and beyond habitat interfaces are as important as measurements within habitat interiors.
- Phytoplankton biomass provides no information about governing processes such as transport and grazing, so biomass alone is a weak indicator of the ecological value of aquatic habitats.
- From the perspective of carbon consumption, as well as the uptake of phytoplankton-associated particulate selenium into the upper trophic levels, “similar looking” flooded islands and their associated channel systems can function in opposite ways (with clam-dominated consumption/uptake inside and zooplankton-dominated consumption outside, or vice versa).
- Water quality in the Delta’s flooded islands, in channels, and at habitat interfaces varies with large amplitude and high (hourly) frequency. The period of variability can vary between constituents (e.g. conductivity, temperature, chlorophyll), across short spatial scales (even within one small water body), and over time. The reasons for this variability in periodicity are not always easily apparent. This high frequency variability has significant implications for monitoring and for process understanding.
- New scaling relationships allow us to estimate the contributions of individual physical and biological processes in generating observed high frequency variability in water quality.
- Strong diel variability in phytoplankton biomass and other water quality constituents may be governed by physics as much or more than biology or chemistry.
- Despite the Delta being a strongly tidal and river-driven system, wind-driven vertical mixing and horizontal advection are surprisingly significant forcings on water quality and biota in some (esp. broad, open water) environments.
- Despite the large degree of connectivity between Delta habitats, even proximal regions can function very differently on physical and biological levels.

Field studies of selenium distributions and transformations (SED)

The major findings from this research include:

- The Delta transects show that selenium is clearly cycled in the Delta; selenium concentrations and speciation in Suisun Bay are not the same as those in the Sacramento and San Joaquin Rivers. Furthermore, higher flow periods show less dissolved removal in Delta, consistent with a residence time effect. This “Delta Removal Effect” is an important component of the Bay model developed by Meseck (2002).
- Similarly, the monthly samples from Suisun show a rough correlation between the concentrations of particulate selenium and San Joaquin River inputs (with ca. 10x more dissolved Se than the Sacramento River). This trend was predicted by the Bay model simulations.

- Results from the Mildred Island study show that we can resolve *in situ* processes from advective ones, dissolved selenium is rapidly cycled in such an embayment, and sediments are an important repository of particulate selenium in the Delta. The major question is whether these results can be extrapolated to other habitats in the Delta?
- Historical cores show periods of higher and lower selenium deposition (the net result of inputs and cycling), with the highest concentrations occurring in the last 30 years and perhaps during the mid 19th century (gold mining activities?).

Se transformations by phytoplankton and bacteria (SET)

Field measurements of selenite uptake.

i) When algal biomass was high, uptake by particles was capable of removing a significant fraction of the dissolved selenite pool daily. Selenite was removed from solution at a rate of $0.11 \text{ nmol L}^{-1} \text{ d}^{-1}$ in the southwest corner of Mildred Island where phytoplankton biomass ranged between $12.4 - 30 \text{ ug chl-}a \text{ L}^{-1}$ (Fig. SET1). That uptake rate amounts to $>30\%$ of the dissolved selenite pool daily, and corresponds roughly to the observed net change in stable dissolved selenite concentrations observed over the first 48 h of the experiment. Where algal biomass was low, uptake by particles was small relative to the amount of dissolved selenite available. Only about 5% of the dissolved selenite was taken up by particles daily in the Channel where chlorophyll concentrations were only $2-3 \text{ } \mu\text{g Chl } a \text{ L}^{-1}$ Table SET1).

ii) Rates of selenite uptake increased with primary production in both sites sampled. ^{75}Se accumulated in particles linearly over time, allowing us to calculate uptake rates at specific light levels based on the slope of regressions of particulate Se vs. time (Fig. SET2). Selenite uptake rates, much like rates of C fixation, increased with irradiance until reaching an asymptote at relatively low light levels (Fig. SET3). Maximum absolute selenite uptake rates varied between the Mildred Island (Chlmax) and Middle River (Channel) sites in direct proportion to the amount of algal biomass at those sites. Consequently, chlorophyll normalized rates of selenite uptake varied far less among sites than non-normalized values. Chlorophyll-normalized uptake of selenite into particles also declined significantly from morning to afternoon at the Chlmax site (Fig. SET3), as did rates of chlorophyll normalized C-fixation possibly in response to C-limitation (Fig. SET4). This suggested that uptake of selenite into particles can be partly modeled as a function of light, much like primary production.

iii) However, a significant fraction of the overall selenite uptake into particles occurred in the absence of light. Dark uptake of selenite amounted to 40-60% of the maximum uptake of selenite at saturating light intensities (Fig. SET3). Integrated across depth and over the course of a day, dark uptake account for about to 80% of the total uptake of selenite into suspended particles in both the Channel and the Chlmax sites (Table SET1). This uptake may be due to either phytoplankton or bacteria or both. Modeling of this important component of selenite represents a continuing challenge. Long-term average primary productivity within a site as well as the supply of allochthonous organic matter may be good predictors of this component of uptake.

iv) A significant fraction of selenite uptake also occurred into the bacteria size fraction (0.2-1.0 μm). Uptake of selenite into this fraction was not related to light, whereas uptake into the $>1.0\mu\text{m}$ size fraction was positively related to light (Fig. SET5). 40-70% of the dark selenite uptake was due to this size fraction, suggesting that most if not all of the dark selenite uptake was due to bacteria. Integrated over the course of a day, the bacterial size fraction accounted for 50% of the areal selenite uptake in both sites (Table SET1).

v) The radiotracer method for estimating Se:C in recently produced particulate matter using dual isotope tracers agreed well with stable chemical measurements. Stable chemical measurements of Se:C ratios (weight:weight) in particulate matter averaged about $12 \mu\text{g Se g}^{-1} \text{C}$ in the Southwest corner of Mildred Island where living material dominated the suspended particulate organic matter. Se:C uptake ratios integrated over the day indicated a ratio of $15.1 \mu\text{g Se g}^{-1} \text{C}$ which was within the range of error for the chemical measurements (Fig. SET6). This suggests that the primary source of selenium accumulating in biomass was selenite, rather than selenate and organic selenide. This result is surprising considering the large fluctuations in organic selenide during the course of the experiment, which suggested that this fraction was bioavailable.

vi) Bacteria are potentially a very important source of Se to consumers compared to phytoplankton. Estimates of the bacterial Se:C ratio in the Southwest corner of Mildred Island were made by assuming either that only selenite uptake in the < 1.0 fraction was due to bacteria, or that all dark selenite uptake was due to bacteria. The resulting estimates of bacteria Se:C ratios were $33 \mu\text{g Se g}^{-1} \text{C}$, and $58 \mu\text{g Se g}^{-1} \text{C}$, respectively. The phytoplankton uptake under the same assumptions were $11 \mu\text{g Se g}^{-1} \text{C}$ and $3.7 \mu\text{g Se g}^{-1} \text{C}$, or 3- 13-fold lower (Fig. SET6). Thus, even though bacteria are not considered an important source of C and energy to higher trophic levels in the Bay-Delta ecosystem (Sobczak *et al.* 2002), they may be important as vectors of selenium.

Lab experiments on selenite uptake.

Freshwater phytoplankton.

vii) Cultured freshwater phytoplankton species isolated from sites other than the Bay-Delta ecosystem behaved like native phytoplankton with respect to selenite. Two findings support this notion. First, the species which we isolated from Mildred Island (MI-34, unidentified chlorophyte), exhibited similar uptake rates to similar sized species isolated from other localities (Table SET2). Moreover, the Se:C ratios estimated for the cultured phytoplankton species $> 4\mu\text{m}$ in size closely resembled the Se:C uptake ratios measured on intact phytoplankton communities in Mildred Island (Table SET2, Fig. SET6). In fact, Se:C ratios predicted for the phytoplankton in Mildred Island based on a relationship between cell size and Se:C in freshwater cultures fell within the range of Se:C estimates for phytoplankton based on the field radioisotope uptake experiments (see item xii below).

viii). Like marine phytoplankton (Baines *et al.* 2001), cultured freshwater phytoplankton vary a great deal in their ability to accumulate selenite from solution under conditions similar to those in the Delta. Rates of initial uptake ranged by more than two orders of magnitude among the

species in 0.02nM selenite, and nearly two orders of magnitude in 0.45 nM selenite (Table SET1, Fig. SET7).

ix) The Se content of freshwater phytoplankton can respond very quickly to changing selenite concentrations and is probably almost always in equilibrium with ambient conditions *in situ*. Within 24 h, most species exhibited nearly constant Se cellular concentrations (Fig. SET7). In most cases equilibrium concentrations were reached in less than 12 h. As with selenite uptake rates, these “equilibrium” cellular selenium concentrations varied by two orders of magnitude among the freshwater species (Table SET1, Figs. SET7-8).

x) Cell size was the best predictor of equilibrium cellular Se concentrations (at 0.45 nM selenite) for freshwater phytoplankton grown in the presence of radiolabeled selenite and under conditions that are typical of the Delta (Fig. SET9). Selenite uptake varied among taxonomic groups of freshwater phytoplankton, but not in the same way as it does among marine plankton (Baines and Fisher 2001). In particular, green algae take up selenite readily in freshwater, while marine chlorophytes are invariably poor at accumulating selenite. The highest cellular concentrations of Se among the freshwater algae were exhibited by two cyanobacterial species. When cell diameter (D) was used to predict cellular Se concentrations (C_{Se}) using the equation $C_{Se} = aD^{-b}$, the exponent b was approximately 2, indicating that uptake was proportional to cell surface area. Although significant, this relationship still left 10-fold differences between the Se content in *Cyclotella meneghiniana* and *Selanastrum* unexplained. A relationship between surface area and Se uptake does not exist for marine phytoplankton.

xi) VCF's for selenite in freshwater algae do not vary with ambient selenite concentration over the typical concentrations observed in the Bay-Delta ecosystem (Table SET1). This indicates that freshwater phytoplankton accumulate selenite in direct proportion to ambient selenite concentration. When grown at selenite concentrations that differed by 22-fold (0.02nM and 0.45nM), the selenite uptake rates and equilibrium cellular selenium concentrations in the experiments with lower selenite concentrations were typically 22-fold lower (Figure SET8). However, uptake does tend to get saturated at selenite concentrations > 1nM (Fig. SET9)

xii) The concentrations of other nutrient anions (nitrate, phosphate, silicate) had no impact on selenite uptake by living freshwater phytoplankton (Fig. SET11). This indicates that selenite is not taken up by algal cells via the same channels as these other substances. Modeling of selenite uptake does not have to incorporate these aspects of water chemistry.

xiii) Adsorption onto killed cells was minimal in all experiments so uptake appears to be active (Fig. SET12). Thus, the correlation between selenite uptake and cell size does not appear to be driven simply by abiotic adsorptive processes, although that may be the process driving initial uptake before other processes become important. The constant VCF's for selenite is likely to hold true only at the low concentrations that currently characterize the Bay-Delta ecosystem.

xiv) Se:C ratios in a natural community of phytoplankton from Mildred Island were accurately predicted using this relationship. Based on the taxonomic composition of the phytoplankton during the Mildred Island process study, we were able to predict the contribution of each species to the community Se and C (Fig. SET3). To do this, cell size of the various taxa were used to

predict their Se:C ratios at 0.45nM selenite using the relationship in Fig. SET10, and the relative contribution of each taxa to community biomass was used to weight these predictions when calculating community the Se:C ratio. These predictions were then scaled to observed selenite concentrations at the sampling sites based on the assumption that VCF's were constant. The community Se:C ratios estimated for southwest Mildred Island averaged $6.3 \mu\text{g g}^{-1}$, which is between the values of 3 and $11 \mu\text{g g}^{-1}$ estimated from field radioisotope experiments.

Marine Phytoplankton.

xv) In general, VCF's for selenite in marine algae varied inversely with ambient selenite concentration (Table SET4). This is because uptake is *non-linearly and non-proportionately* related to ambient selenite concentrations, especially for those marine species that can concentrate selenite most effectively (Fig. SET13). For example, at concentrations typical of the Bay-Delta ecosystem selenite uptake and equilibrium cellular selenium concentrations are within two-fold of their maximum value for the diatom *Thalassiosira pseudonana*. Uptake of selenite and the equilibrium cellular selenium concentration could be described as a function of ambient concentration using Michaelis-Menten kinetics (Figs. SET14-15). Based on this relationship, the selenite concentrations at which selenite uptake is $\frac{1}{2}$ of the maximum rate is 0.06 nM. For comparison, typical background selenite concentrations in the Bay-Delta are about 0.2-0.4 nM. This pattern suggests an uptake mechanism that is highly selective for selenite.

xvi) Uptake of selenite by species that accumulate it poorly may be directly proportional to ambient selenite concentrations. Selenite VCF's for *Skeletonema costatum*, a diatom that accumulates selenite very poorly and is common to the marine and brackish regions of the Bay, were constant over a wide range of selenite concentrations (Table SET4). This is because this species took up selenite *in direct proportion* to ambient selenite concentrations (Fig. SET16). Such uptake patterns are typical non-selective uptake pathways and cause the VCF's for *S. costatum* to be constant over a wide range of selenite concentrations. Preliminary experiments suggest that this pattern is typical of marine phytoplankton that do not accumulate selenite well.

xvii) Low ambient phosphate concentrations allow species that are typically poor accumulators of selenite to accumulate this form of Se much more effectively. In all species tested, uptake of selenite was inversely related to concentrations of ambient phosphate. Silicate had little or no effect on accumulation of selenite while nitrate sometimes had a slight positive effect that may be related to stimulation of protein synthesis. These patterns have been observed, previously, but we have noted that the effect of phosphate on accumulation of selenite appears to be greatest for those species that don't accumulate selenite effectively. Uptake of selenite by *S. costatum*, for instance, declines in direct proportion to ambient phosphate concentration. By comparison, selenite uptake by *T. pseudonana*, a selenite accumulator, increases by only 20% as phosphate concentrations vary by over 1 order of magnitude. Selenite accumulators appear to have a specific uptake channel that discriminates between the two ions, while non-accumulators appear to acquire selenite incidentally via the phosphate uptake channel.

xviii) Salinity did not affect uptake of selenite from marine phytoplankton until it was <4 ppt, at which point salinity caused marine phytoplankton to take up less selenite (Fig. SET17).

Lab Experiments on organic selenide uptake.

Marine phytoplankton.

xviii) A range of marine phytoplankton species accumulated a portion of the dissolved organic selenium derived from algae (Fig. SET18). When presented with lysates of *Thalassiosira pseudonana* grown on radiolabeled selenite all species accumulated selenium from solution at rates that were similar to those observed for selenite, although species varied dramatically in the rate of uptake and in the total amount taken up. Uptake of lysate radiolabel was only partially inhibited by adding a large surplus of non-radioactive selenite (Fig. SET19). This indicates that dissolved organic selenide was actually taken up as organic selenide, rather than as selenite produced after mineralization of selenide compounds.

xix) Not all of the dissolved organic selenide pool is available. The pattern of uptake over time suggested that only a fraction of the dissolved organic selenium in the algal lysates was actually available to the algae (Fig. SET19). The rest, comprising about 50% of the selenium, appears to be unavailable over the short-term. *In situ*, dissolved organic selenide pools in many places may be dominated by this unavailable fraction. The labile fraction of dissolved organic selenide is probably substantial where phytoplankton biomass and production are highest, and where cell lysis of phytoplankton occurs, such as at the salt front in estuaries. At present, the chemical characteristics of these available and unavailable pools is unknown.

xx) The ability of marine phytoplankton to concentrate dissolved organic Se from solution was strongly correlated with the ability of the same plankton to accumulate selenite from solution (Fig. SET20). This suggests that the ability to concentrate selenite from solution may be linked to the ability to exchange synthesized organic selenide compounds with the environment. This correlation may make it possible to predict which marine phytoplankton species are most likely to accumulate dissolved organic selenide from solution.

Marine bacteria.

xxi) Experiments suggest that marine bacteria are likely to act as remineralizers of organic selenide when ambient nutrient concentrations are low. Exposure of algal lysates radiolabeled with ⁷⁵Se to bacteria resulted in the slow production of selenite from the dissolved organic selenides (Fig. SET21). However, almost none of the radioactivity accumulated in bacterial biomass over the course of the experiment.

xxii) The presence of phosphate greatly enhances the ability of marine bacteria to accumulate, rather than mineralize, organic selenides. We exposed marine bacteria to a range of nutrient conditions in the presence of radiolabeled selenite, ostensibly to determine the degree to which the availability of N compounds for protein synthesis affected uptake of dissolved organic selenide. Only in the treatments to which phosphate was added was there a significant accumulation of radioactivity in bacteria (Fig. SET22). This finding may be important to the Bay-Delta as phosphate is rarely depleted by biological activity throughout the region.

Se in Bay-Delta Food Webs (SEF)

Monthly sampling of Potamocorbula at Carquinez Strait.

- Seasonal trends in Se concentrations of *Potamocorbula* at USGS station 8 in Carquinez St. do not appear to have changed since the time series began in 1995 (Figure SEF2).
- Selenium concentrations in *Potamocorbula* are significantly higher in the fall/winter (maximum value during this project $17 \mu\text{g g}^{-1}$) compared to the spring/summer.
- Stable isotopes of carbon ($\delta^{13}\text{C}$) and nitrogen ($\delta^{15}\text{N}$) in the soft tissues of the clams vary with salinity throughout the year (Figure SEF3).

Spatially intensive field studies of Se in Corbicula in the Delta.

- Nitrogen content (% by weight) explained 60% of the variability in Se concentrations in *Corbicula* throughout the Delta (Figure SEF4).
- Variation in Se concentrations of *Corbicula* could not be related to Se distributions in particles, hydrodynamics or phytoplankton dynamics (except through site specific growth).
- Selenium exposure or bioavailable Se does not appear to vary throughout the central Delta.
- Selenium concentrations in *Corbicula* were significantly higher in the Bay relative to the Delta and higher in *Potamocorbula* relative to *Corbicula* over a similar range in nitrogen content (Figure SEF5).
- Stable isotope signatures of *Corbicula* were distinctly different among the Mildred's Island, Frank's Tract, Sacramento and Bay regions (Figure SEF6).

Se distributions in Delta food webs.

- Selenium concentrations in invertebrates of Mildred's Island and Frank's Tract were similar and did not exceed Se toxicity thresholds identified for fish diets (Lemly 1997) (Figures SEF7&9). Highest invertebrate Se concentrations were found in Oligochaetes in Mildred's Island and *Corbicula* in Frank's Tract.
- Selenium concentrations in fish of Mildred's Island and Frank's Tract did not exceed Se toxicity thresholds identified for fish livers (Lemly 1997) (Figures SEF8&10). Highest fish liver Se concentrations were found in striped bass in Mildred's Island.
- Two distinct food webs, phytoplankton-based and epiphytic-based, were identified in both Mildred's Island and Frank's Tract using $\delta^{13}\text{C}$ signatures (Figure SEF11&12).
- Selenium was significantly biomagnified within the epiphytic-based food web of Mildred's Island (Figure SEF13).
- Selenium concentrations in Frank's Tract fish appeared to decrease with increased reliance on the epiphytic-based food web and size of fish (Figure SEF14(a)&(b)).
- San Francisco Bay food webs had significantly higher Se concentrations than Delta food webs.

Kinetics of Se bioaccumulation.

- Biodynamic constants for Se bioaccumulation in different types of organisms that inhabit the Bay-Delta are shown in Table SEF1.

- The clam Se model predicted Se concentrations within $2 \mu\text{g g}^{-1}$ (Figures SEF16-18, Table SEF2-3).
- The lowest residual errors for the clam model were found for IR_{PHYTOCOM} , an AE of 30% and a F_{SF} of 4.6.
- Se: Phytoplankton & Bacteria C ratios of 4.6 and 56 measured by Baines for the Mildred's Island region may be a reasonable surrogate for the Delta as a whole assuming a range in bacteria: phytoplankton biomass ratios of 8 – 30 % in suspended particulates.

Local scale modeling (ML)

Residence time in shallow water habitats. The transport time scales that best described water circulation within MI were mean residence time and mean exposure time. Please see Figure ML2 for a map of these quantities for the June 1999 period. Please also see the Narrative for an explanation of the significance of these findings. The mean reflects the average value at each particle release point for 24 different simulations. The maximum time of 168 h reflects the end of the simulation rather than the maximum residence or exposure time. Exposure is the measure of the total time a particle spends inside the boundaries of MI during the simulation while residence time reflects the time the particle stayed in the domain before exiting once. (Please see Monsen (2002) for more information.)

Franks Tract---The effect of SAV on hydrodynamics.

A water column model of these processes indicates that the inclusion of distributed drag elements is an effective approach to modeling the vertical structure of flows in the presence of SAV. Modeling of flow and scalar flux in the presence of SAV beds should include consideration of the vertical structure of flows, including the drag force induced by the interaction of the flow with the vegetation. For mean velocity calculations, it appears that a simple bed-friction model can adequately capture the flow resistance of submerged vegetation. For transport purposes, however, this approach will not accurately predict the vertical distribution of scalars, due to the lack of a mid-column peak in turbulent stresses. In view of this shortcoming, the distributed drag parameterization provides a superior alternative to simulate the transport and dispersion of scalars in the presence of submerged aquatic vegetation.

Mildred Island—Modeling with reactions. Our major findings include:

- The effect of wind on advection is significant in shaping phytoplankton biomass distributions within MI.
- Wind-driven advection is critical in driving the export of phytoplankton biomass from otherwise sheltered high-productivity sub-regions to open areas more subject tidal exchange.
- The effect of wind on vertical mixing is not significant in shaping horizontal distributions of phytoplankton biomass.
- Wind driven advection represents a significant mechanism for mixing patches of transported scalars in open water areas.
- Phytoplankton biomass and productivity in the Delta appear to possess a positive relationship with residence time/exposure time.

- Although physical processes may be important in shaping the general features of spatial distributions of reactive scalars like phytoplankton, important interactions between reactions and physics (like those between phytoplankton growth and density stratification) may govern important details of those distributions.
- Modest increases in benthic grazing rates can significantly decrease phytoplankton biomass, and that effect intensifies in shallower areas.
- Benthic grazing may mute high frequency oscillations in phytoplankton biomass concentration.
- Edible particulate selenium distributions are expected to follow distributions of phytoplankton biomass and therefore be governed by a combination of physics, phytoplankton growth and grazing.

Delta scale modeling (MD)

Hydrodynamic modeling.

Understanding the influence of barriers, gate, and pump operations on source distribution.

Gates, barriers, and pump operations significantly alter water quality parameters throughout the Delta by shifting the water source and changing the residence time at key locations.

Interbasin transfers (Pump operations): A significant reduction in export flow at the SWP occurred between 7 Oct and 6 Nov 2001 (Fig. MD5a). During the period of high SWP export, the mean net (tidal residual) north to south flow via Middle River was $100 \text{ m}^3 \text{ s}^{-1}$. This mean flow fell to $56 \text{ m}^3 \text{ s}^{-1}$ when exports were curtailed. Because less water was drawn towards the pumps, the net residual flow in the channels surrounding MI and through MI were reduced. In some locations, the direction of net residual flow reversed. Altering the water balance in the channels around MI, also changes the exchange of salt between this open water region and the surrounding channels. During peak SWP exports in late September, the total salt flux (Fischer and others 1979) through the MI south opening was directed out of MI towards the export pumps (Fig. MD5c). During the period when the pump operations were curtailed, the salt flux reversed indicating salt from the channels adjacent to the southeast corner of MI entered MI.

Gate-controlled flow routing (Delta Cross Channel): The Delta Cross Channel diversion channel is located in a key hydraulic location. Salinity records (Fig. MD6) show that discrete diversions at the DCC (Fig. MD2b) cause rapid downstream changes at the SFB-Delta boundary, especially on the SJR arm of the Delta. Diversion of flow through an artificial channel modifies the system-wide salinity distribution.

Barrier-controlled flow routing:

1) Head of Old River Barrier (HORB): Placement of the HORB barriers significantly changes the volume of San Joaquin flow entering the Stockton Ship channel. When the barrier is in, most of the SJR water is directed north towards the Stockton Ship channel. When the HORB is removed, the SJR entering the Delta is diverted at Old River and flows west towards the pumps (Fig. MD1, inset). This manipulation of regional-scale circulation contributes to the decline of DO in the downstream Stockton Ship Channel (Fig. MD7b). For example, after the HORB was

removed on 15 November 2002, DO concentrations fell below the 6 mg L^{-1} DO standard that is in place to protect biota sensitive to hypoxia.

2) Agricultural barriers: Three barriers are constructed in the south Delta each spring to prevent the draw of export pumps from depleting water in nearby channels that supply irrigation water to local farm tracts. These four barriers (3 agricultural barriers and the HORB) establish a temporary reservoir as segments of Old and Middle rivers and Grant Line Canal (Fig. MD1) isolated from the exports and river inflows. The primary inflow source to this temporary storage region is agricultural return water, which is highly enriched in dissolved organic carbon. When the barriers are removed each autumn, the pumps also draw from the south Delta channels (Fig. MD1, inset) where DOC has progressively accumulated, leading to pulse increases in the DOC concentration of drinking water supplied to metropolitan areas (Fig. MD9). (Please see Monsen (Monsen *et al.* In prep.) for more information.)

Source distribution through the Delta. Changing the gate operations at the Delta Cross Channel significantly alters the water source distribution in the central Delta as illustrated in Figures MD8a-b. Figure MD8a is the source water distribution in the Central Delta when the Delta Cross Channel was open for the majority of the period. Figure MD8b shows what the source water distribution would have been if the Delta Cross Channel had been closed for the same period.

Figure MD8a shows the spatial distribution of Sacramento source water after a 35 day simulation with September 2001 hydrology, a period when the Delta Cross Channel was primarily open. This figure shows that Sacramento water dominates in the Sacramento channel as well as in the waters entering the San Joaquin from the Mokelumne system. This distribution is logical since the purpose of the DCC gate is to transfer Sacramento water into the Mokelumne. Note that the Northeast corner of Franks Tract is red indicating that this region is dominated by Sacramento source water. There is a strong gradient in source water across Franks Tract. The darker colors in Franks Tract in this simulation indicate either bay-derived water or old water in the system. The old water/bay-derived water also dominates the San Joaquin River between Big Break and Three Mile slough.

Figure MD8b shows the spatial distribution of Sacramento source water after a 35 day simulation with September 2001 hydrology with the Delta Cross Channel closed for the entire period. This reproduces what the system would look like if the Delta Cross Channel did not exist. The Sacramento water still dominates the Sacramento channel but also influences the Sherman Lake area and the lower San Joaquin River between Big Break and Jersey Point. Less Sacramento water enters the San Joaquin through the Mokelumne river system. There is still some influence since Georgiana Slough naturally connects the Sacramento and Mokelumne system. In the northeast corner of Franks Tract, Sacramento River water comprises ~60% of the source water rather than the ~85% found in the Delta Cross Channel open case. The gradient in source water across Franks Tract is reduced in this case. In this scenario, more San Joaquin derived water enters the Central Delta.

Modeling with reactions.

- A modest increase in clam grazing in the SJR can dramatically decrease phytoplankton standing stock locally; however, for spring hydrologic and operational conditions, when

Delta flows are dominated by the Sacramento, phytoplankton biomass from the upper SJR may not significantly affect the central Delta.

1. Sharp gradients in benthic grazing may result in sharp spatial gradients in phytoplankton biomass, contributing to large amplitude semidiurnal oscillations in chl *a* at a point in space.
2. For spring conditions, pumping does not significantly affect phytoplankton biomass distributions or magnitudes in the Delta (i.e. if the gates at Clifton Court Forebay remain operational).
3. Pumping may modify the character of high frequency variability in transported scalars in the Delta.
4. Lowest phytoplankton biomass, and therefore edible particulate selenium, may be generally located in the central Delta, where benthic grazing is the highest.
5. Highest phytoplankton biomass, and therefore edible particulate selenium, may be located in the San Joaquin River; however, hydrology and operations may determine whether those high concentrations will enhance phytoplankton biomass, productivity, and availability of edible particulate Se in the greater Delta.

VI. NARRATIVE

Hydrodynamic Measurements in Shallow Water Habitats (HS)

The analysis of the data described in the previous section has focused on identifying the important forcing mechanisms in shallow water habitats and, from that, develop a description of the structure and variability of flows in these habitats. Franks Tract and Mildred Island are characterized by very different geometry (in terms of levee breaches and basin shape) and vegetation development (with FT having extensive SAV development while MI remains relatively open), and have given us the opportunity to explore two strongly contrasting systems. In the first subsection below, we develop a description of the interior dynamics for these two basins; then we examine the nature of channel-shallow habitat exchange.

Interior dynamics. Both MI and FT are characterized by a relatively large tidal range – with surface elevations varying of the order of 1 meter. The tides are strongly semi-diurnal, but with a diurnal inequality characteristic of Northern San Francisco Bay and Delta. The tidal forcing is communicated throughout the Delta by the propagation of the tidal wave in the Delta channels such that at FT the primary tidal gradient is along the east-west axis, while at MI the primary gradient is along the north-south axis. Although the depth variation due to tides at the two sites is similar, the influence of the tides on flows in the interior of each basin is quite different, due to differences in basin geometry and the nature of the levee breaches at each site.

Mildred Island Interior Dynamics. In Mildred Island, the primary connection to the Delta channels is through the north (NOPN, Fig. HS1). There is a second, smaller breach on the south levee (SOPN, Fig. HS1) and numerous smaller connections where the levee intermittently overtops. Tidal flows, however, are mostly a result of the two primary levee breaches (NOPN and SOPN). The details of the tidal exchange adjacent to these openings are described in the next section on exchange; in the interior, the effect of the tides is to modulate a net north-to-

south barotropic flow. The magnitude of this barotropic flow is about 2-3 cm/s, and is created due to the net flow around and through MI to the pumps in the south, but modulated by the tides.

More important to the interior dynamics of Mildred Island is the influence of atmospheric forcing. In many ways, MI is reasonably approximated as a moderately sized lake, with heat and momentum fluxes from the atmosphere dominating the local dynamics. This is most clearly seen at the south island station (MILS, Fig. HS1), where we focus this initial discussion.

In Fig. HS4, the temperature variability is presented, and is seen to be characterized by strong diurnal variability in both the top and bottom temperature sensors. The difference between the top and bottom sensors, which is representative of the temperature stratification, is characterized by “spikes” of short duration during the afternoon periods. This does not mean that stratification in the water column only exists during these short periods; rather, the short duration stratification “events” detected here only reflect the period of time when the thermocline is between the two sensors. That is, the surface layer warms under the action of solar heating starting in the late morning. During the afternoon, the wind begins to blow and the surface layer deepens. As the thermocline moves downwards, it first moves past the upper sensor – at which point stratification “appears” in the data. As it deepens further, the thermocline moves below the lower sensor and the stratification “disappears” from the data. A simple two-layer model of surface mixed layer dynamics (developed as part of another CALFED grant) reinforces this interpretation.

In addition to deepening the mixed layer, the afternoon winds also move the surface waters downwind. This leads to a tilting of the thermocline, with downwelling at the downwind boundary and upwelling at the upwind boundary (Fig. HS5). This results in a diurnal pattern of temperature variation that starts out with vertical gradients, created by solar heating, that are converted into horizontal gradients by the action of wind forcing in the late afternoon. The horizontal temperature gradients, which would be maximum in the early evening and overnight, lead to a relaxation flow when the winds subside. This baroclinic flow would reverse the wind-driven circulation of the afternoon (Fig. HS5). This conceptual model of the diurnal flow pattern under wind and temperature forcing has been referred to as “baroclinic pumping” in shallow lakes, and we would expect these dynamics to be important in MI.

The velocity data from MILS is consistent with this daily pattern (Fig. HS6). In the center panel, the surface velocities are seen to be maximum to the SE (downwind) in the afternoons (days 246.6, 247.6 and 248.6, for example). At the bed (bottom panel, Fig. HS6), there are pulses of flow to the SE during the overnight hours (days 244.0, 245.0 and 247.0, for example), when we would expect the baroclinic relaxation to dominate. This pattern is consistent with the conceptual model of baroclinic pumping, and is likely an important flushing mechanism for the SE corner of the island.

Because diurnal processes are so important in MI, we now focus on the average daily cycle at MILS, where the average has been calculated across all days for a given time block (i.e. 10-11 am data is averaged together across the entire deployment). The resulting temperature and wind patterns are shown in Fig. HS7, where the diurnal heating and cooling and afternoon wind patterns are clear. In the velocity data, we expect the averaging process to remove tidal oscillations due to the fact that the data extends across multiple spring-neap periods. What remains should consist of the mean barotropic flow (expected to be primarily North-to-South) and the wind-driven circulation that has a specific variability within the diurnal cycle. To separate these two components, we focus our analysis on depth-averaged velocity (the barotropic component) and the top-bottom velocity difference (to represent the wind-driven and baroclinic

relaxation. The resulting flow pattern (Fig. HS8) is consistent with the baroclinic pumping process described above. The depth-averaged velocity (left panel, Fig. HS8) is relatively constant across time-of-day (due to the averaging out of tidal modulations), but with a dip during mid-day, perhaps due to the development of stratification. The orientation of the depth averaged flow is primarily to the south, consistent with the expectation of a net north-to-south flow of water. The top-bottom shear (right panel, Fig. HS8), on the other hand, has a strong daily cycle, with flow along the wind direction at the surface during the afternoon and reversing at night due to the baroclinic relaxation. The implications of this process on channel-shallow exchange and on flushing times will be considered below. We note here, however, that the flows due to this process are directed along the axis of the wind – along a NW-SE axis – which makes it an efficient transport mechanism in regions along the east and west levees of MI.

While atmospheric forcing is dominant in south MI, the dynamics of northern MI are more mixed, and are more strongly influenced by tidal forcing. The details of the tidal exchange at the north opening of MI are described below, including the modification of these exchanges by atmospheric forcing. The transition from tidally-forced flows (modified by wind forcing) to atmospheric-forced flows (modulated by tidal forcing) appears to occur around the centerline of MI – or the narrowest section of the island. For considerations of transport below, we will divide the island into North and South sections in order to focus on this transition point.

Franks Tract Interior Dynamics. In Franks Tract (FT), the connection between the shallows and the channel is through a large number of levee breaches (Fig. HS2). In fact, the entire eastern levee has been lost to wind-wave erosion, leaving essentially an open boundary between the shallows and the channel. Along the western and northern boundaries, numerous isolated breaches exist, but the two most prominent ones – one on the western boundary, one on the northern – will be the emphasis of our analysis here. It is important to note the development of submerged aquatic vegetation (SAV) in Franks Tract. Figure HS2 is an aerial photograph of the area from the late summer period; the dark regions represent patches of SAV. It is clear that SAV development is extensive in FT, but is organized into patches that outline a “channel” structure through the basin.

Flows in the interior of FT are primarily driven by tidal forcing; the nature of the flood/ebb tide asymmetry will be addressed in the next section regarding channel-shallow exchange, but we note here that the ebb flow is primarily directed from east to west across the basin. Locally, the details of the flow structure are strongly influenced by the presence and nature of SAV. In Figure HS9, we present the average tidal cycle in the region adjacent to the northern opening of FT. During the ebb tide, the open water site has the expected structure, and velocities of approximately 6-10 cm/s. These velocities are directed toward the vegetated site, for which the vertical structure is shown in the right panel of Figure HS9. In the SAV, the overall velocity is reduced, due to vegetative drag, but at the same time, the mid-column velocity variation is increased. This is more clearly seen in Figure HS10, where the vertical structure of the mean velocity is presented as a profile. In the open water, the velocity is consistent with a logarithmic structure; in the SAV, however, a logarithmic structure applied to the lower three sensors severely underestimates the velocity in the upper water column.

This structure implies the presence of a shear layer – or mixing layer – near the top of the SAV. In this case, it is expected that there would be a mid-column peak in turbulent mixing and turbulent momentum transfer in or around the mixing layer. This is in contrast to the traditional logarithmic structure in the open water, where turbulent energy and stresses would decrease

monotonically away from the bed. In Figure HS11, we present profiles of the turbulent stresses to evaluate this conceptual model for flows in SAV. In the open water (left panel of Fig. HS11), the turbulent stresses have the structure expected in channel flow, with larger stresses at the near-bed sensor. In contrast, the SAV station (right panel, Fig. HS11) shows very small near-bed stresses and large stresses in the mid-column region, near the mixing layer we are hypothesizing. The low stresses in the near-bed region are due to the effects of vegetative drag, which reduces the mean velocity near the bed, leaving less momentum to interact with the bed in the form of bottom stresses.

Atmospheric forcing plays a lesser role in FT than it does in MI, largely due to the dominance of tides and SAV. There are times, however, when wind events are important to net transport; one of these will be discussed below in the section on transport. In terms of atmospheric heating and cooling, the pronounced vertical temperature gradients that were found in MI do not develop in FT, largely due to the shallower depth and more extensive tidal forcing. Instead, temperature variation in FT is most pronounced along the boundary of open and vegetated waters (Fig. HS12). While it is possible that these temperature variations facilitate exchange between the open and vegetated regions, the observations and analysis have not focused on this process to this point, and we leave this consideration as an open question.

Channel-Shallow exchange. Tidal exchange through a narrow opening creates a pronounced tidal asymmetry, with a momentum jet entering the shallow habitat during flood tides and a distributed, radial flow moving towards the opening on ebbs (Fig. HS13). This asymmetry, termed “tidal pumping” by Fischer et al. (1979) and others, leads to a net exchange between the channel and the shallow habitat that can be described by the local geometry and the tidal prism (see Fischer et al. 1979 for details). This pure “jet-drain” structure though is, in general, not evident at the exchange points between channels and shallows, except perhaps at the southern opening of MI and the western opening of FT. Instead, the dynamics in the interior of the shallow habitats lead to modifications to this exchange dynamic. In the subsections that follow, we describe four examples of these modifications.

Deflection of Flood Tide Jet. In the traditional tidal pumping model, the flood tide jet is oriented directly into the shallow habitat. If, however, there is a tidally-induced surface gradient across the habitat in a direction that is at an angle to this jet orientation, then the flood tide jet will be deflected by the associated pressure gradient. The result is an asymmetric jet, which will likely develop a coherent recirculating structure along the side of the jet to which it is being deflected. In shallow habitats in the Delta, this configuration is quite common due to the variety of orientations for levee breaches – only a few of which would actually align with the ambient tidal surface gradients.

The observations described here provide two examples of this structure. First, in Mildred Island, the jet from the northern opening is initially directed East-to-West, while the tidal pressure gradient is primarily North-to-South during the rising tide. As a result, the jet is deflected to a more southerly orientation once it enters the shallow habitat (Fig. HS14); on the south side of the jet, a coherent vortex appears to form that recirculates water along the eastern boundary towards the opening, where it is entrained into the jet. This recirculation during the flood tide leads to a bias in the structure of the ebb tide currents (right panel, Fig. HS14), with flow primarily along the eastern boundary (reinforced by wind-driven flow, discussed further

below). The result is a net flow pattern that exchanges fluid into MI along the center of the northern island, and the return flow is along the eastern boundary.

A similar dynamic occurs in Franks Tract at the northern opening described above; here, the flood tide jet is oriented from North-to-South, while the rising tide surface gradient is oriented West-to-East. In this case, the flood tide jet (Fig. HS15) is deflected to the east, which follows the open water region. There is obviously a feedback between the hydrodynamics and the vegetation, and, while the vegetation certainly constrains the flow (discussed below), the distribution of SAV appears to be dictated by the hydrodynamics. To be specific, we hypothesize that the orientation of the flood tide jet – and the resulting open water region – is set by the interaction of the momentum from the flood tide jet with the ambient tidal surface gradient, which deflects the jet to the east. While this interaction is similar to that in Mildred Island, the net effects on circulation are different in FT due to the presence of multiple levee breaches in the area and the presence of SAV along the perimeter of the jet. These two topics are the subjects of the next two sections.

Interaction of Multiple Openings. In Franks Tract, the presence of multiple levee breaches of various size and orientation alters the tidal pumping structure from that outlined above. On ebb tides, flow is everywhere from east-to-west, as the entire basin responds to the ambient tidal surface gradient (Fig. HS15). Immediately adjacent to individual openings, flow is towards the opening (as is evident in Figure HS15), but the influence of the opening during the ebb tide is limited.

This creates a pronounced asymmetry between flood and ebb tides, with flood tides strongly influenced by the opening nearby and relatively unaffected by the large-scale forcing, whereas ebb tides are more strongly influenced by the large-scale pressure gradient. This is to be expected due to the inertial effects of the flood tide jet, which are not a factor during the ebb tide.

Submerged Aquatic Vegetation. The presence of submerged aquatic vegetation in Franks Tract alters the lateral influence of the flood tide jet, particularly the formation of vortices along the perimeter of the jet. As is seen in Figure HS16, the flood jet in Franks Tract still produces vortices along its edge, as is expected due to the instability of the shear layer. Whereas in Mildred Island, this vortex leads to a large-scale recirculation (Fig. HS14), here the development of the vortex is limited in scale by the edge of the SAV. The result is that lateral mixing of the flood tide jet is reduced in the presence of SAV, which would, by itself, increase the tidally-averaged channel-shallow exchange. In this case, the effects of multiple levee breaches, as outlined in the previous section, confounds the analysis of local exchanges, and a more global approach would be required to quantify the tidally-averaged exchange.

Atmospheric Forcing. Finally, we return to consideration of the influence of atmospheric forcing (winds and heating/cooling) on channel-shallow exchange. As was outlined above when considering the interior dynamics, we expect the afternoon flows to be downwind at the surface and upwind at the bed. Because the flood tide jet in the absence of wind (Fig. HS17, left panel) is oriented almost exactly perpendicular to the dominant wind direction, we expect the wind-driven flows to split the jet and spread it laterally. This is exactly what is seen in Figure HS17 (right panel), where an afternoon flood tide is shown to be deflected to the east at the surface and to the west at depth. The implications of this structure on net exchange could be profound: because return flow to the opening on ebb tides is biased towards the eastern shore, these flows

will be preferentially transporting surface waters from the flood tide jet back towards the opening on the ebb. That is, when afternoon winds act to deflect a flood tide jet, there is more net exchange of the near-bottom waters than surface waters. Because the timing of the tides shifts by about 40 minutes per day, the phasing of flood tides relative to afternoon winds should be periodic with about a 2 week return period.

Transport considerations. We now turn to three specific analyses of scalar transport and fluxes. Several of these analyses have been supported by another grant (also CALFED), but we summarize the results here for completeness.

Mildred Island Flushing Time. Using a calibrated, three-dimensional hydrodynamic model of Mildred Island that includes atmospheric forcing due to both wind stresses and heating/cooling, we are able to quantify flushing times for the shallow habitat as a whole – as well as for subhabitats within the basin. To be specific, we have initialized the island (or a portion of the island) with a passive scalar at a uniform concentration. As the hydrodynamic model transports scalar out of the initialized region, the time variability of scalar mass within the habitat (or subhabitat) is fit to simple reactor model to estimate the flushing time. The results of these calculations are summarized in Table HS2.

The most pronounced effect of atmospheric forcing is in the southeast corner of Mildred Island, where the flushing time when atmospheric forcing is included is almost half what it is when only tidal forcing is considered (2.8 days versus 4.9 days). The contribution of atmospheric forcing to flushing is also important to the southern portion of the island, where the flushing time is reduced by about 30% (7.6 days to 5.4 days). Interestingly, the flushing time for north island is actually *increased* when atmospheric forcing is included. This is due to the fact that wind-driven flow moves scalar from north island into south island, where it is retained and gradually re-released into north island. Essentially, a purely tidal model would severely underestimate exchange between north and south island – and between the central part of the island and pockets along its perimeter, such as the southeast corner.

Sediment Fluxes in Franks Tract. A strong ebb-flood asymmetry in Franks Tract is created due to both the presence of SAV and the presence of multiple levee breaches (details described above). This asymmetry also manifests itself in the net flux of suspended sediment. In Figure HS18, the average tidal cycle of mean velocity and suspended sediment is presented. Not only are the velocities much larger on the ebb tides, but so are the suspended sediment concentrations. This is likely due to the fact that flood tide waters are coming from deeper channels, and are likely preferentially sampling the upper part of the channel water column, while the ebb tide waters are coming across the broad shallows of Franks Tract. Because the ebb tide currents are oriented to the west, into the SAV, this covariability between velocity and suspended solid concentration leads to a net flux of sediment into the SAV (bottom panel). While it is generally accepted that vegetation beds are effective as sediment traps, we have here a tidal asymmetry that reinforces the trapping effectiveness of the vegetation. We should note, however, that we are not able to define a control volume for this case since we are just sampling along one edge of the SAV, so we can't quantify the sediment that remains in the SAV. It is unlikely, however, that sediment that enters the SAV bed during the ebb tide traverse the entire bed, and we expect a significant portion to be retained.

Chlorophyll Fluorescence Variation in Franks Tract. Finally, we consider the effects of a large wind event on chlorophyll fluorescence as detected by two SCUFAs deployed in Franks Tract. One was located in the SAV bed, while the second was in the adjacent open water. In Figure HS19, the effect of a large wind storm on days 72-74 is clear in the chlorophyll signal (top panel) and in the backscatter signal (third panel). This time variability was similar at both the SAV (shown) and the open water (not shown) stations. A more detailed comparison of the two suggests that the source of the high concentrations of chlorophyll was likely the SAV. In Figure HS20, it is clear that during the period of high chlorophyll concentrations, the concentration in the SAV was higher than in the adjacent open water. Because the high concentrations were triggered by a large wind storm, we don't expect local growth to be the driving mechanism. Instead, it is likely that particles were dislodged from the SAV by the windstorm, these particles were then advected from the SAV into the open water, a hypothesis that is reinforced by the comparison between chlorophyll concentrations at the two stations.

Regional Hydrodynamic Field Investigations (HR)

Delta-Scale Hydrodynamics. At a very basic level there are three primary factors that control transport in the Delta; (1) river inputs (hydrology), (2) water project operations (including reservoir releases, gate operations, barriers placement/removal and export rates), and the (3) the tidal currents. All of these factors change at daily, seasonal and longer timescales and interact, to a greater or lesser degree, depending on where you are in the Delta. Delta hydrodynamic and transport processes are complex, yet certain large scale features are clear, and these features form the hydrodynamic environment in which Mildred Island and Franks Tract reside.

The average annual inflows to the Delta are on the order of 28,800 thousand acre-feet (TAF). The inflows enter the Delta on its eastern border through three primary sources: the Sacramento River (17,220 TAF) to the north, the San Joaquin River (4,300 TAF) to the south and the east-side streams (1,360 TAF) (Figure HR6). Delta outflow, the amount of water that exchanges between the Delta and the bay is on average 21,020 TAF, and is computed as Delta inflow less the in-delta diversions (primarily the SWP and CVP pumping facilities). The figures given above are averaged values. River inputs, export rates and ultimately the net exchange of water between the bay and Delta changes significantly seasonally and between years. Seasonal and year-to-year variability in river inputs and export rates, to a large degree, control the net, or tidally averaged flows in the Delta; tidal non-linearities and meteorological forcing (wind, atmospheric pressure changes) account for the rest.

North Delta. Sacramento River water, by far the largest source of fresh water in the Delta, enters from the north east and is distributed among the north delta channels depending on the Sacramento River flow rate and Delta Cross Channel (DCC) gate position (Figure HR9). Two major flow paths exist in the North Delta: (1) a combination of Sutter and Steamboat Sloughs conveys Sacramento River water directly to Rio Vista, bypassing the central Delta altogether, and (2) the so-called Delta Transfer flow, made up of the combined flow in Georgiana Slough and the Delta Cross channel. The Delta transfer flow delivers Sacramento River water directly to the central Delta through the Mokelumne system. Somewhat surprisingly, up to half of the Sacramento River water flowing past Freeport is conveyed down the Sutter-Steamboat Sloughs during high flow (Figure HR9). As can be seen in figure HR10, significant reductions in fresh water input to the central Delta occur through the Mokelumne River when the DCC gates are

closed, which can have a dramatic effect on the net flows and salt field in the western and central Delta, including Mildred Island and Franks Tract.

South Delta. The export rates at the SWP and CVP pumping facilities exert a strong influence on the net flows in the south Delta and on the boundary between the central and south Delta, as can be seen in data from Old and Middle Rivers (Figure HR11). Middle River consistently carries roughly 60% of the water heading towards the south Delta export facilities while Old River carries the remaining 40%. This flow split is surprisingly consistent over a wide range of export rates, where the total tidally averaged flows ranged from -12,500 cfs to -31,000 cfs over the period of record considered. The net flows in these channels were towards the export facilities over 90% of the time. Moreover, if periods of high flow on the San Joaquin River ($Q_{sjr} > 10000 \text{ cfs}$ -- approximately 8% of the record) are excluded, then the flows are towards the export facilities over 98% of the time. Under high export conditions, 80% to 85% of the water entering the south Delta is delivered from the North through Old River and Middle River. Under low export rates, the proportion of the flows entering the South Delta is contingent upon the configuration of the South Delta barriers.

The Bay – The salt field. The Delta is usually completely fresh in the late winter, yet becomes saltier as the summer progresses because of salinity intrusion on its western and southern boundaries (Figure HR10). Salinity intrudes into the western Delta from the bay and salty agricultural drainage water enters the southern Delta from the San Joaquin River and local sources. Sandwiched between these salinity intrusions exists a “fresh water corridor” that connects the fresh water supplies that enter the central Delta through the Mokelumne system (via the DCC and Georgiana Slough) with the export facilities in the southern Delta (Figure HR2). From modeling studies (Resource Management Associates, 2005b) we know that salinity intrudes into the central Delta through three primary pathways (Franks Tract, the Lower San Joaquin, and Turner Cut) and secondarily through Dutch Slough and Columbia Cut (Figure HR1).

How salty the Delta gets, and when, is a balance between tidal dispersion, river inflows and export rate. Salinity intrusion varies with the seasons, although its maximum intrusion into the Delta is constrained by water quality regulations that specify the maximum allowable salinity levels at a variety of locations in the Delta: the most important of these are at Jersey Point, Rock Slough, Emmaton (Figure HR6). Water project operators are generally concerned about salinity mixing into the fresh water corridor during the summer/fall period.

Salinity intrusion into the fresh water corridor from both the bay and the San Joaquin River is strongly controlled by dispersive processes. Yet these processes are generally poorly understood in concept, and, in how these processes work within specific regions in the Delta. In the next few sections we discuss specific dispersive processes at a handful of locations in the Delta.

Delta scale dispersive mixing: Where is it important and why? Dispersion within many of the narrow prismatic channels of the Delta is generally weak, although shear flow dispersion in the wide, and bathymetrically complex Sacramento and San Joaquin Rivers in the western Delta is an important transport mechanism there. Dispersion occurs primarily in the tidally influenced regions of the Delta and can be quite large in regions that have one of the following three geometric features: (1) junctions, (2) locations where the channel length < tidal excursion, (3)

where shallow/channel exchange processes occur. To fix ideas we discuss two examples where dispersion is important: (1) in False River, a location where the channel length is less than the tidal excursion and where channel/shallow exchange processes occur, and (2) Threemile Slough, a location where the channel length is less than the tidal excursion and junction dynamics play a role in dispersive mixing. Finally, the geometry in a location where dispersion is not important, on the Mokelumne River, is discussed.

Dispersion example 1: False River. In False River, high saline water flows into Franks Tract on a flood tides and is relatively efficiently mixed with ambient fresher water because of the bathymetric complexity (Figure HR12) water from False River experiences along its tidal excursion trajectory (Figure HR13). The path of drifters released on 2/19/2003 shows that the tidal excursion for water flowing through False River from the San Joaquin River is on the order of 9.3 km and involves, for spring tides, the complete transit of Franks Tract. Therefore, the water traveling through False River on a flood tide is confined to the relatively deep (~ 10m), straight, narrow (~ 180m) channel for ~ 5 km, then is ejected into Franks Tract, which is relatively shallow (< 2 m), through a series of levee breaches (Figure HR12). The net effect of the sum of mixing processes that occur along this tidal excursion trajectory is that water is less saline on ebbs over floods (Figure 14) as it passes a sampling location in False River (for location see Figure HR12). Similarly, the fresh water that exchanges into the San Joaquin River from False River on ebb is mixed with the ambient saltier water in the San Joaquin through shear-flow dispersion in the bathymetrically complex San Joaquin (Figure HR15). Thus, overall, the dispersive flux is a measure of mixing efficiency (primarily lateral) within a tidal excursion of the sampling location, for a given spatial concentration gradient. In the case of the False River location (Figure HR12), the complexity of the local bathymetry in both the flood and ebb directions coupled with a relatively strong salinity gradient (in the fall) create tidally-averaged dispersive specific conductance fluxes that are large or roughly half the total specific conductance flux (Figure HR16).

Dispersion example 2: Threemile Slough. Threemile Slough (Figure HR15) is another location where the local geometry can promote large dispersive fluxes. Threemile Slough can have large dispersive transports because: (1) the tidal excursion within Threemile Slough is longer than the length of Threemile Slough (Figure HR13), and (2) Threemile Slough connects two wide (~ 1000 m) and relatively bathymetrically complex channels – the Sacramento and San Joaquin Rivers (Figure HR15). In the case of Threemile Slough, water that enters the Slough from the San Joaquin is advected all the way through the Slough in about an hour and exits into the Sacramento River where it is efficiently mixed, because the Sacramento is wide (~ 1100m) and carries a much larger tidal discharge [~ 100,000 cfs in the Sacramento River (measured @ Rio Vista) compared to ~ 25,000 cfs in Threemile Slough]. When the tides turn on the Sacramento River, very little, if any, of the water that came through Three-mile Slough from the San Joaquin makes it back to the San Joaquin on the next tide. This process is illustrated through time-series data collected at Three-mile Slough as is shown in figure HR17. The end result of this process is the dispersive flux is greater than, and in the opposite direction of the advective salt flux (Figure HR18). The total salt flux, dominated by the dispersive flux, in the end, is from the San Joaquin to the Sacramento River. In an identical way, relatively fresh Sacramento River water is also dispersively exchanged through Threemile Slough into the San Joaquin.

Spatial and Temporal variations in Dispersive Mixing. Both False River and Threemile Slough are our best *known* examples in the Sacramento/San Joaquin Delta where dispersive transport mechanisms are important. Dispersive transport is large in these locations because the tidal flows are strong, the tidal excursions are long and run over complex bathymetry. And finally, because spatial gradients in water quality constituents, such as specific conductance, regularly occur there. The way in which these factors interact at any given point in the Delta determines the amount of dispersive mixing that occurs. Therefore, not all locations (channels, or junctions) can support large dispersive transports and, moreover, the ability of an area to support dispersive transports will likely change seasonally as the tides are mediated by high river flows and as the spatial gradients in water quality change.

For example, in places where the tides are weak, tide induced lateral and vertical mixing is correspondingly weak. Moreover, with weaker tides, the tidal excursions are shorter which reduces the *possibility* that a given water parcel will experience significant changes in bathymetric conditions over a tidal excursion. Therefore, a critical factor that determines the degree of dispersive mixing at a given point in the Delta's channel network system is the ratio of the local tidal excursion to some appropriate (and as yet to be determined) measure of bathymetric variability that occurs over a given tidal excursion. In some cases, for example, the combination of tidal forcing and bathymetric complexity in a given area may be conducive to dispersive mixing, yet a constituent gradient may be lacking, in which case, dispersive transport of that constituent will not occur. For example, water quality gradients regularly occur in the Mildred Island and Franks Tract areas because they are more or less situated at the confluence of the three major water sources in the Bay/Delta system: (1) ocean derived salty water from Bay intrudes into the central Delta in the late fall/early winter period and likewise, (2) salty water from the San Joaquin mixes from the south Delta into the Franks Tract during the same period, and, meanwhile (3) fresh water from Georgiana Slough and the Delta Cross Channel is injected into the Central Delta where the Mokelumne River meets the San Joaquin (Figure HR19). Yet, even though we know large dispersive transports of specific conductance are possible through False River into Franks Tract, for example, there are nonetheless long periods where specific conductance gradients don't exist there and thus dispersive transport of specific conductance does not occur (see for example day 100 to day 160 in figure HR16). The main reason relatively small changes to Franks Tracts apparently have a greater impact on Delta salinities, when compared to changes made to other flooded islands, such as Sherman Lake and Big Break (see figure HR15 for location), could be its strategic geographic position within the specific conductance gradient. For example, both Big Break and Sherman Lake are seaward of Franks Tract and are therefore more strongly tidally forced than Franks Tract and both are fairly bathymetrically complex, especially in their connections with the channels, yet modifications to these islands in modeling studies have shown a lesser affect on Delta salinities than modification to Franks Tract (Resource Management Associates, 2005).

Finally, where the flows are unidirectional, on the upland fringes of the Delta, for example, dispersive transports can't happen, at least in the way we have defined them. Thus, transport due to dispersive mixing begins where the flows transition from unidirectional to bi-directional flow. This transition moves seasonally with changes in river discharge, and, to a lesser extent, with the spring/neap cycle. The bay/Delta system becomes less dispersive, overall, during periods of high river discharges because: (1) the residual currents are greater during this period, which (2) reduces the tidal flows and thus the tidal excursions, and (3) the transition from unidirectional to bidirectional flow moves seaward during high flows. Where this transition

occurs, and when, is likely important for ecosystem function because this location determines the degree of dispersal (mixing) of river derived: (1) food (chlorophyll, organic carbon, zooplankton, etc.), (2) outmigrating organisms (zooplankton, salmon smolts), (3) toxicants (pesticides, herbicides, mercury, selenium, etc.). The complexity of bathymetry where this transition occurs, and when, may be important in determining seasonal changes in the ecology of the Bay/Delta system.

Example where dispersive mixing isn't important and why: Mokelumne River @ the San Joaquin River. Places where large dispersive transports regularly occur may actually be rare in the Delta because they depend upon an apparently uncommon combination of local spatial constituent gradients, tidal forcing and geometric variability. The Mokelumne River, where it joins the San Joaquin River, is an example of a location that is fairly bathymetrically complex - this reach includes a four-way junction (Figure HR19) - and is fairly strongly tidally forced (Figure HR20A) and yet dispersive mixing is weak (Figure HR21). Flows in Georgiana rarely, if ever, reverse, so it is virtually impossible for constituents, including specific conductance, to mix from the central Delta into Georgiana Slough. However, the flows in the N. and S. forks of Mokelumne River can be bidirectional, particularly under conditions when the Delta Cross Channel gates are closed. The key to the weak dispersive mixing at this location is the tidal excursion from the mouth of the Mokelumne River (Figure HR20) falls short of the North-South Mokelumne junction (Figure HR19), even under conditions when the Delta Cross Channel gates are closed. Moreover, bathymetric variability within the lower Mokelumne River is relatively weak (Figure HR19), which creates relatively little mixing due to shear-flow dispersion. Therefore, when one decomposes the salt flux at this location, the dispersive flux is negligible (Figure HR21) because very little mixing occurs in the Mokelumne River within a tidal excursion of this location. Any salt that is advected into the Mokelumne on a flood tide simply returns on the following ebb (Figure HR20). Another reason "what goes in comes out" at this location are the combined net flows from Georgiana Slough and the Delta Cross channel (Figure HR22C) contribute to flush specific conductance out of this reach every single tidal cycle. Thus, any dispersive mixing from lateral shear that could have "mixed" salinity landward within this reach is completely overcome by the net flows at this location on each tide.

Central Delta Hydrodynamics. The tides have a strong influence in the central Delta and thus the influence of water project operations on transport is less direct and more subtle than elsewhere in the system. In the following section we discuss the details of the regional scale hydrodynamics in Mildred Island.

Mildred Island hydrodynamics. To our knowledge, virtually nothing was known about the hydrodynamics and transport characteristics of the Mildred Island region prior to this study. Therefore, we begin with a very basic description of the transport characteristics of Mildred Island, based primarily on fixed-site measurements of water level, discharge (velocity inside the island) and salinity at 8 sites in the Mildred Island area (Figure HR3). We also released a handful of drifters and mapped the velocity distributions in the north of the Island for a 30 hour period, using methods described in Dinehart and Burau (2005), as part of this investigation.

Mildred Island is a small ($3.8 \times 10^6 \text{ m}^2$) flooded tract that exchanges with its surrounding channels through numerous levee breaches (Figure HR23). Two of the breaches in the Island are large enough to accommodate small boat traffic. The northern breach is 150 m

across and is ~14 m deep. The southern breach is smaller, at 90 m, and is only accessible by small boats at high water. Tidal exchange dominates transport and mixing processes in the northern half of the Island. In the southern half of the island, tidal forcing is significantly less and wind driven circulation can be important in the exchange of constituents, such as salinity and chlorophyll (see Section HS).

Mildred Island is part of the central axis of the Fresh water corridor (Figure HR2) where three distinct sources of fresh water mix: salty water from the bay and San Joaquin river mix with fresh Sacramento River water that enters the central Delta from the Mokelumne system. Exchange and mixing of salt, and other water quality parameters, is complex in this region because of temporal changes in source water quantity and quality and because of the geometric complexity of the Mildred Island region.

Transport in the Mildred Island region is primarily controlled by the regional scale net flows that create a persistent draw of water from north to the south around and through Mildred Island. These net flows vary mostly in concert with south Delta pumping rates. Tidal transports are also important in the region, particularly as a mechanism that contributes to the observed spatial variability in salinity in the region. Nevertheless, the influence of the tides on transport in Mildred Island, under most export conditions, is secondary to the influence of the net flows (see salt flux decomposition section). In particular, Mildred Island itself is a significant residual timescale regional conveyance pathway, in part, because of numerous small levee breaches on its southern border. Based on mass balance calculations, Mildred Islands southern levees are much more porous than we originally thought; significant exchanges through the southern levee occur at both the tidal and residual timescales.

In this section we first discuss, as basic background information, tidal timescale factors that control exchange in the Mildred Island area, including the tidal range, tidal prism, and the tidal flows. We then discuss the residual timescale dynamics, and, finally address salt transport in the region. For clarity, time series plots in this section consistently use the color scheme shown in figure HR24.

Tidal range. The tidal range is a measure of the temporal variation in water level caused by the tides. The tidal range can be computed by subtracting the tidally-averaged water-level from the measured stage, $\zeta' = \zeta - \langle \zeta \rangle$, where ζ are the measured water level fluctuations, ζ' are the tidal fluctuations, and $\langle \zeta \rangle$ is the tidally averaged water level. Variations in water levels due to hydrologic influences, spring-neap cycle and atmospheric pressure affects, by definition, don't contribute to the tidal range, although these factors can change it. In particular, river flows in the upland fringes of the Delta can have a strong influence on the tidal range. The tidal range sets the upper limit on the magnitude of tidal exchanges that can occur in a given region; the interaction between the spatial gradients in water levels and the local system geometry control the actual observed tidal exchanges. The tidal range varies significantly within the Bay and Delta; typically varying inversely with distance from the Golden Gate. Even though Mildred Island is ~75 miles from the Golden Gate, it is nevertheless strongly tidally forced: the maximum (spring) tidal range is on the order of 120 cm (~4ft); during neap tides the tidal range is about 75 cm (~2.4 ft) (Figure HR25). Therefore, tidal forcing within Mildred Island is significant, and varies with the spring/neap cycle; on the order of 45 cm (1.5 ft). Within Mildred Island the tide wave changes very little (Figure HR26), primarily because Mildred is small (3 km [1.9 mi] long) compared to the wave length of the tides (wave length = $\lambda_{M2} \sim T_{M2} \sqrt{gH} \sim 450$ km, where

$T_{M_2} \sim 12.42hrs$, is the M2 tidal period, $g=9.91 \text{ m/s}^2$ is gravity, and $H \sim 10\text{m}$ is the depth), and because very little dissipation occurs within the island - except, most notably, through the levee breaches where there is likely a significant, yet unknown, head loss.

Tidal Flows. The temporal variations in water level shown in figure HR25 create spatial water level gradients which ultimately drive tidal exchanges in the channels that surround Mildred Island and create exchanges into and through the Island. In the north, the tidal flows from Connection Slough and Middle River (Figure HR27E,F) enter northern Mildred Island through a 150 m wide levee breach on flood tides. This creates a pressure gradient that, at the same time, pushes water out the southern breaches (Figure HR27E,F). On ebb tides (Figure HR27B) the distribution of the flows in the channels adjacent to Mildred Island are reversed. The tidal flows change at roughly the same time in the northern channels (Figure HR27C,D), except for Connection Slough, which changes from flood to ebb roughly an hour ahead of the rest of the channels in the area (Figure HR27A).

The tidal flows in the Mildred Island region are dominated by the flows in Middle River (station MIDCOL) which have peak discharges on the order of 625 cms (Figure HR27D). The total discharge at MIDCOL on flood is divided between the channels that surround Mildred Island and Mildred Islands northern opening. In order of decreasing magnitude, the flows in Mildred Island are approximately 300 cms at MIDCON, 250 cms at LATH, CONSL, and at the northern opening, and a paltry 60 cms in the southern opening (Figure HR27C,D). Interestingly, a mass balance using the data from the northern stations indicates the tidal flows in the northern opening are highly correlated with the flows in Connection Slough (Figure HR28). And similarly, the flows at MIDCOL are highly correlated with the sum of the flows in MIDCON and LATH. One possible explanation for this observation is that north/south tidal exchanges are primarily driven by north-south barotropic pressure gradients, and in a somewhat decoupled fashion, the east-west barotropic gradients drive exchanges between Connection Slough and the northern opening. This observation brings up the interesting question of how flows in a channel network respond to pressure gradients that are oblique to the prevailing channel orientations.

Finally, Connection Slough has a persistent short-lived peak in flow that occurs during the beginning of ebb that partly contributes to an ebb-directed net flow in Connection Slough (dashed circle in figure HR27D) (more on this later). Similarly, a persistent short-lived spike in the exchange into Mildred Island's northern opening occurs at the beginning of ebb, at low water (red circle in figure HR27C). To explain this spike we hypothesize that a number of breaks in the northern levees contribute to exchange into Mildred Island throughout most of the tidal range, except at extreme low water (Figure HR29). As water levels decrease, the exchange through minor levee breaches is reduced, limiting the overall exchange to the northern opening. This serves to increase the barotropic pressure gradient across the northern opening at low water (Figure HR29B) creating a short-lived spike in discharge through the opening as can be seen in figure HR29.

Tidal Prism. A portion of the water that tidally exchanges into and out of Mildred Island simply fills and drains the Island itself; this exchange is known as the tidal prism. The remainder of water entering the Island flows through the Island, contributing to the overall conveyance in the region. The maximum tidal prism, the volume of water stored and released over a single tidal cycle, in Mildred Island, can be estimated as

$$\Delta S = \Delta h A = (1.2\text{m})(3.82\text{km}^2) = 4.58 \times 10^6 \text{m}^3 \text{ (3716 acre-ft)},$$

where Δh is the maximum tidal range and A is the surface area of the Island. However, this is bulk estimate because the tidal prism can change appreciably with the spring/neap cycle. An estimate of the mass flux needed to fill and drain a given area, A , in the Delta, over a tidal cycle is

$$Q_{\Delta S} = -\frac{\partial \zeta'}{\partial t} A$$

Where $\zeta' = \zeta - \langle \zeta \rangle$, ζ are the measured water level fluctuations, ζ' are the tidal fluctuations, and $\langle \zeta \rangle$ is the tidal mean.

A time series estimate of the tidal prism, if one assumes a perfectly horizontal water surface (a reasonable assumption given (1) the length of Mildred Island relative to the tidal wave length and (2) weak frictional dissipation in the Island overall), is:

$$\Delta S = -A \int \frac{\partial \zeta'}{\partial t} dt$$

A time series plot of Mildred Islands tidal prism is given in figure HR30. Given the mean-tide volume of Mildred Island is $22.9 \times 10^6 \text{m}^3$ (assuming a mean-tide depth of 6m and an area of 3.82km^2), between 15-22% of the mean-tide volume of Mildred Island exchanges with the channels every single tide cycle, depending on where you are in the spring–neap cycle. Therefore, a significant fraction of Mildred Island’s volume exchanges on every single tide (e.g. twice a day), suggesting that Mildred Island, as a whole, isn’t a completely distinct pelagic habitat separate from the channels that surround it. On a percent volume basis, Mildred Island, particularly the northern Island, is strongly coupled with its surrounding channels. So, how do large daily exchanges, and the spring/neap variability in these exchanges, affect the ecology of these shallow water habitats?

Figure HR31A shows that a significant fraction of the water that enters Mildred Island through the northern opening is simply filling and draining the Island, as estimated by $Q_{\Delta S}$. Figure HR31 also shows that the southern opening exchanges significantly less than is needed to fill and drain the Island, which suggests a significant amount of water is exchanging through the southern levees in addition to the southern opening. So how leaky is Mildred Island? An estimate of the tidal exchange through the remainder of the levee breaches is simply the difference between the northern and southern opening discharges and the change in storage within the Island. Based on this calculation, the peak tidal discharge through the unmeasured levee breaches is approximately 70 cms (Figure HR31C), on the order of the flow through the southern opening.

Stokes Drift. Stokes drift, the tidal correlation between water levels and velocities, can contribute significantly to the tidally averaged exchange of constituents in shallow water systems, like Mildred Island. For example, if there are daily phytoplankton blooms in Mildred Island, Stokes drift could potentially preferentially exchange higher chlorophyll concentration water through the southern levees at high water. This could result in a significant daily exchange of phytoplankton biomass between the island and channels, when high water is correlated (in

phase) with daily phytoplankton production in locations where levee breaches occur. The direction of the exchange would depend on whether an incoming or outgoing current were in phase with high water. For Stokes drift to play a significant role in net transport, water level and velocity variations must be generally in phase. In Mildred Island they are not in phase, water level variations and the currents are very nearly in quadrature (Figure HR32), and, therefore, Stokes drift is an insignificant transport mechanism (Figure HR33). Given the wavelength of the tides, the stage velocity phase relation is likely to be approximately regionally consistent, so we assume the other levee breaches in the south respond in a manner similar to the southern opening.

Net flows – Channels. The net flows through the Mildred Island area are dominated by the hydraulic connection between the Sacramento River water entering the central Delta through the Mokelumne system and the south Delta export facilities. A persistent net flow enters the northern Mildred Island region through Middle River and is split between Connection Slough, Middle River, Latham Slough and Mildred Island itself (Figure HR34). The pervasive north-to-south transport of water around and through Mildred Island, is primarily driven by changes in export rates (Figure HR35). Stations MIDCOL and LATH appear to respond more directly to changes in exports than the other locations (Figure HR35). Interestingly, and importantly for salt transport in the region, the net flows in Middle River drive a persistent net flow toward Franks Tract through Connection Slough (Figure HR34), an observation that partially accounts for Middle River functioning as the central axis of the fresh water corridor (see salinity section).

When the export rate exceeds ~ 75 cms, Middle River carries the majority of the water in the region, roughly 50% of the net flow: Mildred Island and Latham Slough carry roughly ~25% of the remaining net flows each (Figure HR36). Therefore, at least at the higher flow rates, Mildred Island functions as a significant conveyance pathway through the region, comparable to Latham Slough. When the export rate falls below ~75 cms, the net flows in the Mildred Island area are proportionately reduced and the net flows around Mildred Island can create a counterclockwise gyre (Figure HR34E) that can bring salty San Joaquin River water from Empire Cut northward in Latham Slough into Mildred Island's northern opening (see salt transport section).

Net flows – Island exchange. The net flow through Mildred Island's boundaries accounts for roughly 25% of the tidally averaged flow in the region. So how is this accomplished given the small capacity of the southern opening? A mass balance on the net flows can be calculated as $Q_{leaky} = Q_{nopn} - Q_{sopn} - Q_{\Delta S}$, where Q_{leaky} is the amount of net discharge through the unmeasured minor levee breaches in southern Mildred Island and $Q_{\Delta S}$ is the storage of water due to changes in tidally-averaged water level. Firstly, the contribution of the tidally-averaged water level to the net flows is relatively minor: Mildred Island and the tidally averaged water level variations in the region are small (Figure HR39). Secondly, based on this mass balance, only 25% of the water that enters the northern opening leaves through the southern opening at export rates of ~200 cms, which suggests that roughly 75% of the net flows exit Mildred Island through numerous levee breaches in the south of the Island (Figure HR37). At export rates < 150 cms, most of the net discharge entering the northern opening leaves through the levee breaches not the southern opening (Figure HR37). Question: How are ecosystem processes affected by large net exchanges out of Mildred Island through the highly vegetated (mostly tules) shallow levee

openings in the south during high water? For example, corbicula thrive in the channels south of Mildred Island (Janet Thompson, USGS, personal communication).

Local Salt Field – Description. Model results (Figure HR1) and salinity data collected during our experiments (Figure HR39C) show that Mildred Island is situated at the confluence of 3 distinct sources of water. Local salinity variations in the Mildred Island area are set by a combination of these source water distributions (quantity and quality), by changes in export rates and river inputs and by exchanges and mixing within the region. We begin by discussing the as-measured and tidally averaged salinity time-series as a means of discussing the regional salt field. We discuss spatial variability in the salt field through direct comparisons of tidally averaged salinity time-series collected at different locations and by comparing tidal timescale changes in salinity with changes in flow direction. We then discuss the tidally averaged changes in the time-series, which, during the summer period of the experiment, are mostly a function of Delta-scale anthropogenic manipulations. We finish the section by describing the details of some of the complex tidal timescale interactions that, when integrated over days, control tidal and residual timescale salinity variations in the Mildred Island region. Tidal timescale interactions are often complex in this region because of the strong tidal currents, multiple source waters which create salinity gradients on two fronts, and complex geometry.

Regional scale spatial variability. The highest salinities in the Mildred Island region occur in Connection Slough; these are bay-derived salts that are mixed into, and transported through Franks Tract into Connection Slough (Figure HR38B, HR39C). San Joaquin River derived salts enter the Mildred Island through the southern opening and through other numerous levee breaches in the south of the Island and into Latham Slough through Empire Cut (Figure HR39C). Relatively fresh Sacramento River water, conveyed into the central Delta through the Mokelumne River system, enters the Mildred Island area through Middle River (station MIDCOL) (Figure HR39C). Therefore the highest salinities occur in Mildred Island's NW corner (Figure HR39C), followed by moderately high salinities from Empire Cut in the SE corner, while Mildred Island's NE corner remains relatively fresh, owing to its proximity to the Mokelumne River system. The salinities are greater overall in Connection Slough, and, based on the assumption that advection dominates transport in the channels and the tidal currents in the channels are of the same order of magnitude, we can deduce the salinity gradient in Connection Slough is greater than elsewhere in the system because the tidal timescale salinity variations are greatest at this location. Similarly, the salinity gradient in Latham Slough is low overall but increases dramatically during the period of reduced exports (days 285-300) based on tidal timescale salinity variability at this location. The salinity gradients, and thus dispersive mixing, is greatly reduced when the Sacramento River flow and export rates increase after day 300. The salinity at station MIDCOL is considerably less than elsewhere in the region with minimal tidal timescale changes in salinity and thus weaker salinity gradients.

Tidal timescale changes in salinity not only allow us to look at the magnitude of the gradient, but, when salinity variations are compared with flow direction, the direction of the gradient can also be deduced. For example, even though Empire Cut was not instrumented, we can deduce that salinities were higher there because salinities increase at stations LATH (Figure HR40) and at the southern opening, station SOPN, (Figure HR41) on ebbs. For example, peaks in salinities correspond to the end of ebb tides at station LATH indicating a higher concentration in Empire Cut. Moreover, higher salinities in Mildred Island's southern opening occur during

incoming tides. Therefore, San Joaquin River derived salts enter the fresh water corridor through Empire Cut, but mostly pass south of Mildred Island because of the pervasive north-to-south draw from the export facilities. Finally, the Mildred Island region is saltier, overall, than the water in Middle River north of the Island, as can be seen in figure HR42.

Salinity - Tidally averaged variations. The regional tidally averaged salinity variations in figure HR43 show a remarkable coherence between stations and remarkably stable spatial gradients (differences between curves) across the Island under a wide range of hydrologic conditions. This suggests that channels in the immediate vicinity of Mildred Island are highly coupled from a transport perspective. The length of the channels that flank Mildred Island are on the order of the tidal excursion within each channel, and, thus, the Mildred Island region is strongly advectively coupled at the tidal timescale. One can estimate the distance a water parcel would travel, L , over the period of record, T , based on the measured cross-sectionally averaged velocity, \bar{u} , at each of our flow stations as

$$L = \int_0^T \bar{u} dt .$$

To obtain the tidal excursion, L_{tide} , one simply subtracts the tidally averaged distance, $\langle L \rangle$, from L :

$$L_{tide} = L - \langle L \rangle .$$

For stations LATH and MIDCOL, the tidal excursion shown in figure HR44 varies with the spring/neap cycle, as expected, where the peak excursions are 2.5 km and 3.2 km, respectively. Therefore, the tidal excursions are on the order of their respective channel lengths: 3 km and 4 km. And, thus, these stations are relatively “close” from an advective transport perspective and one would expect these proximate measurement locations to closely track one another. In the channels north of Mildred Island, changes in salinity are primarily related to the flows in Connection Slough, the primary source of salinity in the region. This observation speaks to the importance of geometry as a key factor in governing transport processes in the Delta.

Salinities in the northern opening are relatively low, because (1) this breach is located on the east side of the Island, a location that is highly coupled with the fresh water flows that enter the region from Middle River and (2) because dispersive mixing of salt into the region from Connection Slough is relatively weak compared to the tidally averaged advective transport of fresh water from Middle river in Connection Slough. If Mildred Island had been breached on the north-west part of the island, the Island would likely be considerably more salty and could have played a greater role in increasing salinities in the fresh water corridor through increased dispersive mixing of salt from Connection Slough into Mildred Island.

The salt field in the Mildred Island region during the summer of 2001 changed character roughly five times, primarily in response to changes in Sacramento River flow, export rates, and the placement of the Head of Old River Barrier (Figures HR39, HR43). We discuss each of the five regime changes in the salt field shown in figure HR43 individually, in what follows. Since salinity is a conservative tracer, changes in salinity at tidally averaged timescales at fixed locations correspond to movements - dispersive intrusions and advective retreats - of the salt field. Generally, then, increases in salinities at our fixed stations are indicative of a compression

of the fresh water corridor, and conversely, a decrease in salinities indicates an expansion of the fresh water corridor. Specific conditions for each of the salinity regimes indicated in figure HR43 are as follows:

- (1) This period is characterized by relatively constant Sacramento River flows and export rates and a similar gradual increase in salinity in the region from both Connection Slough and Empire Cut (similar slopes in figure HR43C) corresponding, overall, to a contraction in the fresh water corridor.
- (2) This period is characterized by a brief drop in salinity followed by a dramatic rise in salinity from the Connection Slough. The increase in salinity from the west corresponds directly to a period when the net flow in Connection Slough was atypically toward Mildred Island and the flow at station MIDCOL was substantially decreased (Figure HR43D). At the same time salinities from the San Joaquin drop during this period creating an east-west divergence in the salinity time-series indicative of a shift in the fresh water corridor to the east during this period.
- (3) During this period of relatively constant pumping and river inputs both the bay and San Joaquin river derived salinities generally decreased, although the bay-derived salts decreased faster, corresponding to an expansion of the fresh water corridor and slight shift to the east.
- (4) During this period exports and Sacramento River flows were curtailed, San Joaquin River flows slowly increased and the Head of Old River Barrier (HORB) was completed which lead to a step function change in salinity response from decreasing to increasing salinities at all stations. Increasing salinities correspond to a contraction of the fresh water corridor. The closure of the HORB barrier reduces the draw of San Joaquin River water to the pumps through Old River, and, as a consequence, salinities increase in Empire Cut as is evidenced by a rise in salinity at station LATH, relative to the other stations during this period. The net flows in Connection Slough remained relatively constant, though variable throughout the entire record, yet, during this period the fresh water input from northern Middle river substantially declined.
- (5) This period is characterized by declining salinities due to an increase in exports and Sacramento River flow which increases the fresh water moving through the Mildred Island region overall, including increases in fresh water towards Franks Tract through Connection Slough (Figure HR43F). The increase in the north-to-south fresh water exchange decreases dispersive mixing of salt into the fresh water corridor and an expansion of its borders.

Salinity - Tidal timescale variations. Tidal timescale variations in specific conductance within the Mildred Island region can be complex due to a combination of the complex geometry, evolving specific conductance gradients and the relative timing of the tidal currents within the region. In this section we give three examples that highlight the complexities of tidal timescale salinity variations within the Mildred Island region. The first two examples focus on exchange between the island and its surrounding channels, the third explains why the tidally-averaged salinities in Latham Slough are often greater than Connection Slough, even though Connection Slough is the source of salinity in the region. We begin with a simple example, the southern opening:

Example 1---Southern opening exchange: Tidal timescale variability in specific conductance in the southern opening is driven by higher salinity water in Empire Cut, which enters Mildred Island on incoming tides (Figure HR41). Higher salinity water is ejected into the Island (Figure HR45) and is mixed with lower salinity ambient water in the Island, and, thus, the water that exits the Island is considerably fresher than the water that enters the Island. The exchange of moderately high salinities through the SOPN on incoming tides maintain a persistent south-to-north salinity gradient across Mildred Island, despite higher overall salinities in Connection Slough and despite the large net flow through the Island (Figure HR45).

Example 2---Northern opening exchange: The exchange of salt through the northern opening is more complex than the southern opening because it involves exchanges between two channels (CONSL, MIDCOL) and mixing within Mildred Island. The northern opening remains relatively fresh overall, because of its proximity to the fresh water entering the region from northern Middle River (station MIDCOL). Nonetheless, at the beginning of flood tide, a spike of high saline water enters Mildred Island from Connection Slough, followed by a relatively longer period of fresh water from MIDCOL (Figure HR46). The water that leaves Mildred Island on ebb is almost a perfect arithmetic average of specific conductance concentrations that enter the Island during the flood as just described, suggesting near complete mixing within the Island. The gyre that forms in northern Mildred Island on incoming tides, shown in figures HR47 and HR48, is apparently very effective at mixing water that enters through the northern opening. For example, drifters released in the opening on spring flood tides made two complete transits of northern Mildred Island on a single flood tide (Figure HR49) highlighting the extensive mixing that occurs in the north of the Island. From a regional perspective, this mixing process creates a situation where water returning in CONSL on ebb is significantly fresher than the water that entered the region on flood and therefore contributes to a dispersive flux of salt from Franks Tract into the fresh water corridor through Connection Slough (more on this later).

Example 3---Salinity variations at MIDCON: The tidally averaged salinity at station MIDCON is often greater than Connection Slough, even though Connection Slough is the source of salty water in this region. This occurs because Connection Slough is more strongly coupled with MIDCOL than is MIDCON and thus Connection Slough sees periods of relatively fresher water from MIDCOL on ebb tides than does MIDCON. The phenomenon is illustrated in figure HR50, where salty water passes the CONSL stations on flood immediately followed by a fresh water pulse from MIDCOL, and finally, the tidal cycle is finished by a pulse of moderately salty water from MIDCON. This example demonstrates that salinity variations in a channel network involve the phase and duration of exchanges between multiple channels that can have different constituent loads. Connection Slough has larger peak salinities than does station MIDCON, yet, because of the salinity gradients and tidal current phases in the area, MIDCON can have, at times, higher tidally averaged salinities than CONSL.

Salt fluxes. The salt fluxes in the Mildred Island region respond to the regional salinity gradients (higher salinities in the NW and SE corners of the island) the dominant north-to-south net flows and, finally, the tidal currents. We begin our discussion of the salt fluxes in the channels first, beginning with Connection Slough. The total salt flux in Connection Slough is always toward Franks Tract, reflecting the strong net flow in that direction there (Figure HR51). The salt flux in Connection Slough is somewhat complex, where the advective component is predominantly

toward Franks Tract and the dispersive component is into the Mildred Island region, reflecting tidal timescale mixing of the local salinity gradient. A portion of the salinity entering the Mildred Island region from Connection Slough is transported down Middle River (station MIDCON) (Figure HR52) towards the pumps and most of the remainder enters Mildred Island on flood tides spikes through the northern opening (Figure HR53A). The total salt flux in Connection Slough dramatically increases towards Franks Tract, (advective flux increases AND dispersive flux decreases because of a reduction in the local salinity gradient) when the export rates and Sacramento River flows increase on day 300, heralding an expansion of the fresh water corridor. The salt flux in MIDCON, NOPN and SOPN are advection dominated and also, therefore, roughly follow changes in the export rates and Sacramento River flows. However, the salt flux at station MIDCON has a weak, though significant, dispersive component which corresponds to increased salinity gradients in the region (day 255, 267, 283 in Figure HR38). The salt flux in Latham Slough is dominated by the net flows towards the pumps (Figure HR54). However, a significant dispersive flux from Empire Cut is present in Latham Slough during periods of reduced exports. Interestingly, the total salt flux from Empire Cut is northward on day 297 in response to a virtual curtailment of pumping, which physically corresponds to a counter-clockwise gyre setup around Mildred Island (Figure HR34E). This suggests that the residual circulation in general, and transport of constituents in the Mildred Island area, specifically, is very different when the south Delta pumps are off. Finally, even though the total advective specific conductance flux is out of the Island (Figure HR53B), the dispersive flux into the Island is sufficient to maintain a persistent specific conductance gradient, from north-to-south, across the Island (Figure HR45).

Bivalve distribution and grazing rates (B)

Delta Scale Benthic Grazing Rates for Use in Models. *C. fluminea* grazing rates in excess of 1m/d occurred in the central delta in spring, ranged from 1 to ≈ 20 m/d in October, and were coincident with low phytoplankton biomass in this region. The populations of *C. fluminea* in the delta are very dynamic with biomass of populations more than doubling and in some cases increasing by an order of magnitude between spring and fall. The upper Sacramento River and southern San Joaquin both have small populations of *C. fluminea* but show opposite trends in phytoplankton biomass with phytoplankton blooms occurring in the San Joaquin but not the Sacramento River. Although *C. fluminea* was most common in the central delta it is difficult to relate their distribution to the temperature and salt conditions in that section of the delta because the populations persisted into fall. It is likely that *C. fluminea*, as an opportunistic clam which has been reported as food limited in this system (Foe and Knight 1985), is concentrating in areas of the delta where primary production is highest. If this is so, its apparent lack of success in the San Joaquin River is a puzzle. Researchers working on *C. fluminea* in shallow streams find a relationship between *C. fluminea* abundance and grain size where most individuals are found in sand and the least in fine muds. We did not find any such relationship, in fact, the commonly held belief (numerous personal communications during presentations) that *C. fluminea* does not do well in peat sediments is disproved by its success in the very peaty sediment of Franks Tract.

Regional Scale Benthic Grazing Rates for Process Studies – Mildred Island Process Studies. Our findings on the grazing rate of *C. fluminea* within the island were consistent with our

findings published in Lucas et al (2002). However, the inclusion of the external channels may change our perceptions of the island as a producer of phytoplankton for the pelagic system. The large populations of *C. fluminea* in the external boundary channels and connecting rivers and canals may consume much of the phytoplankton produced within the lake. The size of animals may show that *C. fluminea* growth is food limited in most locations around the island except where populations are very small (Empire Cut). Proximity to the island water at the northern boundary and in the southeast corner resulted in large animals despite large populations where competition for food was likely to be greatest. In further support of the food limitation hypothesis, when animals are successful within the lake, the clams are few in number and grow to quite large sizes. The small size of animals at Connection Slough may show that bivalves get little benefit from phytoplankton produced in Mildred Island and the increasing size with distance from the lake in the southern arm of Middle River may show either a food source within the oxbow on that river or to the south of our study area.

Channel Scale Benthic Grazing Rates – Is There a Distribution Pattern? Bivalve grazing rates were low in deep-water channels compared to adjacent banks and in general compared to other habitats. Our hypothesis on the location of highest densities of bivalves held true in the Sacramento River but not in the San Joaquin River and in Threemile Slough. Grazing rates were mostly less than 1 m/d and bivalve effect on phytoplankton may therefore be less important in these habitats than in the other habitats studied here. It has been shown by Lucas et al in prep, that similar grazing rates in the channels of southern San Francisco Bay are sufficient to reduce phytoplankton biomass in the channel but not control the occurrence of phytoplankton blooms in the system.

Spatial Variability in Benthic Grazing Rates – Franks Tract Processes. Grazing rates within Franks Tract were consistent with those reported by Lucas et al (2002). The sloughs and rivers connecting to Franks Tract to the south had higher grazing rates than to the north, with the smallest populations occurring in False River and in the slow moving sloughs (based on the sediment that we observed) to the southwest of the Tract (eg. Taylor Sl). The high grazing rates in the rivers and sloughs external to, but connected to the Tract, shows that grazing in these connecting environments may be important determinants of the productivity and sinks for particulate Se in Franks Tract.

Temporal Variability in Benthic Grazing Rates – Franks Tract Processes. Grazing rates within Franks Tract near the eastern and western channels of the median traverse varied a relatively small amount when compared to the external channels. Although the internal island grazing rates tripled in the year we saw grazing rate increases of an order of magnitude in channels connected to the Tract.

Carbon field studies (C)

Spatial variability. High resolution spatial variability of phytoplankton in the Mildred Island region is depicted in Figure C3. These mappings were conducted on five consecutive slack tides during the 30 hour process experiment in 2001. Predominant features include: 1) general north-to-south increase in chl *a* within MI; 2) maximum chl *a* in southeast corner ; 3) significantly

lower concentrations in adjacent channels compared to MI interior; 4) maximum mean concentrations for interior and channels occurs at approximately 6 PM; relative to the other channels, Empire Cut had generally higher chl *a* than the other channels. The spatial gradients in chl *a* across the MI region are relatively sharp. Similar spatial maps of water temperature, specific conductivity, and dissolved oxygen were also generated. Temperature showed similar spatial patterns as chl *a*. Sample interpolated SC, T, and chl *a* maps are shown in Figure C4.

Discrete samples of chl *a*, zooplankton biomass, irradiance, depth, water temperature, and nutrients across the MI and FT regions were pooled with previous measurements from across the Delta (see Fig. C1 for sampling locations) and analyzed to develop a suite of biological indicators across a gradient of habitat depth. This analysis forms the basis of a paper by Lopez et al. (Lopez *et al.* In press). The purpose of this analysis was to test the hypothesis that plankton biomass, production and pelagic energy flow vary systematically with habitat depth, since phytoplankton growth rate in nutrient-rich aquatic systems is controlled by light availability, which varies inversely with habitat depth. Dissolved inorganic nutrients did not approach concentrations that limit phytoplankton growth in any of the > 200 samples we collected during 1997-1999 and 2001. Dissolved reactive phosphorus concentrations averaged 2.3 μM and were never lower than 0.5 μM (Figure C5a). Dissolved inorganic nitrogen averaged 34 μM and never fell below 3 μM (Figure C5b). Dissolved silica concentrations were never below 130 μM (data not shown). These results are consistent with monitoring data collected across the Delta from 1968-1998 (Jassby et al. (2002)) showing that potential nutrient limitation was extremely rare (DIN, DRP) or nonexistent (DSi), and consistent with our assumptions that phytoplankton growth rate in the Delta is limited by light availability and not nutrient resources.

Results showed that phytoplankton biomass and production are only weakly related to phytoplankton growth rates and that other processes (transport, consumption) are important controls. Figure C6 demonstrates that, as expected, phytoplankton growth rate ($P\mu$) is highly correlated with depth but phytoplankton biomass (Chl *a*), derived from high resolution spatial mapping in the MI region, is not. Instead, chl *a* displays a complex non-monotonic relationship with habitat depth, with highest biomass occurring at depths between ~3.5 m and 5.5 m. Biomass was extremely variable among habitats within that depth range. This chl *a* vs. depth pattern was further demonstrated with discrete samples across the Delta over several years: variability of chl *a* was irregular along the habitat depth gradient and unrelated to growth rate (Fig. C7a). High phytoplankton biomass was common at only 3 of 24 sampling locations (at Mossdale Marina and Mildred Island). Net primary production (PP) was also variable and weakly related to depth of the water column or specific growth rate (Fig. C7b). This robust data set leads to rejection of our hypothesis that phytoplankton biomass varies systematically across gradients of habitat depth.

The phytoplankton community was dominated by a few taxa including centric diatoms (*Cyclotella* spp., *Actinocyclus normanii*, *Skeletonema potamos*), cryptophytes (*Plagioselmis* sp., *Teleaulax amphioxeia*), *Cyanobium* sp., *Nannochloropsis* sp., and smaller components from other divisions (Table C1). Diatoms and cryptophytes have higher nutritional value than other algal taxa, partly because of their enrichment in essential fatty acids (e.g. Brett *et al.* (2000)). Their large contributions (diatoms 53% and cryptophytes 25%) to cumulative biomass in all samples, and small contributions from cyanobacteria, indicate that phytoplankton biomass is an accessible, high quality food resource for consumers in the Delta.

Zooplankton biomass was also dominated by a few taxa, primarily the calanoid copepods *Pseudodiaptomus forbesi* and *Sinocalanus doerri* (Table C2). The cumulative biomass of all

copepod life stages contributed 49% of zooplankton biomass in/around Mildred Island and 80% of biomass in/around Franks Tract. Rotifers (e.g. *Hexarthra* sp., *Brachionus* sp., *Filinia* sp.) contributed 49% of zooplankton biomass in MI but only 8% in FT. Cladocerans (*Diaphanosoma brachyurum*, *Bosmina longirostris*, *Daphnia* sp.) were minor components in MI and contributed 11% of biomass in FT.

We hypothesized that zooplankton biomass would covary with phytoplankton biomass because zooplankton are food limited in many Delta habitats. Zooplankton biomass (ZB) ranged from 4 to 55 mg C m⁻³ and was uncorrelated with phytoplankton biomass (Fig. C8a) or habitat depth. Estimated rates of zooplankton community grazing were similarly variable. We used two indices to explore the apparent decoupling between phytoplankton and zooplankton biomass. The ratio ZB:PB, which measures the proportion of consumer to producer biomass, was highly variable where phytoplankton biomass was low, but ZB:PB was always < 0.1 where PB exceeded ~ 200 mg C m⁻³ (Fig. C8b). The ratio ZG:ZB measures the mean daily ration (ingestion rate as a proportion of biomass) of zooplankton, and this index was also stable in high-PB habitats and variable in low-biomass habitats (Fig. C8c). A third ratio (ZG:PB, not shown) revealed that zooplankton consumed less than 20% of the phytoplankton standing stock daily at most stations, even where PB was less than the presumed food-saturation algal biomass of 300 mg C m⁻³.

We used biomass measures and rate estimates to compute two indices of the balance between primary production and consumption. First, the ratio ZG:PP measures the fraction of daily primary production grazed by mesozooplankton. Although ZG and PP did not vary systematically across habitat types, this ratio was significantly and positively correlated with habitat depth (Fig. C9a). At most habitat depths < 8 m, ZG:PP was usually less than 1, but at the deepest habitat ZG:PP usually exceeded 1 (daily zooplankton consumption exceeded phytoplankton production). The median ZG was only 40% of median PP, implying that zooplankton grazing is not fast enough to control phytoplankton biomass in most habitats. The significant linear relation implies that the pelagic component of shallow habitats functions as a (large) net source of algal biomass. However, deep pelagic systems are net consumers of primary production because algal respiration consumes a large fraction of photosynthetic production in the deep aphotic zone, leaving a small residual insufficient to meet the zooplankton grazing demand.

A second index was developed from a simple daily budget of phytoplankton biomass: $PP_{Res} = PP + \Delta PB - ZG - CG$, where PB is the daily increment of phytoplankton biomass in a water parcel, CG is the clam grazing term, and PP_{Res} is a residual term representing the balance between all processes. (CG was evaluated based on clam biomass and grazing rates estimated and discussed in the Section B). If daily changes in biomass ΔPB are small, we can assume steady state and estimate the residual term as $PP_{Res} = PP - ZG - CG$. The residual PP_{Res} was positive and highly correlated with PP where *Corbicula* was absent (bottom-up control of biomass), but it was small or negative and uncorrelated with PP where *Corbicula* was abundant (top-down control, Figure C10). The daily phytoplankton balance was uncorrelated with zooplankton grazing, regardless of *Corbicula* presence. The residual PP_{Res} was generally negative and highly correlated with *Corbicula* grazing where the clam was present. Thus, despite higher phytoplankton growth rates in shallow habitats, consumption by *Corbicula* rendered nearly all colonized shallow habitats a phytoplankton sink.

Current velocity measurements (see Section HF) were combined with high frequency time series of chl *a* (see below) to calculate chl *a* flux through the northern opening of MI.

Superimposed on an ambient advective flux of Chl *a* through the Delta system driven by hydrology and operations was a significant dispersive flux of Chl *a* (Fig. C11c) caused by tidal timescale pumping of higher Chl *a* water from MI to the channel. On average, this dispersive flux was oriented *out* of MI, meaning that phytoplankton biomass transported to the channel on northerly-flowing ebb tides did not all return on the subsequent flood tide. The mean daily dispersive flux through this opening between Mildred Island and the surrounding channel was 1.9 kg Chl *a* d⁻¹ (60.8 kg C d⁻¹). The combination of tidally oscillating currents within a domain of spatially-variable chl *a* thus drives a dispersive transport of phytoplankton from producing habitats to consuming habitats.

To understand the relative amounts of phytoplankton carbon and phytoplankton-associated particulate selenium consumed by pelagic and benthic grazers, we calculated the ratio CG:ZG (the ratio of *Corbicula* grazing rate to zooplankton grazing rate). This method was employed because any model prediction would require specification of these exact data and would yield the same result. We used the measurements described above from the FT and MI open water regions and several adjacent channel and slough environments for these calculations. The results are shown in Figure C12. CG:ZG >> 1 suggests *Corbicula* dominated consumption and CG:ZG << 1 suggests zooplankton grazing dominated. For CG:ZG on the order of 1, benthic and pelagic grazing were comparable. Not surprisingly, zooplankton grazing dominated within the MI interior, but clam grazing dominated within the FT interior, reinforcing the concept that “similar looking” shallow open water habitats can function in opposite ways, from the perspectives of both carbon consumption and selenium uptake by primary consumers. Because the channels around MI had generally high clam biomass, we see domination by benthic consumption in northern and southern Middle River and comparable benthic and pelagic consumption in Connection Slough and Empire Cut; these trends are extremely different from those in MI’s interior. The channels around FT display a range of consumption ratios, with Fisherman’s Cut and Taylor Slough dominated by zooplankton consumption, False River, Old River and Holland displaying comparable benthic and pelagic consumption rates, and Sand Mound Slough, a small quiescent dead end channel, dominated by benthic consumption. Over the entire calculation area and the times sampled, benthic grazing varied over three orders of magnitude and zooplankton grazing varied over two. These data in several Delta environments show: 1) that adjacent environments (e.g. shallow habitat and adjacent channel) can function oppositely in terms of carbon and contaminant uptake by primary consumers; 2) similar looking shallow habitats (e.g. FT and MI) can also function oppositely in this manner; 3) this variability in function can be due both to variations in clam grazing and zooplankton grazing, with the most widely variable component being the clams.

Temporal Variability. High frequency time series of chl *a*, specific conductivity (SC), and water temperature (T) were collected at two locations in Mildred Island during the summer-fall of 2001. These data were analyzed in conjunction with concurrent high-frequency hydrodynamic and meteorological data, as well as spatial maps of water quality and biological process (photosynthesis, zooplankton grazing, benthic grazing) information. The analysis of this data forms the basis of a manuscript by Lucas et al. which will imminently be resubmitted for publication.

Why is the measurement and understanding of high frequency variability in surface waters important? One reason is that long-term or time-averaged quantities and trends can be governed by interactions occurring at the high frequencies. An example is in the calculation of

scalar fluxes. Tidal dispersive fluxes can significantly contribute to or even dominate the overall net flux of a water quality constituent in a tidal system, but dispersive fluxes can only be assessed with high frequency velocity and concentration data. Understanding the genesis of high frequency variations in the quantities used to calculate flux helps us dissect how those fluxes are generated and thereby allows us to better predict and understand system changes that are ecologically, socially, and geologically significant (Jay *et al.* 1997). As we demonstrate below, high frequency measurements, though not always practical, can help guide the design of a temporally coarser field sampling program and aid in the interpretation of lower frequency measurements.

Figures C13 and C14 show excerpts of the time series data relevant to the Northern MI and Southern MI sites, respectively. The bottom three panels are calculated time derivatives for SC, T, and chl *a*, respectively. Visual inspection of the top three and bottom three panels reveals intradaily variability in water quality that in some cases is coherent between constituents and sometimes not. Chl *a* appears to be more tightly coupled to T than to SC. Power spectra quantitatively identify the dominant periods of variability for the three scalars, velocity, atmospheric heat flux, and wind speed (Fig. C15). SC has a 12.4 h (semidiurnal tidal) period in the north but a 24.0 h (diurnal) period in the south. T is diurnal in both locations. Chl *a* is mixed diurnal-semidiurnal in the north and diurnal in the south. Streamwise and transverse current velocity in the north was predominantly tidal; in the south, velocity in the streamwise direction (toward the SW) was semidiurnal and velocity in the transverse direction (out of the SE corner) was diurnal. Wind and atmospheric heat flux were diurnal. Dominant intradaily periods are summarized in Table C3. The sliding 3-day autocorrelations shown in Figure C16 show the evolving nature of the period of variability for chl *a* in the north: the periodicity oscillates between diurnal and semidiurnal over weekly timescales. These data demonstrate that 1) several physical forcings were acting on water quality constituents, representing different periods of variability; 2) periodicity in water quality varied a) between constituents at a location; b) over short spatial scales for a single constituent; and c) over time for a single constituent at a location.

How can we better understand the physical and biological processes controlling the observed high frequency variability in water quality at MI? We developed scaling relationships that estimate the size of fluctuation (ΔC , where C is either SC, T, or chl *a*) that individual processes can potentially cause (ΔC is the oscillation magnitude from peak to trough). Our scaling expressions are shown Table C4. Scalar oscillations caused by transport processes depend on the amplitude of a velocity scale (u' , v' , u_*') and on a spatial gradient in the scalar. The heating and evaporation scales depend on the amplitude of fluctuating atmospheric heat flux ($\Delta H'$) and evaporation (E_v'), respectively. The phytoplankton growth and zooplankton grazing scales depend on the amplitude of growth (μ') and zooplankton grazing rate (μ_{zp}'), respectively. All scaling expressions depend on the period of variability, τ . The scaling results are presented quantitatively in Table C5 and graphically in Figure C17. The ΔC for each scalar, process and period is shown, as well as $\Sigma \Delta C$, the sum of the oscillation magnitudes for a particular scalar and period (represented graphically as the total height of each stacked histogram). $\Sigma \Delta C$ represents the total amount of scalar variability driven by processes sharing a given period, assuming all like-frequencied processes are in phase. This quantity is then compared in size and period to the order of magnitude and period of the observed ΔC identified with spectral analysis to evaluate whether the scaling is consistent with the observed variability (observed range is shown with gray shading).

For all scalars and both locations, the magnitude and period of the scaled $\Sigma\Delta C$ matched the observed ΔC very well, except in the case of northern T, whose scaling analysis would suggest at least some semidiurnal tidal effect and perhaps a slightly smaller magnitude of oscillation than the purely diurnal one observed. The individual ΔC s tell us about the important processes operating on these water quality constituents to cause the observed variability. In the north, tidal advection is predicted to be important for all scalars, most significantly for SC (agreeing with the observed semidiurnal variability in northern SC), next most importantly for chl *a* (agreeing with the mixed diurnal-semidiurnal signal observed), and least importantly, relative to other processes, for T. So, in the northern strongly tidal levee breach, tidal transport is generally important but its impact may be modulated by other processes acting on individual scalars (e.g. heating for T, growth and wind-driven mixing for chl *a*). In the south, it appears the combination of several diurnal processes dominate, including advection (wind- and density-driven), vertical mixing, and, for chl *a*, additionally growth and zooplankton grazing. It is important to note that, although the biological processes are not insignificant for chl *a* variability in southern MI, the sum of the physical processes is adequate to produce the order of magnitude oscillations observed for that scalar. These physical processes are largely driven by the diurnal wind.

Figure C18 shows an example of the errors and misinterpretations that can occur due to discrete sampling where the measured variable actually varies at higher frequency than the sampling frequency. This figure shows the same NOPN chl *a* time series discussed above, the day-average of that time series, and three sub-sampled time series that represent systematic daily discrete sampling at set times of the day (noon, 6 AM, and 6 PM). We see that the noon and 6 AM sampling replicate the day-average reasonably well, but that the 6 PM sampling causes a large amount of error relative to the day-average. For example, the 6 PM samples suggest a sizeable bloom developing between days 239 and 242, but the daily mean suggests, if anything, a decline during this period. This particular sampling error is due to the apparent tendency for this phytoplankton population to increase in chl *a* in approximate phase with the uptake of carbon through photosynthesis, peaking in chl *a* content around sundown (early evening). In general, this figure shows us that 1) discrete sampling can inject spurious structure (e.g. false peaks) into a time series that may have no---or even the opposite---relationship to the daily mean trend; 2) peak concentrations may display temporal offsets on the order of days, relative to the peak in daily mean. The size of the subsampling error for this case is quantified in Figure C19, which shows the percent error between the day-averaged value and the discrete sub-sample. Again, for this case and constituent, peak errors could be as high as 60% and oscillate in time, according to the timing of the tides relative to the photoperiod. Even preliminary high frequency sampling, if impractical in the long-term, can aid the design and interpretation of temporally coarse discrete field measurement programs.

Time series measurements of chl *a* fluorescence from the Franks Tract vicinity in Spring-Summer 2002 are shown in Figures C20 and C21. Visual inspection of these time series reveals that bloom events (i.e. increased chl *a*) are not necessarily seen by all instruments in the region. For example, the bloom during late May/early June was seen at all stations except for Taylor, Holland, and Sand Mound Slough. We do not yet have an explanation for this, but note that the three stations that did not experience that bloom were infested with *Egeria densa* at the time. Possible relationships between SAV and bloom dampening could have to do with SAV effects on flow, nutrient uptake or shading. These three stations are located on the west and south side of FT; therefore, if the main source of phytoplankton carbon to the region was from the north

and/or east, then it is possible that the large biomass of *Corbicula* within FT acted as a filter for the imported phytoplankton carbon, removing it from suspension and causing only phytoplankton-depleted water to be delivered to these stations. Large bloom events do not coincide with increased OBS; this assures us that the fluorometers are not being affected by turbidity and that the observed blooms are in fact real and “biological.” Chl *a* concentrations were typically highest at Fisherman’s Cut, Old River, western FT, and False River and lowest at Holland, Mandeville, and Taylor (Table C6). This may be indicative of the San Joaquin River acting as a source and conduit for phytoplankton in the central Delta. As for the scalar time series at Mildred Island, we calculated power spectra for the chl *a* and OBS time series in the FT region (Fig. C22), and summarized the results in Table C7. Franks Tract reaffirms the lessons we learned at Mildred: 1) scalars in this system can vary with large amplitude and high (hourly) frequency; 2) the periodicity for a particular scalar may vary between nearby locations (e.g. OBS at FISH vs. FTW); 3) two scalars at a location may have very different periodicities, indicating different dominant processes for each (e.g. chl *a* and OBS at FALSE). Only at MAN and OLDR did chl *a* and OBS display the same periodicity. In most cases, chl *a* and OBS displayed a mixed semidiurnal-diurnal signal. The semidiurnal component is likely due to tidal advection. The diurnal component could, depending upon the local environment, be due to wind or baroclinically driven advection, diurnal stratification and wind-driven mixing, wind-driven resuspension, or, for chl *a*, diurnal phytoplankton growth or zooplankton grazing. Some of the observed periodicities were a surprise to us. For example, chl *a* at FALSE was expected to be semidiurnal due to its proximity to the San Joaquin River and its strong tidal influence; instead, chl *a* at FALSE was clearly and strongly diel. Chl *a* at HOL displayed an unclear period of variability, which may be due to the strong effect of gates, barriers and pumps on this location. An analysis of phytoplankton species composition is shown in Table C8. Only taxa that represented at least 15% of the biovolume at a minimum of one station on one date are shown individually (there are only 12 such taxa); the rest are combined under “other” (there are 55 such taxa). In most cases, “other” represented $\leq 10\%$ of the total biovolume.

Delta Scale. Please see Section B for discussion of Delta scale chl *a* measurements in the context of benthic grazing information.

Field studies of selenium distributions and transformations (SED)

Delta transects. A crucial problem with studying any reactive trace element in the Delta is that transport processes (river and tidal flows; dispersion) are dominant and tend to mask in situ behavior (e.g., uptake or regeneration as in Fig. SED1). Moreover, the water sources in the Delta (“end-members”), including the Sacramento and San Joaquin Rivers, and Suisun Bay are difficult to trace and distinguish. With respect to the latter, we have used chloride as a mixing tracer since the San Joaquin is weathering a more arid watershed in comparison to the Sacramento, but this is applicable only when Suisun influences are minimal (see below). From 1984 to 2000, total dissolved Se in the Sacramento River has averaged $0.91 \pm 0.27 \text{ nmol l}^{-1}$, with selenate being 47% of the total while organic selenide is 40% (Cutter and Cutter 2004). In contrast, the San Joaquin has an average of $15.8 \pm 10.5 \text{ nmol l}^{-1}$ total dissolved Se and selenate is 70% of the total (Cutter and Cutter 2004). From 2000 to 2004, we performed six transects in the Delta between the 3 end-members (Rio Vista on the Sacramento, Antioch representing the top of

Suisun Bay, the San Joaquin River where it enters the Stockton Deep Water Ship Channel); Figure SED2 presents data from 2 of these transects and the entire data set is in Table SED1.

Three conclusions can be drawn from these data, the first being the obvious removal of Se in the Delta as evidenced in the concavity of the mixing line between the San Joaquin and Antioch end-members in January 2003 (Fig. SED2). Secondly, input from the San Joaquin is marked by the total dissolved Se concentration alone, and this concentration is higher when the River is entering the Delta in April 2003 (Fig. SED2). Finally, the utility of chloride as a mixing tracer in the Delta is compromised when Suisun Bay (high salinity) water is moving into the Delta, as seen in April 2003 when the San Joaquin and Antioch chlorides were similar but their Se concentrations were quite different (Fig. SED2). On a larger scale, Table SED1 compares dissolved, suspended particulate, and sedimentary Se in the Delta with those in Suisun Bay. The Mildred Island data will be discussed in detail below, but in general only the total sedimentary Se concentrations are statistically different (higher) from those in Suisun Bay, although the dissolved concentrations can certainly be higher (e.g., Fig. SED2). The processes that attenuate Se inputs from the San Joaquin, thereby making the overall Delta Se “signature” similar to that in the estuary and presumably account for the higher sedimentary Se values in Mildred, need to be quantified.

Monthly selenium and bivalve monitoring - selenium results. The complete data set for this work is found in Table SED3, while the time series results are shown in Figure SED3. Total dissolved selenium ranged from 1.4 – 2.7 nmol l⁻¹, consistent with the long term record in the estuary (Cutter and Cutter, 2004), while suspended particulate Se (SPSe) ranged from 0.25-2.4 µg g⁻¹, also consistent with literature values (Cutter 1989; Doblin *et al.* Submitted submitted). The first observation from these data is that the concentration of selenium in suspended particles bears no resemblance to total dissolved selenium, likely due to the multiple sources of suspended particulate selenium (in situ production, riverine transport, sediment resuspension; Fig. SED1). Secondly, the concentration of suspended particulate Se appears to respond to higher SJ River flows (as a ratio of the total inflow), consistent with simulation model forecasts (Meseck (2002); Meseck and Cutter, in prep) that predict increasing concentrations of suspended particulate Se in the Suisun Bay and Carquinez Strait with increases in SJ River flow to the estuary.

Process studies in Mildred's Island. From a biogeochemical perspective, small embayments and flooded island habitats in the Delta are very interesting since they can change hydrologic residence time and thus have the potential to influence transport and fate of dissolved and particulate materials (e.g., Mosen et al. (2002)). Further, these shallow-water habitats are diverse with respect to their overall function in the Delta - water bodies of similar volume can act as a source or sink for phytoplankton biomass (Lucas *et al.* 2002), with resultant effects on the transformation and cycling of nutrients and trace elements. In September 2001 we sampled Mildred Island (MI) and adjacent channels over a 48 hour period (2 complete tidal cycles) in order to measure the uptake, recycling, and transformation rates of dissolved and particulate Se and nutrients; the complete data set is in Table SED4. In this respect, the best way for studying in situ processes is a Lagrangian approach where measurements are made in the same water mass. However, sampling logistics (e.g., staff, sufficient boats, water mass drogues running aground) prevented us from using this method. Instead, we sampled in the extreme southeast corner of MI where high concentrations of chlorophyll accumulate (Lucas *et al.* 2002), implying minimal transport/longer residence time.

Since the biogeochemical studies were not conducted using a Lagrangian approach, the integrity of the water mass (i.e., influence of physical mixing) was assessed by monitoring the chloride concentration during the 48 hour experiment. Figure SED4 displays the chloride data at the southeast corner station ("Chl Max"), at the northern entrance to MI ("Entrance"), and in the channel 1 km north of the entrance ("S2"). These data indicate that for at least the first 36 hours, and perhaps for 40 hours, the water mass at the Chl Max station appears quite uniform/stable. During this stable period at the Chl Max site, nitrate (Figure SED5) shows a daily (early afternoon) drawdown of ca. $8 \mu\text{mol N l}^{-1}$ and corresponding increase in chlorophyll *a* (Figure SED6). Unfortunately, ammonium concentrations were not monitored, so the nitrogen cycle was not fully revealed. None of these behaviors are observable at the other, more physically-dominated stations (Figs. SED4-6). The chlorophyll decreases in the evening can be due to grazing, particle sinking, and physical mixing (vertical since horizontal transport was low according to the chloride data). To assess these possibilities, natural log-transformed values of the chlorophyll data were computed, with the slopes of linear regressions reflecting the instantaneous rates of increase and decrease (exponents) of the model $N_t = N_0 e^{(k-g)t}$, with N_0 being the initial amount of chl *a* and N_t the amount at time *t*. The loss due to grazing is *g*, and assuming that grazing during the day remains at the same level as during the night, the grazing rate was 0.06 h^{-1} while the mean gross growth coefficient of phytoplankton during the day is $k+g=0.173 \text{ h}^{-1}$. These values are consistent with a coupled and diurnal cycle of primary production and removal by grazing as significant processes in the SE corner of MI (Doblin *et al.*, in prep.), but physical mixing is just as significant (i.e., the observed changes with time are a mixture of both physical and in situ biogeochemical processes).

During this same 40 hour period, dissolved Se at the Chl Max (Figure SED7) station also shows drawdown and regeneration, but unlike nitrate, the uptake appears in the evening. Significantly, the chemical form being taken up is organic selenide (Fig. SED8). Rates of uptake from this pool ($0.04\text{-}0.06 \text{ nmol l}^{-1}\text{h}^{-1}$) were much greater than that of selenite measured at the same time using incubations (Baines *et al.* 2004). These data are contrary to literature reports that find organic selenide to be largely "inert" in the open ocean (e.g., Cutter and Bruland, 1984), and uptake rates in lab studies that are no larger than those of selenite (Baines *et al.* 2001). Indeed, organic selenide in Mildred may have been as free amino acids, but were not sampled during the experiment. Like nitrate and chlorophyll, the drawdown in dissolved organic selenide

was complimented by an increase in particulate Se (Fig. SED9), albeit with only a 30% efficiency (particulate Se is also being grazed and sinking like organic carbon during this nighttime increase). The regeneration of dissolved organic selenide occurs at rates consistent with the literature (Cutter (1982); Cutter and Bruland (1984)).

Immediately after the detailed process studies, sediments were sampled in Mildred Island using a box corer. Organic carbon and nitrogen at the Chlorophyll Max station are substantially higher than at other Delta locations (by ca. a factor of 2; Table SED2), but show a typical diagenetic loss with depth until the old soil horizon is reached (Figure SED8). By assuming steady state, a flux of ca. $380 \text{ g C m}^{-2} \text{ y}^{-1}$ would be required to maintain the observed surface concentration of organic carbon. In terms of selenium, pore water profiles (Figure SED9) show that Mildred Island sediments are a minor source of dissolved organic selenide to the water column, and sink for selenite + selenate, consistent with anoxic sediments below the upper, bioturbated mixed layer. Depth profiles of solid phase selenium in Mildred Island sediments (Figure SED10) are very similar to those of organic carbon and nitrogen, with surface maxima and losses with depth (until the former soil horizon is reached). These profiles are very similar to those reported in the literature (e.g., Velinsky and Cutter (1991)), although the concentrations are slightly higher than other Delta locations (see Table SED2); selenium in Mildred Island is being lost to the sediments.

In summary, the nutrient elements nitrogen and carbon (Chl *a*), and Se, undergo tremendous cycling in Mildred, but more significantly, we are able to observe these transformations and measure their rates. However, they are still influenced by physical processes, and in particular vertical sampling wasn't conducted that would have allowed diurnal mixing effects to be observed, nor were mixing tracers sufficiently robust to detect minor horizontal inputs used. The MI results demonstrate our ability to study such flooded island habitats, the surprising physical and biogeochemical dynamics of these ecosystems, and the likely importance of such shallow waters in terms of trophic interactions (and habitats for species of interest to CALFED).

Historical records of selenium inputs to the Delta contained in sediment cores. In order to study the longer term history of selenium inputs and cycling in the Delta, paired box and gravity cores were taken in 2002 at a site near Little Mandeville Island ($38^{\circ} 00.518' \text{ N}$, $121^{\circ} 33.749' \text{ W}$), in Potato Slough ($38^{\circ} 05.078' \text{ N}$, $121^{\circ} 32.427' \text{ W}$), and off the northeast side of Sherman Island ($38^{\circ} 03.222' \text{ N}$, $121^{\circ} 47.947' \text{ W}$) on the Sacramento River. Sediment accumulation rates at Little Mandeville and Potato Slough were determined using ^{210}Pb , but insufficient material was collected at Sherman Island to measure its accumulation rate. Data for total selenium are shown in Figure SED12 and Table SED5, and based on the measured accumulation rates, the Little Mandeville core has the best temporal resolution. Based on the Mandeville profile, there are 2 periods of higher net selenium accumulation, the most recent period (shown as reaching maxima in ca. 1996 and 1968), and in the mid 19th century; 1910 is marked simply as the selenium minimum between these two periods. Interestingly, the Potato Slough core also has the highest selenium concentrations in the last 30 years, and appears to show an 1855 maximum, albeit not as pronounced. Although no dates are available, the Sherman Island core has its highest selenium concentrations in the uppermost sections (likely representing the last 30 years). Diagenetic effects cannot be discounted, but if the solid phase selenium preserved in these cores is the net result of inputs and outputs, with outputs (i.e., bacterial respiration) likely being constant, then

the greatest selenium inputs appear to have occurred most recently, and in the mid 19th century, perhaps coinciding with the gold rush period.

Se transformations by phytoplankton and bacteria (SET)

Our research on the uptake of dissolved selenium by phytoplankton and bacteria have revealed several surprises that should help guide future attempts to model Se contamination in aquatic food-webs. First, we have discovered that bacteria and phytoplankton in the Delta seem to be very different in their Se content. Bacteria may contain somewhere between 3 and 13 times more Se per unit C than do phytoplankton. So while it appears we can model phytoplankton uptake of selenite as a function of light, much as we can model photosynthesis, this does not help to predict the 50-80% of particulate selenium that is in living bacteria in situ. Bacteria are not considered to be important sources of energy or C to higher trophic levels in the Bay-Delta ecosystem, but their relative abundance may have a large impact on the Se content of zooplankton and bivalves that may feed upon them. In particular, bivalves such as *Corbicula* or *Potamocorbula*, which we know can consume bacteria, may be affected.

We have also discovered that selenite uptake by freshwater and marine phytoplankton is controlled by very different processes. In marine systems, many algae appear to have highly efficient and specific pathways for taking up selenite. Consequently, these species can accumulate selenite very effectively at concentrations that are typical of the Bay Delta ecosystem. Moreover, for these selenite accumulating species at least, higher than typical concentrations of selenite are unlikely to result in much higher cellular selenite concentrations. Another group of species in marine species are very poor at accumulating selenite from solution, although when ambient phosphate levels are low they can accumulate more than when phosphate levels are above 1 μ M, as they typically are in the Bay-Delta ecosystem. These species do increase their uptake of selenite in direct proportion to ambient concentrations. However, because they accumulate selenite so little, their effect on selenium concentrations in particulate matter is forecast to be minimal. Thus, a critical component to any successful model of selenium contamination of marine foodwebs will need to account for interspecific variability in Se uptake. Specifically, species that are most effective at accumulating selenite should be identified and monitored as if they were potentially toxic forms.

In freshwater, the patterns in selenite uptake, and the models to describe them, are different. It appears that selenite is taken up by phytoplankton in proportion to their surface area. Thus, small phytoplankton, such as most cyanobacteria, accumulate selenite much more readily than larger forms. Moreover, at typical natural concentrations of 0.2-0.4 nM selenite, uptake seems to increase proportionately with selenite concentrations. While these patterns suggest that selenite uptake may be via abiotic adsorption to cell surfaces, we have found that cells must be living to take up selenite effectively. Together, these findings suggest that uptake of selenite by freshwater phytoplankton, and perhaps bacteria, can be modelled as a simple function of selenite concentration (assuming a constant concentration factor) and algal cell size. Indeed, when we took such a model developed from our culture studies and tested it against field data, it reproduced the Se:C ratios observed in the field quite well. Such a model might also explain why bacteria have much higher Se:C ratios in the Delta than do the larger phytoplankton.

In most of the delta where phytoplankton abundance is low (2-5 μ g chl-a L⁻¹), selenite is taken up slowly by phytoplankton and bacteria relative to the size of the dissolved pool. Only

5% of the pool was utilized per day in the channels near Mildred Island, for example, which means a turnover rate on the order of a month. Thus, selenite largely acts as a conservative tracer as it moves through the Delta, its concentrations determined by inputs and remineralization. Only in places where flow rates slow enough to allow phytoplankton biomass to increase substantially can selenite concentrations be depleted. In Mildred Island, removal rates suggest that the average selenite atom has at most a week before it is assimilated by planktonic organisms. The fate of this selenite is likely to be organic selenides either in particulate or dissolved phase.

Although we are able to predict Se:C ratios in suspended matter by considering only selenite uptake, dissolved organic selenium may be a very bioavailable form of selenium that may affect exposure of higher trophic levels to Se. Dissolved organic selenium pools were very dynamic during our process study in Mildred Island, suggesting much faster production and mineralization rates than could be supported by selenite uptake and loss rates measured using radioisotopes. This suggests that places where labile forms of organic selenide can accumulate, as in Mildred Island where long residence times allow algal biomass to build up, it may play a substantial role in determining Se content of phytoplankton, and especially bacteria. Laboratory experiments suggest that marine bacteria only accumulate organic Se when phosphate is abundant; phosphate levels are indeed high through almost all of the Delta because the phytoplankton which would consume it are largely light limited. The characteristics and fate of the dissolved organic selenide needs to be analyzed in situ to provide a better understanding of this problem. Mildred Island represents an ideal situation to conduct such studies.

Se in Bay-Delta Food Webs (SEF)

Monthly sampling of Potamocorbula at Carquinez Strait. Monthly variation in Se concentrations of *Potamocorbula* at Carquinez St. is shown in Figure SEF2. Selenium concentrations are significantly higher in the fall/winter (September through February) and lowest in the spring/summer (March through August) ($F = 36.5, p < 0.0001$). Monthly samples of *Corbicula* collected over 1 year from April 1985 through November 1986, also shown in Figure SEF2, show virtually no seasonal variation in Se concentrations and are equivalent to the lowest Se concentrations measured in *Potamocorbula* in the spring/summer.

Seasonal variation in stable isotopes of carbon ($\delta^{13}\text{C}$) and nitrogen ($\delta^{15}\text{N}$) are shown in Figure SEF3. Both isotopes co-varied with each other and with bottom salinity at USGS station 8, although the relationship was stronger with $\delta^{15}\text{N}$. Both carbon and nitrogen were progressively depleted in the clam tissues as salinities decreased with increased water flow into Suisun Bay.

Spatially intensive field studies of Se in Corbicula in the Delta.

Overall relationships between Se content and clam growth. Selenium concentrations were found to be significantly related to the size of the clams and more specifically their nitrogen content and not to the location they were collected from in the Delta. Nitrogen content of *Corbicula* was inversely related to clam size, whereby smaller clams had proportionally more nitrogen than carbon (by weight) than larger clams (Figure SEF4(a) and (b)). The constancy of this relationship with nitrogen content implies that Se exposure or bioavailable Se does not vary

significantly throughout the Delta. The relationship between Se concentrations and nitrogen content in clams also held for *Potamocorbula* collected at USGS station 8 during the fall/winter (Figure SEF5). Nitrogen content explained 60% of the variability in Se concentrations in *Corbicula* in the entire Delta and 40% of the Se variability in *Potamocorbula* in the fall/winter. The overlap *Corbicula* (SJR) and clams from the mouth of Montezuma Sl. (MTZ0607) had higher Se concentrations for a given amount of nitrogen compared to the other Delta clams. Frank's Tract clams also tended to have slightly higher Se concentrations than the other Delta clams for a given amount of nitrogen.

Stable isotope signatures of the clams collected throughout the Delta are shown in Figure SEF6. Clams from the different regions of the Delta are characterized by distinct isotopic signatures. *Corbicula* from the Mildred's Island region had isotopic signatures enriched in nitrogen and depleted in carbon, while those from the Sacramento region had values depleted in nitrogen and carbon. *Corbicula* from the Bay (overlap sites) had intermediate nitrogen values and enriched carbon values relative to the other clams and Frank's Tract clams had values in between the other sites (Mildred's, Sacramento and Bay). The submerged aquatic vegetation (SAV) clams from both Mildred's and Frank's had intermediate nitrogen signatures and highly enriched carbon signatures.

Se distributions in Delta food webs.

Selenium distributions in the food web. Selenium concentrations in invertebrates and fish from Mildred's Island and Frank's Tract are shown in Figures SEF7-10. Selenium concentrations in invertebrates from Mildred's Island ranged from $0.5 \mu\text{g g}^{-1}$ in a dipteran species to $5 \mu\text{g g}^{-1}$ in *Oligochaetes* collected at the base of the SAV. A similar range was observed for invertebrates in Frank's Tract ranging from $1 \mu\text{g g}^{-1}$ *Gammarus* sp. collected from open water sites to $4 \mu\text{g g}^{-1}$ in *Corbicula* collected at the base of the SAV. Selenium concentrations in fish muscle from Mildred's Island ranged from 1 to $1.8 \mu\text{g g}^{-1}$ and from 1.8 to $10 \mu\text{g g}^{-1}$ in fish livers with striped bass having the highest concentrations. Fish muscle Se concentrations were slightly higher in Frank's Tract ranging from 1.8 to $2.5 \mu\text{g g}^{-1}$ with the highest levels measured in Inland silversides.

Stable isotopes. Stable isotope plots for invertebrates and fish from Mildred's Island and Frank's Tract are shown in Figures SEF11&12. Both food webs show depletion in $\delta^{13}\text{C}$ in those organisms that are collected in the open water habitat and/or rely on phytoplankton as a carbon source and an enrichment in $\delta^{13}\text{C}$ in those organisms that live in the SAV and/or rely on epiphytic material (algae, bacteria protozoa) found on the surface of the submerged aquatic plants. The majority of the fish species sampled in this study were found within the epiphytic-based food web. Only Inland silversides and Threadfin shad appeared to rely in part on a phytoplankton based food web.

Relationship between trophic dynamics and Se accumulation. Selenium concentrations in the Mildred's Island epiphytic-based food web were significantly enriched or biomagnified with trophic position ($\delta^{15}\text{N}$) ($R^2 = 0.81$, $p < 0.0001$, Figure SEF13). Similar biomagnification within the phytoplankton-based food web did not occur (data not shown). In Frank's Tract fish Se concentrations showed a negative relationship with $\delta^{13}\text{C}$ and standard length (Figure SEF14(a)&(b)).

The relationship between Se concentration and trophic position of San Francisco Bay clam-based and crustacean-based food web and the crustacean-based food web of Mildred's Island is shown in Figure SEF15. All three food webs biomagnified Se with trophic level, however, the San Francisco Bay food webs had significantly higher Se concentrations than the Mildred's Island food webs.

Kinetics of Se bioaccumulation

Biodynamic constants for Se bioaccumulation in different types of organisms that inhabit the Bay-Delta are shown in Table SEF1. A notable consistency among all organisms is the slow uptake rate from solution. For example, uptake rates for silver under similar conditions are 10 to 100 times faster (*M. edulis* 1.8, *T. longicornis* 10.4, *N succinea*, 1.9). Assimilation efficiencies always were greater than 20% and often exceeded 50%; Se is the only metal or metalloid, other than methylmercury, where it is common that >50% of the ingested element is assimilated. The variability within species reflects different food sources. Predators (mysids and fish) assimilate Se just as efficiently from prey as herbivores do from plants. Rate constants of loss are much faster in crustaceans (mysids and copepods) than for other species. As a result the predators of these animals (e.g. striped bass) will be exposed to less Se than will the predators of other species. All authors concluded that food was strongly predominant as the source of Se uptake for all these organisms, and dissolved uptake was typically minimal compared to food.

Clam Se model. Sensitivity of the model to changes in parameter constants is shown in Figures SEF16-18 and Table SEF2. Root mean square (RMS) of model - measured clam residuals (Se $\mu\text{g g}^{-1}$) ranged from 1.98 for an $\text{IR}_{\text{PHYTOCOM}}$, an F_{SF} of 4.6 (Se contributions from phytoplankton alone) and AE of 30% to 8.45 for an IR_{SPM} , an F_{SF} of 9.08 (Se contributions from phytoplankton and bacteria) and AE of 70%. The sum of the residual errors for each of the model parameters are shown in Table SEF3. The lowest residual errors for the model were found for $\text{IR}_{\text{PHYTOCOM}}$, an AE of 30% and a F_{SF} of 4.6. Although the simulations using $\text{IR}_{\text{PHYTOCOM}}$ yielded the lowest residual errors, these simulations also resulted in increasing residual errors for middle and southern Mildred's Island sites. Why the model over-predicts clam Se concentrations in middle and southern Mildred's Island is unclear. There is a strong positive relationship between the model - measured clam Se residuals and chlorophyll that increases from northern Mildred's through southern Mildred's that is similar to gradients observed in other parameters including stable isotopes of carbon and nitrogen (Figure SEF6) and average clam soft tissue dry wt (g) (Figure SEF4(b)). Inverse relationships for these same parameters are observed for the Delta Boogie and Frank's Tract datasets. Given that the Mildred Island clam Se concentrations follow the same pattern as the Delta Boogie and Frank's Tract datasets of increasing concentration with increasing percent nitrogen (surrogate for growth) this bias may be due to a seasonal or temperature affect on community biomass and/or pumping rate. Mildred Island clams were sampled in the fall when Thompson reports and significantly higher grazing rate compared to the spring when the Delta Boogie and Frank's Tract clams were collected.

Using the $[\text{Se}_{\text{clam}}]^{\text{SF}}$ model, an AE of 70% and $\text{IR}_{\text{PHYTOCOM}}$ and measured Se concentrations in the clams we predicted F_{SF} to range from 3 to 39 with a median value of 8.2 for the entire dataset ($n = 26$). If clam AE is presumed to be lower (30% - measured for sediment particles) our predicted F_{SF} has a much larger range from 6 to 92 with a median value of 19. This suggests that the Se: Phytoplankton & Bacteria C ratios of 4.6 and 56 measured by Baines for the

Mildred's Island region may be a reasonable surrogate for the Delta as a whole assuming a range in bacteria: phytoplankton biomass ratios of 8 – 30 % in suspended particulates.

Local scale modeling (ML)

Residence time in shallow water habitats. Field experiments revealed that Mildred Island is characterized by substantial spatial and temporal variability in currents and mixing. Drifter studies showed that tidal excursions and dispersion are greater in the north, where the levee opening is wider and deeper than in the south. Lucas et al. (2002) measured sharp north-south gradients in temperature, specific (i.e. standardized to 25° C) conductivity, chlorophyll *a*, and dissolved oxygen, with maxima for all in southeast MI, suggesting longer retention of water, dissolved substances, and particles in the south than in the north. Our interest in quantifying transport time scales in MI was stimulated by the search for a mechanistic understanding of this spatial variability, which is consistent with the notion of spatially-variable transport time scales.

Application of the residence time concept to MI illustrates one of the complications in applying idealized transport time scale definitions to tidal systems. Here, we define residence time as the time for a particle to leave MI once and assign values of residence time to the locations of particle release. This definition does not include consideration of oscillating tidal transport of water and scalars into and out of the lake over multiple tide cycles. The total amount of time a particle spends in the domain (“exposure time”) may be a more relevant time scale than residence time for some geochemical or biological processes. For example, the long term net growth of phytoplankton depends on the full range of growth-consumption conditions along tidal trajectories and these conditions vary along bathymetry gradients (Lucas et al. (1999b)). Therefore, the growth dynamics of a patch of phytoplankton in a tidal flow may be a strong function of the total amount of time spent in a particular (e.g. high growth) environment. In Figure ML2b, we see that the exposure time of particles is longer than the residence time in many regions because particles that exit the system may subsequently re-enter MI. Therefore, the influence of MI habitat may be greater on the particle than would be indicated by the formal residence time concept.

Maps depicting spatial variability of residence and exposure times (Figure ML2) provide strong clues about the importance of transport processes in shaping the spatial patterns of nonconservative quantities such as temperature, specific conductivity, chlorophyll *a*, and dissolved oxygen. The strong north-south gradients of these quantities reflect the gradients of residence time, suggesting that heat, plankton and dissolved substances accumulate in the southeastern region because of slow tidal mixing but not in the northeast region where tidal exchanges with the outer channel system are rapid. Integrative time scales, such as flushing time, provide no information about the connections between transport and spatial heterogeneity of these scalars. (Please see Monsen (2002) for more information.)

Franks Tract---The effect of SAV on hydrodynamics. For the approach of specifying an elevated bed drag coefficient, the comparison with the mean flow data from Franks Tract (Figure ML3a) indicates reasonable agreement between the model prediction and the observations for this simple approach. The details of the turbulence, however, are not accurately reproduced with the use of only a bed friction term (Figure ML3b). In the observations, the turbulent stresses have a mid-column peak around the top of the SAV. With only a bed drag, however, the peak stress will necessarily appear at the bed, as is shown in Figure ML3b.

The second approach to modeling the effects of SAV involves the use of a distributed drag parameterization, with the resistance to flow being applied throughout the portion of the water column filled with SAV. Again, there is excellent agreement between the model results and observations for the mean velocities (Figure ML4a). Unlike the bed stress formation, however, the distributed drag parameterization more closely matches the observed structure of the turbulent stresses with the prediction of a mid-water column peak in turbulent stress (Figure ML4b).

Franks Tract---Regional hydrodynamics. Volumetric flow rate calculated by the hydrodynamic model is compared with flow calculated from measurements at six channel locations surrounding Franks Tract. The model does extremely well in capturing tidal phase---a difficult feat in a complex environment such as this where there exist multiple routes to a point. The tidal wave propagates through each route but, due to the length of the channel segment, may take longer or shorter than another route to reach a given point. Calculated magnitudes also compare well with measurements. (See Figures ML15 and ML16.)

Mildred Island—Modeling with reactions. Our TRIM-MILLIE “base case” is that case with the parameter values, initial conditions, and boundary conditions described above. This case matches measured phytoplankton biomass (as chl *a*) quite well. Figure ML5 shows a) model-calculated phytoplankton biomass distributions as chl *a* for the base case at time=14 days, which is at midnight during a low slack tide; b) a spatial map of measured chl *a* during the MI process study for a similar time of day and tide cycle. The model performs well in capturing the observed spatial patterns, including: the overall north-to-south increase in chl *a* inside MI; magnitudes ranging from approximately 5 ug/L or less in the northern interior to concentrations on the order of 20 ug/L in the southern interior; concentrations ranging from approximately 5 ug/L or less in Connection Slough, northern Middle River, and southern Middle River to between 6 and 10 ug/L in Empire Cut; maximum concentrations in the SE and SW coves; in the northern half of the interior, a generally increasing east-to-west gradient and elevated concentrations along the eastern shore; elevated chl *a* in Empire Cut immediately outside the southern levee break.

We also compare time series of model-calculated chl *a* to time series measured by our SCUFA stations in southern and northern MI during our 2001 process study. Figure ML6 shows a) the comparison between chl *a* in the two grid cells nearest the elevation of the upper SCUFA and the upper measurements, and b) a similar comparison of chl *a* in the grid cell corresponding with the lower SCUFA elevation and the lower measurements for southern MI. Concentration magnitudes (e.g. average values) are generally captured well, and some of the high-frequency variability is captured also. Although on some occasions the amplitude of hourly scale variability is matched well, generally the size of modeled oscillation is somewhat smaller than that measured. We show similar data for the northern MI SCUFA station in Figure ML7. For northern MI, the model again captures the typical chl *a* concentrations for the upper and lower water column as well as some of the high frequency variability. In this case, if anything, the modeled amplitude of oscillation is typically larger than that observed. This could be due to the advection of artificially sharp gradients near the northern opening generated by the close proximity of two open model boundaries to that location and the specification of a constant concentration on inflowing tides.

With a model base case that is capturing much of the observed chl *a* (esp. spatial) variability for the study period, we can then use the model as a learning tool to help us understand the significance of various physical and biological processes in the MI region and why the observed distributions of phytoplankton biomass developed. In Figures ML8 and ML9 we compare, for a consecutive high water tidal stage and lower water stage respectively: a) the base case described above (driven by tides, wind, and heating) to b) a case where we turn off the effect of wind on advection and c) a case where we turn off the effect of wind on vertical turbulent mixing. The point of this numerical experiment is to explore the importance of wind to the observed spatial distributions of phytoplankton biomass in MI and, if wind appears to make a difference, dissect the effect of the different wind-driven processes. The chl *a* maps in these figures are all for the exact same conditions except for the inclusion or non-inclusion of wind. The maps are all for the computational cell approximately 1 m from the surface. The concentration scale is the same for all plots for ease of comparison, although the maximum concentration is not the same in all cases. During high water (Fig. ML8), we see distinctly different spatial patterns for phytoplankton biomass, although all three contain a general north to south increase in chl *a*. With no wind on advection (b), the flood tide jet/gyre in northern MI is very well defined; the remnants of a southern jet and associated gyres are also well defined. For the cases of no wind on vertical mixing (c) and all hydrodynamics turned on (a), the spatial patterns are similar but increasingly more diffuse. In these cases, gyres and jets are not as clear, especially in the all-hydrodynamics case. For these two cases, there is higher biomass in the northwest than in the no-wind-on-advection case. This may be due to the density-driven “relaxation” mechanism (referred to in Section HS) that sometimes occurs during the nighttime following wind set-up during the afternoon. That wind set-up/relaxation mechanism is absent in the no-wind-on-advection case (b), resulting in overall lower concentrations in the northern half of MI. The largest maximum chl *a* concentrations were associated with no-wind-on-advection, with most concentrated biomass accumulating in the corners and coves. Similar relationships between wind and phytoplankton distributions in MI are evident in the chl *a* maps for the low water tidal phase (Fig. ML9). In this case, it appears more clearly evident that, without a wind driven component of advection, much less high biomass water from southern MI reaches the northern opening and becomes exported. These results suggest that 1) the effect of wind on advection is significant in shaping phytoplankton biomass distributions within MI; 2) wind-driven advection is critical in driving the export of phytoplankton biomass from otherwise sheltered high-productivity sub-regions to open areas more subject tidal exchange; 3) the effect of wind on vertical mixing is not significant in shaping horizontal distributions of phytoplankton biomass; 4) wind driven advection is a significant source of mixing energy for patches of transported scalars in open water areas.

Figure ML10 compares calculated phytoplankton biomass for the base case to a conservative passive tracer (e.g. “dye”) for the same hydrodynamic conditions. At time = 14 d in the simulation, we see some similarities between the phytoplankton biomass and the tracer. For example, we see a general north-to-south increase in concentration. We also see maximum concentrations in the corners and coves. However, one major difference is that by far the maximum tracer concentration is seen in the southwest corner; whereas, comparably large phytoplankton biomass concentrations are seen in the southeast and southwest corners. Therefore, we can conclude that, on a large scale, the phytoplankton distributions within MI are largely governed by physical processes. However, some of the details, such as the precise locations of maximum concentration, may be governed by a combination of biological and

physical processes. One major consideration is the fact that the tracer does not react to its surroundings; whereas, phytoplankton react to the light and grazing conditions they encounter as they are transported. Therefore, the differences in locations of maximum concentration could be related to issues such as stratification dynamics: a tracer does not “care” whether the water column is stratified, but phytoplankton do care because stratification can assist phytoplankton in remaining near the water surface where light is plentiful.

In Figure ML11 we compare phytoplankton for the base case to phytoplankton calculated for a case in which we raised the benthic grazing rate inside MI uniformly to 1.0 m/d. This benthic grazing rate is a value typical of the greater Central Delta region and, actually, low compared to many estimated grazing rates in the region. As a result of the intensification of grazing, the maximum concentration over the domain was reduced by more than half, although the overall shape of the phytoplankton distribution remained. Time series for these two cases are shown in Figures ML12 and ML13. Instantaneous chl *a* as well as 24-hour median filtered chl *a* are shown for each case and for the upper and lower water column. For southern MI, the difference between the two cases grows over all with time; at the end of the simulation, filtered biomass for the increased grazing case is about half that for the base case. Also, the amplitudes of short timescale oscillations appear attenuated with benthic grazing is increased. For northern MI, the difference between cases was much smaller than for southern MI; this difference was greatest in the lower portion of the water column and appeared to grow over time. This result is consistent with previous work that has shown that the effect of benthic grazing on a suspended algal population is inversely proportional to the water column depth (Lucas *et al.* 1999a).

Calculations of edible particulate selenium (Se_p^{ed}) are shown in Figure ML14. Values are shown for locations at which measurements were taken for selenium in clams. Our estimates of the minimum and maximum values are shown. Relative maxima are expected to occur in the interior of MI and in Empire Cut, due to the higher phytoplankton biomass in those locations; smaller concentrations are expected to occur in the other surrounding channel regions. These distributions are due to hydrodynamics, water depth and clarity, and benthic grazing rates, which collectively control phytoplankton production and accumulation and, consequently, the conversion of dissolved Se to edible particulate Se.

Delta scale modeling (MD)

Hydrodynamic modeling.

Understanding the influence of barriers, gate, and pump operations on source distribution.

Interbasin transfers: Coherent variability of flow around MI, salinity and pump operations illustrates the general principle that diversions can generate system-scale responses. In this example, flows (and salinity) at one geographic location responded almost instantaneously to export diversions occurring 25 km away because those diversions altered regional flows, local exchanges, and source mixture of water in the central Delta. The implications of this diversion effect extend beyond salinity. As SJR-derived salt input increases, so does the input of substances including nutrients and selenium that are highly enriched in this river. Results of our hydrodynamic measurements imply that mass loadings of nutrients and contaminants from the SAC-SJR watersheds to San Francisco Bay are influenced by diversions as they alter the source mixture of water transported downstream to the estuary from the Delta.

Gate-controlled flow routing (Delta Cross Channel): Diversion of flow through an artificial channel modifies the system wide salinity distribution, a key attribute of estuarine habitat quality for biota at multiple trophic levels (Jassby et al (1995)), and the spatial distribution and susceptibility of migrating and resident fishes to entrainment mortality.

Barrier-controlled flow routing:

1) Head of Old River Barrier: This barrier-controlled diversion directly alters regional flows and hydraulic residence time and indirectly influences the local-scale balance between oxygen sources and sinks, leading to hypoxia that impedes salmon spawning migration.

The Stockton Ship Channel is a deep section of the San Joaquin River that receives large loadings of ammonia from local municipal waste and algal biomass produced upstream (Lehman et al (2004)). Metabolism of these exogenous inputs consumes oxygen faster than it is replaced by advection and mixing when the HORB is removed and net flows approach zero, so removal of this barrier slows flushing and promotes development of hypoxia in the lower San Joaquin River.

2) Agricultural barriers: The agricultural barriers in conjunction with the Head of Old River Barrier create the isolated reservoir in the south Delta which temporarily raises DOC concentrations delivered to municipal consumers via the export pumps. The Southern California municipalites (principly Metropolitan Water District) are concerned about elevated DOC levels because carcinogenic trihalomethanes (THM) are formed when high-DOC water is chlorinated for disinfection. Untreated Delta water currently has total THM formation potential 3 to 9 times higher than the THM standard for treated water. As DOC concentrations increase, more disinfection by-products are produced in the treatment process. Therefore, increases in DOC concentrations increases the cost of water treatment (Lam and others 1994). (Please see Monsen (Monsen *et al.* In prep.) for more information.)

Source distribution through the Delta. Each manipulation by gates, barriers and pumps alters the source distribution throughout the Delta. Our simulations depicting the influence of Delta Cross Channel showed that one gate by itself can change the source water distribution throughout the Central Delta.

Modeling with reactions. The base case simulation of the Delta-scale coupled model implemented Monsen's April 2002 hydrodynamics and the biological and geochemical parameters shown in Figure MD3 and described above. Spring chl *a* predicted by the model for this base case and discrete chl *a* measurements from the Benthic Boogie are shown in Figure MD10 for comparison. Additionally, time series of chl *a* from the 14-day simulation are shown in Figure MD11 (blue curves) along with level lines representing the Benthic Boogie discrete samples, where available (red curves). Generally, measured chl *a* concentration magnitudes and distributions are matched quite well by the model. Both model and measurements show that all stations west of MIB302 (Empire Cut) had concentrations ≤ 10 ug/L. Highest concentrations were in the upper San Joaquin River (SJR27 and upstream). Lowest concentrations were in and around Franks Tract. SJR27, where the model significantly underestimates chl *a*, represents the largest difference between model and measurement. This could be due to differences in

hydrology or operations between the April 2002 hydrodynamic model period and the May 2003 Benthic Boogie period, causing San Joaquin flows and phytoplankton to more dramatically affect downstream areas in 2003. Maximum and minimum predicted Edible Particulate Selenium concentrations for the base case are shown in Figure MD12. Maximum values are in the upper San Joaquin River and southern Delta; lowest values are in and around Franks Tract.

We ran a second model case, for which the benthic grazing rate in the upper San Joaquin River was raised to 1.0 m/d while keeping all physics and biology the same as for the base case. Results are in Figure MD13 (presented with the base case for comparison, and with an inset showing benthic grazing input regions) and Figure MD14. The only station that changed noticeably in response to the increase in SJR grazing was SJR32; chl *a* at this location decreased to approximately one quarter of the value calculated in the base case. This suggests one important reason for the high chl *a* concentrations in the upper San Joaquin River, relative to most of the rest of the Delta, is the paucity of clams. A relatively modest increase in clam grazing in the SJR could dramatically decrease phytoplankton standing stock locally; however, for these hydrologic and operational conditions, phytoplankton biomass from the upper SJR does not significantly affect the central Delta.

The third model case was the same as the base case, except that we turned off the state and federal pumps. The gates at Clifton Court Forebay remained operational. Therefore, semidiurnal flow into Clifton Court still occurred due to barotropic flow set up by the flood tide (i.e. surface tilt between the water outside the Forebay and the water inside) but was damped due to the lack of pumping-related drawdown within the Forebay. Results are shown in Figures MD15 and MD16. Comparison with the base case reveals that no significant change in chl *a* magnitude occurred at any of the time series stations anywhere as a result of turning the pumps off. The largest changes in mean magnitude included modest chl *a* decreases at SMS and FALSE and a slight increase at MDR04. Overall, the most noticeable change from the base case was in the character (usually amplitude) of the high frequency variability at some sites (e.g. MIB302, SMS). At SMS, for example, the large semidiurnal oscillations in the base case were muted to a large degree when pumps were turned off; this was likely due to a muted tidal flow into Clifton Court Forebay since any barotropic flow would be due only to tidal surface tilt---not pumping. The enhancement of the amplitude of oscillation at MIB302 is not fully understood, it may be related to the fact that this station was situated just near the edge of a benthic grazing input area boundary and therefore likely in the midst of a sharp chl *a* gradient. If diurnal flow was somehow enhanced in the case of no pumps, then sloshing of a sharp spatial gradient in chl *a* could cause a local large amplitude oscillation in that scalar.

VII. RECOMMENDATIONS

Hydrodynamic Measurements in Shallow Water Habitats (HS)

The findings described in the previous section point towards several specific recommendations when analyzing shallow water habitats, and the potential for ecosystem restoration.

- First, as is evident in both Mildred Island and Franks Tract, the geometry of the basin, particularly with respect to the primary wind and tidal axes, is critically important to the dynamics in the interior. Based on this, we recommend that:
 - Analysis of shallow habitats include consideration of atmospheric forcing

- The ecological and water quality effects of “pockets” in the basin geometry that are not exposed to wind or tidal forcing should be carefully considered.
 - Estimates of flushing times (or residence times) should take into account spatial variability in the flushing time so as to identify high retention-time areas within the habitat.
- Secondly, the presence of *Egeria densa* fundamentally alters the flow dynamics by creating a shear layer near the top of the canopy. We therefore recommend:
 - The particular species of vegetation, including its structure and interaction with flow, must be considered when analyzing a habitat. Buoyant species will interact with the flow in a different way from rigid species – and emergent species will have very different effects on transport and mixing, due to the lack of a mixing layer.

Regional Hydrodynamic Field Investigations (HR)

Flux Measurements. The ability to predict the long-term changes in the flux of constituents at key locations in the Delta in response to both natural and anthropogenic influences should become a key tool in helping to manage the bay/Delta system for water quantity, water quality and ecosystem function because fluxes can help uncover the *processes* that control exchanges within the system. Fluxes are not only useful in helping managers determine how much of a given constituent passes a given location, but they could also help managers understand *how* these transports are accomplished through the calculation of the flux decompositions. Since these fluxes, and the processes they represent, are essential to the creation, maintenance, and evolution of Bay/Delta habitats and contribute to the movement and distribution of organisms, as well as water quality constituents they should be routinely calculated as part of CALFED funded monitoring programs.

Moreover, because fluxes help us get at transport processes, fluxes directly quantifying how modifications to the system change transport processes within the modified area. For example, modifications to the Franks Tract area have been proposed as a means of reducing salinities at the export facilities: most of the changes have been aimed at changing dispersive mixing of salt into Franks Tract. Changes in the dispersive to advective salt flux ratio through False River could be used to assess the impacts of these proposed changes to the system.

Moreover, a given modification strategy could be optimized, in a mechanistic way, on the basis of the change it makes in salt fluxes at key locations. For example, in the case of proposed modifications to Franks Tract, changes in salt flux in False River could be determined. Similarly, changes in the local *transport mechanisms* that occur as a result of changes to the system can be quantified, in a general way, using salt flux decompositions. Thus, fluxes can be used as a “mechanistic” metric in the evaluation of different modification scenarios.

Finally, if CALFED hopes to use adaptive management strategies that depend upon evaluating incremental changes to portions of the bay/Delta system, then metrics must be developed that are water-year-type invariant so that incremental changes to the system can be evaluated in a reasonable time frame, say, on a yearly basis. For example, if evaluative metrics are dependent on water year type, say wet versus dry years, then the collection of a wet and dry year data sets would be necessary to assess project impacts. This need could delay project implementation in cases where the hydrology during the implementation period were

characterized by a string of either wet or dry years. Process-based metrics, like the advective to dispersive transport ratio, for example, could reduce water-year type dependency in projects that need to be adaptively managed.

Spatial Scales. A cascade of scales need to be considered when managing the system for water quality, water supply and ecosystem function. Depending on the question, exchange within islands habitats, such as exchange between the SAV and open water areas; shallow-channel exchange processes; and regional processes such as river inputs, gate operations, barrier installation and removal, and changes in export rate must all be considered, to a greater and lesser degree, in this highly interconnected system.

Breach geometry and location. Breach geometry and location are critical factors controlling within Island mixing and exchange processes that can translate into regional effects and therefore should be carefully considered in the restoration of shallow water habitats in the Delta.

Project operations as a component of experiments in the future. We were fortunate to have a broad range of operational changes in export rates, Sacramento and San Joaquin River flows and barrier placements during our studies. These rather dramatic changes, in particular a brief complete cessation of exports, allowed us the opportunity to study the hydrodynamics and transport characteristics under a broad range of hydrologic conditions. This, to a large extent, was pure luck. In the future, resource managers and water project operators should be engaged in the planning and execution of these large scale experiments, so that operational changes become an explicit part of the experimental design. Moreover, it would be useful if changes in various operations were not made simultaneously. For example, the Head of Old River barrier was completed and exports and Sacramento River flows were curtailed simultaneously during our Mildred Island experiment. Changing operations of several factors simultaneously makes it virtually impossible to determine the response of the system to each of the changes individually through analysis of field data. If changes could be made several days apart, the time necessary for the system to reach some sort of dynamic steady state, the analysis of the field data would be much more illuminating – specific responses could be tied to specific operational changes in the system. Finally, dramatic step function changes in operations are useful. The virtual cessation of the south Delta pumps (for maintenance) was incredibly useful in understanding system response. In particular, transport in the Mildred Island area is remarkably different in the absence of the persistent draw to the pumps.

Bivalve distribution and grazing rates (B)

Delta Scale Benthic Grazing Rates for Use in Models.

- Seasonal changes in grazing rate are sufficiently large in most of the delta that field studies to assess these rates need to occur during the period of study.
- Studies need to be carried out to determine why *C. fluminea* are not successful in the southern San Joaquin River where their grazing might be a benefit to the system.

Regional Scale Benthic Grazing Rates for Process Studies – Mildred Island Process Studies.

- This study has confirmed that *C. fluminea* do not successfully establish large populations within Mildred Island. Because this clam is an important consumer of phytoplankton it is important for studies to be done that can answer why they are not in the island and if these conditions can be replicated in restoration areas.
- Studies on habitats believed to be net producers of phytoplankton need to include adjoining channels to determine the extent of benefit to the pelagic foodweb from the production.

Channel Scale Benthic Grazing Rates – Is There a Distribution Pattern? Although we need to examine these strongly advective systems to insure that the bivalves in them are not important to the processes in the system, it is unlikely that the grazing rates observed here are sufficient to greatly affect phytoplankton biomass in the delta. The most significant effects of this habitat on phytoplankton production and particulate Se consumption, if seen, will be due to grazing in the shallow areas, adjacent to the channels which are the hardest to sample and model. The only way to adequately determine the effect of these shallow water bivalves on phytoplankton growth and particulate Se consumption is in a model that can resolve these small areas.

Spatial Variability in Benthic Grazing Rates – Franks Tract Processes. The high grazing rates consistently observed in this region of the Delta show bivalve grazing is important in the production and consumption of phytoplankton and particulate Se in the central delta. Ecological models in the central and southern delta will likely be more successful if this important region of the delta is carefully modeled, with attention being paid to the areal differences in benthic grazing rates.

Temporal Variability in Benthic Grazing Rates – Franks Tract Processes. For years like 2002, when freshwater flow was less than average, it may be possible to sample seasonally (quarterly) to estimate average grazing rates within the island. The external channels appear to be much more dynamic and will require more frequent sampling. This fact is magnified by the finding that the peak grazing rates at some of these locations are higher than those seen in the island.

Carbon field studies (C)

- A regional perspective including considering habitat connectivity should be employed in any study, assessment, or design of individual habitats.
- If enhanced primary productivity is a goal of restoration, then top-down and physical processes must be considered as well as bottom-up processes.
- Restoration decision-making must recognize the possibility that “similar looking” habitats (e.g. habitats with approximately the same depth) may be functionally opposite.
- To predict ecosystem responses to future intended and unintended change in the Delta, further detailed study of the invasive clam *Corbicula fluminea* and its population and colonization dynamics is recommended.
- Due to the uncertainty associated with key species in the Delta (e.g. *Corbicula*), truly adaptive management strategies---i.e. changeability and even *reversibility* of restoration actions---are necessary.

- Monitoring should be as process-oriented as possible, so that understanding of habitat function and connectivity is enhanced. Where process measurements are not feasible, indices of process rates and ratios should be derived and estimated to improve mechanistic understanding of the system.
- Where possible, high frequency measurements (taken on timescales of minutes to hours) should be obtained for quantifying and understanding connectivity between Delta habitats and sub-habitats.
- Preliminary reconnaissance of high resolution temporal variability in water quality should be conducted before coarser discrete measurement based field programs are designed, so that periods and amplitudes of hourly variability can be assessed and aliasing, biasing, and misinterpretation of discrete measurements minimized.
- Preliminary reconnaissance of high resolution spatial variability should be conducted before more spatially coarse field programs are designed, so that regions of distinct functionality within a study area are identified.
- Knowledge of spatial gradients is critical to understanding the impact of transport on measured temporal variability in water quality and waterborne biota.
- In a highly dynamic system such as the Delta, physical processes (hydrodynamics, transport) should be assessed in any study of chemical or biological constituents.
- Design of discrete measurement programs for waterborne constituents should acknowledge the fact that periods of variability may be different for different constituents; therefore, one sampling scheme may not fit all.

Se transformations by phytoplankton and bacteria (SET)

- Models of selenium contamination in the brackish and marine portions of the Bay-Delta ecosystem need to identify which of the hundreds of native species are “accumulators.” These species must be monitored and their abundance related to Se contents of critical herbivores.
- Models of selenium contamination in the freshwater portion of the Bay-Delta ecosystem need to account for the relative abundance of bacteria as a proportion of living biomass since these organisms appear to have very high selenium contents. Temporal and spatial variability in the Se content of consumer species which feed on bacteria should be related to this variable.
- Size distributions of phytoplankton, and possibly bacteria, should be used to predict Se content in living plankton and the Se content of consumers that feed upon this material.
- The chemical nature of dissolved organic selenide needs to be assessed in a range of habitats to help understand its likely role in Se dynamics.

Se in Bay-Delta Food Webs (SEF)

Further work is needed to understand the higher Se bioavailability in San Francisco Bay relative to the Delta. Methods used to date (total particulate Se analysis normalized to carbon content) have been able to identify differences in Se bioavailability in suspended particles, but not the underlying mechanisms driving those differences. Attached is a proposal that could identify these mechanisms (Calfed Potamocorbula Monitoring Proposal 2005).

Local scale modeling (ML)

Residence time in shallow water habitats. In order to understand how the sub-region works, we need to take a systems (full Delta) view that includes all the management manipulations throughout the Delta. We learned that the configuration of levee breaks around shallow water habitats significantly influences circulation patterns within the shallow water habitat and the exchange with the surrounding channels.

Franks Tract---The effect of SAV on hydrodynamics. Modeling of flow in the presence of SAV beds should include consideration of the vertical structure of flows, including the drag force induced by the interaction of the flow with the vegetation. When modeling transport of scalars, such an approach should include a distributed drag force within the water column.

Mildred Island—Modeling with reactions.

- When the transformation, accumulation, distribution, and transport of scalar quantities in open water areas are studied or new open water areas designed, the effect of wind driven advection must be considered, despite the strongly tidal nature of the Delta.
- Because benthic grazing can radically reduce phytoplankton standing stock and, therefore, productivity and availability of edible particulate selenium, further research on the invasive clam is necessary for understanding and predicting the functioning of the food web base and contaminant uptake in the Delta
- If a restoration goal were to be enhancement of phytoplankton biomass and productivity, then one strategy toward that goal may be the creation of habitats with (sub-habitats with) increased residence and/or exposure times relative to the fast moving channels that dominate most of the Delta. However, flushing would have to be adequate for export to unproductive habitats to occur and nuisance blooms in the donor habitats to be avoided.

Delta scale modeling (MD)

Hydrodynamic modeling. The key information that we learned from the modeling in this task was that the Delta is very inter-connected. In order to understand how a sub-region works, we need to take a systems (full Delta) view that includes all the management manipulations throughout the Delta. Management actions that are intended to benefit a local region such as the placement of agricultural barriers in the south Delta affect the circulation patterns for the entire region. Likewise, regional operations such as export pumping affect the exchange rates of small openings in Mildred Island 25 km away. To determine the source of water in any part of the Delta, we must know all the manipulations that are occurring in the system.

Modeling with reactions.

- Because benthic grazing can radically reduce phytoplankton standing stock and, therefore, productivity and availability of edible particulate selenium, further research on the invasive clam is necessary for understanding and predicting the functioning of the food web base and contaminant uptake in the Delta.
- Because phytoplankton biomass and productivity are very low in the Delta but important to supporting upper trophic levels and to contaminant transfer and availability, the

detailed coupling between physics and biological kinetics which governs biomass and productivity is an area for continued study.

VIII. CONCLUSIONS

Hydrodynamic Measurements in Shallow Water Habitats (HS)

The dynamics in southern Mildred Island are dominated by wind and atmospheric heating/cooling. In northern Mildred Island, the hydrodynamics are produced by mixture of tidal and atmospheric forcing. The importance of atmospheric forcing in MI is particularly pronounced when considering flushing times for sub-habitats along the perimeter of the island. Franks Tract circulation is set by a combination of local forcing (from local openings) and larger-scale forcing (the background tidal pressure gradient). The circulation in Franks Tract is strongly influenced by the seasonal development of SAV, which ‘channelizes’ the basin. The vertical structure of flows in the presence of SAV is characterized by a strong shear layer at the top of the SAV canopy. Channel-shallow exchange is strongly tidal, but the traditional tidal pumping structure is modified by 1) the orientation of the ambient tidal gradient relative to the opening; 2) the presence of multiple openings; 3) the presence of SAV; and 4) atmospheric forcing.

Regional Hydrodynamic Field Investigations (HR)

The data from the Mildred Island and Franks Tract investigations have been extensively used in the calibration of multidimensional numerical model in the context of a multi-agency task force. The insights gained from this data collection effort guided the development of a series of proposed physical changes to the Franks Tract region aimed at reducing electrical conductivity at the export facilities. Preliminary modeling results suggest that reductions of 25% in the peak electrical conductivity concentrations are possible at the pumps by making physical changes to the Franks Tract region, without the need for increasing reservoir releases or reducing exports.

Some of the proposed modifications to Franks Tract will give the water project operators explicit control over the distribution of salinity intrusion among the primary and secondary salt transport pathways shown in Figure HR9. From a management perspective, one can think of using operable gates in the central Delta to blend the water from the various channels in the central Delta. Through analysis of these data, gate operations could be optimized to achieve a variety of management objectives, such as minimizing salinity at the export facilities, in much the same way water is blended when filling San Luis reservoir. The difference between blending water in the central Delta and in San Luis reservoir is the operational timescale – manipulations of central Delta salt fluxes will be managed at the tidal timescale, whereas, the blending of water in San Luis reservoir is accomplished at seasonal timescales. Today, for example, the water project operators are heuristically manipulating the salt field to meet water quality standards at Jersey Point, Rock Slough and Emmaton through reservoir releases, DCC gate operations and changes in export rates. The monitoring data proposed here will give the project operators explicit knowledge, based on quantitative analysis, of how the flows, salt fluxes and spatial structure of the salt field in the central Delta are responding to these manipulations.

Bivalve distribution and grazing rates (B)

C. fluminea is a common filter-feeder in the Delta with the potential to affect the availability of phytoplankton in most of the system. It is likely a significant sink for particulate Se in most locations where it is available with the exception of the northern Sacramento River (with a boundary just beyond Freeport) and in the southern reach of the San Joaquin (from north of Stockton to Vernalis). *C. fluminea* is most abundant and has the highest grazing rates in the central Delta with the most seasonally consistent grazing rates occurring in the interior of Franks Tract. A comparison of biomass and grazing rates in spring and fall throughout the Delta showed, at most, a doubling and tripling of biomass in fall relative to spring but an order of magnitude increase in grazing rates due to a combination of larger animals, higher biomass, and higher pumping rates due to the elevated temperatures in fall. Higher resolution spatial studies established the importance of connectivity of habitats: phytoplankton biomass and particulate Se produced in one habitat, such as a flooded island, can be reduced by consumption within adjoining habitats by *C. fluminea* that may find the adjoining habitat better for their needs.

Carbon field studies (C)

- Because the benefits of some ecosystem functions can be displaced by water movements, the benefits and impacts of individual habitat types can only be revealed through a regional perspective that includes connectedness among habitats.
- Phytoplankton production is not a simple function of habitat depth and light availability. Benthic grazing and transport may override light-driven phytoplankton growth.
- Within the 3.5-5.5 m habitat depth range, phytoplankton biomass and productivity is extremely variable. Therefore, within this range, there is no “generic” or “typical” habitat, from the perspective of primary productivity.
- The invasive clam *Corbicula fluminea* can play a dominant role in habitat functionality, including carbon (food) and contaminant uptake, but much is still not understood about this organism (e.g. conditions that promote or deter its colonization of Delta habitats). The unexplained patchy distribution of this clam in the Delta implies high uncertainty in the outcomes of creating new aquatic habitats.
- Successful adaptive management requires that monitoring provide information for both *measuring* and *understanding* the outcomes of habitat modification so that subsequent phases can incorporate improved mechanistic knowledge of the linkages between habitats and the functions they provide. Thus, process measurements are very useful. However, in the absence of process measurements, derived indices (e.g. process ratios) may be used to provide valuable information to improve our mechanistic understanding of ecosystem function and to benefit adaptive management strategies.
- Adjacent habitats can often function in opposite ways (e.g. the interior of Mildred Island as a phytoplankton source, the exterior channels as phytoplankton sinks). For this reason, the dynamics at habitat interfaces is critical to understanding habitat interior dynamics, inter-habitat mass exchange, and standing stock concentrations of chemical constituents and suspended biota.

- High frequency monitoring of currents and concentrations may be critical to quantifying and understanding connectivity (i.e. fluxes) between habitats, especially within geometrically complex, dynamic environments.
- If the amplitude of high frequency variability in water quality is on the order of the amplitude of the seasonal variability, aliasing, biasing, and the introduction of artificial structure into measured time series may cause substantial error in discretely sampled data.
- High resolution spatial and temporal variability in water quality can reveal the periods and amplitudes of high frequency variability in measured variables and aid in the assessment of any aliasing, biasing, or other error associated with discrete measurements.
- Physical processes can be as or more important than biological processes in governing the variability of biological constituents.
- High frequency variability of water quality can vary in space, over time, and between constituents.
- New scaling techniques can reveal the processes underlying high frequency variability in water quality.

Field studies of selenium distributions and transformations (SED)

- The Delta transects show that selenium is clearly cycled in the Delta; selenium concentrations and speciation in Suisun Bay are not the same as those in the Sacramento and San Joaquin Rivers. Furthermore, higher flow periods show less dissolved removal in Delta, consistent with a residence time effect. This “Delta Removal Effect” is an important component of the Bay model developed by Meseck (2002).
- Monthly samples from Suisun show a rough correlation between the concentrations of particulate selenium and San Joaquin River inputs (with ca. 10x more dissolved Se than the Sacramento River). This trend was predicted by the Bay model simulations.
- Results from the Mildred Island study show that we can resolve *in situ* processes from advective ones, dissolved selenium is rapidly cycled in such an embayment, and sediments are an important repository of particulate selenium in the Delta. The major question is whether these results can be extrapolated to other habitats in the Delta?
- Historical cores show periods of higher and lower selenium deposition (the net result of inputs and cycling), with the highest concentrations occurring in the last 30 years and perhaps during the mid 19th century (gold mining activities?).

Se transformations by phytoplankton and bacteria (SET)

Our research on the uptake of dissolved selenium by phytoplankton and bacteria have revealed several surprises that should help guide future attempts to model Se contamination in aquatic food-webs.

- Bacteria and phytoplankton in the Delta seem to be very different in their Se content.

- Selenite uptake by freshwater and marine phytoplankton is controlled by very different processes. Thus, a critical component to any successful model of selenium contamination of marine foodwebs will need to account for interspecific variability in Se uptake.
- Uptake of selenite by freshwater phytoplankton, and perhaps bacteria, may be modeled as a simple function of selenite concentration (assuming a constant concentration factor) and algal cell size.
- In places where labile forms of organic selenide can accumulate, as in Mildred Island where long residence times allow algal biomass to build up, it may play a substantial role in determining Se content of phytoplankton, and especially bacteria.

Se in Bay-Delta Food Webs (SEF)

- Selenium concentrations in *Potamocorbula* have not changed since 1995.
- Selenium concentrations in clams in the Delta are highly dependent on growth (nitrogen content).
- Selenium exposure does not appear to vary throughout the Delta and is higher in the Bay.
- Frank's Tract and Mildred Island invertebrates have Se concentrations that are below dietary toxicity thresholds of predators ($\ll 10 \mu\text{g g}^{-1}$ dry weight).
- Fish Se concentrations are low relative to those in estuarine fish and are below fish liver toxicity thresholds.
- There are two distinct food webs (phytoplankton-based and epiphytic-based) in Mildred's Island and Frank's Tract.
- Selenium concentrations are enriched at higher trophic levels. Carbon source (phytoplankton vs. epiphytic algae) may influence Se concentrations in fish from Frank's Tract.
- Selenium concentrations in Delta food webs are lower than in San Francisco Bay food webs.

Local scale modeling (ML)

Residence time in shallow water habitats. Our *Limnology and Oceanography* paper about transport time scales (Monsen *et al.* 2002) looks at what happens to that source water if it gets trapped in shallow water habitats within the Delta.

Franks Tract---The effect of SAV on hydrodynamics. Using the GOTM model with distributed water column drag elements, we are able to reproduce the mean flows at the vegetated site, and produce the correct structure for the turbulent stresses. It is important to note that other modeling approaches to SAV drag would be able to reproduce the depth-averaged velocities (through elevated drag coefficients or through an adjustment of the bed elevation, for example), but the detailed vertical structure of the flow, including through-canopy flow, and the turbulent mixing in the water column will not be accurately predicted by these approaches. To resolve the mixing layer at the top of the SAV, and to successfully model both the vertical structure of flows and the turbulent stresses, a modeling approach must be applied that includes vertical variability and distributed drag due to vegetation.

Mildred Island—Modeling with reactions.

- Because the TRIM-MILLIE model captures well the spatial distributions of phytoplankton biomass but currently misses some aspects of the high frequency temporal variability, some high frequency interactions may not be critical in determining the overall spatial distribution of phytoplankton biomass in environments like Mildred Island.
- The effect of wind on advection can be significant in mixing and shaping phytoplankton biomass distributions within open water regions of the Delta. The effect of wind on vertical mixing may not be significant in shaping horizontal distributions of phytoplankton biomass.
- Phytoplankton biomass and productivity in the Delta appear to possess a positive relationship with residence time/exposure time.
- Wind-driven advection is critical in driving the export of phytoplankton biomass from otherwise sheltered high-productivity sub-regions to open areas more subject tidal exchange.
- The effect of wind on vertical mixing may not be significant in shaping horizontal distributions of phytoplankton biomass.
- Wind driven advection represents a significant mechanism for mixing patches of transported scalars in open water areas.
- Although physical processes may be important in shaping the general features of spatial distributions of reactive scalars like phytoplankton, important interactions between reactions and physics (like those between phytoplankton growth and density stratification) may govern important details of those distributions (like where biomass is highest).
- Modest increases in benthic grazing rates can significantly decrease phytoplankton biomass, and that effect intensifies in shallower areas.
- Since edible particulate selenium distributions are expected to follow distributions of phytoplankton biomass, they are therefore expected to be governed by a combination of physics, phytoplankton growth and grazing.

Delta scale modeling (MD)

Hydrodynamic modeling. As fresh water transits the Delta, there are a variety of obstacles that will alter its path. Our *Water Resources Research* manuscript (Monsen *et al.* In prep.) outlines the changes in Delta circulation patterns caused by each of the major operations in the Delta.

One goal for this task was to determine the conditions under which San Joaquin water had the potential of reaching Suisun Bay. The configuration most likely to allow San Joaquin river water to reach Suisun Bay would involve:

- 1) A larger San Joaquin River to Sacramento River flow ratio.
- 2) Temporary barriers in
- 3) Export pumping reduced
- 4) Delta Cross Channel closed

These conditions would most likely occur in the late spring during a salmon migration period.

Modeling with reactions.

- Clam grazing on phytoplankton can dramatically decrease phytoplankton biomass within the Delta; however, depending on the hydrology and operations, this effect may be only local.
- Sharp gradients in benthic grazing may result in sharp spatial gradients in phytoplankton biomass, contributing to large amplitude semidiurnal oscillations in chl *a* at a point in space.
- Hydrology and other operational conditions may determine whether pumping will significantly affect phytoplankton biomass distributions or magnitudes in the Delta (i.e. if the gates at Clifton Court Forebay remain operational).
- Pumping may modify the character of high frequency variability in transported scalars in the Delta.
- Lowest phytoplankton biomass, and therefore edible particulate selenium, may be generally located in the central Delta, where benthic grazing is the highest.
- Highest phytoplankton biomass, and therefore edible particulate selenium, may be located in the San Joaquin River; however, hydrology and operations will determine whether and to what extent those high concentrations will enhance phytoplankton biomass, productivity, and Se uptake by primary consumers in the greater Delta.

IX. REFERENCES

A. List of products

Documentary Film

USGS Film Documentary: “Delta Revival: Restoration of a California Ecosystem” 2003. This video documents the field, modeling and laboratory science performed by the scientists under this grant and how science fits in with the restoration process. Footage of field work and interviews with the scientists are included.

Ph.D. Theses

Sereno, D. M. “Hydrodynamics of shallow water habitats in the Sacramento-San Joaquin Delta.” Ph.D. Thesis, University of California, Berkeley. Expected completion: August 2005.

Baek, S. “The role of atmospheric forcing in determining transport in shallow tidal lagoons.” Ph.D. Thesis, University of California, Berkeley. Expected completion: August 2005.

Methodology

PI's at SUNY have developed and tested two new means of assessing the Se content of living, as opposed to detrital, particles *in situ*. These two products will be useful to future evaluations of Se contamination in the Bay-Delta ecosystem.

Papers in the peer-reviewed literature

Baines, S.B., Fisher, N.S., Doblin, M.A., Cutter, G.A. 2001. Accumulation of dissolved organic selenides by marine phytoplankton. *Limnol. Oceanogr.* 46(8): 1936-1944.

Baines, S.B., N.S. Fisher and R. Stewart. 2002. Assimilation and retention of selenium and other trace elements from crustacean food by juvenile striped bass (*Morone saxatilis*). *Limnology and Oceanography* 47: 646-655.

Baines, S. B., Fisher, N.S., Doblin, M.A., Cutter, G.A., Cutter, L.S., and Cole, B. 2004. Light dependence of selenium uptake by phytoplankton and implications for predicting selenium incorporation into food-webs. *Limnol. Oceanogr.* 49: 566-578.

Baines, S.B. and N.S. Fisher. Evidence of specific and non-specific selenite uptake pathways in marine phytoplankton and implications for management of selenium in estuaries. *In prep.*

Baines, S.B., B.S. Twining, G.A. Cutter and N.S. Fisher. Use of synchrotron based x-ray fluorescence microscopy to measure selenium and arsenic in individual protists. *In prep.*

Baines, S.B. and N.S. Fisher. Factors controlling uptake of selenite uptake by freshwater phytoplankton: development of a predictive model. *In concept.*

- Baines, S.B. and N.S. Fisher. The accumulation of organic and inorganic selenium by aerobic bacteria. *In concept*.
- Brown, L., Thompson, J.K., Lucas, L.V. *Corbicula fluminea* Limits Algal Import from Watershed Into the San Joaquin River, California. Journal of the North American Benthological Society. *In review*.
- Croteau, M-N, Luoma, S.N., Stewart, A.R. Trophic transfer of metals along freshwater food webs: Evidence of cadmium biomagnification in nature. *Limnology and Oceanography. In press*.
- Cutter, G.A. and Cutter, L.S. 2004. The biogeochemistry of selenium in the San Francisco Bay estuary: changes in water column behavior. *Estuarine Coastal Shelf Sci.* 61: 463-476.
- Dinehart, R. and J. Burau. 2005. Repeated surveys by acoustic Doppler current Profiler for flow and sediment dynamics in a tidal river. *Journal of Hydrology. In press*.
- Doblin, M.A., Cutter, L.S., Baines, S.B., and Cutter, G.A. Transformation and cycling of nutrients and selenium in a semi-enclosed freshwater ecosystem. *Limnology and Oceanography. In review*.
- Doblin, M.A., Baines, S.B., Cutter, L.S. and Cutter, G.A. Sources and biogeochemical cycling of particulate selenium in the San Francisco Bay estuary. *Estuarine, Coastal and Shelf Science. In review*.
- Doblin, M.A., S.B. Baines, Cutter, L.S., and Cutter, G.A. Selenium biogeochemistry in the San Francisco Bay estuary: seston and phytoplankton. *Estuarine Coastal and Shelf Science. In review*.
- Lopez, C, Cloern, J, Schraga, T.S., Little, A.J., Lucas, L.V., Thompson, J.K., and Burau, J.R. Ecological Values of Shallow-Water Habitats: Implications for Restoration of Disturbed Ecosystems. *Ecosystems. In press*.
- Lucas, L.V., T. Schraga, C.B. Lopez, J.R. Burau, and A.D. Jassby. 2002. Pulsey, Patchy Water Quality in the Delta: Implications for Meaningful Monitoring. Newsletter, Interagency Ecological Program for the Sacramento-San Joaquin Estuary, 15(3), 21-27.
- Lucas, L.V., J.E. Cloern, J.K. Thompson, and N. E. Monsen. 2002. Functional variability of habitats in the Sacramento-San Joaquin Delta: restoration implications. *Ecological Applications.* 12(5): 1528-1547.
- Lucas, L. V., D. M. Sereno, J. R. Burau, T. S. Schraga, C. B. Lopez, M. T. Stacey, K. V. Parchevsky, V. P. Parchevsky. High frequency variability in a small tidal habitat: indications of underlying processes. *In prep*.
- Lucas, L.V. and J.E. Cloern. 2002. "Effects of tidal shallowing and deepening on phytoplankton production dynamics: a modeling study." *Estuaries*, 25(4A), 497-507.

Lucas, L.V., J.R. Burau, and T.S. Schraga. Scalar fluxes at the boundaries of a shallow tidal habitat. *In concept*.

Lucas, L.V., A.R. Stewart, and N.E. Mosen. Organic carbon source tracing in a complex freshwater tidal ecosystem. *In concept*.

May, C., J. R. Koseff, L. V. Lucas, J. E. Cloern, and D. H. Schoellhamer. 2003. Effects of spatial and temporal variability of turbidity on phytoplankton blooms. *Marine Ecology Progress Series*, 254, 111-128.

Monsen, N.E., J.E. Cloern, L.V. Lucas, and S.G. Monismith. 2002. A comment on the use of flushing time, residence time, and age as transport time scales. *Limnology and Oceanography* 47(5): 1545-1553.

Monsen, N.E., J.E. Cloern, J.R. Burau. Water diversion as an ecosystem disturbance: examples from the Sacramento-San Joaquin River Delta, California. *In prep*.

Orsi, J. J. 2002. Zooplankton production in shallow water and channel habitats: an example from Mildred Island. Newsletter, Interagency Ecological Program for the Sacramento-San Joaquin Estuary. IEP Newsletter 15(3), 27-32.

Parchaso, F. and Thompson, J. Distribution and Grazing Potential of *Corbicula fluminea* in the Sacramento-San Joaquin Delta. *In prep*.

Purkerson, D., Doblin, M.A., Schleckat, C.E., Luoma, S.N., Bollens, S.M. and Cutter, G.A. 2003. Selenium in San Francisco Bay Zooplankton: Potential effects of hydrodynamics and food web interactions. *Estuaries* 26(4a): 956-969.

Sereno, D. M., Baek, S. and Stacey, M. T. "Wind-driven and density-driven circulation in a shallow tidal basin." *In prep*.

Sereno, D. M. and Stacey, M. T. Exchanges between vegetated and unvegetated subhabitats within a shallow tidal system. *In prep*.

Stewart, R., Luoma, S.N., Schleckat, C.E., Doblin, M.A., Hieb, K.A. 2004. Food web pathway determines how selenium affects aquatic ecosystems: A San Francisco Bay Case Study. *Environ. Sci. Technol.* 38: 4519-4526.

Stewart, R. Luoma, S.N. Understanding Selenium variability in migratory top predators in San Francisco Bay. *In prep*.

Stewart, R. Luoma, S.N., Doblin, M.A. Differences in bioavailability and accumulation of Selenium in food webs from the San Francisco Bay and Delta. *In concept*.

Twining, B.S., S.B. Baines, N.S. Fisher, J. Maser, S. Vogt, C. Jacobsen, A. Tovar-Sanchez, and S.A. Sañudo-Wilhelmy. 2003. Quantifying trace elements in individual aquatic protist cells with a synchrotron x-ray fluorescence microprobe. *Analytical Chemistry* 75:3806-3816.

Reports

Cuetara, J.I., J.R. Burau and C.A. Ruhl. Water, temperature and salt transport in the Mildred Island region of the Sacramento/San Joaquin Delta, California, 2002. USGS Water Resources Investigation Report. *In prep.*

Cuetara, J.I., J.R. Burau and C.A. Ruhl. Water, temperature and salt transport in the Franks Tract region of the Sacramento/San Joaquin Delta, California, 2002, USGS Water Resources Investigation Report. *In prep.*

Presentations

Baines, S.B., N.S. Fisher, L.S. Cutter, M.A. Doblin, and G.A. Cutter. 2003. Evidence for direct uptake of dissolved organic selenium by riverine phytoplankton for prediction of Se incorporation into food-webs. Calfed Science Conference. Sacramento, CA.

Baines, S.B., N.S. Fisher, L.S. Cutter, M.A. Doblin, and G.A. Cutter. 2003. Direct uptake of dissolved organic selenium by riverine phytoplankton inferred from selenite:C uptake ratios and Se:C in suspended particles. American Society of Limnology and Oceanography Meeting. Salt Lake City, UT.

Brown, L.R., J.K. Thompson, and L.V. Lucas. 2005. Possible effects of filter-feeding by an invasive clam *Corbicula fluminea* in the Lower San Joaquin River Watershed. Interagency Ecological Program Annual Workshop, Asilomar, CA. (Poster)

Burau, J.R. 2004. Transport in Suisun Marsh – Why do we care and what do we know. San Francisco Bay-Delta Science Consortium workshop “Making Science work for Suisun Marsh.” (Invited)

Burau, J.R. 2004. Water management in the Delta at daily timescales – The next frontier? Water Education Foundation (WEF) 21st Annual executive briefing “New directions on the water front.” (Invited)

Burau, J.R., J. DeGeorge, and C. Enright. 2004. Salinity Transport in Franks Tract: Physical Processes and Alternatives Analysis. Annual IEP workshop.

Burau, J.R. Transport in the Delta: Where Does Stuff Go and How Does it Get There?, Presentation at the charter meeting of the CALFED Independent Science Board at the request of Sam Luoma, CALFED lead Scientist. (Invited)

Burau, J.R. Tides and hydrodynamics in the estuary. The 6th Biennial State of the Estuary Conference.

Burau, J.R. 2003. New science and understanding of physical process in the central and south Delta: How can this information helping us manage the Delta? Year Three Technical Review of the Environmental Water Account and Science Symposium on Environmental and Ecological Effects of Proposed Long-term Water Project Operations. (Invited)

Burau, J.R. 2003. Franks Tract: water quality benefits, presentation at the University of the Pacific meeting of the exporters and south delta interests (“UOP accord”), at the request of Tim Quinn, Vice President of Metropolitan Water District. (Meeting included most of the directors of the agencies, including Patrick Wright, executive director of CALFED, Mike Spear director of DWR, Kirk Rogers, regional director of the USBR, Dianna Jacobs, deputy director of CA Fish and Wildlife service, Tom Glover, deputy director of DWR).

Burau, J.R. 2003. Franks Tract: water quality and ecological benefits. Presentation to the CALFED Bay-Delta Authority program managers, including Patrick Wright, executive director of CALFED.

Burau, J.R. 2003. Water movements in the vicinity of the DCC. 2003 EWA Salmon Workshop. (Invited)

Burau, J.R. 2003. Management implications of DCC study results, 2003 EWA Salmon Workshop, 7/16/2003

Burau, J.R. 2003. Transport in the Delta – Implications for managing fish migration and salinity intrusion. CALFED Science symposium on environmental and ecological effects of proposed long-term water project operations. (Invited)

Burau, J.R. 2003. Effects of the tides, geometry, meteorology, and project operations on circulation and mixing in a flooded island environment: Lessons from Mildred Island. CALFED Science Conference.

Burau, J.R. 2002. Exports and the zone of influence: What do we know. CALFED Environmental Water Account Review. (INVITED by Sam Luoma, CALFED Lead Scientist)

Burau, J.R. 2002. On transport mechanisms in the Bay/Delta system. CALFED Adaptive Management Workshop. Tiburon, CA.

Burau, J.R. 2001. How the Delta works: results from recent hydrodynamic investigations. CALFED Policy Group Briefing (audience included Mary Nichols, Resources Secretary for California and Bennett Raley, Asst. Secretary of the Interior)

Burau, J.R. 2001. Sills and Cells: A New Conceptual Model of Gravitational Circulation and the Null Zone Concept in Suisun Bay. Fifth Biennial State of the Estuary conference.

Burau, J.R. 2001. Transport processes in the Bay and Delta: Implications for sampling design.

Interagency Ecological Program Environmental Program Review. Sacramento, CA.

Cloern, J.E. 2003. Science in support of ecosystem restoration: A tribute to Aretha Franklin. CALFED Science Conference. Sacramento, CA. (Invited Plenary)

Cloern, J.E., L.V. Lucas, F. Parchaso, A.R. Stewart, and J.K. Thompson. 2004. Delta Revival: Restoration of a California Ecosystem. Video presentation and panel discussion for public. U.S. Geological Survey. Menlo Park, CA.

Cloern, J.E. A. Jassby, L. Lucas, A. Mueller-Solger, and W. Sobczak. 2001. Integrated Science in Support of Ecosystem Restoration: An Example from the San Francisco Bay-Delta. 16th Biennial International Conference of the Estuarine Research Federation. St. Pete Beach, FL.

Cutter, L.S., Cutter, G.A., and Luoma, S.N. 2000. The biogeochemistry of selenium in San Francisco Bay: Water column trends. AGU Ocean Sciences Meeting.

Cutter, G.A., Cutter, L.S., Meseck, S., and Doblin, M. 2003. Dissolved and particulate selenium dynamics in Mildred's Island: biotic controls on a trace element cycle. CALFED Science Conference. Sacramento, CA.

Cutter, G.A., Cutter, L.S., and Doblin, M.A. 2003. Dissolved organic selenide cycling in contrasting ecosystems: open ocean versus tidal freshwaters. ASLO Aquatic Sciences Meeting.

Doblin, M., Baines, S.B. Cutter, L.S., Fisher, N.S., and Cutter, G.A. 2000. The biogeochemistry of selenium in San Francisco Bay: Seston and phytoplankton. AGU Ocean Sciences Meeting.

Doblin, M.A., Baines, S., and Cutter, G.A. 2001. Particulate selenium in the San Francisco Bay: concentrations and implications for foodweb accumulation. ASLO Aquatic Sciences Meeting.

Doblin, M.A., Cutter, L.S., Cutter, G.A. 2003. Biogeochemical cycling of nutrients and trace elements in flooded island habitats. CALFED Science Conference. Sacramento, CA.

Doblin, M.A., Cutter, L.S. and Cutter, G.A. 2004. Nutrient and selenium dynamics in a shallow water system. ASLO Ocean Research Conference.

Doblin, M.A. 2004. Biogeochemical cycling of particulate selenium in the San Francisco Bay and the importance of an introduced clam in determining foodweb toxicity. CSIRO Division of Marine Research, Hobart, Tasmania, Australia. (Invited seminar)

Doblin, M.A. 2004. Biogeochemical cycling of particulate selenium in the San Francisco Bay and the importance of an introduced clam in determining foodweb toxicity. Center for Coastal Physical Oceanography, Old Dominion University, Norfolk, Virginia, USA. (Invited seminar)

Koseff, J.R., L.V. Lucas, J.E. Cloern, S.G. Monismith, J.K. Thompson. 2004. Modeling and field observations of algal blooms in South San Francisco Bay, 1: Philosophy and initial approaches.

American Society of Limnology and Oceanography Aquatic Sciences Meeting, Honolulu, HI.
(Invited)

Lopez, C.B. and T.S. Schraga. 2002. Revealing Patterns of Phytoplankton Dynamics in a Delta Habitat: A Billion Diatoms Can't Be Wrong! U.S. Geological Survey. Menlo Park, CA.

Lopez, C.B., L.V. Lucas, J.E. Cloern, and T.S. Schraga. 2003. Spatial Variability of Phytoplankton Dynamics in a Tidal Flooded Island. CALFED Science Conference. Sacramento, CA. (Invited)

Lopez, C.B., L.V. Lucas, J.E. Cloern, and T.S. Schraga. 2003. Spatial Variability of Phytoplankton Dynamics in a Tidal Flooded Island. 17th Biennial International Conference of the Estuarine Research Federation, Seattle, WA.

Lopez, C.B., T.S. Schraga, A.J. Little, J.E. Cloern, L.V. Lucas, and J.J. Orsi. 2004. Ecological values of shallow water habitat in the Delta. CALFED Science Conference, Sacramento, CA.

Lucas, L.V. 2002. Delta phytoplankton dynamics: time scales, spatial scales, and processes of variability." Organic Matter Estuarine Ecology Team Meeting, Interagency Ecological Program. Romberg-Tiburon Center. Tiburon, CA.

Lucas, L.V. 2002. Unraveling variability and revealing uncertainty: a role for science in ecosystem restoration. UC Berkeley Civil Engineering Department. Berkeley, CA. (Invited)

Lucas, L.V. 2002. Unraveling variability and revealing uncertainty: a role for science in ecosystem restoration. U.S. Geological Survey. Menlo Park, CA.

Lucas, L.V., J.E. Cloern, J.K. Thompson, and N.E. Mosen. 2002. Frank and Millie's Secrets Revealed: Comparison of "Similar" Shallow Tidal Habitats in the Sacramento-San Joaquin River Delta. Interagency Ecological Program Annual Workshop. Asilomar, California. (Poster)

Lucas, L.V. 2005. Connections across space, time, and process---ecosystem based science in support of restoration and management in the Sacramento-San Joaquin Delta, California. To be presented at 18th Biennial International Conference of the Estuarine Research Federation, Norfolk, VA.

Lucas, L.V. 2003. Unraveling variability and revealing uncertainty: a role for science in ecosystem restoration. CALFED-ERP Brown-bag seminar. Sacramento, CA.

Lucas, L.V. 2003. High Frequency Periodic Physical Processes Can Have Long-Term Effects on Water Quality. 17th Biennial International Conference of the Estuarine Research Federation. Seattle, WA.

Lucas, L.V., J.E. Cloern, J.K. Thompson. 2003. Science and Ecosystem Restoration. Sixth Biennial State of the Estuary Conference, San Francisco, CA. (Poster)

- Lucas, L.V. 2003. Unraveling variability and revealing uncertainty: a role for science in ecosystem restoration. California State University, Hayward, Department of Geology. Hayward, CA. (Invited)
- Lucas, L.V., J.R. Koseff, J.E. Cloern, S.G. Monismith, J.K. Thompson. 2004. Modeling and field observations of algal blooms in South San Francisco Bay, 3: Intratidal physical processes. American Society of Limnology and Oceanography Aquatic Sciences Meeting. Honolulu, HI. (Invited)
- Lucas, L.V. 2005. Modeling hydrodynamics, reactions, and transport of “stuff”---one tool in the integrated science toolbox. Lecture at the Museum of Nebraska History. Lincoln, NE. (Invited)
- Lucas, L.V. 2005. Modeling hydrodynamics, reactions, and transport of “stuff”---one tool in the integrated science toolbox. Lecture at the U.S. Geological Survey Colorado Water Science Center. Lakewood, CO. (Invited)
- Lucas, L.V. 2005. Modeling hydrodynamics, reactions, and transport of “stuff”---one tool in the integrated science toolbox. Lecture at the U.S. Geological Survey Texas Water Science Center. Austin, TX. (Invited)
- Lucas, L.V. 2005. Modeling hydrodynamics, reactions, and transport of “stuff”---one tool in the integrated science toolbox. Lecture at the U.S. Geological Survey Connecticut Water Science Center. East Hartford, CT. (Invited)
- Lucas, L.V. 2005. Modeling hydrodynamics, reactions, and transport of “stuff”---one tool in the integrated science toolbox. Lecture at the U.S. Geological Survey Alabama Water Science Center. Montgomery, AL. (Invited)
- May, C.L., L.V. Lucas, J.R. Koseff. 2001. The Influence of Wind Events on Turbidity and Phytoplankton Dynamics. 16th Biennial International Conference of the Estuarine Research Federation. St. Pete Beach, FL.
- May, C.L., J.R. Koseff, L.V. Lucas, and J.E. Cloern. 2003. Modeling of phytoplankton blooms in shallow turbid estuaries: a generic study. 8th International Conference on Estuarine and Coastal Modeling. Monterey, CA.
- May, C.L., J.R. Koseff, L.V. Lucas, J.E. Cloern, D.H. Schoellhamer. 2004. Modeling and field observations of algal blooms in South San Francisco Bay, 2: Spatial and temporal variability in light. American Society of Limnology and Oceanography Aquatic Sciences Meeting, Honolulu, HI. (Invited)
- Meseck, S.L., Cutter, L.S., and Cutter, G.A. 2000. The biogeochemistry of selenium in San Francisco Bay: Sediment cycling. AGU Ocean Sciences Meeting.
- Meseck, S.L. and Cutter, G.A. 2001. Biogeochemical cycle of selenium in the San Francisco Bay: a modeling approach. ASLO Aquatic Sciences Meeting.

- Meseck, S. and Cutter, G.A. 2003. Modeling the biogeochemical cycle of selenium in the San Francisco Bay. CALFED Science Conference. Sacramento, CA.
- Monsen, N.E., J.R. Burau, and J.E. Cloern. 2004. Water diversion as an ecosystem disturbance: Four examples from the Delta. CALFED Science Conference. Sacramento, CA.
- Monsen, N.E. 2004. Lessons learned from specific Delta habitats: when, where, and how I use a multi-dimensional model. California Water and Environmental Modeling Forum. Asilomar, CA.
- Monsen, N.E. 2003. Transport Timescales: What do they really mean? Estuarine Research Federation Conference. Seattle, WA. (Invited)
- Monsen, N.E. 2003. Circulation and Mixing within Delta Flooded Island Habitats: Implications for Ecosystem Restoration. CALFED Science Conference. Sacramento, CA. (Invited)
- Monsen, N.E., L.V. Lucas, J.E. Cloern, and S.G. Monismith. 2002. Transport Timescales: No Two Approaches are Alike. ASLO/AGU Ocean Sciences Conference. Honolulu, HI.
- Monsen, N.E. 2001. The Importance of Tidal Dispersion with Application to the Sacramento-San Joaquin Delta, CA. Estuarine Research Federation Conference. St. Pete Beach, FL.
- Purkerson, D.G., Doblin, M.A., Schlekot, C.E., Luoma, S.N., Bollens, S.M., and Cutter, G.A. 2000. Selenium in San Francisco Bay zooplankton. AGU Ocean Sciences Meeting.
- Parchaso, F. and Thompson, J. 2003. Distribution and Grazing Potential of *Corbicula fluminea* in the Sacramento-San Joaquin Delta. IEP Annual Meeting. Asilomar, CA. (Poster)
- Parchaso, F. and Thompson, J. 2004. Distribution and Grazing Potential of *Corbicula fluminea* in the Sacramento-San Joaquin Delta. CALFED Science Conference. Sacramento, CA.
- Schraga, T.S., L.V. Lucas, J.E. Cloern, and C.B. Lopez. 2003. Strong Diel Patterns of Phytoplankton Biomass in a Tidal Flooded Island: High Frequency and "Fast Biology." CALFED Science Conference. Sacramento, CA.
- Schraga, T.S., C.B. Lopez, L.V. Lucas, and J.E. Cloern. 2003. Strong Diel Patterns of Phytoplankton Biomass in a Tidal Lake: High Frequency and "Fast Biology". 17th Biennial International Conference of the Estuarine Research Federation, Seattle, WA. (Poster)
- Schraga, T.S., C.B. Lopez, L.V. Lucas, and J.E. Cloern. 2003. Strong Diel Patterns of Phytoplankton Biomass in a Tidal Lake: High Frequency and "Fast Biology". Sixth Biennial State of the Estuary Conference. San Francisco, CA. (Poster)
- Schraga, T.S., J.E. Cloern, L.V. Lucas, and C.B. Lopez. 2005. Fast biology: spatial variability of diel phytoplankton biomass patterns in the Sacramento-San Joaquin Delta (California, USA). ASLO Summer Meeting. Santiago de Compostela, Spain.

Stacey, M.T., D.M. Sereno, S. Baek, and J.R. Burau. 2003. Spatial and seasonal variability in the hydrodynamics of shallow water habitats in the Sacramento-San Joaquin Delta. CALFED Science Conference. Sacramento, CA. (Invited)

Sereno, D.M., M.T. Stacey. 2003. Circulation and exchange in shallow, subtidal habitats of the Sacramento-San Joaquin Delta. 17th Biennial Conference of the Estuarine Research Federation. Seattle, WA. (Invited)

Sereno, D.M., M.T. Stacey. 2004. The influence of submerged aquatic vegetation on the hydrodynamics in Franks Tract – Observations and Modeling. CALFED Science Conference. Sacramento, CA

Stewart, A.R. 2002. Case Study: Bioaccumulation of Selenium in the Food webs of the San Francisco Bay/Delta: Importance of feeding relationships and location. USGS National Contaminants Review, Biological Research Division, Stevenson, Washington. (Invited)

Stewart, A. R., Luoma, S.N., Doblin, M., Hieb, K. 2002. Contrasting selenium and mercury bioaccumulation in the food web of San Francisco Bay. 3rd International Conference of Applications of Stable Isotope Techniques to Ecological Studies. Flagstaff, AZ, USA.

Stewart, R.A., Doblin, M.A., Grimaldo, L., Luoma, S., and Lucas, L. 2003. Understanding selenium bioaccumulation in shallow-water habitats of the Sacramento/San Joaquin Delta: Importance of trophic pathways, biogeochemistry, and hydrodynamics. CALFED Science Conference. Sacramento, CA.

Stewart, A.R. 2004. Food web impacts of contaminants. Calfed Bay-Delta Science Program's Contaminant Stressors in the Bay-Delta Watershed Workshop, Sacramento, CA. (Invited)

Stewart, A.R., Luoma, S.N., and Hieb, K. 2004. Stable isotopes unravel the mystery of intraspecific contaminant variability in top predators in San Francisco Bay. CALFED Science Conference. Sacramento, CA.

Stewart, A.R., Luoma, S.N., and Hieb, K. 2004. Stable isotopes unravel the mystery of intraspecific contaminant variability in top predators in San Francisco Bay. 25th Annual Meeting of the Society of Environmental Toxicology and Chemistry, World Congress, Portland, OR.

Thompson, J. Parchaso, F., Shouse, M, and Peterson, H. 2002. The distribution and temporal trends in *Corbicula fluminea* biomass and what they tell us about the function of habitats. CALFED Science Conference. Sacramento, CA.

Thompson, J. 2003. Bivalve grazers as ecosystem engineers in the future. A CALFED Workshop on Scenarios of Change. Sacramento, CA

Thompson, J.K. 2004. What we know about the Benthic-Pelagic Ecosystems in the Delta. CALFED Science Board Seminar. (Invited)

Thompson, J.K. 2004. The benthic community in the context of the ecosystem in the Delta. Two-day briefing and discussion with J. Moore, new lead scientist. (Invited)

Thompson, J.K. 2005. Bivalves in a System with Low Production Limit and are Limited by Phytoplankton Productivity. To be presented at the Estuarine Research Federation Conference. (Invited)

Thompson, J.K. and L. Lucas. 2002. The San Francisco Bay experience... a different problem. Suspension feeders: A workshop to assess what we know, don't know, and need to know to determine their effects on water quality. Baltimore, MD.

Thompson, J.K., J.R. Koseff, S.G. Monismith, L.V. Lucas. 2004. Modeling and field observations of algal blooms in South San Francisco Bay, 4: Integration of numerical models and field observations. American Society of Limnology and Oceanography Aquatic Sciences Meeting. Honolulu, HI.

B. Service to Calfed and Bay-Delta Community

- CALFED Science Board Workshop on Adaptive Management, March 19-20, 2002, Tiburon, CA. Invited to assist drafting adaptive management plan for Delta restoration that could be funded by the CALFED Science Board. (Monsen, Lucas)
- Interagency Ecological Program Annual Meeting, February 28, 2002, Pacific Grove, CA, February 28, 2002: Showed a video of the Mildred Island September 2001 Field Experiment at the poster session to inform other agencies of this field program. (Monsen)
- North Delta Science Panel (Bureau)
- Presentations at CALFED Science Conference II, January 2003 (Bureau)
- Presentation at State of the Estuary, October 2003 (Bureau)
- Presentation at Science Symposium: Environmental and Ecological Effects of Proposed Changes in Water Operations June 19-20, 2003 (Bureau)
- Presentation at State of the Estuary, October 2001 (Bureau)
- Presentation at CALFED Science Conference I, October 2000 (Bureau)
- Making science work for Suisun Marsh, March 1-2, 2004 (Bureau)
- Presentation at EWA review workshop 2003, October 15-17, 2003 (Bureau)
- Presentation at Adaptive management workshop, March, 19-20, 2001 (Bureau)
- Presentation at 2003 EWA Salmon Workshop, June 15-16, 2003 (Bureau)
- Presentation at Mercury science strategy for the Bay-Delta system and watershed, October 8-9, 2002 (Bureau)
- Presentation at Water operations and environmental protection in the Delta: Scientific issues panels, April 22-23, 2002 (Bureau)
- Presentation at Hydrodynamic Modeling Workshop, June 27-28, 2001 (Bureau)
- Manuscript review for *San Francisco Estuary and Watershed Science*, 2004 (Monsen)
- Clarified assumptions about flow routing through the Delta (influence of temporary barriers and export pumps) for the CALFED Science Board, March 15, 2001 (Monsen)
- Stockton teachers workshop about the Delta, Stockton, CA, March 13, 2001. Gave a

general overview of Delta hydrodynamics to Elementary, Jr. High, and High School science teachers who were developing a science curriculum (K-12) based on the Delta. (Monsen)

- Interagency Ecological Program Estuary Ecology Team Project Work Team meeting, Tiburon, CA, August 24, 2000. Presented an overview of numerical modeling results. (Monsen)
- Participant on a committee that was tasked with developing a strategic plan for exotic species in the restoration design. Most recently this committee has planned and facilitated a workshop on adaptive management with exotic species. (Thompson)
- CALFED-ERP Brown-bag seminar, March 2003, Sacramento, CA. (Lucas)
- CALFED-ERP Brown-bag seminar, May 2003, Sacramento, CA. (Thompson)
- CALFED-ERP Brown-bag seminar, March 2003, Sacramento, CA. (Sereno)
- Contributions to Rubissow-Okamoto, A., and many others. 2001. "Science in Action: Puzzling over the Shallows." Newsletter, CALFED Bay-Delta Program & San Francisco Estuary Project. (Lucas, Cloern, Thompson, Monsen)
- Co-chair and Member, Technical and Scientific Panel Reviewing the Water Quality and Environmental Aspects of In-Delta Storage. July 2002 to August 2003. (Lucas)
- Advised USGS and CDWR scientists and Metropolitan Water District representatives on the design of a study of organic carbon dynamics and hydrodynamics at Jones Tract, the accidentally flooded island in the Delta. June 2004. (Monsen, Lucas)
- Invited by CALFED Ecosystem Restoration Program Science Panel to participate in a workshop considering the feasibility of "Low-Resolution Modeling" for projecting impacts of future physical, climatological, and management changes on the Delta. December 2004. (Lucas)
- Member, Science Advisory Group to provide input for and review a Draft Feasibility Study of the Ecosystem and Water Quality Benefits Associated with Restoration of Flooded Islands in the Sacramento-San Joaquin Delta. May 2004 to May 2005. (Burau, Lucas)
- Grant Proposal Review for CALFED Ecosystem Restoration Program. February 2002. (Lucas)
- Suisun Marsh Scalar Transport Conceptual Model Review for CALFED Ecosystem Restoration Program. April 2005. (Lucas)
- Organizer and Chair, Flooded Islands Session, CALFED Science Conference. January 2003. (Lucas)
- Two-day briefing and discussion with J. Moore, new lead scientist. Presentation: The benthic community in the context of the ecosystem in the Delta. 2004. (Thompson, Stewart, Burau, invited)
- Numerous presentations of research at 2003 and 2004 CALFED Science Conferences, State of the Estuary Conference, and IEP Annual Meetings. (All PI's)
- Presentation and participation on the science panel at the Calfed Bay-Delta Science Program's Contaminant Stressors in the Bay-Delta Watershed Workshop, Sacramento, CA. (Stewart, Invited)

"Extending" the Data:

Benthic data of this spatial resolution are extremely valuable and difficult to collect. Therefore, upon receiving this grant we contacted the Environmental Monitoring Program (EMP) of the California Department of Water Resources (DWR, Anke Mueller-Solgar) to see if they would be interested in collaborating with us on these samples. We agreed that the USGS would remove all of the *Corbicula* and *Corbula* as promised in the grant but that DWR could then have the remaining sample to sort, identify, and enumerate the benthic invertebrates. These data are now being used in the 10 year review of the benthic monitoring program for the EMP to determine if their long-term stations are good representations of the regional data. These data are presently being compiled and analyzed and show great promise in their present use but will also serve as a baseline dataset to examine changes in the benthic community with time.

We submitted and received a small proposal to CALFED with Liz Canuel, Virginia Institute of Marine Sciences, to examine lipid biomarkers in the sediment that was collected coincident with our samples. We had hoped these biomarkers would help us determine the conditions required by *Corbicula*. This report has recently been submitted and this preliminary data looks promising as a means of determining what food sources *Corbicula* are consuming – ie although they are capable of deposit feeding, feeding on bacteria and on phytoplankton, we don't know which carbon source determines their distribution. It appears from our early analyses of these data that largest populations are found in areas with highest phytoplankton biomass and that the sediment in much of the upper Sacramento River is sufficiently low in non-bacterial carbon that the only source of carbon available to them may be the small amount of bacteria living in the sediment. These biomarker data may also prove to be useful in DWR's analyses of the distribution of the deposit feeding benthic communities in the Delta.

C. Bibliography

- Atwater, B.F., Conard, S.G., Dowden, J.N., Hedel, C.W., MacDonald, R.L., and Savage, W. 1979. History, landforms, and vegetation of the estuary's tidal marshes. *In* San Francisco Bay, The Urbanized Estuary. Edited by T.J. Conomos. Pacific Division of the American Association for the Advancement of Science, pp. 347-385.
- Baines, S.B., Doblin, M.A., Fisher, N.S., and Cutter, G.A. 2001. Uptake of dissolved organic selenides by marine phytoplankton. *Limnol. Oceanogr.* 46: 1936-1944.
- Baines, S.B. and Fisher, N.S. 2001. Interspecific differences in the bioconcentration of selenite by phytoplankton and their ecological implications. *Mar. Ecol. Prog. Ser.* 213: 1-12.
- Baines, S.B., Fisher, N.S., Doblin, M.A., Cutter, G.A., Cutter, L., and Cole, B.E. 2004. Light dependence of selenium uptake by phytoplankton and implications for predicting selenium incorporation into food-webs. *Limnol. Oceanogr.* 49: 566-578.
- Bender, M., Martin, W., Hess, J., Sayles, F., Ball, L., and Lamber, C. 1987. A whole core squeezer for interfacial pore-water sampling. *Limnol. Oceanogr.* 32: 1214-1225.
- Bennett, W.A. and Moyle, P.B. 1996. Where have all the fishes gone? Interactive actors producing fish declines in the Sacramento-San Joaquin Estuary. *In* San Francisco Bay:

The Ecosystem. *Edited by* J.T.Hollibaugh. Pacific Division, American Association for the Advancement of Science, San Francisco, CA pp. 519-542.

- Brett,M.T., Müller-Navarra,D.C., and Park,S.K. 2000. Empirical analysis of the effect of phosphorus limitation on algal food quality for freshwater zooplankton. *Limnol.Oceanogr.* 45: 1564-1575.
- [CALFED] Calfed Bay-Delta Program 2000. Programmatic record of decision.
- [CDFA] California Department of Food and Agriculture 2002. Resource directory.
- [CDWR] California Department of Water Resources 1998. California water plan update.
- Casulli,V. and Cattani,E. 1994. Stability, accuracy and efficiency of a semi-implicit method for three-dimensional shallow water flow. *Computers and Mathematics with Applications* 27: 99-112.
- Cloern,J.E., Grenz,C., and Lucas,L.V. 1995. An empirical model of the phytoplankton chlorophyll:carbon ratio - the conversion factor between productivity and growth rate. *Limnol.Oceanogr.* 40: 1313-1321.
- Cole,B.E., Thompson,J.K., and Cloern,J.E. 1992. Measurement of filtration rates by infaunal bivalves in a recirculating flume. *Mar.Biol.* 113: 219-225.
- Croteau,M.-N., Luoma,S.N., and Stewart,A.R. 2005. Trophic transfer of metals along freshwater food webs: Evidence of cadmium biomagnification in nature. *Limnol.Oceanogr.* In press.
- Cuetara, J.I, and J.R. Burau. Water, temperature, and salt transport in the Mildred Island region of the Sacramento/San Joaquin Delta, California, 2001. USGS Water Resources Investigation Report. *In press.*
- Cuetara, J.I, and J.R. Burau. Water, temperature, and salt transport in the Franks Tract region of the Sacramento/San Joaquin Delta, California, 2002. USGS Water Resources Investigation Report. *In press.*
- Cutter,G.A. 1978. Species determination of selenium in natural waters. *Anal.Chim.Acta.* 98: 59-66.
- Cutter,G.A. 1982. Selenium in reducing waters. *Science* 217: 829-831.
- Cutter,G.A. 1983. Elimination of nitrite interference in the determination of selenium by hydride generation. *Anal.Chim.Acta.* 149: 391-394.
- Cutter,G.A. 1985. Determination of selenium speciation in biogenic particles and sediments. *Anal.Chem.* 57: 2951-2955.
- Cutter,G.A. 1989. The estuarine behaviour of selenium in San Francisco Bay. *Estuar.Coast.Shelf Sci.* 28: 13-34.

- Cutter,G.A. and Bruland,K.W. 1984. The marine biogeochemistry of selenium: A re-evaluation. *Limnol.Oceanogr.* 29: 1179-1192.
- Cutter,G.A. and Cutter,L.S. 2004. The biogeochemistry of selenium in the San Francisco Bay estuary: changes in water column behavior. *Est.Coast.Shelf Sci.* 61: 463-476.
- Cutter,G.A. and Radford-Knoery,J. 1991. Determination of carbon, nitrogen, sulfur, and inorganic sulfur species in marine particles. *In Marine particles: Analysis and characterization. Edited by D.Hurd and D.Spencer.* American Geophysical Union, Washington, D.C. pp. 57-63.
- Dinehart, R. and J. Burau. Repeated surveys by acoustic Doppler current Profiler for flow and sediment dynamics in a tidal river, *Journal of Hydrology. In press.*
- Doblin, M. A., Baines, S. B., Cutter, L. S., and Cutter, G. A. The biogeochemistry of selenium in San Francisco Bay: seston and phytoplankton. *Est.Coast.Shelf Sci.* Submitted.
- Dronkers, J.J. and J. Van De Kreeke, 1986, Experimental determination of salt intrusion mechanisms in the Volkerak Estuary. *The Netherlands Journal of Sea Research* 20:1-19.
- Dyer, K.R., 1974. The salt balance in stratified estuaries. *Estuarine and coastal marine science*, 2, pp. 273-281.
- Fischer,H.B., List,E.J., Koh,R.C.Y., Imberger,J., and Brooks,N.H. 1979. Mixing in inland and coastal waters. Academic Press, Inc., San Diego, California, USA.
- Foe,C. and Knight,A. 1985. The effect of phytoplankton and suspended sediment on the growth of *Corbicula fluminea* (Bivalvia). *Hydrobiologia* 127: 105-115.
- Foe,C. and Knight,A. 1986. Growth of *Corbicula fluminea* (Bivalvia) fed on artificial and algal diets. *Hydrobiol.* 133: 155-164.
- Geyer, W.R. and H. Nepf. 1996. Tidal pumping of salt in a moderately stratified estuary. *Coastal and Estuarine Studies* 53: 213-226
- Gross,E.S., Koseff,J.R., and Monismith,S.G. 1999. Three-dimensional salinity simulations of South San Francisco Bay. *Journal of Hydraulic Engineering* 125: 1199-1209.
- Guillard,R.R.L. 1975. Culture of phytoplankton for feeding marine invertebrates. *In Culture of Marine Invertebrates. Edited by W.L.Smith and M.H.Chanley.* Plenum Press, New York pp. 26-60.
- Harrison,P.J., Yu,P.W., Thompson,P.A., Price,N.M., and Phillips,D.J. 1988. Survey of selenium requirements in marine-phytoplankton. *Mar.Ecol.Prog.Ser.* 47: 89-96.
- Herren,J.R. and Kawasaki,S.S. 2001. Inventory of water diversions in four geographic areas in California's Central Valley. *In Contributions to the biology of Central Valley Salmonids.*

Volume 2, Fish Bulletin 179. *Edited by* R.L.Brown. California Department of Fish and Game, Sacramento, CA pp. 343-355.

- Jassby, A.D. and Cloern, J.E. 2000. Organic matter sources and rehabilitation of the Sacramento-San Joaquin Delta (California, USA). *Aquatic Conserv. Mar. Freshw. Ecosyst.* 10: 323-352.
- Jassby, A.D., Cloern, J.E., and Cole, B.E. 2002. Annual primary production: patterns and mechanisms of change in a nutrient-rich tidal ecosystem. *Limnol. Oceanogr.* 47: 698-712.
- Jassby, A.D., Kimmerer, W.J., Monismith, S.G., Armor, C., Cloern, J.E., Powell, T.M., Schubel, J.R., and Vendlinkski, T.J. 1995. Isohaline position as a habitat indicator for estuarine populations. *Ecol. Appl.* 5: 272-289.
- Jay, D.A., Uncles, R.J., Largier, J.L., Geyer, W.R., Vallino, J., and Boynton, W.R. 1997. A review of recent developments in estuarine scalar flux estimation. *Estuaries* 20: 262-280.
- Johns, C., Luoma, S.N., and Elrod, V. (*Editors*). 1988. Selenium accumulation in benthic bivalves and fine sediments of San Francisco Bay, the Sacramento-San Joaquin Delta, and selected tributaries. *Estuar. Coast. Shelf Sci.* 27.
- Lacy, J.R., Schoellhamer, D.H., and Burau, J.R. 1996. Suspended-solids flux at a shallow-water site in South San Francisco Bay, California: Proceedings of the North American Water and Environment Congress, Anaheim, California, June 24-28, 1996.
- Lehman, P.W., Sevier, J., Giulianotti, J., and Johnson, M. 2004. Sources of oxygen demand in the lower San Joaquin River, California. *Estuaries* 27: 405-418.
- Lemly, A.D. 1997. A teratogenic deformity index for evaluating impacts of selenium on fish populations. *Ecotox. Environ. Safety* 37: 259-266.
- Linville, R. Selenium Effects on Health and Reproduction of White Sturgeon in the Sacramento-San Joaquin Estuary. In prep.
- Linville, R. and Luoma, S. N. Selenium in the invasive bivalve *Potamocorbula amurensis* in the San Francisco Bay-Delta: Spatial distribution, temporal variability, and comparisons to other species. *Aquat. Toxicol.* In press.
- Linville, R.G., Luoma, S.N., Cutter, L., and Cutter, G.A. 2002. Increased selenium threat as a result of invasion of the exotic bivalve *Potamocorbula amurensis* into the San Francisco Bay-Delta. *Aquat. Toxicol.* 57: 51-64.
- Lopez, C. B., Cloern, J. E., Schraga, T. S., Little, A. J., Lucas, L. V, Thompson, J. K., and Burau, J. R. Ecological values of shallow-water habitats: Implications for restoration of disturbed ecosystems. *Ecosystems.* In press.
- Lucas, L.V. and Cloern, J.E. 2002. Effects of tidal shallowing and deepening on phytoplankton production dynamics: A modeling study. *Estuaries* 25: 497-507.

- Lucas,L.V., Cloern,J.E., Thompson,J.K., and Monsen,N.E. 2002. Functional variability of habitats within the Sacramento-San Joaquin Delta: Restoration implications. *Ecol.Appl.* 12: 1528-1547.
- Lucas,L.V., Koseff,J.R., Cloern,J.E., Monismith,S.G., and Thompson,J.K. 1999a. Processes governing phytoplankton blooms in estuaries. I: The local production-loss balance. *Mar.Ecol.Prog.Ser.* 187: 1-15.
- Lucas,L.V., Koseff,J.R., Monismith,S.G., Cloern,J.E., and Thompson,J.K. 1999b. Processes governing phytoplankton blooms in estuaries. II: The role of horizontal transport. *Mar.Ecol.Prog.Ser.* 187: 17-30.
- Luoma,S.N. and Fisher,N. 1997. Uncertainties in assessing contaminant exposure form sediments. *In Ecological risk assessment of contaminated sediments. Edited by C.G.Ingersoll, T.Dillon, and G.R.Biddinger.* SETAC Press, pp. 211-237.
- Luoma,S.N., Johns,C., Fisher,N.S., Steinberg,N.A., Oremland,R.S., and Reinfelder,J.R. 1992. Determination of selenium bioavailability to a benthic bivalve from particulate and solute pathways. *Environ.Sci.Tech.* 26: 485-491.
- Luoma, S. N. and Presser, T. 2000. Forecasting Selenium Discharges to the San Francisco Bay-Delta Estuary: Ecological Effects of a Proposed San Luis Drain Extension. US Geological Survey Open-File report 00-416, <http://pubs.water.usgs.gov/ofr00-416/>.
- McKee, L., Ganju, N., Schoellhamer, D., Davis, J., Yee, D., Leatherbarrow, J., and Hoenicke, R., 2002. Estimates of suspended sediment flux entering San Francisco Bay from the Sacramento and San Joaquin Delta. Report prepared for the Sources Pathways and Loading Workgroup (SPLWG) of the San Francisco Bay Regional Monitoring Program for Trace Substances (RMP). SFEI contribution 65. San Francisco Estuary Institute, December 2002. 28pp.
- Meseck,S.L. Modeling the biogeochemical cycle of selenium in the San Francisco Bay. PhD Dissertation thesis, Old Dominion University.
- Monsen,N.E. A study of sub-tidal transport in Suisun Bay and the Sacramento-San Joaquin Delta, Ca. Stanford University.
- Monsen, N. E., Cloern, J. E., and Burau, J. R. Water diversion as an ecosystem disturbance: examples from the Sacramento-San Joaquin River Delta, California. *Water Resources Research.* In prep.
- Monsen,N.E., Cloern,J.E., and Lucas,L.V. 2002. A comment on the use of flushing time, residence time, and age as transport time scales. *Limnol.Oceanogr.* 47: 1545-1553.
- Morlock, S.E., 1994, Evaluation of acoustic Doppler current profiler measurements of river discharge: U.S. Geological Survey Water-Resources Investigations Report 95-4218, 37 p.

- Morlock, S.E., Nguyen, H.T., and Ross, J.H., 2002, Feasibility of acoustic Doppler velocity meters for the production of discharge records from U.S. Geological Survey Streamflow-Gaging Stations: U.S. Geological Survey Water-Resources Investigations Report 01-4157, 56 p.
- Mueller-Solger, A.B., Jassby, A.D., and Muller-Navarra, C.D. 2003. Nutritional quality of food resources for zooplankton (*Daphnia*) in a tidal freshwater system (sacramento-san joaquin river delta). *Limnol.Oceanogr.* 45: 1468-1476.
- Officer, C.B., 1976, *Physical Oceanography of Estuaries*, Wiley, New York, 465 pp.
- O'Riordan, C.A., Monismith, S.G., and Koseff, J.R. 1995. The effect of bivalve excurrent jet dynamics on mass transfer in a benthic boundary layer. *Limnol.Oceanogr.* 40: 330-344.
- Ohlendorf, H.M., Hoffman, D.J., Saiki, M.K., and Aldrich, T.W. (*Editors*). 1986. Embryonic mortality and abnormalities of aquatic birds; apparent impacts by selenium from irrigation drainwater. *Sci.Tot.Environ.* 52.
- Ohlendorf, H.M., Lowe, R.W., Harvey, T.E., and Kelly, P.R. 1989. Selenium and heavy metals in San Francisco Bay diving ducks. *J.Wild.Manag.* 50: 64-71.
- Oremland, R.S., Hollibaugh, J.T., Maest, A.S., Presser, T.S., Miller, L.G., and Culbertson, C.W. 1989. Selenate reduction to elemental selenium by anaerobic bacteria in sediments and culture: biogeochemical significance of a novel, sulfate-independent respiration. *App.Environ.Microbiol.* 55: 2333-2343.
- Parsons, T.R., Maita, Y., and Lalli, C.M. 1984. *A manual of chemical and biological methods for seawater analysis*. Pergamon Press, Oxford, United Kingdom.
- Presser, T.S. and Ohlendorf, H.M. 1987. Biogeochemical cycling of selenium in the San Joaquin Valley, California, USA. *Environ.Manag.* 11: 805-821.
- Price, N.M., Harrison, G.I., Hering, J.G., Hudson, R.J., Nirel, P.M.V., Palenik, B., and Morel, F.M.M. 1988. Preparation and chemistry of the artificial algal media medium Aquil. *Biological Oceanography* 6: 443-461.
- Rantz, S.E., 1982, *Measurement and computation of streamflow: vol. 2. Computation and discharge*: U.S. Geological Survey Water-Supply Paper 2175, 2 v., 631 p.
- Reinfelder, J.R., Fisher, N.S., Luoma, S.N., Nichols, J.W., and Wang, W.X. 1998. Trace element trophic transfer in aquatic organisms: A critique of the kinetic model approach. *Science Of the Total Environment* 219: 117-135.
- Riedel, G.F., Ferrier, D.P., and Sanders, J.G. 1991. Uptake Of Selenium By Fresh-Water Phytoplankton. *Water Air and Soil Pollution* 57-8: 23-30.

- Riedel, G.F. and Sanders, J.G. 1996. The influence of pH and media composition on the uptake of inorganic selenium by *Chlamydomonas reinhardtii*. *Environmental Toxicology and Chemistry* 15: 1577-1583.
- Riedel, G.F., Sanders, J.G., and Gilmour, C.C. 1996. Uptake, transformation, and impact of selenium in freshwater phytoplankton and bacterioplankton communities. *Aquatic Microbial Ecology* 11: 43-51.
- Resource Management Associates, 2005a, Flooded Islands Pre-Feasibility Study: RMA Delta Model Calibration
- Resource Management Associates, 2005b, Flooded Islands Pre-Feasibility Study: Alternatives Modeling Report
- Ruhl, C.A. and M.R. Simpson, 2005, Computation of Streamflow in Tidally Affected Areas Using the Index Velocity Method, Scientific Investigations Report, 2005-5004, 41 p.
- Ruhl C.A. and D.H. Schoellhamer, 1999, Time series of suspended-solids concentration in Honker Bay during water year 1997, SFEI. 1999. 1997 Annual Report: San Francisco Estuary regional Monitoring Program for Trace Substances. San Francisco Estuary Institute, Richmond, CA. <http://www.sfei.org/rmp/1997/c0304.htm>
- Schlekat, C.E., Dowdle, P.R., Lee, B.G., Luoma, S.N., and Oremland, R.S. 2000. Bioavailability of particle-associated Se to the bivalve *Potamocorbula amurensis*. *Environmental Science & Technology* 34: 4504-4510.
- Schlekat, C.E., Lee, B.-G., and Luoma, S.N. 2001. Dietary metals exposure and toxicity to aquatic organisms: Implications for ecological risk assessment. *In Coastal and estuarine risk assessment. Edited by M.C. Newman, M.H. Roberts, and R.C. Hale.* CRC Press, Boca Raton pp. 151-188.
- Schlekat, C.E., Purkerson, D.G., and Luoma, S.N. 2004. Modeling selenium bioaccumulation through arthropod food webs in San Francisco Bay. *Environ. Toxicol. Chem.* 23: 3003-3010.
- Simpson, M.R., 2001, Discharge measurements using a broad-band acoustic Doppler current profiler: U.S. Geological Survey Open-File Report 01-1, 123 p.
- Simpson, M.R. and Bland, Roger, 1999, Techniques for accurate estimation of net discharge in a tidal channel: IEEE Sixth Working Conference on Current Measurement, San Diego, Calif., March 11-13, 1999, Proceedings p. 125-130.
- Simpson, M.R., and Oltmann, R.N., 1993, Discharge-measurement system using an acoustic Doppler current profiler with applications to large rivers and estuaries: U.S. Geological Survey Water-Supply Paper 2395, 32 p.

- Skorupa, J. P. 1998. Constituents of concern: selenium, in Guidelines for interpretation of the biological effects of selected constituents in biota, water, and sedimen. National Irrigation Water Quality Program Information Report No. 3.
- Sobczak, W. V., Cloern, J. E., Jassby, A. D., Cole, B. E., Schraga, T. S., and Arnsberg, A. 2005. Detritus fuels ecosystem metabolism but not metazoan food webs in San Francisco Estuary's Freshwater Delta. *Estuaries* 28: 124-137.
- Sobczak, W. V., Cloern, J. E., Jassby, A. D., and Muller-Solger, A. B. 2002. Bioavailability of organic matter in a highly disturbed estuary: the role of detrital and algal resources. *PNAS* 99: 8101-8105.
- Stewart, A. R., Luoma, S. N., Schlekot, C. E., Doblin, M. A., and Hieb, K. A. 2004. Food Web Pathway Determines How Selenium Affects Aquatic Ecosystems: A San Francisco Bay Case Study. *Environ.Sci.Tech.* 38: 4519-4526.
- Teh, S. 2004. Effects of dietary selenium on early life stages of Sacramento splittail., In press.
- Twining, B. S., Baines, S. B., and Fisher, N. S. 2004a. Element stoichiometries of individual plankton cells collected during the Southern Ocean Iron Experiment (SOFEX). *Limnology and Oceanography* 49: 2115-2128.
- Twining, B. S., Baines, S. B., Fisher, N. S., and Landry, M. L. 2004b. Cellular iron contents of plankton during the Southern Ocean Iron Experiment (SOFEX). *Deep-Sea Research I* 51: 1827-1850.
- Twining, B. S., Baines, S. B., Fisher, N. S., Maser, J., Vogt, S., Jacobsen, C., Tovar-Sanchez, A., and Sanudo-Wilhelmy, S. A. 2003. Quantifying trace elements in individual aquatic protist cells with a synchrotron X-ray fluorescence microprobe. *Analytical Chemistry* 75: 3806-3816.
- Urquhart, K. A. F and Regalado, K. 1991. Selenium Verification Study, 1988–1990. California State Water Resources Control Board Report 91-2-WQWR.
- Velinsky, D. J. and Cutter, G. A. 1990. Determination of elemental and pyrite-selenium in sediments. *Anal.Chim.Acta.* 235: 419-425.
- Velinsky, D. J. and Cutter, G. A. 1991. Geochemistry of selenium in a coastal salt marsh. *Geochim.Cosmochim.Acta.* 55: 179-191.
- Verity, P. G. 1981. Effects of temperature, irradiance and daylength on the marine diatom *Leptocylindricus danicus* Cleve. 1. Photosynthesis and cellular composition. *J.Exp.Mar.Biol.Ecol.* 55: 79-91.
- Walters, R. A. and C. Heston, 1982, Removing tidal-period variations from time-series data using low-pass digital filters, *Journal of Physical Oceanography*, V.12, No.1. pp. 112-115.

- Walters, R.A. and J.W. Gartner, 1984, Subtidal sea level and current variations in the Northern reach of San Francisco Bay,
- Warner J.C., D.H. Schoellhamer, J.R. Burau, 1997, A sediment transport pathway in the back of a nearly semi-enclosed subembayment of San Francisco Bay, California, In: environmental and coastal hydraulics: Protecting the aquatic habitat, edited by: Wang S.Y. and T. Carstens, proceeding of the 27th Congress of the International Association of Hydraulic Research, August 10-15, 1997, San Francisco, California. pg. 1096-1101.
- Wang, J. and Cheng, R.T. 1993, On low-pass digital filters in oceanography, *Acta Oceanologica Sinica* 12, 183-196
- Winters, J.W. 1978. A review on the knowledge of suspension-feeding lamellibranchiate bivalves, with special reference to artificial aquaculture systems. *Aquaculture* 13: 1-33.
- Zhang, L., Walsh, R.S., and Cutter, G.A. 1998. Estuarine cycling of carbonyl sulfide: production and sea-air flux. *Mar. Chem.* 61: 127-142.

X. EXHIBITS

Table HS1. Summary of Franks Tract hydrodynamic experiments.

Experiment	Dates	Veg.ADV's	OpenADVs	ADCP	Mapping Days
FT1	3/22/02-4/10/02	4	0	1	4
FT2	4/30/02-5/23/02	4	0	1	4
FT3	6/10/02-6/25/02	4	0	1	2
FT4	9/11/02-9/26/02	4	0	1	5
FT5	3/7/03-3/25/03	4	2	1	4

Table HS2. Flushing times (in days) based on three-dimensional hydrodynamic simulations, columns compare the effects of including atmospheric forcing (“All Forcing”) versus just tidal processes.

Flushing Time (days)	Forcing	
	All	Tides Only
MI	4.8	5.8
MI-North	4.2	3.7
MI-South	5.4	7.6
MI-SE corner	2.8	4.9

Table B1. Station location and date used for delta-wide grazing analysis.

Location	Date	# Stations Sampled
Mildred Island Channels	August 2001	21
Franks Tract Channels	April 2002	89
Three Mile Slough	August 2002	14
San Joaquin River	August 2002	13
Sacramento River	August 2002	14
Delta-Wide	May 2003	156
Delta-Wide	October 2003	42

Table B2. Results of Delta-wide sampling in May 2003.

Region	Station Number	Habitat Description	Depth		Sample Description	<i>Corbicula fluminea</i>			<i>Corbula amurensis</i>			TOTAL
			ft	m		#/0.05 m ²	g AFDW/0.05m ²	Grazing Rate (m/d)	#/0.05 m ²	g AFDW/0.05m ²	Grazing Rate (m/d)	Grazing Rate (m/d)
Lower San Joaquin (>22°C)												
1a	N-Southern Middle River; 3° river											
	MIB400	S-	13.6	4.1	very soupy mud	13	0.0	0.01	0	0.0	0.00	0.01
	MIB403	S-Shallow - east shore	18.1	5.5	coarse beach sand	15	0.0	0.04	0	0.0	0.00	0.04
1b	S-Southern Middle River; 3° river; near export pumps - barriers down											
	MDR06	S-Shallow - east shore	17.4	5.3	very sandy sediment sandy with patches of	9	0.0	0.01	0	0.0	0.00	0.01
	MDR07	M-	16.0	4.9	mud	21	0.4	0.52	0	0.0	0.00	0.52
	MDR08	S-	?			19	0.4	0.50	0	0.0	0.00	0.50
2	Victoria Canal - man made canals; near export pumps											
	VIC001		9.2	2.8	soft silty mud, no clams	19	0.0	0.01	0	0.0	0.00	0.01
	VIC002		12.2	3.7	soft mud with sand and peat sandy with patches of	60	0.3	0.37	0	0.0	0.00	0.37
	MDR07		16.0	4.9	mud	21	0.4	0.52	0	0.0	0.00	0.52
3	Cross Delta Canals/Woodward - Man Made Canals - Junction with Old River, Middle River; near export pumps											
	MIB403		18.1	5.5		15	0.0	0.04	0	0.0	0.00	0.04
	MDR02		48.6	14.8	muddy with peat	15	0.0	0.01				0.01
4	Southern Old R.@Clifton Court; 3° river; near export pumps - barriers down											

	OLD28.5	M- Shallow - east shore	46.4	14.1	hard packed peaty sediment, lots of organic matter (chunks of wood) soft mud in spots	108	0.2	0.19	0	0.0	0.00	0.19
	OLD29A	S- Eastern Channel	15.2	4.6	sand with a bit of mud	16	0.0	0.01	0	0.0	0.00	0.01
	OLD29B	S- Central Channel	15.8	4.8	sand with a bit of mud	0	0.0	0.00	0	0.0	0.00	0.00
	OLD29C	S- Western Channel	16.8	5.1	sandy	2	0.0	0.00	0	0.0	0.00	0.00
	CC3	S - Channel	20.5	6.2	sandy mud with clams (big fat happy clams)	12	0.0	0.01	0	0.0	0.00	0.01
	OLD30	M -Shallow	9.1	2.8	hard pack with sandy mud patches at very surface	7	0.0	0.01	0	0.0	0.00	0.01
5	Middle Old River; 3' river											
	OLD20	S - Channel	20.2	6.2	soft mud with lots of clams	47	0.1	0.10	0	0.0	0.00	0.10
	OLD26	M- Channel	32.1	9.8	chunky peaty sed with mud, sponge covering the surface	26	0.0	0.02	0	0.0	0.00	0.02
6	Coney Is. Canal - around island, near export pumps											
	CNY001	M	15.5	4.7	goopy mud	20	0.0	0.02	0	0.0	0.00	0.02

	CNY002	S	13.9	4.2	sand and mud with small amount of peat (peat layer under sand)	62	0.1	0.06	0	0.0	0.00	0.06
	CC3	at Clifton Court	20.5	6.2	sandy mud with clams (big fat happy clams)	12	0.0	0.01	0	0.0	0.00	0.01
	VIC001	M - at junction	9.2	2.8	soft silty mud, no clams	19	0.0	0.01	0	0.0	0.00	0.01
7	Grant Line Canal - man made canal ; near export pumps											
	FBC01	S	16.4	5.0	sandy mud, no clams	30	0.0	0.02	0	0.0	0.00	0.02
	FBC02	S	5.8	1.8	sand, no clams	8	0.0	0.01	0	0.0	0.00	0.01
	MDR07	S - at junction Middle River	16.0	4.9	sandy with patches of mud	21	0.4	0.52	0	0.0	0.00	0.52
8	Empire cut - - man made canal											
	MIB300	SE of Mildred Is. - S	21.7	6.6	fine gooey mud with peat underneath then layer of clay under that	37	0.1	0.08	0	0.0	0.00	0.08
9	Whiskey Slough - slough; near export pumps											
	ISL001	M	11.8	3.6	sandy mud	63	0.0	0.05	0	0.0	0.00	0.05
10	San Joaquin R to Stockton - 4' river											
	SJR27A	S- east end of transect	8.7	2.7	sandy mud with sticks, no clams	2	0.0	0.03	0	0.0	0.00	0.03

	SJR27B	S - center of transect	4.7	1.4	gooey mud with sand and egeria roots, some shells, no live clams	6	0.0	0.01	0	0.0	0.00	0.01
	SJR27C	S - west end of transect	38.9	11.9	sandy mud, some shells but no live clams	6	0.0	0.04	0	0.0	0.00	0.04
	SJR28	S	12.0	3.7	soupy mud, O2 surface, below anoxic, no clams	1	0.0	0.00	0	0.0	0.00	0.00
	SJR30	S	5.8	1.8	soupy mud, looks dead	1	0.0	0.00	0	0.0	0.00	0.00
11	Southern Tributaries of SJR - 2* rivers											
	CAL001	S	1.4	0.4	sandy, no clams	10	0.0	0.00	0	0.0	0.00	0.00
	SMC001	S	2.0	0.6		21	0.0	0.01	0	0.0	0.00	0.01
	FCS001	S	1.5	0.5	fine med sand	8	0.0	0.01	0	0.0	0.00	0.01
12	San Joaquin R to Old River - 4* river											
	SJR32	S - Shallow - west shore	3.9	1.2	sandy with clam shells hard hard concrete, living large corbicula in 4	18	0.0	0.01	0	0.0	0.00	0.01
	SJR33	M -Shallow - east shore	3.0	0.9	grabs	72	0.1	0.13	0	0.0	0.00	0.13
	SJR36	S	2.3	0.7		8	0.0	0.01	0	0.0	0.00	0.01
13	Rough and Ready - slough, man-made?											
	SJR28	S	12.0	3.7	soupy mud, O2 surface, below anoxic, no clams	1	0.0	0.00	0	0.0	0.00	0.00
14	Southern San Joaquin R. - 4* river											

	Overlap with L. Brown Station- USGS											
SJR/LB1		0.7	0.2	coarse sand, no clams	21	0.0	0.01	0	0.0	0.00	0.01	
SJR37		15.0	4.6	coarse sand	31	0.0	0.02	0	0.0	0.00	0.02	
SJR38		4.0	1.2	coarse sane and gravel	35	0.0	0.01	0	0.0	0.00	0.01	
SJR39		6.0	1.8	coarse sand	27	0.0	0.01	0	0.0	0.00	0.01	

Mildred Island (>21°C)

1 **Rock Slough - man-made**

RSC001	S	10.6	3.2	gooey soft mud	16	0.0	0.01	0	0.0	0.00	0.01
PLM001	S	10.6	3.2	gooey mud and peat	4	0.0	0.00	0	0.0	0.00	0.00
PLM002	S	12.8	3.9	sandy mud with some HUGE clams	20	0.0	0.02	0	0.0	0.00	0.02

2 **Holland Cut to Old River -3° connection**

HOL	S	29.1	8.9	sand	5	0.6	0.81	0	0.0	0.00	0.81
OLD08	S	18.1	5.5	muddy sand with some detritus	39	1.6	1.78	0	0.0	0.00	1.78

3 **Connection Sl./L. Mandeville -3° connection**

MAN03	M	12.1	3.7	muddy sand	95	0.5	0.63	0	0.0	0.00	0.63
-------	---	------	-----	------------	----	-----	------	---	-----	------	------

4 **Old R. out of Franks Tract - 3° river**

OLDR		29.0	8.8	soft silty mud	3	0.0	0.01	0	0.0	0.00	0.01
------	--	------	-----	----------------	---	-----	------	---	-----	------	------

5 **Old R. from Holland - 3° river**

OLD09	west shore	32.1	9.8	silty mud gooey mud with some	37	1.3	1.39	0	0.0	0.00	1.39
OLD16	west shore	27.6	8.4	peat	1	0.0	0.00	0	0.0	0.00	0.00

7 **Around Mildred Island - 3° - mixed origin rivers**

	MIB126	S - near western waist of island	28.2	8.6	uniform fine mud, no obvious clams	32	0.0	0.02	0	0.0	0.00	0.02
	MIB109	S - near eastern waist of island	28.2	8.6	fine sandy mud with loose fluffy layer on top	37	0.6	0.82	0	0.0	0.00	0.82
8	N. Middle R. out of MI - 3° river - advective highway when pumps on											
	MIB102	M - exiting northern Middle River	41.7	12.7	fine mud with peat mixed in, very oxidized with clams	26	0.7	0.79	0	0.0	0.00	0.79
	MIB203	S - north of first meander in river, north of Mildred Is.	13.2	4.0	soft fluffy sandy mud and surface with some organic in it and clams	12	0.4	0.46	0	0.0	0.00	0.46
9	San Joaquin R - 4° river											
	HDC001-C		24.5	7.5	firm thick oxidized mud, no clams	22	0.0	0.03	0	0.0	0.00	0.03
12	White Slough - 2° slough											
	WHT001		16.5	5.0	soft silty mud, no clams	5	0.0	0.00	0	0.0	0.00	0.00
13	King Is, Rindge Tract - East - 2° man made canal											
	BPC001	S	10.7	3.3	greyish black fine grained firm sediment, very sticky, no clams	0	0.0	0.00	0	0.0	0.00	0.00

Franks Tract (20.5-21°C)

1 **Franks Tract - inside of flooded island**

				soupy gooey mud with baby clams	17	0.7	0.84	0	0.0	0.00	0.84
		7.9	2.4								
		FTI09									
		FTI14		soupy mud	1	0.0	0.01	0	0.0	0.00	0.01
		8.4	2.6								
		FTI23	in Egeria	sandy dark sediment	0	0.0	0.00	0	0.0	0.00	0.00
		6.5	2.0								
		FTI17		soupy peaty mud with clams	10	1.7	2.03	0	0.0	0.00	2.03
		8.0	2.4								
		FTI01	in Egeria	gooey soupy mud	4	0.0	0.00	0	0.0	0.00	0.00
		9.0	2.7								
2		Fishermens Cut - man-made canal									
		FISH	S	gooey silty mud	3	0.0	0.00	0	0.0	0.00	0.00
		14.3	4.4								
		FSH01	S	gooey silty	6	0.0	0.00	0	0.0	0.00	0.00
		7.4	2.3								
		FSH03	S	soft silty	2	0.0	0.00	0	0.0	0.00	0.00
		17.1	5.2								
3		False River 3° river									
		FALSE	S		0	0.0	0.00	0	0.0	0.00	0.00
		8.0	2.4								
		FLR07	S	lots of shells and clams in sandy mud	1	0.0	0.00	0	0.0	0.00	0.00
		29.0	8.8								
		FLR03	S	hard packed	36	3.9	4.50	0	0.0	0.00	4.50
		7.3	2.2								
4		Taylor,Dutch,Sandmound Sloughs - around Franks Tract									
		TYLR	Shallow - east shore	goopy mud, no clams	0	0.0	0.00	0	0.0	0.00	0.00
		20.0	6.1								
		TLR02		goopy mud fine grained, sandy sediment	1	0.0	0.00	0	0.0	0.00	0.00
		13.8	4.2								
		DTCO4			1	0.0	0.01	0	0.0	0.00	0.01
		10.3	3.1								
		SMS03	Shallow - west shore	sandy mud	0	0.0	0.00	0	0.0	0.00	0.00
		9.3	2.8								
		SMS		sandy gooey mud	31	2.7	3.10	0	0.0	0.00	3.10
		12.2	3.7								
5		San Joaquin R east of Threemile SI - 4° river									

	SJR23A	southern end of transect	41.5	12.6	very fine sand	1	0.0	0.01	0	0.0	0.00	0.01
	SJR23B	middle of transect	7.2	2.2	silty mud with some sand	1	0.2	0.23	0	0.0	0.00	0.23
	SJR23C	northern end of transect	4.9	1.5	sandy soupy mud, no clams	11	0.0	0.02	0	0.0	0.00	0.02
6	Potatoe Slough											
	PT005		31.8	9.7	hard packed mud with thin layer of soft mud at the surface with sponges at the surface	41	0.2	0.27	0	0.0	0.00	0.27
7	S. Fork Mokelumne - 3° river											
	SMK003	M	9.4	2.9	soupy mud with corbicula shells, sandy mud with hard pan clay many clams but they seem unhappy	8	0.0	0.02	0	0.0	0.00	0.02
	SMK005	S	2.9	0.9	poorly sorted muddy sand	47	0.2	0.31	0	0.0	0.00	0.31
7a	Mokelumne R - 3° river											
	MKR04	S	3.8	1.2	sand with stick coarse sand, maybe baby corbicula	59	2.1	2.59	0	0.0	0.00	2.59
	MKR05	S	2.0	0.6		16	0.0	0.01	0	0.0	0.00	0.01
8	San Joaquin R west of Threemile Sl - 4° river											
	SJOL6	S	14.2	4.3	sand	0	0.0	0.00	0	0.0	0.00	0.00
	SJR19	S	12.3	3.7		1	0.0	0.01	0	0.0	0.00	0.01
	SJR18	S - shallow	na			8	0.0	0.01	0			0.01

	SJOL15A	east shore	6.6	2.0		8	0.5	0.60	20	0.2	1.06	1.66
	SJOL15A-MID	transect	7.2	2.2	sandy mud	6	0.5	0.61	9	0.0	0.27	0.88
					sandy, trouble getting sediment, too many clams							
	SJOL15B	transect	14.2	4.3		10	0.3	0.33	12	0.1	0.75	1.08
	SJOL15C	west shore?	9.8	3.0		6	0.0	0.00	0	0.0	0.00	0.00
	SJOL20	Shallow - west shore				2	0.0	0.05	1	0.0	0.05	0.10
9	Sherman Lake - flooded island, estuarine											
	SHI001	inner island	1.0	0.3	soupy mud & egeria pieces	2	0.0	0.00	0	0.0	0.00	0.00
	SHI002	inner island	1.5	0.5	soupy, o2 surface	56	0.0	0.02	0	0.0	0.00	0.02
	SHI003	inner island	1.1	0.3	soupy mud	19	0.0	0.01	0	0.0	0.00	0.01

Sacramento River (19.5-20°C)

1	S. Sacramento River - 4° river											
	SR105	S	15.6	4.8	sand, few clams	1	0.0	0.00	0	0.0	0.00	0.00
	SR106	S	20.3	6.2	sand	2	0.0	0.00	0	0.0	0.00	0.00
	SR107	S	33.2	10.1	sand	2	0.0	0.00	0	0.0	0.00	0.00
4	Sacramento R. South of Locke - 4° river											
	SR111A	west end of transect	18.8	5.7	sand with small pebbles	23	0.0	0.04	0	0.0	0.00	0.04
	SR111B	transect	18.2	5.5	sand, no clams	15	0.1	0.20	0	0.0	0.00	0.20
	SR111C	transect	21.0	6.4	sand	1	0.0	0.00	0	0.0	0.00	0.00
	SR112B	at Sacramento	27.0	8.2	sand	4	0.0	0.01	0	0.0	0.00	0.01
	SR113		15.0	4.6	sand	2	0.0	0.00	0	0.0	0.00	0.00
5	Upper Sacramento River - 4° river											
	SR108	M	32.8	10.0	sand	4	0.0	0.00	0	0.0	0.00	0.00

	SR109	M - South of Hood	22.0	6.7	sand with stone and plant material at surface, small clams present	3	0.0	0.00	0	0.0	0.00	0.00
	SR110	S - about at Hood	31.7	9.7	coarse sand with mica and a few baby clams	7	0.0	0.00	0	0.0	0.00	0.00
6	Elk Slough - off of Sacramento R.											
	ELK001	S	10.1	3.1	soft silty mud, no clams	0	0.0	0.00	0	0.0	0.00	0.00
7	Miner/Sutter Sl. - off of Sacramento R.											
	MSL002	M	4.2	1.3	sand	0	0.0	0.00	0	0.0	0.00	0.00
	SUS001	S	19.2	5.9	medium grain sand with clams	2	0.0	0.00	0	0.0	0.00	0.00
8	Steamboat Sl. - off of Sacramento R.											
	SBT001	M	3.6	1.1	sand with small corbicula	0	0.0	0.00	0	0.0	0.00	0.00
	SBT002	S	3.9	1.2	sand with baby corbicula	4	0.0	0.00	0	0.0	0.00	0.00
	SBT003	S	12.9	3.9	sand with stone rocks and debris, and clams	0	0.0	0.00	0	0.0	0.00	0.00
9	Georgiana Sl. - off of Sacramento R. at Delta Cross Channel											
	GSL001		95.1	29	gravel with a thin layer of sand over something hard and/or all sand	1	0.0	0.00	0	0.0	0.00	0.00

				dense mud with sandy mud at surface	135	0.0	0.06	0	0.0	0.00	0.06
	GSL002	62.0	18.9								
	GSL003	77.8	23.7	muddy sand	321	1.3	1.56	0	0.0	0.00	1.56
10	N. Mokelumne River - 3° river										
				silty mud with a clay base	7	0.0	0.00	0	0.0	0.00	0.00
	NMK002	3.4	1.0								
				at 10M solid sand with clay and corbicula and insect larvae -> we moved to the side of the channel where the sed was							
	NMK003	6.8	2.1	soft mud	2	0.0	0.00	0	0.0	0.00	0.00
11	Delta Cross-Channel - man- made canal with gate										
	SR108	S	32.8	10.0	sand	4	0.0	0.00	0	0.0	0.00
15	Ship Channel - man made off of Sacramento R.										
	DWC001	S	8.7	2.7	mud	5	0.0	0.00	0	0.0	0.00
	DWC002	S	9.8	3.0	mud	3	0.2	0.26	0	0.0	0.26
	DWC003	S	96.0	29.3	soupy, no clams, O2	0	0.0	0.00	0	0.0	0.00

Yolo Bypass (20-20.5°C)

1 **Cache C, Prospect, Lindsay Sl. - 3° sloughs, rivers**

				solid hard- pack patches with soft parts							
	PS001	9.8	3.0	too	66	0.0	0.04	0	0.0	0.00	0.04
	CAS003	10.6	3.2	goeey mud	15	0.0	0.01	0	0.0	0.00	0.01
	LS002	3.1	0.9		2	0.0	0.00	0	0.0	0.00	0.00

5 **Sacramento River - 4° river**

SR104	29.6	9.0	coarse sand, one small clam	12	0.0	0.02	0	0.0	0.00	0.02
CAS002	14.7	4.5	clay balls, baby corbicula	78	0.1	0.14	0	0.0	0.00	0.14

Carquinez Straits (19-19.5°C)

1 **Deep channel**

BEN4.1				0	0.0	0.00	23	0.1	0.77	0.77
BEN6.1				0	0.0	0.00	30	0.1	0.88	0.88
BEN8.1				0	0.0	0.00	65	0.3	1.98	1.98

2 **New York Slough**

MDS001	30.5	9.3	muddy sand	3	0.0	0.00	0	0.0	0.00	0.00
NYS001	11.7	3.6	sand	0	0.0	0.00	1	0.0	0.04	0.04
NYS002	13.8	4.2	sand	0	0.0	0.00	0	0.0	0.00	0.00

3 **SJR at Confluence**

SJOL01	2.0	0.6		60	0.0	0.05	0	0.0	0.00	0.05
SJOL02	22.6	6.9	sandy mud	14	0.1	0.09	1	0.0	0.02	0.11
SJOL03	21.7	6.6	sandy mud	18	0.0	0.04	5	0.0	0.18	0.22
SJOL06	46.6	14.2	sand	0	0.0	0.00	0	0.0	0.00	0.00

Suisun Cut (19-19.5°C)

5 **Suisun Slough to Suisun Cut**

SSS005	3.4	1.0	soupy mud	0	0.0	0.00	173	0.1	0.78	0.78
SSS006	2.7	0.8	thin O2 surface, semi- solid mud underneath	0	0.0	0.00	327	0.2	0.92	0.92
BEN415				0	0.0	0.00	89	0.1	0.63	0.63

Suisun Marsh (20-20.5°C)

1	Shallow Grizzly											
	BEN417				0	0.0	0.00	11	0.0	0.12	0.12	
2	Near Channel Shoal											
	BEN408				0	0.0	0.00	32	0.1	0.42	0.42	
5	Shallow Honker Bay											
	BEN433				0	0.0	0.00	2	0.0	0.14	0.14	
6	Suisun Slough -4°											
	SSS01	2.6	0.8	goopy mud	0	0.0	0.00	40	0.0	0.33	0.33	
	SSS02	2.4	0.7		0	0.0	0.00	13	0.0	0.16	0.16	
	SSS03	17.7	5.4	soupy mud	1	0.0	0.01	23	0.0	0.16	0.17	
	SSS04	7.6	2.3	soupy mud	0	0.0	0.00	7	0.0	0.04	0.04	
	SSS05	3.4	1.0	soupy mud	0	0.0	0.00	173	0.1	0.78	0.78	
7	Cutoff Slough -3°											
	SSS04	7.6	2.3	soupy mud	0	0.0	0.00	7	0.0	0.04	0.04	
				soupy mud, few bugs in sss, cts series								
	CTS001	1.7	0.5		0	0.0	0.00	0	0.0	0.00	0.00	
	CTS002	5.0	1.5		1	0.0	0.00	0	0.0	0.00	0.00	
8	Montezuma Slough -4°; man-made											
	MTZ001	Grizzly Bay end of slough	9.4	2.9		0	0.0	0.00	469	1.6	7.13	7.13
	MTZ002		7.0	2.1	very sticky mud with potamocorbula	0	0.0	0.00	213	1.2	6.77	6.77
	MTZ003		6.0	1.8	O2 mud on surface w/sticky clay below	0	0.0	0.00	161	0.7	3.81	3.81
	MTZ004		8.3	2.5	sandy mud and gravel peaty mud, some	5	0.0	0.02	0	0.0	0.00	0.02
	MTZ005		4.1	1.2	corbicula	0	0.0		0	0.0	0.00	0.00

	MTZ006	6.1	1.9	sandy mud with lots of corbicula	2	1.5	2.04	5	0.0	0.21	2.25
9	MTZ007	4.8	1.5		10	0.0	0.00	86	0.3	1.65	1.65
	Nurse Slough -3°										
	NRS001	9.0	2.7	soupy mud, no clams	0	0.0	0.00	3	0.0	0.02	0.02
	NRS002	5.0	1.5		0	0.0	0.00	0	0.0	0.00	0.00
	NRS003	2.3	0.7	soupy mud, no clams	0	0.0	0.00	0	0.0	0.00	0.00
	NRS004	1.5	0.5		0	0.0	0.00	1	0.0	0.00	0.00
10	Luca, Denverton Slough - 3°										
	DEN001	2.2	0.7	solid sand	0	0.0	0.00	0	0.0	0.00	0.00
	DEN002	1.4	0.4	soupy anaerobic mud	0	0.0	0.00	0	0.0	0.00	0.00

Table B3. Results of delta-wide sampling in October 2003.

Region	Station Number	Habitat Description	Depth		Sample Description	<i>Corbicula fluminea</i>		<i>Corbula amurensis</i>		TOTAL		
			ft	m		#/0.05 m ²	g AFDW/0.05m ²	#/0.05 m ²	g AFDW/0.05m ²	Grazing Rate (m/d)	Grazing Rate (m/d)	Grazing Rate (m/d)
Lower San Joaquin (>22°C)												
1a	N-Southern Middle River; 3° river											
	MIB403	S-Shallow - east shore	20.1		sand	330	1.0	2.90	0	0.0	0.00	2.90
1b	S-Southern Middle River; 3° river; near export pumps - barriers down											
	MDR07	M-	14.9		sand	250	0.3	1.00	0	0.0	0.00	1.00
2	Victoria Canal - man made canals; near export pumps											
	MDR07		14.9		sand	250	0.3	1.00	0	0.0	0.00	1.00
3	Cross Delta Canals/Woodward - Man Made Canals - Junction with Old Rvier, Middle River; near export pumps											
	MIB403		20.1		sand	330	1.0	2.90	0	0.0	0.00	2.90
4	Southern Old R.@Clifton Court; 3° river; near export pumps - barriers down											
	OLD28.5	M- Shallow - east shore	45.2		some sands; lots of shells and a few small clams - gates open?	48	2.2	7.40	0	0.0	0.00	7.40
5	Middle Old River; 3° river											
	OLD20	S - Channel	18.1		fine mud - dark	32	3.5	11.90	0	0.0	0.00	11.90
6	Coney Is. Canal - around island, near export pumps											
	CNY002	S	13.5		soft mud	69	0.0	0.10	0	0.0	0.00	0.10
7	Grant Line Canal - man made canal ; near export pumps											
	MDR07	S - at junction Middle River	14.9		sand	250	0.3	1.00	0	0.0	0.00	1.00

9	Whiskey Slough - slough; near export pumps											
				goeey mud - full grab; leaked out of door								
	ISL001	M	11.8		63	0.0	0.06	0	0.0	0.00	0.06	
10	San Joaquin R to Stockton - 4° river											
	SJR27C	S - west end of transect	38.9	dark sandy mud	4	0.0	0.01	0	0.0	0.00	0.01	

Mildred Island (>21°C)

2	Holland Cut to Old River -3° connection											
				muddy sand with <i>Corbicula</i>								
	OLD08	S	18.4		147	3.8	11.70	0	0.0	0.00	11.70	
3	Connection Sl./L. Mandeville -3° connection											
	MAN03	M	40.1	soft mud	69	2.3	7.70	0	0.0	0.00	7.70	
7	Around Mildred Island - 3° - mixed origin rivers											
		S - near eastern waist of island		hard pack mud -little penetration								
	MIB109		31.1		16	0.1	0.40	0	0.0	0.00	0.40	
8	N. Middle R. out of MI - 3° river - advective highway when pumps on											
		S - north of first meander in river, north of Mildred Is.		muddy sand layer into sticky mud								
	MIB203		18.7		243	13.0	28.30	0	0.0	0.00	28.30	
9	San Joaquin R - 4° river											
	HDC001- C		29.3	thick dark gray mud	12	0.0	0.02	0	0.0	0.00	0.02	

Franks Tract (20.5-21°C)

1	Franks Tract - inside of flooded island											
---	--	--	--	--	--	--	--	--	--	--	--	--

			finer sediment with some <i>Corbicula</i> ; <i>Egeria</i> on top of grab	42	2.0	6.80	0	0.0	0.00	6.80
			<i>Corbicula</i> on surface, some peat, no <i>Egeria</i>	48	4.3	14.50	0	0.0	0.00	14.50
			soft silty mud with filamentous algae and egeria	1	0.0	0.00	0	0.0	0.00	0.00
3			False River 3° river							
			sandy, some fine mud with at least one <i>Corbicula</i>	116	8.89	23.60	0	0.0	0.00	23.60
4			Taylor,Dutch,Sandmound Sloughs - around Franks Tract							
			SMS	100	4.5	12.30	0	0.0	0.00	12.30
			gooey with clams	283	2.3	6.60	0	0.0	0.00	6.60
			coarse sand - no visible clams	8	0.0	0.01	0	0.0	0.00	0.01
5			Old R. from Franks; 3° river							
			sandy mud with a few clams	36	1.8	6.20	0	0.0	0.00	6.20
5.5			San Joaquin R east of Threemile Sl - 4° river							
			sandy mud	16	0.1	0.20	0	0.0	0.00	0.20
			northern end of transect							

6	Potatoe Slough										
	PT005		32.8	muddy sand with clams	123	10.0	26.20	0	0.0	0.00	26.20
7	S. Fork Mokelumne - 3° river										
	SMK003	M	26.2	soupy mud	64	0.5	1.70	0	0.0	0.00	1.70
7a	Mokelumne R - 3° river										
	MKR04	S	14.3	fine grain sand with clams	65	0.0	0.05	0	0.0	0.00	0.05
8	San Joaquin R west of Threemile Sl - 4° river										
	SJR19	S	12.1	2 grabs for success; solid gravel and cobble, at least 1 clam	13	0.1	0.03	0	0.0	0.00	0.03
	SJOL15B	transect	13.4	3 grabs for success; very hard pack sand; some small clams	14	0.0	0.05	0	0.0	0.00	0.05
	SJOL20	Shallow - west shore	16.0	sand no visable clams	8	0.0	0.01	0	0.0	0.00	0.01
9	Sherman Lake - flooded island, estuarine										
	SHI002	inner island	1.2	gooey mud with some clams	27	0.4	1.30	0	0.0	0.00	1.30
	SHI003	inner island	1.1	fine mud; no visable clams	9	0.4	1.40	0	0.0	0.00	1.40

Sacramento River (19.5-20°C)

1	S. Sacramento River - 4° river										
	SR106	S	5.7	fine sand with some <i>Corbicula</i>	67	0.7	2.40	0	0.0	0.00	2.40

5 **Upper Sacramento River - 4° river**

SR108	M	9.4	fine sand with some Corbicula	80	1.4	4.70	0	0.0	0.00	4.70
Georgiana Slough										
GSL002		6.4	fine sand some Corbicula	140	0.2	0.60	0	0.0	0.00	0.60
GSL003		6.1	fine sand some Corbicula	329	0.2	0.50	0	0.0	0.00	0.50

10 **N. Mokelumne River - 3° river**

NMK002		28.2	sandy mud with peat	75	0.7	2.30	0	0.0	0.00	2.30
NMK003		13.1	sandy	2	0.0	0.00	0	0.0	0.00	0.00

11 **Delta Cross-Channel - man- made canal with gate**

SR108	S			80	1.4	4.70	0	0.0	0.00	4.70
-------	---	--	--	----	-----	------	---	-----	------	------

Yolo Bypass (20-20.5°C)

1 **Cache C, Prospect, Lindsay Sl. - 3° sloughs, rivers**

PS001		10.1	hard pack bottom - no visable clams	7	0.0	0.00	0	0.0	0.00	0.00
CAS003		10.0	soft goeey mud- no clams visable	5	0.0	0.01	0	0.0	0.00	0.01

5 **Sacramento River - 4° river**

SR104		7.0	fine goeey mud with peat	61	0.9	3.00	0	0.0	0.00	3.00
-------	--	-----	--------------------------------	----	-----	------	---	-----	------	------

CAS002	16.7	channel marker 45 not 48; very hard, packed clay hard to get grab not much in it	4	0.0	0.00	0	0.0	0.00	0.00
--------	------	--	---	-----	------	---	-----	------	------

Carquinez Straits (19-19.5°C)

1	Deep channel								
	4.1		0	0.0	0.00	332	1.0	6.27	6.27
	6.1		0	0.0	0.00	194	1.7	7.71	7.71
	8.1		0	0.0	0.00	165	0.9	4.45	4.45
2	New York Slough								
	NYS002	12.3	thick mud with some peat	0	0.0	0.00	20	0.0	0.00

Suisun Cut (19-19.5°C)

5	Suisun Slough to Suisun Cut								
	BEN415		0	0.0	0.00	289	0.8	4.13	4.13

Suisun Marsh (20-20.5°C)

1	Shallow Grizzly								
	BEN417		0	0.0	0.00	80	0.3	2.51	2.51
2	Near Channel Shoal								
	BEN408		0	0.0	0.00	160	0.6	4.46	4.46
3	Channel								
	BEN657	10.8	sandy with many <i>Corbicula</i>	42	2.0	6.17	0	0.0	0.00
5	Shallow Honker Bay								
	BEN433		0	0.0	0.00	62	0.1	0.72	0.72

Table B4. Field notes for Mildred Island spatial study.

Station Number	Location	Habitat Details	Date	Depth		Grab description, sediment; Washed sample description	Benthic Chlorophyll ($\mu\text{g}/\text{cm}^2$)	Benthic Phaeophytin ($\mu\text{g}/\text{cm}^2$)
				ft	m			
MIB001	Inner Lake	NC	28-Aug-01	10	3	fine sed, goopy on top peaty, sticky, mucky, slimy newly-settled layer, on top; lots of thistles	2.3	30.6
MIB002	Inner Lake	NW N entrance channel	28-Aug-01	8.5	2.6		3.1	25.4
MIB003	Inner Lake	N entrance channel	28-Aug-01	12	3.7	fine, smooth, silty-clay, little peat	3.1	22.2
MIB004	Inner Lake	N entrance channel	28-Aug-01	20	5.9	fine clay with slightly more sand; clams near	4.5	24.3
MIB004	Inner Lake	N entrance channel	28-Aug-01		0	surface and larger than at MIB03	4.5	24.3
MIB005-1	Inner Lake	N entrance channel	28-Aug-01	20	6.2	compact peat - grab and harpoon bounced	4.4	28.4
MIB005-2	Inner Lake	N entrance channel	28-Aug-01	19	5.8	fine silty clay		
MIB006	Inner Lake	N entrance channel	28-Aug-01	17	5.2	silty clay with lots of veg detritus surface fine with mucky veg	3.3	28.4
MIB007	Inner Lake	NW	28-Aug-01	10	3.1	detritus below	3.8	35.6
MIB009	Inner Lake	NC	28-Aug-01	15	4.7	fine silty clay	2.7	32.6
MIB010	Inner Lake	NE	29-Aug-01	11	3.4	silty clay - very nice	1.3	18.0

Station Number	Location	Habitat Details	Date	Depth ft	Depth m	Grab description, sediment; Washed sample description	Benthic Chlorophyll ($\mu\text{g}/\text{cm}^2$)	Benthic Phaeophytin ($\mu\text{g}/\text{cm}^2$)
MIB011	Inner Lake	NE	29-Aug-01	15	4.5	silty clay smooth small amount of peat	0.2	13.7
MIB012	Inner Lake	NC	29-Aug-01	14	4.3		2.4	22.7
MIB013	Inner Lake	CW	29-Aug-01		0	very gritty w/lots of peat - not chunks	0.6	13.8
MIB014	Inner Lake	CE	28-Aug-01	17	5.1	fine, dark silty clay w/ veg detritus	1.4	22.6
MIB015	Inner Lake	CC	28-Aug-01	16	4.8	fine dark silty-sandy slay w/ Tule roots	4.9	48.6
MIB016	Inner Lake	CW	28-Aug-01	12	3.8	silty clay with detritus grit	1.3	34.8
MIB018	Inner Lake	CC	29-Aug-01	5	1.5		2.5	35.7
MIB019	Inner Lake	CW	28-Aug-01	16	4.8		3.0	15.9
MIB020	Inner Lake	CC	28-Aug-01	17	5.2	fine sand/silt with little veg grit	3.9	18.1
MIB021	Inner Lake	CE	29-Aug-01	15	4.6	fine sed, veg detritus chunks at lower depth	2.5	24.1
MIB022	Inner Lake	CE	29-Aug-01	15	4.5	fine sed with peat detritus chunks	2.6	28.2
MIB023	Inner Lake	CC	29-Aug-01	14	4.2	peat with silt	1.1	14.4
MIB025	Inner Lake	SW	29-Aug-01	11	3.4	fine sed with little peat	2.9	21.1
MIB026	Inner Lake	SC	29-Aug-01	13	4	silty clay, anoxic	1.3	15.2
MIB027	Inner Lake	SC	29-Aug-01	14	4.1	fine sed with peat detritus chunks		
MIB028	Inner Lake	SE	29-Aug-01	15	4.6	silty		
MIB029	Inner Lake	SW	29-Aug-01			fine seds	0.0	10.6
MIB030	Inner Lake	SC	29-Aug-01	14	4.3	fine silt with peat chunks (25%)	1.1	21.2
MIB031	Inner Lake	SC	29-Aug-01	14	4.3	fine silt sed with peat chunks	2.9	10.2
MIB032	Inner Lake	SC	29-Aug-01	14	4.3	fine silt sed with peat chunks	1.4	12.6
MIB033	Inner Lake	SE	29-Aug-01	14	4.3	silty anoxic	0.8	9.2
MIB034	Inner Lake	SW	28-Aug-01	10	3	mucky fine sed	3.9	47.1
MIB035	Inner Lake	SC	29-Aug-01	13	3.9	peat chunks and silt	0.7	9.1
MIB036	Inner Lake	SE	29-Aug-01	12	3.7	silty	2.7	23.2
MIB100	Peripheral Channel	N	29-Aug-01	23	7.0	fine grained silty	4.6	32.5

Station Number	Location	Habitat Details	Date	Depth		Grab description, sediment; Washed sample description	Benthic Chlorophyll ($\mu\text{g}/\text{cm}^2$)	Benthic Phaeophytin ($\mu\text{g}/\text{cm}^2$)
				ft	m			
MIB131	Peripheral Channel	WN	29-Aug-01	25	7.6	sandy mud; few empty shells	2.1	16.2
MIB124	Peripheral Channel	WC	29-Aug-01	11	3.2	fine clay, slightly silty, pieces of SAV no bugs	3.1	16.3
MIB120	Peripheral Channel	SW	29-Aug-01	20	6.2	soft, fine silty clay; lots shells, some clams	1.1	8.9
MIB117	Peripheral Channel	S	29-Aug-01	33	10.1	sandy bottom, no live animals in first grab	4.6	33.6
MIB115	Peripheral Channel	SE	29-Aug-01	25	7.6	very sandy, some mud, lots of clams		
MIB109	Peripheral Channel	EC	29-Aug-01	32	9.8	sandy sed, pure sand no mud mixed in	0.8	4.6
MIB105	Peripheral Channel	EN	29-Aug-01	36	11.0	sandy, peaty mud lots of dead clams	2.6	23.8
MIB102	Peripheral Channel	NE	29-Aug-01	42	12.8	fine sand, med clams near ag diversion/pipe		
MIB104	Peripheral Channel	NE	29-Aug-01	19	5.8	silty, with clams	1.1	21.8
MIB118	Peripheral Channel	S	29-Aug-01				4.0	30.8
MIB200	N Middle River	S	28-Aug-01	39	11.9	very sandy	4.2	30.1
MIB201	N Middle River	W meander	28-Aug-01	47	14.3	clay/mud lots shells/big dead clams	1.0	23.7
MIB202	N Middle River	E meander	28-Aug-01	37	11.3	hard packed clay	0.1	1.6
MIB203	N Middle River	N	28-Aug-01	24	7.3	sand and mud		
MIB300	Empire Cut	W	28-Aug-01	24	7.2	dark clay/mud with small amt sand all oxy	4.2	33.7

Station Number	Location	Habitat Details	Date	Depth		Grab description, sediment; Washed sample description	Benthic Chlorophyll ($\mu\text{g}/\text{cm}^2$)	Benthic Phaeophytin ($\mu\text{g}/\text{cm}^2$)
				ft	m			
MIB301	Empire Cut		28-Aug-01	17	5.2	dark mud/clay, stinky, very few bugs	3.9	31.1
MIB302	Empire Cut	E	28-Aug-01	24	7.3	mud/clay, dark gray brown, oxy; few bugs	1.4	25.1
MIB400	S Middle River	N	29-Aug-01	17	5.1	thick soft fine silty clay, no compact layer	2.3	21.8
MIB401	S Middle River	W meander	29-Aug-01	22	6.7	fine sand	1.8	25.2
MIB402	S Middle River	E meander	29-Aug-01	32	9.9	fine sand/ mostly clams	2.4	11.1
MIB403	S Middle River	S	29-Aug-01	11	3.5	fine sand		
MIB500	Connection Slough	E	28-Aug-01	33	10.0	peat and shells; sandy sediment	0.8	9.0
MIB501	Connection Slough		28-Aug-01	28	8.5	dark mud w/some sand lots of clams	2.0	28.7
MIB502	Connection Slough	SW meander	28-Aug-01	13	4.1	mud with little bit of sand; all oxy	2.7	14.0
MIB503	Connection Slough	NE meander	28-Aug-01	26	7.9	sandy w/chunks of peat; lots of clams	1.5	6.0

Table B5. Density, biomass, and grazing rate for *Corbicula fluminea* in Mildred Island spatial study.

<i>Corbicula fluminea</i>								
Station Number	Date	Depth		#/0.05 m ²	g AFDW/0.05m ²	Grazing Rate (m/d)	# < 10mm/sample	# > 10mm/sample
		ft	m					
MIB001	28-Aug-01	10.0	3.0	0	0.0	0.0	0	0
MIB002	28-Aug-01	8.5	2.6	0	0.0	0.0	0	0
MIB003	28-Aug-01	12.1	3.7	1	0.4	1.0	0	1
MIB004	28-Aug-01	19.5	5.9	3	0.9	2.4	0	3
MIB005	28-Aug-01	20.2	6.2	1	0.1	0.2	0	1
MIB006	28-Aug-01	17.0	5.2	0	0.0	0.0	0	0
MIB007	28-Aug-01	10.3	3.1	0	0.0	0.0	0	0
MIB008	28-Aug-01			0	0.0	0.0	0	0
MIB009	28-Aug-01	15.4	4.7	1	0.2	0.6	0	1
MIB010	29-Aug-01	11.3	3.4	1	0.3	0.8	0	1
MIB011	29-Aug-01	14.6	4.5	0	0.0	0.0	0	0
MIB012	29-Aug-01	14.0	4.3	1	0.2	0.6	0	1
MIB013	29-Aug-01		0.0	0	0.0	0.0	0	0
MIB014	28-Aug-01	16.6	5.1	0	0.0	0.0	0	0
MIB015	28-Aug-01	15.6	4.8	0	0.2	0.6	0	0
MIB016	28-Aug-01	12.4	3.8	0	0.0	0.0	0	0
MIB017	28-Aug-01			0	0.0	0.0	0	0
MIB018	29-Aug-01	5.0	1.5	0	0.0	0.0	0	0
MIB019	28-Aug-01	15.7	4.8	0	0.0	0.0	0	0
MIB020	28-Aug-01	17.0	5.2	0	0.1	0.2	0	0
MIB021	29-Aug-01	15.1	4.6	0	0.0	0.0	0	0
MIB022	29-Aug-01	14.9	4.5	0	0.0	0.0	0	0
MIB023	29-Aug-01	13.7	4.2	0	0.0	0.0	0	0
MIB024	29-Aug-01			0	0.0	0.0	0	0
MIB025	29-Aug-01	11.3	3.4	0	0.0	0.0	0	0
MIB026	29-Aug-01	13.0	4.0	0	0.0	0.0	0	0
MIB027	29-Aug-01	13.6	4.1	0	0.0	0.0	0	0
MIB028	29-Aug-01	15.0	4.6	0	0.0	0.0	0	0
MIB029	29-Aug-01			0	0.0	0.0	0	0
MIB030	29-Aug-01	14.0	4.3	0	0.0	0.0	0	0
MIB031	29-Aug-01	14.1	4.3	0	0.0	0.0	0	0
MIB032	29-Aug-01	14.2	4.3	0	0.0	0.0	0	0
MIB033	29-Aug-01	14.1	4.3	0	0.0	0.0	0	0
MIB034	28-Aug-01	10.0	3.0	0	0.0	0.0	0	0
MIB035	29-Aug-01	12.9	3.9	0	0.0	0.0	0	0
MIB036	29-Aug-01	12.0	3.7	0	0.0	0.0	0	0
MIB100	29-Aug-01	23.0	7.0	0	0.0	0.0	0	1
MIB102	29-Aug-01	42.0	12.8	16	2.3	5.5	4	12
MIB104	29-Aug-01	19.0	5.8	7	1.2	2.9	0	7
MIB105	29-Aug-01	36.0	11.0	15	2.2	5.3	2	13
MIB109	29-Aug-01	32.0	9.8	7	1.4	3.6	0	7

Corbicula fluminea

Station Number	Date	Depth		#/0.05 m ²	g AFDW/0. 05m ²	Grazing Rate (m/d)	# < 10mm/ sample	# > 10mm/ sample
		ft	m					
MIB115	29-Aug-01	25.0	7.6	23	8.6	22.2	1	22
MIB117	29-Aug-01	33.0	10.1	0	0.0	0.0	0	0
MIB118	29-Aug-01			0	0.0	0.0	0	0
MIB120	29-Aug-01	20.3	6.2	11	2.5	6.8	0	11
MIB124	29-Aug-01	10.5	3.2	0	0.0	0.0	0	0
MIB131	29-Aug-01	25.0	7.6	31	3.0	7.7	1	30
MIB200	28-Aug-01	39.0	11.9	80	12.6	25.3	12	68
MIB201	28-Aug-01	47.0	14.3	81	12.4	24.8	0	81
MIB202	28-Aug-01	37.0	11.3	16	0.6	1.5	11	5
MIB203	28-Aug-01	24.0	7.3	57	6.4	13.6	6	51
MIB300	28-Aug-01	23.7	7.2	1	0.4	1.2	0	1
MIB301	28-Aug-01	17.0	5.2	2	0.8	2.2	0	2
MIB302	28-Aug-01	24.0	7.3	1	0.4	1.2	0	1
MIB400	29-Aug-01	16.7	5.1	11	2.6	7.0	0	11
MIB401	29-Aug-01	22.0	6.7	24	5.4	13.9	1	23
MIB402	29-Aug-01	32.4	9.9	130	6.6	13.6	108	22
MIB403	29-Aug-01	11.4	3.5	100	6.8	14.6	92	8
MIB500	28-Aug-01	32.7	10.0	8	0.9	2.6	1	7
MIB501	28-Aug-01	28.0	8.5	22	1.9	4.9	0	22
MIB502	28-Aug-01	13.3	4.1	5	0.3	0.9	1	4
MIB503	28-Aug-01	26.0	7.9	5	0.5	1.3	0	5

Table B6. Field notes for advective channels spatial studies.

Station Number	Location	Transect	Habitat Details	Date	Depth ft	Depth m	Grab description, sediment Washed sample description
SR101a	Sacramento R.	#1 Mid-Decker Is.	NW Shore	8/21/2002	21.1	6.4	sticky mud with some sand, <i>Corbicula</i>
SR101b	Sacramento R.	#1 Mid-Decker Is.	Mid-Channel	8/21/2002	21.7	6.6	coarse sand with <i>Corbula</i>
SR101c	Sacramento R.	#1 Mid-Decker Is.	SE Shore	8/21/2002	17.5	5.3	sand
SR102a	Sacramento R.	#2 N Entrance Horseshoe Bend	NW Shore	8/21/2002	9	2.7	sticky mud with <i>Corbicula</i>
SR102b	Sacramento R.	#2 N Entrance Horseshoe Bend	Mid-Channel	8/21/2002	31.2	9.5	ship channel, fine clay clumps, coarse sand, some wood debris
SR102c	Sacramento R.	#2 N Entrance Horseshoe Bend		8/21/2002	12.2	3.7	sand with shells, clams
SR102d	Sacramento R.	#2 N Entrance Horseshoe Bend	SE Shore	8/21/2002	42.3	13	sand, clams
SR103a	Sacramento R.	#3 W Entrance Threemile Sl.	Mid-Channel	8/21/2002	32.5	9.9	coarse sand 1 clam
SR103b	Sacramento R.	#3 W Entrance Threemile Sl.		8/21/2002	17.3	5.3	sand with <i>Corbicula</i>
SR103c	Sacramento R.	#3 W Entrance Threemile Sl.	Mouth of Threemile Sl.	8/21/2002	19.2	5.9	silty mud with <i>Corbicula</i>
SR104a	Sacramento R.	#4 Upstream of Threemile Sl.	NW Shore	8/21/2002	12.3	3.7	sandy mud coarse sand with some wood debris; 10+ medium size
SR104b	Sacramento R.	#4 Upstream of Threemile Sl.	Mid-Channel	8/21/2002	31.2	9.5	<i>Corbicula</i>
SR104c	Sacramento R.	#4 Upstream of Threemile Sl.		8/21/2002	21.3	6.5	sand with <i>Corbicula</i>
SR104d	Sacramento R.	#4 Upstream of Threemile Sl.		8/21/2002	19	5.8	sand with <i>Corbicula</i> and shells

SR104e	Sacramento R.	#4 Upstream of Threemile Sl.	SE Shore	8/21/2002	12.2	3.7	silty sand with clams, shells
SJR101a	San Joaquin R	#1 S of Threemile Sl.	W Shore	8/21/2002	9.2	2.8	sand with <i>Corbicula</i>
SJR101b	San Joaquin R	#1 S of Threemile Sl.	W Channel Edge	8/21/2002	2.5	0.8	muddy sand with <i>Corbicula</i>
SJR101c	San Joaquin R	#1 S of Threemile Sl.	E Channel Edge	8/21/2002	35.8	11	sand no clams
SJR101d	San Joaquin R	#1 S of Threemile Sl.	E Shore into Threemile Sl. conjunction	8/21/2002	36.7	11	silty sand no clams
SJR102b	San Joaquin R	#2 at mouth of Threemile Sl.	SJR & Threemile Sl.	8/21/2002	21.4	6.5	silty sand
SJR102c	San Joaquin R	#2 at mouth of Threemile Sl.	SJR Channel	8/21/2002	23.3	7.1	sand no clams
SJR102d	San Joaquin R	#2 at mouth of Threemile Sl.	SE of Channel N Edge of Channel;	8/21/2002	42.1	13	sand
SJR103a	San Joaquin R	#3 west of first bend	outside of bend	8/21/2002	51.9	16	sand with lots of <i>Corbicula</i>
SJR103b	San Joaquin R	#3 west of first bend	Mid-Channel S Edge of Channel;	8/21/2002	28.9	8.8	sand with a few shells
SJR103c	San Joaquin R	#3 west of first bend	inside of bend N Shore;	8/21/2002	18.7	5.7	sand with layers of mud (oxic sediment with anoxic layer)
SJR104a	San Joaquin R	#4 peak at first bend	outside of bend	8/21/2002	29.4	9	fine grain sandy mud with <i>Corbicula</i>
SJR104b	San Joaquin R	#4 peak at first bend	Mid-Channel	8/21/2002	39.8	12	sandy mud

SJR104c	San Joaquin R	#4 peak at first bend	S Shore; inside of bend	8/21/2002	20.4	6.2	dense mud with <i>Corbicula</i>
TMS101a	Threemile Sl.	#1 at Sacramento R.	S Shore	8/21/2002	42.4	13	peaty, sandy clay with <i>Corbicula</i>
TMS101b	Threemile Sl.	#1 at Sacramento R.	Mid-Channel	8/21/2002	13.5	4.1	sand
TMS101c	Threemile Sl.	#1 at Sacramento R.	N Shore S Shore-	8/21/2002	14.5	4.4	sand with clumps of mud; <i>Corbicula</i>
TMS102a	Threemile Sl.	#2 E of First Bend	outside of bend	8/21/2002	27.9	8.5	sand
TMS102b	Threemile Sl.	#2 E of First Bend	Mid-Channel N Shore -	8/21/2002	18.1	5.5	coarse sand; possibly hard pack under
TMS102c	Threemile Sl.	#2 E of First Bend	inside of bend S Shore-	8/21/2002	23.1	7	hard pack clay with surface sand layer some <i>Corbicula</i>
TMS103a	Threemile Sl.	#3 W of First Bend	outside of bend	8/21/2002	29.3	8.9	sand and shells
TMS103b	Threemile Sl.	#3 W of First Bend	Mid-Channel N Shore -	8/21/2002	45.1	14	sand
TMS103c	Threemile Sl.	#3 W of First Bend	inside of bend	8/21/2002	11.2	3.4	sand with detritus hard pack clay with surface
TMS104a	Threemile Sl.	#4 Out of Bend	SE Shore	8/21/2002	19.5	5.9	peat layer
TMS104b	Threemile Sl.	#4 Out of Bend	Mid-Channel	8/21/2002	16.1	4.9	sand
TMS104c	Threemile Sl.	#4 Out of Bend	NW Shore	8/21/2002	28.2	8.6	cemented hard sand with thin shell layer
TMS105a	Threemile Sl.	#5 Between Bends	SE Shore	8/21/2002	18.2	5.5	sand
TMS105b	Threemile Sl.	#5 Between Bends	Mid-Channel	8/21/2002	20.8	6.3	sand
TMS105c	Threemile Sl.	#5 Between Bends	NW Shore	8/21/2002	28.0	8.5	sand with rocks, shells, and some clams

TMS106a	Threemile Sl.	#6 Northern Bend	SW Shore - inside of bend	8/21/2002	19.6	6	sandy with mica flakes
TMS106b	Threemile Sl.	#6 Northern Bend	Mid-Channel	8/21/2002	46.4	14	sand with some mud and clams
TMS106c	Threemile Sl.	#6 Northern Bend	NE Shore - mouth of Sevenmile Sl.	8/21/2002	20	6.1	muddy sand
TMS107a	Threemile Sl.	#7 S of Sevenmile Sl.	W Shore	8/21/2002	23	7	sand with <i>Corbicula</i>
TMS107b	Threemile Sl.	#7 S of Sevenmile Sl.	Mid-Channel	8/21/2002	26.4	8	sand with <i>Corbicula</i>
TMS107c	Threemile Sl.	#7 S of Sevenmile Sl.	E Shore	8/21/2002	20.6	6.3	mudy peat with some sand
TMS108a	Threemile Sl.	#8 Straightaway	W Shore	8/21/2002	21	6.4	lots of sand
TMS108b	Threemile Sl.	#8 Straightaway	Mid-Channel	8/21/2002	20.1	6.1	sand with woody debris
TMS108c	Threemile Sl.	#8 Straightaway	E Shore	8/21/2002	24.8	7.6	sand
TMS109a	Threemile Sl.	#9 at San Joaquin R	SW Shore	8/21/2002	33.1	10	sand
TMS109b	Threemile Sl.	#9 at San Joaquin R	Mid-Channel	8/21/2002	19.6	6	sand with mica near inside bend of confluence
TMS109c	Threemile Sl.	#9 at San Joaquin R	NE Shore	8/21/2002	8.3	2.5	with SJR

Table B7 Summary of spatial studies in Sacramento River, San Joaquin River, and Threemile Slough.

Station	Location	Transect	Habitat	<i>Corbicula fluminea</i>				
				#/0.05 m ²	g AFDW/0.05m ²	Grazing Rate (m/d)	# < 10mm/sample	# > 10mm/sample
Number			Details					
SR101a	Sacramento R.	#1 Mid-Decker Is.	NW Shore	47	1.78	2.16	23	24
SR101b	Sacramento R.	#1 Mid-Decker Is.	Mid-Channel	27	1.68	2.04	4	23
SR101c	Sacramento R.	#1 Mid-Decker Is.	SE Shore	3	0.02	0.03	2	1
SR102a	Sacramento R.	#2 N Entrance Horseshoe Bend	NW Shore	73	1.77	2.09	47	26
SR102b	Sacramento R.	#2 N Entrance Horseshoe Bend	Mid-Channel	3	0.00	0.00	3	0
SR102c	Sacramento R.	#2 N Entrance Horseshoe Bend		4	0.17	0.25	1	3
SR102d	Sacramento R.	#2 N Entrance Horseshoe Bend	SE Shore	343	1.05	1.20	330	13
SR103a	Sacramento R.	#3 W Entrance Threemile Sl.	Mid-Channel	12	0.06	0.09	11	1
SR103b	Sacramento R.	#3 W Entrance Threemile Sl.		26	0.51	0.73	20	6
SR103c	Sacramento R.	#3 W Entrance Threemile Sl.	Mouth of Threemile Sl.	134	0.70	0.90	122	12
SR104a	Sacramento R.	#4 Upstream of Threemile Sl.	NW Shore	86	0.78	1.05	68	18

SR104b	Sacramento R.	#4 Upstream of Threemile Sl.	Mid-Channel	40	0.28	0.39	35	5
SR104c	Sacramento R.	#4 Upstream of Threemile Sl.		8	0.37	0.53	2	6
SR104d	Sacramento R.	#4 Upstream of Threemile Sl.		84	0.84	1.12	71	13
SR104e	Sacramento R.	#4 Upstream of Threemile Sl.	SE Shore	130	0.87	1.13	117	13
SJR101a	San Joaquin R	#1 S of Threemile Sl.	W Shore	14	0.13	0.19	12	2
SJR101b	San Joaquin R	#1 S of Threemile Sl.	W Channel Edge	104	0.38	0.50	99	5
SJR101c	San Joaquin R	#1 S of Threemile Sl.	E Channel Edge E Shore	13	0.01	0.02	13	0
SJR101d	San Joaquin R	#1 S of Threemile Sl.	into Threemile Sl.	2	0.00	0.00	2	0
SJR102b	San Joaquin R	#2 at mouth of Threemile Sl.	conjunction SJR & Threemile Sl.	173	0.43	0.54	168	5
SJR102c	San Joaquin R	#2 at mouth of Threemile Sl.	SJR Channel	20	0.02	0.03	24	2
SJR102d	San Joaquin R	#2 at mouth of Threemile Sl.	SE of Channel N Edge of Channel;	112	0.12	0.16	103	0
SJR103a	San Joaquin R	#3 west of first bend	outside of bend	86	0.65	0.87	58	28

SJR103 b	San Joaquin R	#3 west of first bend	Mid- Channel	0	0.00	0.00	0	0
SJR103 c	San Joaquin R	#3 west of first bend	S Edge of Channel; inside of bend	0	0.00	0.00	0	0
SJR104 a	San Joaquin R	#4 peak at first bend	N Shore; outside of bend	75	0.59	0.80	67	8
SJR104 b	San Joaquin R	#4 peak at first bend	Mid- Channel	6	0.10	0.15	4	2
SJR104 c	San Joaquin R	#4 peak at first bend	S Shore; inside of bend	31	0.39	0.55	25	6
TMS10 1a	Threemile Sl.	#1 at Sacramento R.	S Shore	147	0.09	0.11	146	1
TMS10 1b	Threemile Sl.	#1 at Sacramento R.	Mid- Channel	98	0.02	0.03	96	2
TMS10 1c	Threemile Sl.	#1 at Sacramento R.	N Shore	66	0.13	0.18	64	2
TMS10 2a	Threemile Sl.	#2 E of First Bend	S Shore- outside of bend	3	0.00	0.00	3	0
TMS10 2b	Threemile Sl.	#2 E of First Bend	Mid- Channel	0	0.00	0.00	0	0
TMS10 2c	Threemile Sl.	#2 E of First Bend	N Shore - inside of bend	3	0.15	0.22	0	3
TMS10 3a	Threemile Sl.	#3 W of First Bend	S Shore- outside of bend	229	0.01	0.01	229	0
TMS10 3b	Threemile Sl.	#3 W of First Bend	Mid- Channel	0	0.00	0.00	0	0
TMS10 3c	Threemile Sl.	#3 W of First Bend	N Shore - inside of bend	66	0.00	0.00	66	0
TMS10 4a	Threemile Sl.	#4 Out of Bend	SE Shore	26	0.00	0.00	26	0
TMS10 4b	Threemile Sl.	#4 Out of Bend	Mid- Channel	1	0.00	0.00	1	0
TMS10 4c	Threemile Sl.	#4 Out of Bend	NW Shore	4	0.00	0.00	4	0
TMS10 5a	Threemile Sl.	#5 Between Bends	SE Shore	4	0.18	0.25	2	2

TMS10 5b	Threemile Sl.	#5 Between Bends	Mid- Channel	0	0.00	0.00	0	0
TMS10 5c	Threemile Sl.	#5 Between Bends	NW Shore	2	0.15	0.21	0	2
TMS10 6a	Threemile Sl.	#6 Northern Bend	SW Shore - inside of bend	0	0.00	0.00	0	0
TMS10 6b	Threemile Sl.	#6 Northern Bend	Mid- Channel	139	1.28	1.64	127	12
TMS10 6c	Threemile Sl.	#6 Northern Bend	NE Shore - mouth of Sevenmile Sl.	200	0.01	0.01	200	0
TMS10 7a	Threemile Sl.	#7 S of Sevenmile Sl.	W Shore	5	0.00	0.00	5	0
TMS10 7b	Threemile Sl.	#7 S of Sevenmile Sl.	Mid- Channel	9	0.10	0.15	8	1
TMS10 7c	Threemile Sl.	#7 S of Sevenmile Sl.	E Shore	41	0.01	0.01	41	0
TMS10 8a	Threemile Sl.	#8 Straightawa y	W Shore	1	0.00	0.00	1	0
TMS10 8b	Threemile Sl.	#8 Straightawa y	Mid- Channel	0	0.00	0.00	0	0
TMS10 8c	Threemile Sl.	#8 Straightawa y	E Shore	5	0.07	0.10	4	1
TMS10 9a	Threemile Sl.	#9 at San Joaquin R	SW Shore	5	0.00	0.00	5	0
TMS10 9b	Threemile Sl.	#9 at San Joaquin R	Mid- Channel	0	0.00	0.00	0	0
TMS10 9c	Threemile Sl.	#9 at San Joaquin R	NE Shore	0	0.00	0.00	0	0

Table B8. Field notes for Franks Tract spatial study.

Station Number	Location	Habitat Details	Date	Depth		Grab description, sediment Washed sample description
				ft	m	
FTI 01	north interior	near False River	4/1/02	10.1	3.08	soupy mud
FTI 02	north interior	near False River	4/1/02	7.7	2.35	soupy mud with <i>Egeria</i>
FTI 03	north interior	near False River	4/1/02	8.8	2.68	soupy mud with <i>Egeria</i>
FTI 04	north interior	west north transect	4/1/02	8.1	2.47	soupy mud
FTI 05	north interior		4/1/02	8.4	2.56	soupy mud
FTI 06	north interior		4/1/02	8.7	2.65	soupy mud with <i>Egeria</i>
FTI 07	north interior	east north transect	4/1/02	8.7	2.65	muddy
FTI 08	central transect	west/near False River	4/1/02	10.6	3.23	sand and <i>Corbicula</i> ; hard; 2 grabs to succeed
FTI 09	central transect		4/1/02	8.5	2.59	soupy mud
FTI 10	central transect		4/1/02	9.1	2.77	soupy mud
FTI 11	central transect		4/1/02	NA		fine mud, peat and <i>Corbicula</i>
FTI 12	central transect		4/1/02	NA		fine mud with bits of <i>Egeria</i>
FTI 13	central transect	mid transect	4/1/02	9	2.74	fine mud with bits of <i>Egeria</i>
FTI 14	central transect		4/1/02	9.5	2.9	soupy mud
FTI 15	central transect		4/1/02	8	2.44	<i>Egeria</i> with fine mud and clams; <i>Egeria</i> with peat
FTI 16	central transect		4/1/02	7	2.13	fine mud with <i>Corbicula</i>
FTI 21	central transect		4/1/02	7	2.13	fine mud with <i>Corbicula</i>
FTI 17	central transect		4/1/02	7	2.13	muddy with <i>Corbicula</i>
FTI18	central transect		4/1/02	8.2	2.5	soupy mud
FTI 22	central transect	East; near Old River	4/1/02	NA		goopy mud
FTI 19	south interior	west	4/1/02	5	1.52	mud with clam(s)
FTI 20	south interior		4/1/02	6	1.83	slightly solid mud with bits of <i>Egeria</i>
FTI 23	south interior		4/1/02	5	1.52	sandy mud with <i>Egeria</i> , at least 1 clam
FTI 24	south interior	East; near Sandmound	4/1/02	5	1.52	mud with <i>Egeria</i> , fine mud
FLS01	False River	at San Joaquin R; meter	4/1/02	28.7	8.75	sand min center; mud on north edge

Station Number	Location	Habitat Details	Date	Depth		Grab description, sediment Washed sample description
				ft	m	
FLS02	False River		4/1/02	28	8.53	hard sand; strong currents; 5 grabs to get 1
FLS03	False River	w/in Franks	4/1/02	33	10.1	sand, peat;
FLS04	False River	w/in Franks	4/1/02	25	7.62	loose mud
FLS05	False River	w/in Franks	4/1/02	28	8.53	loose mud
FLS06	False River	nearest Old River	4/1/02	30	9.14	soupy mud; overpenetrated
SJR04	San Joaquin R.		4/2/02	34.5	10.5	sand w/some mud and mica (fools gold)
SJR05	San Joaquin R.	at 3 Mile Slough	4/2/02	47.1	14.4	sandy - 2 grabs to succeed
SJR06	San Joaquin R.		4/2/02	32.1	9.78	mud and shells/no babies
SJR07	San Joaquin R.		4/2/02	15	4.57	mud; dead adults live babies
SJR08	San Joaquin R.		4/2/02	55.1	16.8	sand w/baby clams
SJR09	San Joaquin R.	at 7 Mile Slough	4/2/02	27.5	8.38	mud -moved towards mouth of 7MS -too deep
SJR10	San Joaquin R.	at Mokelumne R.	4/2/02	40.1	12.2	mud and clams
SJR11	San Joaquin R.		4/2/02	18.5	5.64	mud and clams
SJR12	San Joaquin R.	at Potato Sl.	4/2/02	41.1	12.5	sand
SJR13	San Joaquin R.		4/2/02	38.5	11.7	muddy sand
SJR14	San Joaquin R.	in oxbow (14-17)	4/3/02	42	12.8	muddy sand, clams and shells
SJR15	San Joaquin R.		4/3/02	41.3	12.6	mud clams
SJR16	San Joaquin R.		4/3/02	45.5	13.9	sandy mud, little gravel, clams
SJR17	San Joaquin R.	Venice Cut/Middle R.	4/3/02	11.3	3.44	mud, no clams
DTC01	Dutch Slough	at San Joaquin R	4/2/02	12	3.66	soft mud
DTC02	Dutch Slough		4/2/02	6	1.83	
DTC03	Dutch Slough		4/2/02	NA		very coarse sand
DTC04	Dutch Slough		4/2/02	NA		coarse sand with peat
DTC05	Dutch Slough	at Sand Mound Sl.	4/2/02	14	4.27	solid peat with sand on surface
BBK01	Big Break	west	4/2/02	4	1.22	fine mud with <i>Corbicula</i>
BBK02	Big Break	east	4/2/02	4	1.22	v soft mud w/babies on surface
TLR01	Taylor Slough	at meter (north end)	4/2/02	18	5.49	soupy mud with 3 clams in about 10 grabs

Station Number	Location	Habitat Details	Date	Depth		Grab description, sediment Washed sample description
				ft	m	
TLR02	Taylor Slough	mid slough	4/2/02	12	3.66	goopy mud
PPR01	Piper Slough	NW end	4/1/02	25		v coarse sand, 1 <i>Corbicula</i> , current ripping
PPR02	Piper Slough	mid slough	4/1/02	8.202	2.5	goopy mud
PPR03	Piper Slough	near Sugar Barge	4/1/02	8.202	2.5	muddy, fine peat
SMS01	Sand Mound Sl.	north/at Franks Tract	4/1/02	15	4.57	fine mud;oxidized on surface with <i>Corbicula</i>
SMS02	Sand Mound Sl.	meter SMS	4/2/02	7	2.13	sandy w/lots of clams
SMS03	Sand Mound Sl.	confluence w/Dutch Sl	4/2/02	6	1.83	coarse sand with lots of clams
SMS04	Sand Mound Sl.	south/near Rock Sl.	4/2/02	9	2.74	goopy mud
MKR01	Mokelumne R.	upriver	4/2/02	11.4	3.47	sandy
MKR02	Mokelumne R.	near Franks	4/2/02	17.1	5.21	muddy
PTO01	Potato Slough	near San Joaquin R.	4/2/02	7.9	2.41	mud
PTO02	Potato Slough		4/2/02	16.4	5	mud w/shells
PTO03	Potato Slough	upslough	4/2/02	21.2	6.46	shells and mud
MDR01	N. Middle River	near Connection Sl	4/3/02	13.1	3.99	mud, peat, no clams
MIB203	N. Middle River		4/3/02	27.7	8.44	peaty, mud, clams; <i>Egeria</i> bits from washing
MIB202	N. Middle River	East of 5 Fingers	4/3/02	29.4	8.96	muddy, clams
MIB201	N. Middle River	West of 5 Fingers	4/3/02	37	11.3	peat, rocks, no clams; near Tules away from rip rap
MIB200	N. Middle River	near Mildred's Is.	4/3/02	37	11.3	clams, mud, peat
MIB500	Old River at MI	near Mildred's Is.	4/3/02	36.2	11	peaty, clams
MIB501	Old River at MI		4/3/02	23	7.01	soupy mud and clams
MIB502	Old River at MI		4/3/02	20.1	6.13	mud,peat,clams,shells
MIB503	Old River at MI	near Connection Sl	4/3/02	30	9.14	thick mud w/clams
MAN	Old R. at Mandeville	meter, near Franks T	4/1/02	29	8.84	peat with a few clams; moved to Tule side of channel
MAN02	Old R. at Mandeville	midway to Little Mand.	4/3/02	14.7	4.48	sandy mud, no clams

Station Number	Location	Habitat Details	Date	Depth		Grab description, sediment Washed sample description
				ft	m	
LMI01	Little Mandeville Is.	N boundary slough	4/3/02	11.1	3.38	mud w/peat
LMI02	Little Mandeville Is.	east inside	dropped			couldn't see a safe way into island
LMI03	Little Mandeville Is.	west inside	dropped			couldn't see a safe way into island
LMI04	Little Mandeville Is.	S boundary slough	4/3/02	6.9	2.1	peat, egeria, muc
OLD01	Old River	N. of Franks at meter	4/2/02	28.9	8.81	mud clams and trash
OLD02	Old River	east side of Franks	4/1/02	15	4.57	soupy mud
OLD03	Old River	east side of Franks	4/1/02	13	3.96	soupy mud
OLD04	Old River	at NE Middle R junction	4/1/02	10.1	3.08	soupy mud with lots of peat when washed
OLD05	Old River		4/1/02	8	2.44	soup mud
OLD06	Old River	at HOL meter	4/3/02	9	2.74	soft mud w/lots of shells and clams
OLD07	Old River	at Little Mandeville Is.	4/3/02	25	7.62	fine sand w/few animals
OLD08	Old River		4/3/02	25	7.62	soft fine silty mud; a few clams
OLD09	Old River	at confluence/ Rock Sl.	4/3/02	25	7.62	soft fine silty mud; very little sediment;no live clams
OLD11	Old River	in oxbow	4/3/02	25	7.62	very little penetration, sand washed out, few clams
OLD13	Old River	in oxbow	4/3/02	25	7.62	hard pack with few clams, very little penetration
OLD16	Old River	in oxbow	4/3/02	20	6.1	soft mud with peat - no clams
OLD19	Old River	in oxbow	4/3/02	27	8.23	sand, washing out of grab some clams,shells
OLD20	Old River	in oxbow	4/3/02	18	5.49	soft mud with small clams
OLD21	Old River	in oxbow	4/3/02	25	7.62	sandy mud with lots of clams
OLD24	Old River	southern boundary	4/3/02	27	8.23	sand and clams (some dead)
FSH01	Fisherman's Cut	N Fisherman's Cut	4/2/02	13.1	3.99	mud; loosely packed
FSH02	Fisherman's Cut	S at meter	4/2/02	18.8	5.73	mud
TMS01	Threemile Slough	mouth at Sacramento R.	4/2/02	25.3	7.71	mud
TMS02	Threemile Slough	inside of bend	4/2/02	29.3	8.93	sand
TMS03	Threemile Slough	towards San Joaquin R.	4/2/02	30.3	9.24	sand

Table B9. Data summary for Franks Tract spatial study.

Station	Location	Depth		<i>Corbicula fluminea</i>				
		ft	m	#/0.05 m ²	g AFDW/ 0.05m ²	Grazing Rate (m/d)	# < 10mm/ sample	# > 10mm/ sample
FTI 01	north interior	10.1	3.08	7	1.2	1.7	0	7
FTI 02	north interior	7.7	2.35	6	0.0	0.0	6	0
FTI 03	north interior	8.8	2.68	32	0.7	1.1	28	4
FTI 04	north interior	8.1	2.47	26	0.7	1.0	23	3
FTI 05	north interior	8.4	2.56	27	1.8	2.3	15	12
FTI 06	north interior	8.7	2.65	59	0.2	0.3	58	1
FTI 07	north interior	8.7	2.65	12	0.6	0.9	8	4
FTI 08	central transect	10.6	3.23	17	1.4	1.9	5	12
FTI 09	central transect	8.5	2.59	42	2.1	2.6	32	10
FTI 10	central transect	9.1	2.77	38	2.6	3.3	20	18
FTI 11	central transect	NA		10	1.2	1.7	6	4
FTI 12	central transect	NA		20	0.0	0.0	20	0
FTI 13	central transect	9	2.74	32	0.0	0.0	32	0
FTI 14	central transect	9.5	2.9	26	1.1	1.4	19	7
FTI 15	central transect	8	2.44	16	2.1	2.9	8	8
FTI 16	central transect	7	2.13	28	3.1	4.0	15	13
FTI 17	central transect	7	2.13	14	0.0	0.0	14	0
FTI 18	central transect	8.2	2.5	44	4.9	6.2	19	25
FTI 19	south interior	5	1.52	3	0.4	0.6	1	2
FTI 21	central transect	7	2.13	91	7.0	8.0	47	44
FTI 22	central transect	NA		38	1.2	1.7	32	6
FTI 23	south interior	5	1.52	171	3.0	3.7	163	8
FTI 24	south interior	5	1.52	3	0.0	0.0	3	0
FLS01	False River	28.7	8.75	38	0.0	0.0	38	0
FLS02	False River	28	8.53	4	0.2	0.3	3	1
FLS03	False River	33	10.1	59	2.1	2.5	45	14
FLS04	False River	25	7.62	27	0.3	0.4	25	2
FLS05	False River	28	8.53	27	1.4	1.9	17	10
FLS06	False River	30	9.14	20	0.2	0.2	19	1
SJR04	San Joaquin R.	34.5	10.5	4	0.1	0.2	3	1
SJR05	San Joaquin R.	47.1	14.4	9	1.0	1.5	3	6
SJR06	San Joaquin R.	32.1	9.78	41	3.3	4.2	16	25
SJR07	San Joaquin R.	15	4.57	68	2.1	2.5	50	18
SJR08	San Joaquin R.	55.1	16.8	25	0.5	0.6	19	6
SJR09	San Joaquin R.	27.5	8.38	10	0.8	1.1	2	8
SJR10	San Joaquin R.	40.1	12.2	70	5.2	6.1	34	36
SJR11	San Joaquin R.	18.5	5.64	13	1.3	1.8	5	8
SJR12	San Joaquin R.	41.1	12.5	5	0.1	0.2	4	1
SJR13	San Joaquin R.	38.5	11.7	34	1.1	1.5	25	9
SJR14	San Joaquin R.	42	12.8	73	1.0	1.3	64	9
Station	Location	Depth		<i>Corbicula fluminea</i>				

		ft	m	#/0.05 m ²	g AFDW/ 0.05m ²	Grazing Rate (m/d)	# < 10mm/ sample	# > 10mm/ sample
LMI01	Little Mandeville Is.	11.1	3.38	3	0.0	0.0	3	0
LMI04	Little Mandeville Is.	6.9	2.1	0	0.0	0.0	0	0
LFT01	Little Franks Tract			2	0.0	0.0	2	0
OLDR	Old River	28.9	8.81	2	0.0	0.0	2	0
OLD02	Old River	15	4.57	13	0.4	0.6	9	4
OLD03	Old River	13	3.96	20	1.1	1.5	9	11
OLD04	Old River	10.1	3.08	17	0.0	0.0	17	0
OLD05	Old River	8	2.44	4	0.0	0.0	4	0
HOL	Old River	9	2.74	76	4.2	4.9	54	22
OLD07	Old River	25	7.62	50	0.7	0.9	47	3
OLD08	Old River	25	7.62	28	0.7	1.0	23	5
OLD09	Old River	25	7.62	2	0.2	0.2	1	1
OLD11	Old River	25	7.62	37	0.4	0.6	34	3
OLD13	Old River	25	7.62	7	0.0	0.0	7	0
OLD16	Old River	20	6.1	12	0.0	0.0	12	0
OLD19	Old River	27	8.23	44	0.2	0.3	42	2
OLD20	Old River	18	5.49	90	1.1	1.5	84	6
OLD21	Old River	25	7.62	187	4.2	4.1	163	24
OLD24	Old River	27	8.23	241	15.3	13.7	160	81
FSH01	Fisherman's Cut	13.1	3.99	1	0.0	0.0	1	0
FISH	Fisherman's Cut	18.8	5.73	4	0.0	0.0	4	0
TMS01	Threemile Slough	25.3	7.71	36	0.8	1.1	30	6
TMS02	Threemile Slough	29.3	8.93	1	0.0	0.0	1	0
TMS03	Threemile Slough	30.3	9.24	1	0.0	0.0	1	0

Table C1. Phytoplankton community composition and percent biovolume by species in Mildred Island and Franks Tract and by taxonomic division for all samples. Only species that made up >1% of total biovolume are listed.

Percent of total		
biovolume	Division	Genus species
Mildred Island		
39%	Bacillariophyta	<i>Cyclotella atomus</i>
15%	Cryptophyta	<i>Plagioselmis sp.</i>
13%	Cyanophyta	<i>Cyanobium sp.</i>
10%	Eustigmatophyta	<i>Nannochloropsis sp.</i>
7%	Cryptophyta	<i>Teleaulax amphioxeia</i>
6%	Bacillariophyta	<i>Skeletonema potamos</i>
3%	Chlorophyta	<i>Choricystis sp.</i>
1%	Cyanophyta	<i>Aphanothece sp.</i>
Franks Tract		
17%	Bacillariophyta	<i>Actinocyclus normanii</i>
15%	Bacillariophyta	<i>Cyclotella striata</i>
7%	Bacillariophyta	<i>Cyclotella atomus</i>
3%	Cryptophyta	<i>Teleaulax amphioxeia</i>
3%	Bacillariophyta	<i>Melosira varians</i>
3%	Bacillariophyta	<i>Skeletonema potamos</i>
2%	Bacillariophyta	<i>Aulacoseira granulata</i>
2%	Bacillariophyta	<i>Cyclotella meneghiniana</i>
2%	Bacillariophyta	<i>Aulacoseira islandica</i>
Percent biovolume by taxonomic division for all samples		
53%	Bacillariophyta	
25%	Cryptophyta	
9%	Eustigmatophyta	
8%	Cyanophyta	
3%	Chlorophyta	
2%	Chrysophyta, Pyrrophyta, Euglenophyta	

Table C2. Zooplankton community composition and percent biomass for Mildred Island, Franks Tract and all samples combined.
 Taxa that made up < 0.5% are not shown.

MILDRED ISLAND					
Copepods	49%	Herbivorous Rotifers	49%	Cladocerans	2%
<i>Pseudodiaptomus forbesi</i>	36.4%	<i>Hexarthra</i> sp.	17.4%	<i>Diaphanosoma brachyurum</i>	1.6%
Nauplii	5.2%	Unidentified	11.0%	<i>Bosmina longirostris</i>	0.6%
<i>Limnoithona tetraspina</i>	3.1%	<i>Brachionus</i> sp.	8.1%	Other species	<0.5%
<i>Sinocalanus doerrii</i>	2.1%	<i>Filinia</i> sp.	4.7%		
<i>Acanthocyclops vernalis</i>	1.4%	<i>Monostyla</i> sp.	1.9%		
<i>Eurytemora affinis</i>	<0.5%	<i>Synchaeta bicornis</i>	1.8%		
		<i>Polyarthra</i> sp.	1.3%		
		<i>Synchaeta</i> sp.	1.3%		
		<i>Keratella</i> sp.	0.9%		
		<i>Rotaria</i> sp.	0.7%		
		Other species	<0.5%		
FRANKS TRACT					
Copepods	80%	Herbivorous Rotifers	8%	Cladocerans	11%
<i>Sinocalanus doerrii</i>	35.6%	Unidentified	7.0%	<i>Bosmina longirostris</i>	4.9%
<i>Pseudodiaptomus forbesi</i>	29.0%	Other species	<0.5%	<i>Daphnia</i> spp.	2.6%
Nauplii	11.3%			<i>Graptolaberis</i> sp.	1.4%
<i>Eurytemora affinis</i>	2.2%			<i>Diaphanosoma brachyurum</i>	0.9%
<i>Acanthocyclops vernalis</i>	1.7%			Unidentified	0.7%
<i>Limnoithona tetraspina</i>	0.6%			Other species	<0.5%
ALL SAMPLES					
Copepods	63%	Herbivorous Rotifers	31%	Cladocerans	6%

Table C3. Summary of intradaily periods of variability for three water quality constituents and environmental forcings at Mildred Island, Summer-Fall 2001. Periods of variability were identified using power spectra calculated for upper water column measurements of each quantity (see Figure C15). Where two values are listed, two periods appeared significant, and the order of periodicities reflects relative power.

Quantity	Dominant intradaily period [h]		
	North	South	MI
Specific Conductance (SC)	12.4/6.2	24.0	-
Water Temperature (T)	24.0	24.0	-
Chlorophyll <i>a</i> (Chl <i>a</i>)	24.0/12.4	24.0	-
Streamwise Velocity (<i>u</i>)	12.4	12.4/24.0	-
Transverse Velocity (<i>v</i>)	12.4	24.0	
Wind Speed (U_{wind})	-	-	24.0
Heat flux (ΔH)	-	-	24.0

Table C4. Scaling expressions derived for estimating scalar oscillation magnitudes associated with various periodic processes.

Scaling expression	Description
$\Delta C_{adv-x} \sim u' \frac{\tau}{\Pi} \frac{\partial C}{\partial x}$	Scalar oscillation magnitude associated with streamwise advection
$\Delta C_{adv-y} \sim v' \frac{\tau}{\Pi} \frac{\partial C}{\partial y}$	Scalar oscillation magnitude associated with transverse advection
$\Delta C_{mix} \sim u'_* \frac{\tau}{\Pi} \left(\frac{0.067 \bar{h} (1 + 3.33 Ri_g)^{-3/2}}{\Delta z} \right) \frac{\partial C}{\partial z}$	Scalar oscillation magnitude associated with vertical turbulent mixing
$\Delta T_{heat} \sim \frac{\Delta H'}{\rho_o c_p \bar{h}} \left(\frac{\tau}{\Pi} \right)$	Temperature oscillation magnitude associated with atmospheric heating
$\Delta SC_{evap} \sim \frac{SC_o}{h_o} \left(E'_v \frac{\tau}{\Pi} \right)$	Specific conductivity oscillation magnitude associated with evaporation
$\Delta Chl_{growth} \sim Chl_o \left[\exp \left(\frac{\tau}{\Pi} \mu' \right) - 1 \right]$	Chlorophyll <i>a</i> oscillation magnitude associated with phytoplankton growth
$\Delta Chl_{zp} \sim Chl_o \left[\exp \left(\frac{\tau}{\Pi} \mu'_{zp} \right) - 1 \right]$	Chlorophyll <i>a</i> oscillation magnitude associated with zooplankton grazing

Table C5. Scaling based estimates of scalar oscillation amplitude (ΔC) caused by individual processes and at individual periods/SCs for either SC, T, or Chl *a*, as indicated. ΔC_{adv-x} , ΔC_{adv-y} , ΔC_{mix-cs} , $\Delta C_{mix-wind}$, ΔC_{evap} , ΔC_{heat} , ΔC_{growth} , and ΔC_{zp} are the oscillation amplitudes caused by streamwise advection, transverse advection, vertical mixing caused by current shear, vertical mixing caused by wind, evaporation (for SC only), atmospheric heating (for T only), growth (for Chl *a* only), and zooplankton grazing (for Chl *a* only), respectively. $\Sigma\Delta C$ is the sum of all ΔC s for a particular constituent and period. "Obs. ΔC " is the order of magnitude ΔC for the observations. Gray shading indicates that that process and period was either irrelevant or insignificant and consequently not shown.

Scalar, C	Location	Period, [h]	ΔC_{adv-x}	ΔC_{adv-y}	ΔC_{mix-cs}	$\Delta C_{mix-wind}$	ΔC_{evap}	ΔC_{heat}	ΔC_{growth}	ΔC_{zp}	$\Sigma\Delta C$	Obs. ΔC	
SC [mS cm ⁻¹]	North	6.2			7.6x10 ⁻⁵						7.6x10 ⁻⁵		
		12.4	0.02								0.02	Order[0.01]	
		24.0				5.9x10 ⁻⁴	4.4x10 ⁻⁵				6.3x10 ⁻⁴		
	South	6.2											
		12.4	2.1x10 ⁻³		4.0x10 ⁻⁴							2.5x10 ⁻³	
		24.0	3.1x10 ⁻³	1.8x10 ⁻³	1.2x10 ⁻³	3.9x10 ⁻³	6.1x10 ⁻⁵					0.01	Order[0.01]
T [deg C]	North	6.2			1.1x10 ⁻³						1.1x10 ⁻³		
		12.4	0.25								0.25		
		24.0				8.6x10 ⁻³		0.47				0.48	Order[1]
	South	6.2											
		12.4	0.066		0.011							0.077	
		24.0	0.10	0.10	0.032	0.11		0.62				0.96	Order[1]
Chl <i>a</i> [μg L ⁻¹]	North	6.2			0.045						0.045		
		12.4	1.4								1.4	Order[1]	
		24.0				0.35			0.41		0.76		
	South	6.2											
		12.4	0.39		0.27							0.66	
		24.0	0.59	1.3	0.8	2.7			1.6	0.27	7.3	Order[1-10]	

Table C6. Summary statistics of chlorophyll *a* concentrations at Franks Tract for all timeseries from 4/12/02 to 5/20/02.

	mean	highest daily average	lowest daily average
FALSE chl	9.8	20.2	3.4
FISH chl	9.7	20.2	5.1
FTW chl	8.5	13.7	5.7
OLD chl	8.1	16.0	5.1
SMS chl	7.9	15.7	5.4
FTE chl	6.9	12.7	4.5
MAN chl	6.4	11.8	2.8
HOL chl	6.2	12.0	3.5
TYL chl	5.5	7.9	4.2

concentration in $\mu\text{g/l}$

Table C7. Summary of spectral patterns for chl *a* and OBS at Franks Tract, 2002.

	diurnal	semi	mixed	unclear
TYL	chl		obs	
OLD		chl+obs		
FTW		obs	chl	
MAN			chl+obs	
FTE			chl	obs
HOL			obs	chl
FALSE	chl	obs		
FISH	obs		chl	
SMS			obs	chl

* bold parameters are most significant

Table C8. Phytoplankton species composition at Franks Tract, 2002.
(percentage based on μ^3/mL)

Date	10-Apr-02						1-May-02						21-May-02						12-Jun-02						9-Jul-02						
* Station	FTE	FTW	HOL	OLD	SMS	FAL	FTE	FTW	HOL	OLD	SMS	FAL	FTE	FTW	HOL	OLD	SMS	FAL	FTE	FTW	HOL	OLD	SMS	FAL	FTE	FTW	HOL	OLD	SMS	FAL	
** Taxon																															
Plagioselmis prolonga var. nordica	39%	9%	7%	22%	37%	16%	23%	18%	15%	17%	17%	4%	56%	24%	11%	18%	28%	45%	26%		24%	25%	19%	28%	52%	49%	21%	1%		12%	
Nannochloropsis	3%	1%	3%	6%	8%	2%	5%		6%	2%	12%	2%	17%	14%		11%	22%	16%	7%	87%	33%	40%	15%	14%	11%	12%	39%	7%	3%	60%	
Rhinomonas	4%	2%	4%	5%	7%	2%	26%	23%	10%	5%	11%	3%	9%	39%	8%	3%	2%	13%	16%	1%	3%	21%	5%	2%	32%	27%	13%	0%		6%	
Cyclotella striata	38%	30%	66%	45%		43%	18%	3%		4%									10%	1%	1%	9%	5%	14%						11%	
Actinocyclus normanii		50%	8%		25%	18%	8%	27%	7%	20%	37%	69%		10%					4%	6%						3%					
Teleaulax amphioxeia	1%		1%						10%	10%	8%				60%	1%		14%	12%		27%		47%	25%			19%			9%	
Cyclotella atomus	2%	1%	3%	1%	4%	1%	9%	7%	18%	28%	11%	11%	2%	13%	4%	5%	18%	11%	11%		10%		4%	8%	0%	7%		0%	12%		
Melosira varians	3%		4%	18%	9%	17%						1%	13%											8%							
Aphanizomenon flos-aquae																									1%			69%			
Aulacoseira islandica							8%					2%					56%														
Rhodomonas marina					1%						1%							22%	1%									3%	21%		
Skeletonema potamos	0%	0%	1%	1%		1%	1%	0%		3%	2%	1%		0%				1%												15%	
Stephanodiscus									15%																						
*** Other	10%	7%	5%	1%	10%	0%	2%	22%	8%	12%	1%	7%	4%	0%	16%	6%	7%	1%	14%	5%	3%	4%	6%	1%	5%	1%	4%	1%	59%	13%	

* FTE: Franks Tract East, FTW: Franks Tract West, HOL: Holland Cut, OLD: Old River, SMS: Sand Mount Slough, FAL: False River

** Taxon shown represent those which were $\geq 15\%$ of the total composition at a minimum of one station on one date.

*** Other includes up to 55 other taxon that were always $< 15\%$ of the total composition at a particular station and date.

Table SED1. Delta transects data.

Station #	Location	Latitude	Longitude	Time local	Dissolved							Particulate			
					Chlorinity mmol/l	NO3+NO2 µmol/l	PO4 µmol/l	SiO4 µmol/l	Se IV nmol/l	Se VI nmol/l	Se -II+0 nmol/l	Total Se nmol/l	TSM mg/l	Chl a µg/l	Total Se nmol/l
Jul 12-13 '00															
1	SJR	37 56.97'	121 20.17'	1025	1.429	163.79	5.6	146.8	1.214	6.487	3.254	10.955	42.245	16.7	0.561
2	Cal R	37 57.99'	121 22.08'	1200	2.491	131.46	4.82	134.5	1.18	6.291	1.656	9.127	21.793	14.9	0.42
3	14 M SI	37 59.74'	121 25.30'	1245	5.139	129.46	5.92	126.2	1.266	5.534	1.549	8.349	19.192	8.32	0.386
4	Ward C	38 02.04'	121 28.94'	845	0.807	15.14	1.37	246.5	0.082	0.661	0.463	1.206	8.268	2.24	0.16
5	Venice C	38 03.08'	121 31.50'	1010	0.999	12.96	1.55	235.8	0	0.683	0.789	1.472	7.257	2.34	0.081
6	Moke R	38 06.07'	121 35.45'	1135	2.172	15.41	1.5	264.5	0.121	0.762	0.227	1.11	13.352	2.28	0.114
7	3 M SI	38 05.14'	121 40.92'	1255	0.823	19.35	1.73	251.9	0.27	0.56	0.419	1.249	22.812	3.84	0.174
8	Mild I S	37 58.53'	121 31.28'	1410	2.035	18.53	1.49	244.2	0.146	0.967	0.362	1.475	11.052	13.4	0.235
9	Mild I C	37 59.26'	121 31.45'	1505	0.814	16.9	1.54	242.7	0.233	0.838	0.363	1.434	12.536	8	0.173
10	Mild I N	37 59.74'	121 30.79'		3.104	16.7	1.58	251.9	0.08	0.544	0.546	1.17	9.621	2.89	0.135
11	Frank T W	38 02 98'	121 37.73'	1750	3.992	19.45	1.86	227.1	0.127	0.792	0.628	1.547	19.475	3.24	0.17
Jan 22 '03															
1	Benicia	38 02.77	122 06.27	835	136.3	28.76	0.86	362.8	0.201	0.865	0.962	2.028	87.266	0.88	0.298
2		38 03.71	122 00.70	952	92	27.07	0.92	375.7	0.141	1.113	1.097	2.351	77.373	0.56	0.571
3		38 02.66	121 54.66	1050	0.45	27.89	0.55	385.4	0.074	0.724	0.608	1.406	75.686	0.74	0.364
4		38 01.27	121 48.50	1140	0.5	34.92	0.32	370.2	0.143	1.14	0.812	2.095	45.1	0.55	0.331
5	Rio Vista	38 09.08	121 04.25	1335	0.17	21.35	0.21	419.7	0.129	1.263	0.717	2.109	47.021	0.78	0.225
6		38 05.30	121 40.77	1430	0.28	30.81	0.48	401.8	0.114	0.827	0.676	1.617	48.759	0.49	0.233
7		38 05.96	121 34.90	1505	0.14	22.45	0.33	431.4	0.12	1.149	0.477	1.746	41.501	0.46	0.141
8		38 02.02	121 28.94	1610	0.66	84.5	0.45	390.2	0.135	1.08	0.506	1.721	19.105	0.46	0.108
9		37 59.73	121 25.30	1640	2.47	119.1	4.62	378.4	0.278	3.599	0.546	4.423	15.813	1.54	0.11
10		37 57.80	121 21.90	1720	3.27	110.89	8.7	410.7	0.707	5.797	0.488	6.992	14.972	2.91	0.058
11	Stockton	37 56.99	121 20.17	1745	3.34	145.53	13.2	283.1	0.608	6.925	0.053	7.586	13.355	5.55	0.063

Apr 22-23 '03

1 Benicia	38 02.77	122 06.89	928	64.3	31.7	2.28	278.2	0.272	1.067	0.257	1.596	25.828	1.17	0.109
2	38 03.83	122 03.65	1010	52.7	28.35	1.69	296.8	0.332	1.118	0.072	1.522	38.468	1.69	0.221
3	38 03.55	121 59.37	1050	13.7	30.12	1.27	294.5	0.212	1.231	0.314	1.757	41.248	2.29	0.201
4	38 02.66	121 54.16	1135	2.71	26.87	0.6	327.6	0.228	1.067	0.179	1.474	54.826	1.69	0.191
5 Antioch	38 01.27	121 48.50	1220	0.83	18.23	0.7	321.3	0.14	1.061	0.33	1.531	28.374	5.43	0.189
6 Rio Vista	38 09.09	121 41.24	1410	0.21	17.58	0.52	382.5	0.281	1.067	0.393	1.741	23.663	1.73	0.159
7 3 mile SI	38 05.34	121 40.73	1510	0.28	20.89	3.1	322.5	0.208	1.181	0.069	1.458	18.227	4.08	0.078
8	38 05.96	121 35.05	1555	0.39	28.98	3.4	320.5	0.237	1.823	0.283	2.343	12.981	3.93	0.102
9	38 02.01	121 28.89	1650	1.79	75.32	3.59	228.9	0.697	9.371	1.471	11.539	21.969	23	0.363
10	37 59.73	121 25.27	1720	1.76	78.45	3.69	228	0.893	9.576	1.41	11.879	19.248	11.3	0.212
11 Stockton	37 56.94	121 20.18	935	1.17	74.81	7.12	243.7	1.017	10.23	1.512	12.761	17.147	6.86	0.243
12 SAV	38 01.53	121 36.51	1140	0.49	0.98	0.21	156.2	0.102	0.041	1.124	1.267	3.634	0.75	0.017
13 Frank's T	38 01.97	121 35.36	1155	0.27	12.25	0.32	298.3	0.131	1.144	0.019	1.294	8.199	1.73	0.028

Jun 17 '03

1, 1m	8.1 38 01.813	122 09.073	525	218.6	15.53	3.83	191.6	0.332	0.743	0.978	2.053	23.612	0.73	0.064
1, 14m				277.1	15.02	5.51	159.8	0.351	0.99	0.264	1.605	34.55	1.23	0.121
2	38 03.279	122 04.562	610	131.2	14.18	4.56	235	0.519	0.724	0.785	2.028	29.579	0.93	0.145
3	38 03.754	122 01.052	640	67.4	15.71	4.72	242.2	0.358	0.99	0.487	1.835	47.245	0.89	0.127
4	38 03.596	121 58.713	700	36.3	12.45	4.4	269.2	0.315	1.054	0.177	1.546	53.376	1.32	0.235
5 Antioch	38 01.269	121 48.509	800	2.09	12.25	3.93	301.5	0.251	0.709	0.675	1.635	34.752	2.1	0.176
6 Rio Vista	38 09.088	121 41.222	940	0.14	10.22	3.1	320.6	0.205	0.745	0.311	1.261	28.72	1.32	0.165
7 3 mile SI	38 05.333	121 40.718	1025	0.28	11.86	3.4	307.3	0.242	0.249	1.141	1.632	23.828	1.99	0.151
8	38 05.958	121 35.066	1100	0.21	10.19	3.59	314.8	0.245	0.439	0.603	1.287	14.708	1.16	0.092
9	38 02.002	121 28.896	1150	0.21	12.51	3.69	282.2	0.281	0.79	0.095	1.166	9.352	1.49	0.058
10	37 59.73	121 25.290	1220	1.93	50.83	3	191.5	1.794	4.677	3.184	9.655	15.909	3.98	
11 Stockton	37 57.065	121 20.148	1255	1.53	73.33	7.12	192.6	2.178	4.059	3.418	9.655	40.39	27.1	0.528

Oct 10, '03

1 Benicia	38 02.578	122 06.63	646	204.5	17.73	5.84	209.5	0.409	0.831	0.207	1.447	50.753	1.51	0.313
2	38 03.802	122 03.760	722	170	17.23	6.14	232.7	0.322	0.851	0.087	1.26	37.756	lost	0.176

3	38 03.831	122 01.858	740	136.2	18.25	5.93	249	0.384	0.867	0.328	1.579	33.482	1.43	0.245
4	38 03.270	121 56.999	820	83.4	18.06	5.32	261.3	0.286	0.665	0.257	1.208	28.254	1.39	0.164
5	38 02.688	121 53.198	850	50.1	15.44	5.35	285.2	0.269	0.592	0.003	0.864	24.111	1.41	0.121
6 Antioch	38 01.246	121 48.533	925	22.6	12.28	4.85	289.8	0.252	0.785	0.017	1.054	17	1.6	0.152
7 Rio Vista	38 09.165	121 41.271	1050	0.3	15.72	4.61	332	0.494	0.581	0.333	1.408	18.158	2.49	0.095
8 3 mile SI	38 05.382	121 40.701	1135	3.9	15.42	4.67	316.4	0.304	0.292	0.561	1.157	10.576	1.67	0.108
9	38 05.900	121 35.201	1210	1.1	14.67	4.62	326.5	0.319	0.374	0.815	1.508	7.225	1.62	0.102
10	38 01.979	121 28.920	1250	1	27.32	4.7	308.5	0.345	0.943	0.238	1.526	6.527	2.88	0.126
11	37 59.734	121 25.264	1325	2.3	56.79	5.18	318.6	2.479	3.751	0.445	6.675	16.473	5.56	0.179
12 Stockton	37 55.973	121 20.188	1400 S-51		55.7	6.47	380	1.958	4.762	0.008	6.728	14.526	14	0.233
Jan. 15, '04														
1 Benicia	38 02.427	122 06.955	905	130.7	18.75	3.83	184.3	0.51	1.432	0.098	2.04	29.263		0.181
2	38 03.791	122 03.763	930	93.5	16.76	4.72	279.5	0.378	1.396	0.406	2.18	38.111		0.124
3	38 03.692	122 00.917	1000	13.65	23.32	8.44	327.1	0.358	1.163	0.099	1.62	35.135		0.255
4	38 03.403	121 57.427	1025	4.63	24.82	8.08	351.8	0.268	1.621	0	1.82	46.287		0.137
5	38 02.685	121 53.206	1055	0.79	26.39	8.48	358.2	0.407	1.148	0.317	1.872	37.408		0.185
6 Antioch	38 01.294	121 48.449	800	0.86	33.23	9.21	354.2	0.473	0.936	0.03	1.439	36.605		0.337
7 Rio Vista	38 09.088	121 41.329	1145	0.2	15.86	10.3	366.4	0.458	1.099	0.132	1.689	31.91		0.169
8 3 mile SI	38 05.305	121 40.685	1225	0.49	29.08	12.3	354.2	0.409	0.802	0.293	1.504	34.076		0.254
9	38 05.900	121 35.201	1255	0.34	23.99	13.7	354.7	0.352	1.211	1.231	2.794	26.223		0.137
11	37 59.730	121 25.266	1345	1.05	69.73	14.6	335.8	0.52	4.28	1.523	6.323	17.631		0.14
12 Stockton	37 56.958	121 20.180	1420	2.68	84.56	16.7	329.5	0.601	4.587	1.433	6.621	23.874		0.3

Table SED2. Summary of Selenium Data for the Delta and Suisun Bay

Location	Dissolved Total Se (nmol/L)	Suspended Particles		Sediments*	
		Total Se (nmol/L)	Se:C Atomic	Total Se (nmol/g)	Se:C Atomic
Suisun Bay 1997-1999	1.89 ± 0.59	0.183 ± 0.055	5.41x10 ⁻⁶ ± 2.13x10 ⁻⁶	3.50 ± 0.37	2.97x10 ⁻⁶ ± 0.75x10 ⁻⁶
Delta from 1998-2004	3.47 ± 3.16	0.195 ± 0.174	5.9x10 ⁻⁶ ± 6.7x10 ⁻⁶	5.94 ± 0.44	2.63x10 ⁻⁶ ± 0.57x10 ⁻⁶
Mildred I. 1998-2000	1.61 ± 0.60	0.159 ± 0.042	2.79x10 ⁻⁶ ± 0.20x10 ⁻⁶	10.31 ± 0.06	1.66x10 ⁻⁶ ± 0.22x10 ⁻⁶
2001 Mildred Island Process Study					
Chl Max	2.08 ± 0.14	0.158 ± 0.028	1.81x10 ⁻⁶ ± 0.70x10 ⁻⁶	10.72 ± 0.46	1.06x10 ⁻⁶ ± 0.05x10 ⁻⁶

* Note: Sediment results are for 0-2 cm

Table SED3. Monthly monitoring of dissolved and particulate selenium in Suisun Bay (USGS Bivalve Station 8.1).

Date	Salinity (ppt, meter)	Dissolved		Particulate		Total Se µg/g	SD µg/g
		Total Se nmol/l	SD nmol/l	Total Se nmol/l	SD nmol/l		
1/11/2000	14.43	1.56	0.05	0.23	0.01	1.26	0.03
2/9/2000	2.00	1.73	0.04	0.35	0.01	0.26	0.01
3/8/2000	0.07	1.56	0.01	0.08	0.00	0.41	0.02
4/5/2000	4.50	1.77	0.04	0.93	0.05	0.47	0.02
5/17/2000	3.00	2.04	0.04	0.95	0.04	0.39	0.02
6/14/2000	6.15	1.90	0.05	0.42	0.02	4.55	0.16
7/12/2000	9.27	2.01	0.06	0.25	0.01	0.41	0.01
8/9/2000	8.99	1.74	0.04	0.13	0.01	0.36	0.02
9/6/2000	8.00	1.96	0.01	0.11	0.01	0.62	0.03
10/11/2000	9.00	1.45	0.10	0.15	0.01	0.36	0.02
11/8/2000	9.00	1.87	0.05	0.20	0.01	0.52	0.03
12/13/2000	13.00	1.54	0.01	0.11	0.00	0.43	0.00
2/7/2001	6.00	1.75	0.05	0.14	0.00	0.41	0.01
2/27/2001	2.00	1.49	0.13	0.15	0.00	0.29	0.00
3/28/2001	4.30	2.20	0.03	0.48	0.01	0.27	0.01
4/25/2001	6.06	1.98	0.02				
5/22/2001	7.00	2.04	0.08				
6/20/2001	9.00	2.88	0.02				
7/18/2001	10.00	1.90	0.11				
8/1/2001	no cruise						
9/12/2001	13.00						
10/17/2001	13.00	1.53	0.03	0.19	0.01	0.30	0.01
11/28/2001	8.00	1.44	0.05	0.11	0.00	0.36	0.01
12/19/2001	no samples						
1/23/2002	8.00	2.18	0.12	0.12	0.01	0.58	0.05
3/20/2002	2.00	2.31	0.00	0.26	0.00	0.32	0.00

4/17/2002	8.00	1.21	0.02	0.46	0.03	0.28	0.02
5/8/2002	4.00	2.49	0.02	0.13	0.00	0.37	0.01
6/5/2002	5.00	1.93	0.04	0.13	0.00	0.43	0.01
7/17/2002	13.00	2.17	0.03	0.11	0.01	0.46	0.03
8/22/2002	9.50	2.19	0.04	0.53	0.01	0.45	0.01
9/11/2002	13.00	2.18	0.01	0.21	0.00	0.76	0.00
10/9/2002	13.00	1.88	0.04	0.16	0.01	0.45	0.01
11/4/2002	14.00	1.82	0.00	0.09	0.00	0.30	0.00
12/11/2002	13.00	1.75	0.04				
1/8/2003	0.00	1.44	0.08				
2/20/2003	0.00	1.30	0.01				
3/19/2003	0.00	1.50	0.05				
4/9/2003	6.00	1.79	0.08				
5/21/2003	0.00	1.29	0.04				
7/16/2003	6.00	1.07	0.05				
8/13/2003	4.00	1.24	0.09				
9/10/2003	5.00	1.09	0.01				
10/16/2003	12.00	1.42	0.07				
12/17/2003	8.00	1.10	0.06				
1/14/2004	0.00	1.12	0.01				
2/11/2004	1.00	1.27	0.04				
3/10/2004	2.00	1.24	0.07				
4/21/2004	0.00	1.07	0.03				

Table SED4. 2001 Mildred Island process study results.

Mildred Island
 9/5-6/2001

Expt. Time hours	Time local	Dissolved					Particulate								
		Cl µmol/l	NO3 µmol/l	PO4 µmol/l	SiO4 µmol/l	Total Se nmol/l	Se IV nmol/l	Se VI nmol/l	Se -II+0 nmol/l	Chl a µg/L	Phaeo µg/L	Total Se nmol/l	Carbon mg C/l	Nitrogen mg N/l	
Channel, S2															
	0	740	1709	21.34	2.11	290	1.053	0.29	0.7	0.063	2.58	1.24	0.067	0.256	0.038
	3.08	1045	1525	18.92	2.09	282	0.981	0.21	0.702	0.072	2.97	1.21	0.106	0.273	0.038
	6.18	1351	1791	20.94	2.17	274	1.045				3.88	1.32	0.076	0.506	0.064
	9.13	1648	1614	21.46	2.17	279	1.105				3.58	1.36	0.076	0.529	0.058
	12.08	1945	1872	20.94	2.17	273	1.035				3.58	1.05		0.368	0.047
	15.22	2253	1702	20.75	2.04	265	1.06				3.54	1.66		0.265	0.031
	18.45	207	2014	21.46	2.17	277	1.045				4.12	1.38	0.082	0.444	0.061
	21	440	1973	21.69	2.09	275	1.104				2.74	1.59		0.403	0.043
	24.1	746	1947	21.53	2.09	185	1.034				2.4	1.52		0.318	0.032
	27.1	1046	2114	21.85	2.17	258	1.109				2.86	1.63		0.354	0.042
	30.03	1342	1998	21.24	2.08	229	1.054				3.95	1.11		0.382	0.044
	33.22	1653	1854	21.32	1.82	229	1.045				3.81	1.02		0.436	0.053
	36.05	1943	1947	20.7	1.97	283	1.094				3.25	1.31		0.379	0.041
	39.13	2248	2009	20.58	2.2	233	1.034				3.31	1.16		0.396	0.051
	42.17	150	2071	20.52	2.11	264	1.109				3.5	1.33		0.612	0.079
	45.05	443	2078	21	2.03	235	1.105				2.91	1.93		0.587	0.049
	48.05	743	2264	21.46	1.94	265	1.08	0.21	0.851	0.024	2.74	2.35	0.088	0.519	0.068
Entrance															
	0	756	2006	21.4	1.9	253	1.213	0.11	0.6	0.505	2.83	2.32	0.105	0.442	0.052
	2.88	1053	1825	18.13	1.96	206	1.171	0.17	0.546	0.458	4.43	0.74	0.078	0.433	0.047
	6.02	1357	2154	20.75	2.04	257	1.121	0.29	0.489	0.346	5.4	0.34	0.059	0.518	0.054
	8.97	1654	1846	20.78	2.14	267	1.06				4.02	1.33	0.097	0.355	0.039
	11.93	1952	1609	21.9	1.97	248	1.17				3.67	1.5		0.337	0.043

15.1	2302	1486	20.99	2.05	272	1.255				5.49	1.5		0.441	0.054
18.32	215	1636	21.1	2	270	1.045				3.81	2.22	0.076	0.307	0.044
20.87	448	1718	21.46	1.81	279	1.105				3.49	1.35		0.559	0.069
23.97	754	1656	22.34	1.81	263	1.034				2.39	2.08		0.273	0.036
26.95	1053	2105	22.2	1.88	275	1.15				3.45	2.23		0.449	0.057
29.9	1350	1843	21.44	1.96	266	1.13				4.46	0.82		0.448	0.052
33.03	1658	1625	21.34	1.97	251	1.109				4	1.1		0.444	0.058
35.87	1948	1599	20.62	1.89	286	1.299				3.37	1.1		0.293	0.038
39.02	2257	1445	18.84	2.04	269	1.019				4.11	1.32		0.436	0.055
42.02	157	1814	20.01	1.94	256	1.155				3.93	1.22		0.447	0.054
44.92	451	2180	21.06	1.96	266	1.189				3.4	1.44		0.438	0.056
47.87	748	1835	20.74	2.09	276	1.233	0.32	0.438	0.478	2.8	1.62	0.092	0.416	0.053
Chl Max														
0	809	1354	22.82	1.81	164	2.157	0.29	1.063	0.802	19.11	3.68	0.193	0.846	0.149
3	1109	1374	24.88	1.89	252	2.093	0.41	0.958	0.723	13.98	4.02	0.175	0.601	0.088
6.02	1410	1407	27.8	1.92	256	2.144	0.34	1.015	0.787	19.12	1.73	0.139	0.817	0.122
8.97	1707	1359	20.58	1.73	252	2.25	0.34	1.034	0.876	31.68	1.69	0.145	1.376	0.182
12.05	2012	1369	19.71	1.73	260	2.281	0.28	1.064	0.936	33.72	0	0.112	1.339	0.184
15.18	2320	1240	19.26	1.69	248	2.208	0.25	1.051	0.905	26.22	1.97	0.167	1.258	0.191
18.42	234	1310	21.57	1.79	258	1.867	0.29	1.062	0.513	21.5	1.29	0.174	1.058	0.169
20.82	458	1335	22.33	1.8	245	1.833	0.24	1.111	0.478	19.06	1.59	0.2	0.880	0.138
24.03	811	1387	21.4	1.75	265	1.997	0.23	1.048	0.719	16.32	2.78	0.154	1.280	0.180
26.95	1106	1336	23.04	1.87	279	2.154	0.21	1.136	0.805	17.67	5.67	0.167	1.302	0.179
29.93	1405	1317	25.28	1.87	236	2.252	0.29	1.092	0.866	29.1	0.62	0.138	1.367	0.205
33	1709	1330	18.05	1.8	248	lost sample				41.13	0	0.114	1.716	0.260
35.83	1959	1307	18.44	1.77	263	lost sample				36.61	0	0.131	1.538	0.237
39.07	2313	1063	16.71	1.62	224	2.06	0.2	1.157	0.704	27.74	0.96		1.157	0.183
42.1	215	1373	23.3	1.72	234	2.029	0.17	1.223	0.64	20.14	2.34	0.138	0.673	0.096
44.92	504	1412	17.53	1.13	204	1.878	0.24	1.112	0.524	22.06	5.81	0.196	1.272	0.187
47.85	800	1671	22.18	1.71	259	2.036	0.37	0.937	0.732	19.8	3.1	0.187	1.279	0.182

Table SED5. Historical Delta cores.

Mandeville			Potato Slough			Sherman Island		
Depth, cm	Avg Tot Se nmol/g	210Pb Date	Depth, cm	Avg Tot Se nmol/g	210Pb Date	Depth, cm	Avg Tot Se	
Box Core			Box Core			Box Core		
0.5	6.91	2001	0.5	3.37	2001	0.5	2.85	
1.5	6.84	2000	1.5	3.12	1999	1.5	5.45	
2.5	7.36	1999	2.5	3.75	1998	2.5	7.81	
3.5	6.61	1998	3.5	5.5	1996	3.5	6.81	
4.5	7.98	1997	4.5	4.47	1994	4.5	8.67	
5.5	4.86	1996	5.5	4.08	1992	5.5	7.92	
6.5	7.07	1995	6.5	5.19	1990	6.5	8.89	
7.5	7.21	1994	7.5	4.67	1989	7.5	6.7	
8.5	6.26	1993	8.5	4.2	1987	8.5	7.29	
9.5	6.44	1992	9.5	4.07	1985	9.5	5.21	
11	7.97	1991	11	5.62	1982	11	5.68	
13	6.84	1988	13	4.39	1979	13	5.11	
15	7.3	1986	15	3.72	1975	15	5.99	
			17	4.85	1972			
			19	4.54	1968			
Gravity Core			Gravity Core			Gravity Core		
1	6.268	2001						
3	6.615	1999						
5		1997						
7	6.185	1995						
9	5.98	1993						
11		1991						
13	4.946	1988						
15		1986						

17	4.212	1984				17	
19		1982	19		1968	19	
21		1980	21		1965	22.5	
23	7.314	1978	23		1961	27.5	
25	6.923	1976	25		1957	32.5	
27		1974	27		1954	37.5	
29	5.619	1972	29		1950	42.5	
31		1970	31		1947	47.5	
33	7.374	1968	33		1943	52.5	
35		1966	35		1940	55.7	
37	5.401	1963	37		1936	62.5	
39	5.289	1961	39		1932	67.5	
41		1959	41	2.8	1929	72.5	
43	6.286	1957	43		1925	77.5	
45	4.977	1955	45		1922	82.5	
47	4.267	1953	47		1918	87.5	
49	4.245	1951	49		1915	92.5	
51		1949	51		1911	97.5	
53.5	5.018	1946	53.5		1906	102.5	
57.5		1942	57.5		1899	107.5	
62.5	4.219	1937	62.5	2.79	1890	112.5	6.45
67.5		1932	67.5		1881	117.5	
72.5	6.035	1926	72.5	2.86	1873	122.5	
77.5		1921	77.5		1864	127.5	
82.5		1916	82.5	4.13	1855	132.5	2.24
87.5	3.092	1911	87.5		1846	137.5	
92.5	3.114	1906	92.5	2.2	1837	142.5	4.38
97.5		1900	97.5	2.68	1828	147.5	
102.5	3.335	1895	101	3.56	1822	152.5	4.09
106		1892	103		1818	157.5	3.3
108		1890	105		1815	162.5	
110		1887	107		1811	167.5	

112		1885	109		1807	172.5	
114	4.649	1883	112.5		1801	177.5	
117.5	3.93	1880	117.5		1792	182.5	
122.5	4.733	1874	122.5		1783	187.5	
127.5		1869	127.5	2.83	1774	192.5	
132.5	5.634	1864	132.5		1765	197.5	
137.5		1859	137.5		1756	202.5	
141	4.313	1855	142.5		1748	207.5	6.07
143		1853	147.5	2.36	1739	212.5	9.13
145		1851	148		1738	217.5	
147	5.72	1849	151.5		1731	222.5	
149		1847	156.5	2.53	1723	227.5	
151	5.171	1845	161.5	2.57	1714	232.5	6.16
154.5		1841				237.5	
159.5		1836				242.5	6.11
164.5	3.932	1831				247.5	
169.5		1825				252.5	
174.5	3.155	1820				257.5	
179.5	6.76	1815				262.5	
						267.5	
						272.5	3.91
						277.5	3.69
						282.5	
						287.5	4.99

Table SET1. Absolute daily rates of selenite uptake into particles and those rates relative to ambient selenite pools during the Mildred Island experiment. Rates are calculated for all particles, for particles < and > 1.0 μm and for dark and light selenite uptake components.

	Channel (Middle River)				Southwest Mildred Island			
	Daily Uptake $\mu\text{mol m}^{-2} \text{d}^{-1}$	[Se IV] $\text{nmol L}^{-1} \text{d}^{-1}$	[Se IV] nM	Turnover % pool d^{-1}	Daily Uptake $\mu\text{mol m}^{-2} \text{d}^{-1}$	[Se IV] $\text{nmol L}^{-1} \text{d}^{-1}$	[Se IV] nM	Turnover % pool d^{-1}
Total	0.073	0.015	0.265	5.5	0.329	0.110	0.345	31.8
<1.0	0.038	0.008		2.9	0.156	0.052		15.1
>1.0	0.035	0.007		2.6	0.173	0.058		16.7
dark	0.057	0.011		4.3	0.270	0.090		26.1
light	0.016	0.003		1.2	0.059	0.020		5.7

Table SET2. Results from laboratory experiments on selenite uptake by freshwater phytoplankton. ESD = equivalent spherical diameter of cells. C_{Se} = equilibrium cellular Se concentration, U_{Se} = uptake rate of selenite, VCF = volume:volume concentrations factor for selenite, Se:C= cellular Se:C ratio at equilibrium.

Species	taxonomic		0.02 nM experiments					0.45 nM experiments			
	division	ESD	C_{Se}	U_{Se}	VCF	Se:C	C_{Se}	U_{Se}	VCF	Se:C	
		μm	$\text{ugC}/\mu\text{m}^3$	$\text{ng Se } \mu\text{m}^{-3}$	$\text{ng-Se } \mu\text{m}^{-3} \text{ d}^{-1}$	vol:vol	$\mu\text{g g}^{-1}$	$\text{ng Se } \mu\text{m}^{-3}$	$\text{ng-Se } \mu\text{m}^{-3} \text{ d}^{-1}$	vol:vol	$\mu\text{g g}^{-1}$
<i>Chlorella vulgaris</i>	green	3	0.2	3.24E-10	1.31E-09	2.05E+05	1.62	8.8E-09	3.56E-08	2.47E+05	43.98
<i>Cyclotella meneghiana</i>	diatom	10	0.13	7.21E-11	2.47E-10	4.56E+04	0.55	1.45E-09	4.96E-09	4.08E+04	11.16
MI-34	green	5.5	0.17	2.72E-11	3.62E-10	1.72E+04	0.16	8.7E-10	3.52E-09	2.45E+04	5.12
<i>Stephanodiscus hantzschii</i>	diatom	7	0.15	3.10E-11	3.25E-10	1.96E+04	0.21	5.96E-10	6.26E-09	1.68E+04	3.98
<i>Synechococcus sp.</i>	bluegreen	2	0.22	8.42E-10	7.64E-09	5.33E+05	3.83	1.3E-08	1.18E-07	3.66E+05	59.22
<i>Synechocystis sp.</i>	bluegreen	2.3	0.22	nd	nd	nd		1.75E-08	1.92E-07	4.92E+05	79.55
<i>Selenastrum sp.</i>	green	4.5	0.2	3.46E-12	nd	8.77E+02	0.02	1.82E-10	nd	5.12E+03	0.91

Table SET3. Summary of calculations of phytoplankton community Se:C ratios during the Mildred Island process experiment in September 2001. Site designations are S1 for northern Mildred Island, C1 for the channel site, and C20 for the southwest corner of Mildred Island. Calculations of Se:C are based on the regression of equivalent spherical cell diameter (ESD) on Se:C ratio of algae in culture at 0.45 nM selenite: $Se:C = 63 * ESD^{-1.95}$. These values are then corrected for the average selenite concentrations at the site assuming a constant volume:volume concentration factor.

Site	Date	Time	Se(IV) nM	<i>Cyanobium sp.</i>			<i>Cyclotella atomus</i>			<i>Skeletonema potamos</i>			<i>Plagioselmis sp.</i>			<i>Teleaulax amphioxeia</i>			<i>Chlorella minutissima</i>			Total Se:C $\mu\text{g g}^{-1}$
				ESD μm	BV %	Se:C $\mu\text{g g}^{-1}$	ESD μm	BV %	Se:C $\mu\text{g g}^{-1}$	ESD μm	BV %	Se:C $\mu\text{g g}^{-1}$	ESD um	BV %	Se:C $\mu\text{g g}^{-1}$	ESD um	BV %	Se:C $\mu\text{g g}^{-1}$	ESD um	BV %	Se:C $\mu\text{g g}^{-1}$	
S1	5-Sep	7:42	0.265	1.2	5.0	24.7	7.1	86.3	0.8	4.8	0.5	1.8	3.6	2.7	3.2	7.2	1.2	0.8	1.7	0.9	13.8	2.0
C1	5-Sep	7:13	0.265	1.2	24.6	24.7	7.1	21.7	0.8	4.8	4.4	1.8	3.4	8.6	3.4	5.3	3.3	1.4	1.5	4.2	16.8	6.7
C20	5-Sep	8:58	0.335	1.2	12.3	31.2	7.1	39.7	1.0	4.8	7.5	2.2	4.8	22.3	2.2	7.0	10.5	1.1	1.7	2.2	16.8	5.0
C20	5-Sep	6:14	0.335	1.2	16.5	31.2	7.1	35.9	1.0	4.8	5.2	2.2	5.6	20.4	2.2	7.0	13.1	1.1	2.0	1.0	16.8	6.9
C20	5-Sep	22:25	0.335	1.2	7.7	31.2	7.1	50.2	1.0	7.9	19.4	2.2	5.1	15.8	2.2	7.0	0.4	1.1	2.0	4.7	16.8	3.4
C20	6-Sep	3:44	0.335	1.2	26.1	31.2	7.1	50.3	1.0	5.5	4.9	2.2	4.9	11.0	2.2	7.2	1.2	1.1	2.0	5.4	16.8	9.0
C20	6-Sep	10:00	0.335	1.2	20.3	31.2	7.1	33.8	1.0	5.5	9.0	2.2	4.9	24.2	2.2	7.2	3.2	1.1	2.0	3.6	16.8	7.4

Table SET4. Volume/volume concentration factors for selenite accumulation by marine phytoplankton at the two experimental concentrations. Ratio is the concentration factor from the 0.15 nM experiment divided by the concentration factor from the 4.5 nM experiment. nd: not determined.

4.5 nM			0.15 nM			Ratio
mean	+95% CI	-95% CI	mean	+95% CI	-95% CI	
2.1×10^3	2.2×10^3	1.9×10^3	2.8×10^4	3.0×10^4	1.0×10^3	13.4
1.1×10^2	1.4×10^2	7.8×10^1	4.2×10^1	6.1×10^1	9×10^0	0.4
2.5×10^4	3.5×10^4	1.6×10^4	4.5×10^5	3.1×10^5	5.9×10^5	17.6
2.8×10^1	3.7×10^1	1.9×10^1	4.0×10^3	5.4×10^3	6.8×10^2	142.8
4.3×10^2	5.0×10^2	3.7×10^2	1.0×10^4	1.2×10^4	6.7×10^2	23.7
2.4×10^1	3.5×10^1	1.4×10^1	4.6×10^3	6.1×10^3	7.2×10^2	192.1
2.4×10^2	3.4×10^2	1.5×10^2	nd	-	-	-
1.1×10^4	1.5×10^4	6.7×10^3	4.1×10^5	5.2×10^5	5.1×10^4	37.6
7.3×10^1	1.2×10^2	2.8×10^1	nd	-	-	-
1.3×10^4	1.7×10^4	9.3×10^3	2.6×10^5	3.4×10^5	3.6×10^4	20.1
1.5×10^5	2.5×10^5	5.5×10^4	nd	-	-	-
1.0×10^4	1.3×10^4	6.8×10^3	nd	-	-	-
8.2×10^4	1.2×10^5	4.3×10^4	2.8×10^6	5.4×10^6	1.2×10^6	34.9
6.8×10^4	1.5×10^5	3.8×10^4	nd	-	-	-

Table SEF1. Biodynamic constants for Se bioaccumulation in different types of organisms that inhabit the Bay-Delta. * Not an inhabitant of the Bay-Delta, but expected to invade. **Not an inhabitant of the Bay-Delta; surrogate for bivalve consuming fish.

Species	Dissolved uptake rate $\mu\text{g g}^{-1}\text{d}^{-1}$ per μgL^{-1}	Assimilation efficiency (%)	Rate constant of loss (d^{-1})	Reference
Freshwater bivalves				
<i>Corbicula fluminea</i>	0.0025	29 – 81	0.010	1
<i>Dreissina polymorpha</i> *	0.14	20 - 30	0.03	3
Estuarine bivalves				
<i>Potamocorbula amurensis</i>	0.009	35 – 54	0.023	1
<i>Mytilus edulis</i>	0.035	20 – 70	0.022	2
Polychaete worm				
<i>Nereis succinea</i>	0.006	30 – 50		2
Copepods				
<i>Acartia tonsa</i>	0.024	55-97	0.16	
<i>Temora longicornis</i>	0.024	50 - 60	0.11	2
<i>Mixed-estuary</i>	0.024	51	0.16	4
Mysid –Crustacean predator				
<i>Neomysis mercedes</i>	0.027	68	0.25	4
Fish – predators				
Striped bass, <i>Morone saxatilis</i>		42	0.08	5
Mangrove snapper**, <i>Lutjanis argentimaculatus</i>	0.008	32 – 67	0.03	6

1. Lee B-G, Lee J-S, Luoma SN. In prep., 2. (Wang and Fisher 1999) 3. (Roditi *et al.* 2000) 4. (Schlekat *et al.* 2004) 5. (Baines *et al.* 2002) 6. (Xu and Wang 2002)

Table SEF2. Sensitivity of model runs with varying parameters including ingestion rate (IR), assimilation efficiency (AE), bioavailable particulate Se (F_{SF}). Sensitivity is quantified as the root mean square of residuals of model – measured Se concentrations in clams ($\mu\text{g g}^{-1}$ dry wt) at individual sites sampled during the Mildred Island Process study (n = 12, August 29, 2001), Frank's Tract Boogie (n = 7, April 1, 2002) and Delta Boogie (n = 7, May 12, 2003).

IR	AE	F_{SF}	RMS
PHYTO/COM	0.7	4.6	2.31
PHYTO/COM	0.7	9.08	2.54
SPM	0.7	4.6	3.02
SPM	0.7	9.08	8.45
Constant 0.029	0.7	4.6	2.09
Constant 0.029	0.7	9.08	6.80
PHYTO/COM	0.3	4.6	3.45
PHYTO/COM	0.3	9.08	1.98
SPM	0.3	4.6	2.48
SPM	0.3	9.08	5.15
Constant 0.029	0.3	4.6	2.48
Constant 0.029	0.3	9.08	3.89
SPM	0.7	Meas. Part. Se ($\mu\text{g/g}$)	3.52

$IR_{PHYTO/COM}$ is the ingestion rate estimated from community consumption of chlorophyll and community biomass ((Pumping Rate ($\text{m}^3 \text{m}^{-2} \text{d}^{-1}$) x Chlorophyll *a* ($\mu\text{g L}^{-1}$))/ Bed biomass (Tissue Ash-free Dry weight g m^{-2})) adjusted for a chlorophyll to phytoplankton C ratio of 32 (Lopez, in press)) ($\text{g C g}^{-1} \text{d}^{-1}$).

IR_{SPM} which is the ingestion rate estimated from site specific SPM ($0.137[\text{SPM mg L}^{-1}]^{0.421}$ x Filtration Rate (temperature specific (Foe and Knight 1986;Reinfelder, Fisher, Luoma, Nichols, and Wang 1998) ($\text{g g}^{-1} \text{d}^{-1}$)).

$IR = 0.029$ ($\text{g g}^{-1} \text{d}^{-1}$), ingestion rate determined empirically for *Corbicula fluminea* in the laboratory (Croteau et al. in prep.).

F_{SF} is the bioavailable particulate Se per unit phytoplankton carbon (constant of 4.6) and Se per unit bacterial carbon (constant of 56 multiplied by a factor accounting for bacterial :phytoplankton cellular ratios (Sobczak, Cloern, Jassby, and Muller-Solger 2002)) developed by Baines ($\mu\text{g g C}^{-1}$)

Table SEF3. Sum of residual errors associated with varying model parameters including ingestion rate (IR), assimilation efficiency (AE), bioavailable particulate Se (F_{SF}) for twelve separate model runs (see Table SEF1). Residual errors are quantified as the root mean square of residuals of model – measured Se concentrations in clams ($\mu\text{g g}^{-1}$ dry wt) at individual sites sampled during the Mildred Island Process study (n = 12, August 29, 2001), Frank’s Tract Boogie (n = 7, April 1, 2002) and Delta Boogie (n = 7, May 12, 2003).

Model Parameter		Sum of residual error
IR	PHYTO/COM	10.28
	SPM	19.10
	0.029	15.26
AE	0.3	19.43
	0.7	25.20
F_{SF}	4.6	15.83
	9.08	28.81

$IR_{PHYTOC/COM}$ is the ingestion rate estimated from community consumption of chlorophyll and community biomass ($\text{g C g}^{-1} \text{d}^{-1}$)

IR_{SPM} which is the ingestion rate estimated from site specific SPM ($\text{g g}^{-1} \text{d}^{-1}$)

$IR = 0.029$ ($\text{g g}^{-1} \text{d}^{-1}$), ingestion rate determined empirically for *Corbicula fluminea* in the laboratory (Croteau et al. in prep.).

F_{SF} is the bioavailable particulate Se per unit phytoplankton carbon (constant of 4.6) and Se per unit bacterial carbon (constant of 56 multiplied by a factor accounting for bacterial :phytoplankton cellular ratios ($\mu\text{g g C}^{-1}$))

AE is the assimilation efficiency (%)

DELTA SCALE HYDRODYNAMICS: *Forcing Mechanisms*

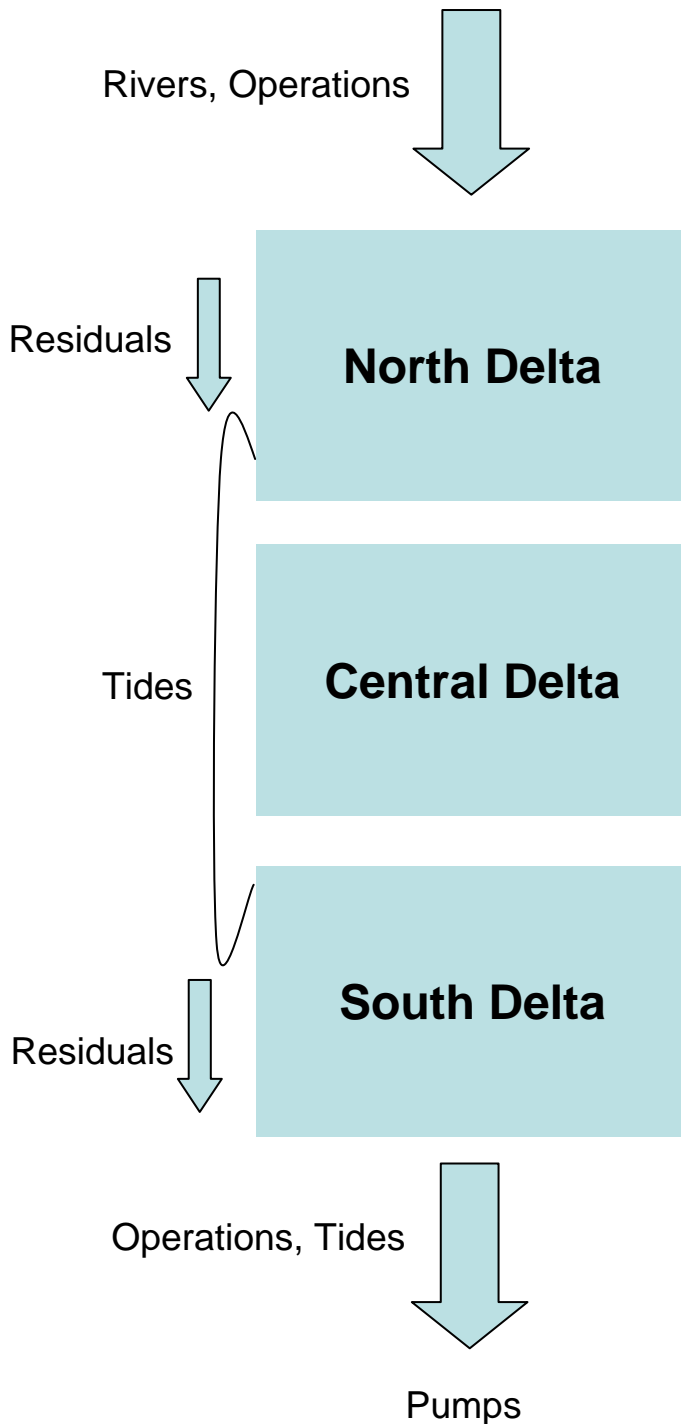


Figure E1. Conceptual model describing predominant forcings on hydrodynamics and transport at a Delta scale.

DELTA SCALE HYDRODYNAMICS: The “Freshwater Corridor”

SEASONAL VARIABILITY

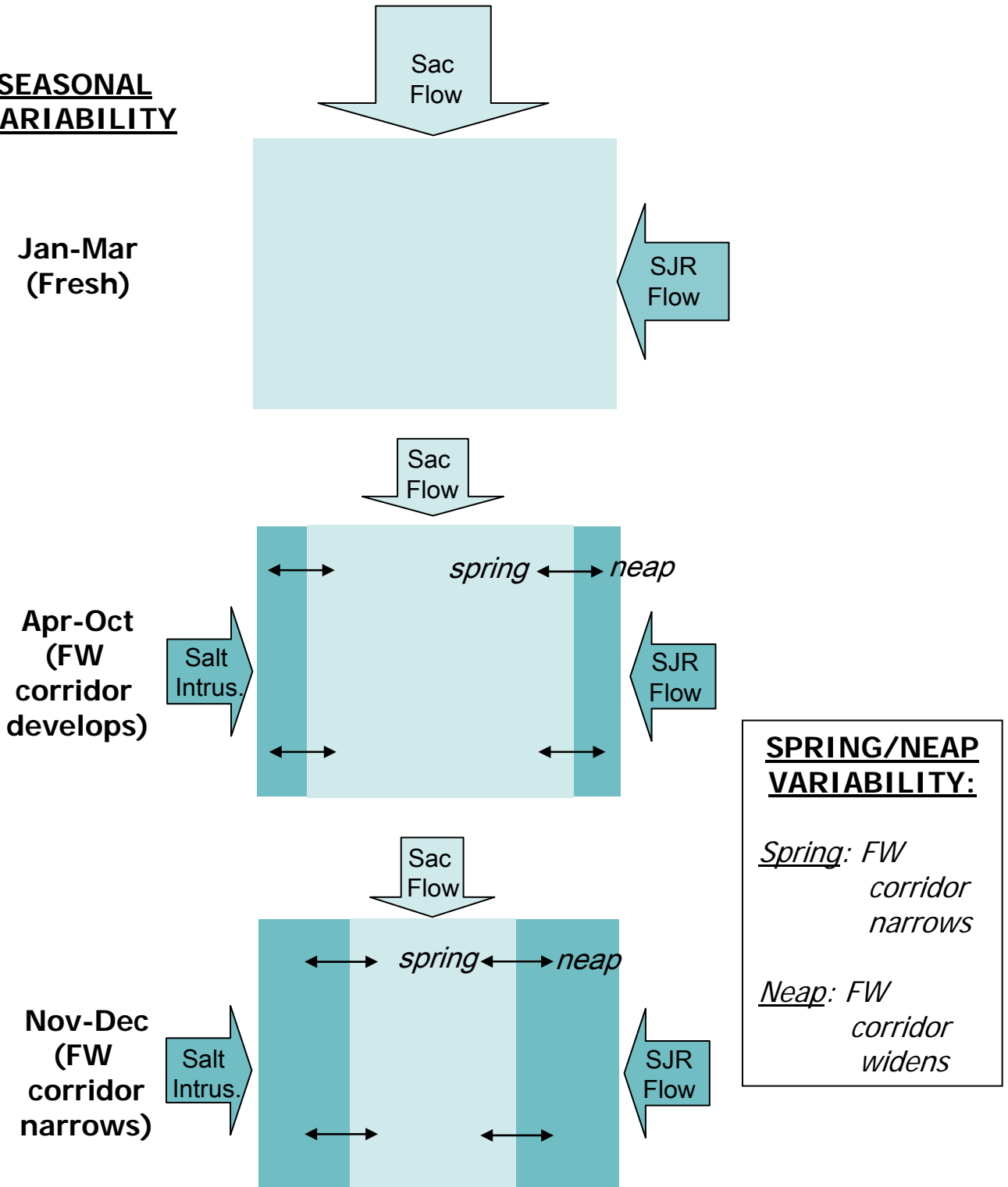


Figure E2. Conceptual model describing modulation of the Delta’s “freshwater corridor.”

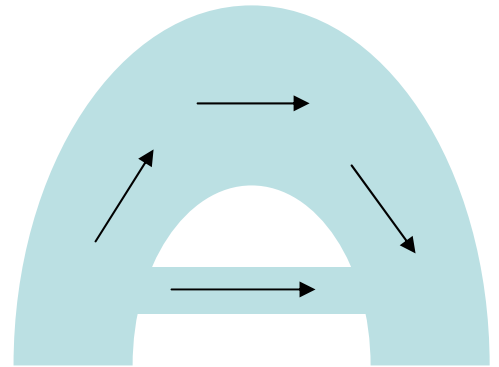
REGIONAL SCALE HYDRODYNAMICS

(e.g. Shallow water habitat and its neighborhood---
the “Loop” Model)

$L_C = \text{channel length}$

$L_U = \text{advective length } (U * T)$

$L_T = \text{tidal propagation length } (c * T)$



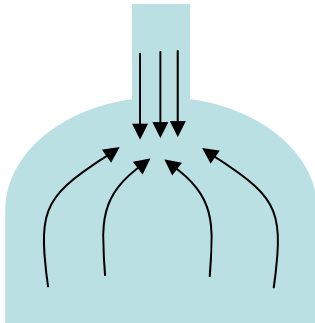
IF $L_C > L_U, L_T \rightarrow$ System acts like a River

IF $L_U > L_C \rightarrow$ System is highly Dispersive

IF $L_T > L_C \rightarrow$ Phasing is more Complicated

Figure E3. Conceptual model describing relationships between geometric, advective, and tidal propagation lengthscales, resulting in different hydrodynamic functionalities.

HYDRODYNAMICS OF SWH-CHANNEL EXCHANGE



TIDAL PUMPING
(classic inflow jet and radial outflow)

BUT...

...MODIFIED BY:

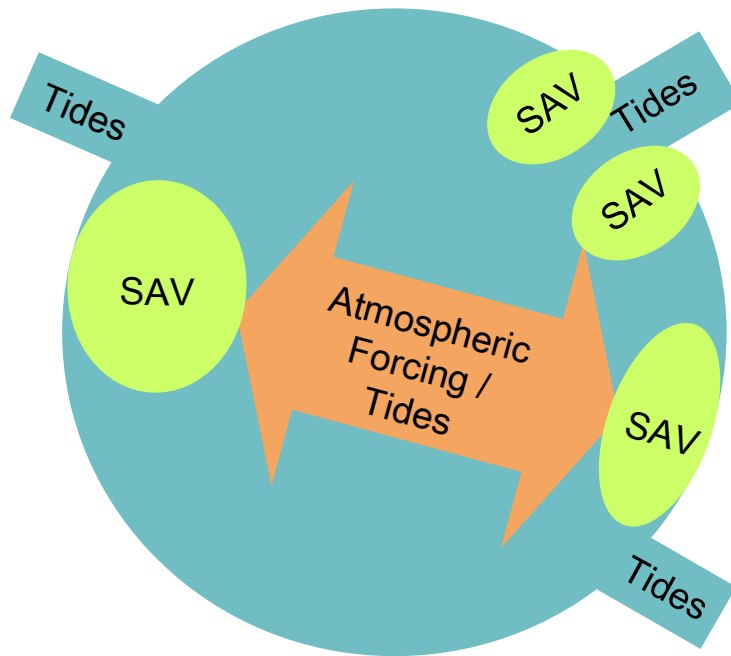
1) Geometry (levee breaches and effects on barotropic pressure gradient)

2) Vegetation (in environments like Franks Tract, SAV constrains jet)

1) Meteorology (in environments like Mildred Island, wind, heating and cooling are important)

Figure E4. Conceptual model describing hydrodynamics at shallow-channel exchange locations.

HYDRODYNAMICS OF SWH INTERIORS



Tidal and atmospherically forced hydrodynamics and transport modified by SAV via:

- *low velocity*
- *low bed stress*
- *limited exchange*

Figure E5. Conceptual model describing hydrodynamics and transport within shallow Delta habitats.

DELTA SCALE CONCEPTUAL MODEL FOR PHYTOPLANKTON

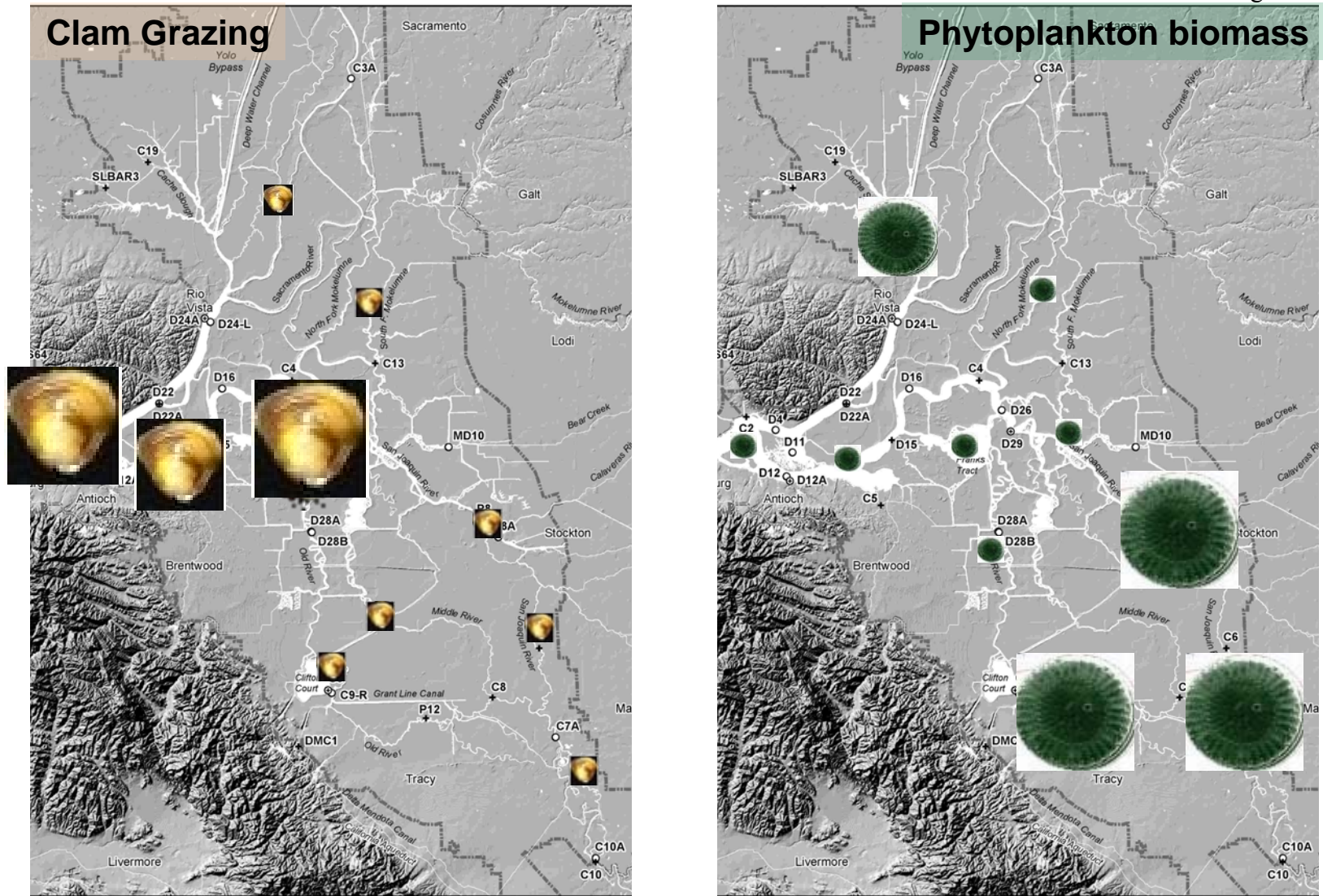


Figure E7. Conceptualization of the relationship between clam grazing and phytoplankton biomass in the Delta (i.e. somewhat of an inverse relationship, based on May 2003 measurements of clam and phytoplankton biomass, see Fig. B9.)

****One* REGIONAL SCALE
CONCEPTUAL MODEL
FOR PHYTOPLANKTON***

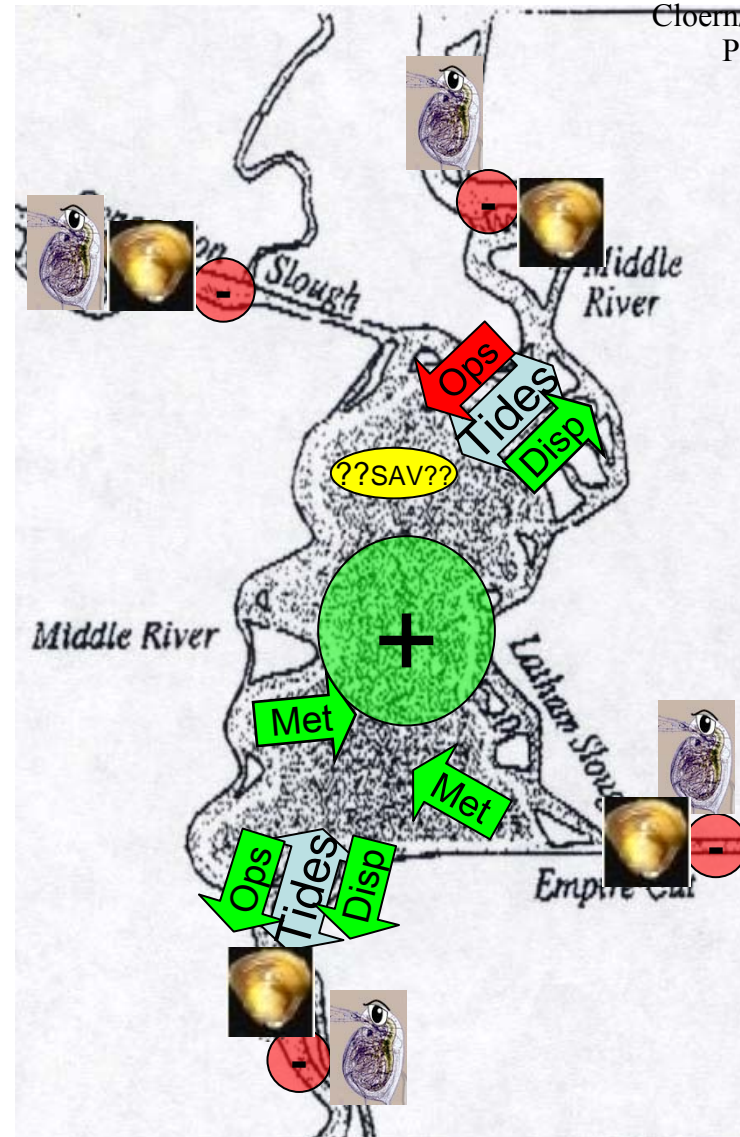
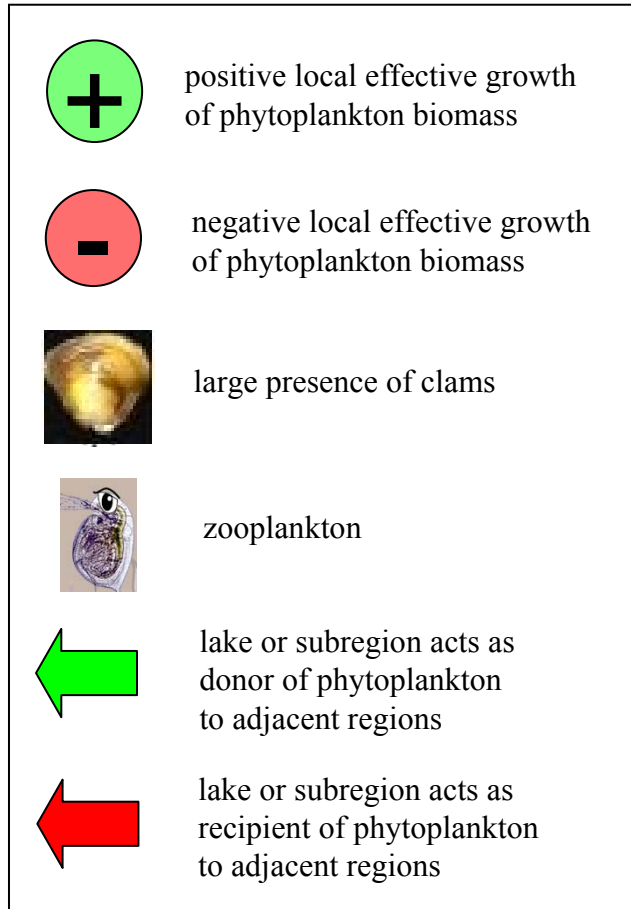


Figure E8. One regional conceptual model for phytoplankton biomass. In the case of Mildred Island, the shallow habitat is a net source for phytoplankton and the adjoining channels are net sinks due to rapid grazing by clams. Although the channels are net phytoplankton sinks, secondary productivity by zooplankton there can still be sustained by the net export of phytoplankton from the donor lake.

****One* REGIONAL SCALE
CONCEPTUAL MODEL
FOR PHYTOPLANKTON***

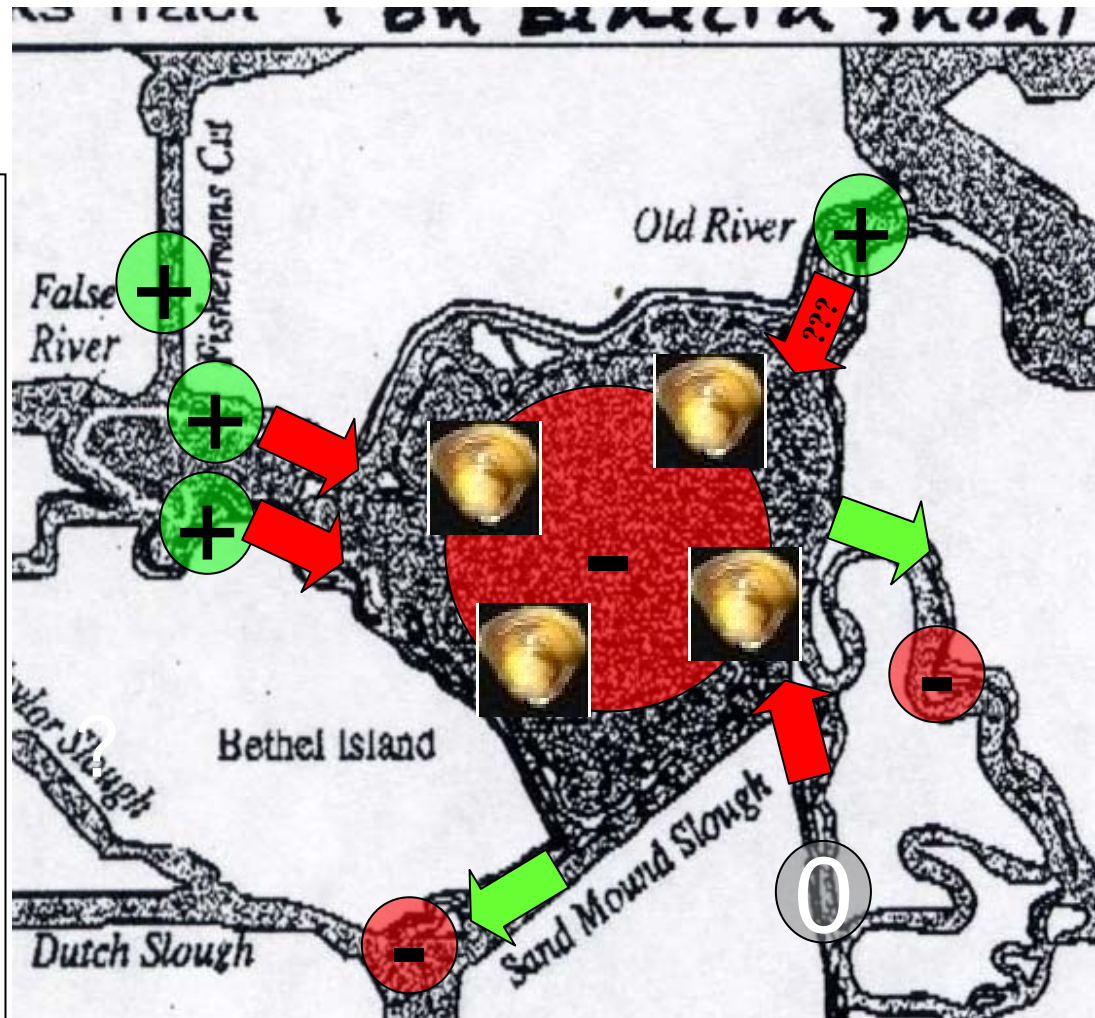
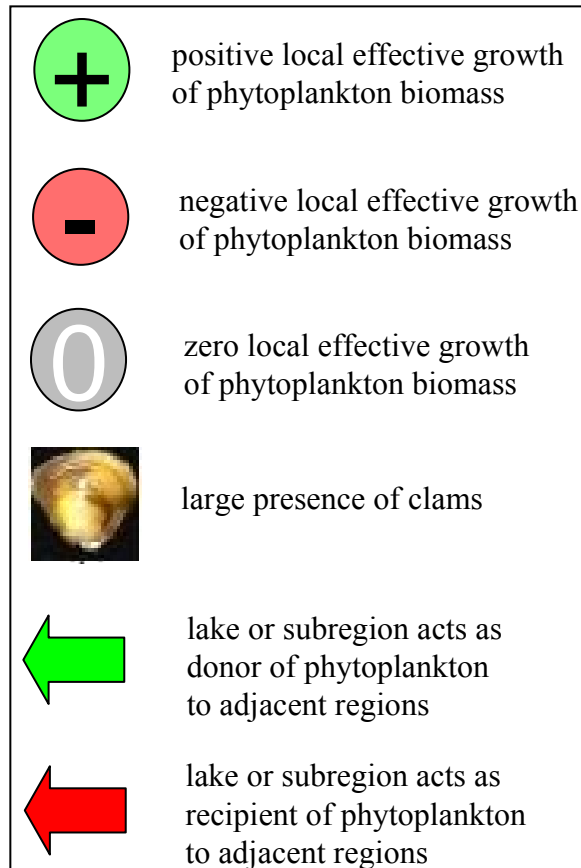


Figure E9. One regional conceptual model for phytoplankton biomass. In the case of Franks Tract, the shallow habitat is a net sink for phytoplankton, due to rapid grazing by clams. Surrounding channels range from net sources, to net sinks. Ongoing work will test quantitatively the hypothesized net fluxes of phytoplankton between lake and adjacent channels.

DELTA SCALE CONCEPTUAL MODEL FOR BIOAVAILABLE SELENIUM

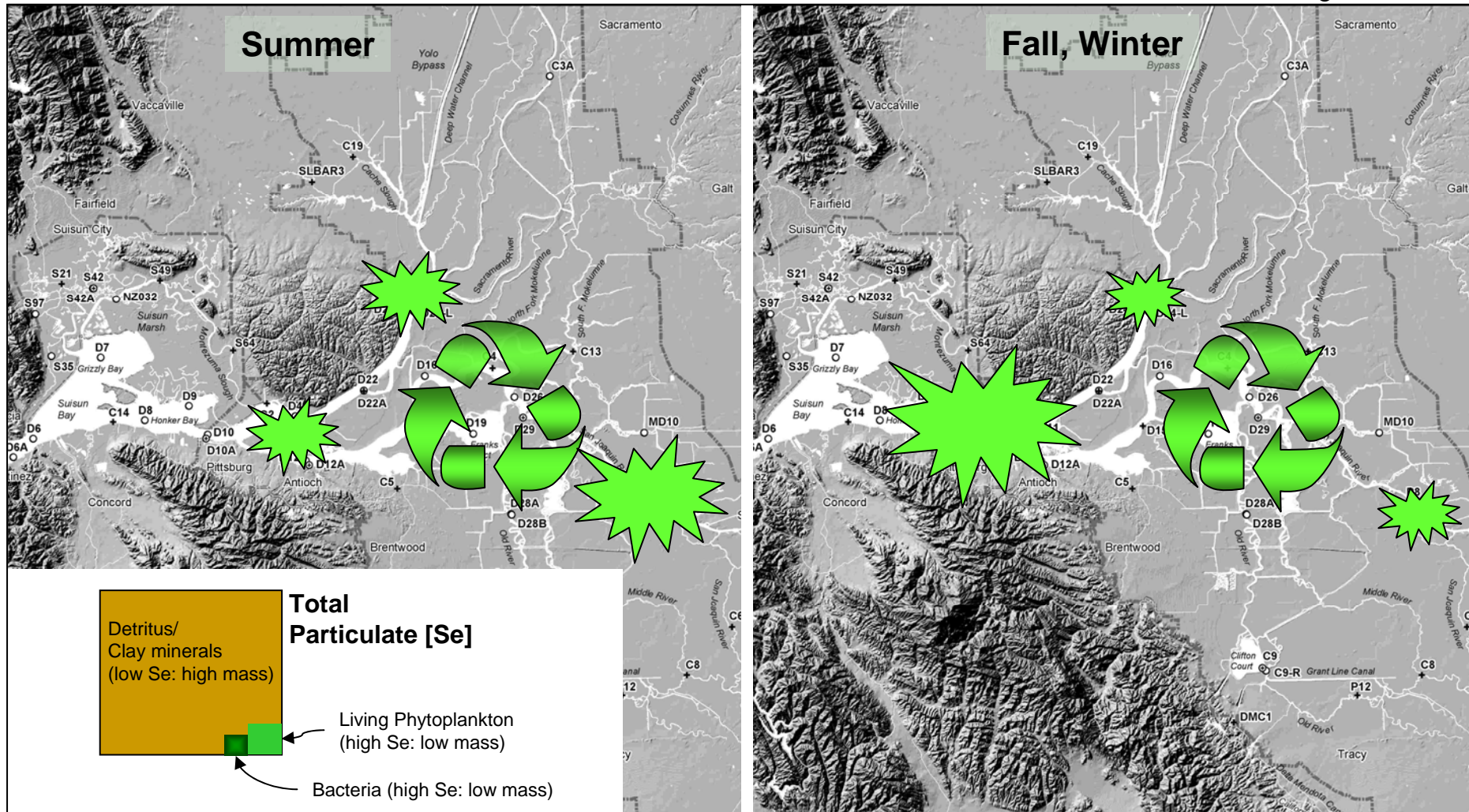


Figure E11. Relative molar Se:C ratios in suspended particulate matter (proxy for Se bioavailability) in the Bay/Delta during the project during summer and fall/winter (2001-2004), based on Cutter et al. (Section SED). Estimates are based on samples collected at Rio Vista, Stockton and Antioch. Corner cartoon illustrates how phytoplankton and bacteria are a relatively small component of the total suspended particulate mass. Changing these proportions could result in higher Se bioavailability.

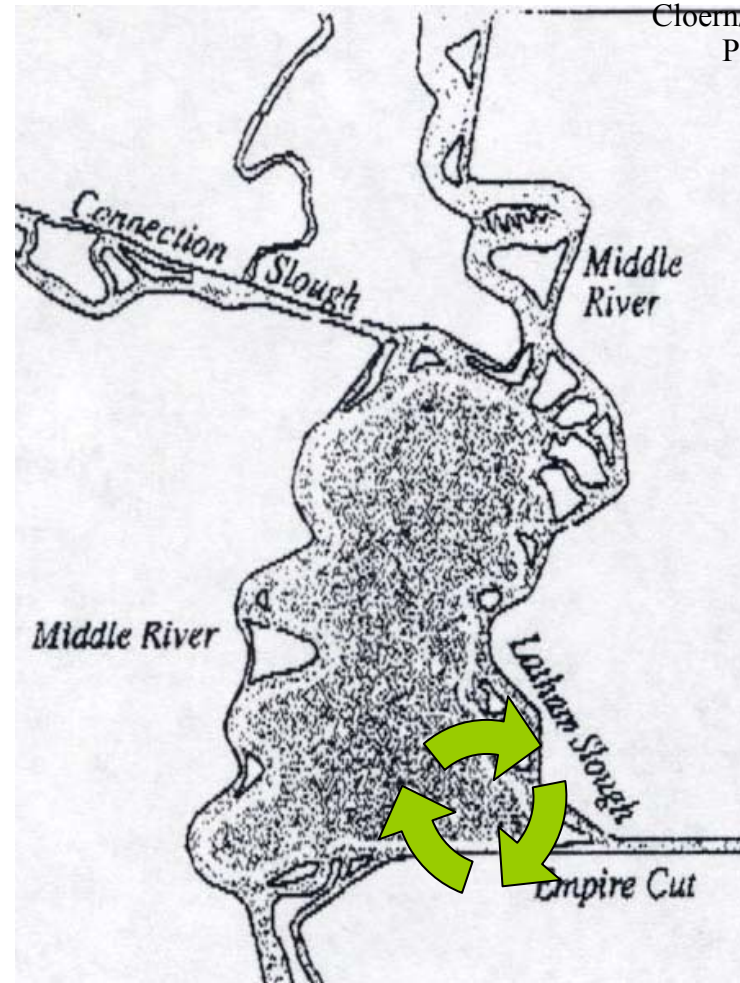
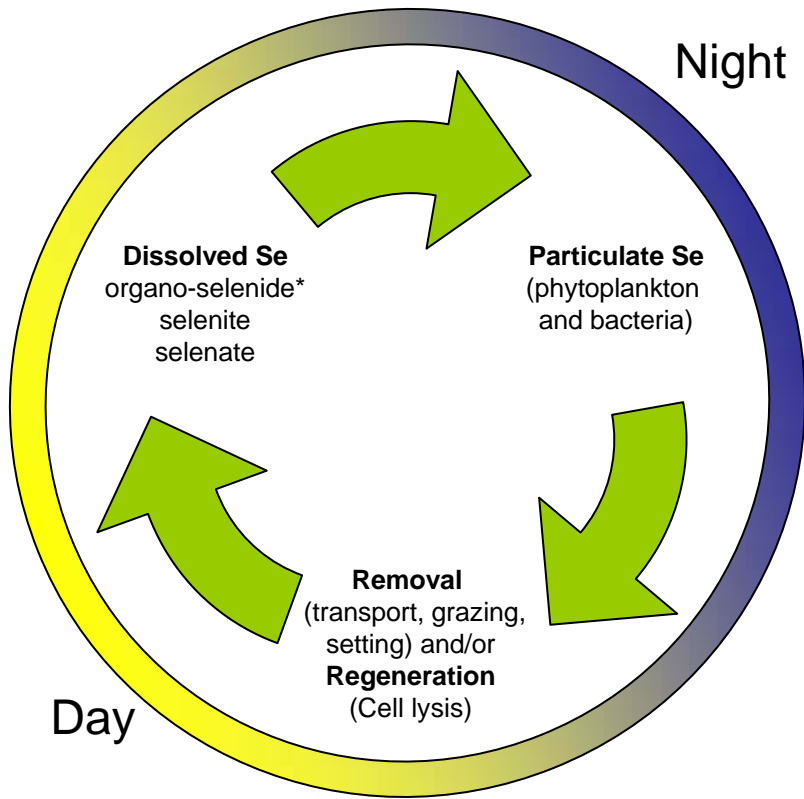


Figure E12. Conceptual model for Se uptake and regeneration in the southwestern Mildred's Island during the 2001 process study. Dissolved Se is taken up by phytoplankton late in the day and by bacteria at night and released by phytoplankton during the day. Laboratory uptake experiments (see Section SET) and cycling during field study (see SED4-8) suggest that dissolved organo-selenide (*) is utilized by the phytoplankton and rapidly exchanges with the selenite pool.

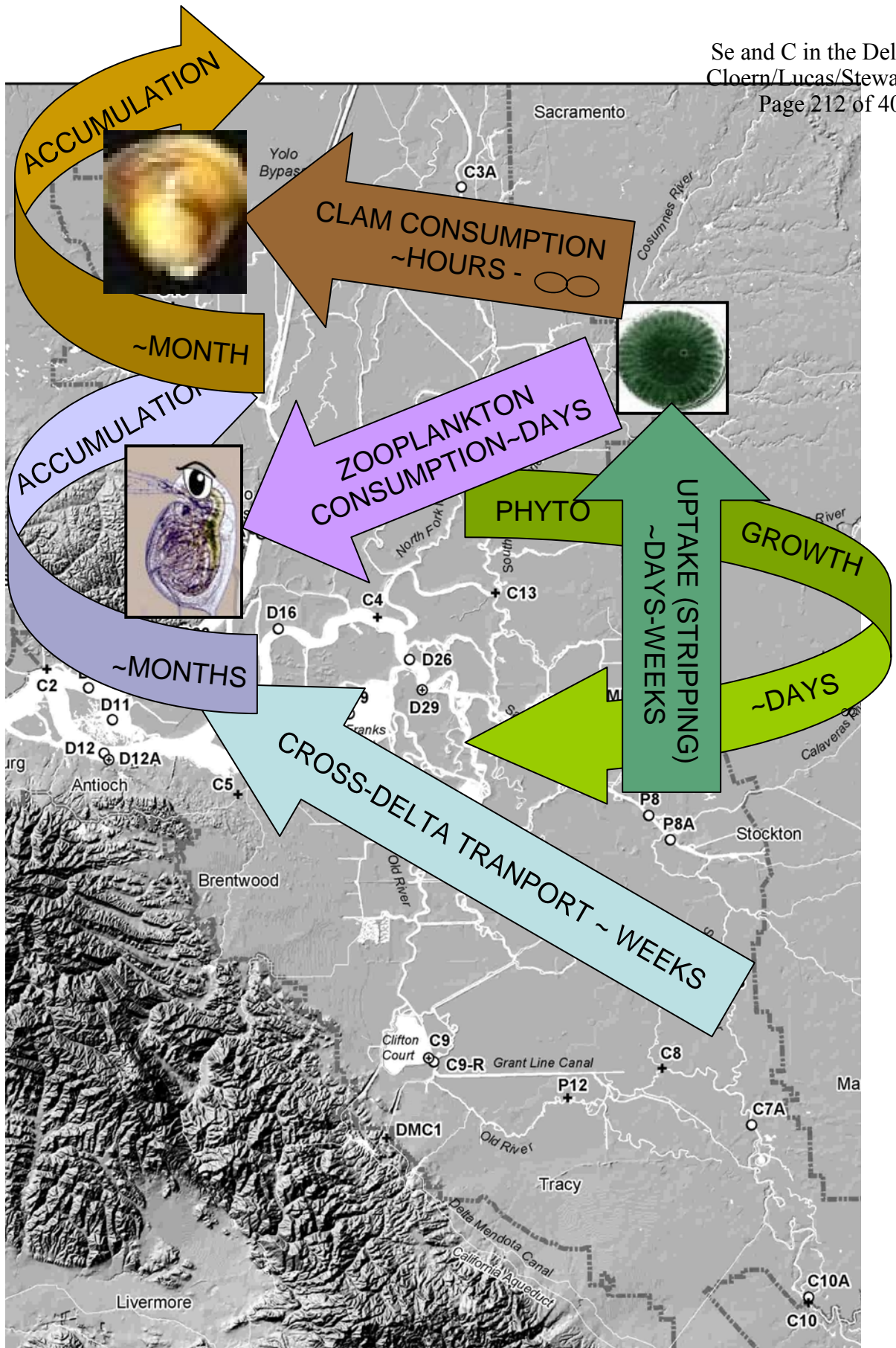


Figure E13. Time scales governing Se distribution, transformation, and export to SF Bay.

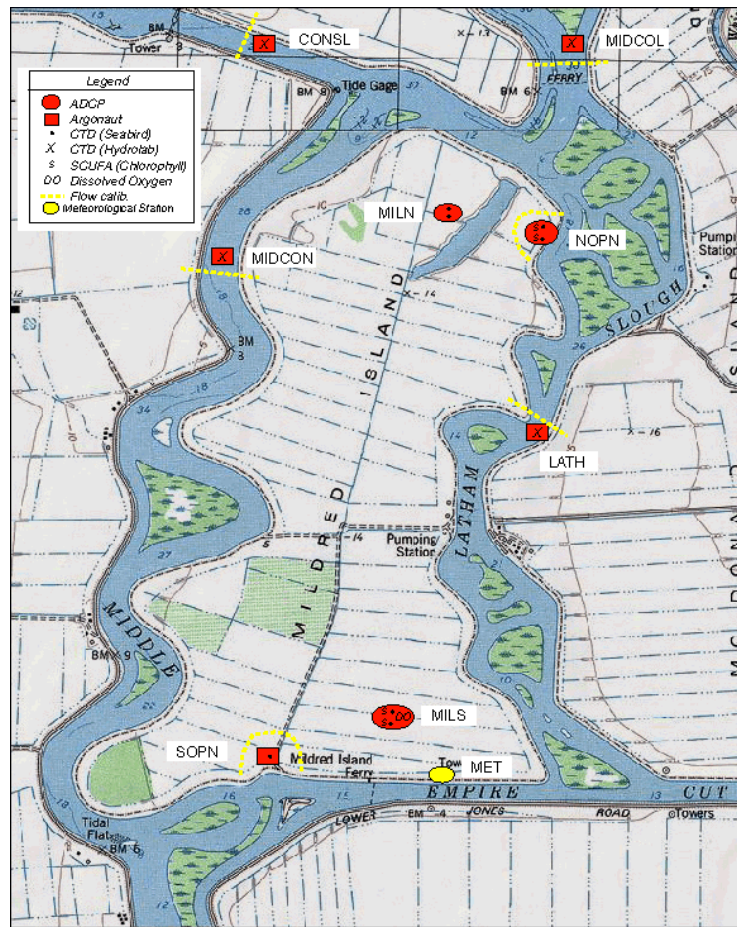


Figure HS1. Mildred Island experiment location map.



Figure HS2. Franks Tract aerial photograph showing levee locations, submerged aquatic vegetation (dark shading). Northern levee breach that is the emphasis of the discussion is highlighted.

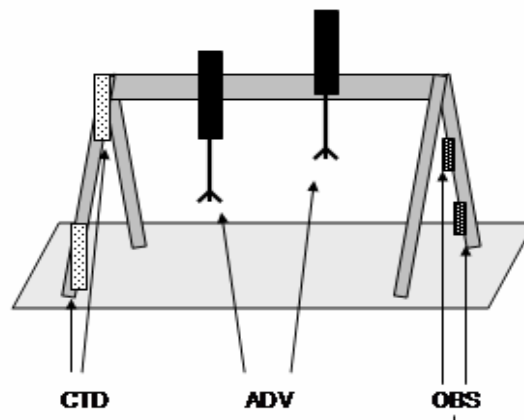


Figure HS3. Sawhorse frame with 2 ADVs, 2 CTDs and 2 OBSs. In most FT experiments, 4 ADVs were deployed from this frame.

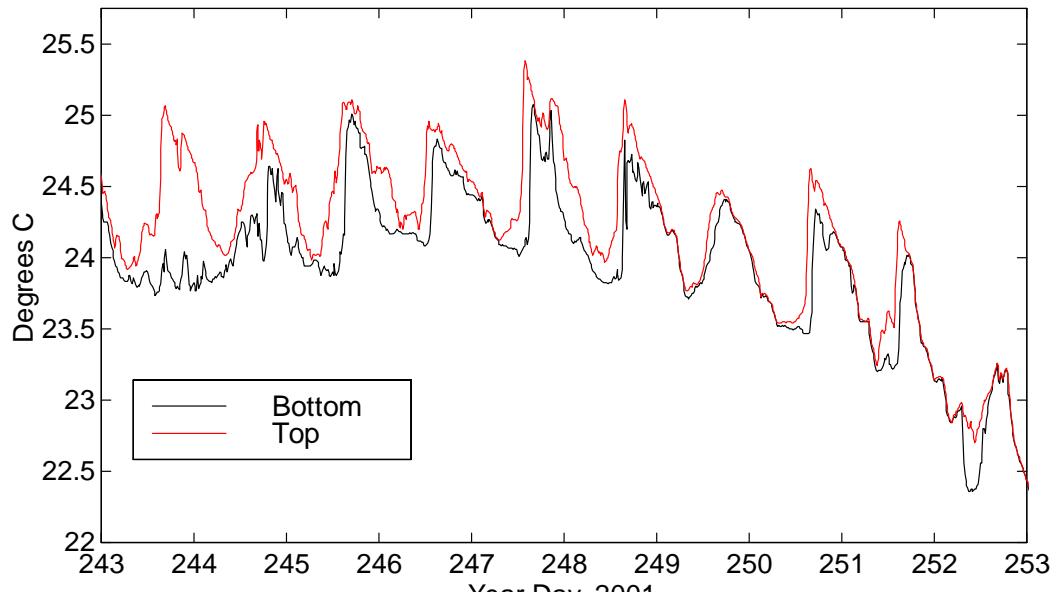


Figure HS4. Top and bottom temperature variability versus year day (2001) at Mildred Island, South Station.

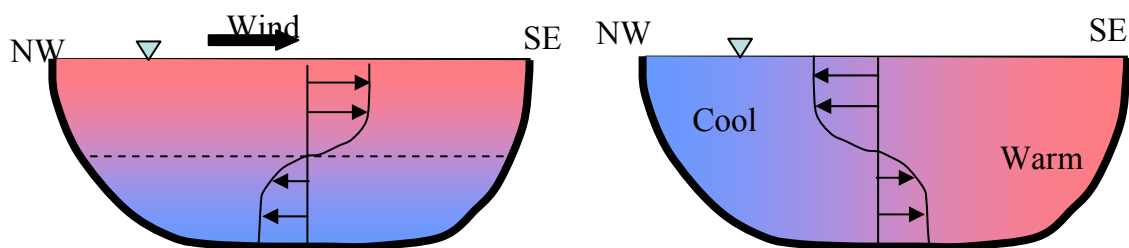


Figure HS5. Schematic of baroclinic pumping process in which vertical temperature gradients, created by solar heating, are converted to horizontal gradients by wind-driven flow. The horizontal gradients then relax back to a stable condition during the night with a reversed flow structure.

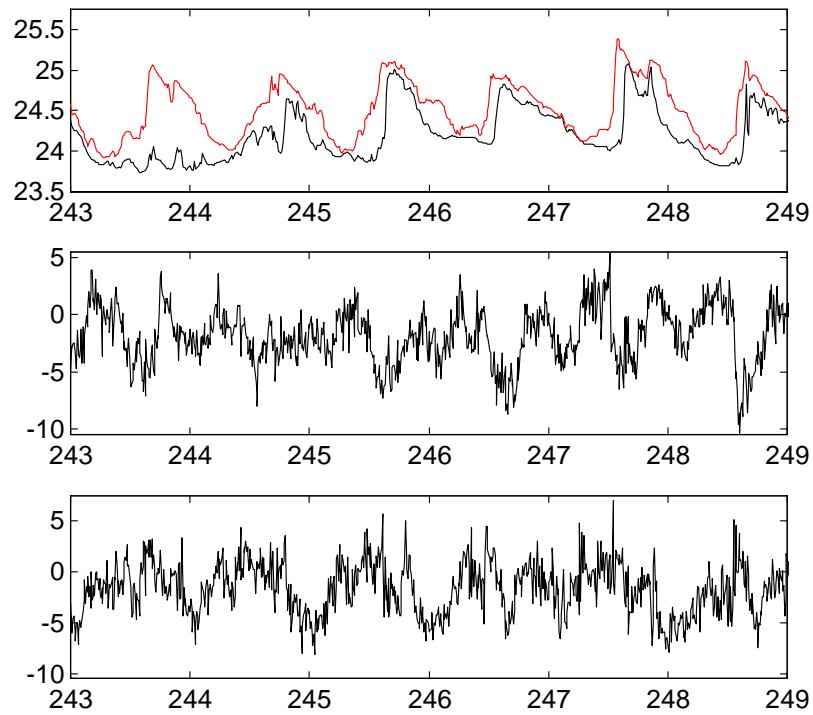


Figure HS6. Top and bottom temperature (top panel), NW-SE component of surface velocity (middle panel) and near-bed velocity (bottom panel).

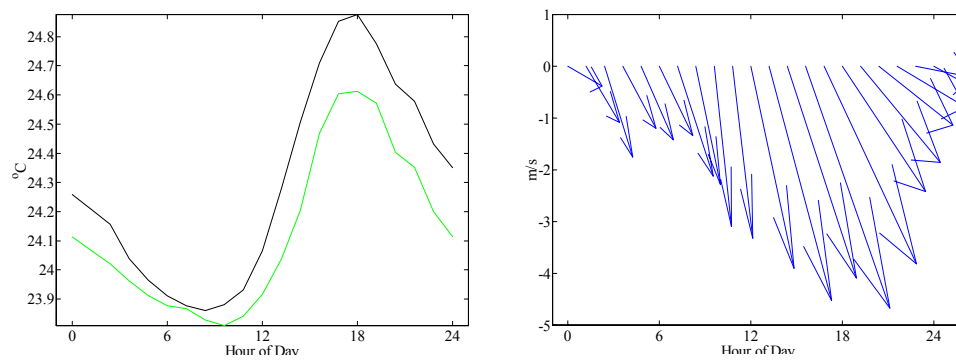


Figure HS7. Average daily cycle of top and bottom temperature (left panel) and wind (right panel).

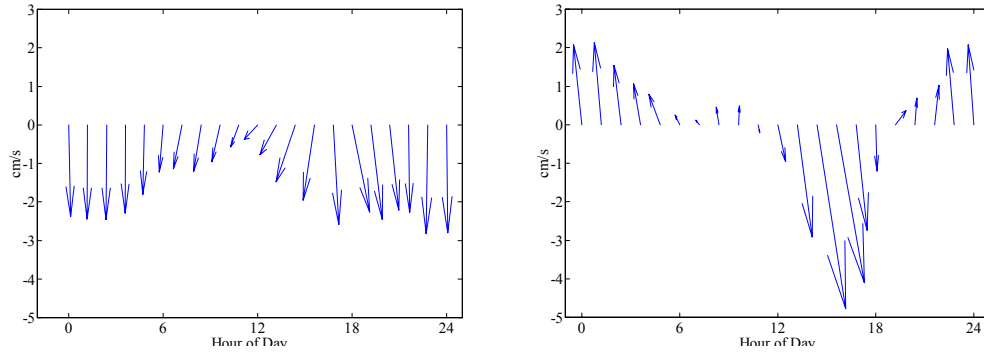


Figure HS8. Average daily cycle of depth-averaged velocity (left panel) and top-bottom velocity difference (right panel). Note that the aspect ratios of the arrows are not accurate, and the large velocities in the right panel at around hour 16 are actually oriented at about 30 degrees east of south.

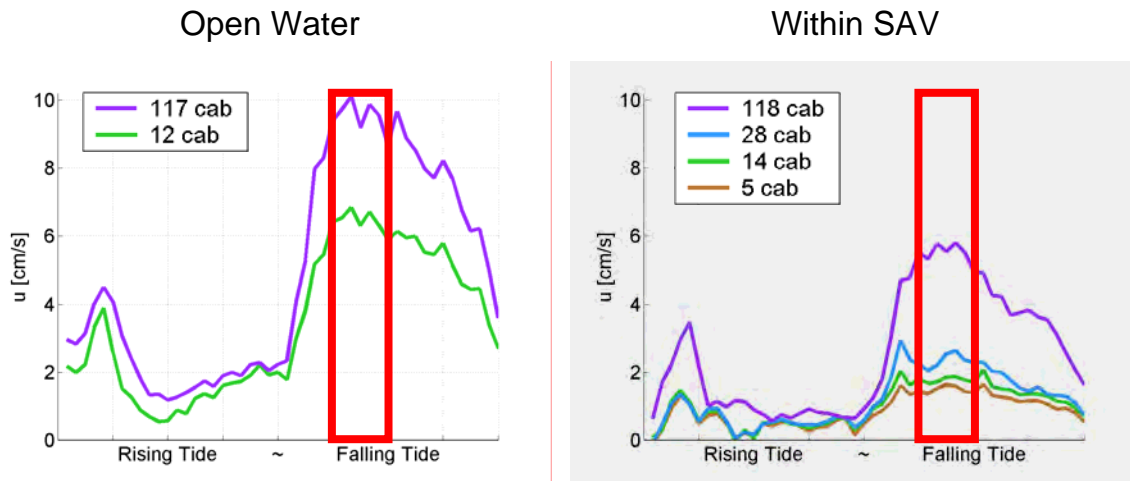


Figure HS9. Average tidal cycle development of mean velocity in open water (left panel) and within submerged aquatic vegetation (right panel).

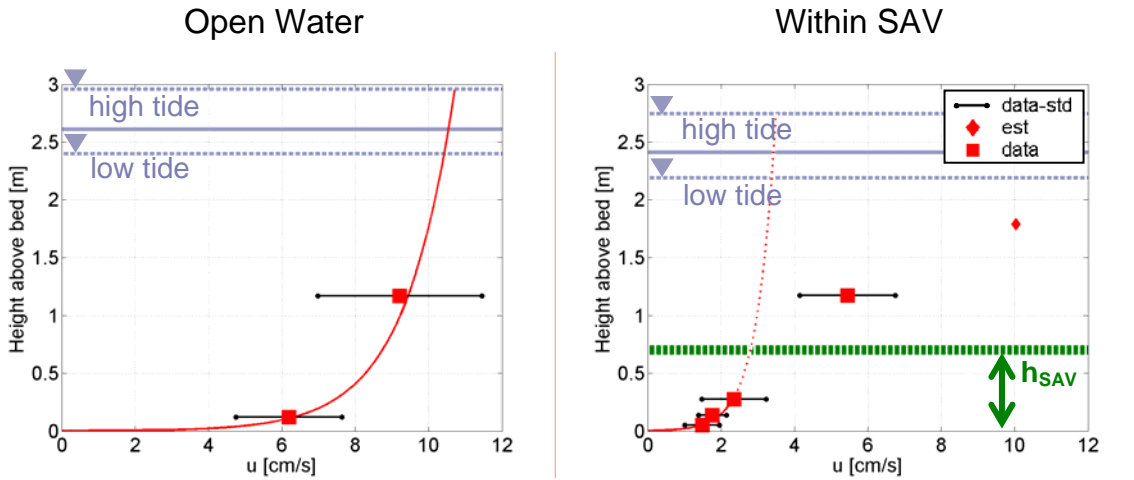


Figure HS10. Vertical structure of flows during ebb tide in open water (left panel) and in submerged aquatic vegetation (right panel).

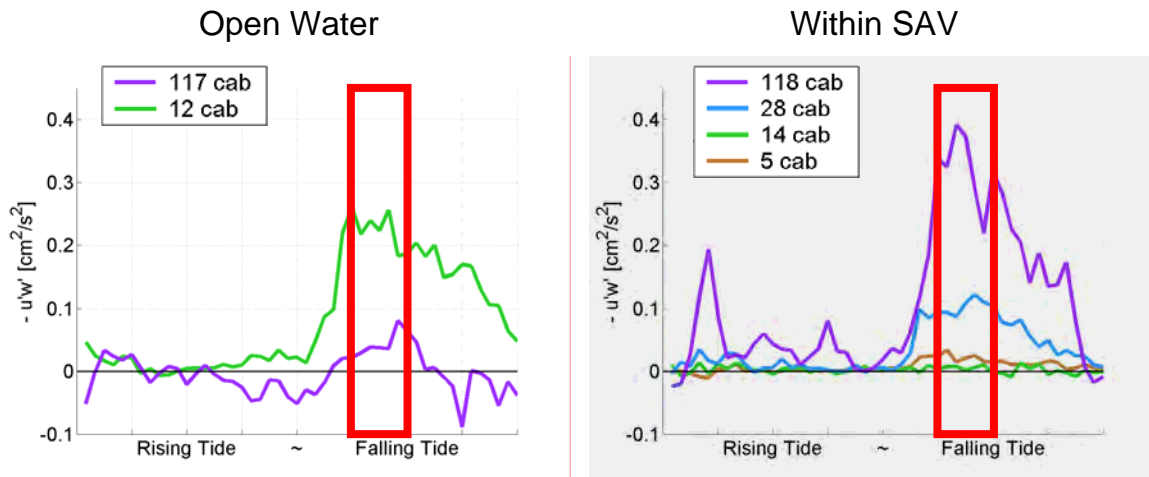


Figure HS11. Average tidal cycle variability of turbulent stresses in open water (left panel) and within submerged aquatic vegetation (right panel). Note that the top sensor in the right panel is just above the top of the SAV canopy.

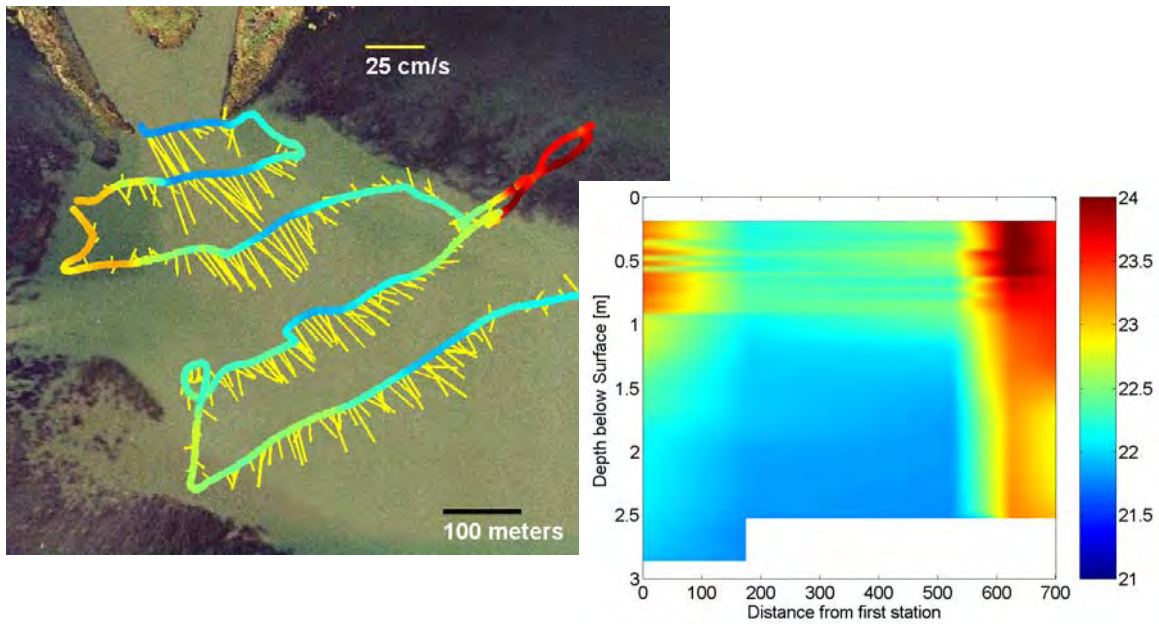


Figure HS12. Transects of temperature variability in Franks Tract demonstrating the pronounced influence of the SAV. Left panel depicts the broad spatial variability of the surface temperature (note color scale is in the right panel); the right panel shows the a lateral cross-section extending into SAV, illustrating that temperature variability is almost entirely horizontal with very limited vertical variability.

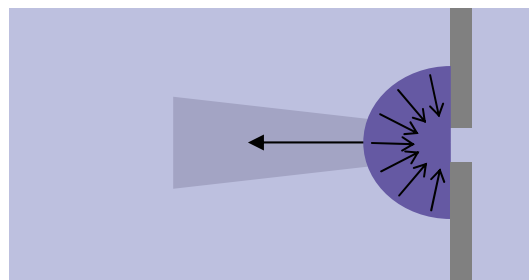


Figure HS13. Idealized tidal pumping mechanism with momentum jet entering habitat (to the left) and radial flow towards the opening on the ebb tide.

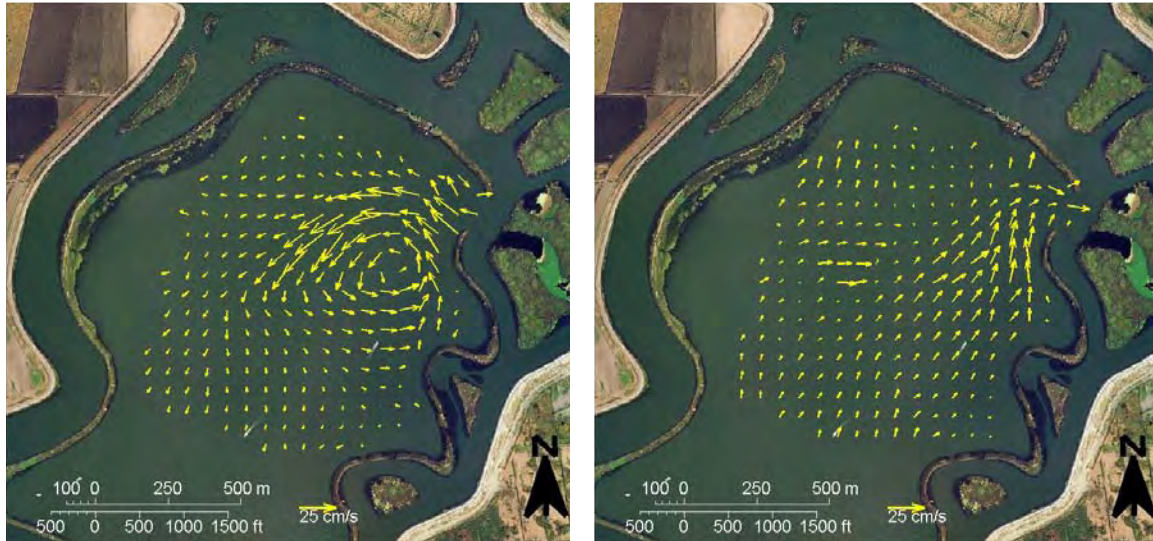


Figure HS14. Flood-ebb asymmetry in northern Mildred Island. Left panel shows flood tide jet deflected to the south, along with the recirculating eddy on the south side of the jet (measured from transect studies). The right panel shows a typical ebb tide velocity distribution, with flow biased towards the eastern shore.

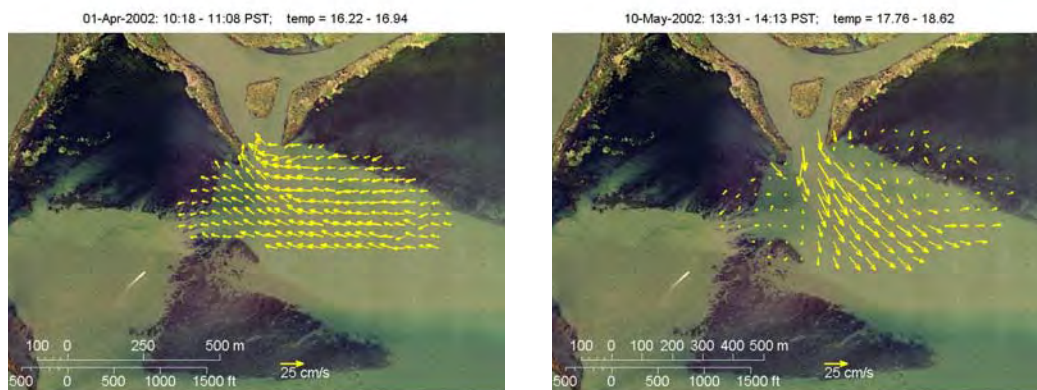


Figure HS15. Flood-ebb asymmetry in northern Franks Tract. Ebb tide (left panel) is largely from east to west, with limited influence of the opening. Flood tide in the same region is strongly dominated by the flood tide jet, which is slightly deflected to the east.

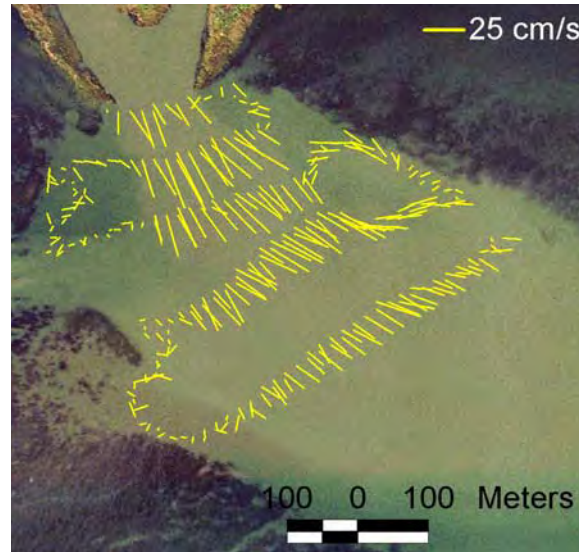


Figure HS16. Effects of SAV on vortex formation. A vortex is created along the northeast side of the flood jet, but it is constrained to within the open water region, and does not extend into the SAV.

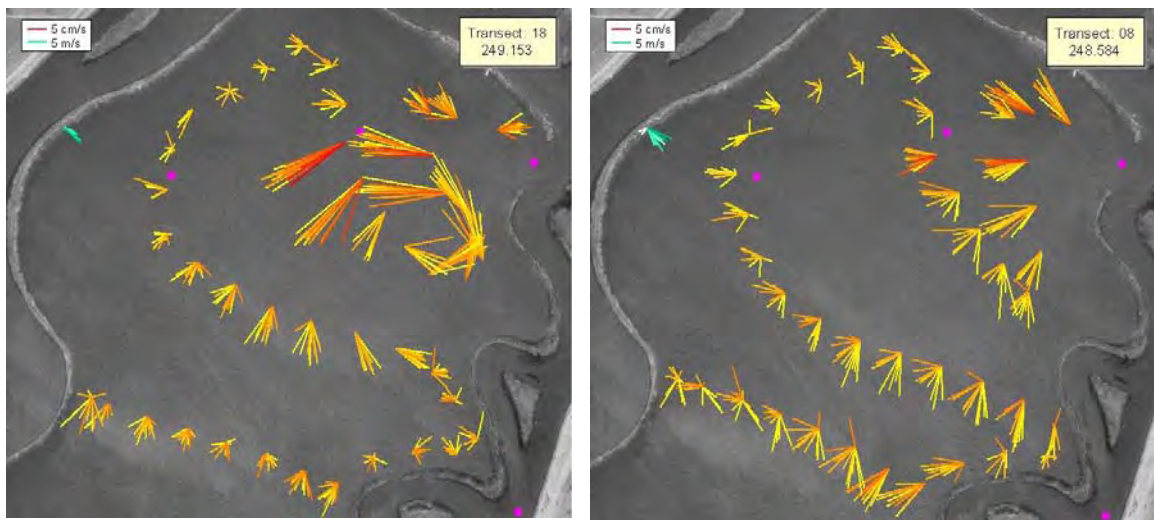


Figure HS17. Influence of wind-driven flow on the flood jet. During calm periods, such as at night (left panel), the flood tide jet maintains its identity well into the interior of MI (deflected to the south by the ambient tidal surface slope). During windy afternoons, however (right panel), the flood jet is overwhelmed by wind-driven flow, and the surface currents move to the south or southeast, while the near-bottom flows are oriented to the west or northwest.

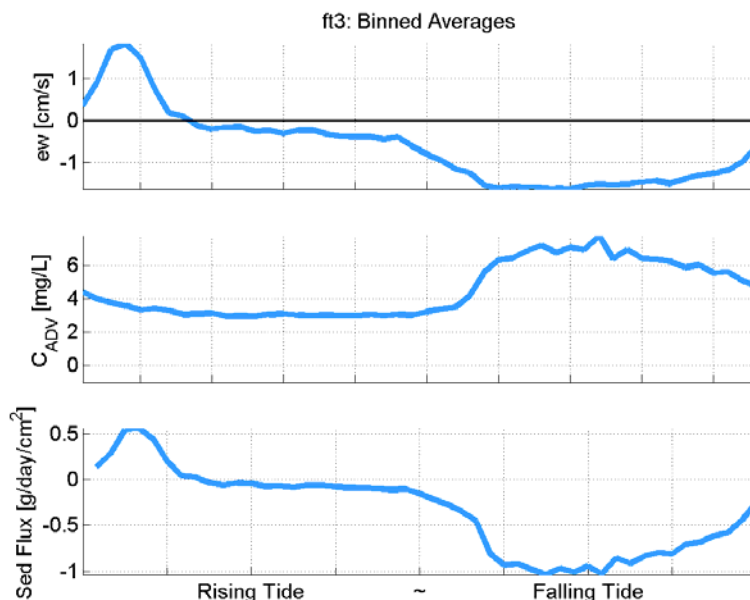


Figure HS18. Tidal cycle variation in sediment flux. Velocity is strongly ebb dominated, except for a positive pulse of flow at the beginning of the flood tide (top panel). Suspended sediment (center panel) is much higher during the ebbing tide such that the net sediment flux (bottom panel) is oriented to the west, into the SAV.

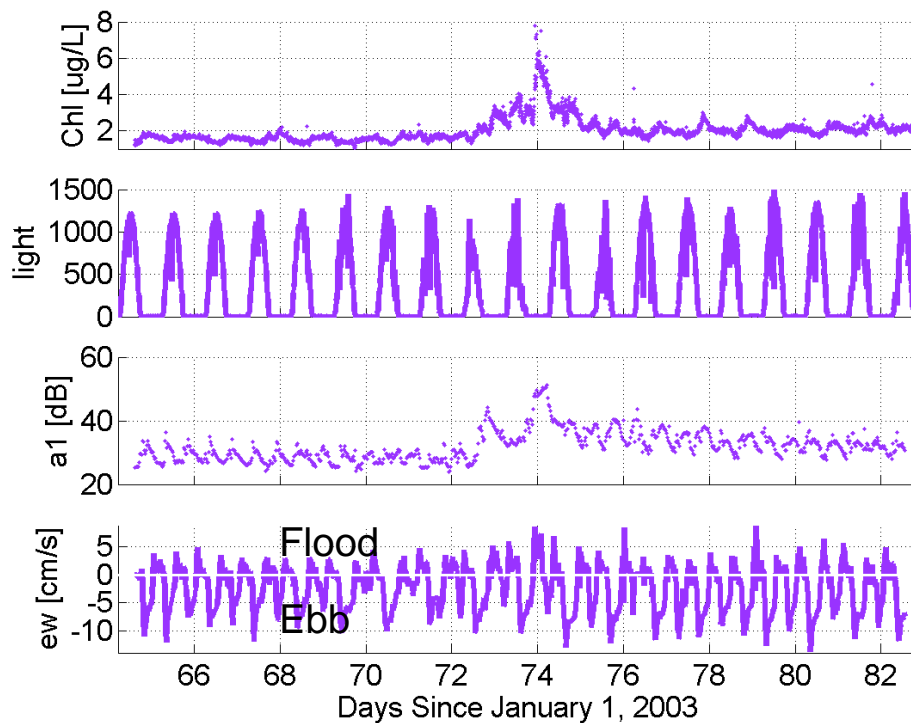


Figure HS19. Effects of wind on chlorophyll fluorescence. A large windstorm on days 73-74 led to a large peak in both chlorophyll fluorescence (top panel) and particles in suspension (third panel).

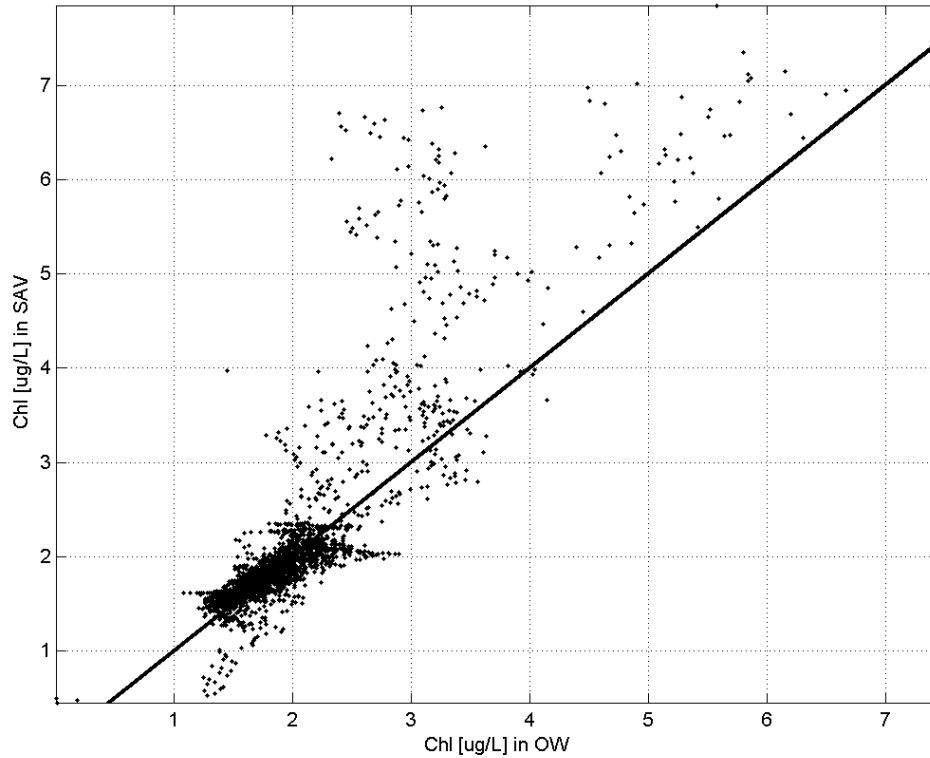


Figure HS20. Comparison of chlorophyll fluorescence in SAV and in open water. During the storm on days 73 and 74, the fluorescence in the SAV exceeds that in the open water; at other times (low fluorescence values), the two are in good agreement.

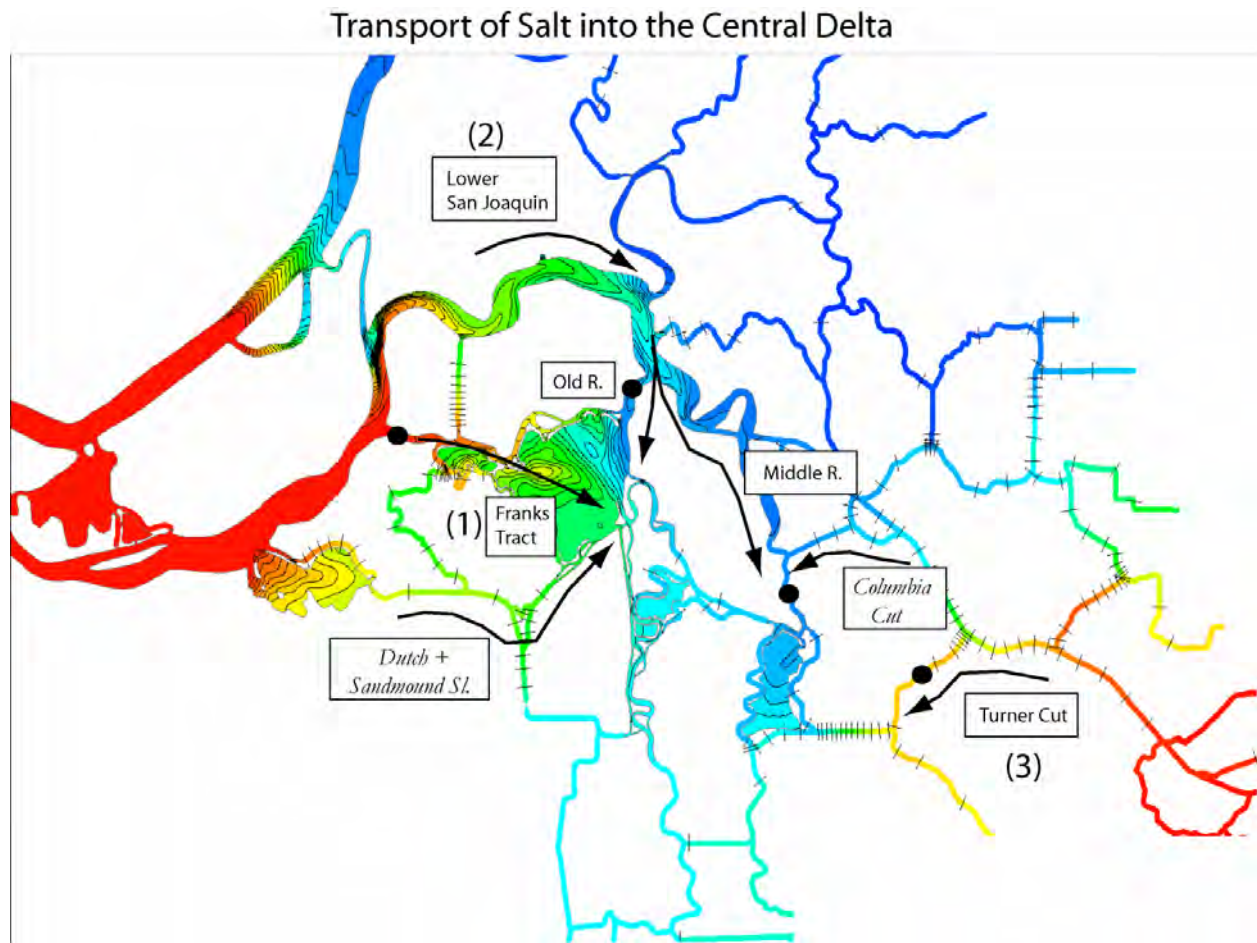


Figure HR1. Salt concentration from a numerical simulation is shown in terms of color – cooler colors (blue) represent relatively fresh water, warmer colors (red) represent saltier water. Salty water is exchanged into the central Delta through three main pathways: (1) through False River into Franks Tract, (2) through the lower San Joaquin River, and (3) Turner Cut. Secondary pathways through (a) Dutch and Sandmound Slough, (b) Old River and Middle River and (c) Columbia Cut also convey salt into the central Delta. (Background image courtesy of John DeGeorge, RMA)

Fresh Water into the Central Delta

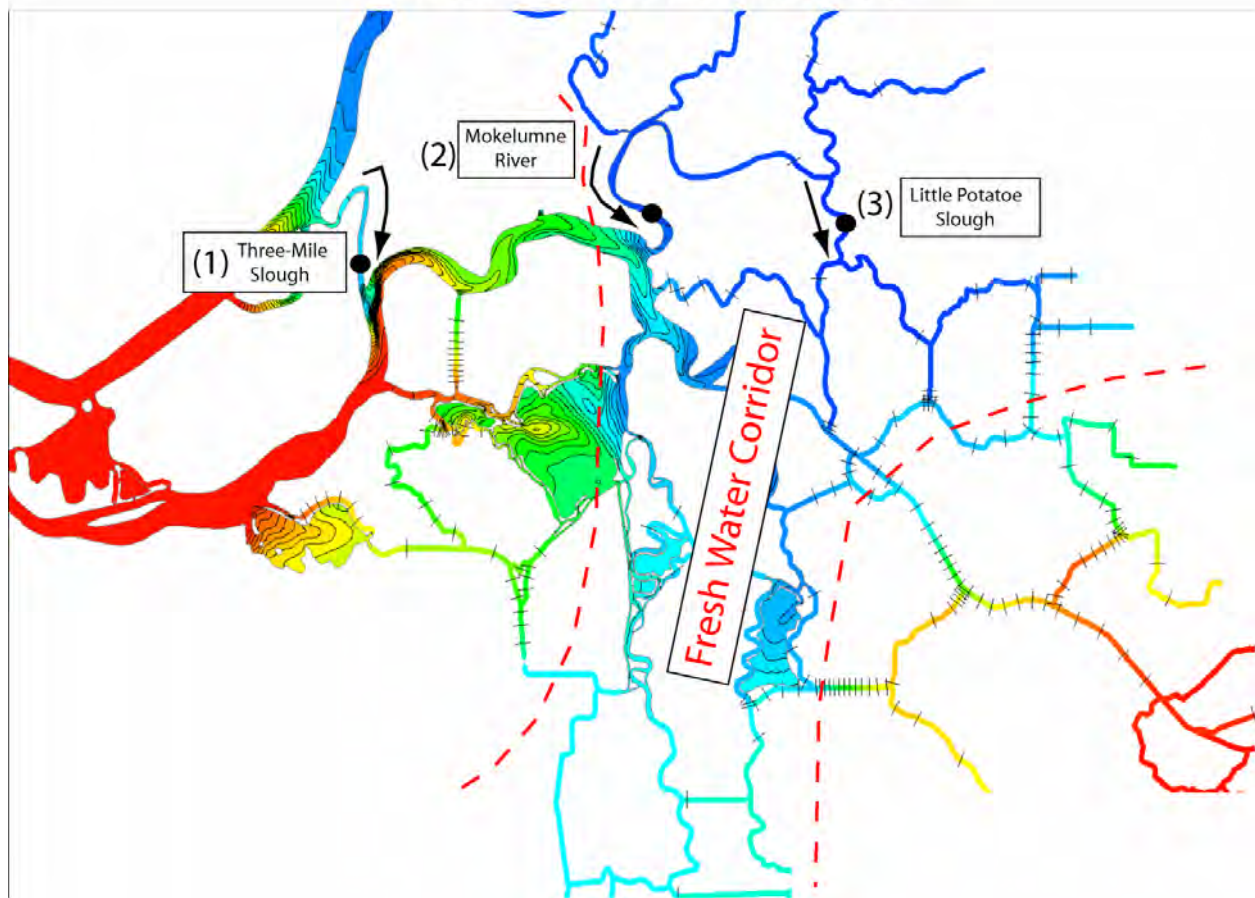


Figure HR2. Salt concentration from a numerical simulation is shown in terms of color – cooler colors (blue) represent relatively fresh water, warmer colors (red) saltier water. Fresh water is exchanged into the central Delta through three paths (1) Threemile Slough, (2) the Mokelumne River, (3) Little Potato Slough. Fresh water from these channels is mixed with saltier water from the west and south creating a “fresh water corridor” represented by the north-to-south blue to cyan band (Background image courtesy of John DeGeorge, RMA)

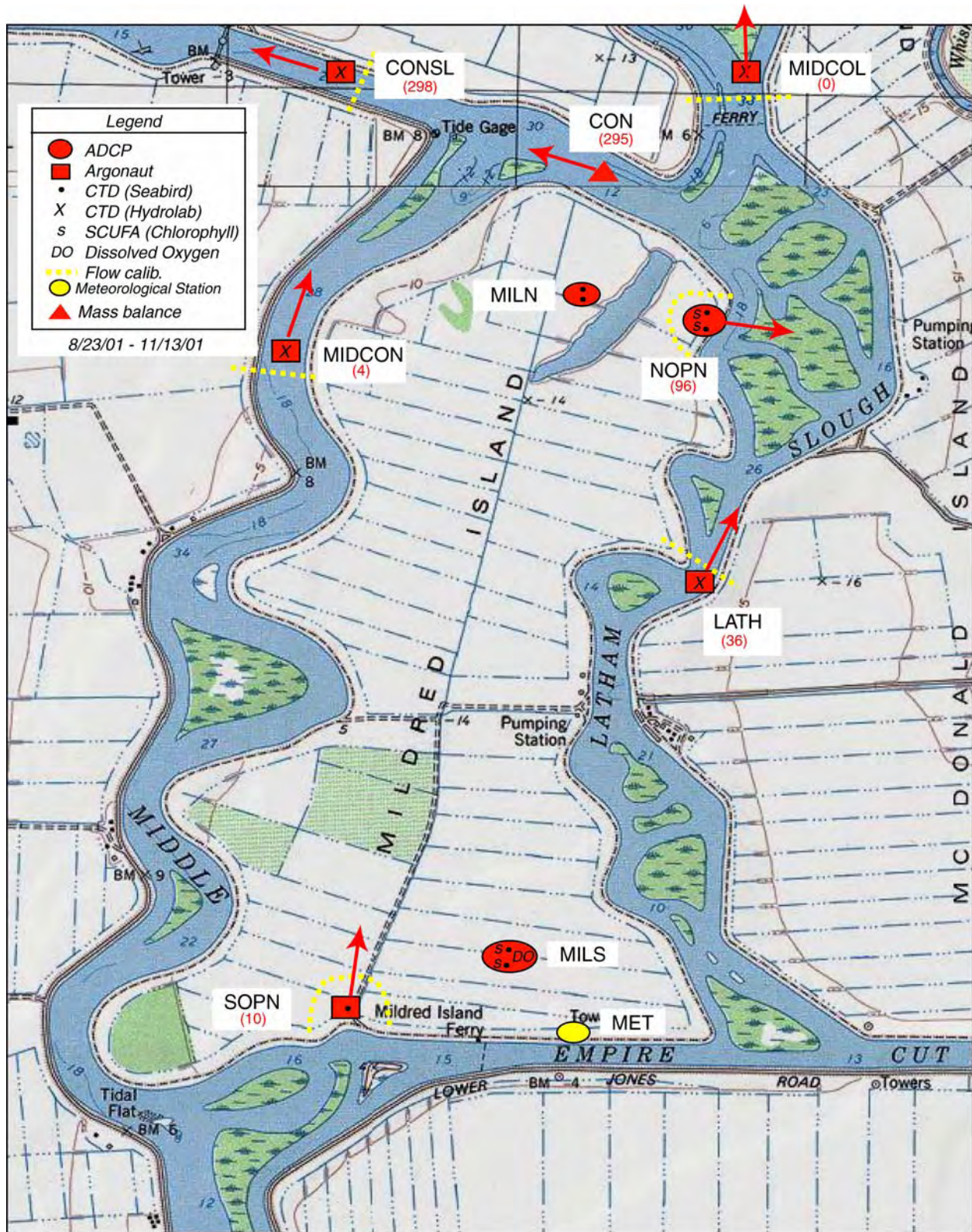


Figure HR3. Data-collection locations, station names and assumed positive flow directions, Mildred Island, California. The flow at station CON is a computed quantity based on a mass balance of surrounding stations.

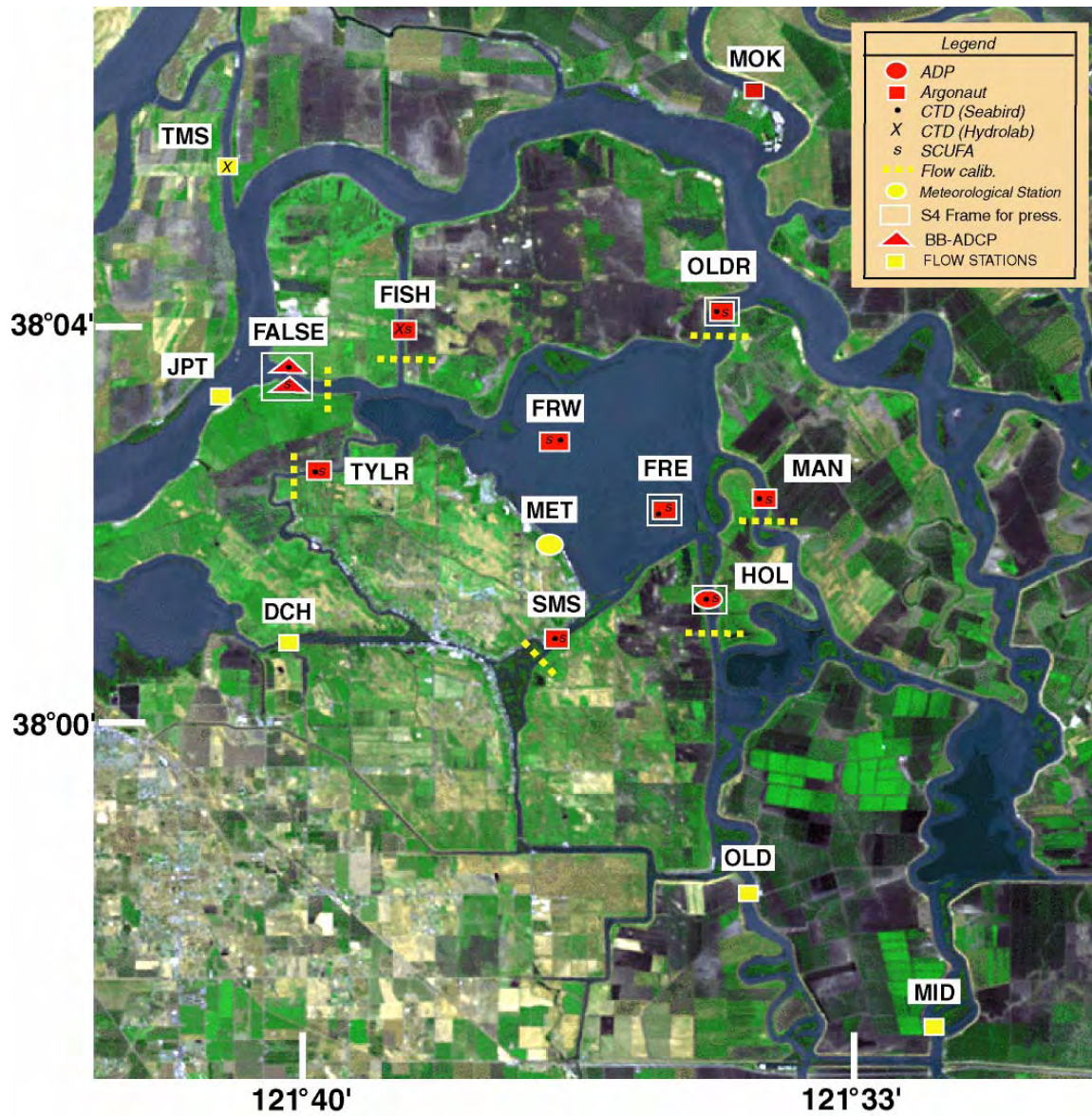


Figure HR4. Data-collection locations and station names, Franks Tract, California, April 10, 2002 through August 27, 2002.

OLDR: 12134738

Lat/Long: 38 04.21 N, 121 34.74 W

VELOCITY STRING

Argonaut: E192 1.5 Mhz (Pinger)
Pinger: 37.5 Khz
Surface Mark: F12

CTD STRING

Seabird-CTD: 0315
Pinger: 45 Khz
Surface Mark (CTD): F16

SCUFA STRING

Scufa: 160
Sub-surface Mark: 201
Surface Mark: M5

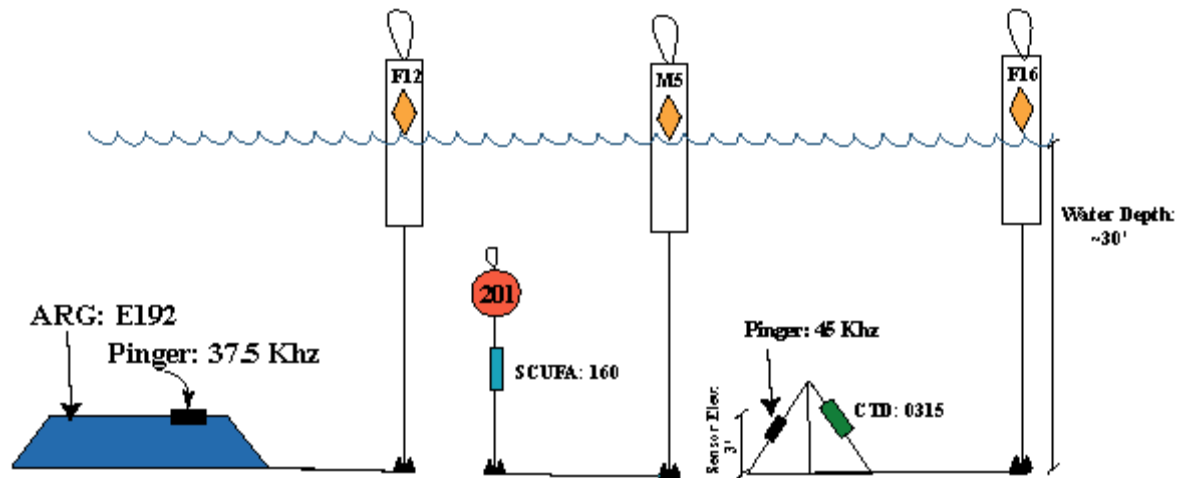
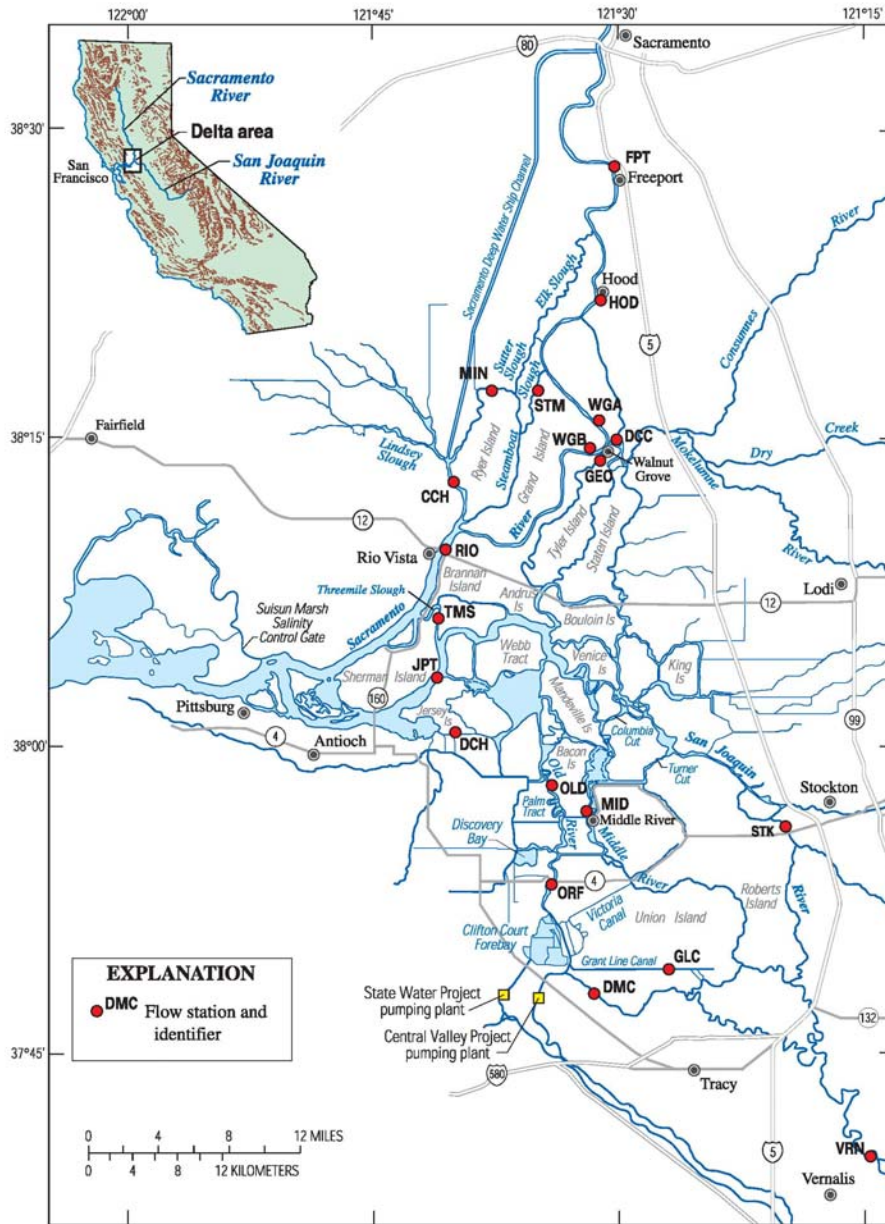


Figure HR5. Typical suite of instruments at each station location in figure HR3 and HR4.



Location of flow station sites in the Delta Area of California.

Figure HR6. Flow monitoring network in the Sacramento/San Joaquin Delta.

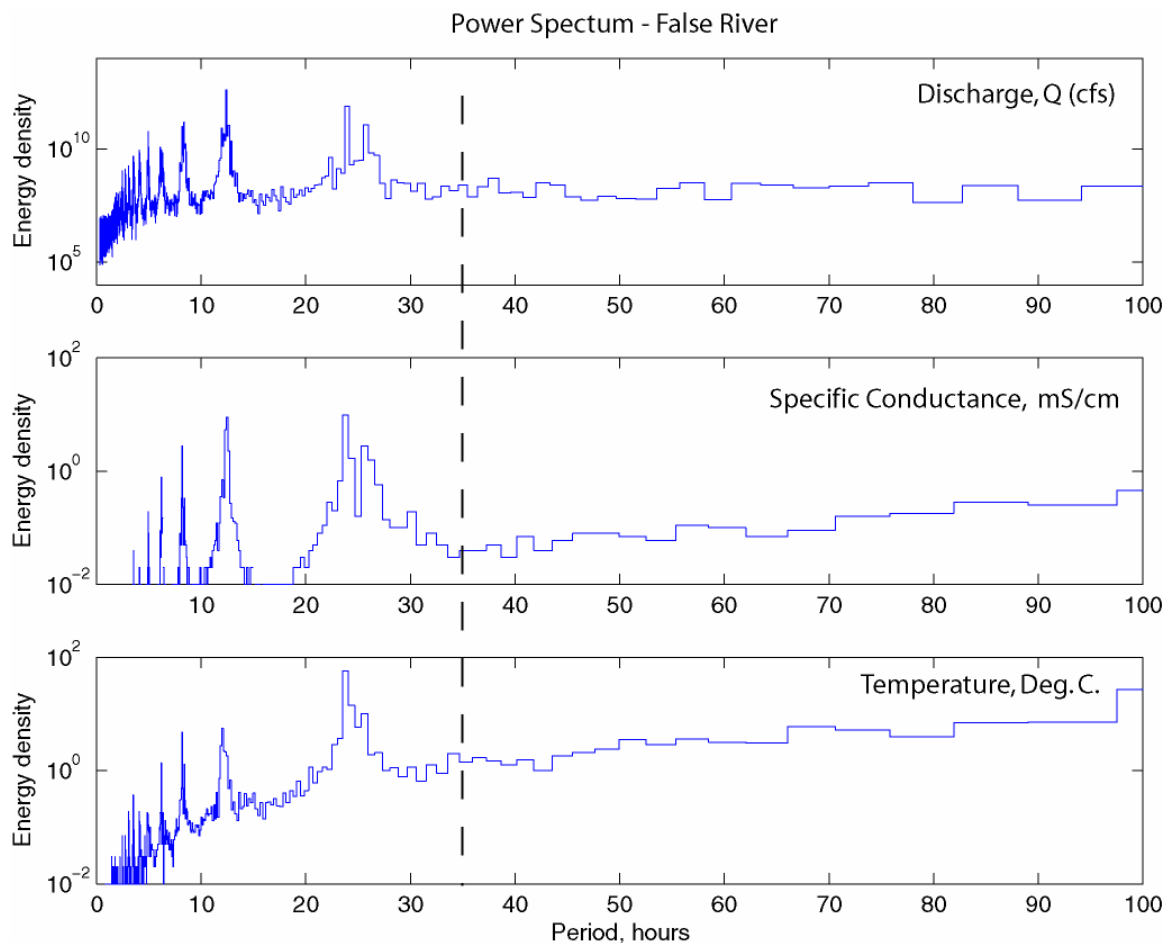


Figure HR7A. Power spectrum of (a) discharge, (b) specific conductance, (c) temperature at based on time-series collected at False River location.

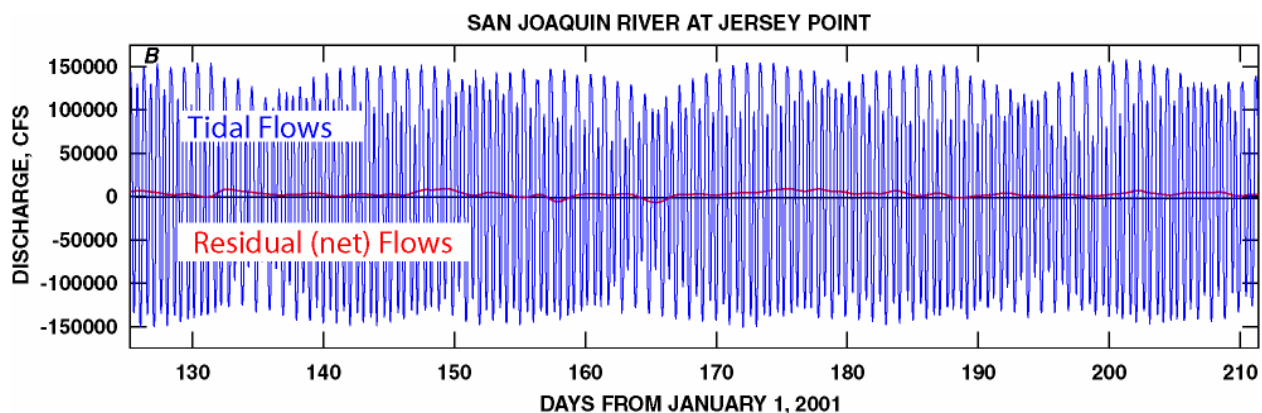


Figure HR7B. Time series plot of the tidal and residual (tidally-averaged) discharge measured at Jersey Point in 2001. By convention, positive flows are seaward. The tides drive the variability in the measured discharge, which is on the order of $\pm 150,000$ cfs. The net flows, computed using the digital filter described in Walters and Heston, 1982, is on the order of 5,000 cfs. Therefore, in this case, the net flows are on the order of 3% of the tidal flows.

Drifter Recovery

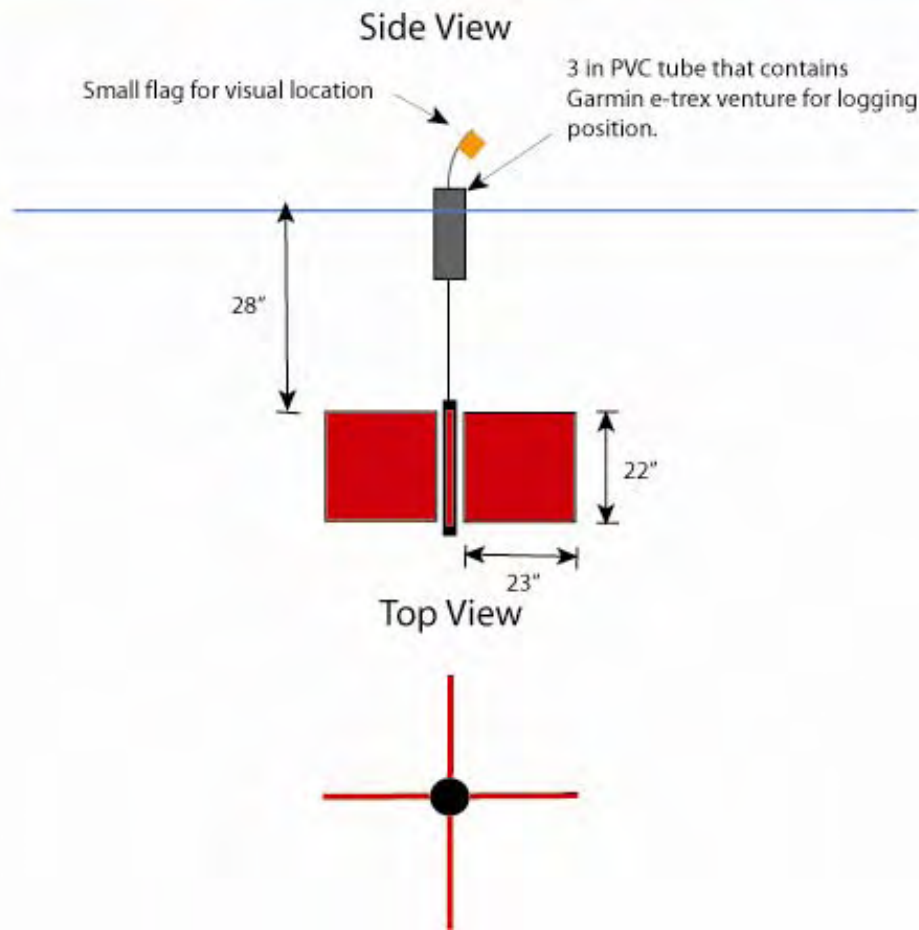


Figure HR8. Photograph and schematic of the drifters used in the Lagrangian experiments.

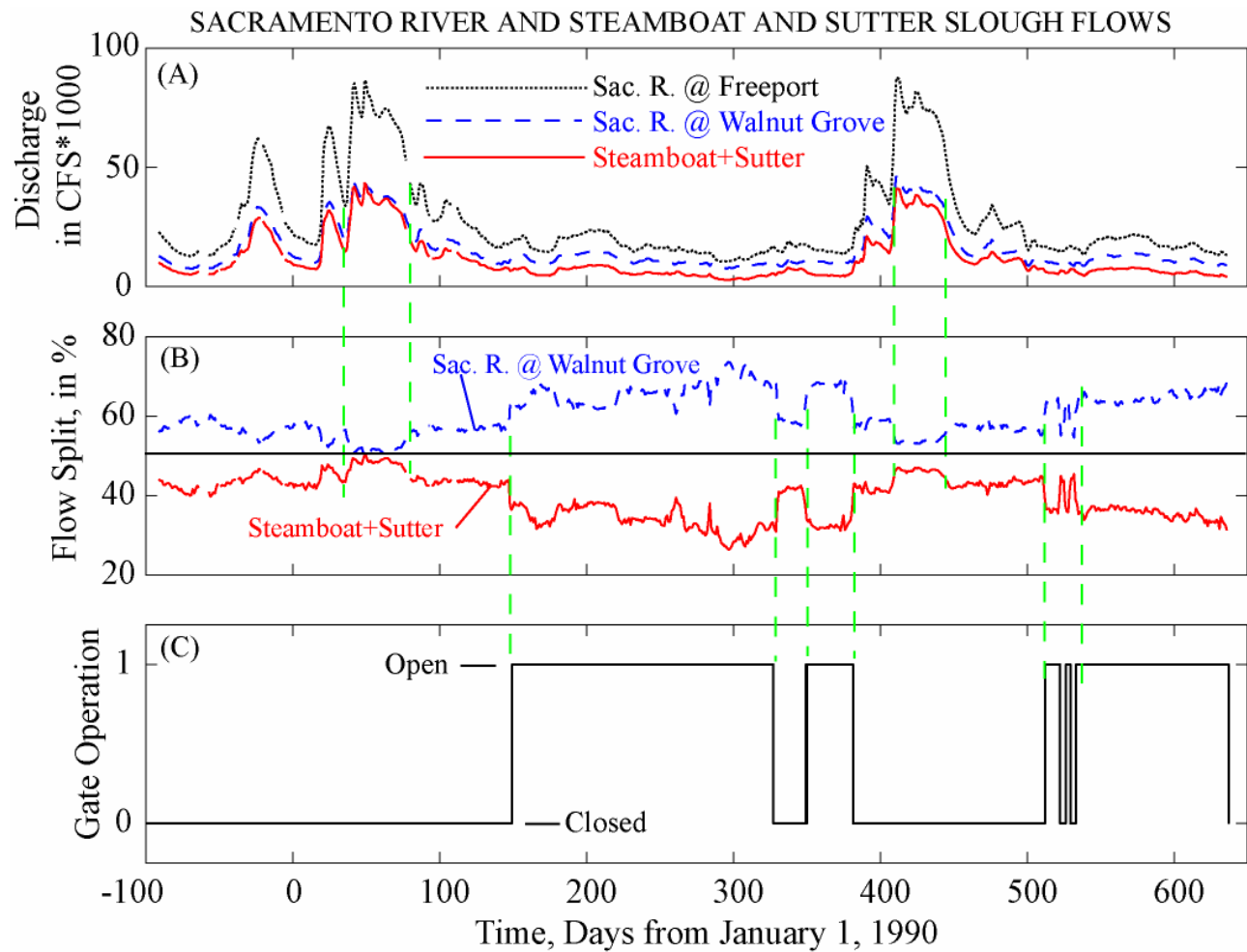


Figure HR9. Time series of (top panel) net flow in the Sacramento River at Freeport, in the Sacramento River above Walnut Grove, and the combined net flow in Sutter and Steamboat Sloughs; (middle panel) the percentage of the net Sacramento River flow as measured at Freeport flowing in the Sacramento River above Walnut Grove and down Sutter and Steamboat Sloughs; and (bottom panel) Delta Cross Channel gate position.

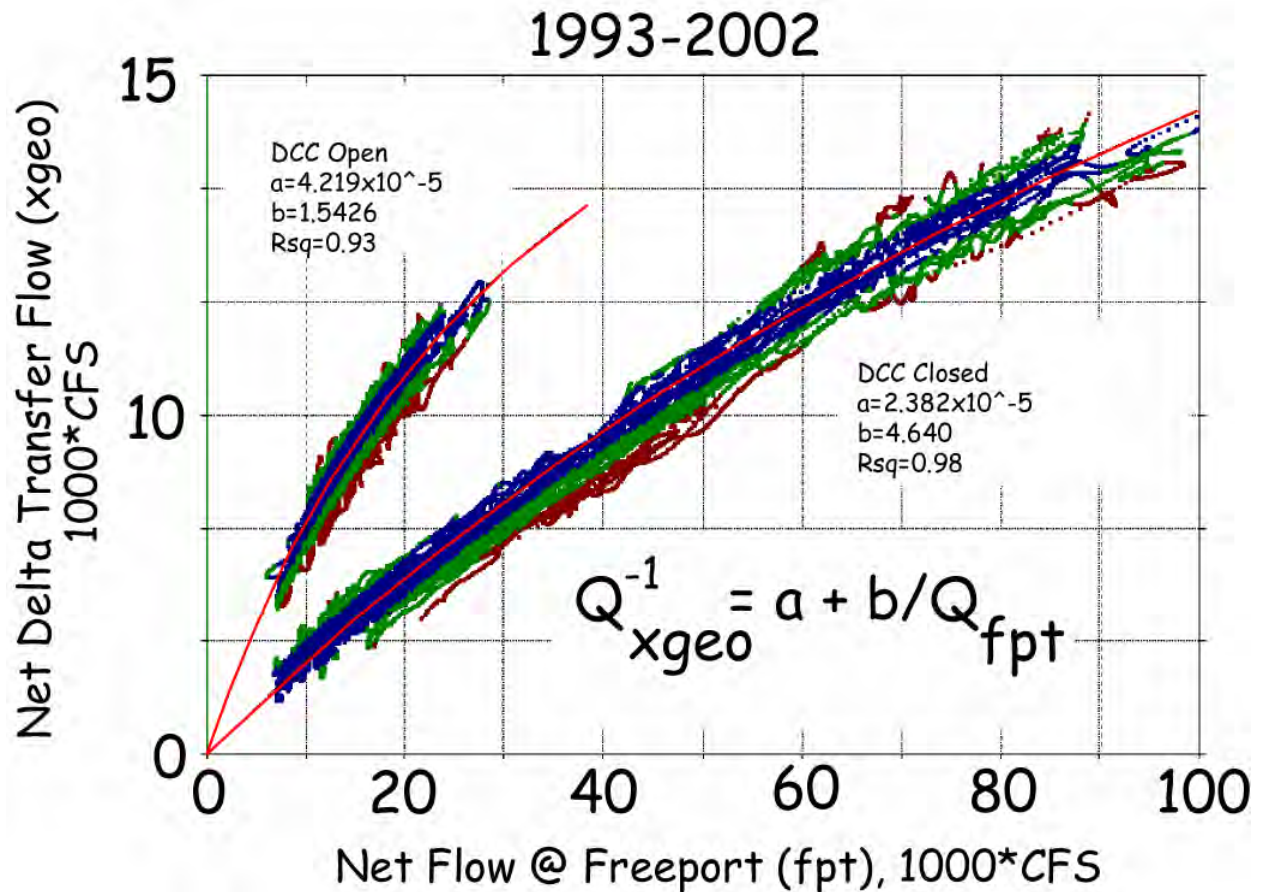


Figure HR10. Net Delta transfer flow, Q_{xgeo} , as a function of the net Sacramento River flow measured at Freeport, Q_{fpt} , and Delta Cross Channel (DCC) gate position. A simple non-linear relation was regressed to the data using a least-squares approach. This relation naturally goes through zero, which allows these relations to predict system response at very low flows (severe drought conditions). The non-linear relation used, $Q_{xgeo}^{-1} = a + b/Q_{fpt}$, fit 10 years of data remarkably well with $Rsq > 0.90$. Based on this graph it is clear that the response of net Delta transfer flow to DCC gate operations is well defined, statistically stationary over the period of record, and clearly bi-modal with respect to DCC gate operations over the full range of Sacramento River flows as measured at Freeport.

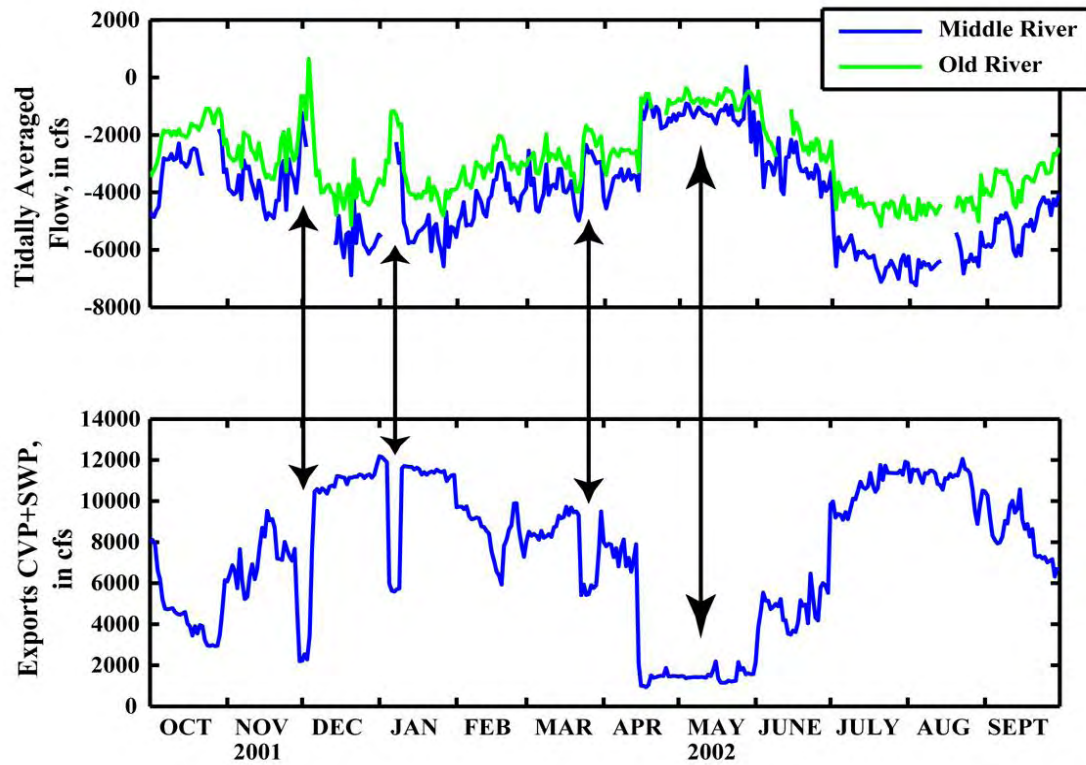


Figure HR11. Time series plots of the tidally-averaged flow in Old and Middle River, where negative flows are toward the export facilities (south). Even short duration reductions in exports have a strong effect on the tidally-averaged flows in Old and Middle River. Negative flows are flows towards the export facilities.

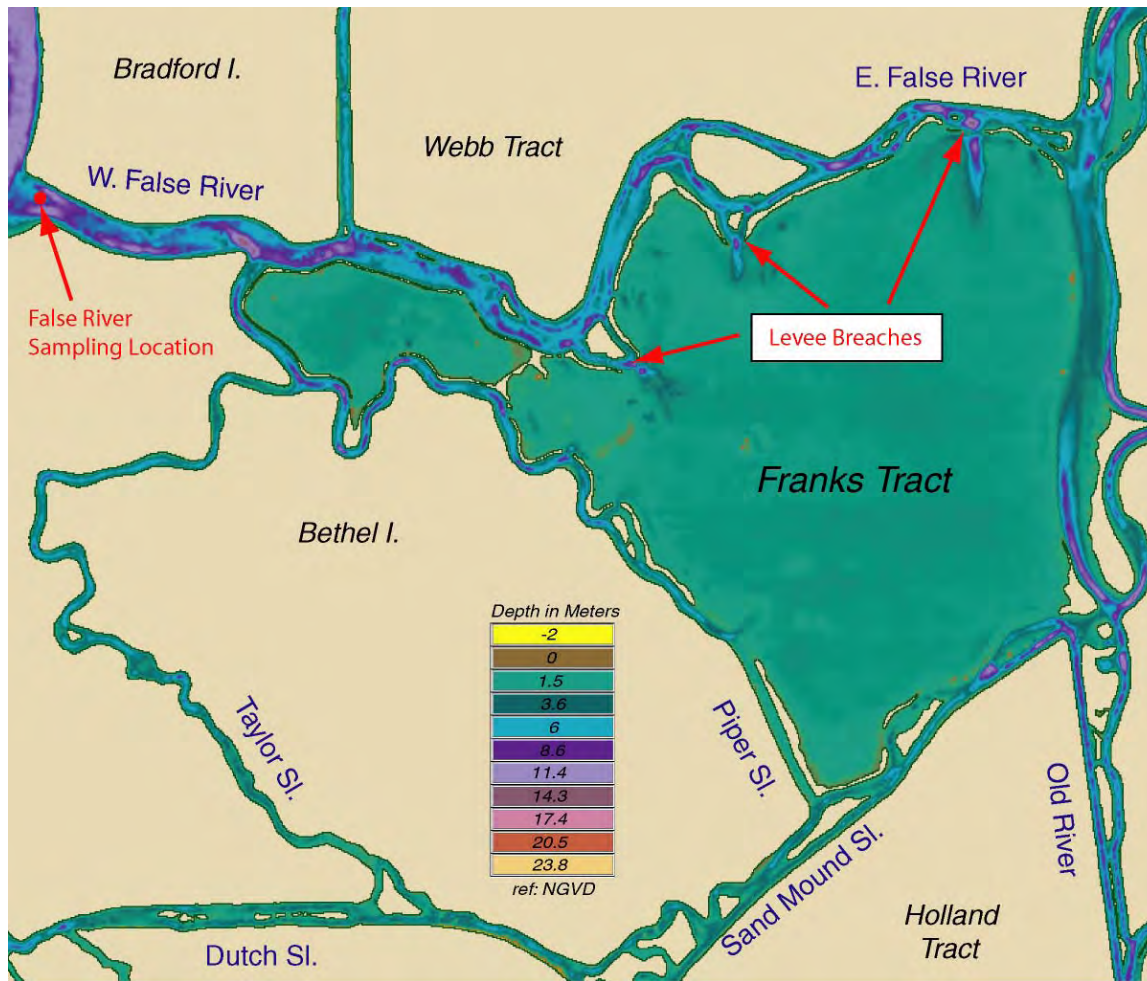


Figure HR12. Bathymetry in the Franks Tract area. Franks Tract is a shallow (depths < 2 m) Flooded Island connected to its surroundings by a series of deep/narrow levee breaches on its western boundary and by a submerged remnant levee to the east. False river is roughly 1000 m wide and has fairly complex bathymetry with a number of well defined deeper areas of intense scour.

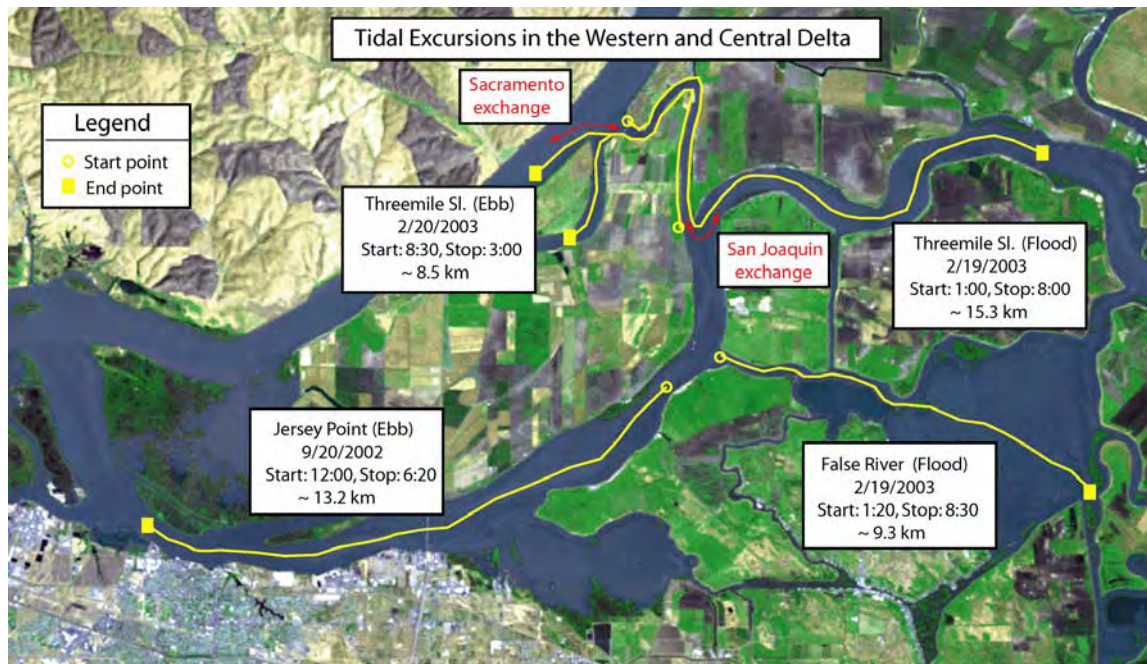


Figure HR13. Tidal excursion data collected using surface drifters outfitted with differential GPS receiver/loggers at the dates and times indicated. Typically, tidal excursions increase seaward as the tidal forcing increases. However, the Threemile floodtide excursion is the exception – note that it is longer than the tidal excursion measured at Jersey Point. The short/long tidal excursion in Threemile Slough during ebb/flood tides, respectively, occurs because the tides turn roughly 50 minutes later on the San Joaquin compared to the Sacramento River at Threemile Slough. Drifters released at the Threemile/San Joaquin junction on flood take about an hour to traverse Threemile Slough and thus pop out on the San Joaquin very near the time the tide turns so they are carried up the San Joaquin by a full tide cycle. Similarly, drifters released on an ebb tide at the Threemile/San Joaquin junction travel about an hour in traversing Threemile slough and pop out several hours into the Sacramento River ebb and thus their tidal excursion is foreshortened. Finally, the tidal excursion of drifters released at the False River/San Joaquin River junction can traverse the entirety of Franks Tract.

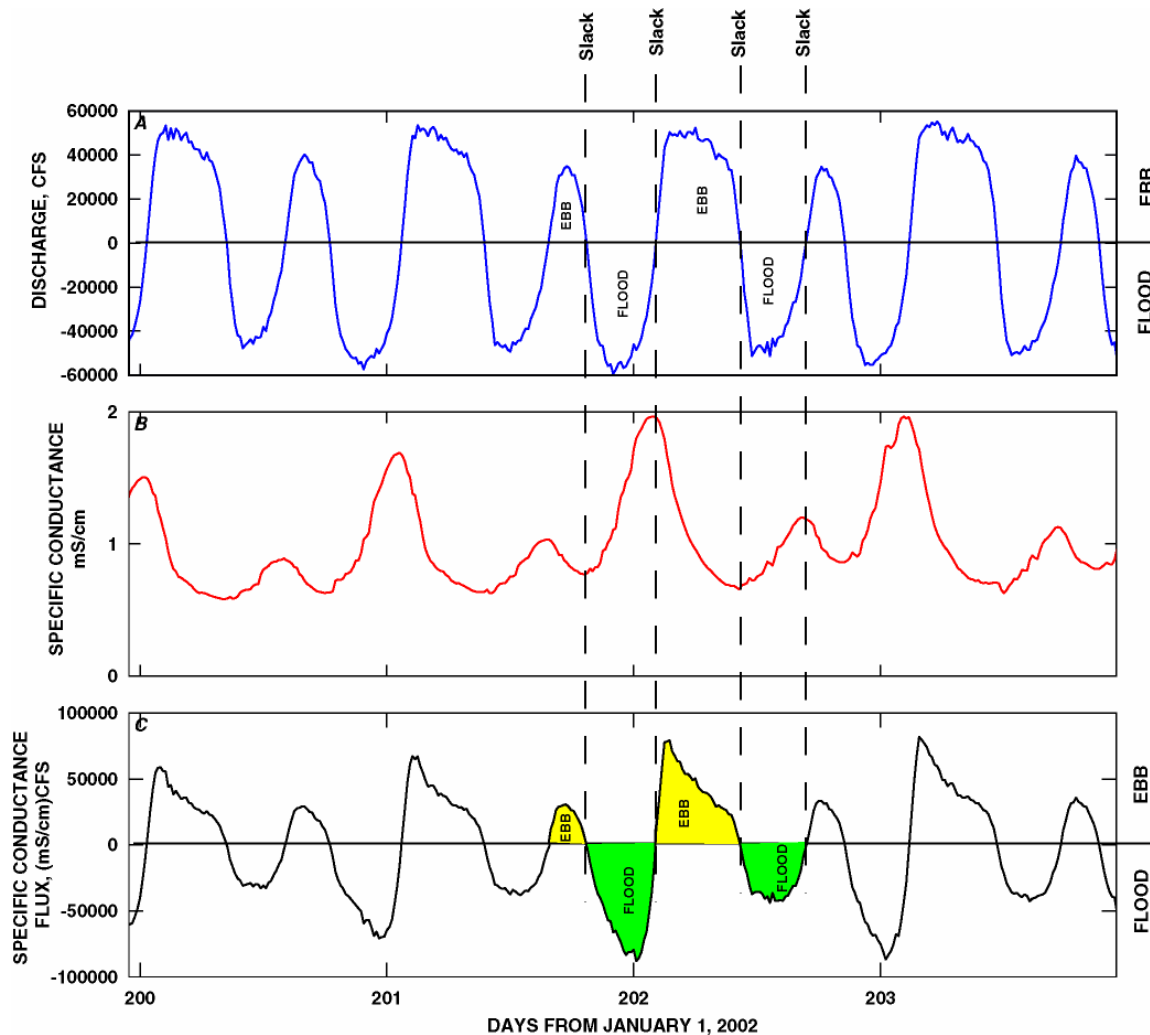


Figure HR14. Discharge, specific conductance, and specific conductance flux time-series measured in False River in 2002. The peaks and troughs in specific conductance correspond to slack water periods (e.g. discharge and specific conductance are in quadrature). This indicates that transport of specific conductance at this location is advection dominated, as it is throughout most of the Delta. Most of the tidal timescale variations in specific conductance are simply due to the translation of a relatively time-stable horizontal specific conductance gradient that moves past our False River by the tidal currents. The area under the specific conductance flux curve is the amount of salt that passed in a given direction, flood or ebb. In this case, the amount of salt moving past this section on flood (green) is greater than ebb (yellow) because the tidally averaged dispersive salt flux is in the flood direction (negative, by convention)(Figure HR13), although this is hard to see visually. Essentially, more salty water goes into Franks Tract through False River (the green area) than comes out (the yellow area) on each tidal cycle.

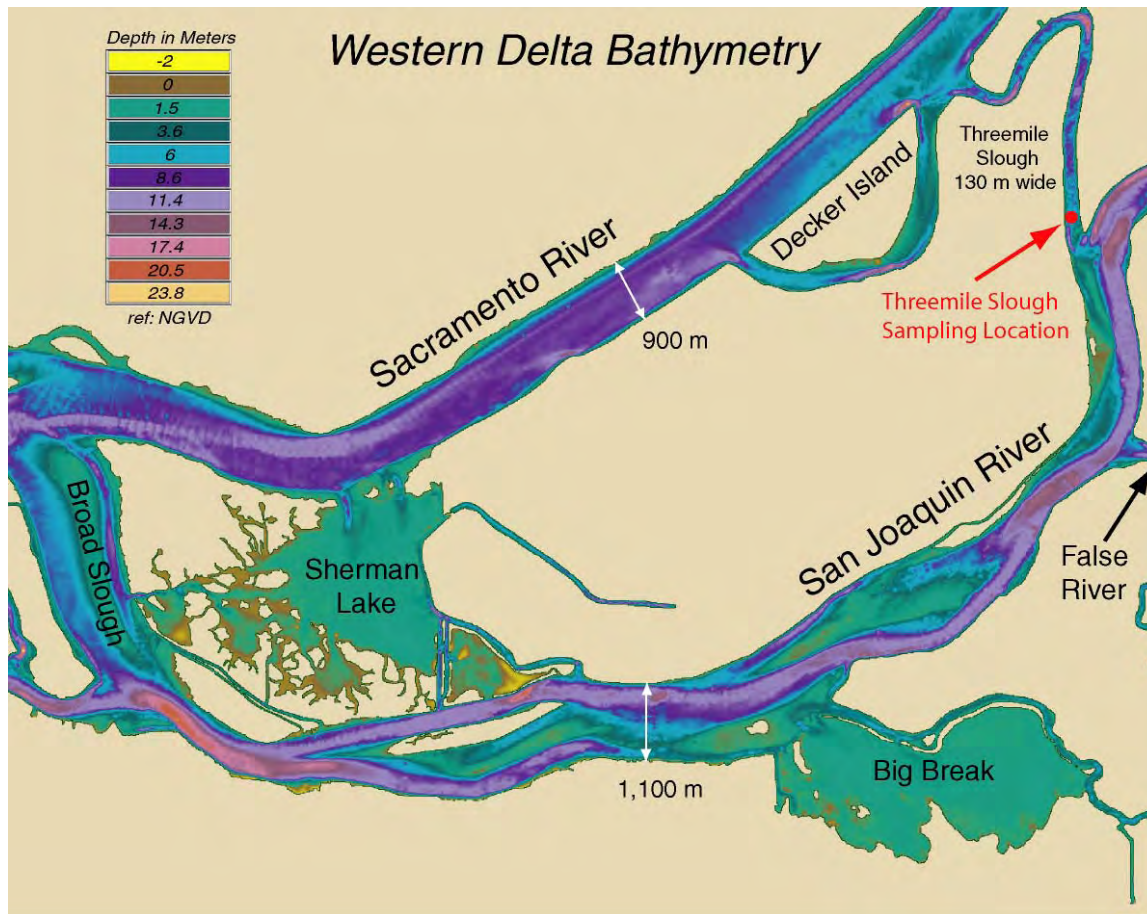


Figure HR15. Western Delta bathymetry. The Sacramento and San Joaquin Rivers are wide and bathymetrically complex. In the case of the Sacramento River, the channel is clearly dredged upstream of Decker Island and becomes deep across its full width downstream of Decker Island. The San Joaquin River has a sinuous deep water channel that weaves its way through numerous shallow bars and islands.

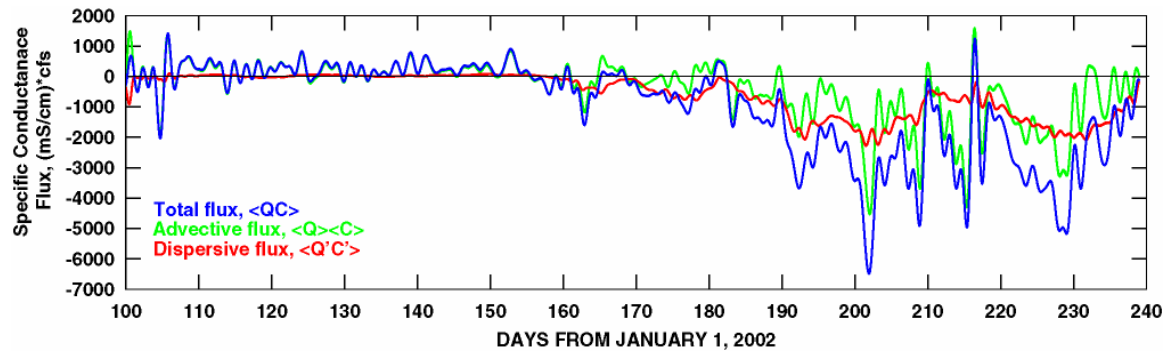


Figure HR16. Time-series of the total (blue), advective (green), and dispersive flux measured in False River in 2002. The dispersive flux contributes roughly half of the total, suggesting that tidal timescale mixing within a tidal excursion of this sampling location significantly contributes to the transport of salt in this region.

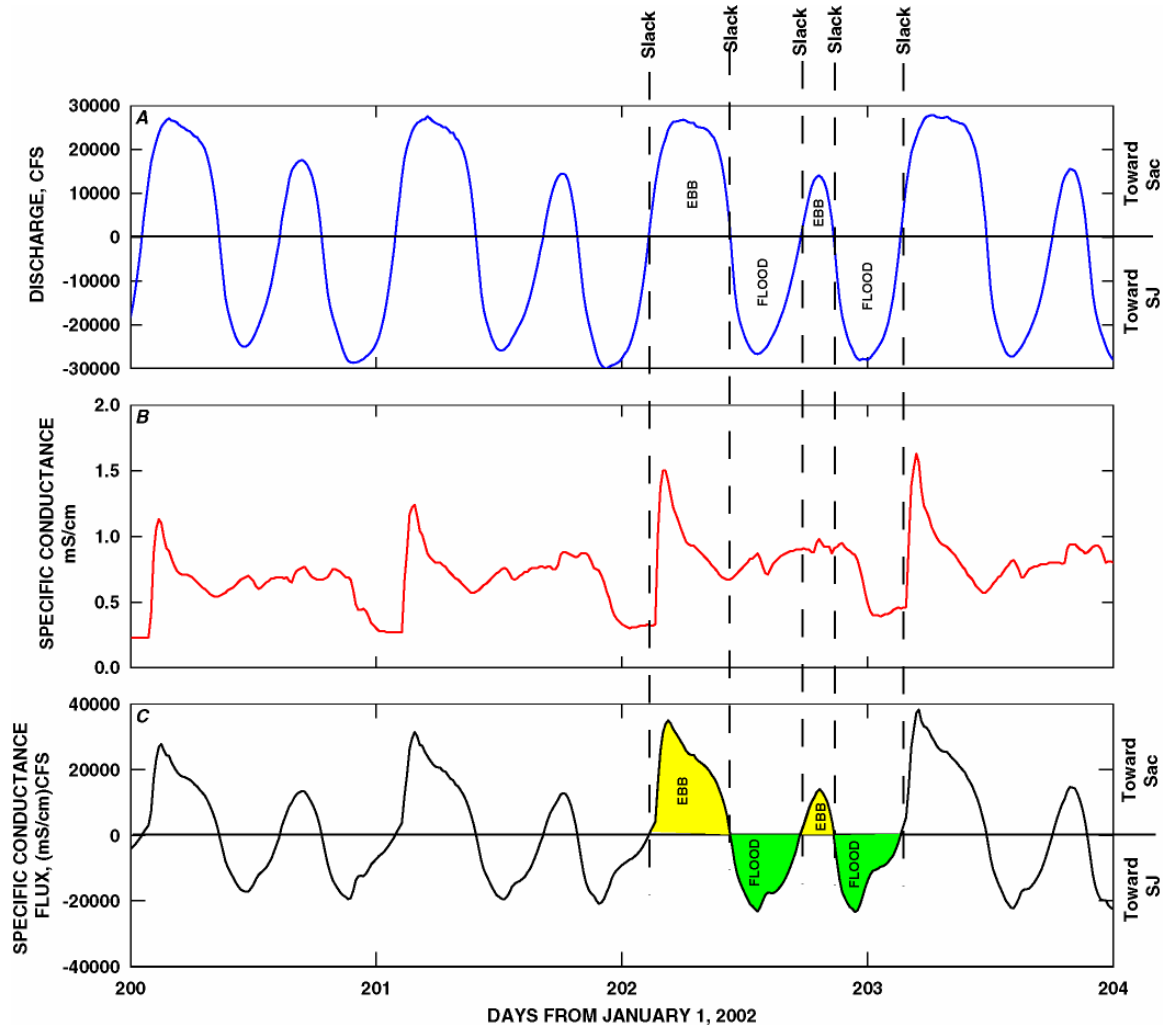


Figure HR17. Discharge, specific conductance, and specific conductance flux time-series measured in Threemile Slough in 2002. The ebb direction is positive from the San Joaquin to Sacramento River. Variation in specific conductance is somewhat more complicated in Threemile Slough compared to other locations in the Delta, reflecting its role as a conduit of exchange between two much larger river systems. The tidal current phase relations between the Sacramento River, San Joaquin River, and Threemile Slough explains the observed specific conductance variation. Water flows through Threemile Slough due to water level differences (barotropic pressure gradients) between the Sacramento and San Joaquin Rivers. Water Level differences between these large rivers are primarily driven by differences in the tidal wave propagation characteristics between them. The tide wave arrives about 50 minutes earlier on the Sacramento River, which drives water through Threemile Slough towards the San Joaquin on flood tides. Therefore, water exiting Threemile Slough into the San Joaquin River is carried landward on flood tides. For similar reasons, water entering Threemile Slough, flowing towards the Sacramento River, comes from upstream and is carried toward Suisun Bay as it enters the Sacramento River. Thus fresh water from the Sacramento River is exchanged through Threemile Slough and is transported in the San Joaquin toward the Mokelumne system on flood tides and salty water from the San Joaquin is ejected into Sacramento River water headed towards the Bay

(see red arrows on Figure HR13). The rapid rise in salinity during ebb tides (leftmost vertical dashed line) as San Joaquin River water begins to enter Threemile Slough is indicative of the strong salinity gradient between the Sacramento and Joaquin River. However, this initial rapid rise in salinity at the beginning of the ebb is shortly followed by a gradual decline throughout the remainder of the ebb. The high saline pulse measured in Threemile Slough on ebb tides is actually high saline water that passed the Slough on the San Joaquin River on the previous flood tide. So the high saline water entering Threemile is coming from upriver on the San Joaquin, which is why it quickly declines as fresh water originally from the Mokelumne enters the Slough. Because the salty pulse from the San Joaquin occurs on the beginning of the ebb, it is ejected into the Sacramento where it is mixed and, for all intents and purposes, does not return on the next flood tide (see figure HR13 for drifter paths). Finally, the drop in salinity that occurs at the end of a flood (prior to the rightmost vertical line) is fresh Sacramento River water that is ejected into the San Joaquin, is rapidly mixed, and does not return. The area under the specific conductance flux curve is the amount of salt that passed in a given direction, flood or ebb. In this case, the amount of salt moving past this section on flood (green) is less than ebb (yellow) because the tidally averaged dispersive salt flux is in the ebb direction (positive, by convention)(Figure HR18), although this is hard to see visually. Essentially, more salty water goes into Franks Tract through False River (the green area) than comes out (the yellow area) on each tidal cycle.

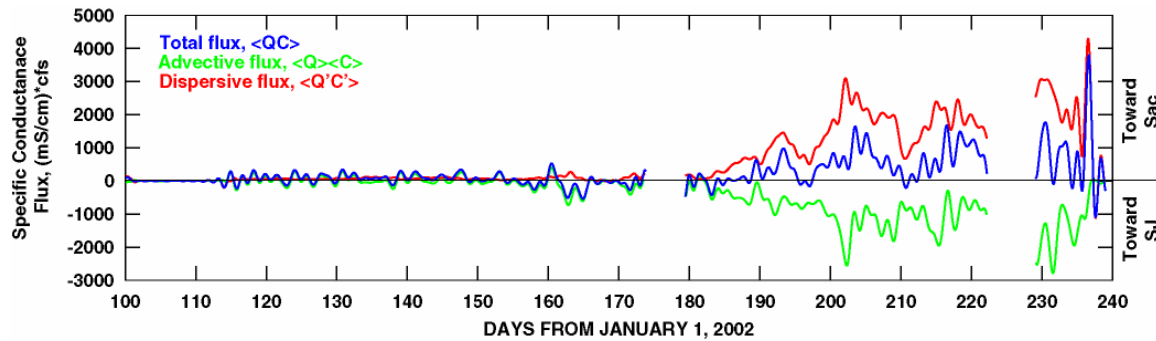


Figure HR18. Time-series of the total (blue), advective (green), and dispersive flux measured in Threemile Slough in 2002. Salt Transport, overall, is toward the Sacramento River through Threemile Slough, since salinities are higher on the San Joaquin. Yet, the advective flux is toward the San Joaquin, in a counter gradient direction because the net flow through Threemile is toward the San Joaquin River. So, Threemile Slough provides an interesting example of where the advective and dispersive fluxes are in opposite directions, the dispersive flux being the larger of the two. Therefore, if one were to take the product of the mean specific conductance concentration and the net flow to compute a net flux, as is commonly done, one would not only get the wrong answer, the answer would be in the wrong direction. This is an extreme example of where the net flows are often poor predictors of transport of constituents in a tidally dominated system like the western Delta.

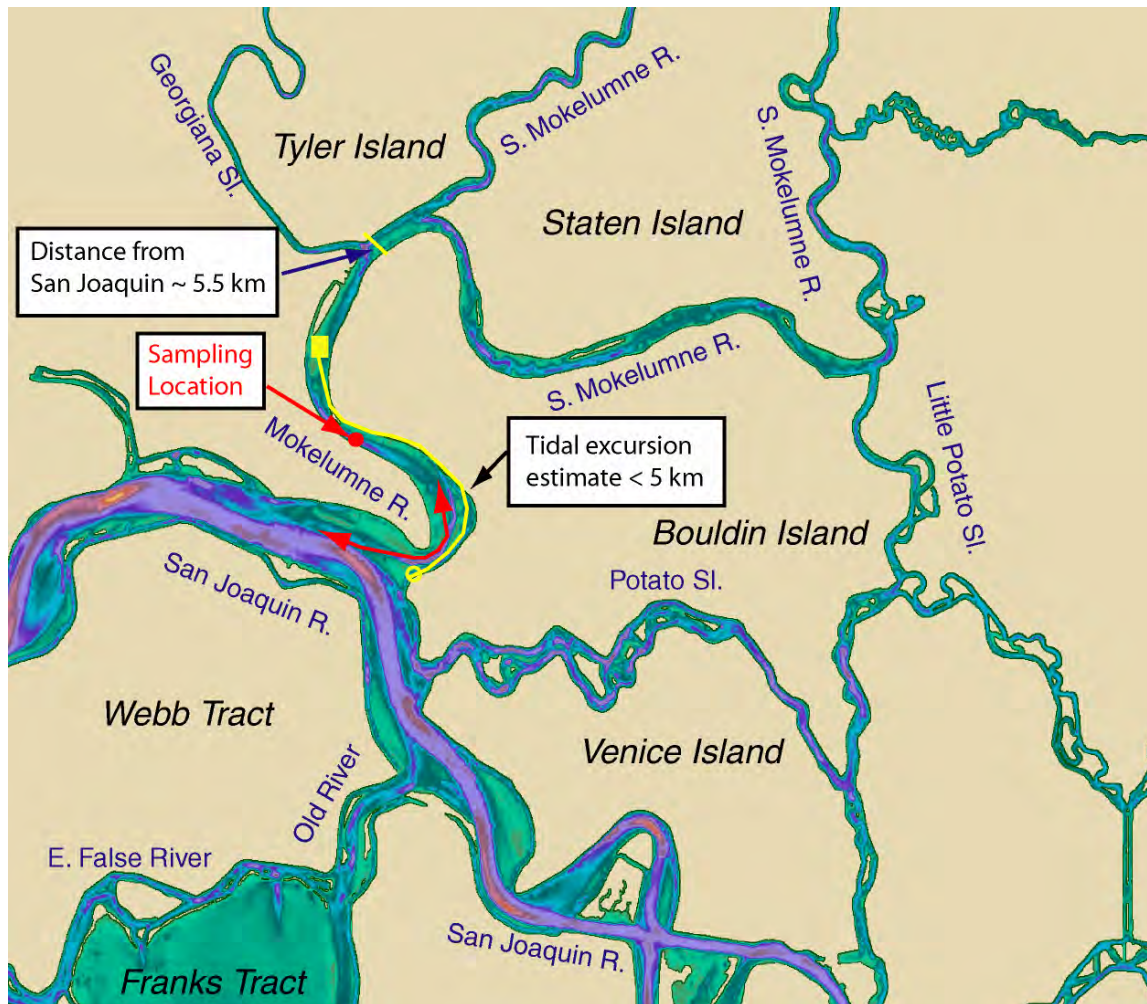


Figure HR19. Central Delta bathymetry. An estimate of the tidal excursion from the Mokelumne/San Joaquin River junction is approximately 5 km, which is less than the distance to Georgiana Slough. The tidal excursion estimate was made using the cross-sectionally averaged velocity (Figure HR20) under DCC gates open conditions. Exchange between the Mokelumne and San Joaquin Rivers occurs as indicated by the red arrows. Therefore, fresh water leaving the Mokelumne River is initially advected towards the Bay.

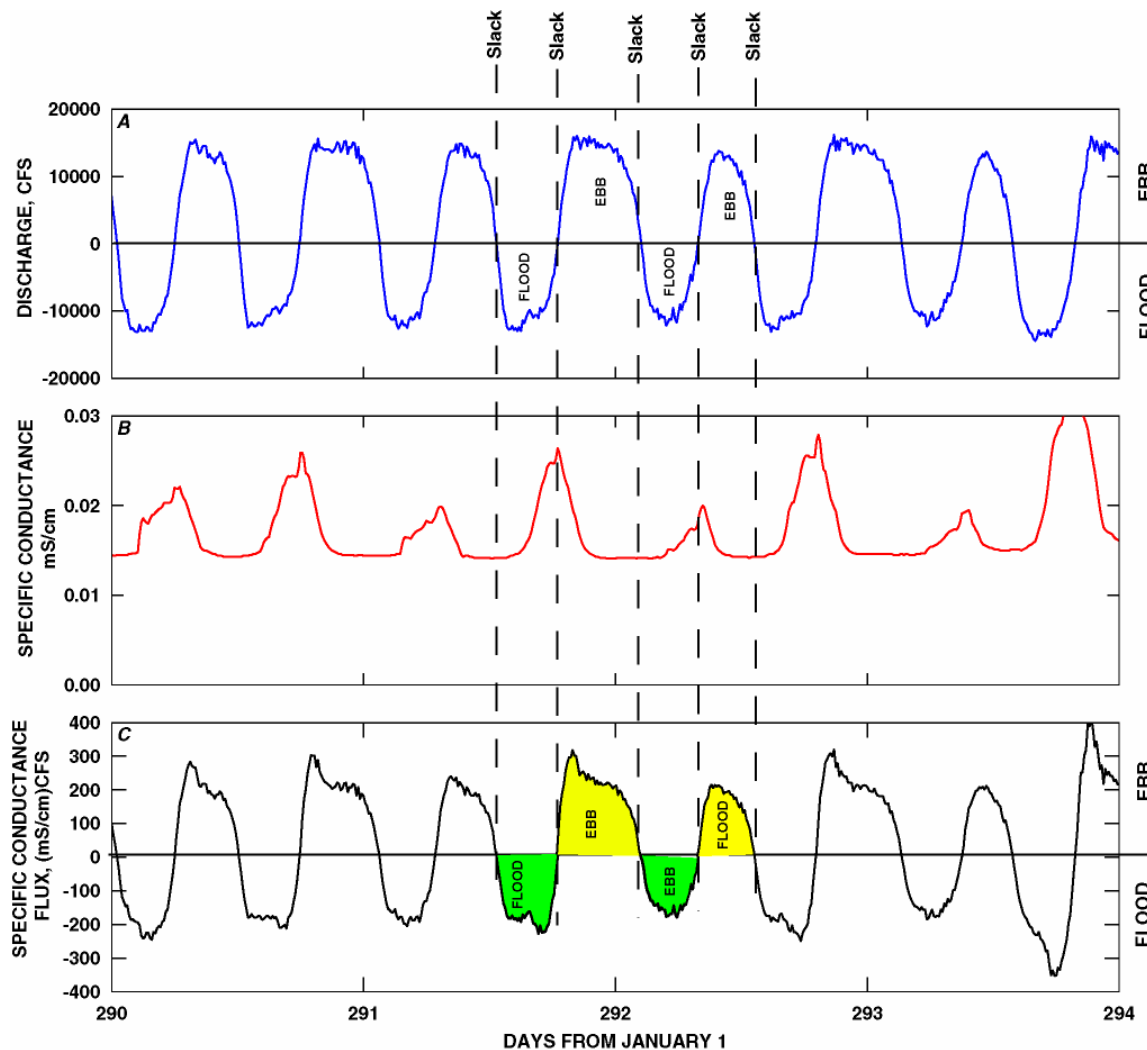


Figure HR20. Discharge, specific conductance, and specific conductance flux time-series measured in the Mokelumne River in 2001 under Delta Cross Channel gates open conditions. The tidal exchange, even under DCC gate open conditions, is on the order of 15,000 cfs even though the Mokelumne River is a relatively narrow channel (0.2 km) and 115 km from the Golden Gate. Specific conductance variations are advection dominated, although the pulses measured at a location between the mouth and Georgiana Slough (Figure HR20), significantly lag the beginning of the flood tide. This lag is basically the time it takes water to travel from the San Joaquin to our sampling location. Specific conductance peaks occur at the end of flood tide and thus the source of the high saline water is likely bay derived. The area under the specific conductance flux curve is the amount of salt that passed in a given direction, flood or ebb. In this case, the amount of salt moving past this section on flood (green) is roughly equal to that of the ebb (yellow) because the tidally averaged dispersive salt flux is small (Figure HR20). Essentially, the salty water that enters the Mokelumne River (the green area) comes out (the yellow area) on each tidal cycle. The advective flux is essentially the movement of the (very low) background specific conductance past our sampling location by the net flow.

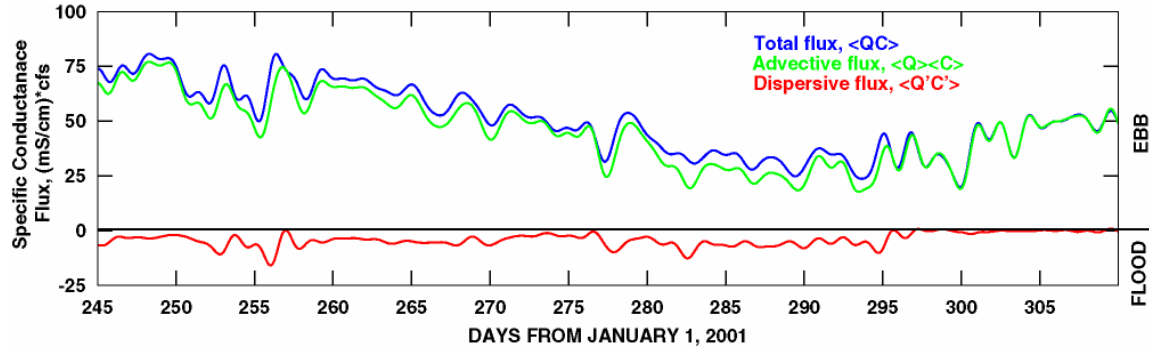


Figure HR21. Time-series of the total (blue), advective (green), and dispersive flux measured in the Mokelumne River in 2001. The total specific conductance flux is toward the San Joaquin river and represents the product of the very low specific conductance in the Mokelumne River and the Georgiana Slough/Delta Cross Channel net flows. The Dispersive flux is very low indicating very little upstream movement of specific conductance due to tidal mixing processes occurs in this reach.

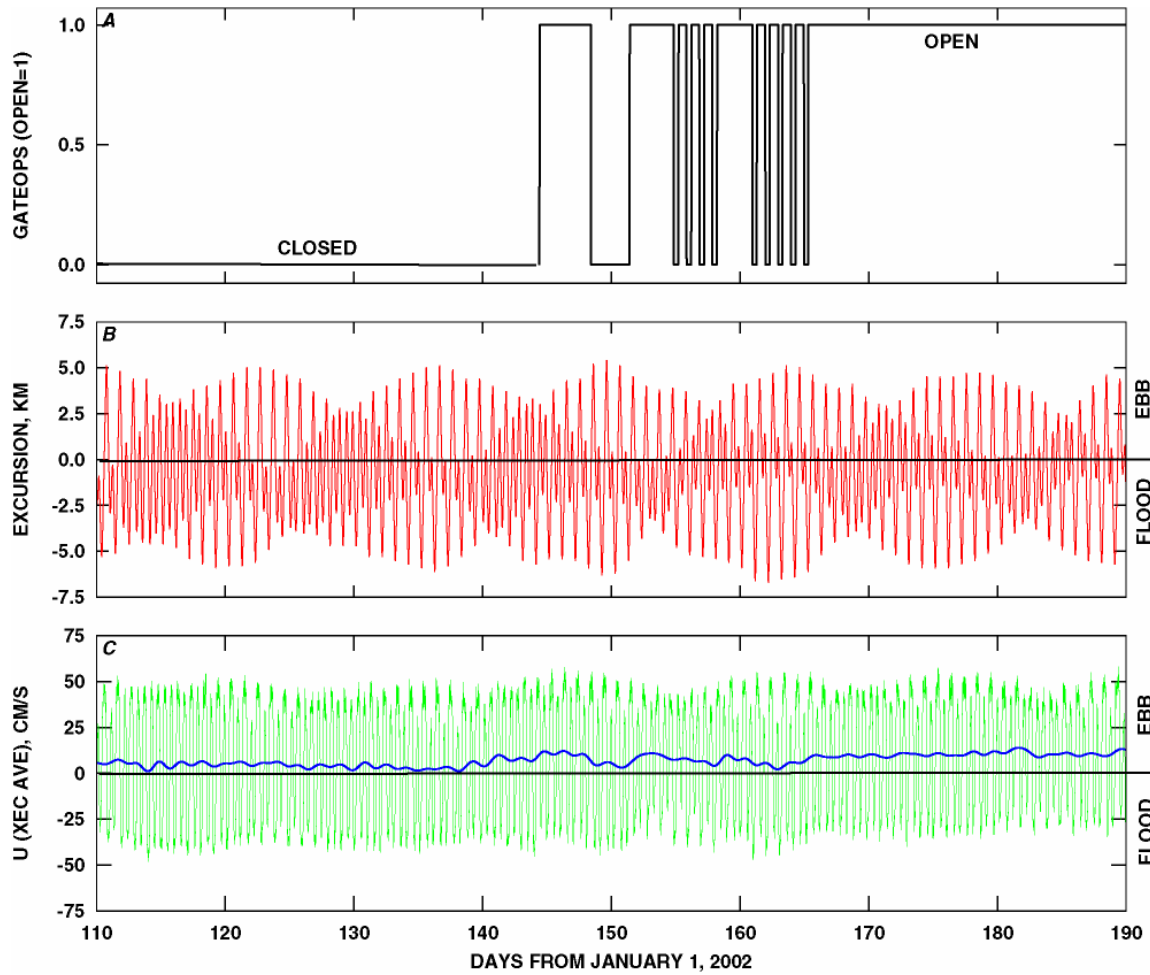


Figure HR22. Time series of (A) Delta Cross Channel gate operations, (B) tidal excursion computed on the basis of the (C) cross-sectionally averaged current. The tidal excursion in the ebb direction is on the order of 5 km. Both the tidal currents and tidal excursion appear to be little affected by gate operations.



Figure HR23. Aerial photograph of Mildred Island. Key geometry features such as planar area, volume, tidal prism, basin dimensions, key channels lengths, etc. are shown.

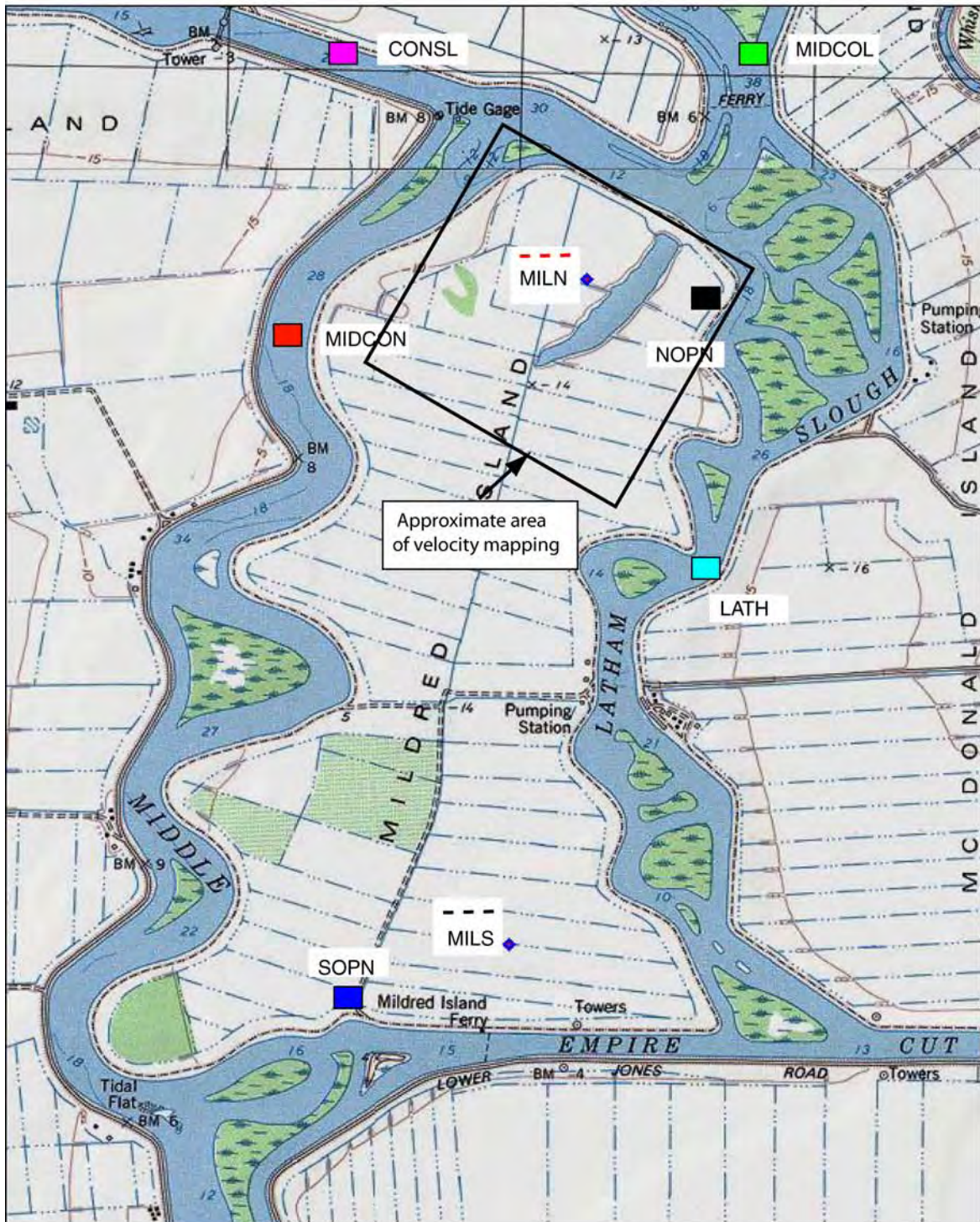


Figure HR24. Color scheme used for time series plots and the approximate area of velocity mapping using a boat-mounted downward-looking ADCP.

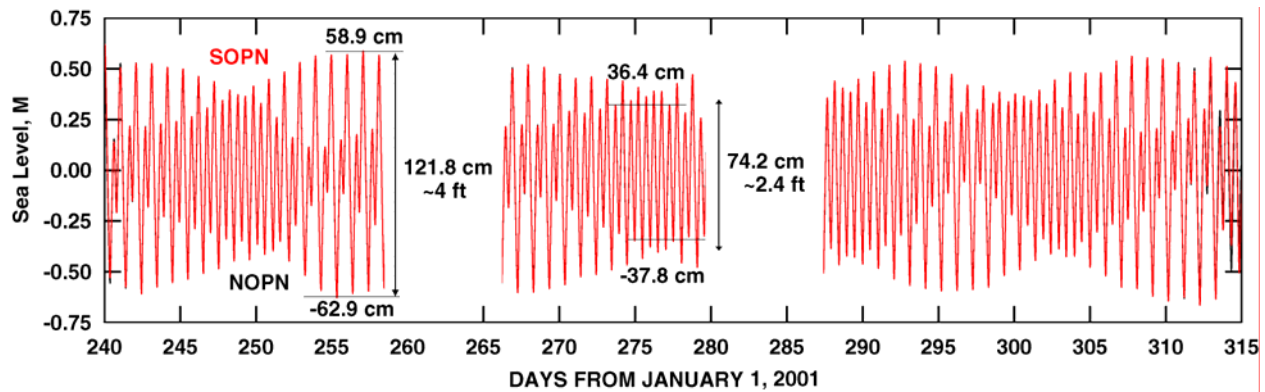


Figure HR25. Time series plots of the tidal variations, ζ' , from pressure sensors at each end of Mildred Island, one at SOPN (red) and the other at NOPN (black). The maximum tidal range is roughly 120 cm and minimum is ~75 cm in MI.

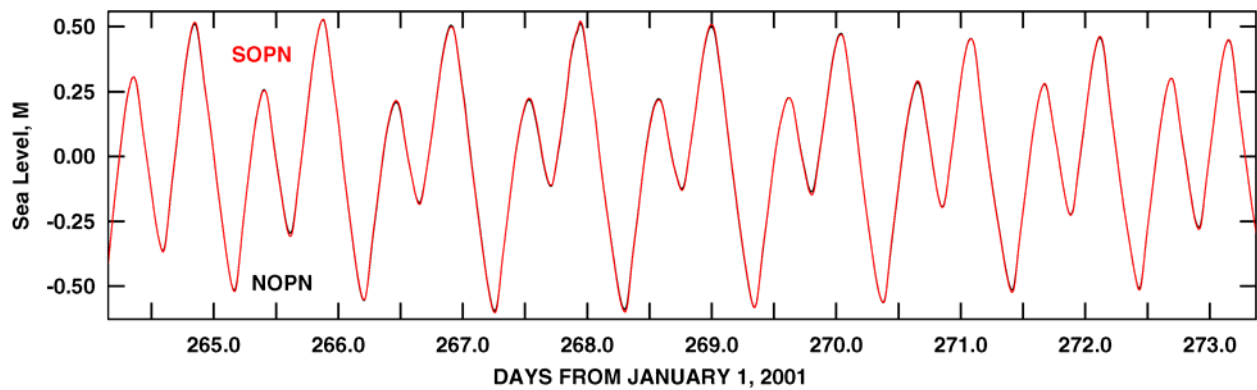


Figure HR26. Time series plots of the tidal variations, ζ' , from pressure sensors at each end of Mildred Island, one at SOPN (red) and the other at NOPN (black). The tidal variations, ζ' , from these two pressure sensors are virtually identical, indicating very little change in the tidal wave as it propagates through Mildred Island and a roughly coherent rise in fall in water levels across the Island, mostly because Mildred Island is small, ~ 3 km long.

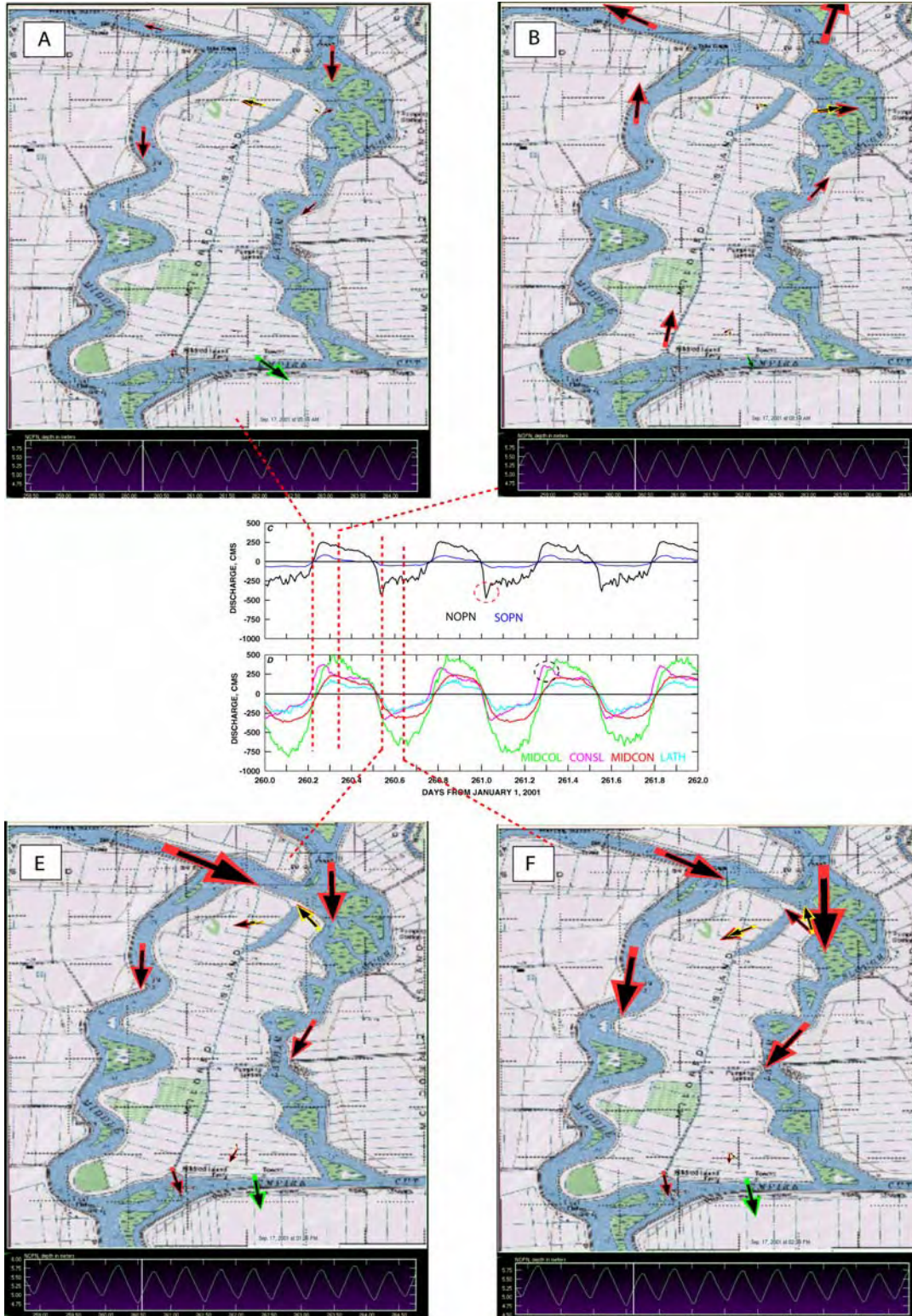


Figure HR27. Tidal variations in the tidal flows in Mildred Island: (A) discharge vector map for slack before ebb tide; (B) discharge map for full ebb tide; (C) discharge time-series for stations NOPN and SOPN; (D) discharge time-series for stations MIDCOL, CONSL, MIDCON, LATH; (E) discharge vector map for early in the flood tide; (F) discharge vector map full flood tide.

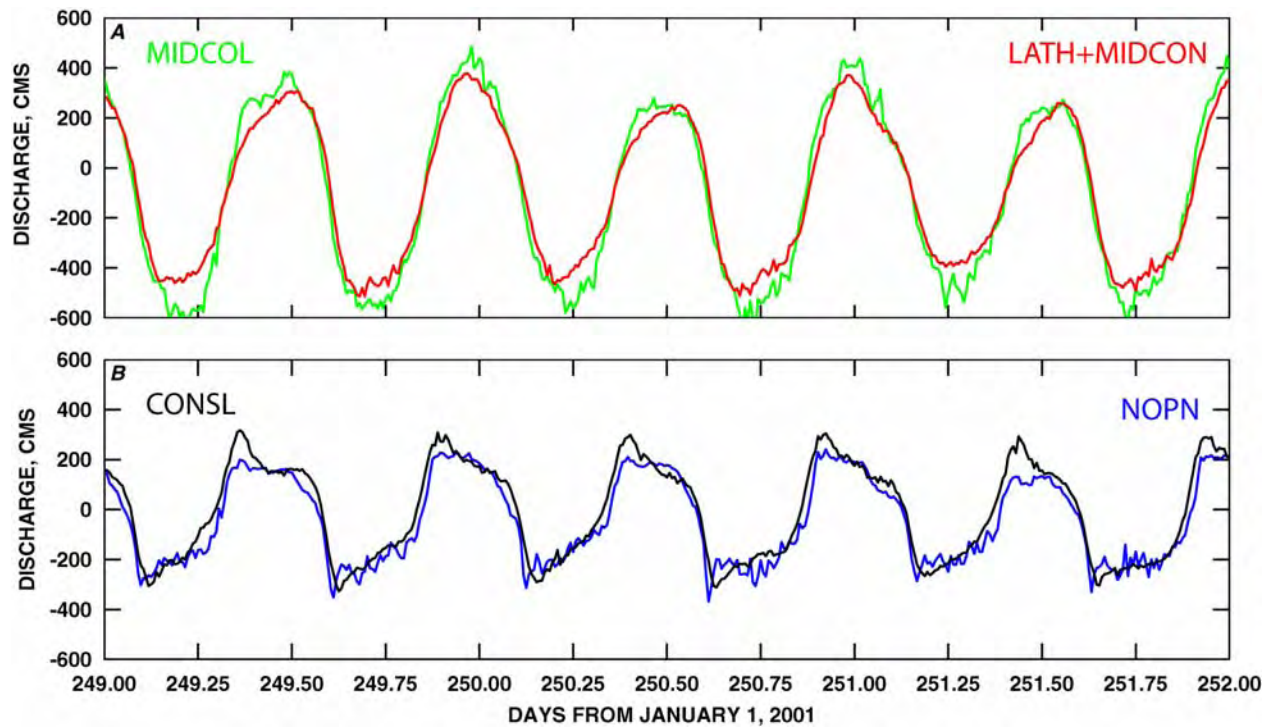


Figure HR28. Time-series of tidal discharges (A) station MIDCOL and the sum of LATH and MIDCON, (B) Connection Slough and northern opening.

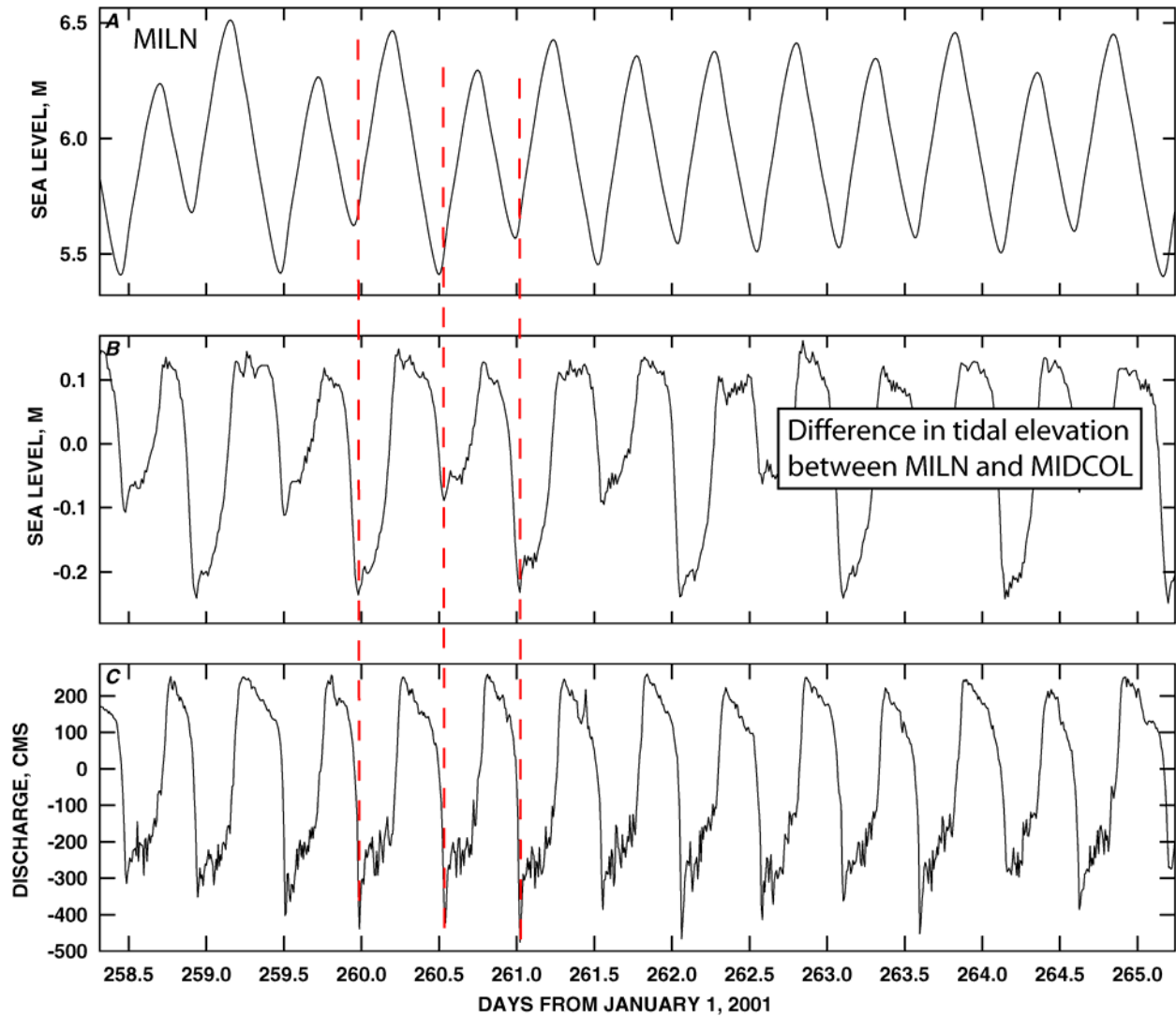


Figure HR29. Time-series plots of (A) sea level at station MILN, (B) the difference in tidal elevation between MILN and MIDCOL (essentially the water surface gradient across the northern opening), (C) Discharge in the northern opening (NOPN). Spikes in the discharge through the northern opening occur at low water during a peak in the water surface gradient across the opening.

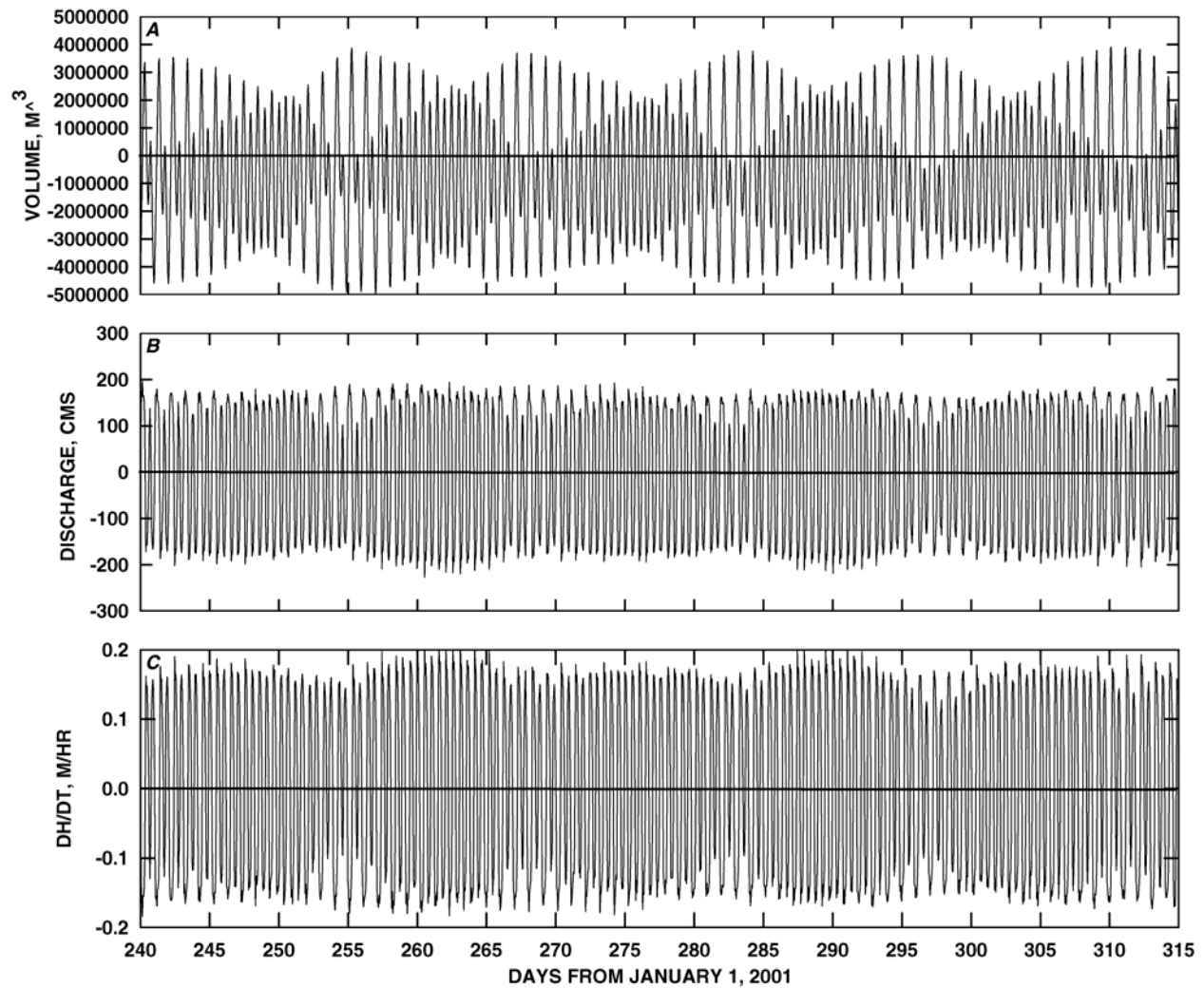


Figure HR30. Time series of (A) Mildred Island tidal prism, in m^3 , (B) an estimate of the discharge needed to fill and drain Mildred Island, and the (C) time rate of change of water level, in m/hr . Mildred Islands tidal prism ranges from $\sim 3,500,000$ (2800 acre-ft) to $5,000,000 m^3$ (4,000 acre-ft) depending on the spring/neap cycle and diurnal inequality. Peak tidal prism discharges are on the order of 200 cms and the maximum rate at which water levels change is 0,2 m/hr .

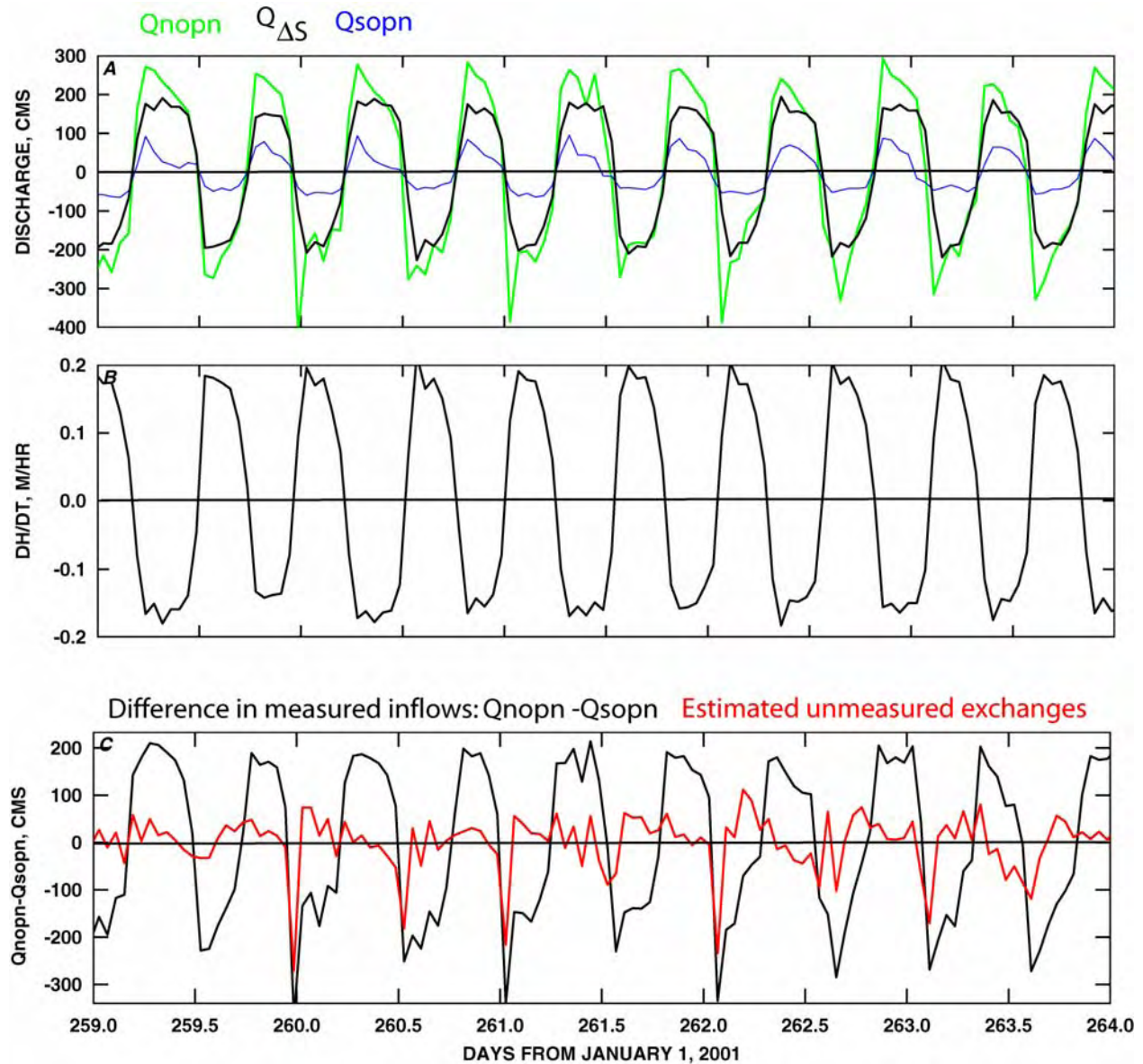


Figure HR31. Time-series of (A) tidal discharge into the Island from the northern opening (Q_{nopn} , green), the southern opening (Q_{sopn} , blue) and an estimate of the amount of exchange needed to fill and drain Mildred Island, $Q_{\Delta S}$, (B) The time rate of change of water level, in meters per hour, and (C) the difference between the measured inflows (black) and an estimate of the unmeasured tidal exchanges (red) based on the difference between the measured inflows and the amount of stage in the island.

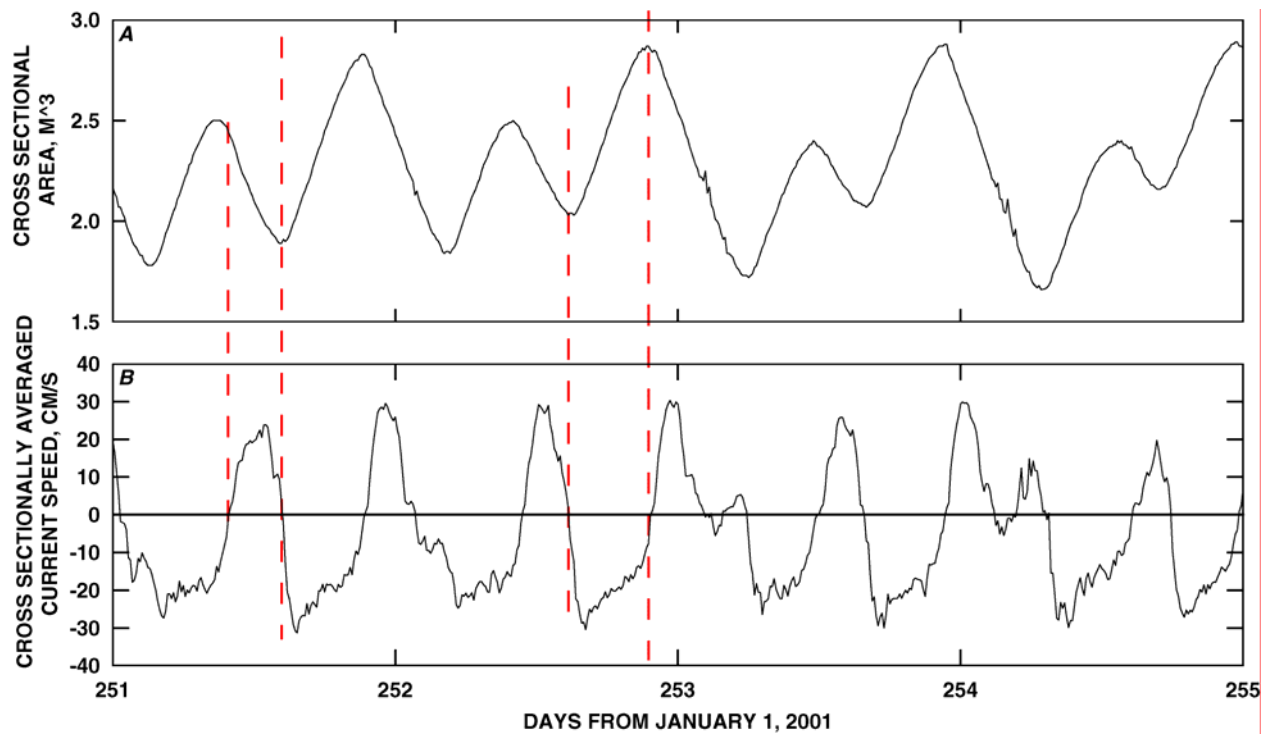


Figure HR32. Time series plot of (A) cross sectional area of the southern opening, (B) cross sectionally averaged current speed. Stokes Drift flux is small, at least compared to the net flow through the Island. because tide waves in Mildred Island are very nearly standing waves where neither the flood tide nor ebb tides are strongly correlated with water level variations: water level variations are in quadrature with the currents out of the southern opening as is indicated by the vertical dashed lines.

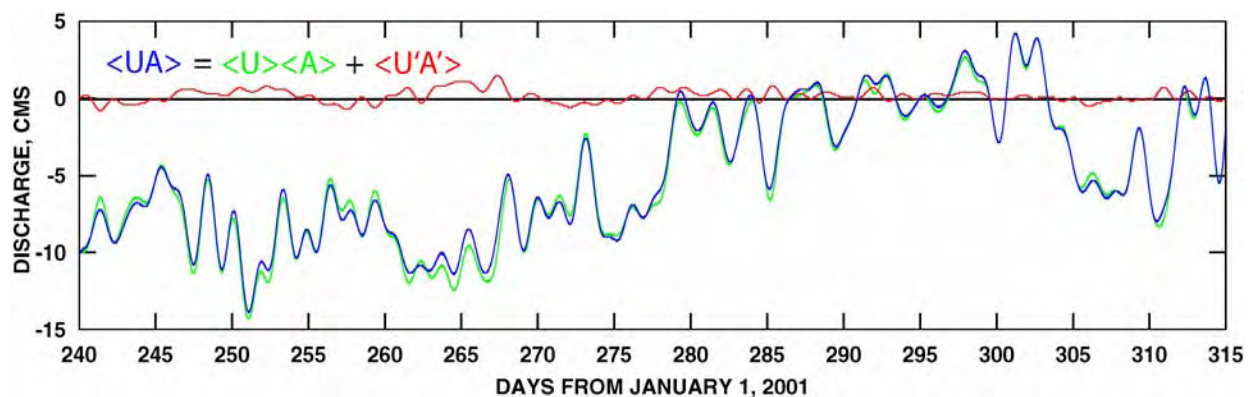


Figure HR33. Mass flux through the southern opening due to Stokes drift, $\langle U'A' \rangle$ is small. Stokes drift was a possible exchange mechanism between the island and the surrounding channels. However, the Stokes Drift flux is small, at least compared to the net flow through the Island. because tide waves in Mildred Island are very nearly standing waves where neither the flood tide nor ebb tides are strongly correlated with water level variations: water level variations are in quadrature with the currents out of the southern opening. The other levee breaches in the south are presumed to respond similarly.

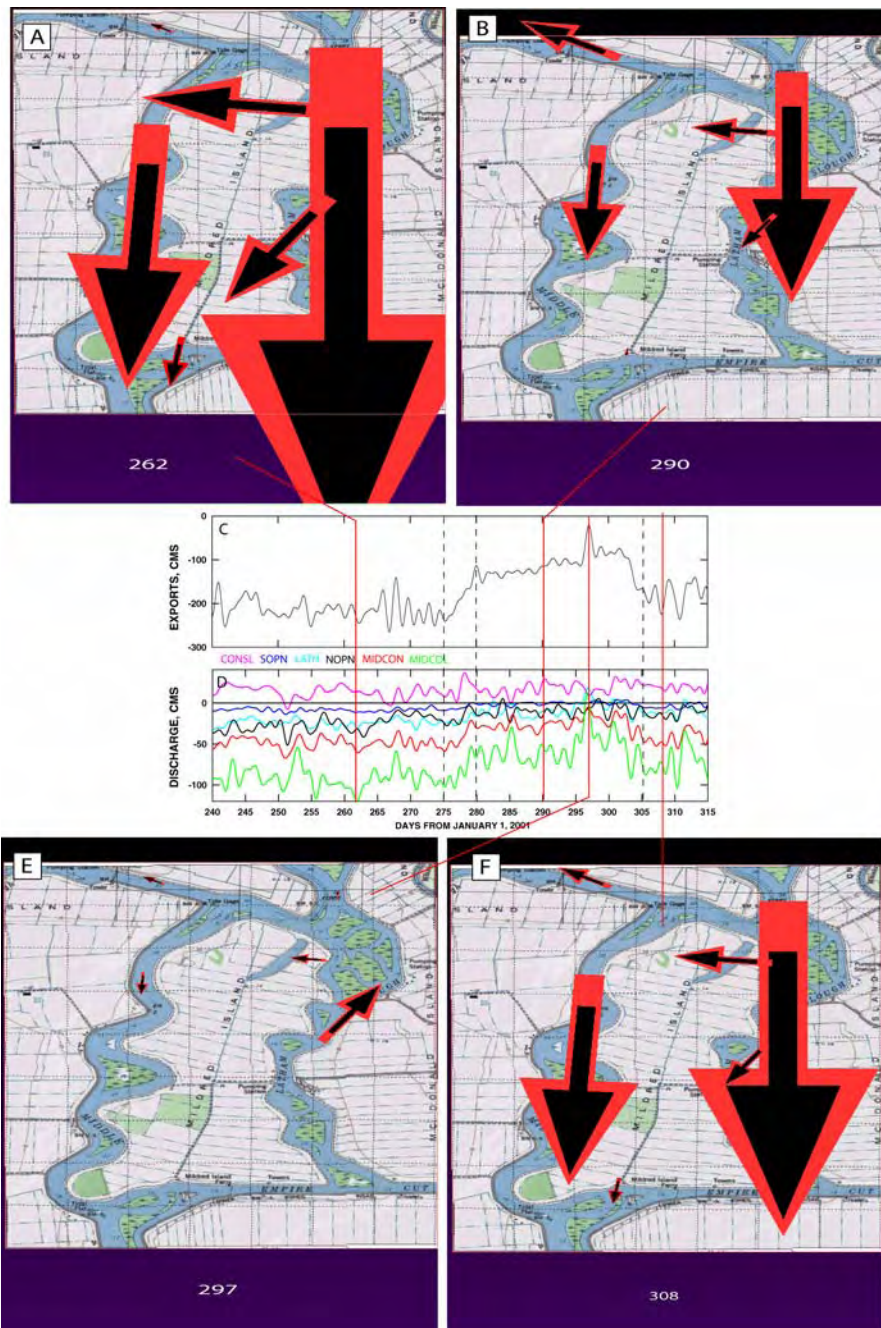


Figure HR34. Example net flow distributions in the Mildred Island region. Four basic net circulation regimes occurred during the study period which were intimately tied to changes in exports: (A) a combined export rate of ~220 cms prior to day 275, (B) a period of combined exports of ~120 cms between days 280-300, (E) a period of near zero exports near day 297, and (F) exports of about 200 cms. Panels (C) and (D) are time series plots of the combined export rate and the net flows in the region, respectively.

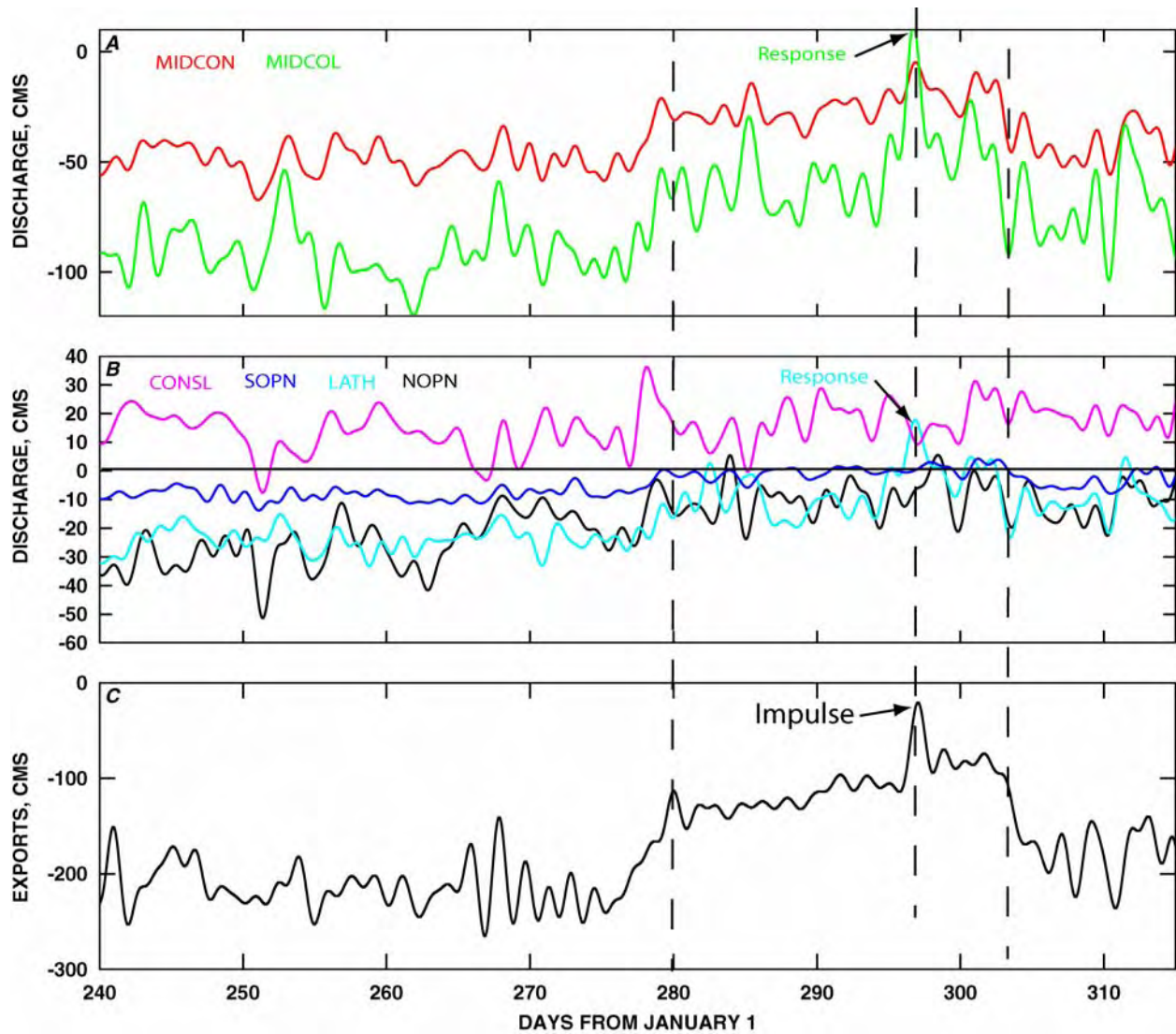


Figure HR35. Time series plots of (A) the net discharge at stations MIDCON and MIDCOL, (B) net discharges at stations CONSLS, SOPN, LATH, NOPN, and (C) the combined export rate.

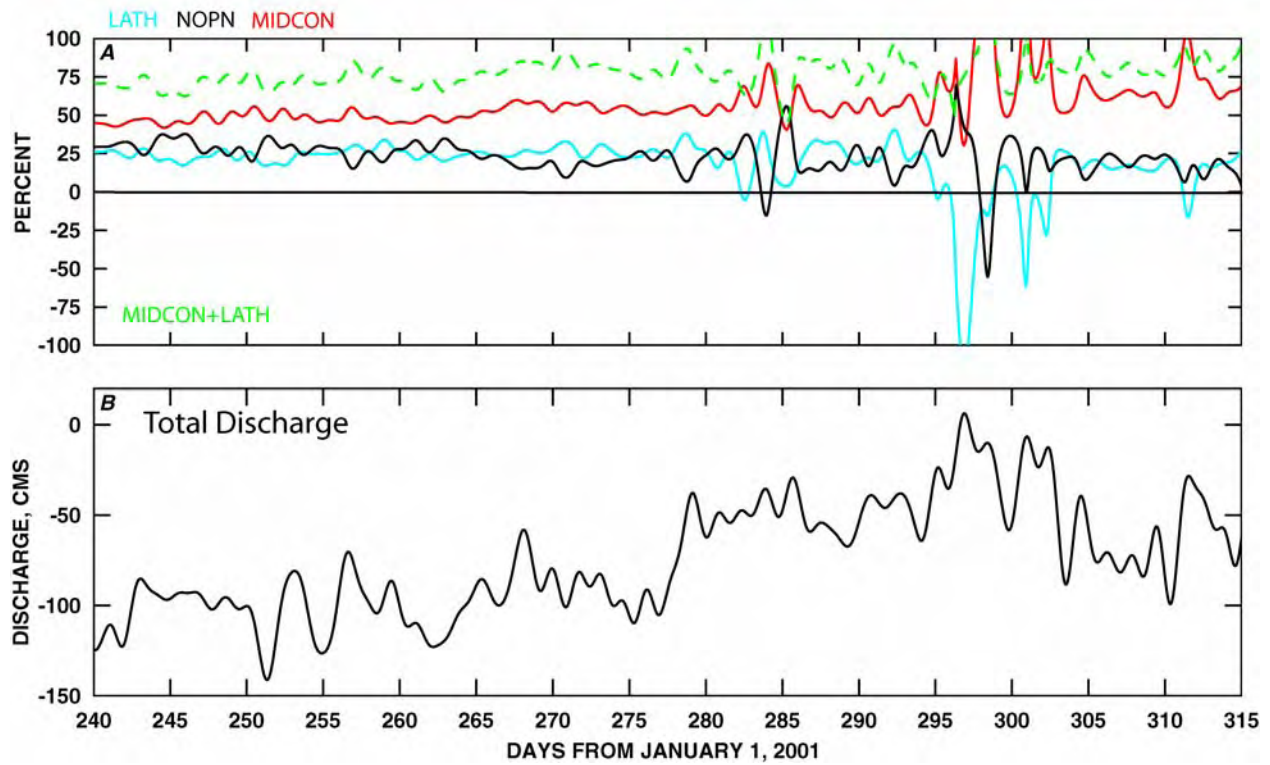


Figure HR36. Time series plots of (A) the percentage of the total net discharge in the Mildred Island region passing through stations LATH, NOPN, MIDCON and (B) the total discharge entering the region (MIDCOL+CONSL).

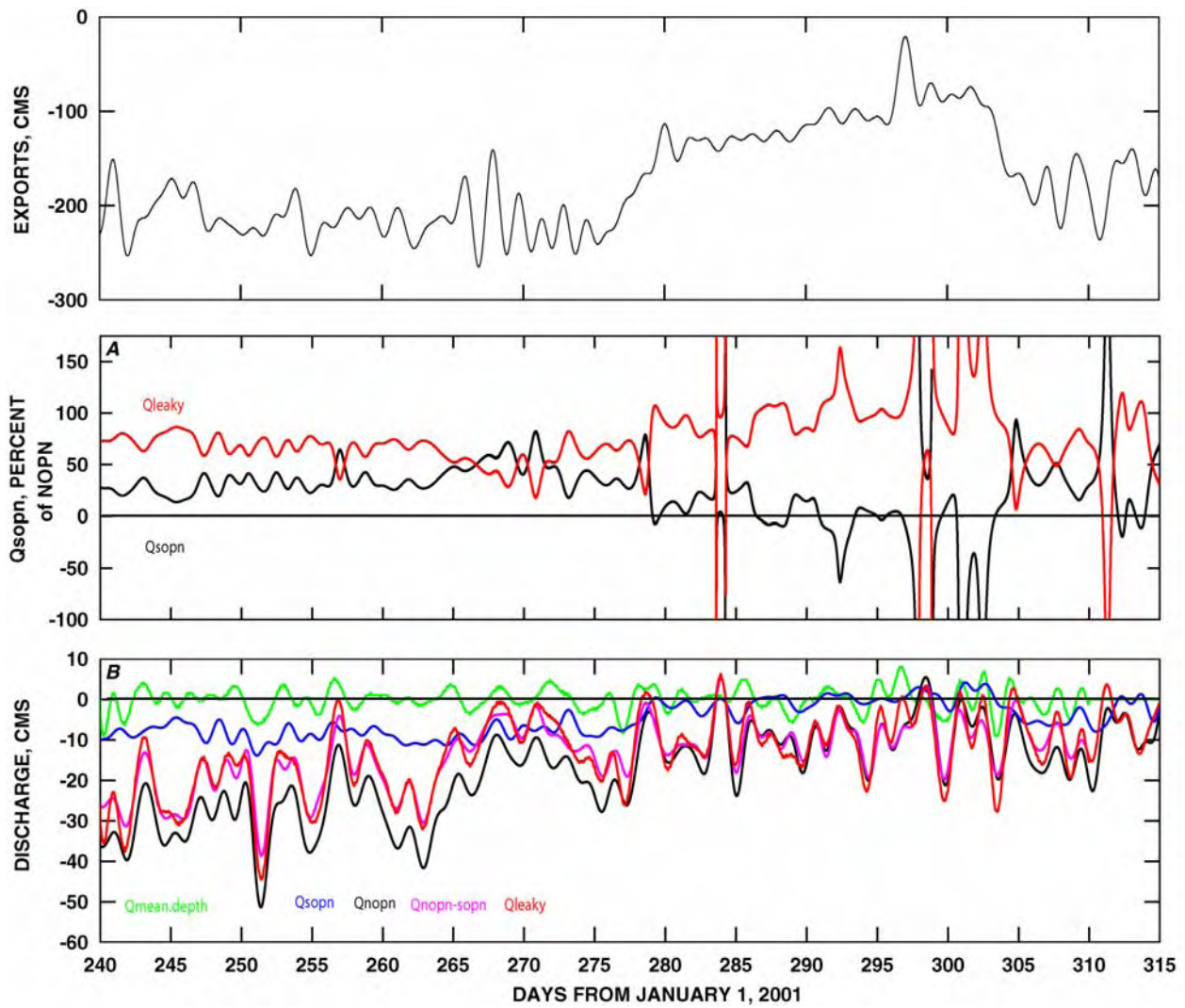


Figure HR37. Time series plots of (A) combined export rate, (B) percent of the flow entering the northern opening, (C) discharge in the southern opening, Q_{sopn} (blue), northern opening Q_{nopn} (black), the difference between the two (magenta), the discharge associated with tidally-averaged water level changes, $Q_{\Delta\zeta}$ (green), the net flow passing through the southern levee Q_{leaky} (red).

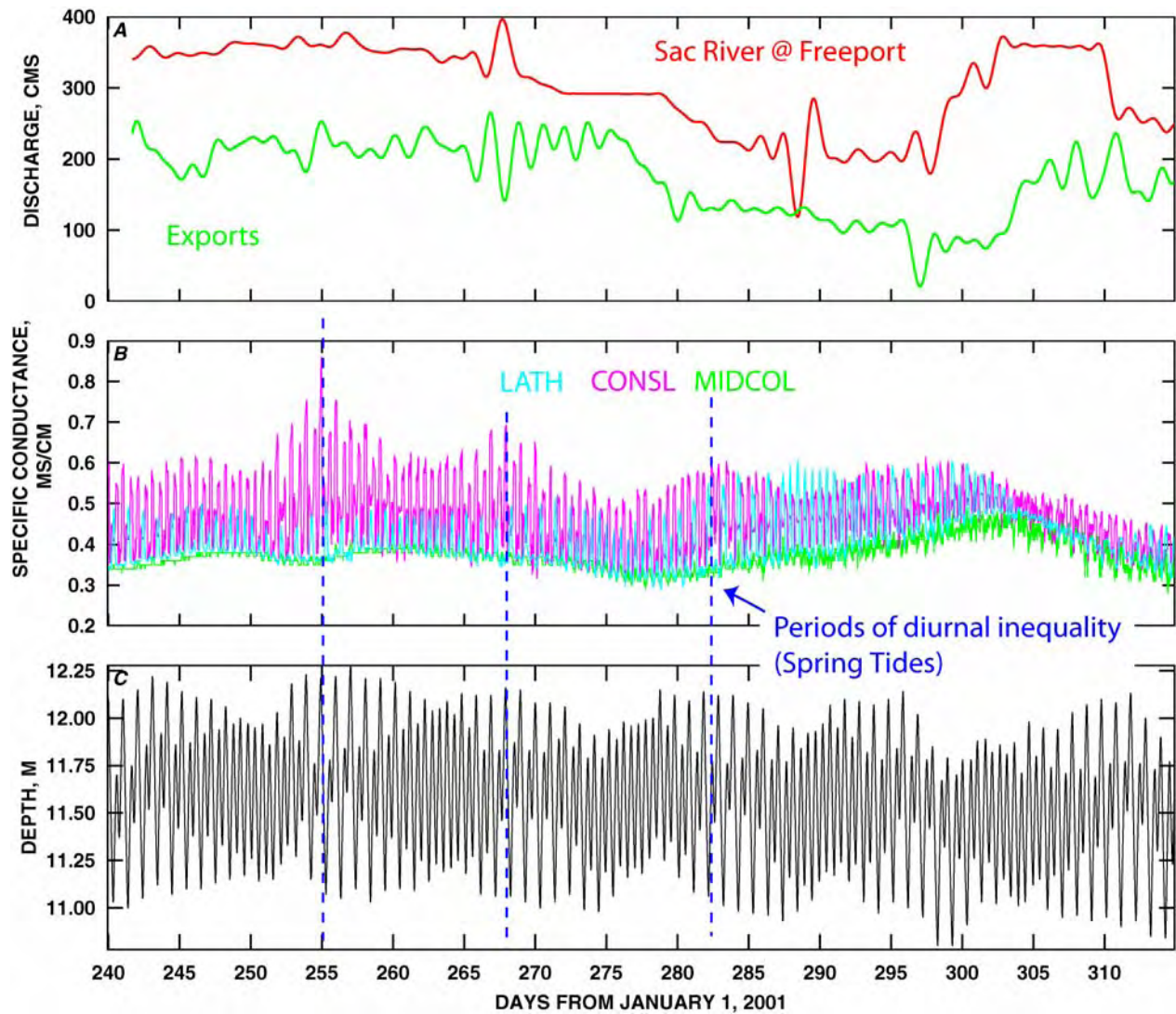


Figure HR38. Time series plots of (A) Sacramento River flow measured at Freeport (red), combined export rate (green), (B) specific conductance measured in Latham Slough (LATH)(cyan), Connection Slough (CONSL)(magenta), Middle River at station MIDCOL (green), (C) Depth measured by a pressure sensor at station MIDCOL. Vertical blue lines indicate spring tide periods which correspond to increased tidal excursions and concomitant salinity variations.

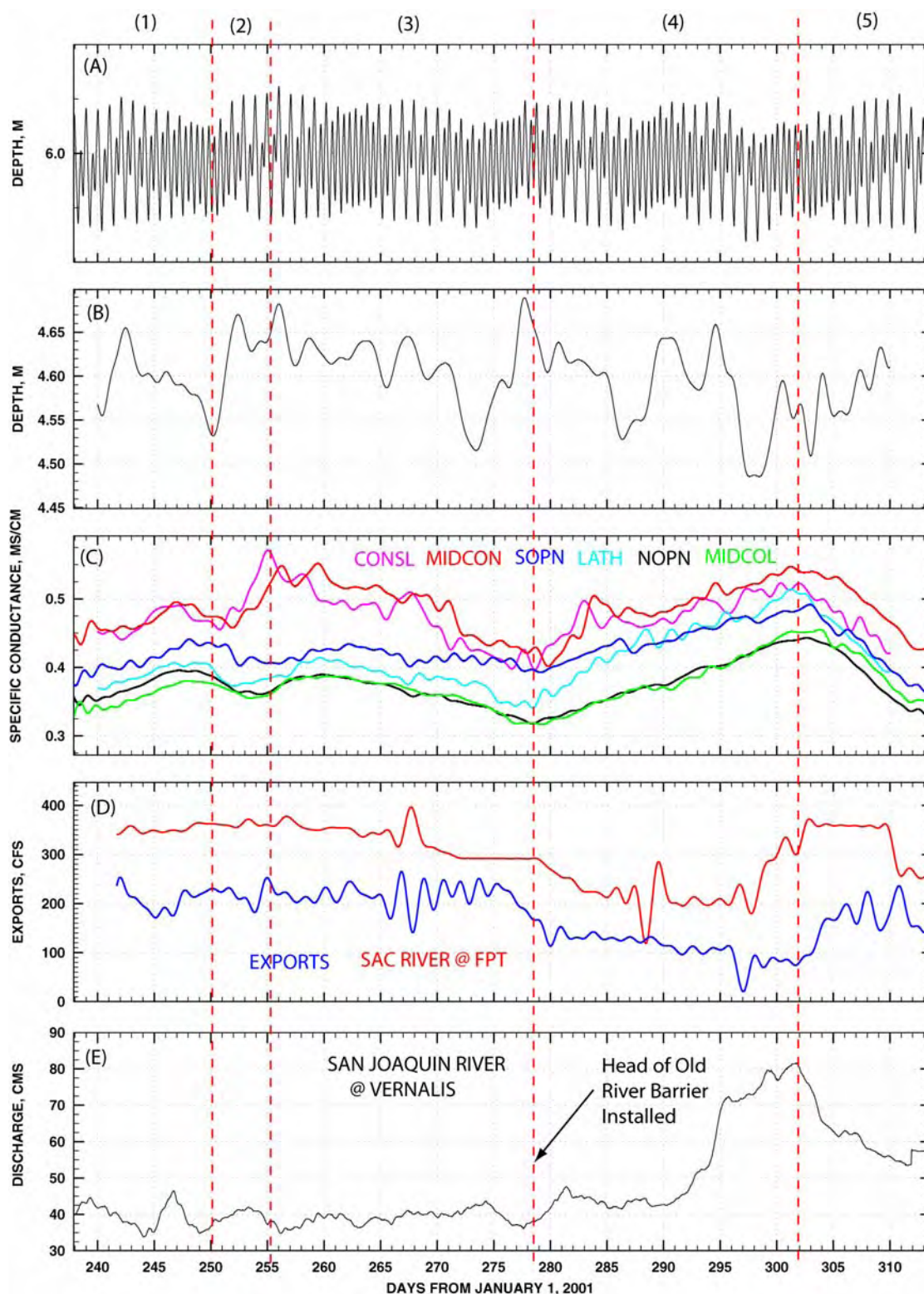


Figure HR39. Time series plots of (A) the as-measured depth at station CONSL, (B) tidally averaged depth at station CONSL, (C) tidally averaged specific conductance, (D) Sacramento River flow measured at Freeport (red), export rate (blue), (E) San Joaquin River flow measured at Vernalis. Vertical dashed red lines indicate times where the salinity time series changed slope.

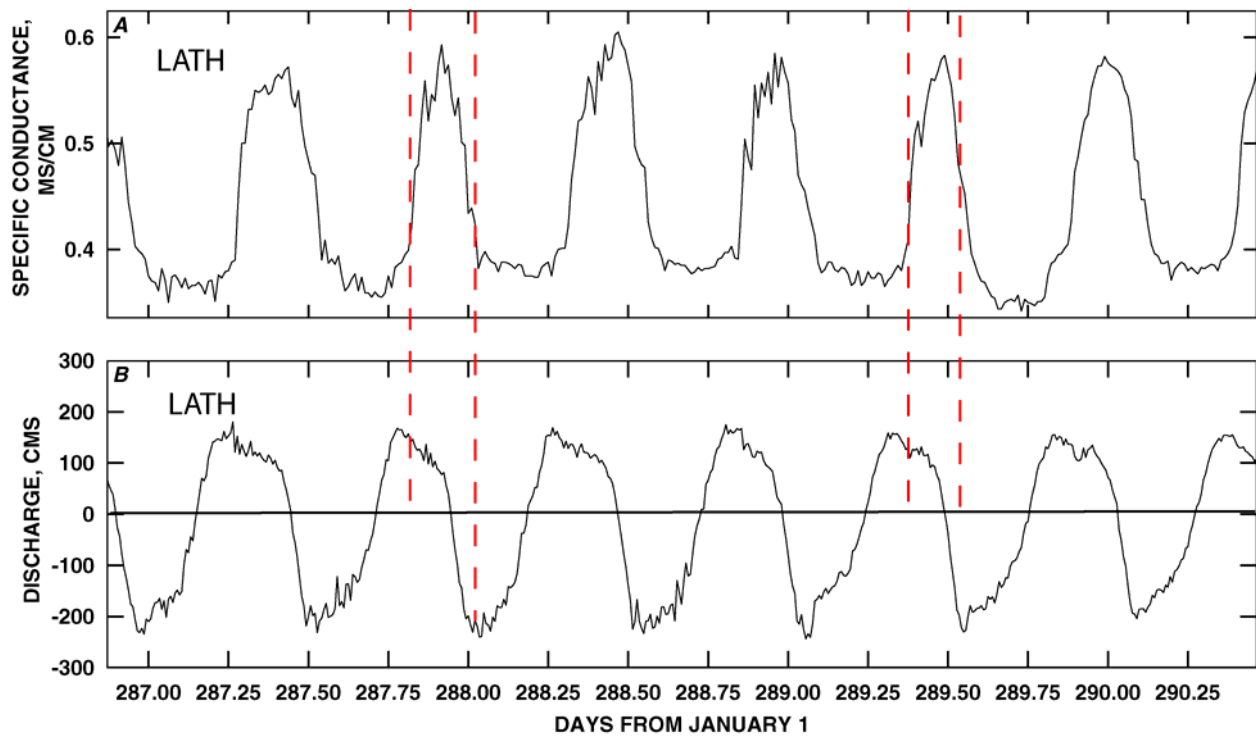


Figure HR40. Time series plot of (A) specific conductance and (B) discharge in Latham Slough (station LATH). Specific conductance is higher on Empire Cut because specific conductance increases during ebbs, when the flows are positive (toward the north).

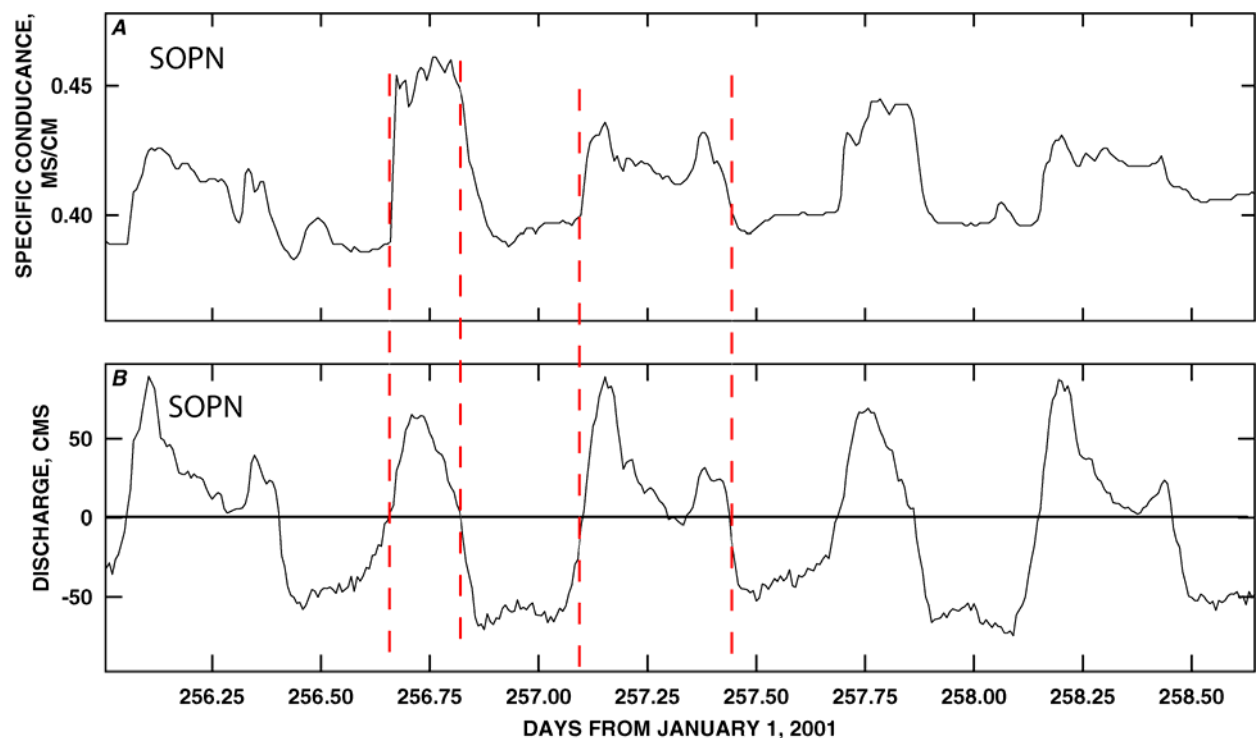


Figure HR41. Time series plot of (A) specific conductance and (B) discharge in the southern opening (station SOPN). Specific conductance is higher on Empire Cut compared to the Islands interior because specific conductance increases during incoming tides, when the flows are positive (toward the north).

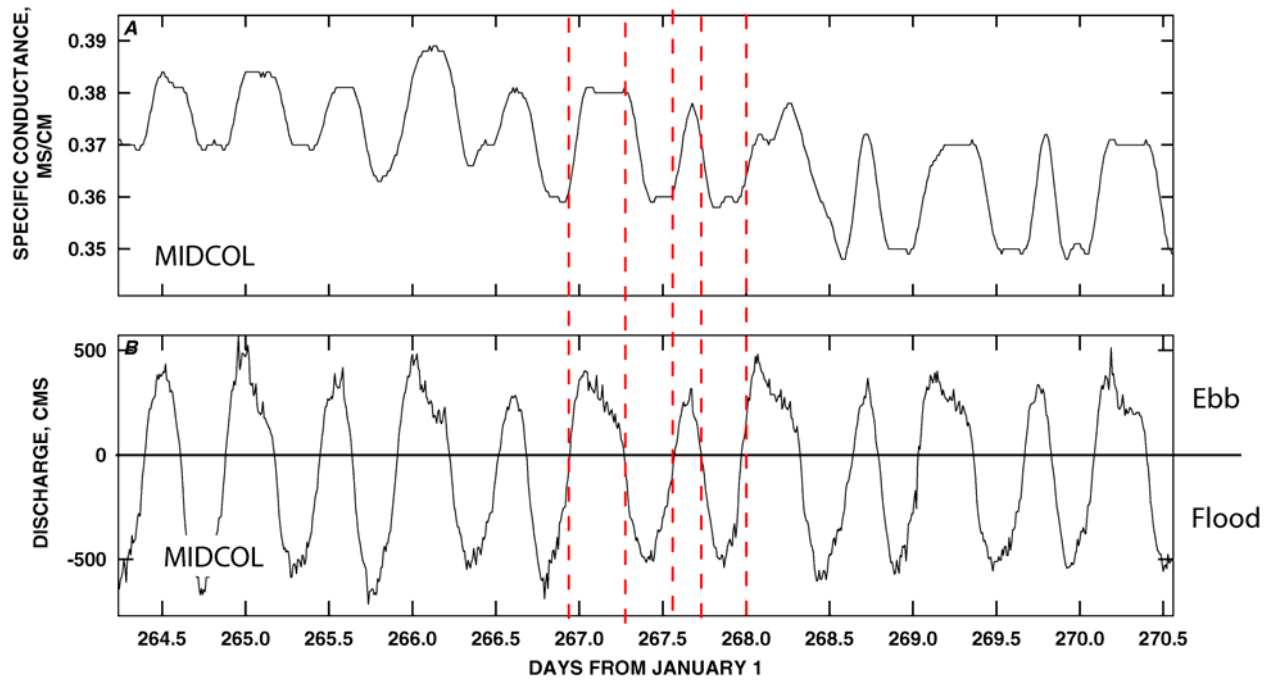


Figure HR42. Time series plot of (A) specific conductance and (B) discharge in northern Middle River (station MIDCOL). Specific conductance is lower north of Mildred Island because specific conductance decreases on flood, when the flows are negative (toward the south).

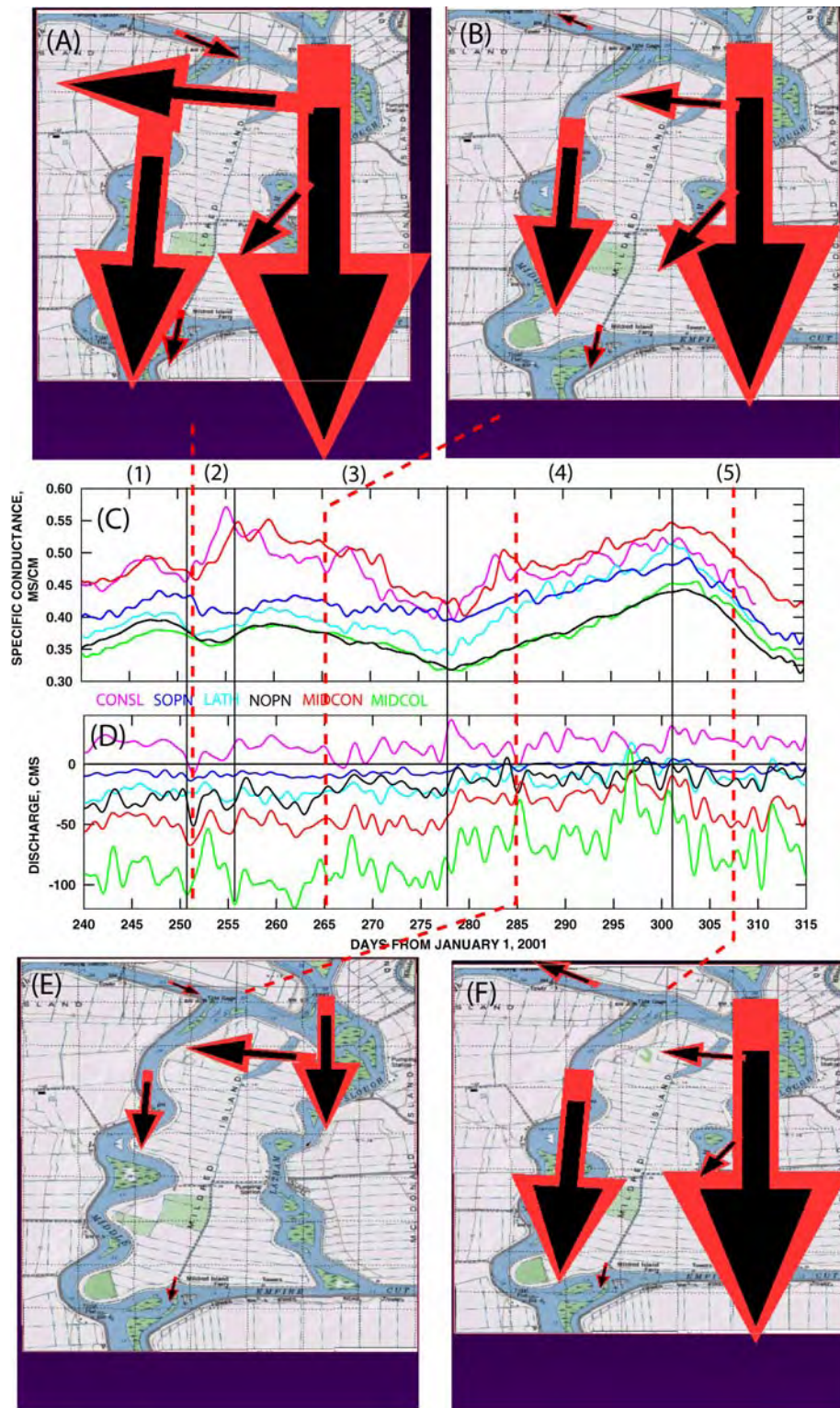


Figure HR43. Vector plots of the net flows at specific characteristic times: (A) Day 251, (B) Day 265, (E) Day 285, (F) Day 307. Time series plots of the tidally averaged (C) specific conductance and (D) net flows in the Mildred Island region.

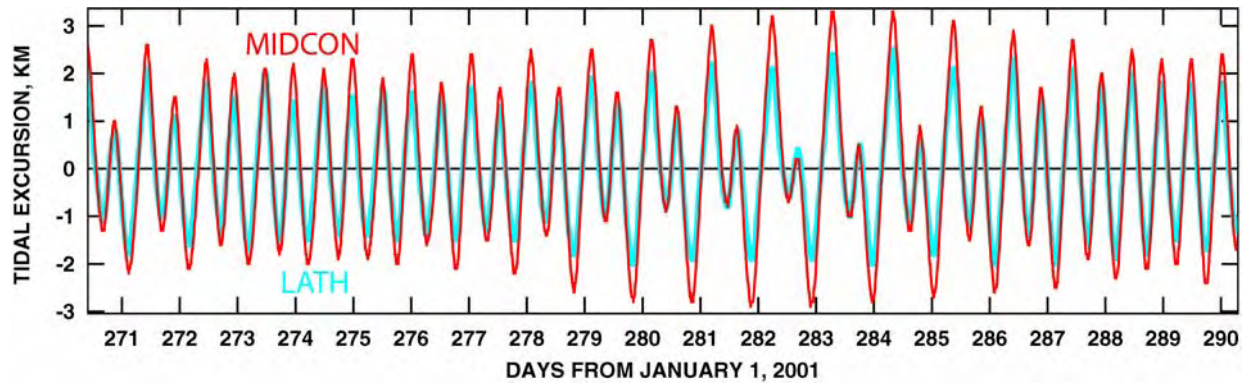


Figure HR44. Time series of tidal excursion estimates at stations MIDCON and LATH.
(file:tide.excur.ai)

circuit 3 - low slack

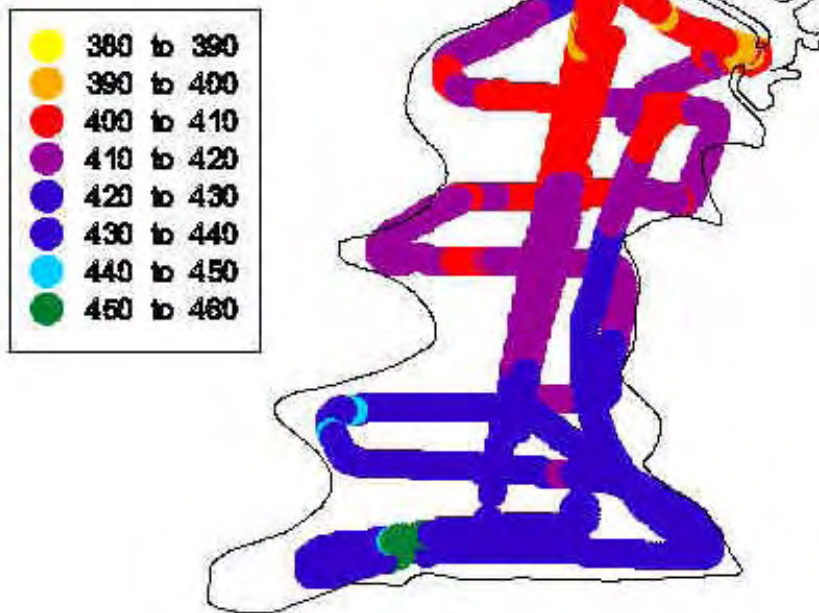


Figure HR45. High specific conductance concentration water injected into Midred Island from the southern opening creates a persistent weak south-to-north gradient in specific conductance across Mildred Island. (Courtesy of Lisa Lucas, USGS)

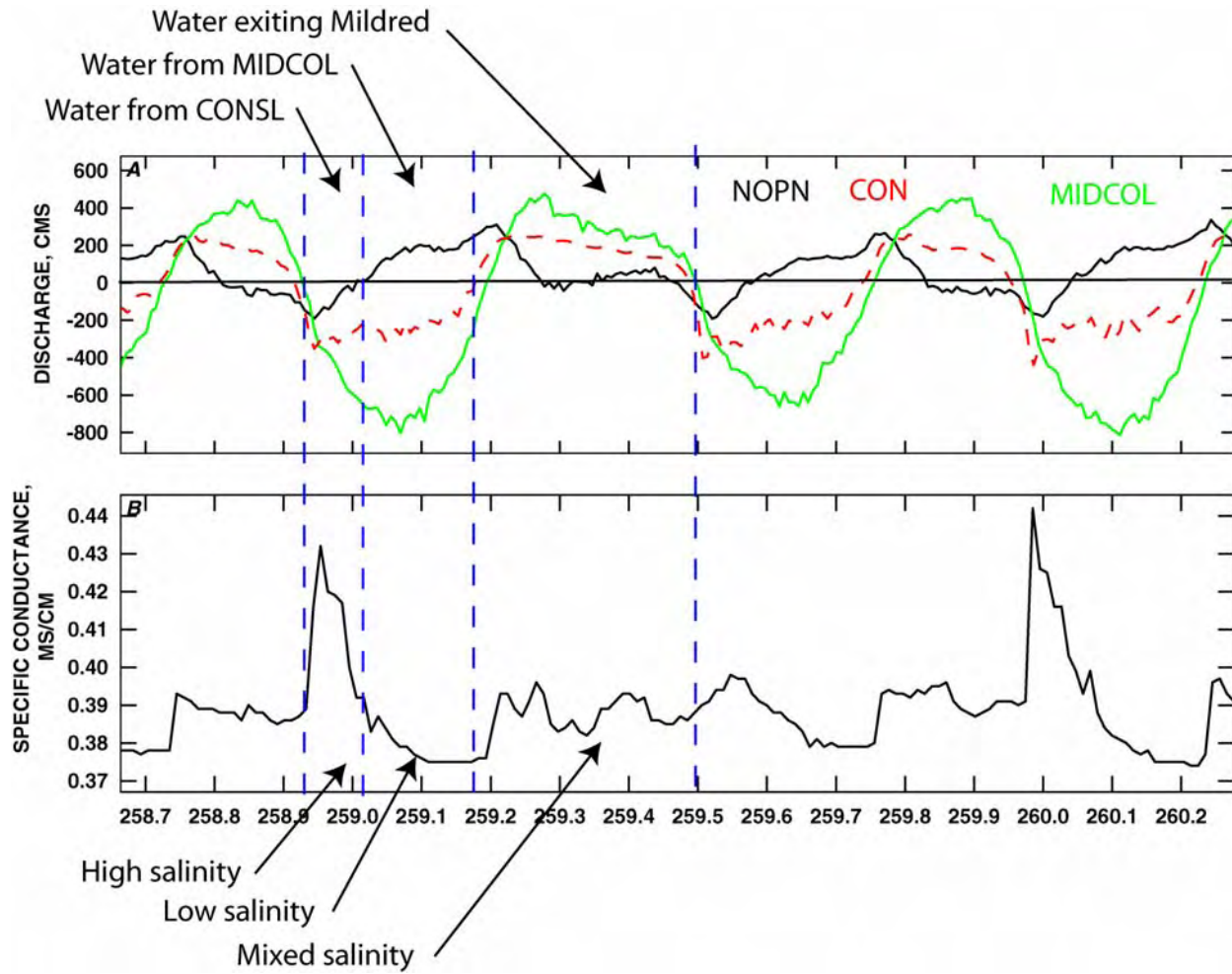


Figure HR46. Time series plots of (A) discharge at the northern opening (NOPN, black), in Connection Slough between Middle River and the Northern Opening (a computed quantity as is shown in figure 3 (red), the flow at MIDCOL (green), (B) specific conductance measure in the northern opening.

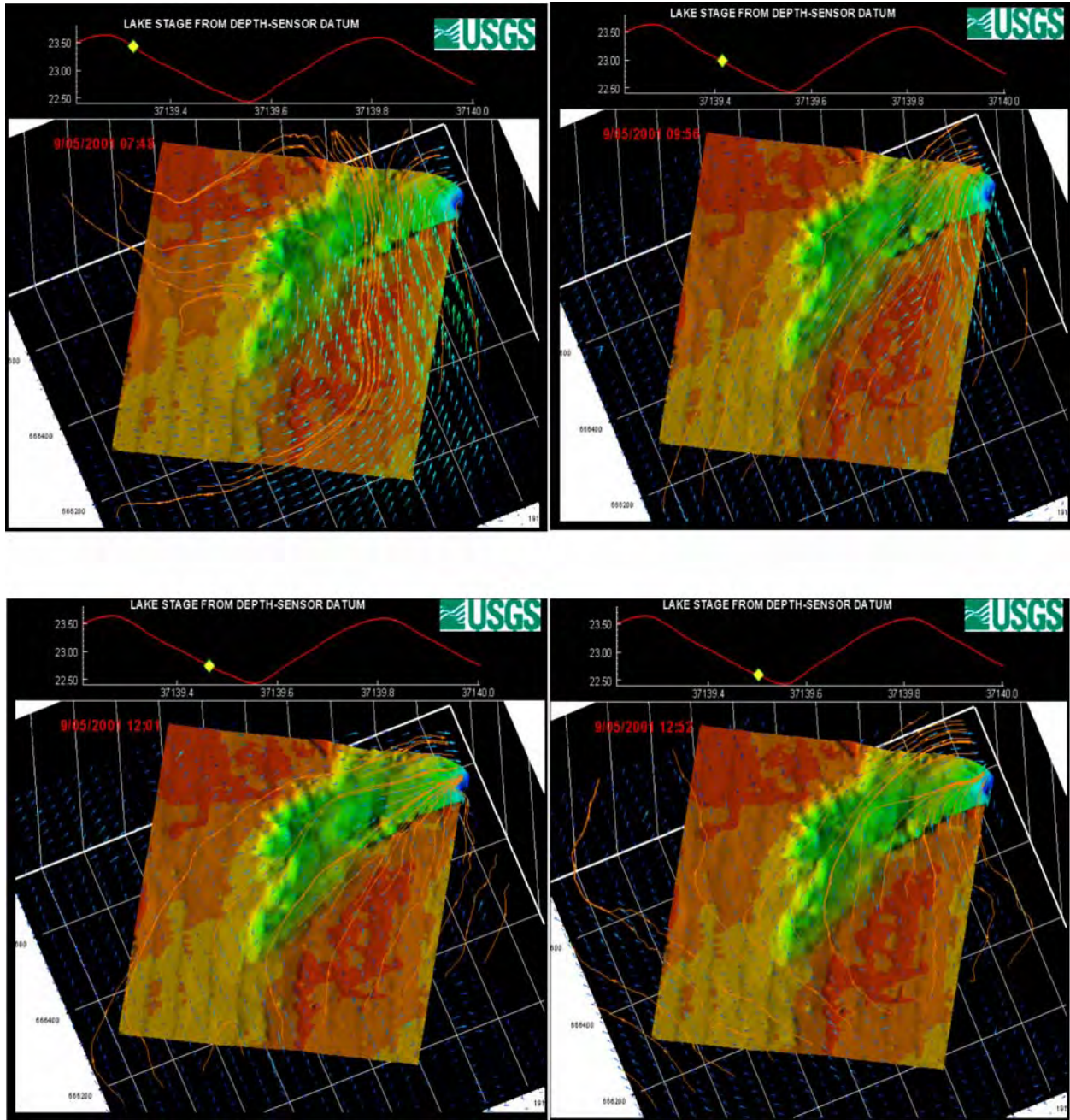


Figure HR47. Mildred Island flow fields – ebb tide progression measured using a method described in Dinehart and Burau, 2005.

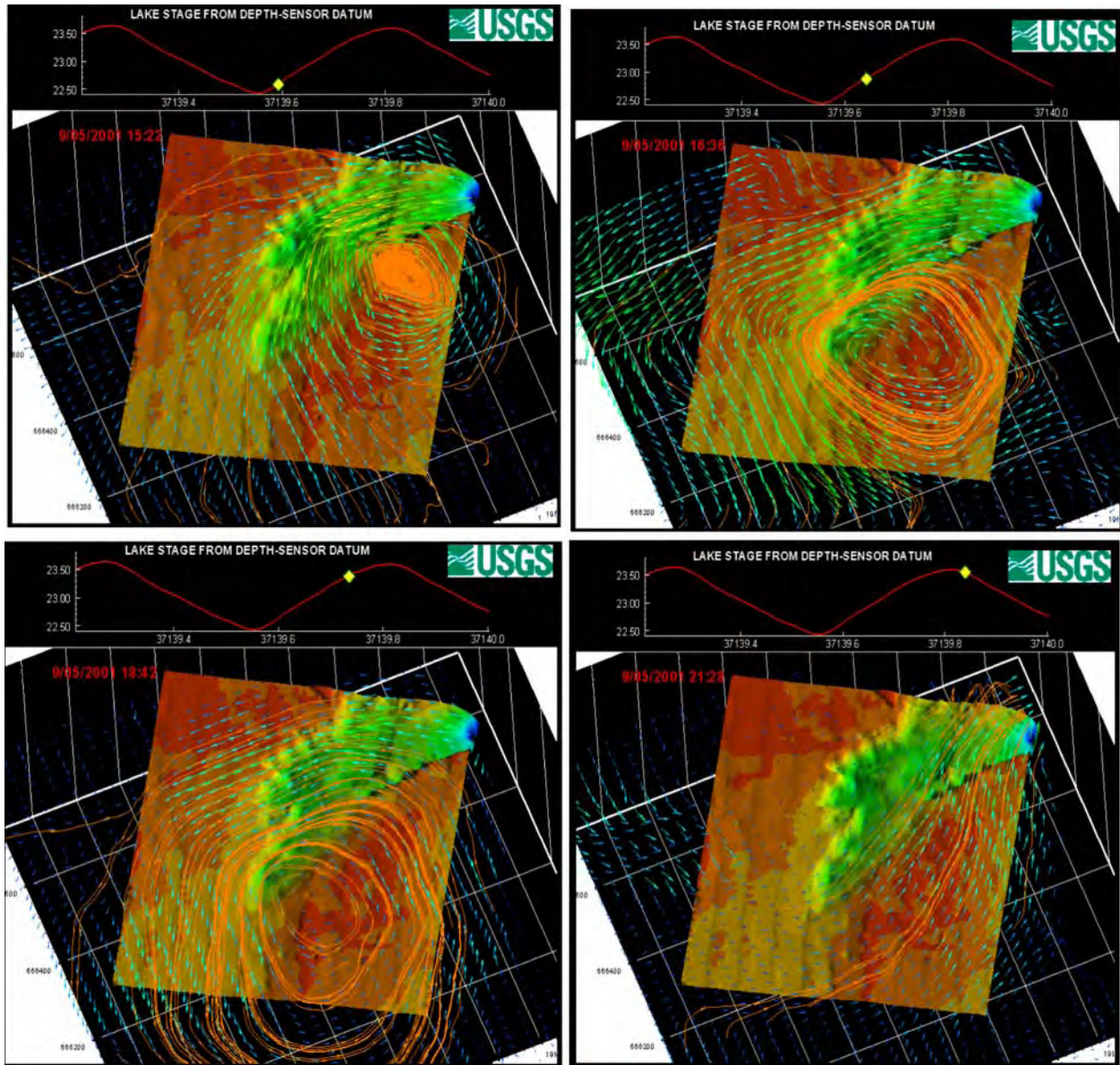


Figure HR48. Mildred Island flow fields – flood tide progression measured using a method described in Dinehart and Burau, 2005.

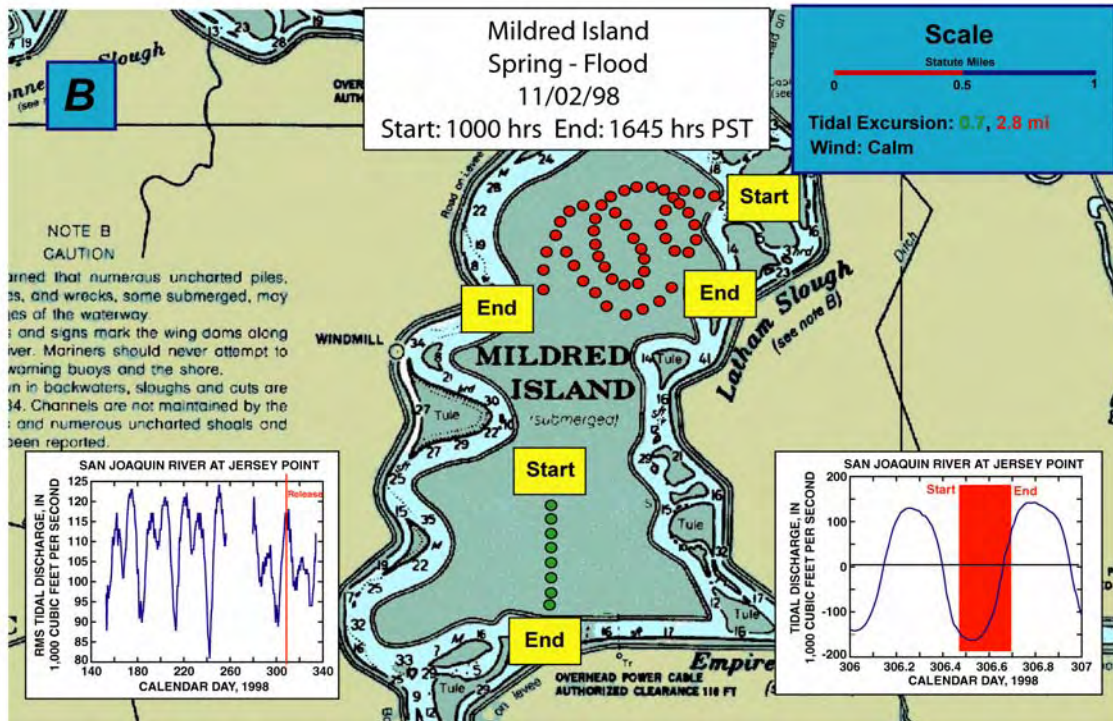
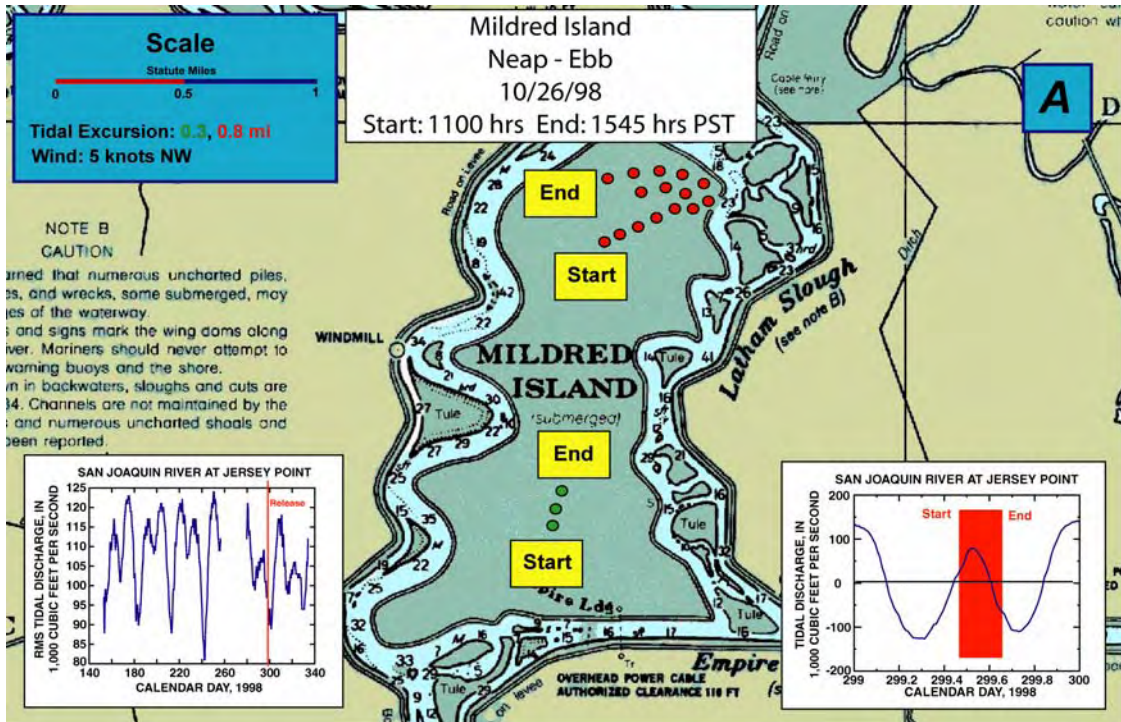


Figure HR49. Mildred Island drifter tracks.

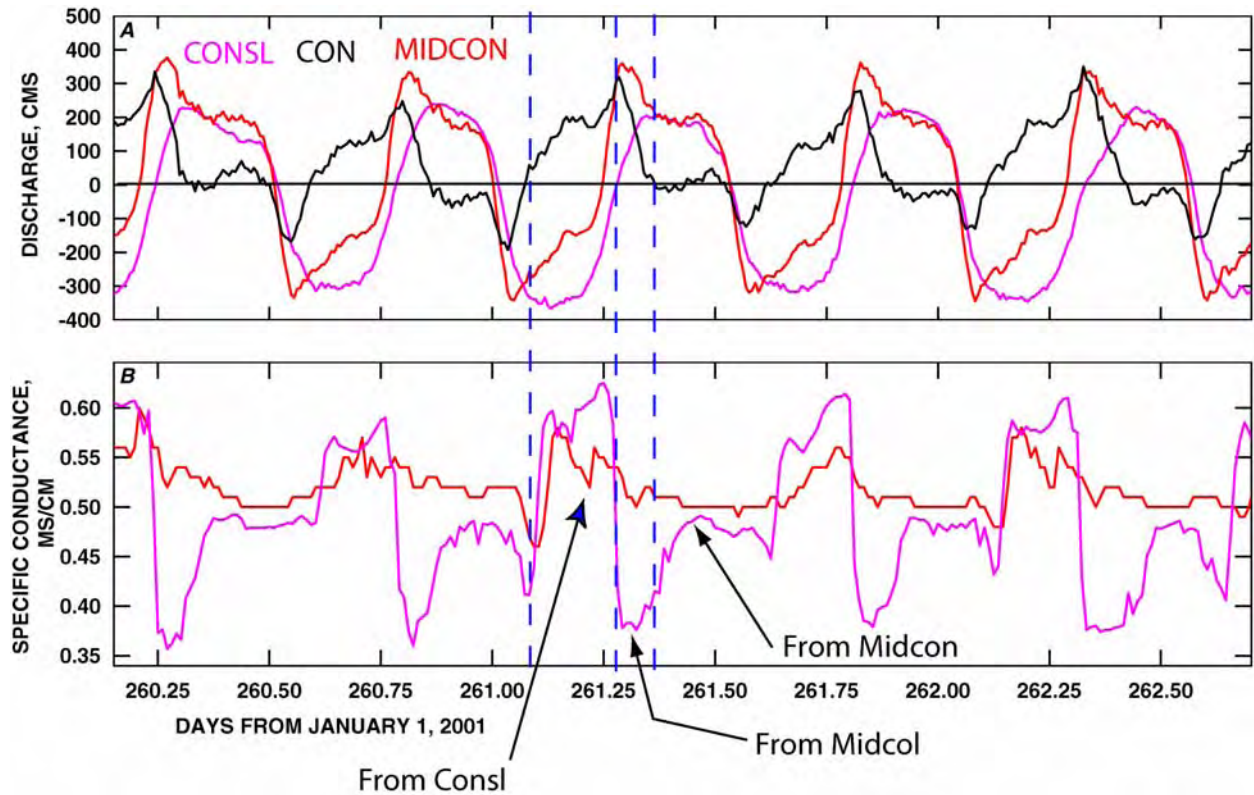


Figure HR50. Discharge at CON; $Q_{con}=Q_{midcon}-Q_{consl}$. Shows that variability at consl is a function of the salinities and phasing of flows in the adjacent channels – high saline water from FT in consl, then big drop in salinity from water coming from midcol, then a average salinity coming from midcon.

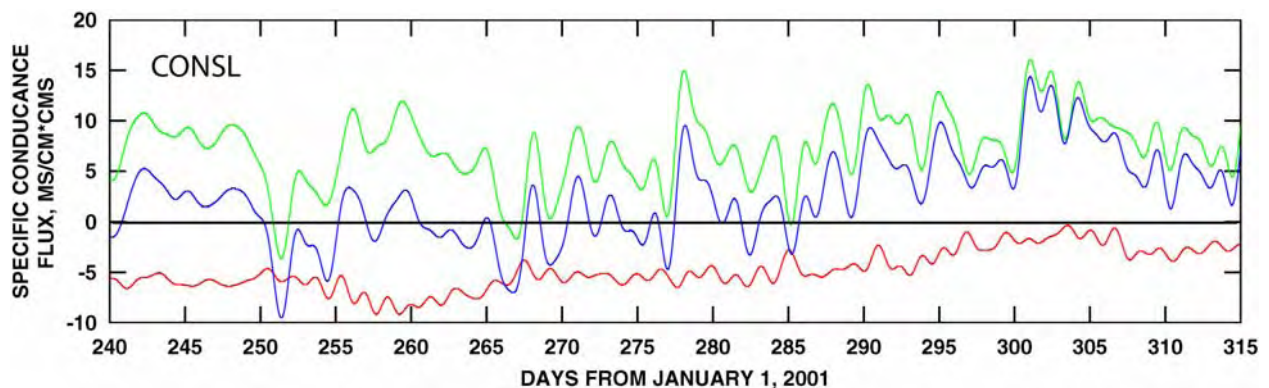


Figure HR51. Time series of salt flux decomposition in Latham Slough. The total specific conductance flux is green, advective flux in blue and the dispersive flux is red.

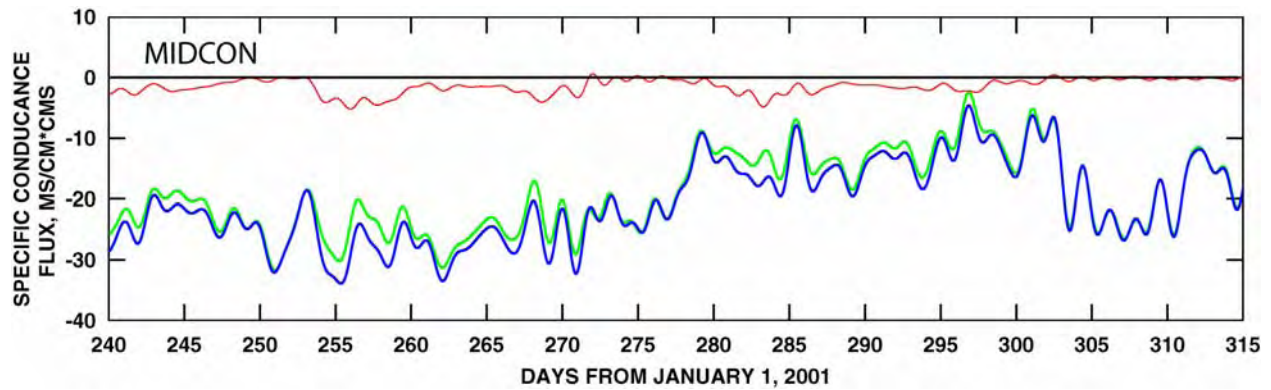


Figure HR52. Time series of salt flux decomposition in Middle River at station MIDCON. The total specific conductance flux is green, advective flux in blue and the dispersive flux is red.

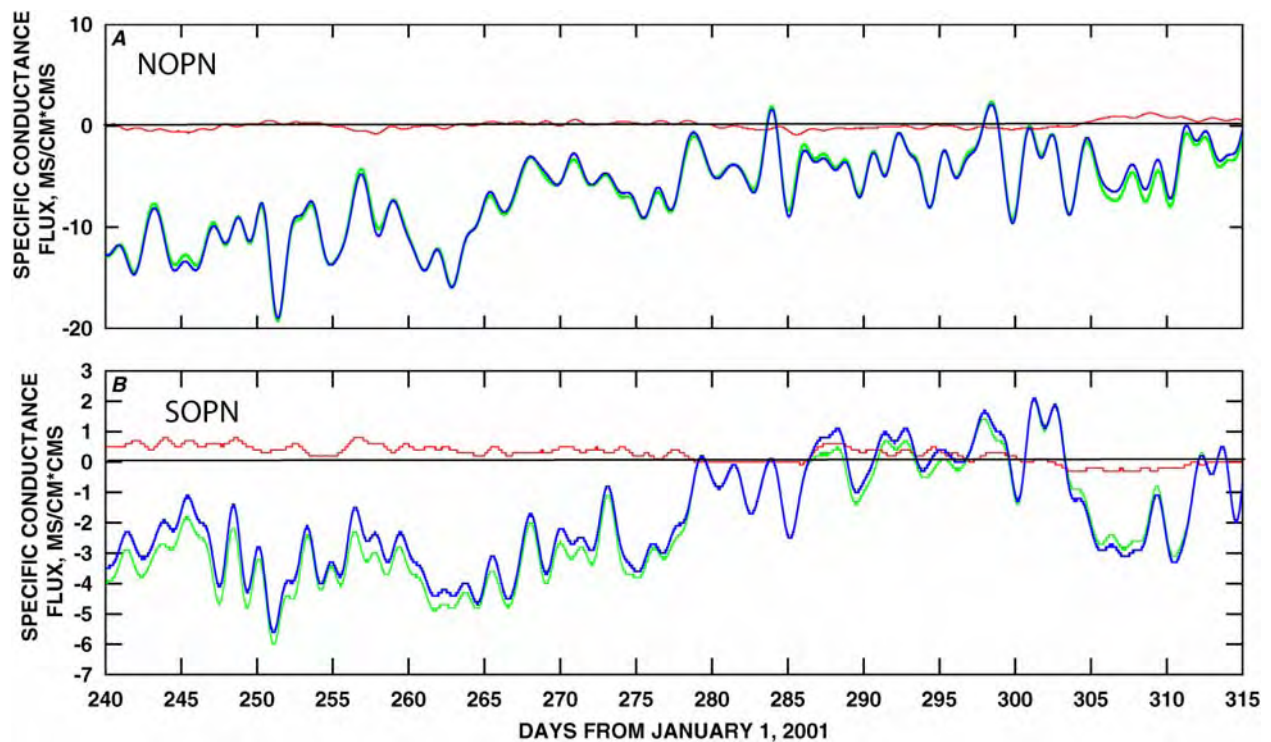


Figure HR53. Time series of salt flux decompositions in the (A) northern opening and (B) southern openings. The total specific conductance flux is green, advective flux in blue and the dispersive flux is red.

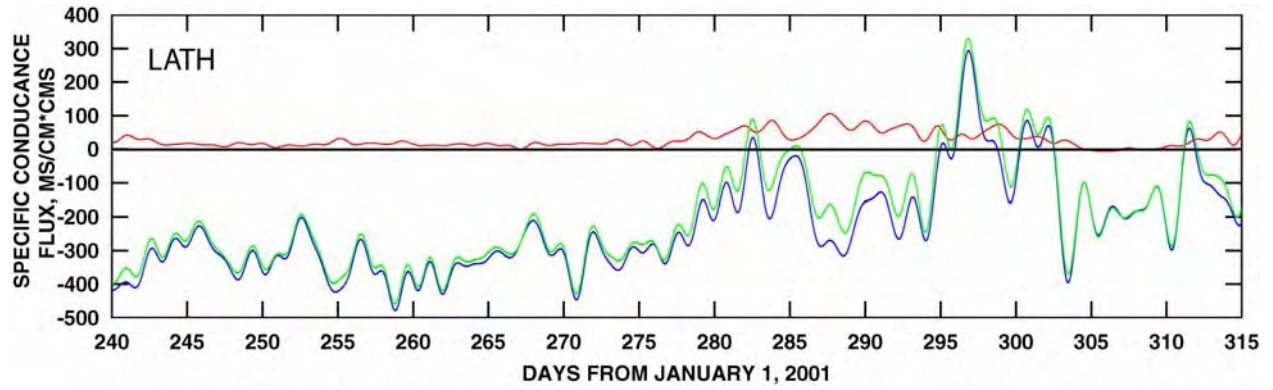


Figure HR54. Time series of salt flux decomposition in Latham Slough. The total specific conductance flux is green, advective flux in blue and the dispersive flux is red.

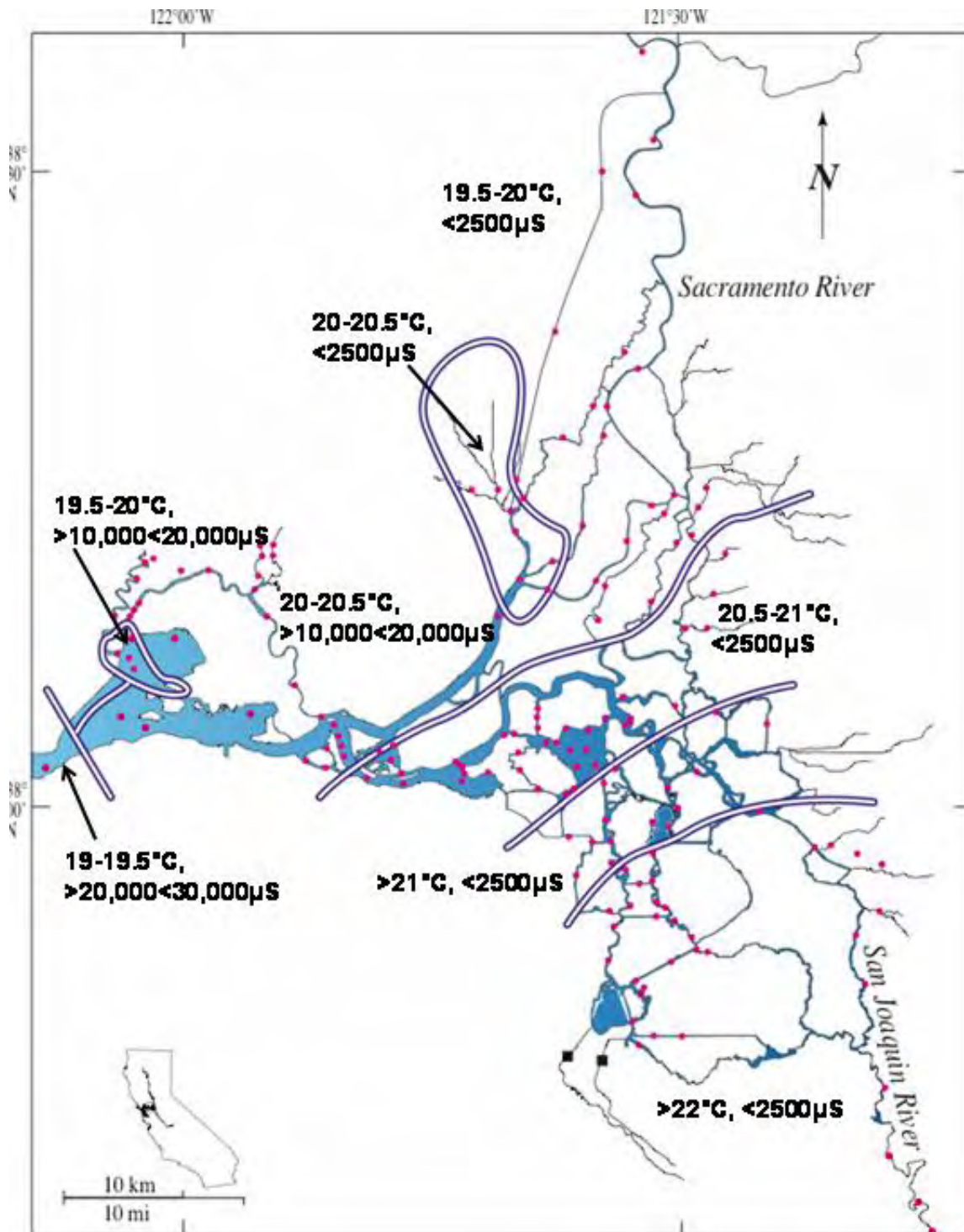


Figure B1. Strata (based on average spring temperatures and electrical conductivity) established for delta-wide benthic sampling. Data provided by A. Jassby and W. Kimmerer.

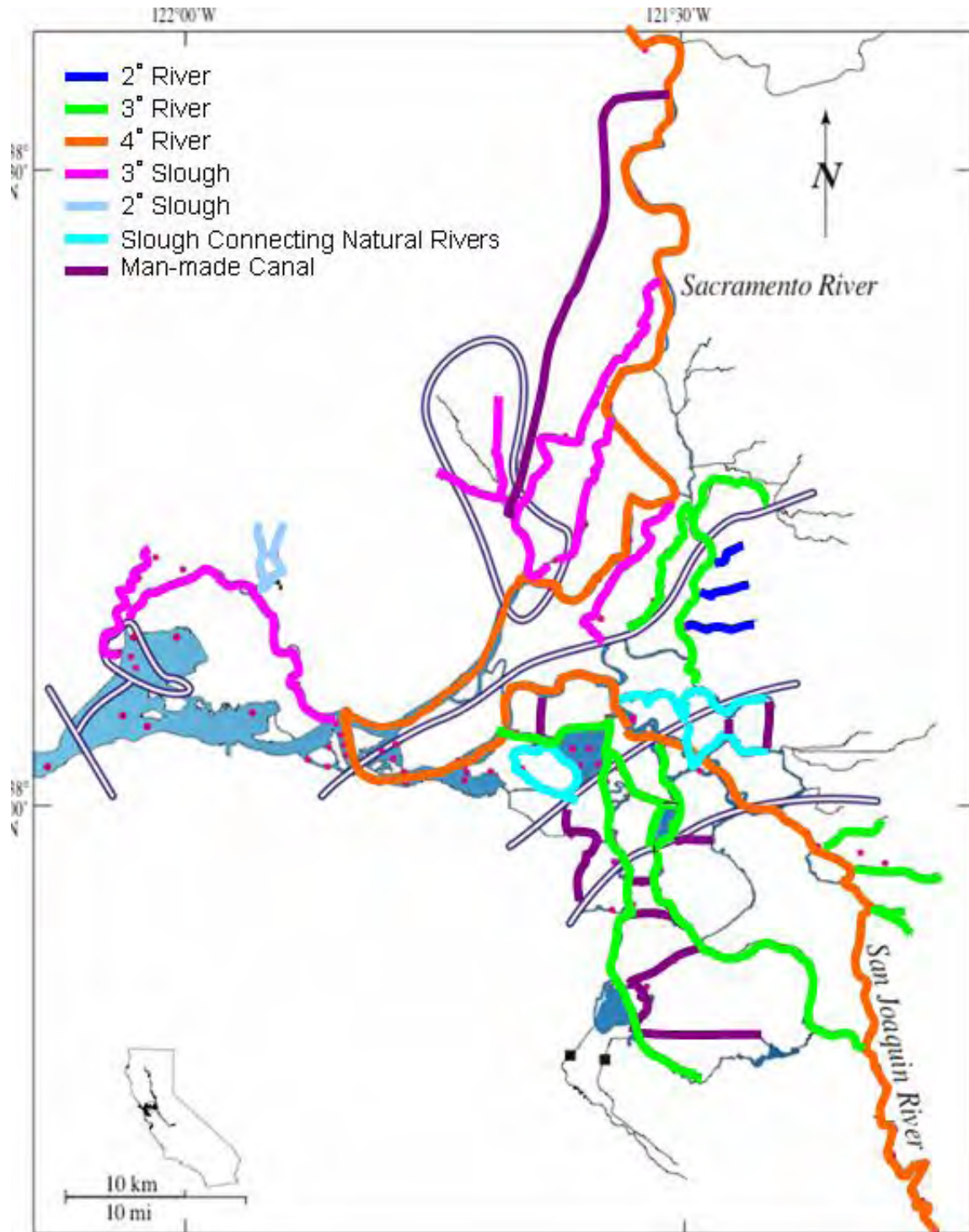


Figure B2. River and slough “classification” used in grouping water bodies by their relative connections to the bay and Sacramento and San Joaquin Rivers (assumed to be fourth degree for this exercise).

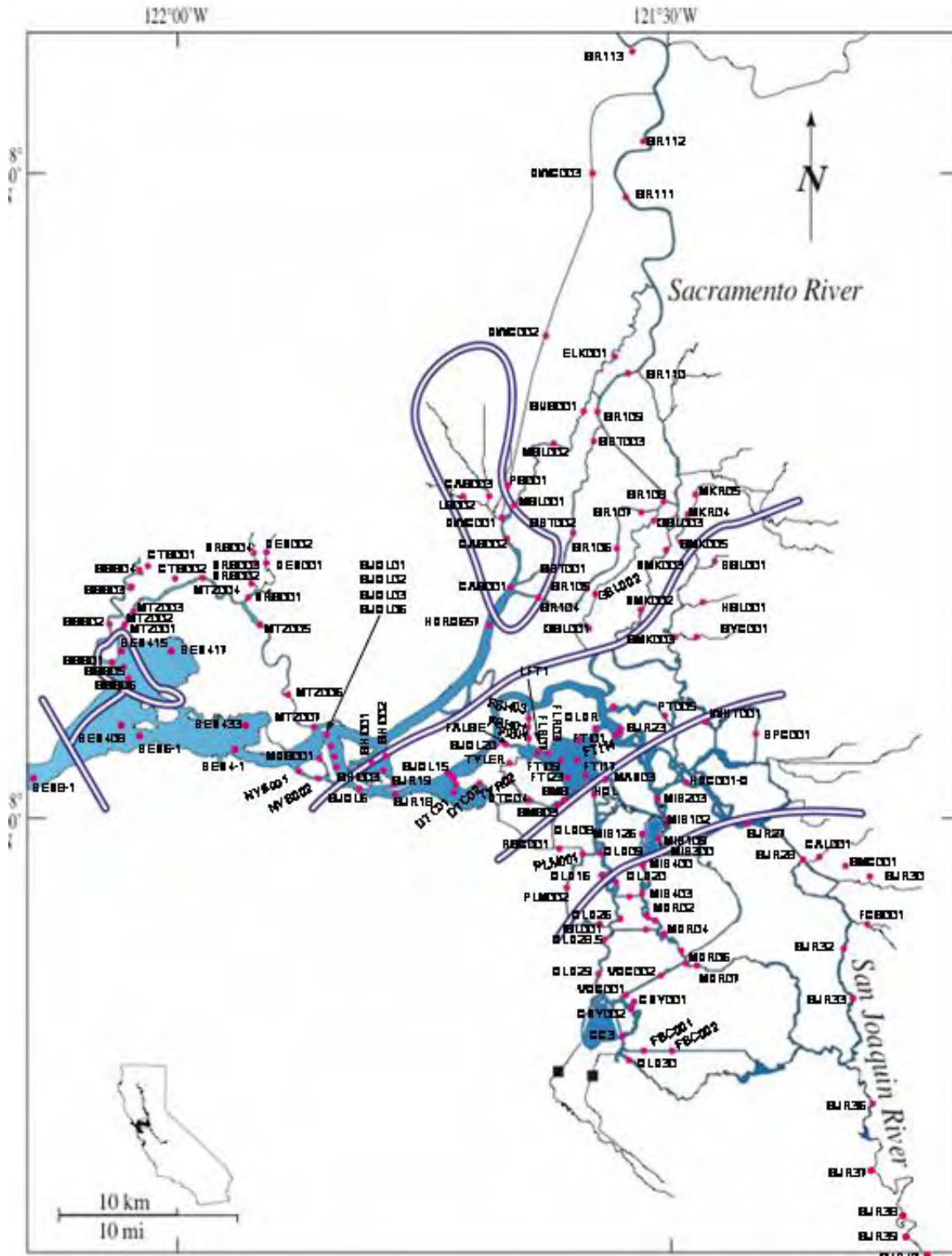


Figure B3. Station locations for delta-wide sampling in May 2003.

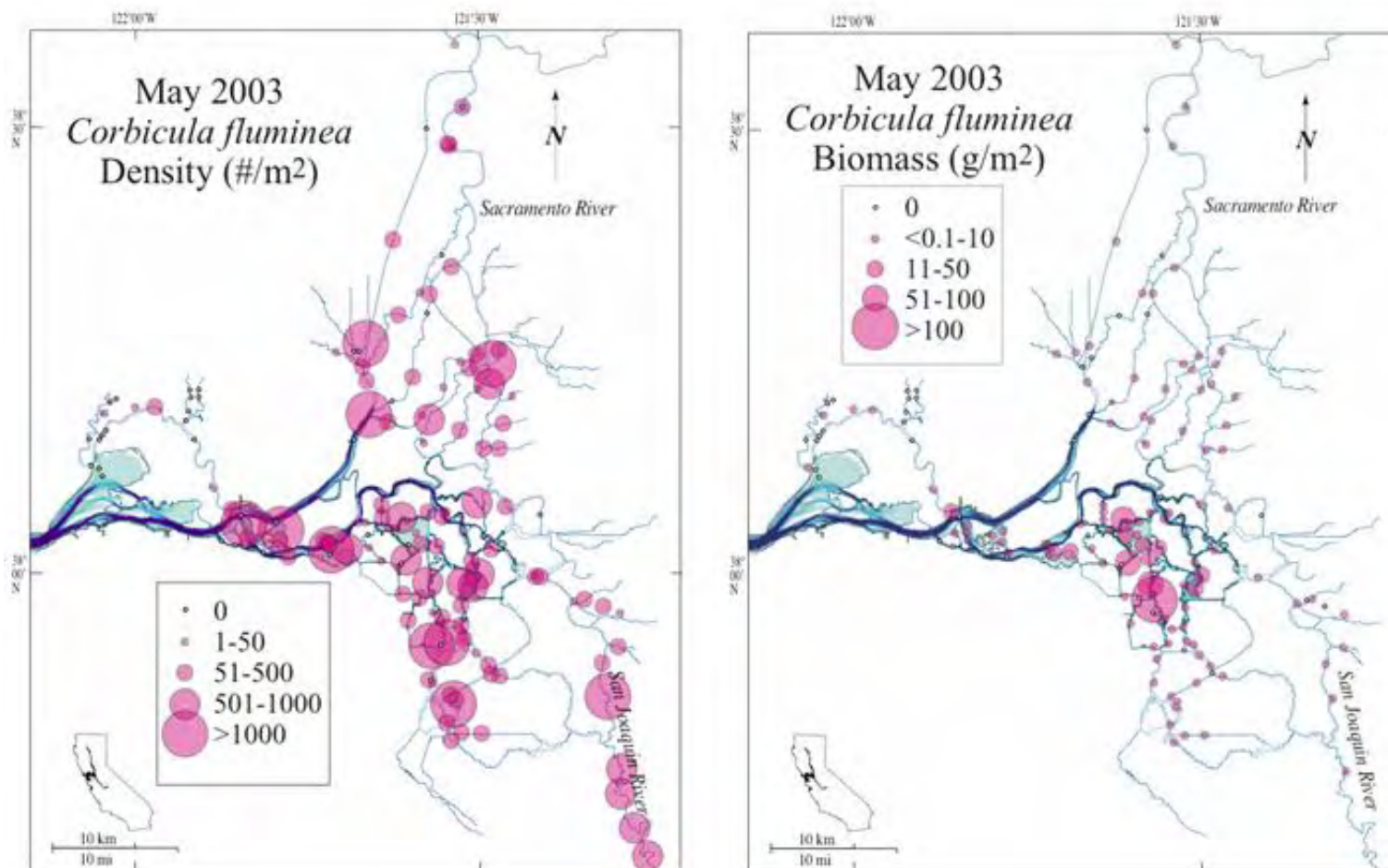


Figure B4. Density and biomass of *C. fluminea* in May 2003.

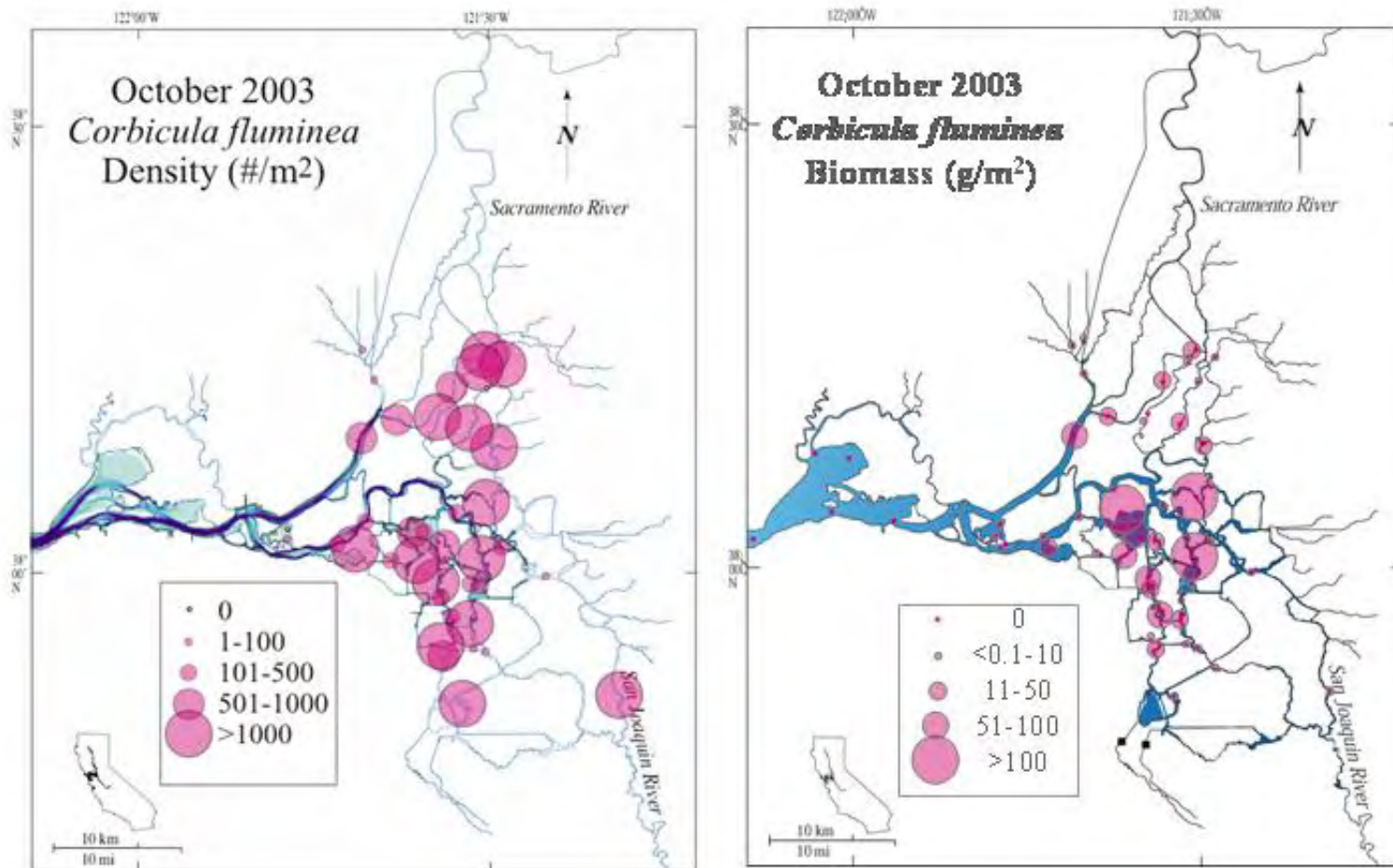


Figure B5. Density and biomass of *C. fluminea* in October 2003.

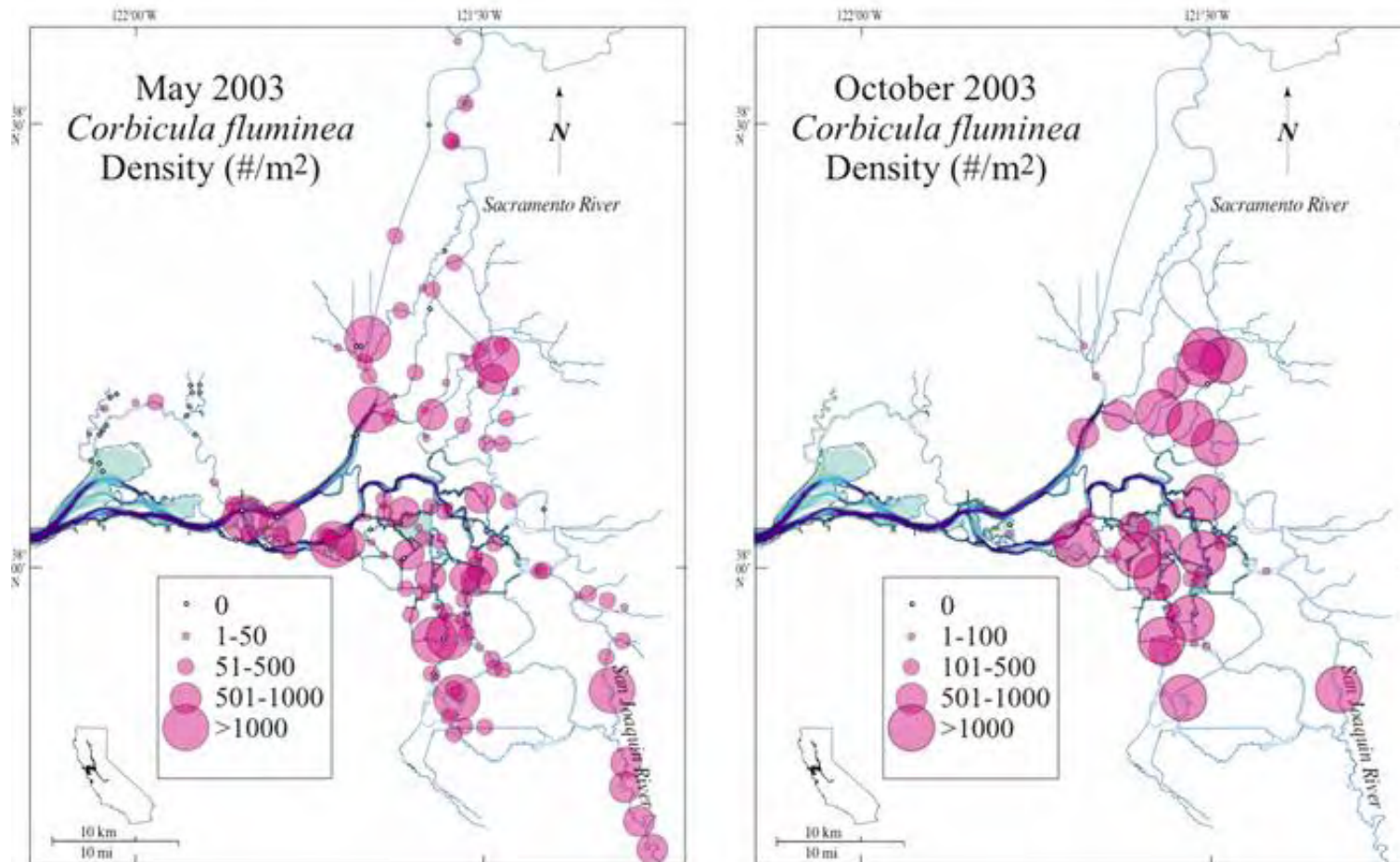


Figure B6. A comparison of density of *C. fluminea* in May and October 2003.

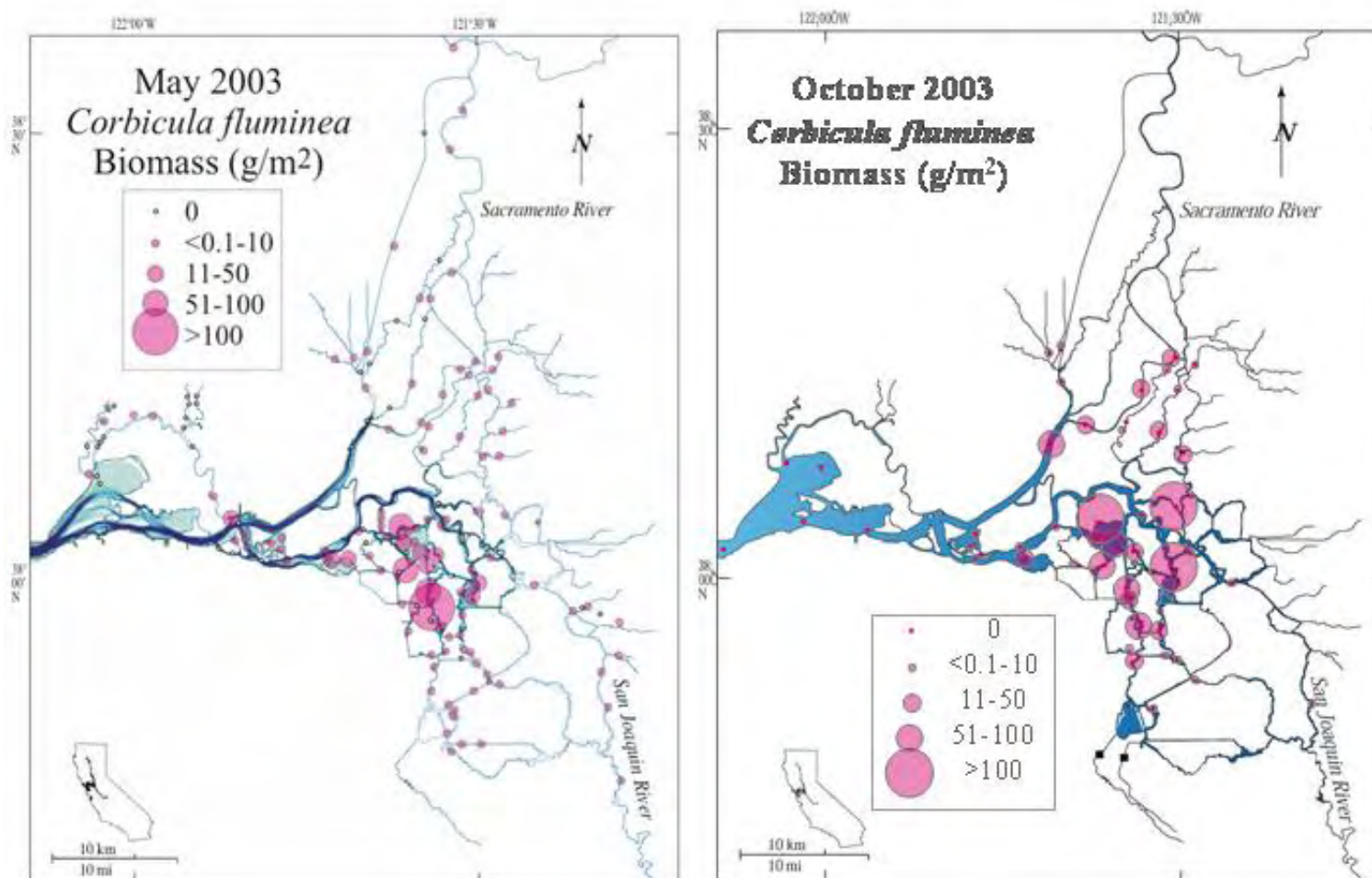


Figure B7. A comparison of biomass of *C. fluminea* in May and October 2003.

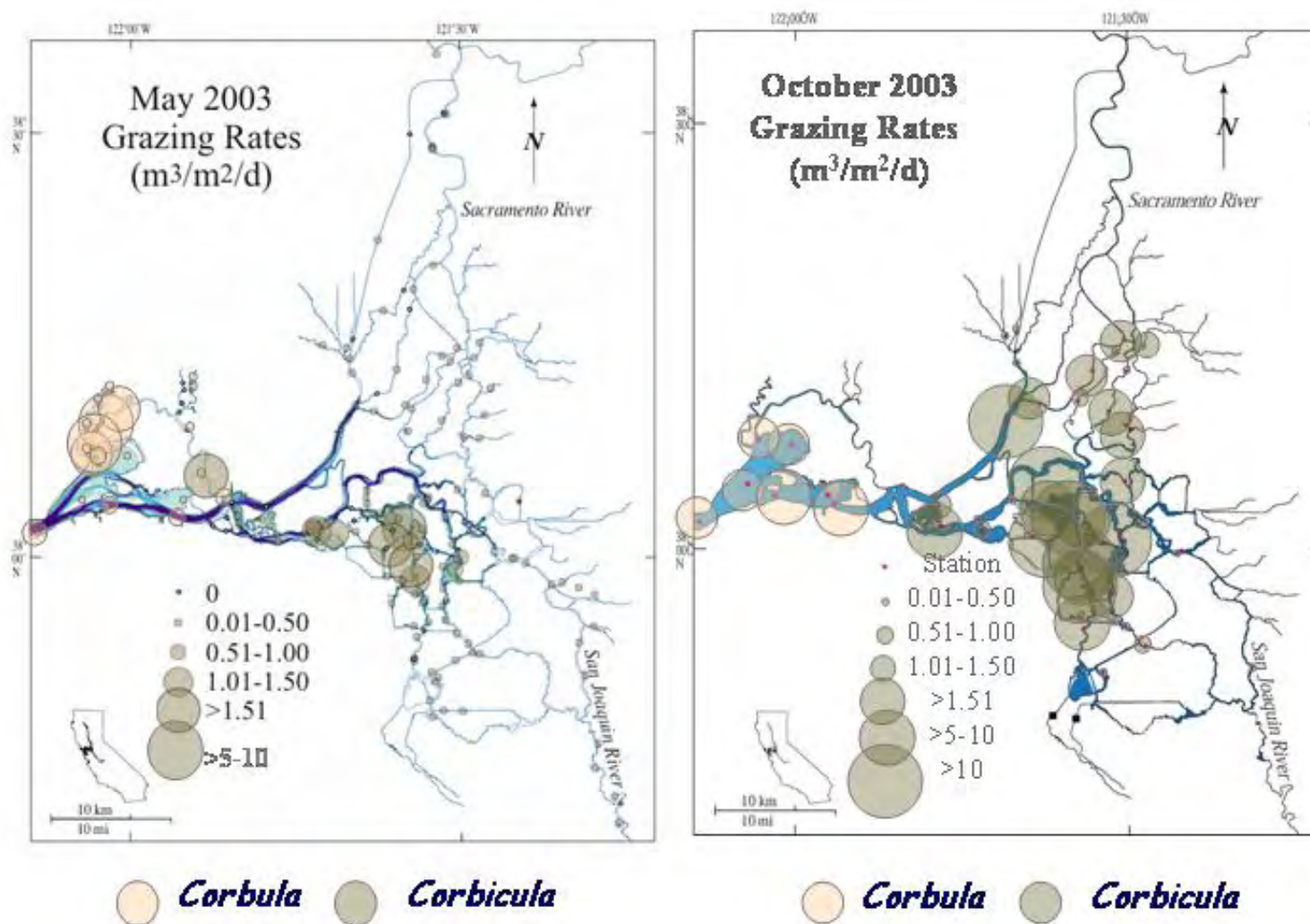


Figure B8. A comparison of grazing rates of *C. fluminea* and *C. amurensis* in May and October 2003

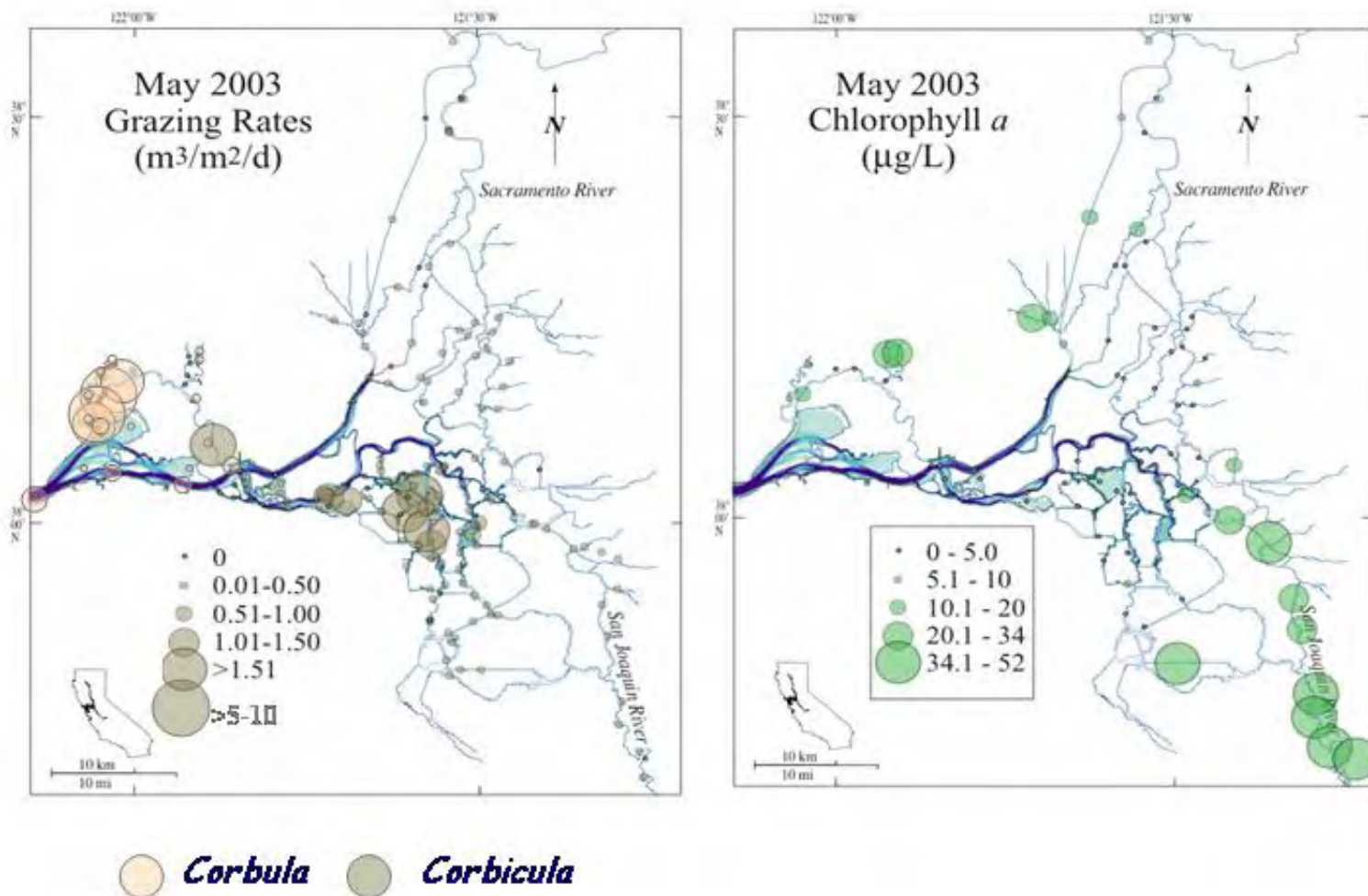


Figure B9. A comparison of grazing rates of *C. fluminea* and *C. amurensis* in May 2003 with concurrently measured chlorophyll *a* concentration.

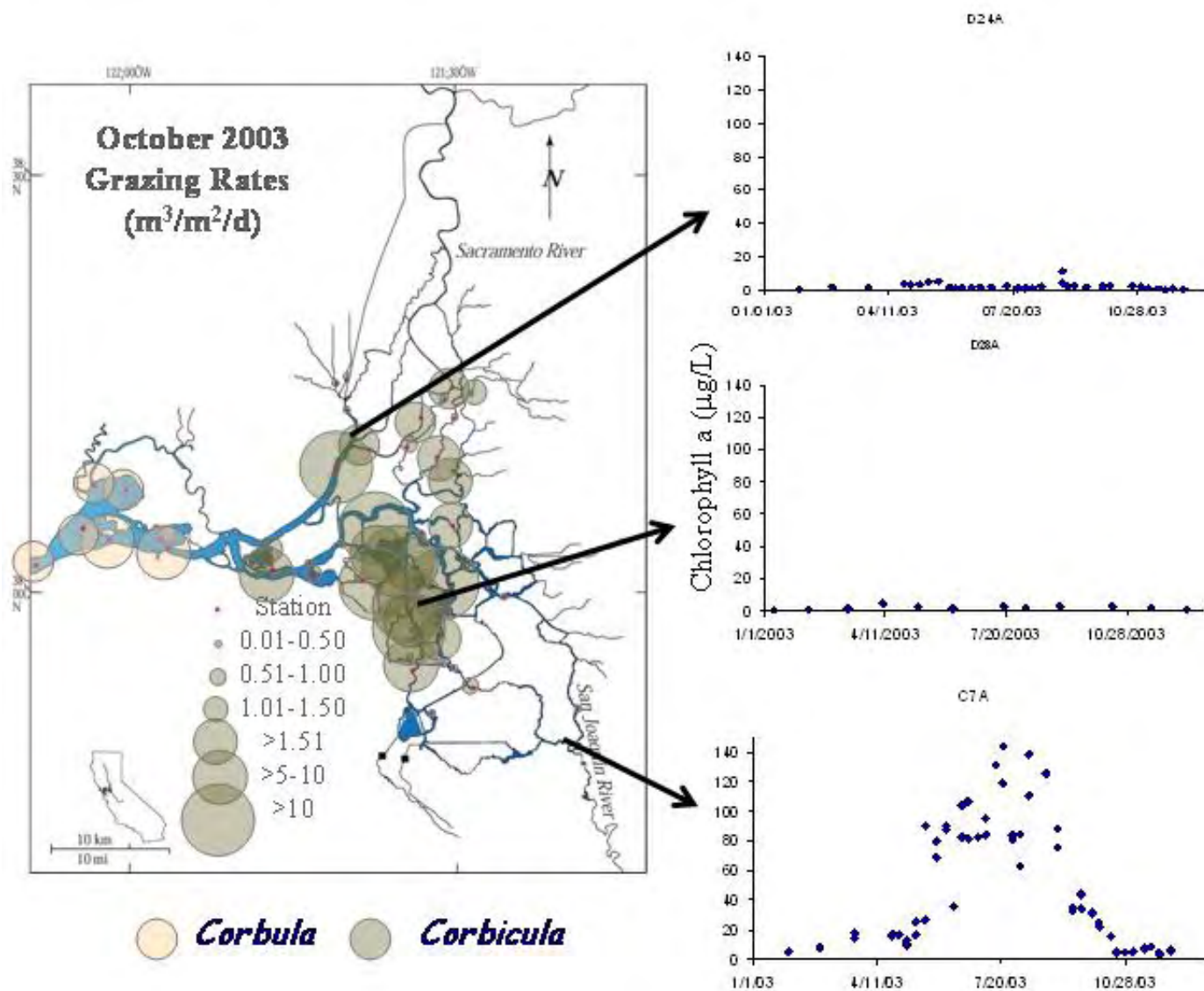


Figure B10. A comparison of grazing rates of *C. fluminea* and *C. amurensis* in October 2003 with chlorophyll a concentration measured throughout the year at three locations in the Delta by the California Department of Water Resources.

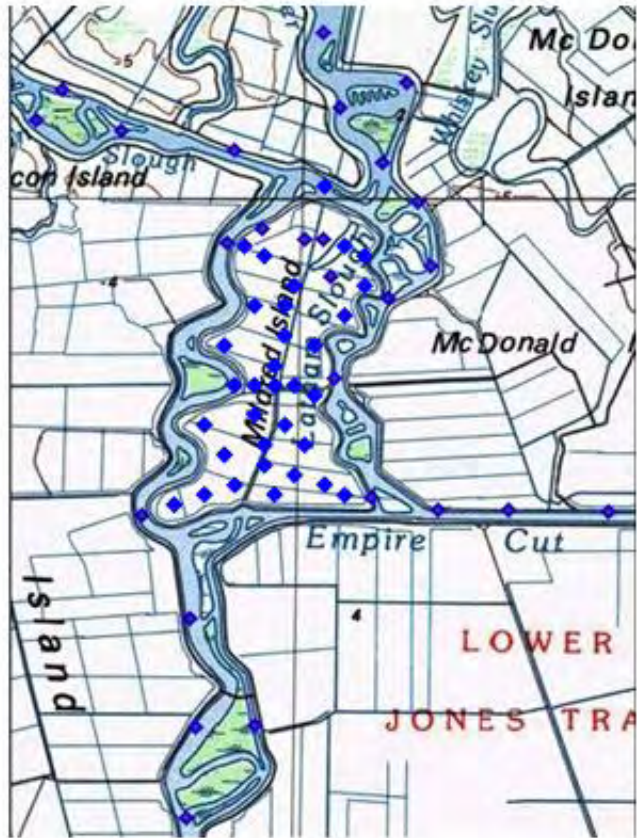


Figure B11. Station locations for the spatial study of *C. fluminea* grazing in Mildred Island in August 2001.

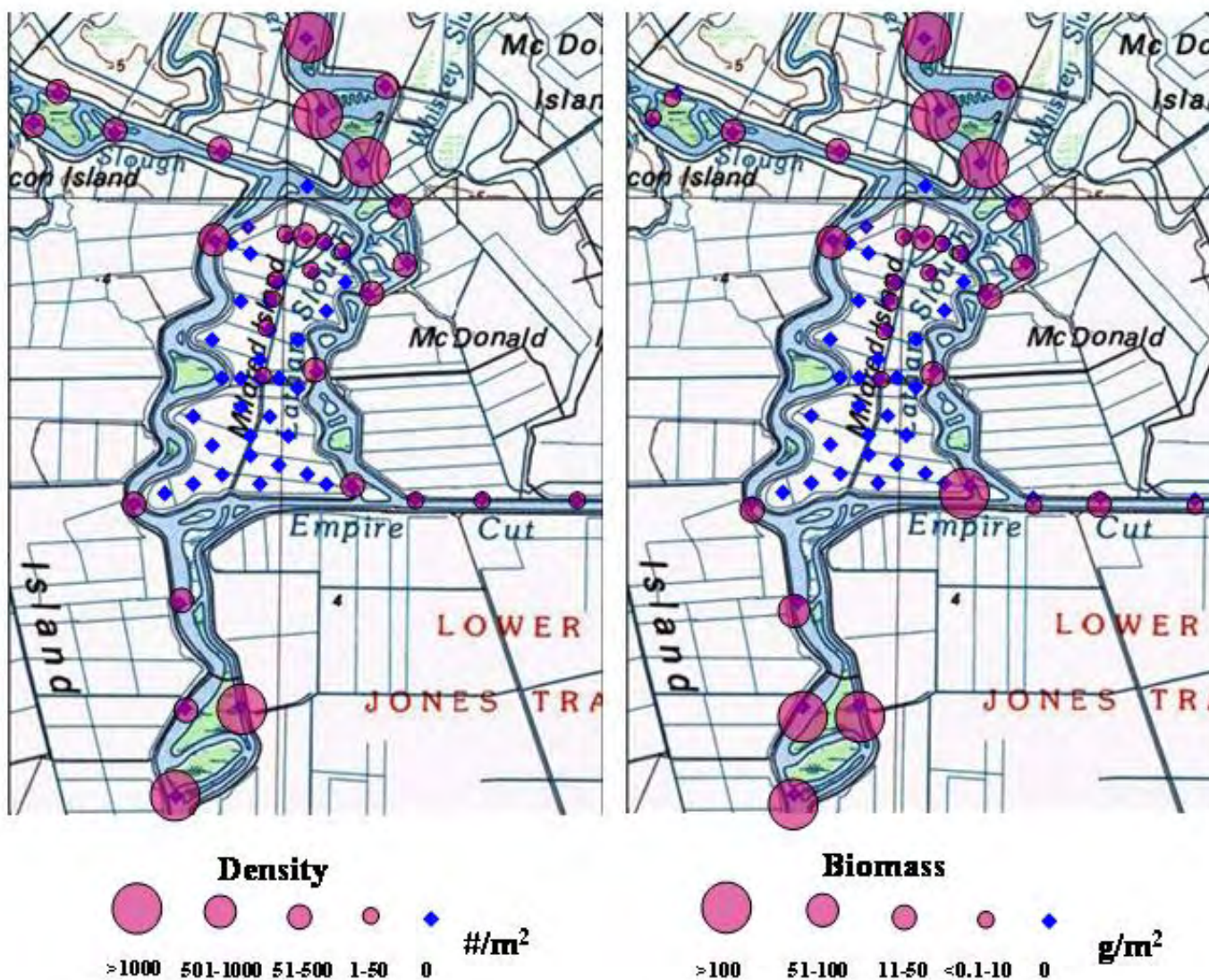


Figure B12. *C. fluminea* abundance and biomass in Mildred Island and connecting channels in August 2001.

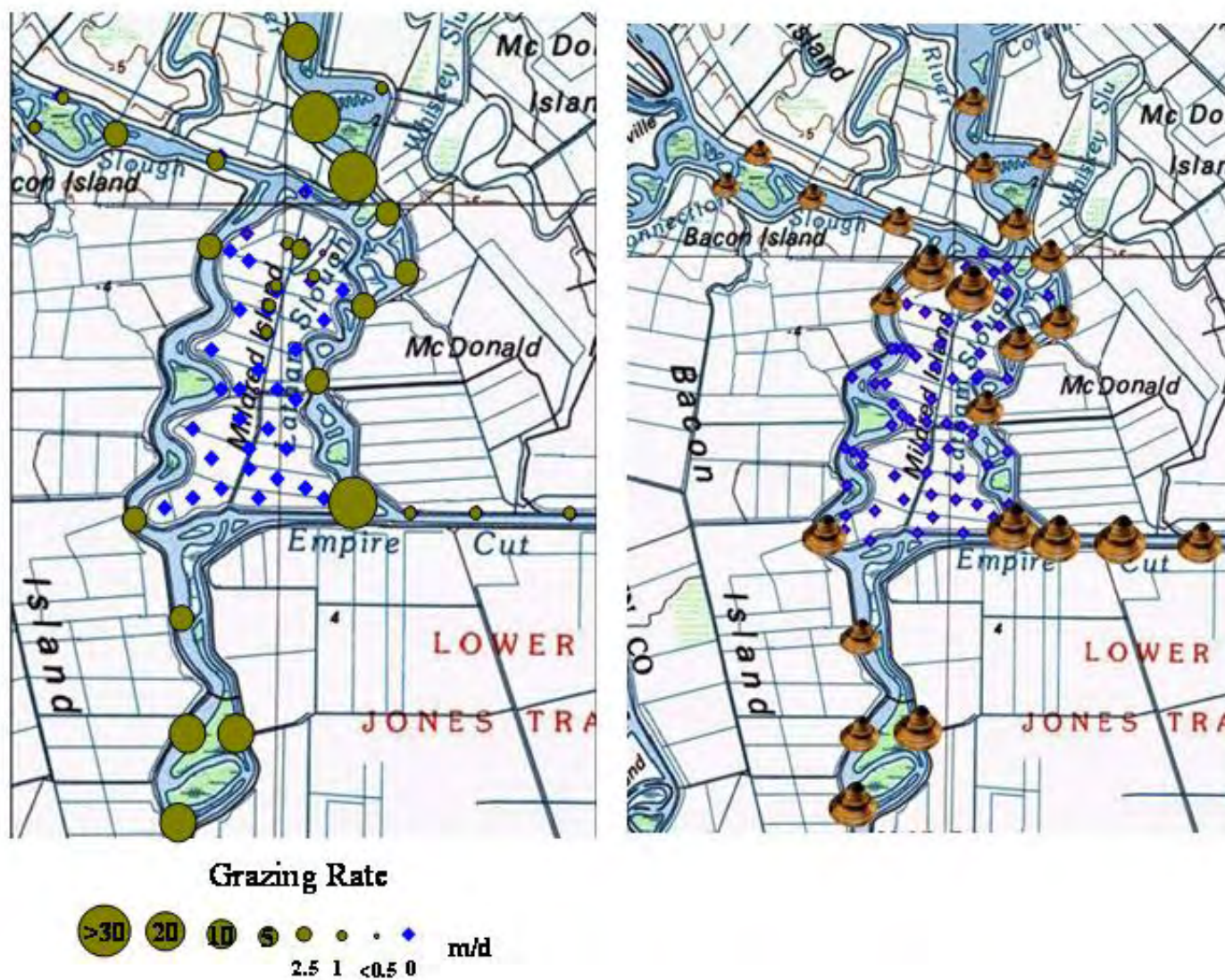


Figure B13. *C. fluminea* grazing rates and median size of oldest year class (out of two year classes) in Mildred Island and connecting channels in August 2001.

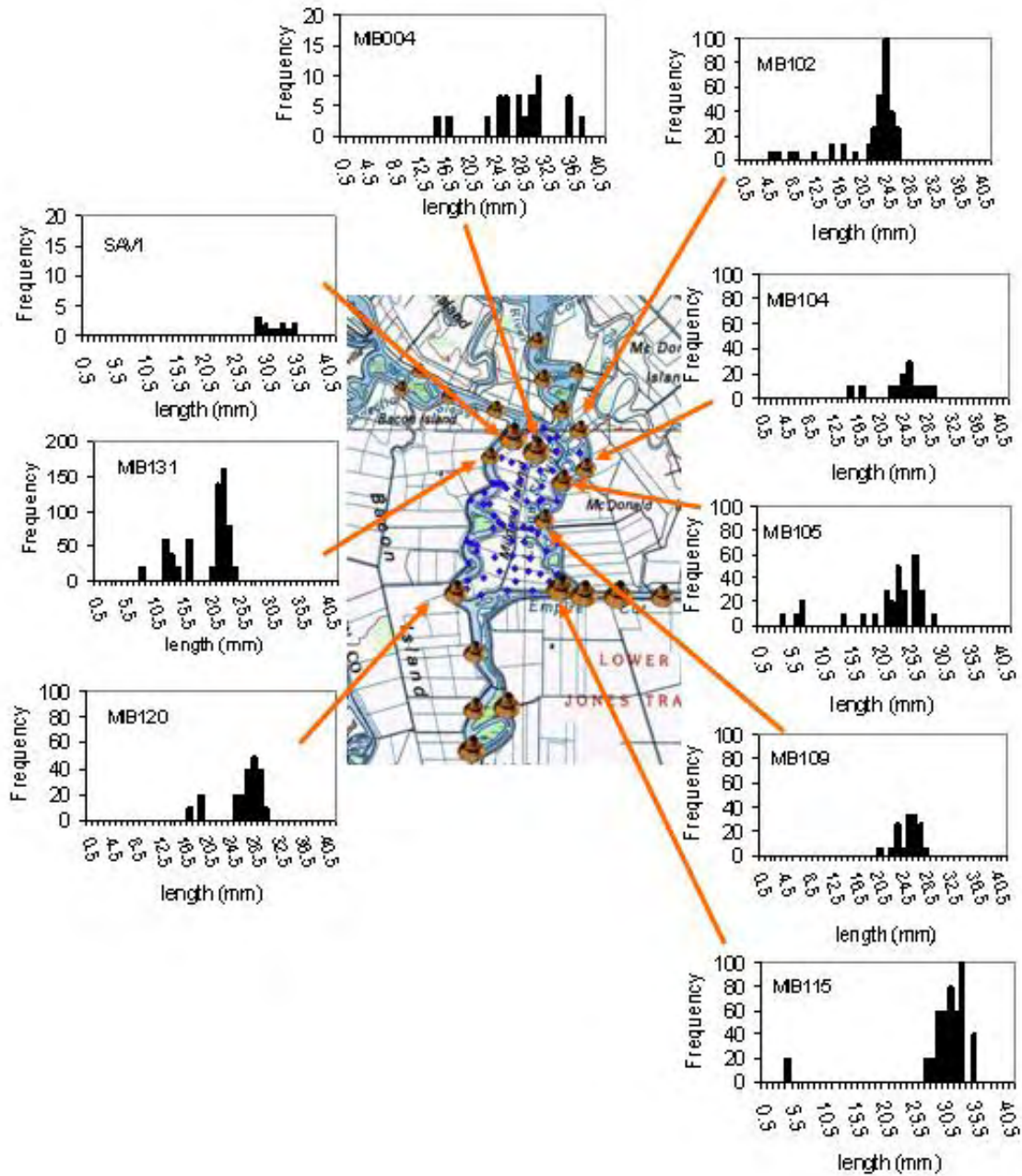


Figure B14. Size frequency distributions of *C. fluminea* collected in the boundary channels of Mildred Island and at two interior island locations (SAV1 and MIB004) in August 2001.

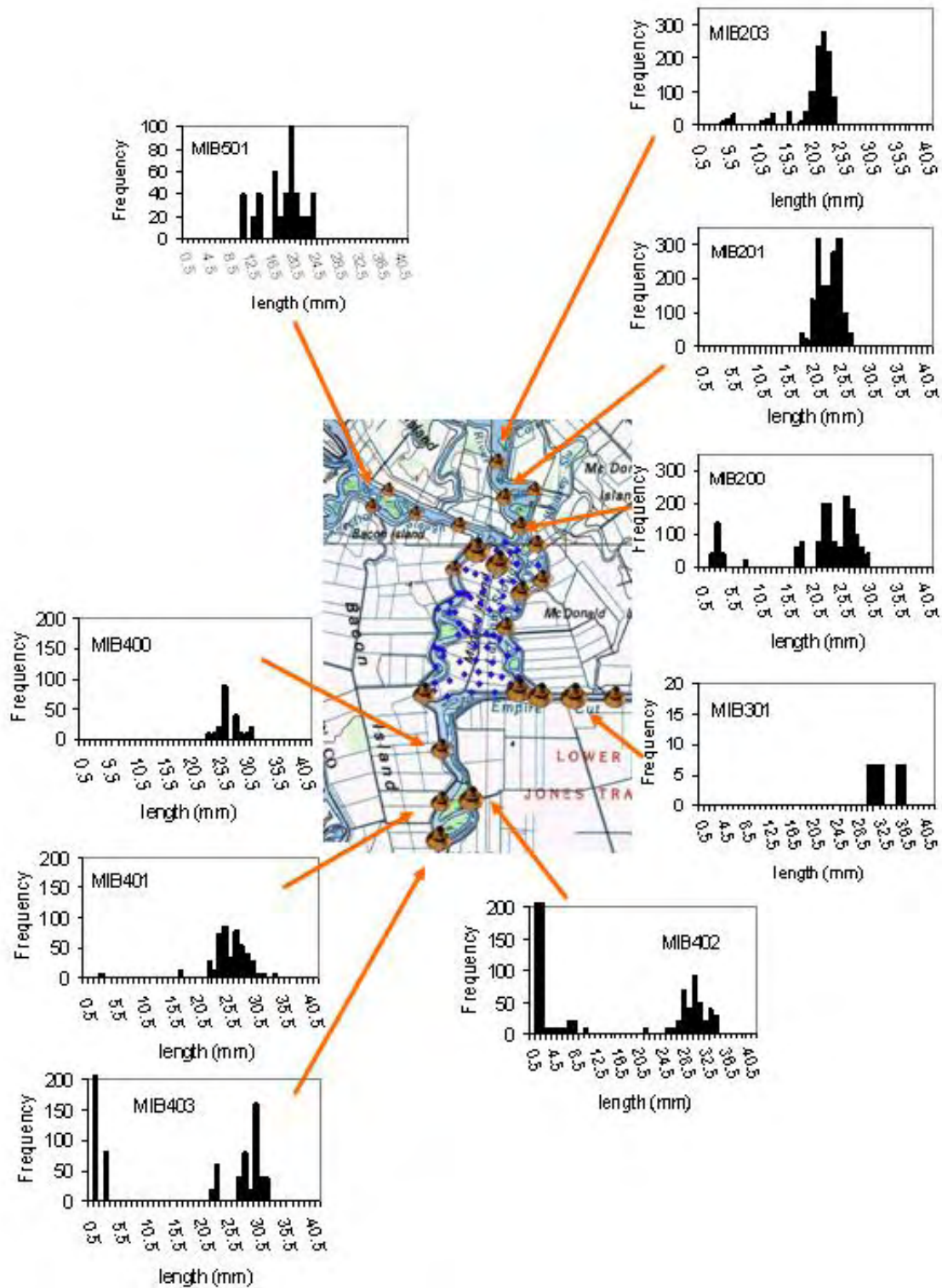


Figure B15. Size frequency distributions of *C. fluminea* collected in the connecting channels to Mildred Island in August 2001.

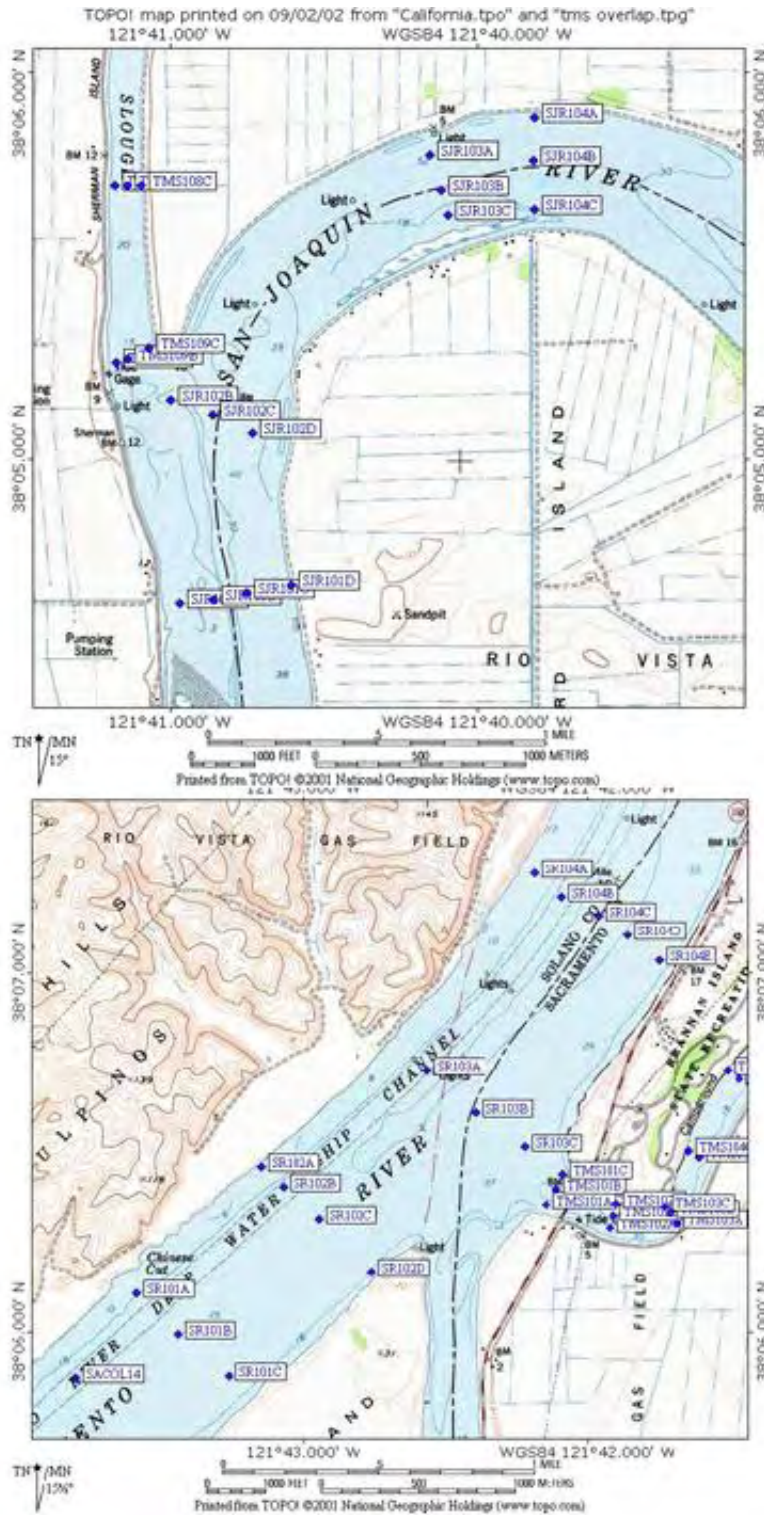


Figure B16. Station locations for the spatially intensive study of *C. fluminea* distribution in the San Joaquin and Sacramento Rivers in August 2002.

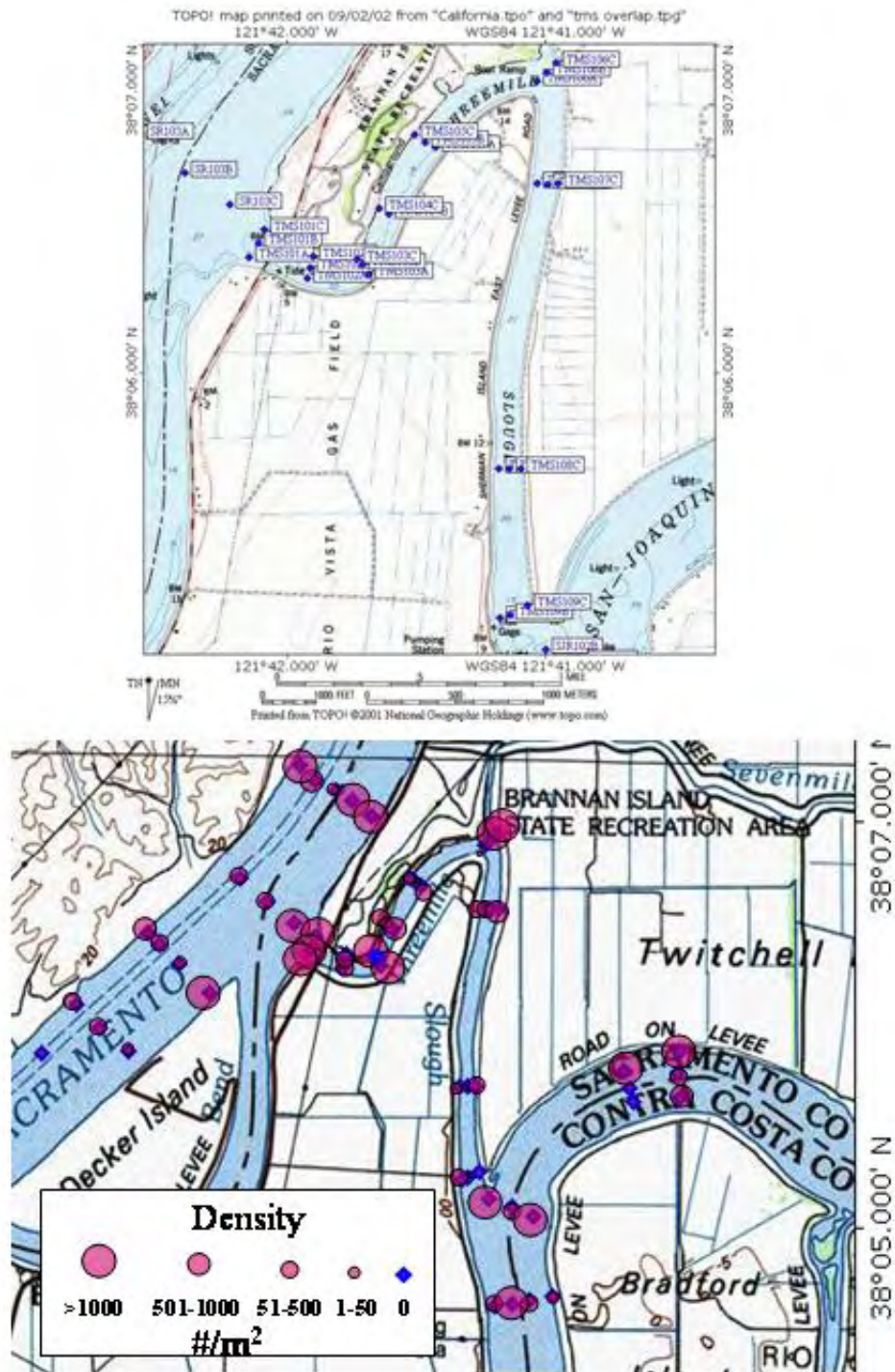


Figure B17. (a) Station locations for the spatially intensive study of *C. fluminea* distribution in Threemile Slough in August 2002. (b) *C. fluminea* densities in the three channels.

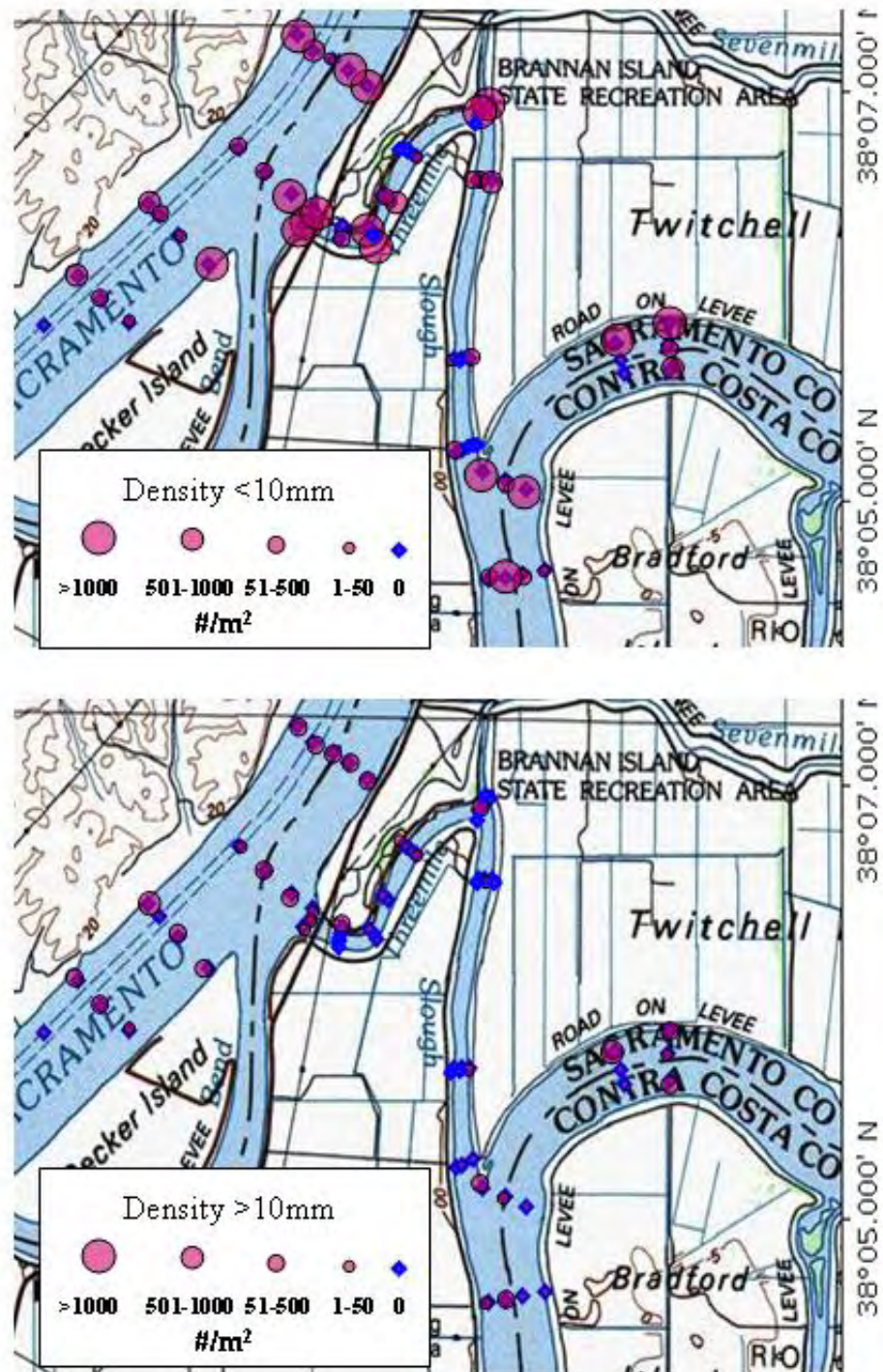


Figure B18. Distribution of *C. fluminea* in the three channels as a function of size.

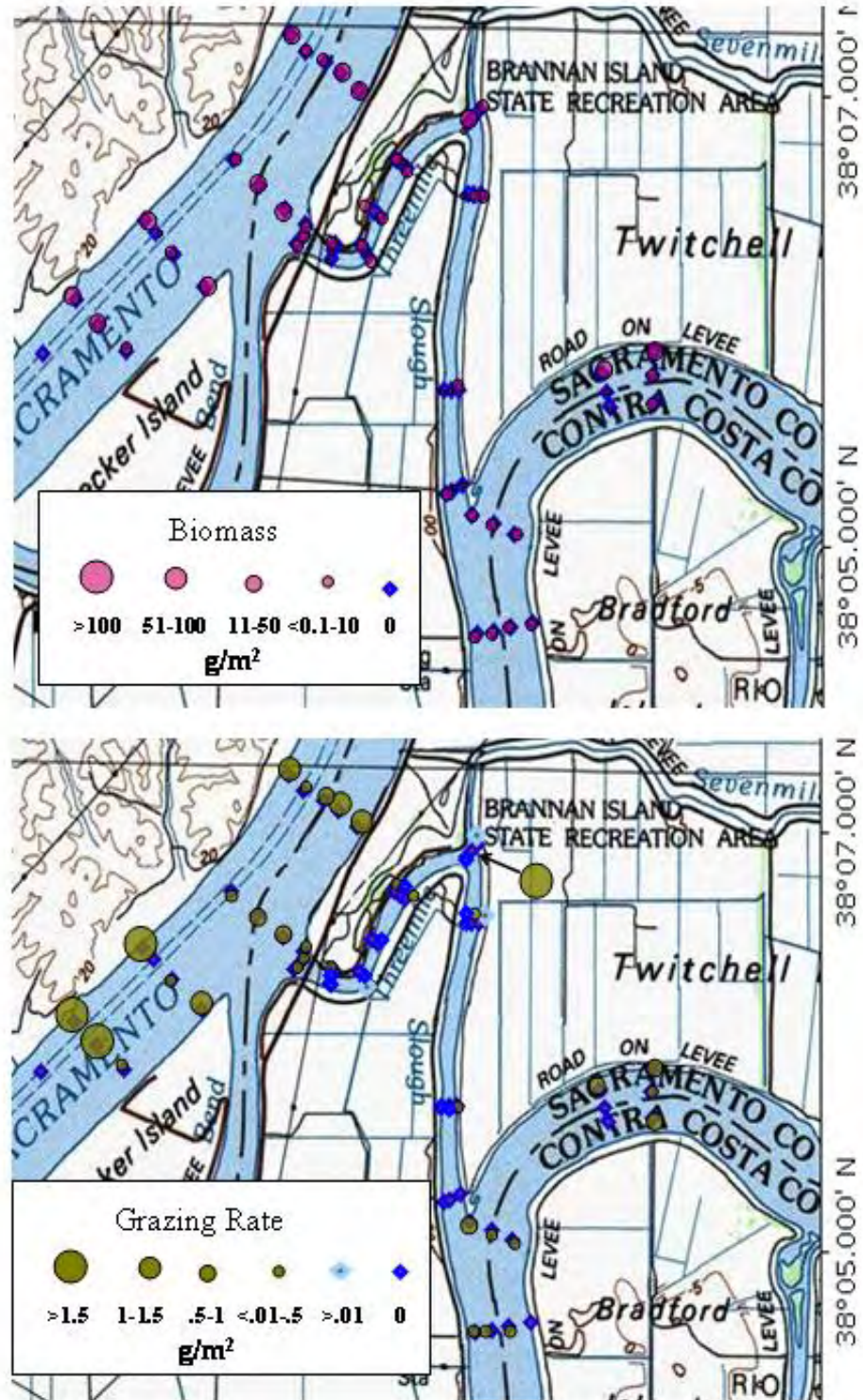


Figure B19. Biomass and grazing rate of *C. fluminea* in the three channels in August 2001.

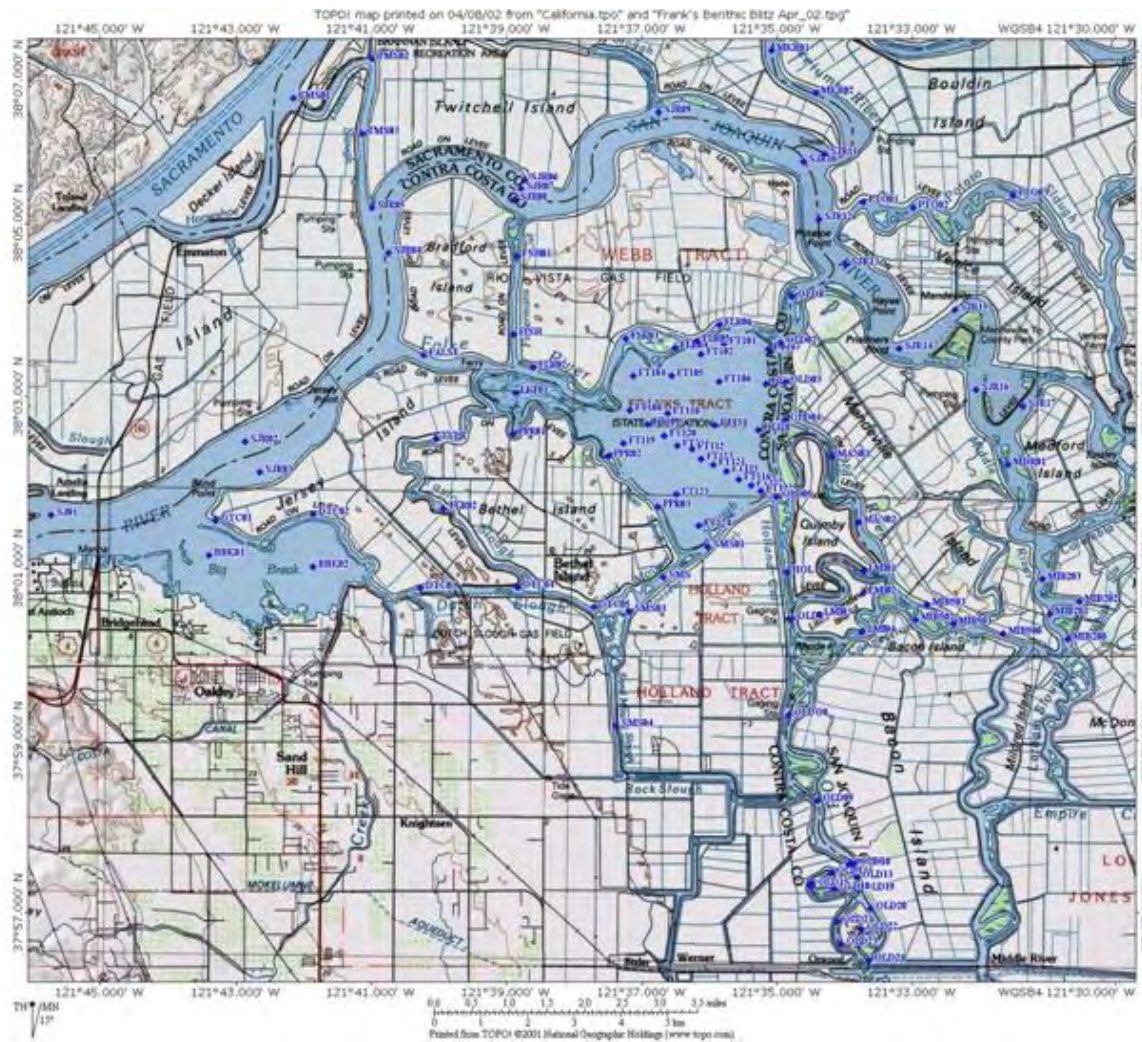


Figure B20. Station locations for benthic samples for the Franks Tract process study in April 2002.

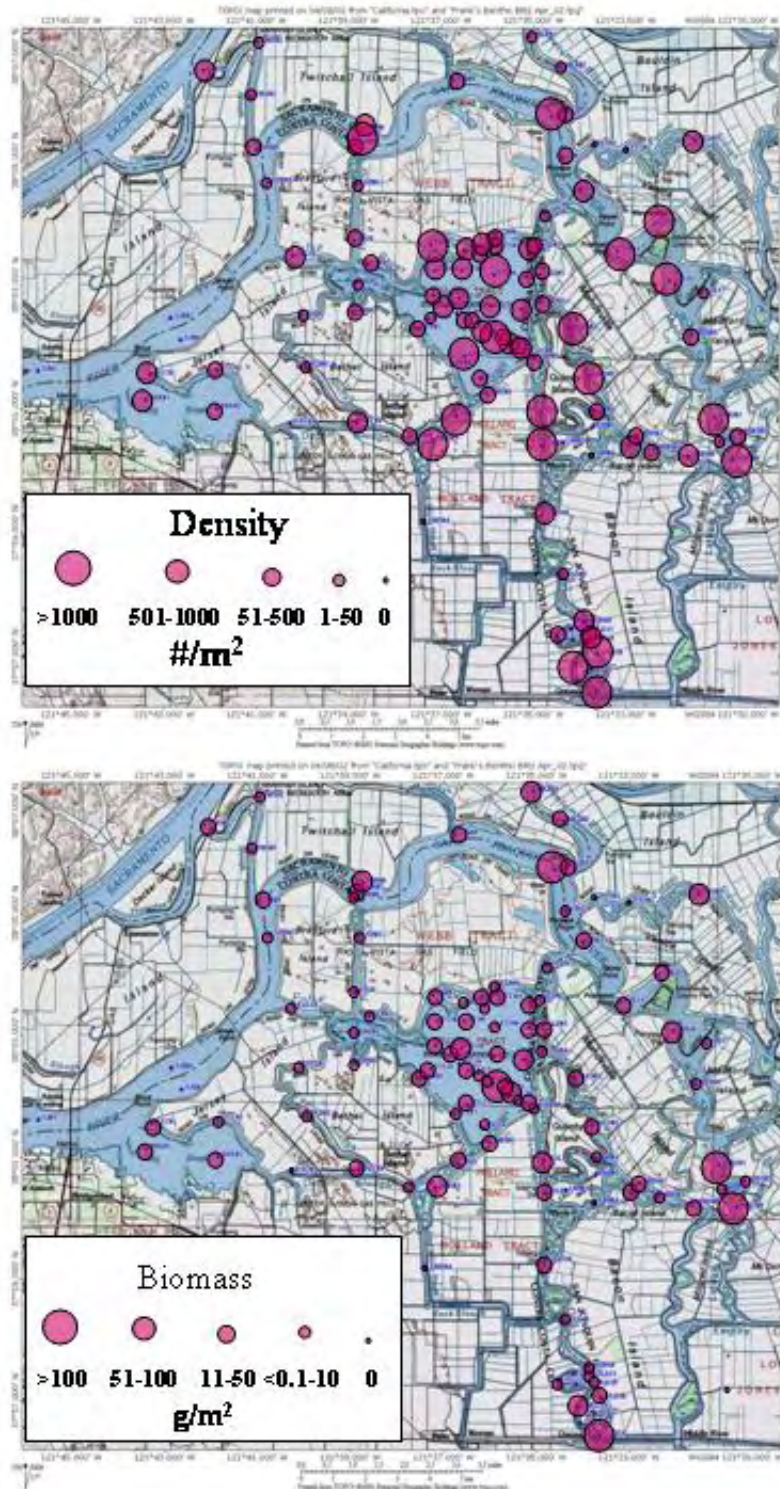


Figure B21. Density and biomass of *C. fluminea* in Franks Tract in April 2002.

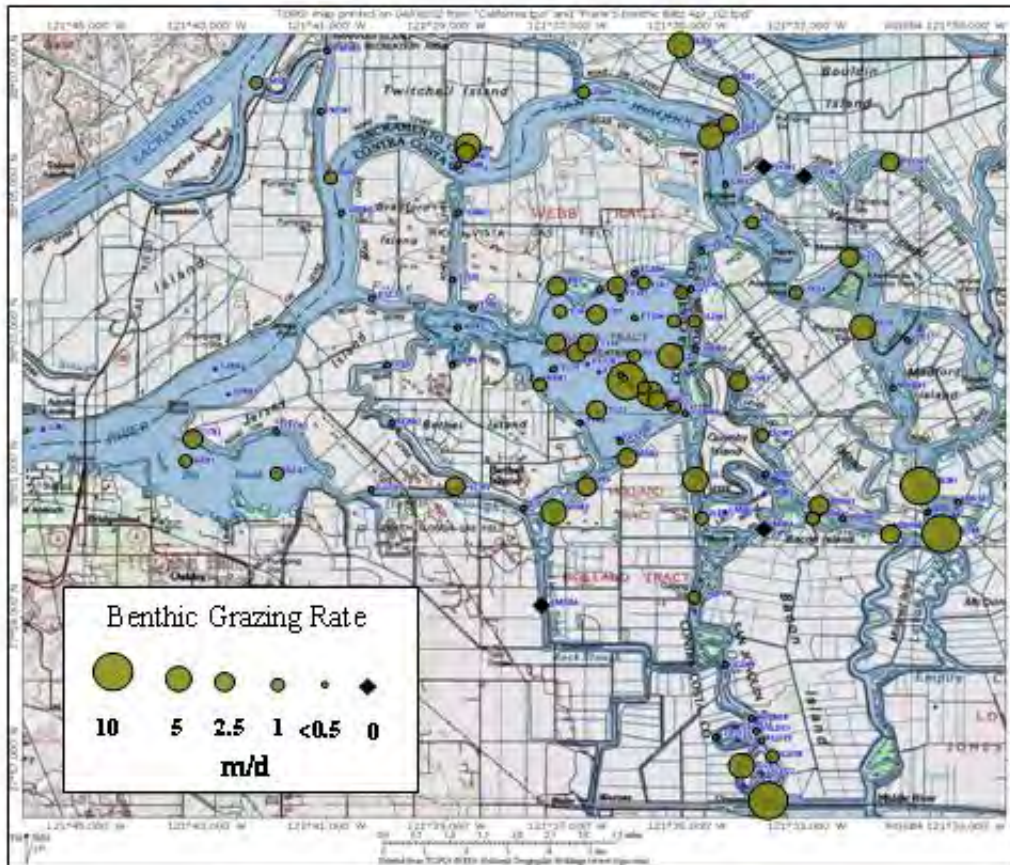


Figure B22. Grazing Rate of *C. fluminea* in Franks Tract in April 2002.

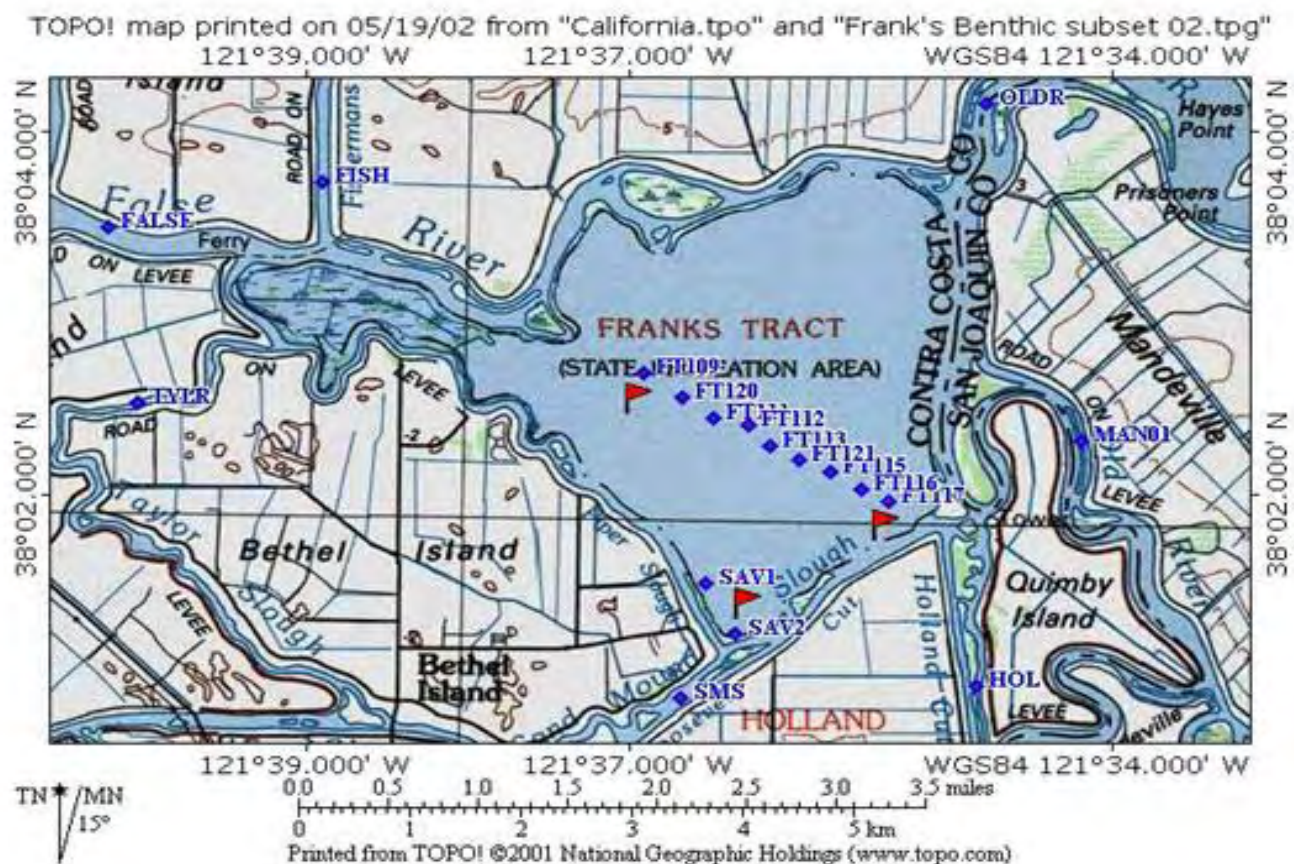


Figure B23. Station locations for seasonal study of *C. fluminea* grazing rate in Franks Tract in 2002.

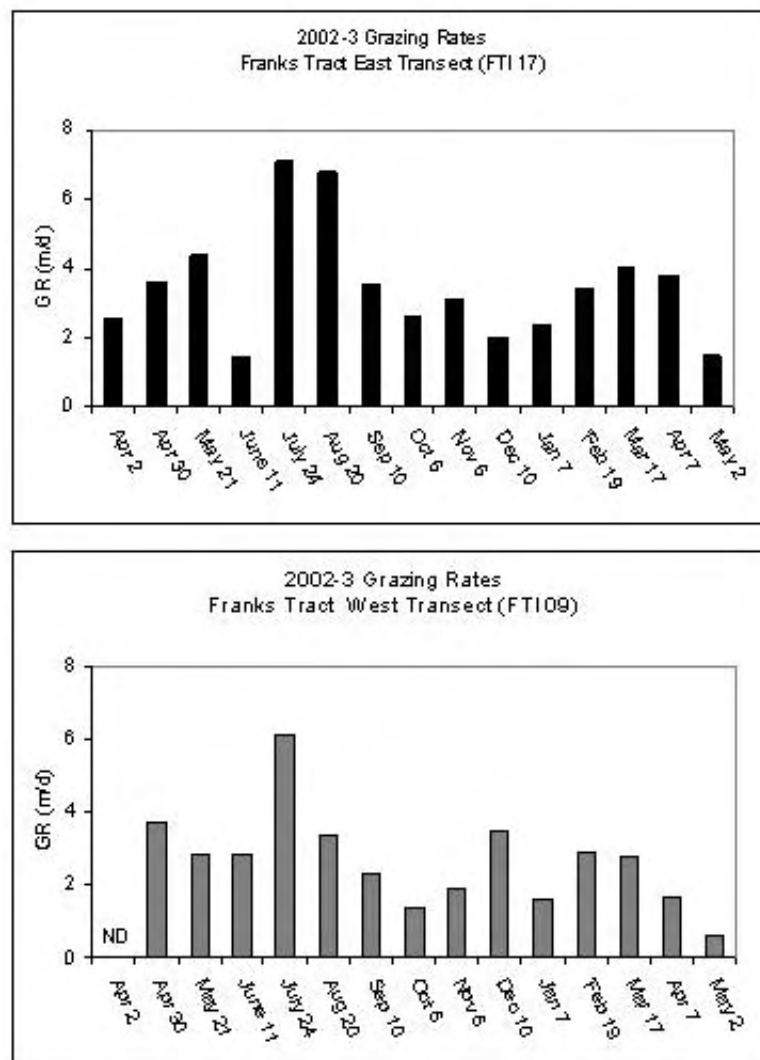


Figure B24. *C. fluminea* grazing rates at two stations sampled for a year within Franks Tract in 2002

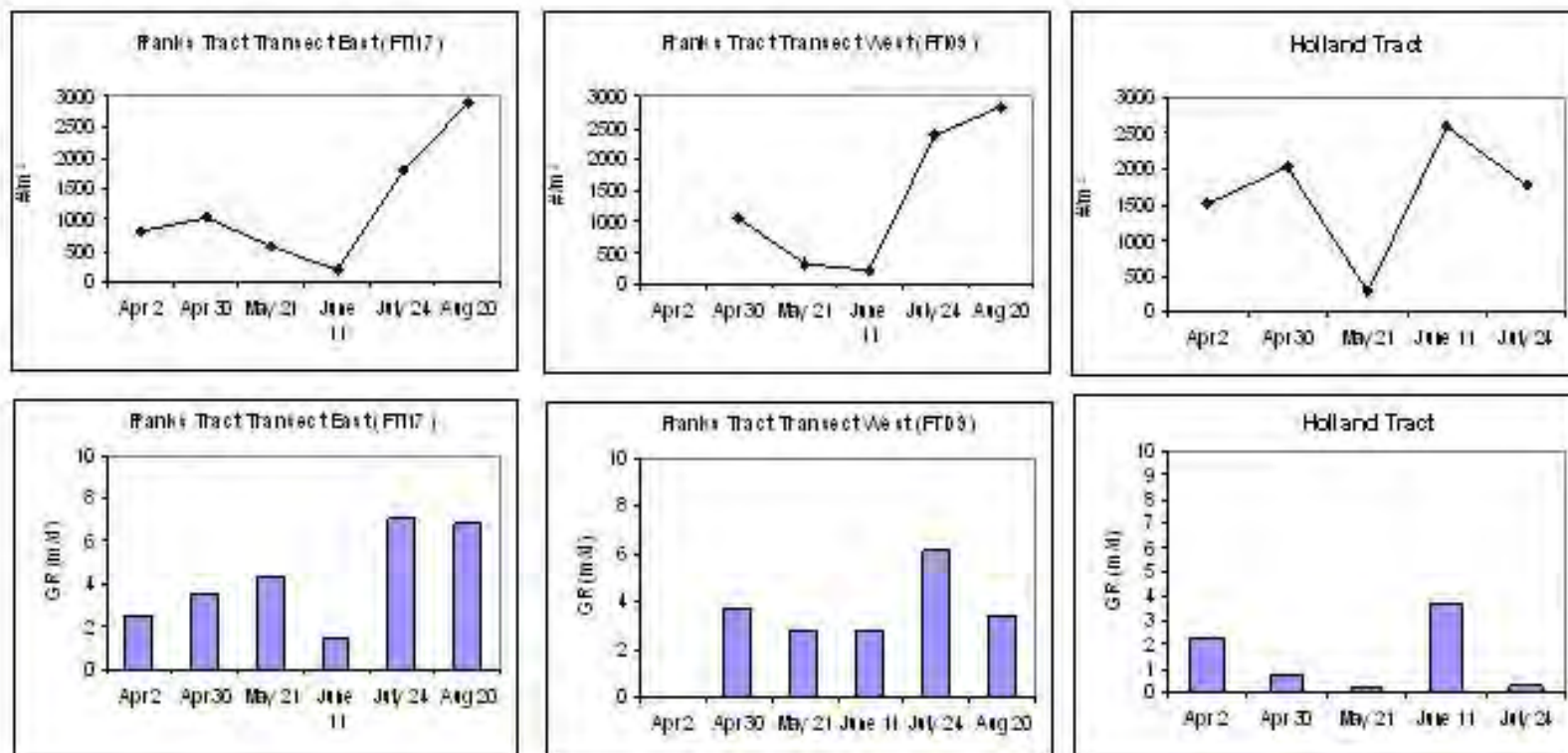


Figure B25. *C. fluminea* abundance and grazing rates at two stations from within Franks Tract and the connecting channel at Holland Tract for April through July 2002.

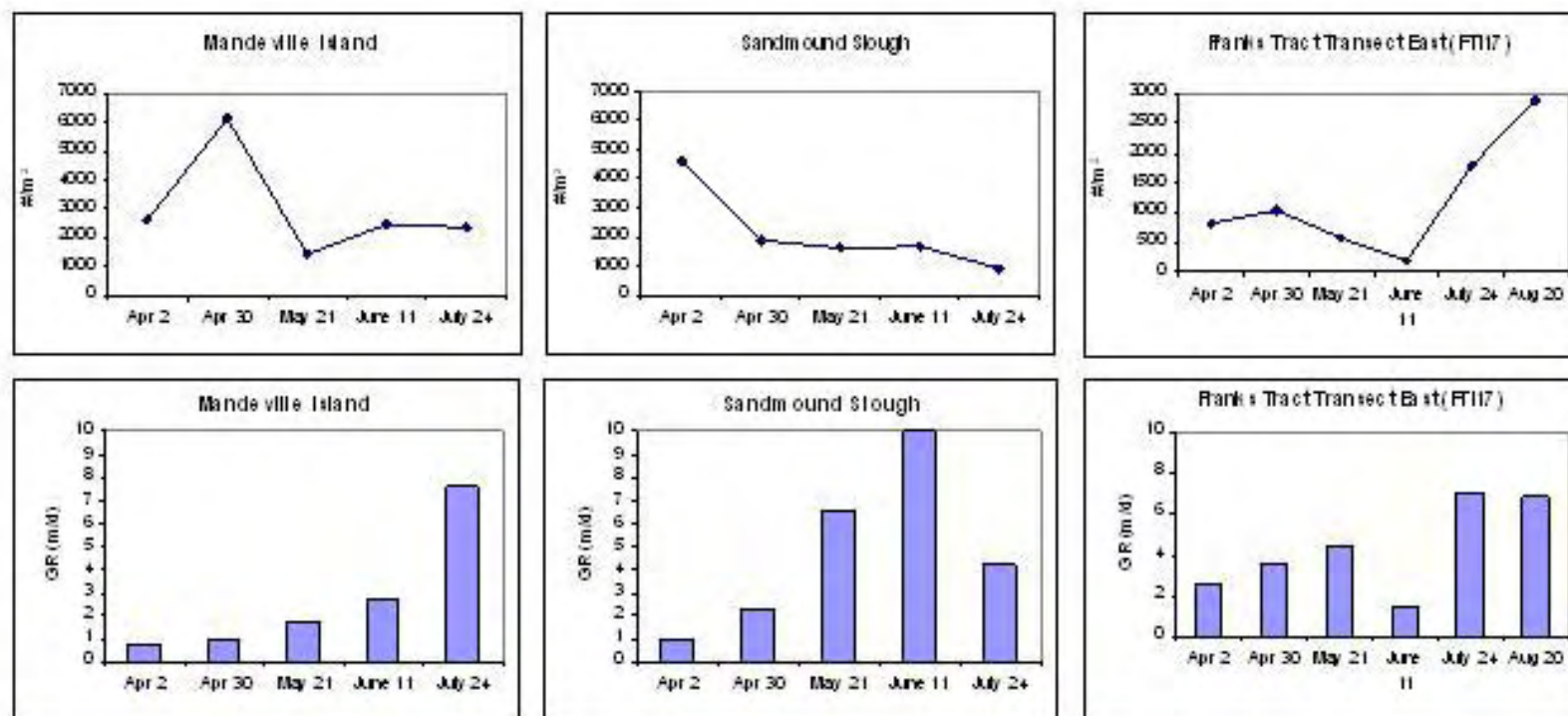


Figure B26. *C. fluminea* abundance and grazing rates at nearest station from within Franks Tract and the connecting channel at Mandeville Island and Sandmound Slough for April through July 2002.

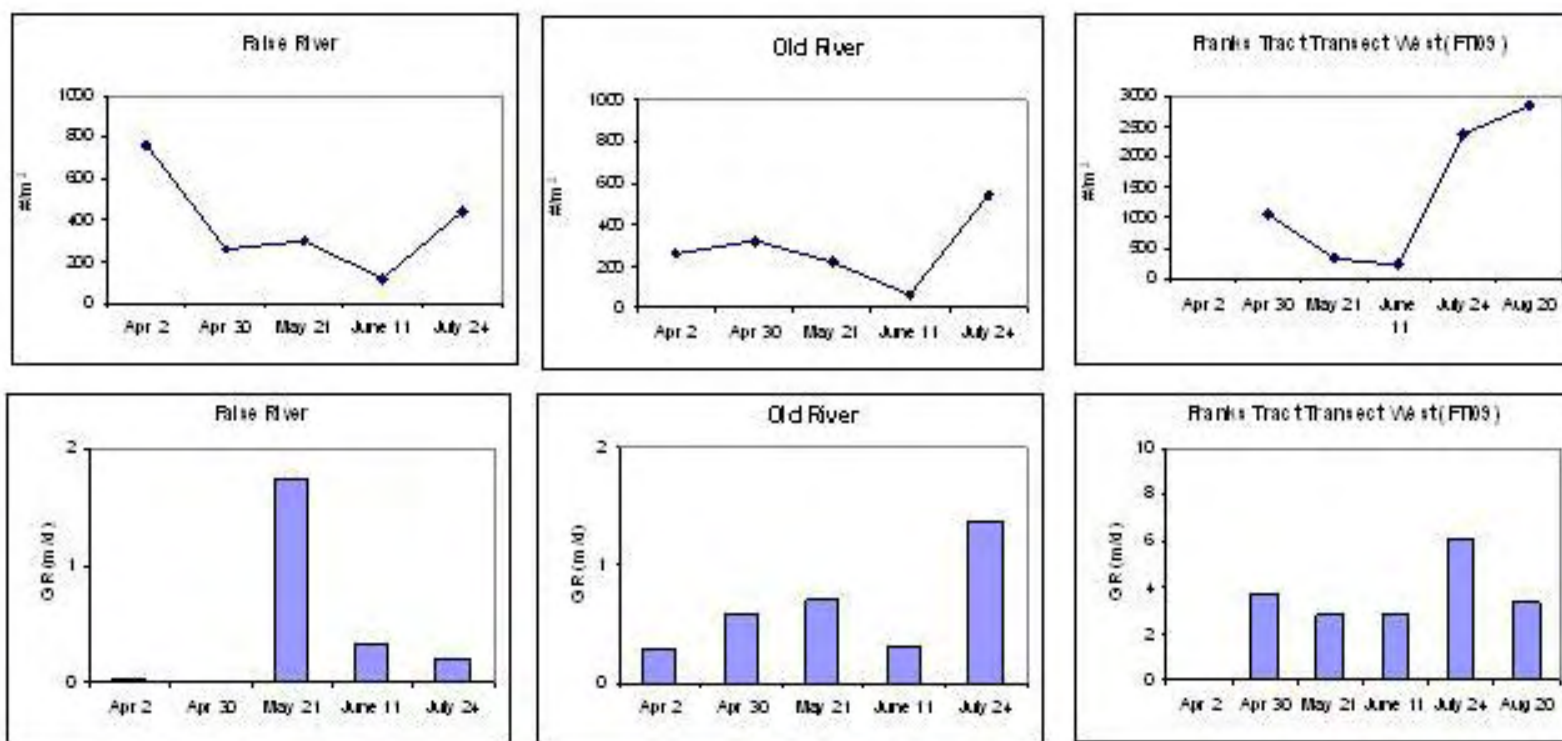


Figure B27. *C. fluminea* abundance and grazing rates at nearest station from within Franks Tract and the connecting channel at Old River and False River for April through July 2002 (note the change in scale).

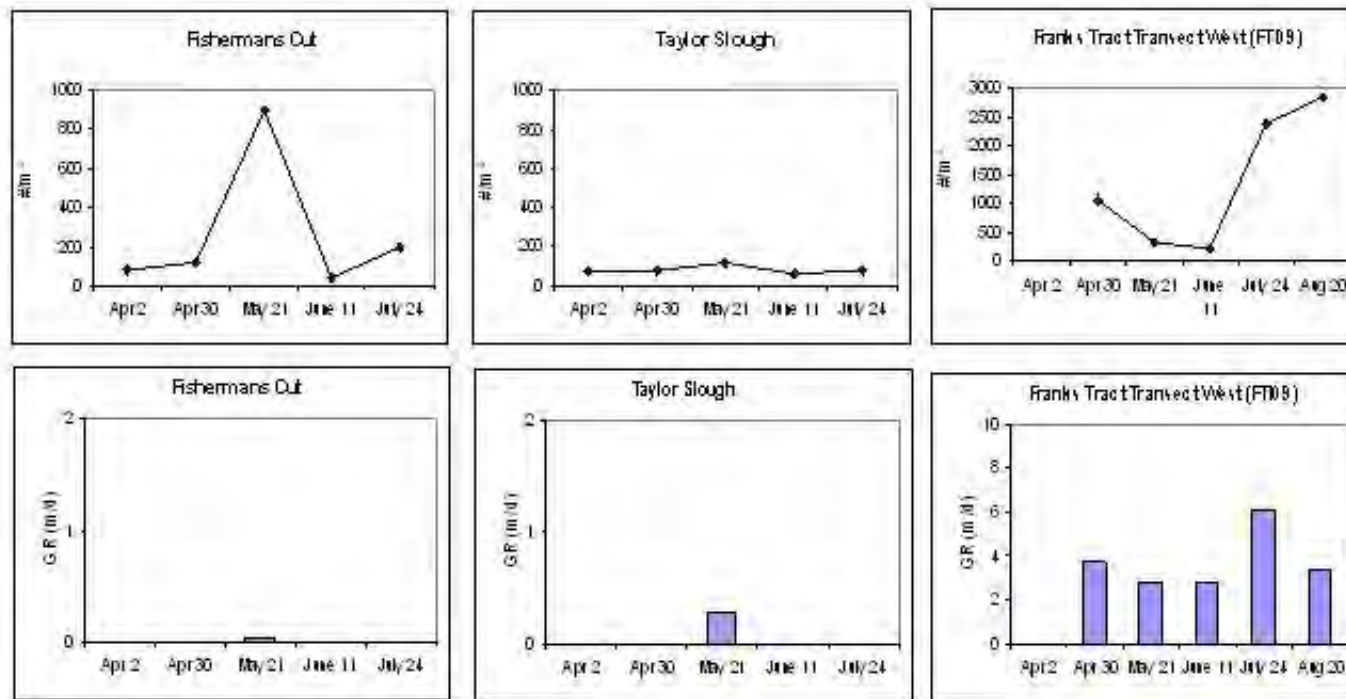


Figure B28. *C. fluminea* abundance and grazing rates at nearest station from within Franks Tract and the connecting channel Fishermans Cut and Taylor Slough for April through July 2002 (note the change in scale).

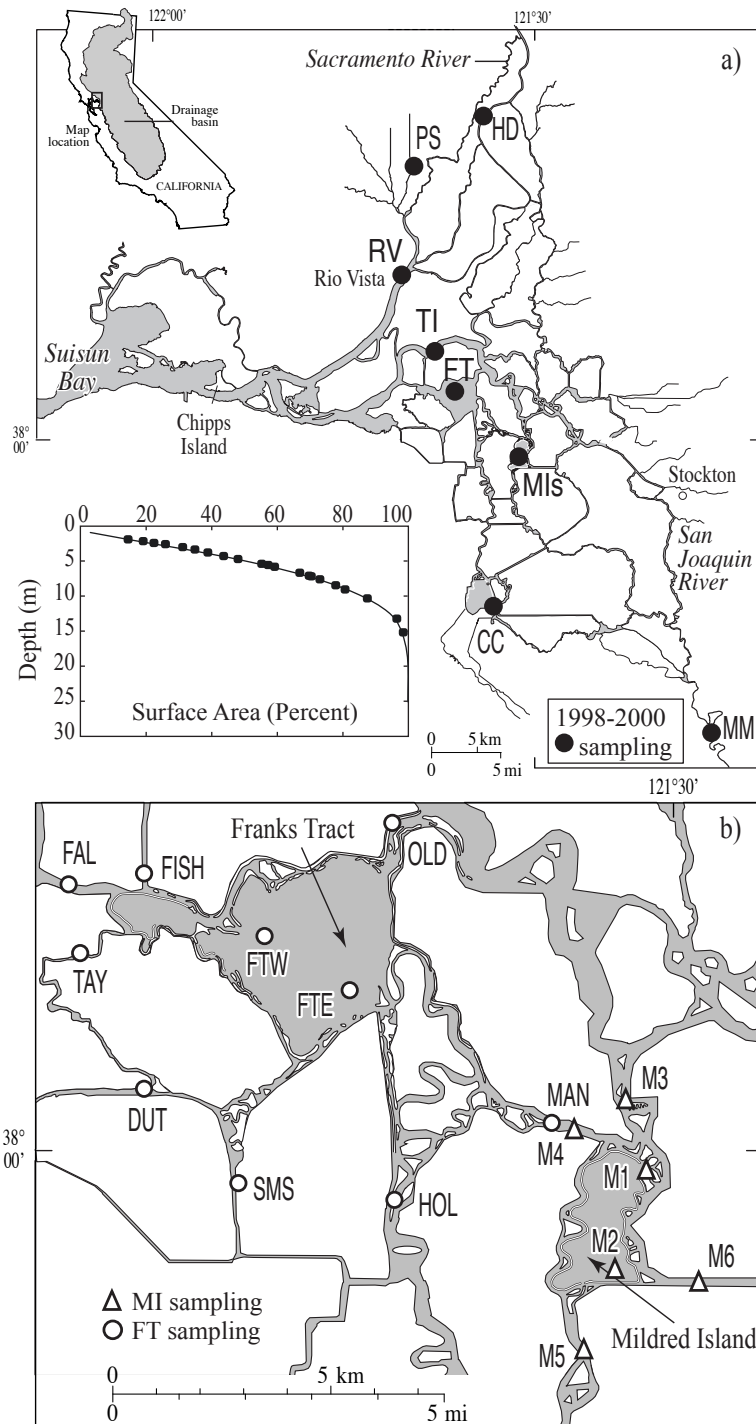


Figure C1. (a) The Sacramento-San Joaquin Delta, California, showing sites sampled by Sobczak and others (2002) during 1998-2000. (Inset): Central Delta tidally averaged habitat depth distribution by surface area. The hypsograph line shows cumulative percent surface area of the central Delta that is shallower than a given depth, and filled circles represent depths of sampling sites in this study. (b) Enlarged view of the study area showing sites sampled in/around Mildred Island (MI) during 2001 (open triangles) and Franks Tract (FT) during 2002 (open circles).

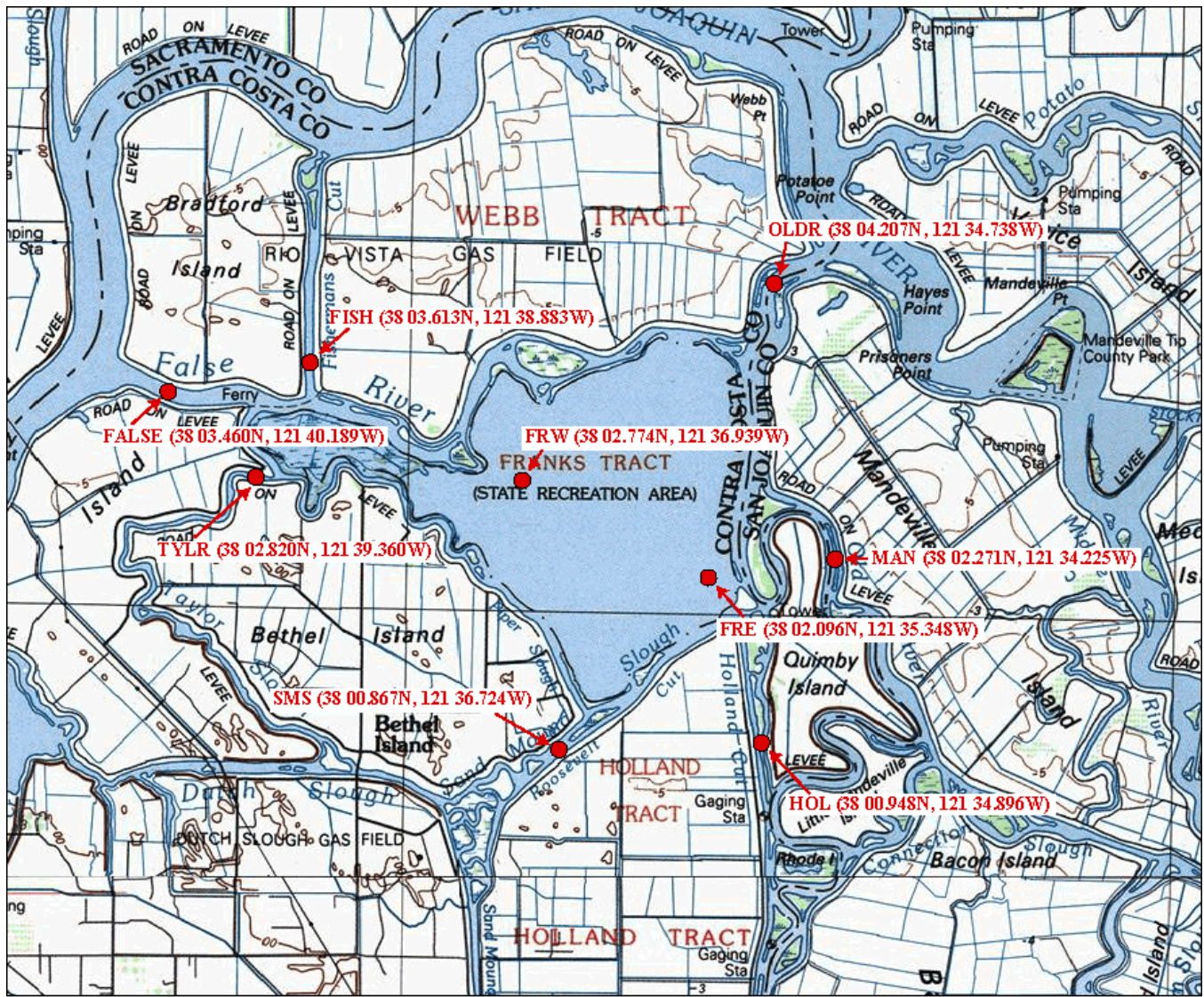


Figure C2. Locations of SCUFA (submerged fluorometers) for Franks Tract Process Study, 2002.

chlorophyll a [ug/l]

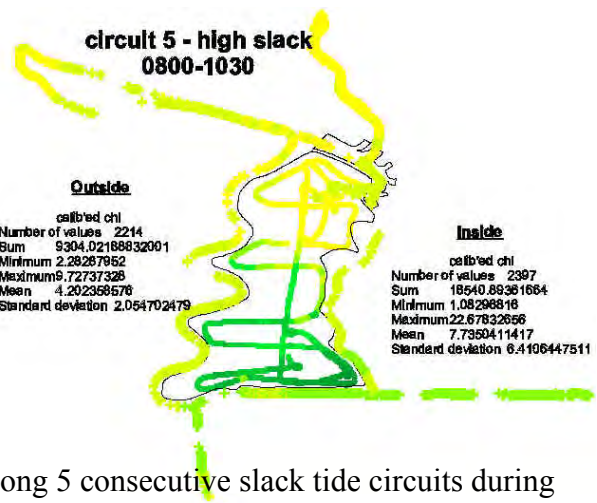
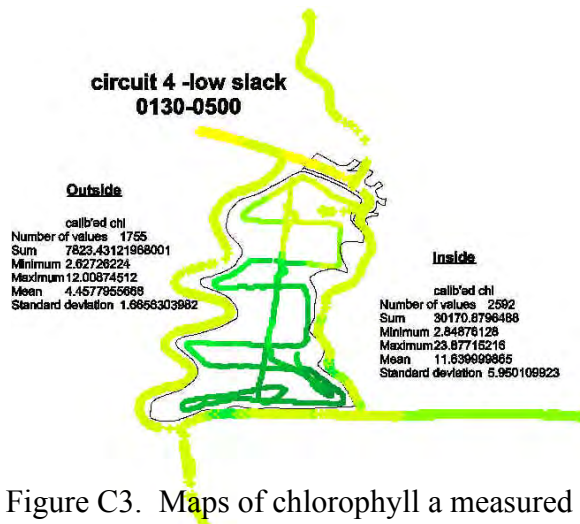
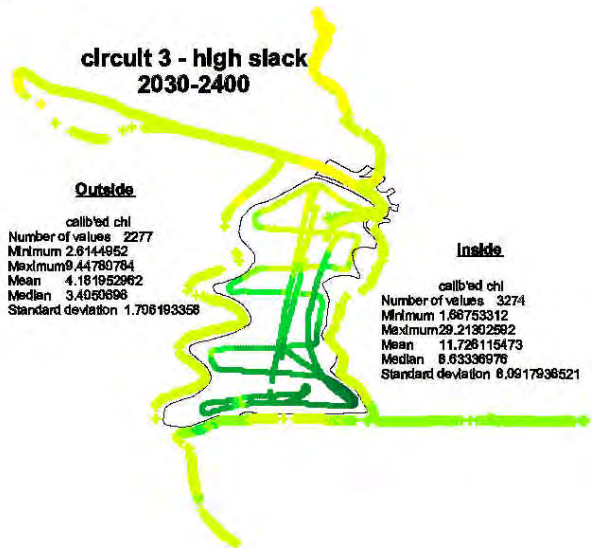
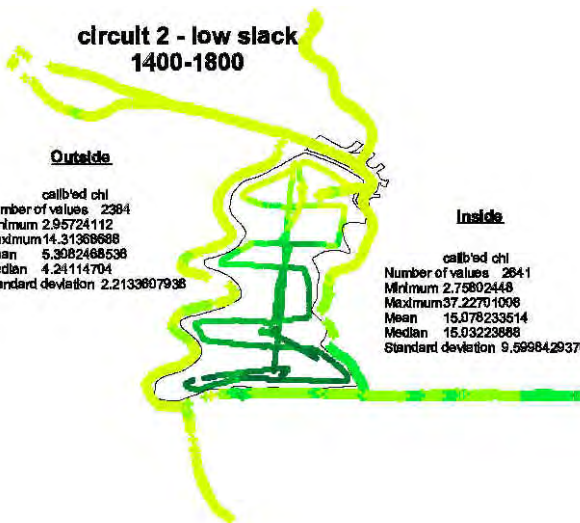


Figure C3. Maps of chlorophyll a measured along 5 consecutive slack tide circuits during Mildred Island Process Study, September 2001.

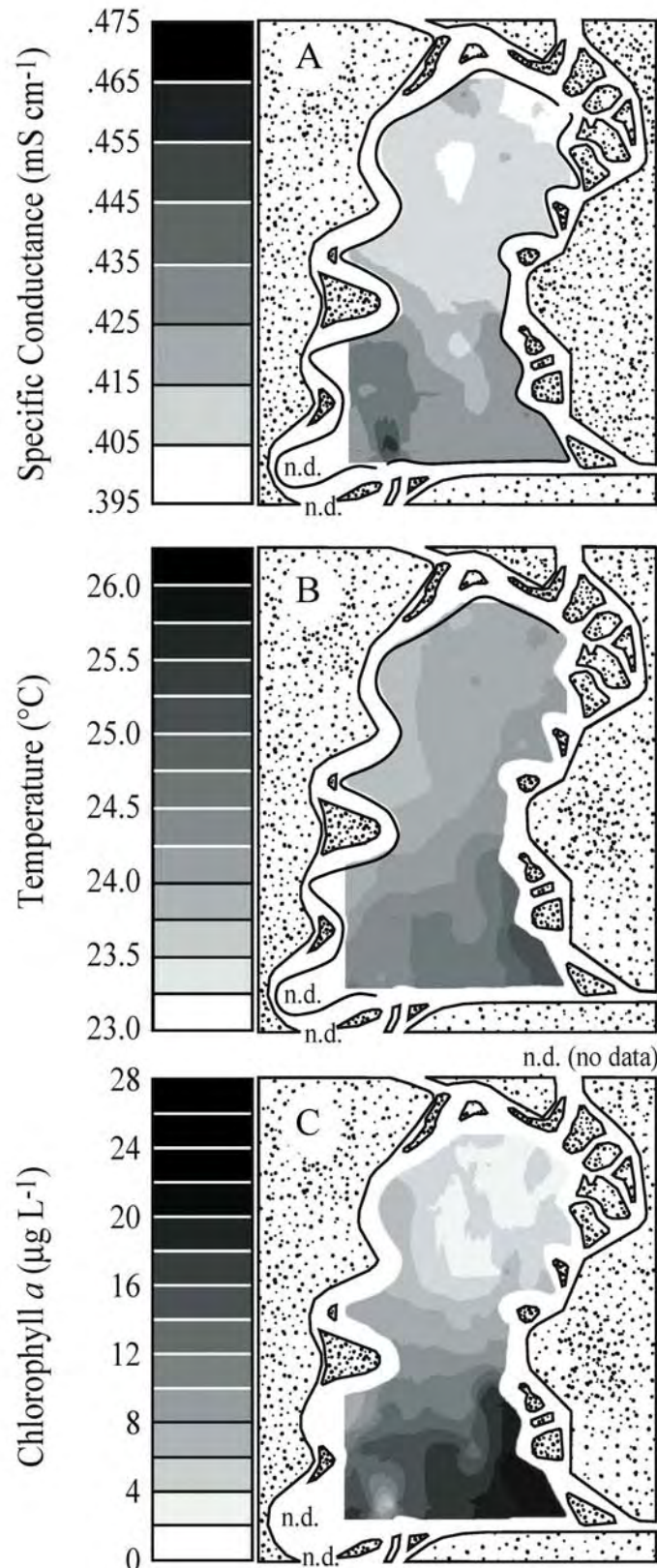


Figure C4. Sample water quality maps interpolated from mapping circuits in Mildred Island during September 2001. The maps shown represent the third of five circuits performed during consecutive slack tides, occurred between 8:45 pm and 10:00 pm PDT on 5 September, and were centered temporally on a slack tide after flood.

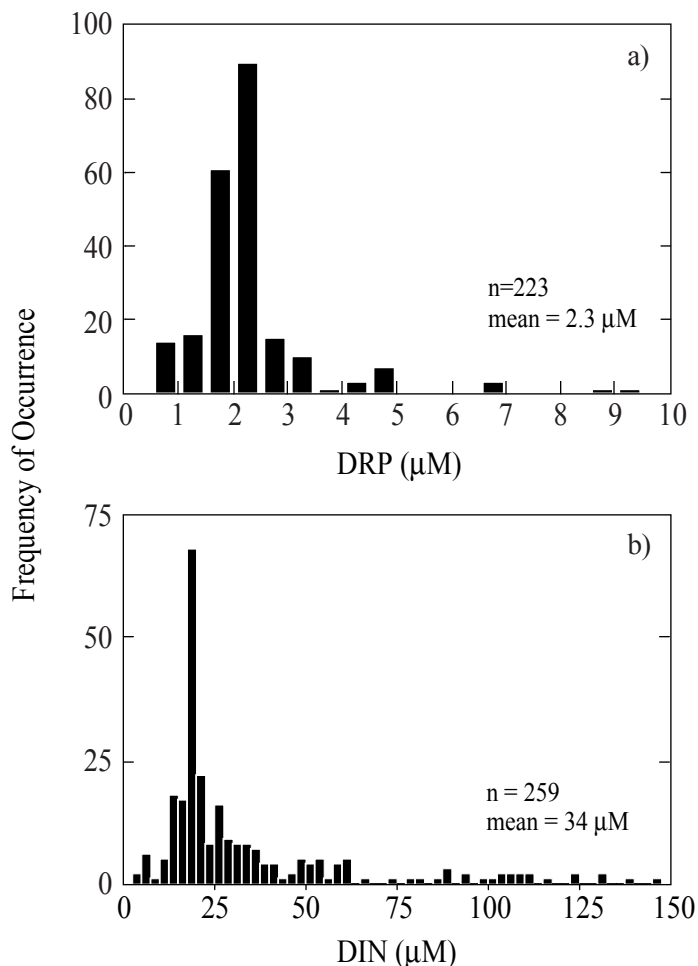


Figure C5. Frequency distributions of (a) dissolved reactive phosphorus (DRP) and (b) dissolved inorganic nitrogen (DIN) concentrations (μM) in the Delta during 1997-1999 and 2001. Samples from 1997-1999 were collected throughout the Delta (including our study area). Samples from 2001 were collected in/around MI during August and September. The number of samples and mean concentrations for the entire sampling period are also displayed for each constituent. requencey distributions of (a) dissolved reactive phosphorus (DRP) and (b) dissolved inorganic nitrogen (DIN) concentrations (μM) in the Delta during 1997-1999 and 2001. Samples from 1997-1999 were collected throughout the Delta (including our study area). Samples from 2001 were collected in/around MI during August and September. The number of samples and mean concentrations for the entire sampling period are also displayed for each constituent.

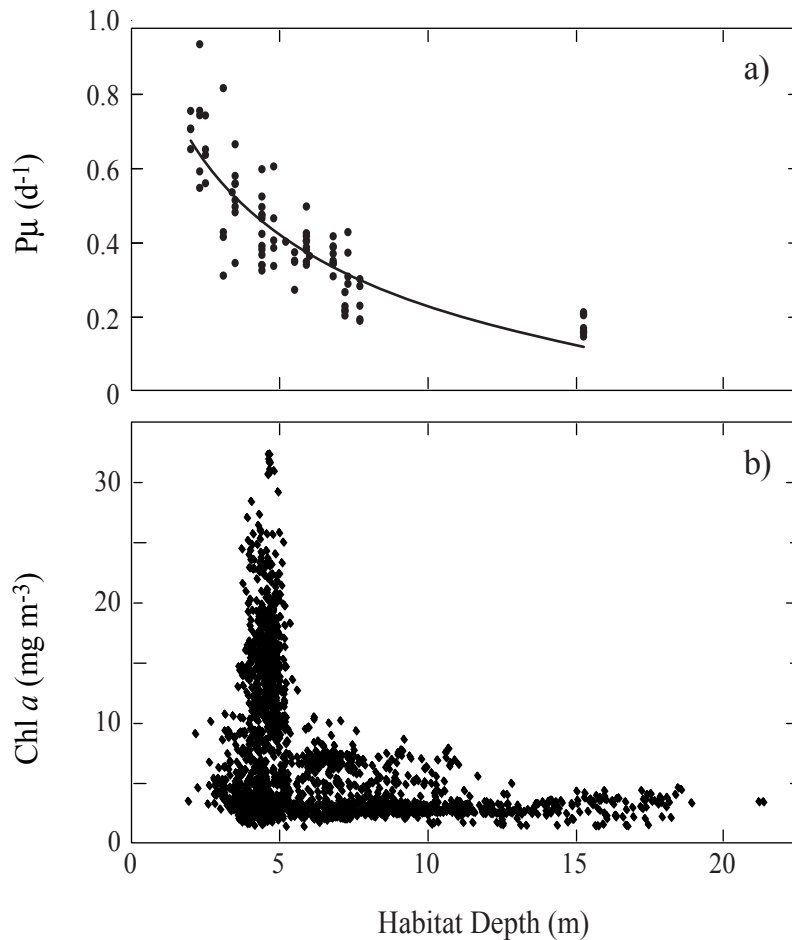


Figure C6. (a) Phytoplankton growth rate $P\mu$ calculated versus mean habitat depth. Growth rate was calculated from measured temperature, irradiance, and light attenuation in MI during 2001 and in FT during 2002. The logarithmic function was fit by least squares regression: $P\mu = 0.86 - 0.27\ln[H]$ ($R^2=0.72$). (b) Chl a concentrations collected during synoptic mapping plotted against habitat depth. Mapping was performed on 5 consecutive slack tides within and around MI during 5,6 September 2001.

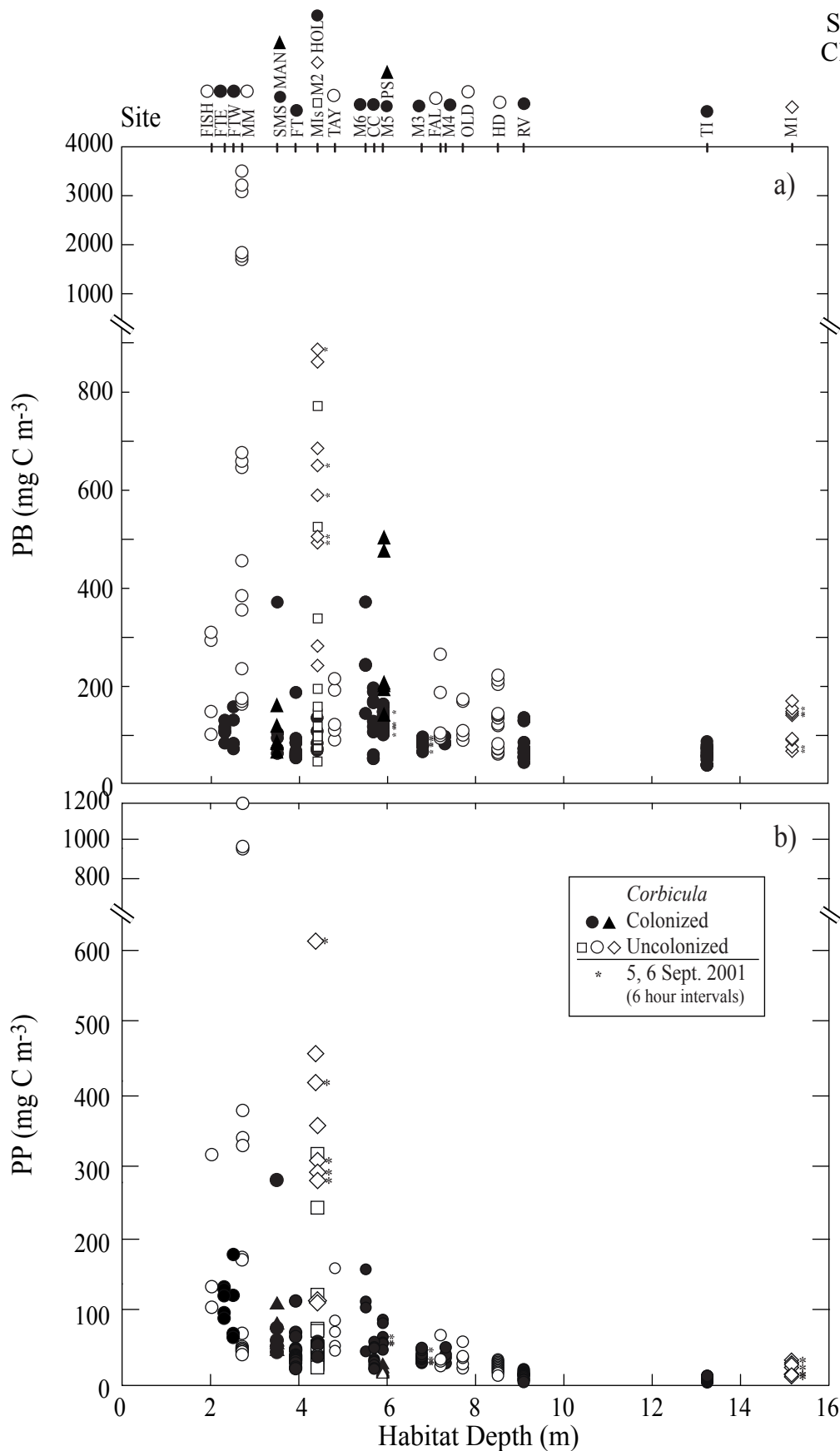


Figure C7. (a) Phytoplankton biomass, PB, and (b) net primary production, PP, versus mean habitat depth. Samples were collected during 1998-2000 (Sobczak and others 2002), 2001 (MI) and 2002 (FT). Open symbols indicate stations where *Corbicula* was rare or absent ("Uncolonized"). Filled symbols indicate stations where *Corbicula* was abundant ("Colonized"). Asterisks (*) next to symbols indicate samples taken every 6 hours over 30 hours during 5,6 September 2001. Stations and corresponding symbols are detailed on the top x-axis at appropriate depths; stations with common depths are distinguished by different symbols.

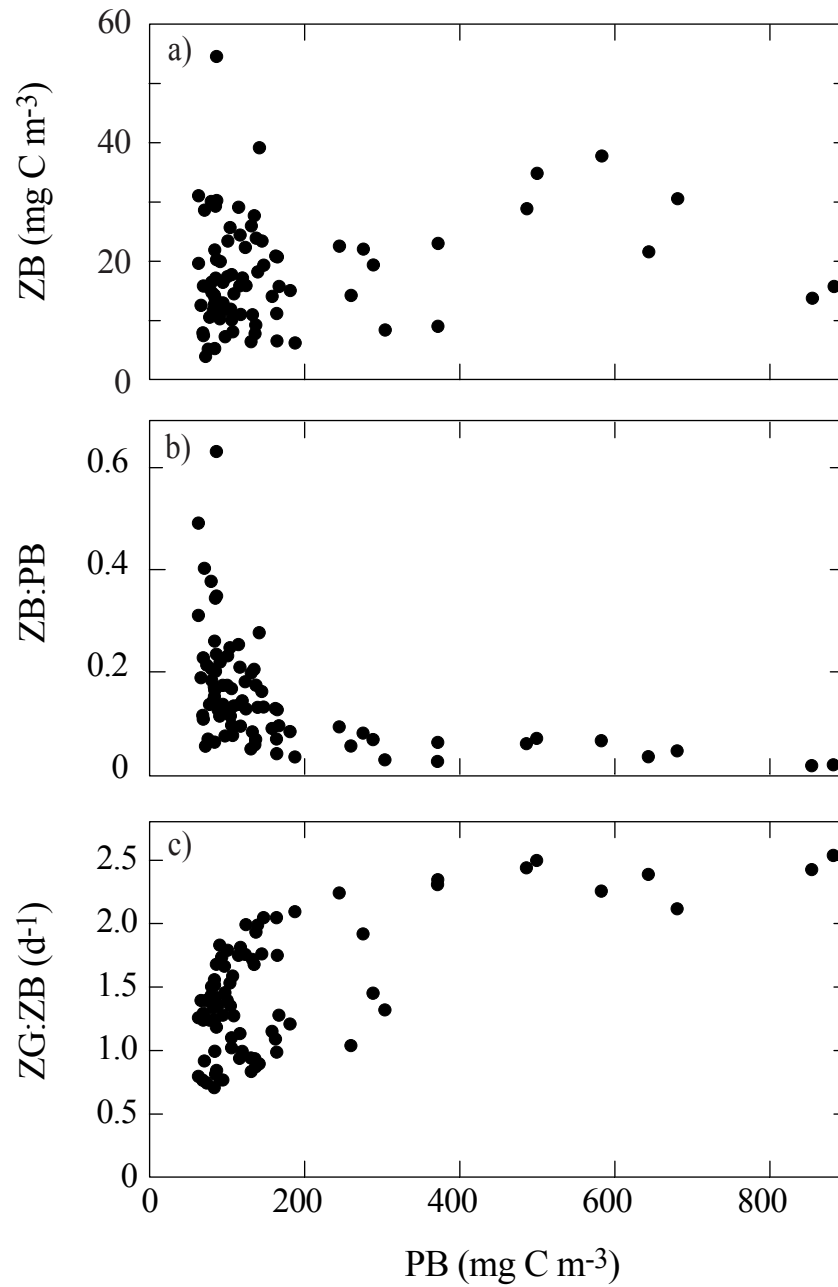


Figure C8. (a) Zooplankton biomass, ZB, (b) the zooplankton daily food ration, ZG:ZB, and (c) potential grazing pressure, ZB:PB, against phytoplankton biomass, PB, from samples collected in/around MI during 2001 and FT during 2002.

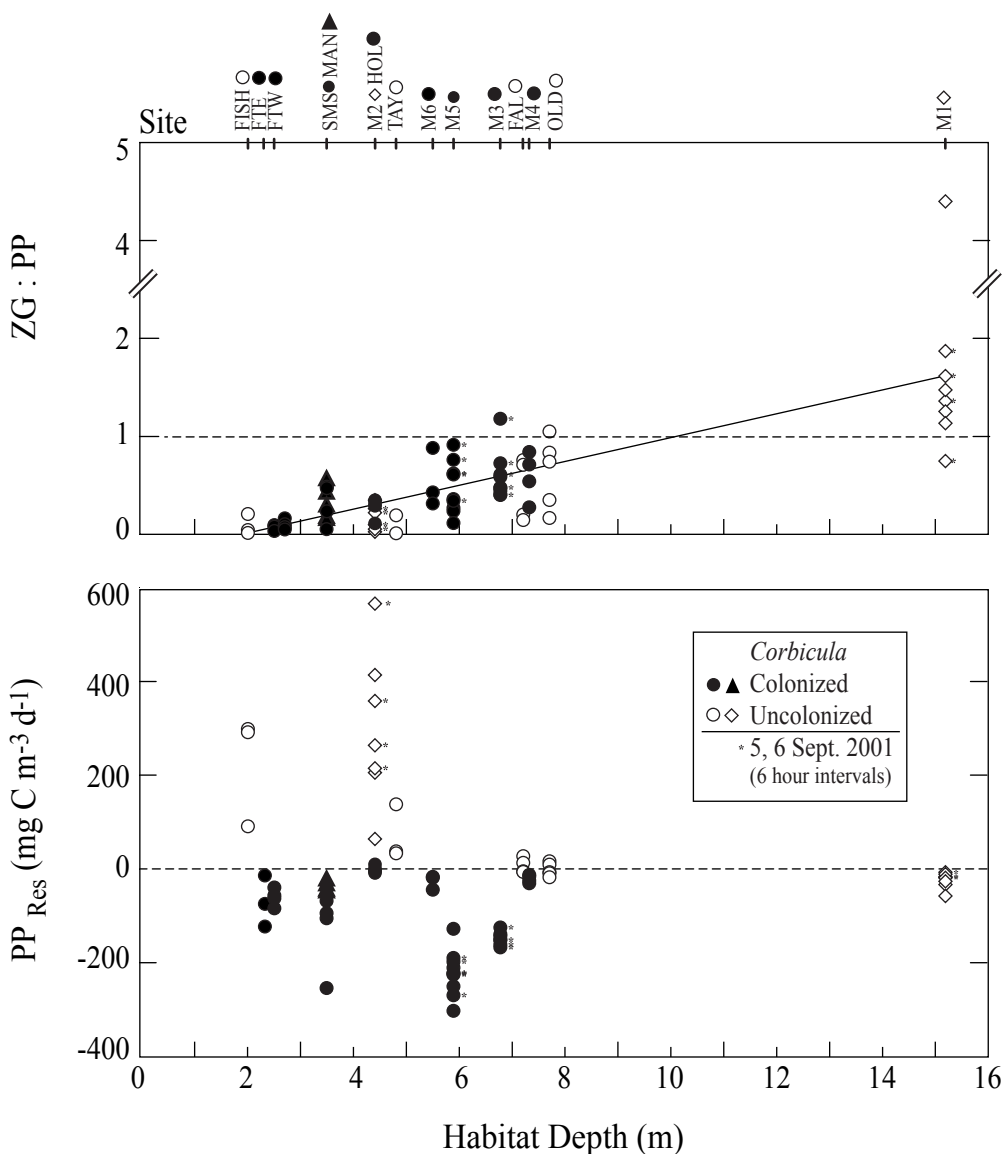


Figure C9. (a) The ratio of zooplankton grazing to primary production and (b) residual primary production, PP_{Res} , versus mean habitat depth from samples collected in/around MI in 2001 and FT in 2002. Open symbols indicate stations where the invasive clam, *Corbicula*, was rare or absent ("Uncolonized"). Filled symbols indicate stations where *Corbicula* was abundant ("Colonized"). Asterisks (*) next to symbols indicate samples taken every 6 hours over 30 hours during 5,6Sept 2001. Station and corresponding symbols are detailed on the top x-axis. (a) The horizontal dashed line divides surplus and deficit habitats based on zooplankton consumption alone. The trendline represents the linear fit of ZG:PP ($y = -0.22 + 0.13x$, $R^2=0.57$) with depth (without station M1, the trend is still significant with a similar slope and intercept). (b) For PP_{Res} , the horizontal dashed line separates potential donor ($PP_{Res} > 0$) and consumer ($PP_{Res} < 0$) habitats when consumption by both zooplankton and *Corbicula* is taken into account.

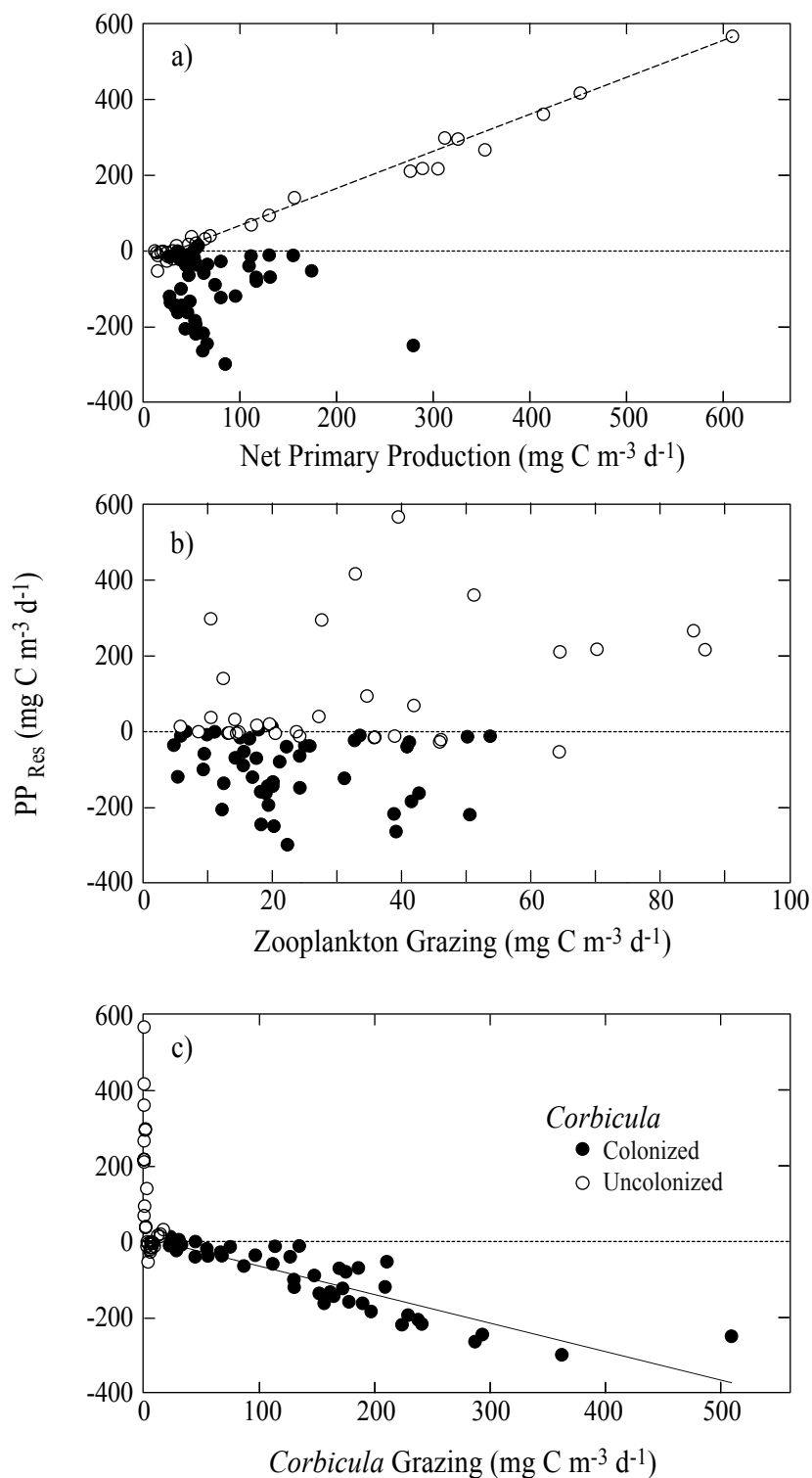


Figure C10. Residual phytoplankton production (PPRes) versus (a) net primary production (PP), (b) zooplankton grazing (ZG) and (c) Corbicula grazing (CG) from samples collected during 2001 (MI) and 2002 (FT). Open circles indicate sites where Corbicula was rare or absent ("Uncolonized"). Filled circles indicate sites where Corbicula was abundant ("Colonized"). Trend lines represent significant correlations of (a) PPRes at uncolonized sites with PP ($R^2=0.99$, $p<0.001$) and (b) PPRes at colonized sites with CG (inverse correlation, $R^2=0.77$, $p<0.001$). residual phytoplankton production (PPRes) versus (a) net primary production (PP), (b) zooplankton grazing (ZG) and (c) Corbicula grazing (CG) from samples collected during 2001 (MI) and 2002 (FT). Open circles indicate sites where Corbicula was rare or absent ("Uncolonized"). Filled circles indicate sites where Corbicula was abundant ("Colonized"). Trend lines represent significant correlations of (a) PPRes at uncolonized sites with PP ($R^2=0.99$, $p<0.001$) and (b) PPRes at colonized sites with CG (inverse correlation, $R^2=0.77$, $p<0.001$).

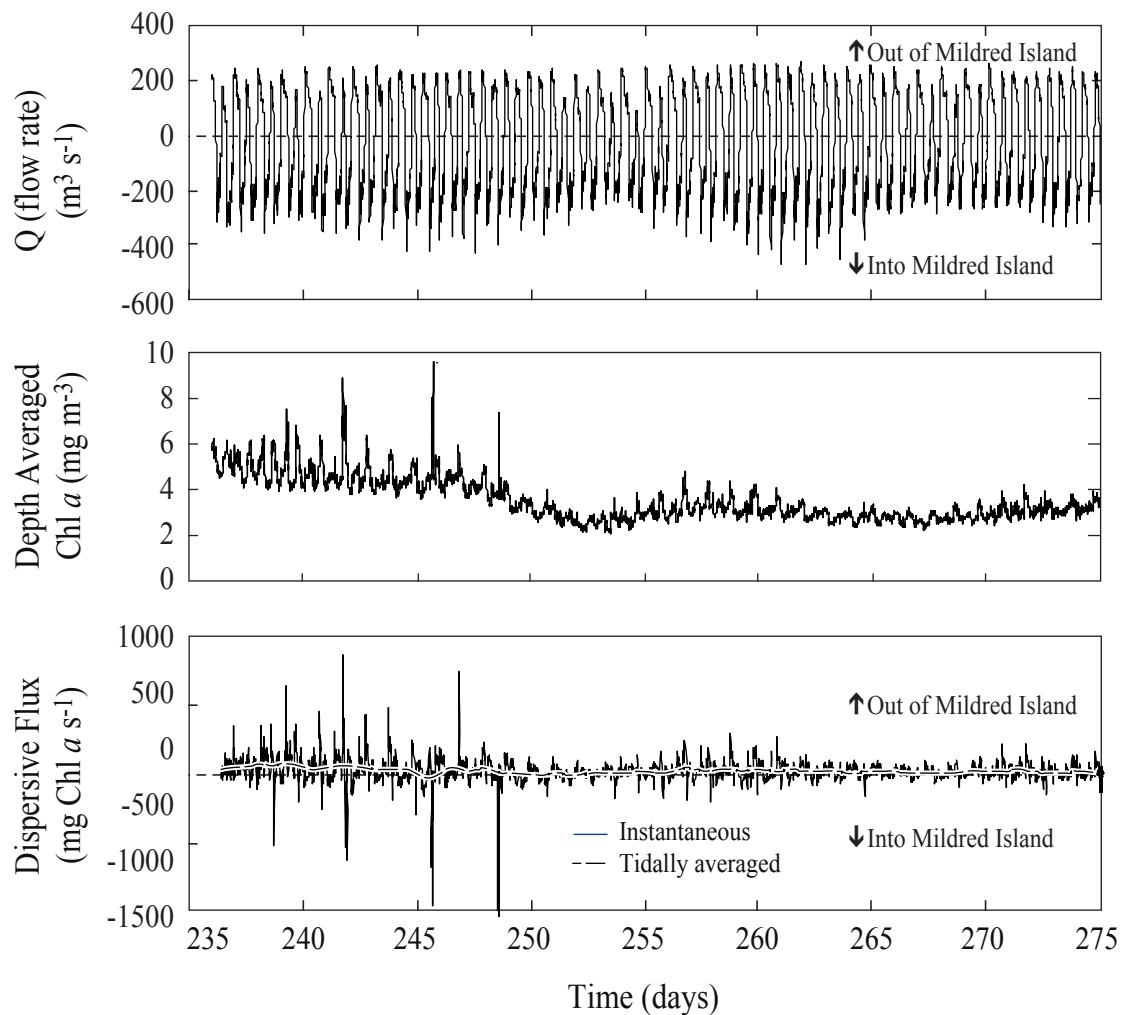


Figure C11. Time series at the northern opening of MI of (a) flow rate, Q , (b) depth-averaged Chl a , and (c) instantaneous and tidally averaged (smoothed line) dispersive flux of Chl a through the northern opening. Data were collected at 10-minute intervals from 23 August to 01 October 2001. Positive values for flow rate and dispersive flux indicate flow or flux out of MI through the northern opening; negative values indicate flow or flux into MI through the northern opening. Tidally averaged dispersive flux (c, smoothed line) was generally positive (or out of MI).

Corbicula Grazing : Zooplankton Grazing
(Mildred Island Stations: 8/23/01-9/20/01, Franks Tract Stations: 4/10/02-7/9/02)

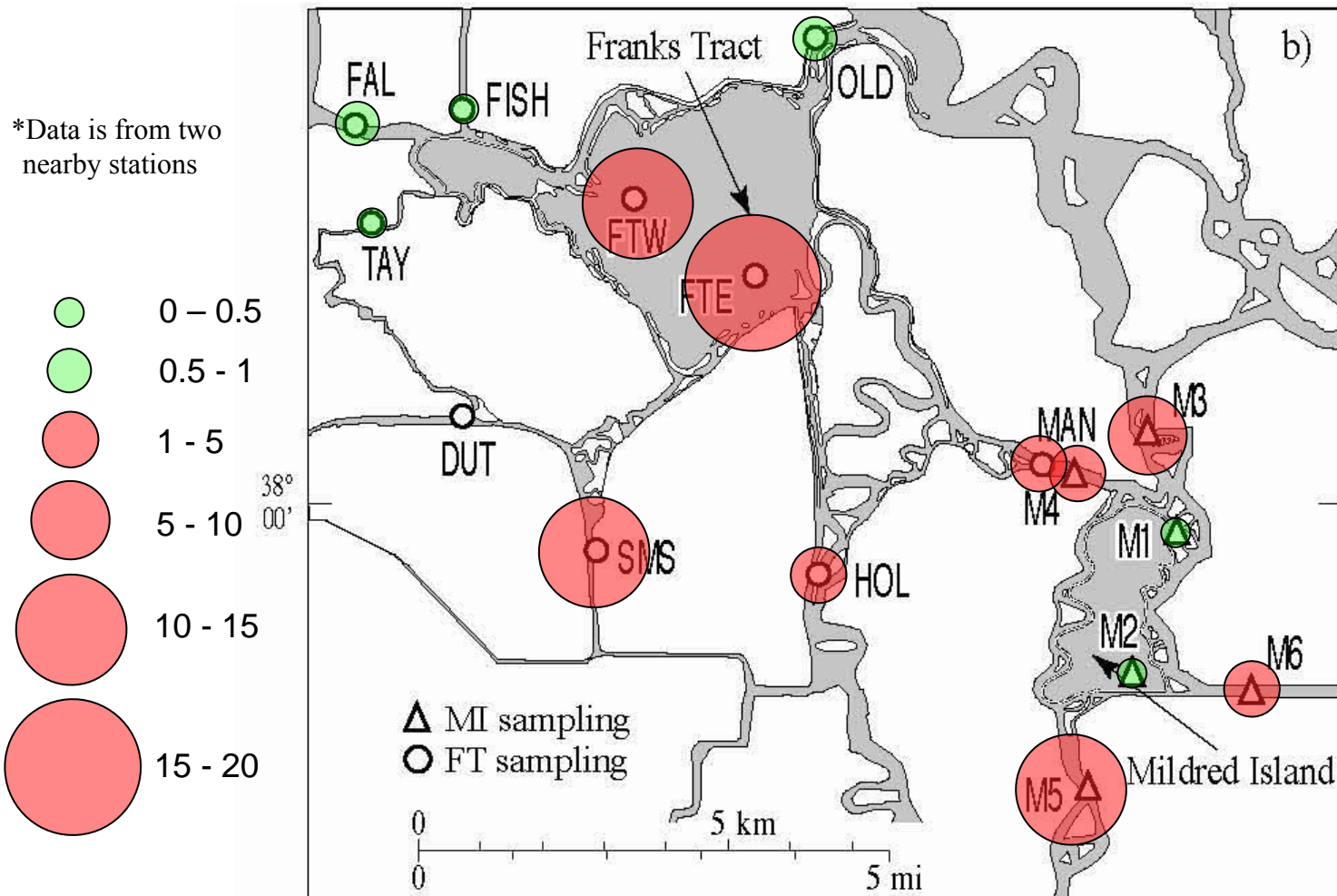


Figure C12. The ratio of grazing/particulate selenium ingestion by *Corbicula* versus zooplankton in the Mildred Island and Franks Tract regions.

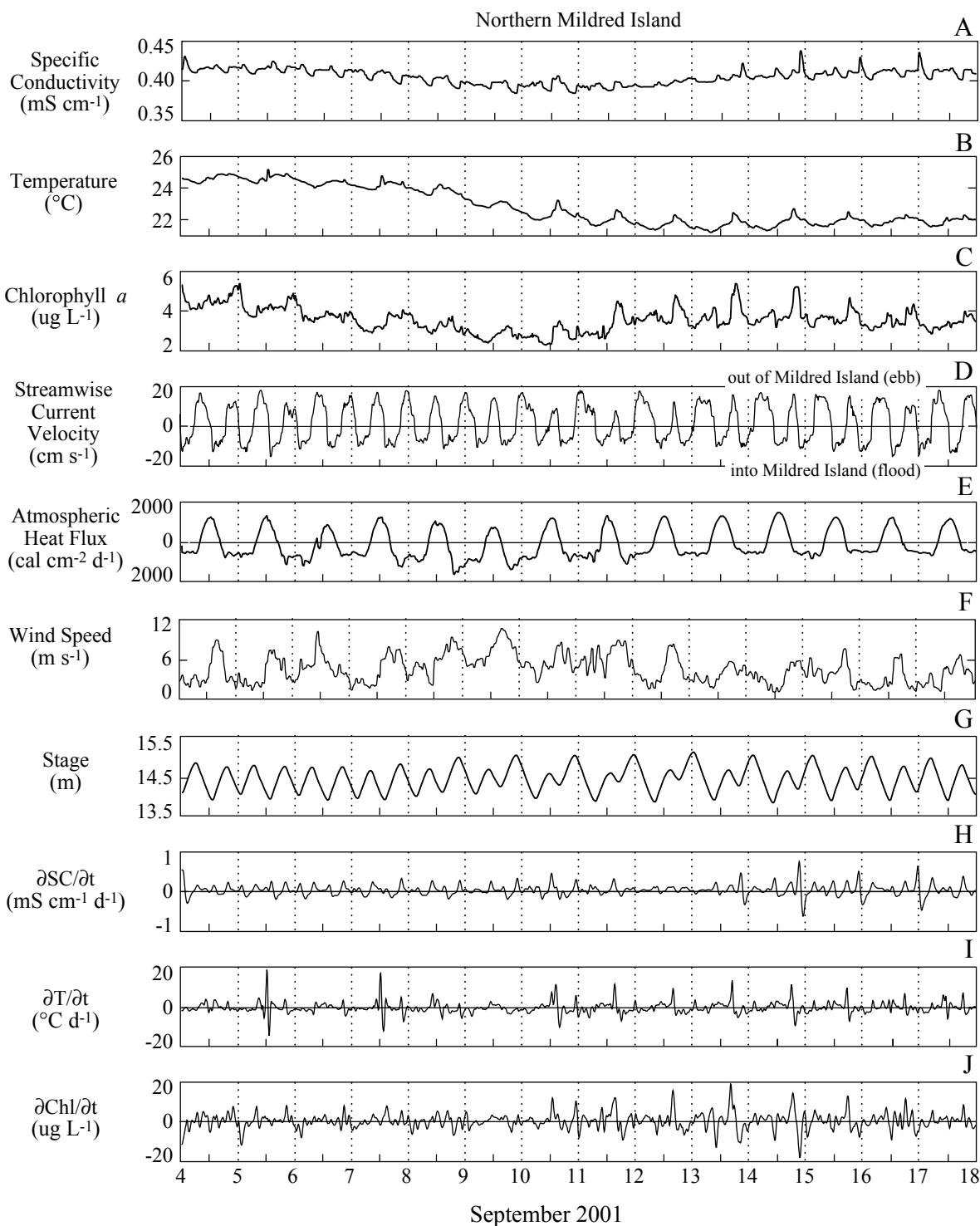


Figure C13. Time series data collected or calculated for northern Mildred Island: specific conductivity (A), water temperature (B), chlorophyll a (C), streamwise current velocity (D), calculated atmospheric heat flux (E), wind speed (F), stage (G), and first time derivatives of specific conductivity (H), water temperature (I), and chlorophyll a (J). Data shown in A-D, F-G were 1-hour median filtered for easier visual identification of dominant frequencies.

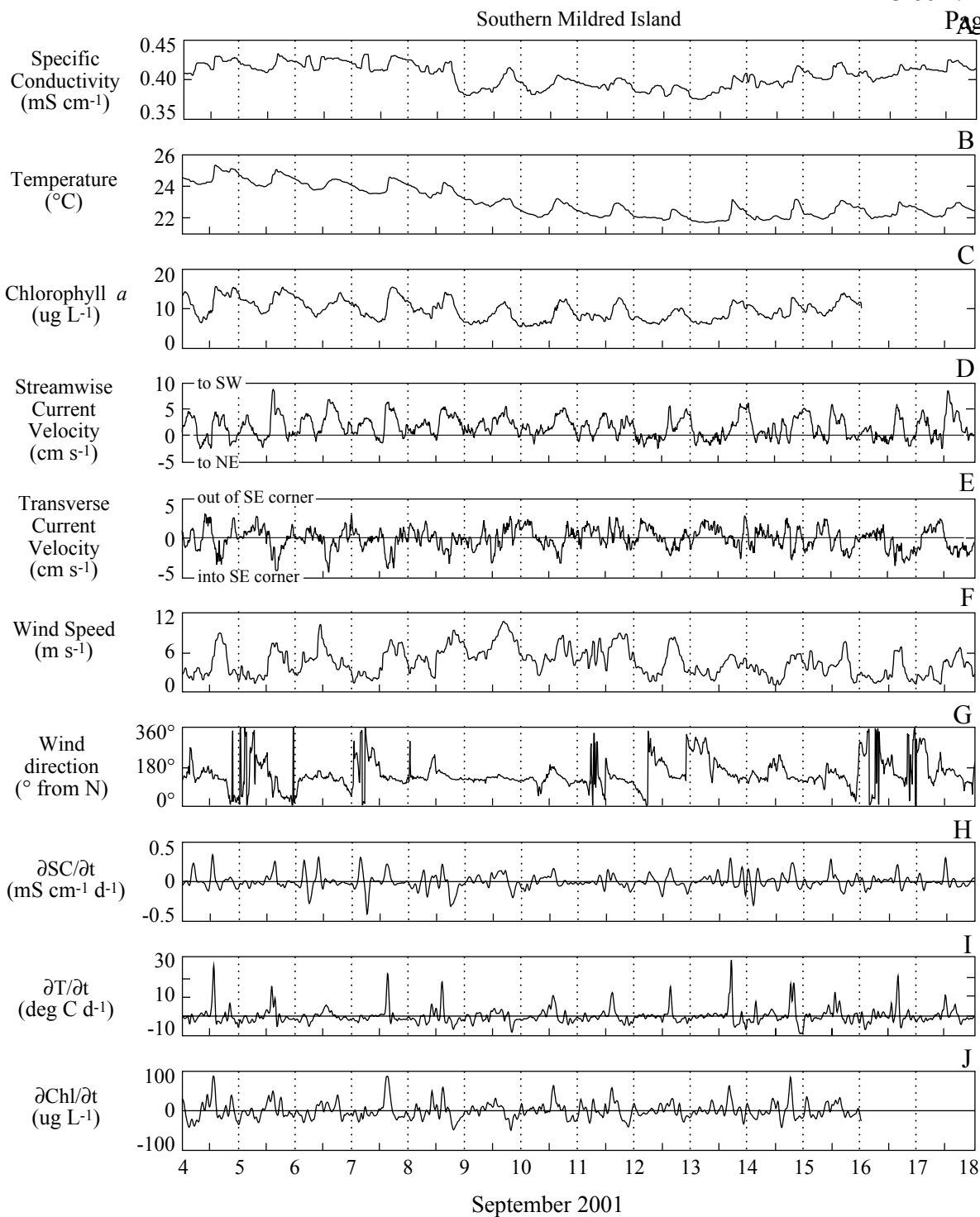


Figure C14. Time series data collected or calculated for southern Mildred Island: specific conductivity (A), water temperature (B), chlorophyll a (C), streamwise current velocity (D), transverse current velocity (E), wind speed (F), wind direction (G), and first time derivatives of specific conductivity (H), water temperature (I), and chlorophyll a (J). Data shown in A-F were 1-hour median filtered for easier visual identification of dominant frequencies.

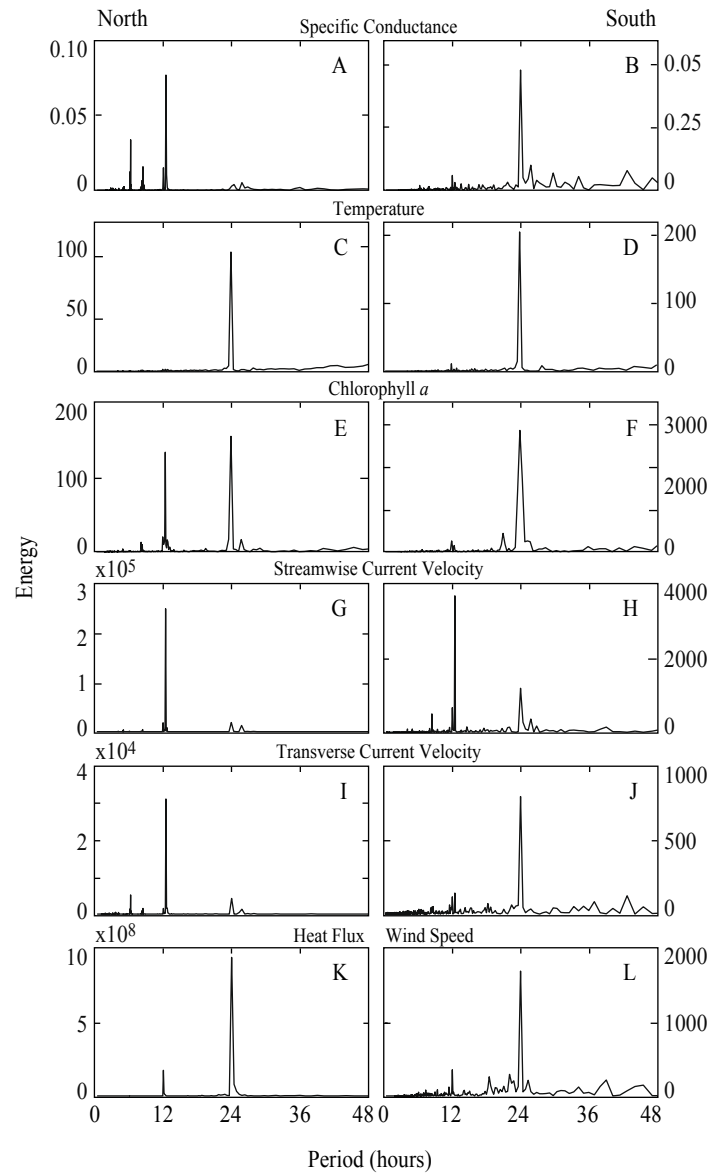


Figure C15. Power spectra at north/south stations for specific conductance (A/B), water temperature (C/D), chlorophyll *a* (E/F), streamwise current velocity (G/H), and transverse current velocity (I/J). Heat flux (K) was calculated for the northern site. Wind speed (L) was measured in southern Mildred Island.

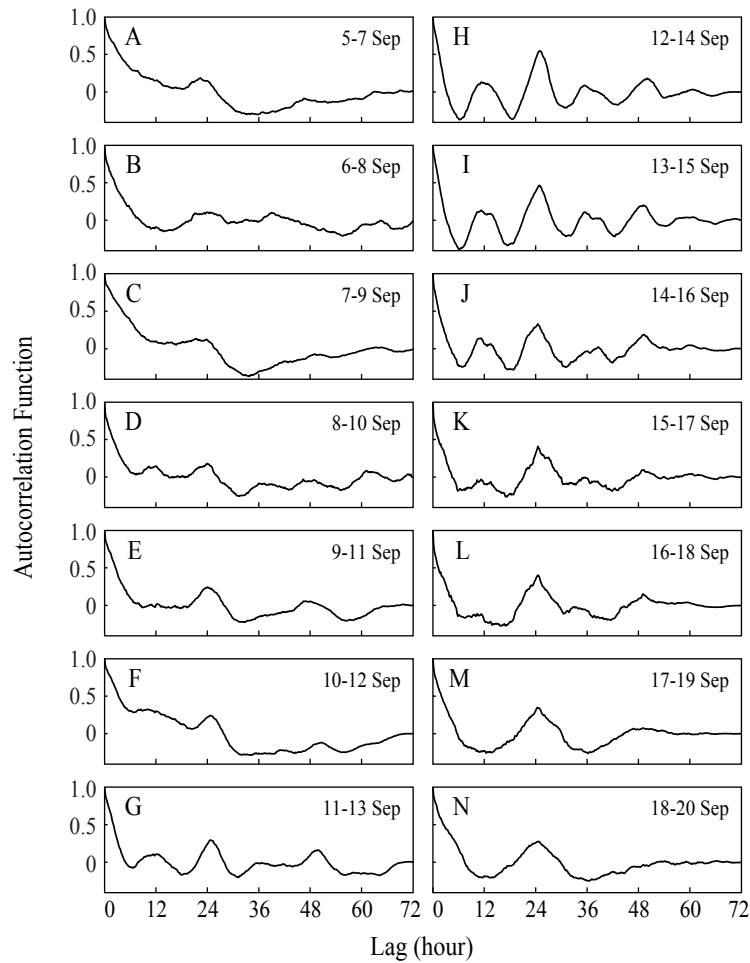


Figure C16. Sliding 3-day autocorrelations calculated for chlorophyll a in the upper water column at the north station. Successive panels demonstrate the evolution in periodicity for this quantity at this location.

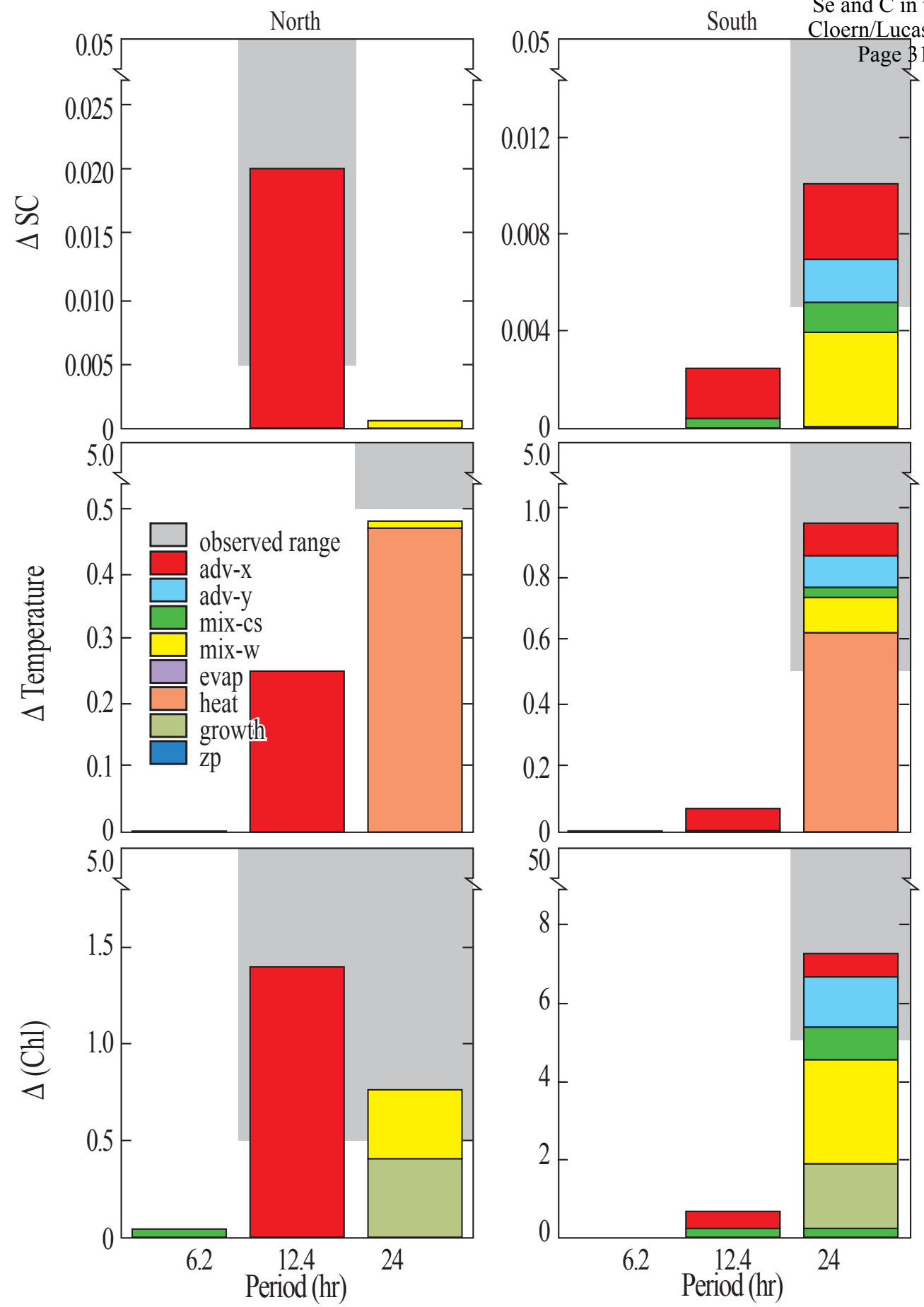


Figure C17. Stacked histograms representing the individual and collective oscillation magnitudes caused by various processes in northern and southern Mildred Island, 2001. Gray shaded regions represent the observed order-of-magnitude range and period of scalar oscillations.

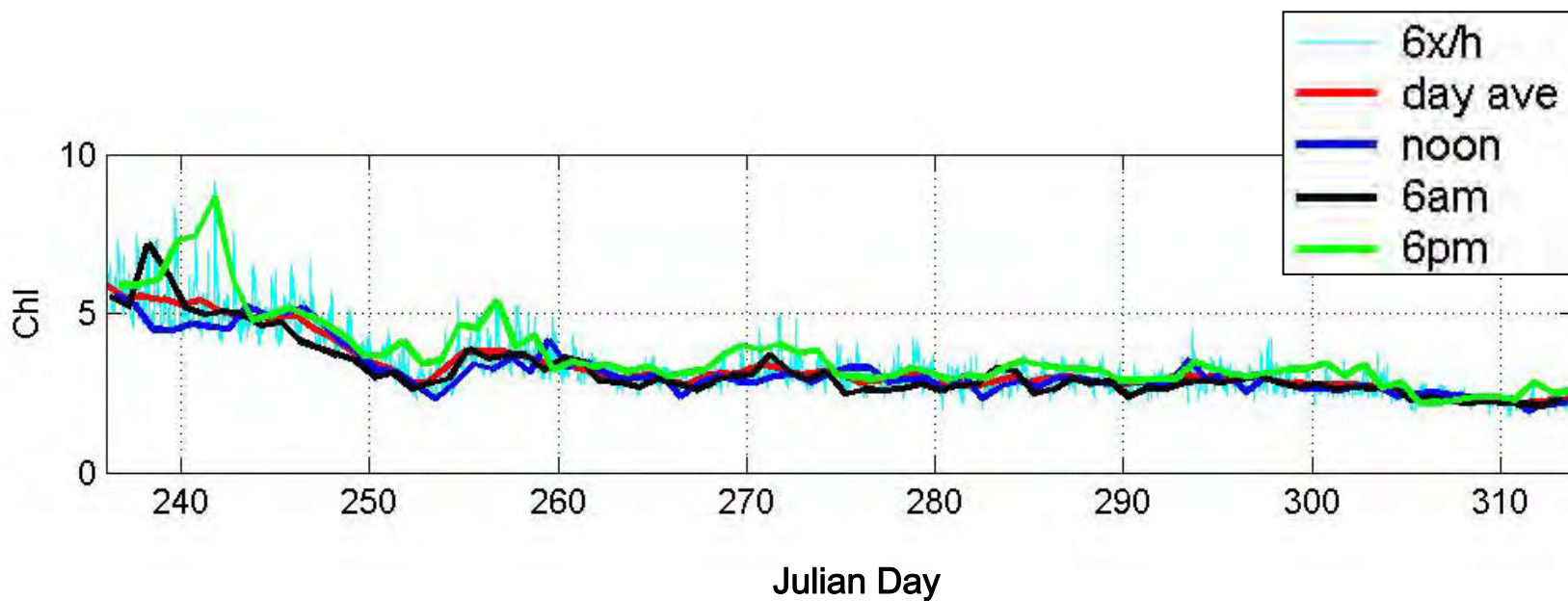


Figure C18. Measured high frequency chl *a* [$\mu\text{g/L}$] time series from northern Mildred Island, 2001 (aqua line) presented with the day-average (red line) and three sub-samplings of the high frequency series. Sub-sampled time series were obtained using a 24 hour sampling period at three different times of day (noon = dark blue, 6 a.m. = black, 6 p.m. = green).

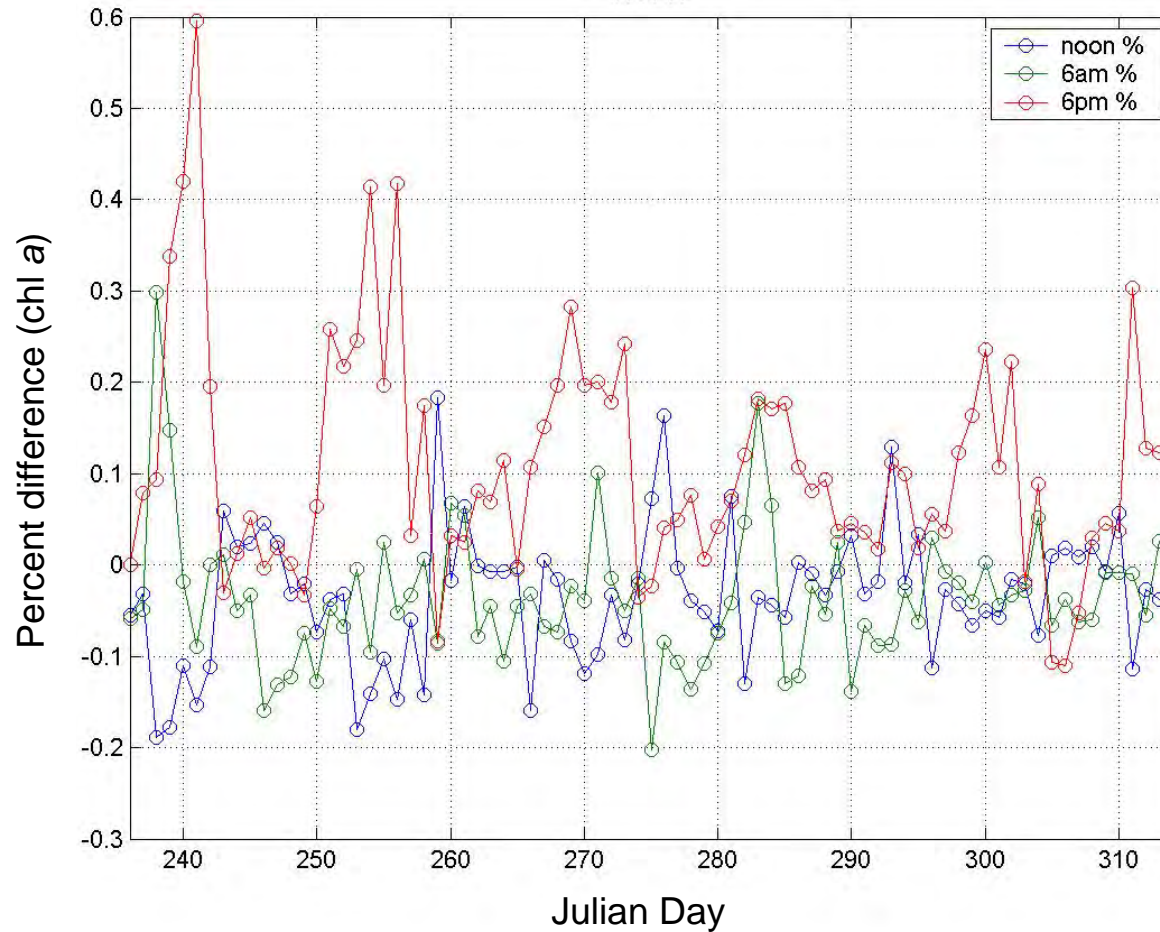


Figure C19. Percent difference between instantaneous sub-sampled chl *a* and day averaged chl *a* at northern Mildred Island. Different curves are for three different daily sub sampling schemes: sampling at noon (blue), sampling at 6 a.m. (green), and sampling at 6 p.m. (red).

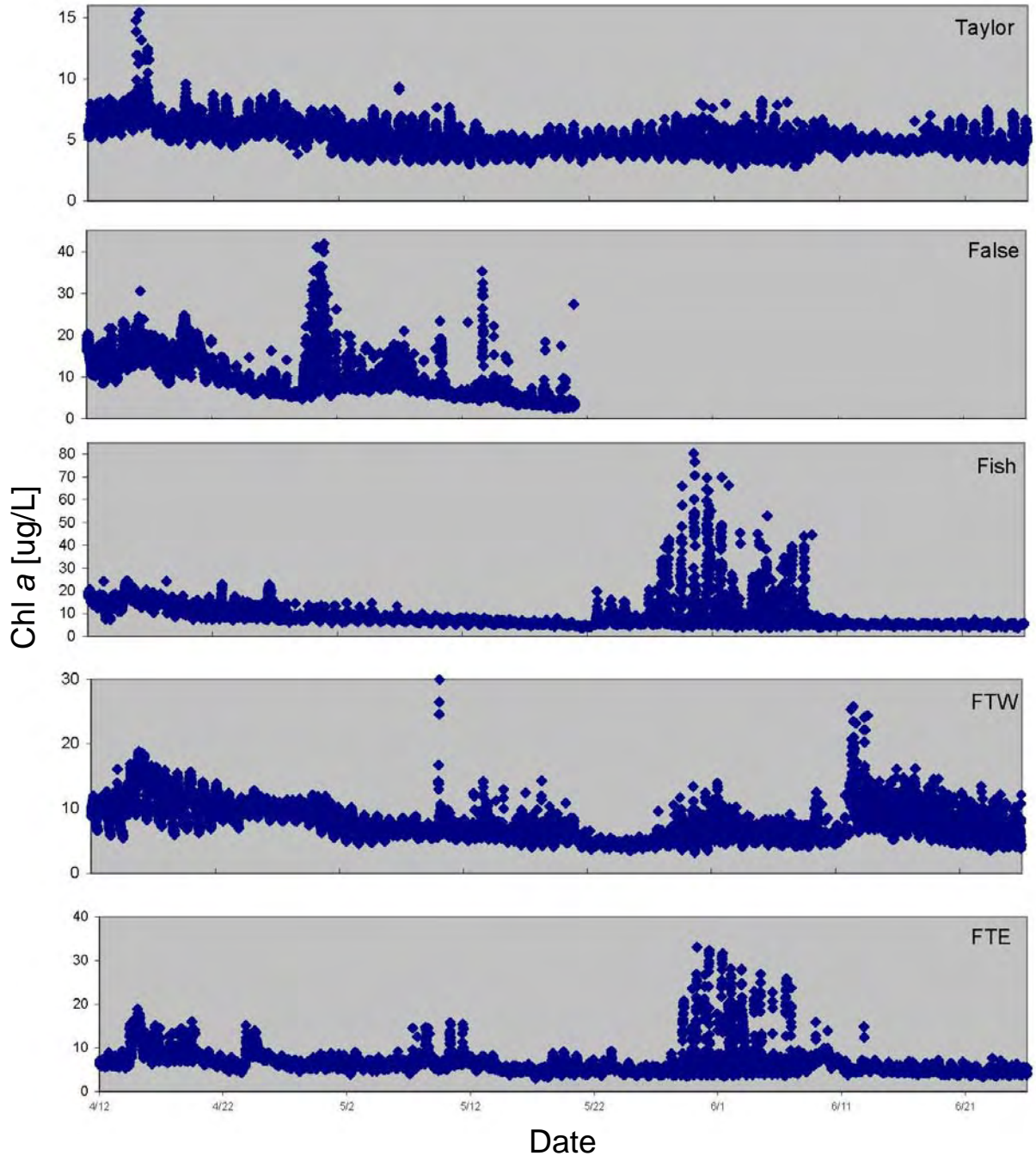


Figure C20a. Measured time series of chl *a* in the Franks Tract region, 2002. See Figure C2 for station locations.

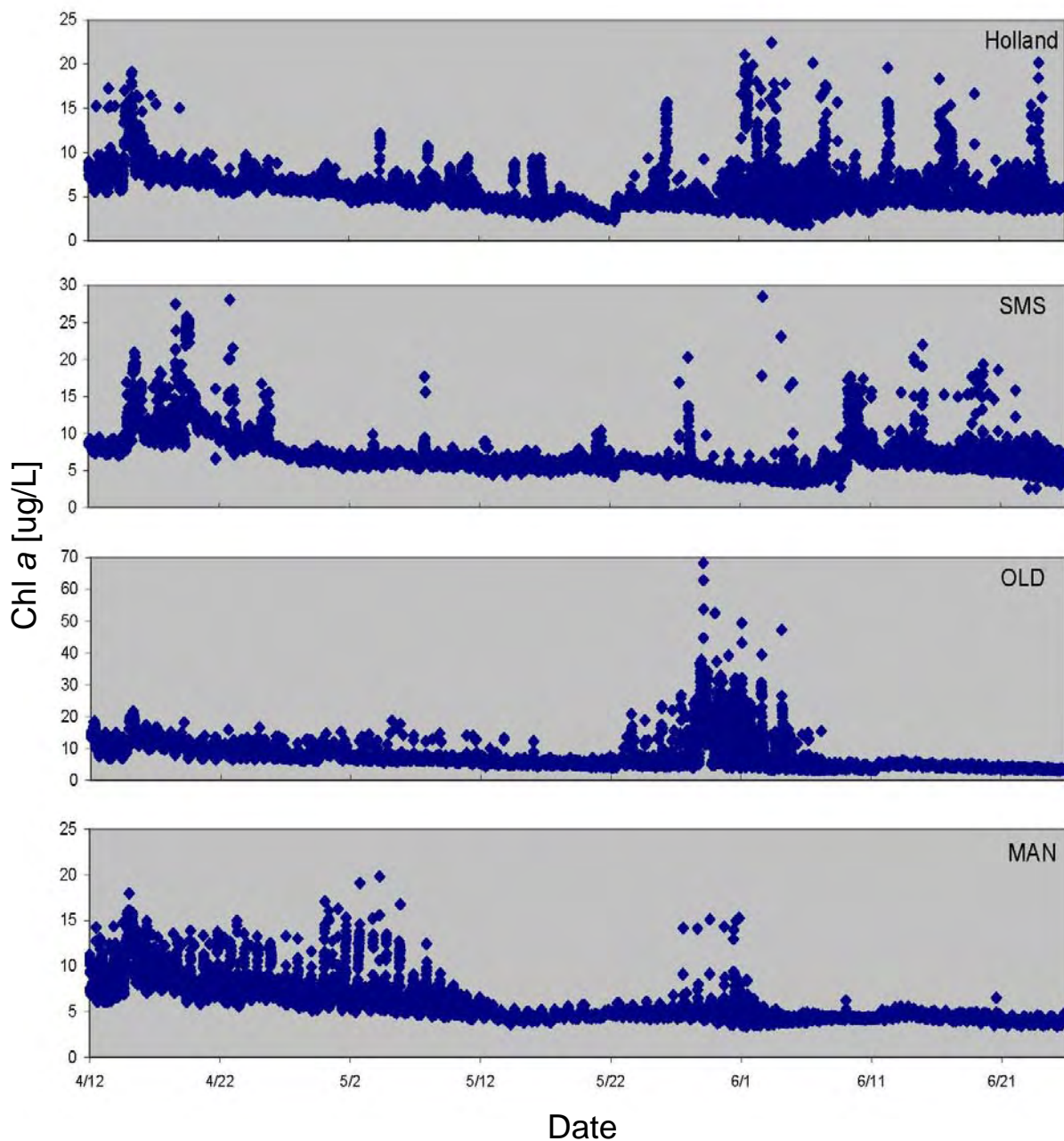


Figure C20b. Measured time series of chl *a* in the Franks Tract region, 2002. See Figure C2 for station locations.

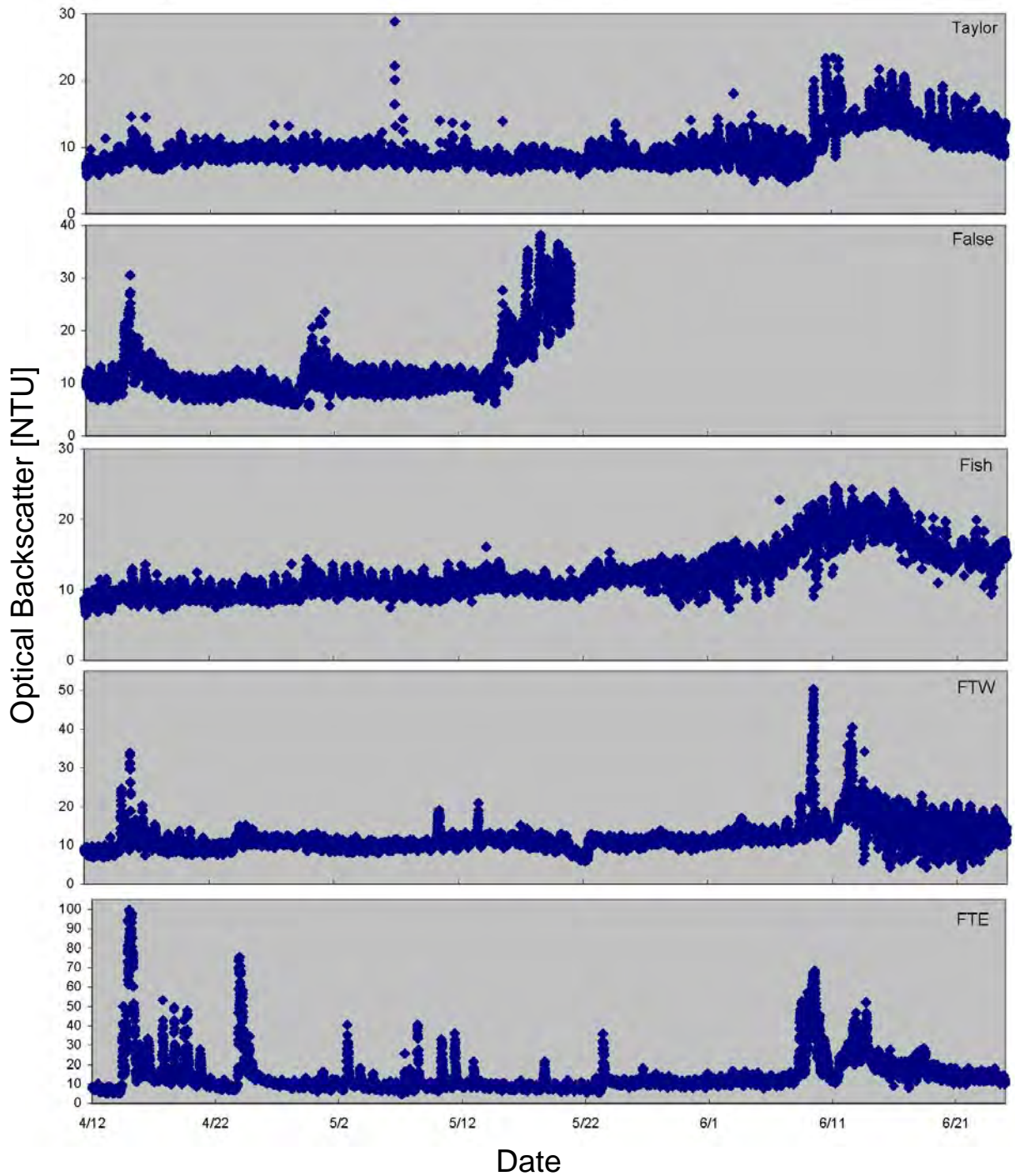


Figure C21a. Measured time series of optical backscatter in the Franks Tract region, 2002. See Figure C2 for station locations.

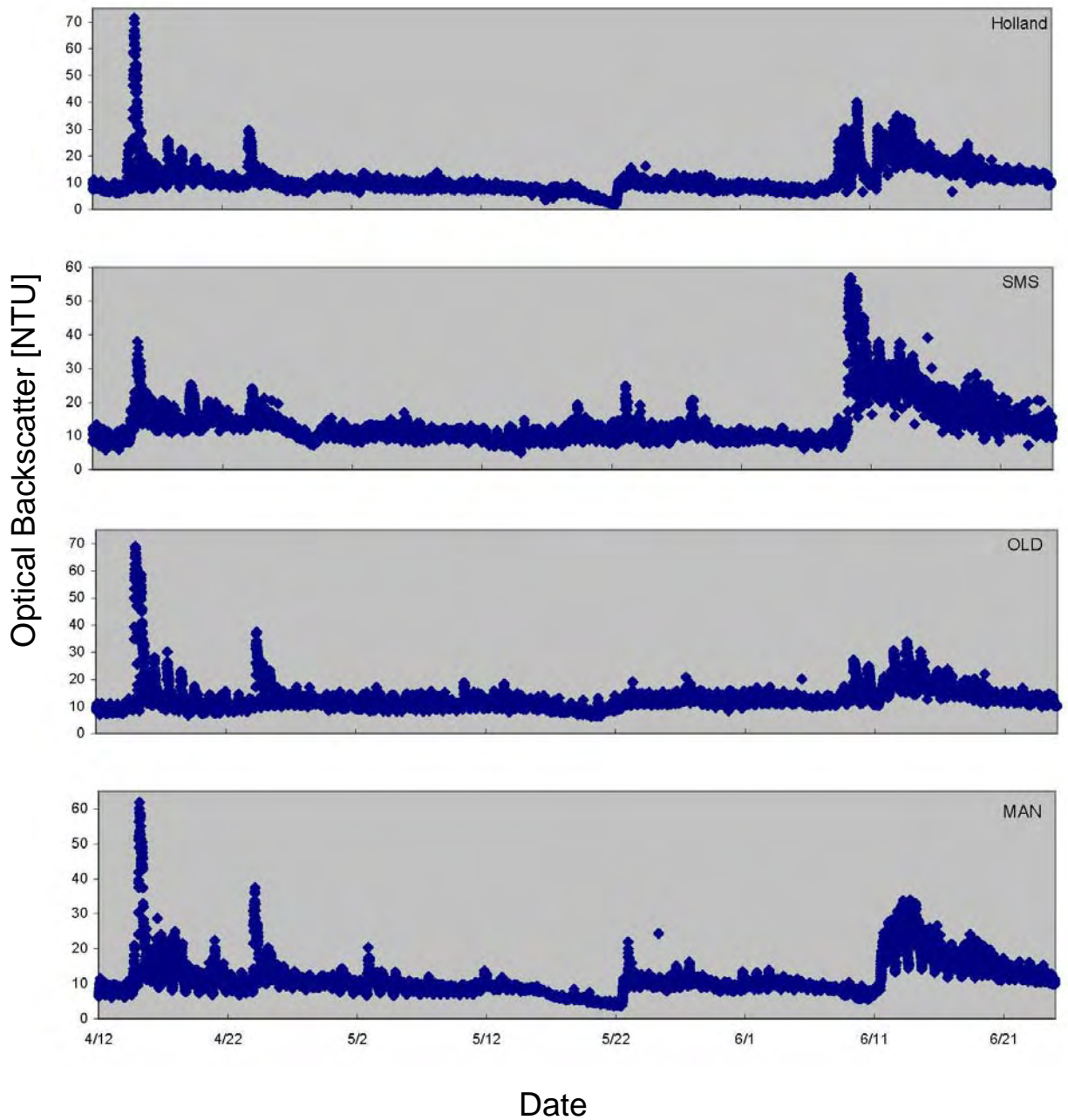


Figure C21b. Measured time series of optical backscatter in the Franks Tract region, 2002. See Figure C2 for station locations.

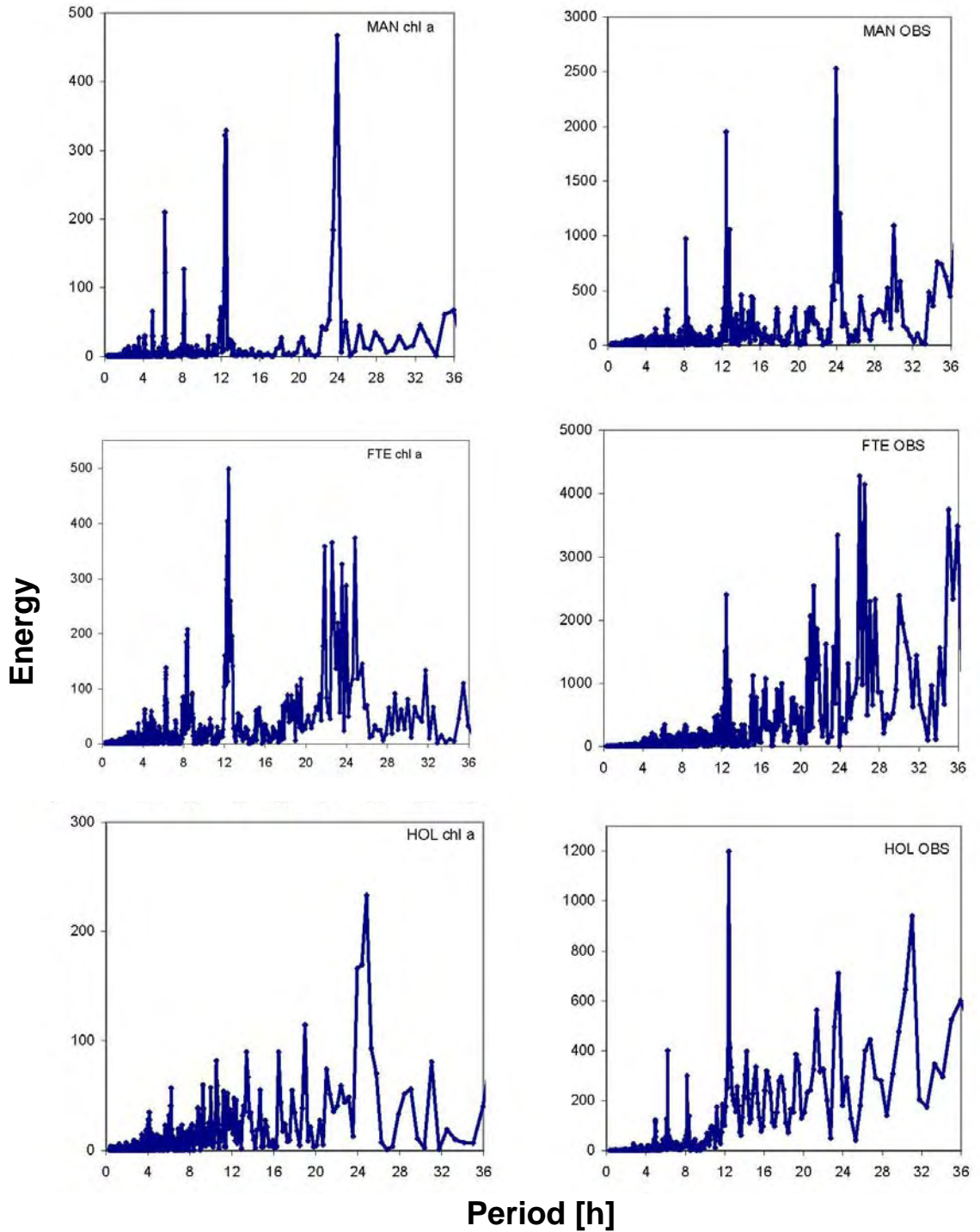


Figure C22a. Power spectra for chl a and OBS in Franks Tract region, 2002. See Fig. C2 for station locations.

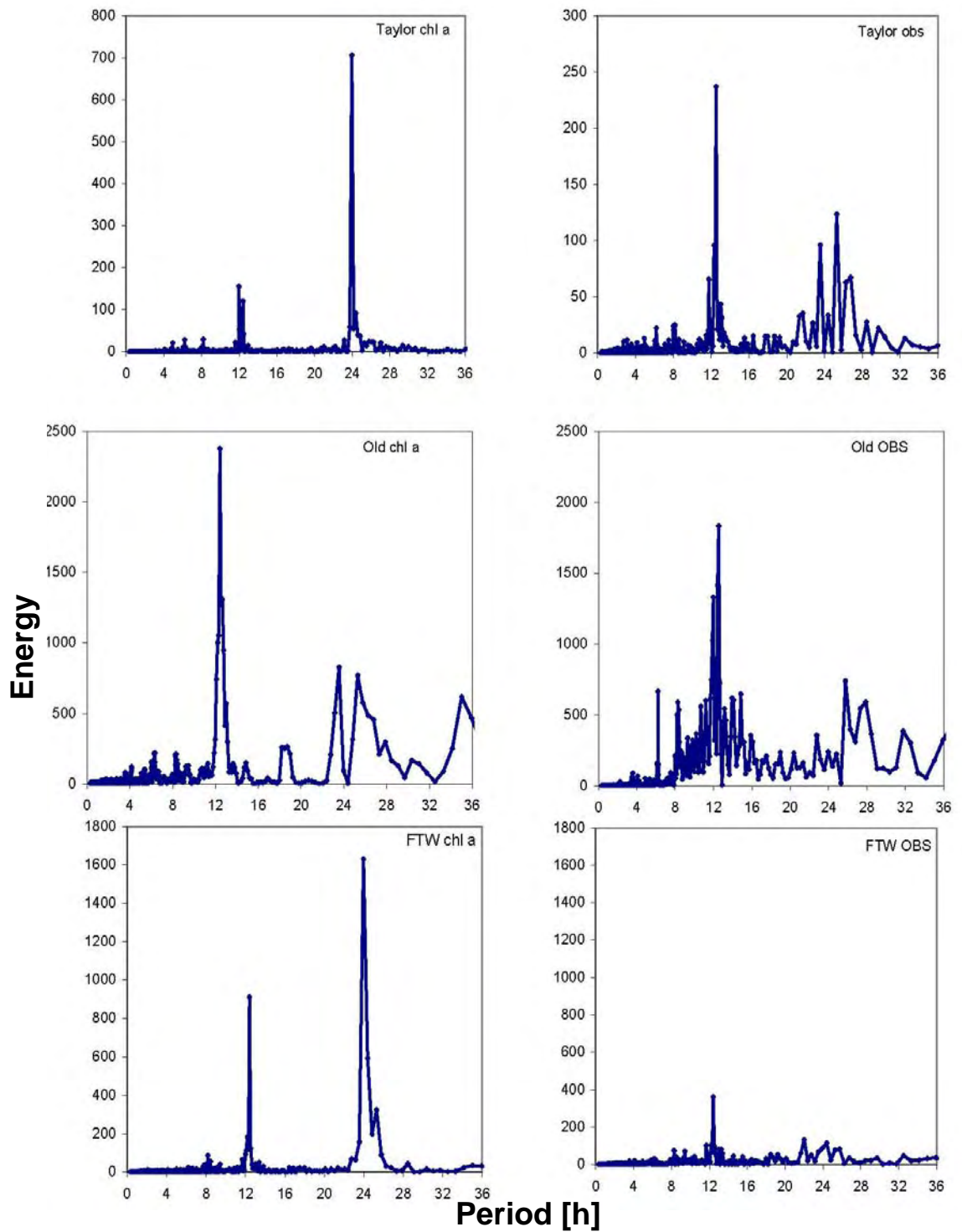


Figure C22b. Power spectra for chl *a* and OBS in Franks Tract region, 2002. See Fig. C2 for station locations.

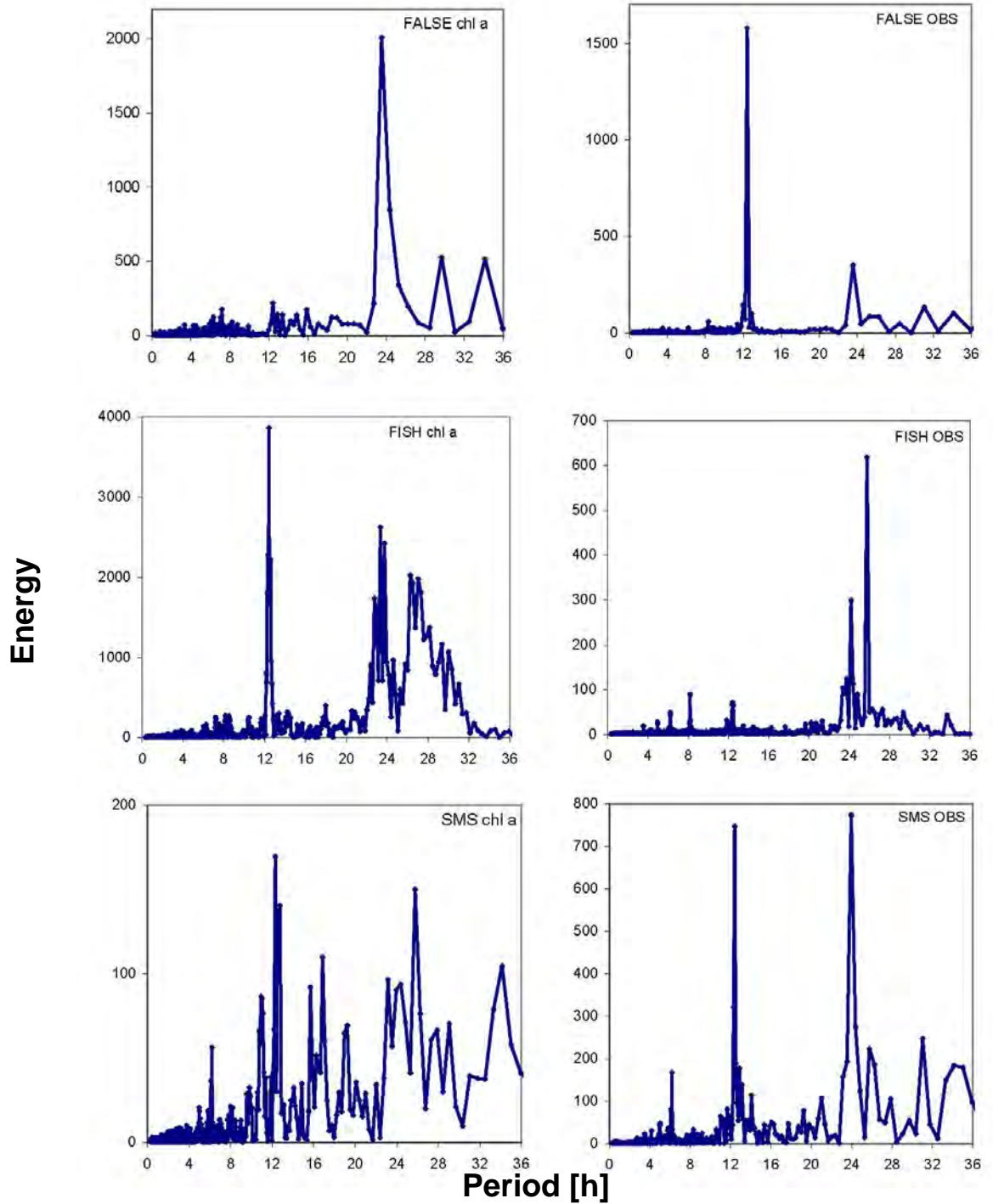


Figure C22c. Power spectra for chl *a* and OBS in Franks Tract region, 2002. See Fig. C2 for station locations.

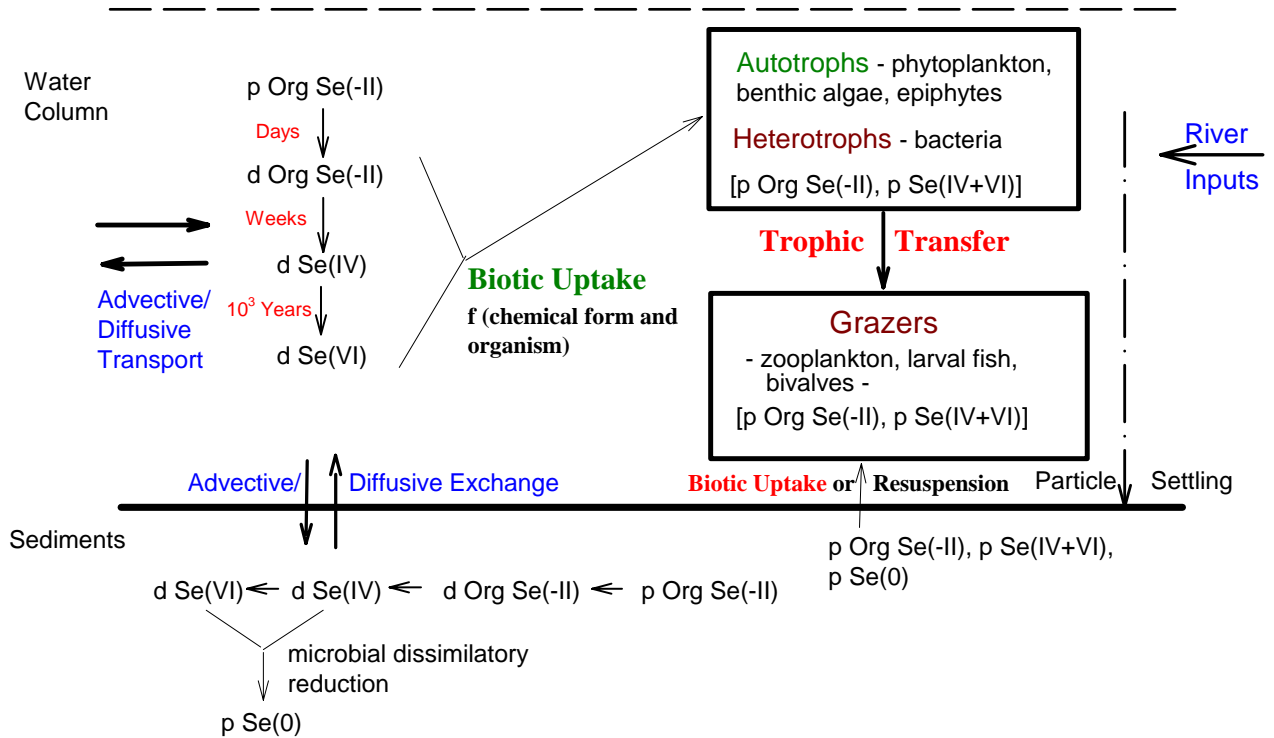


Figure SED1. A conceptual model for selenium cycling in the Sacramento-San Joaquin River Delta. Physical transport processes are labeled in blue while biogeochemical processes are in red and green. The speciation of particulate Se is in [brackets]. p - particulate, d - dissolved.

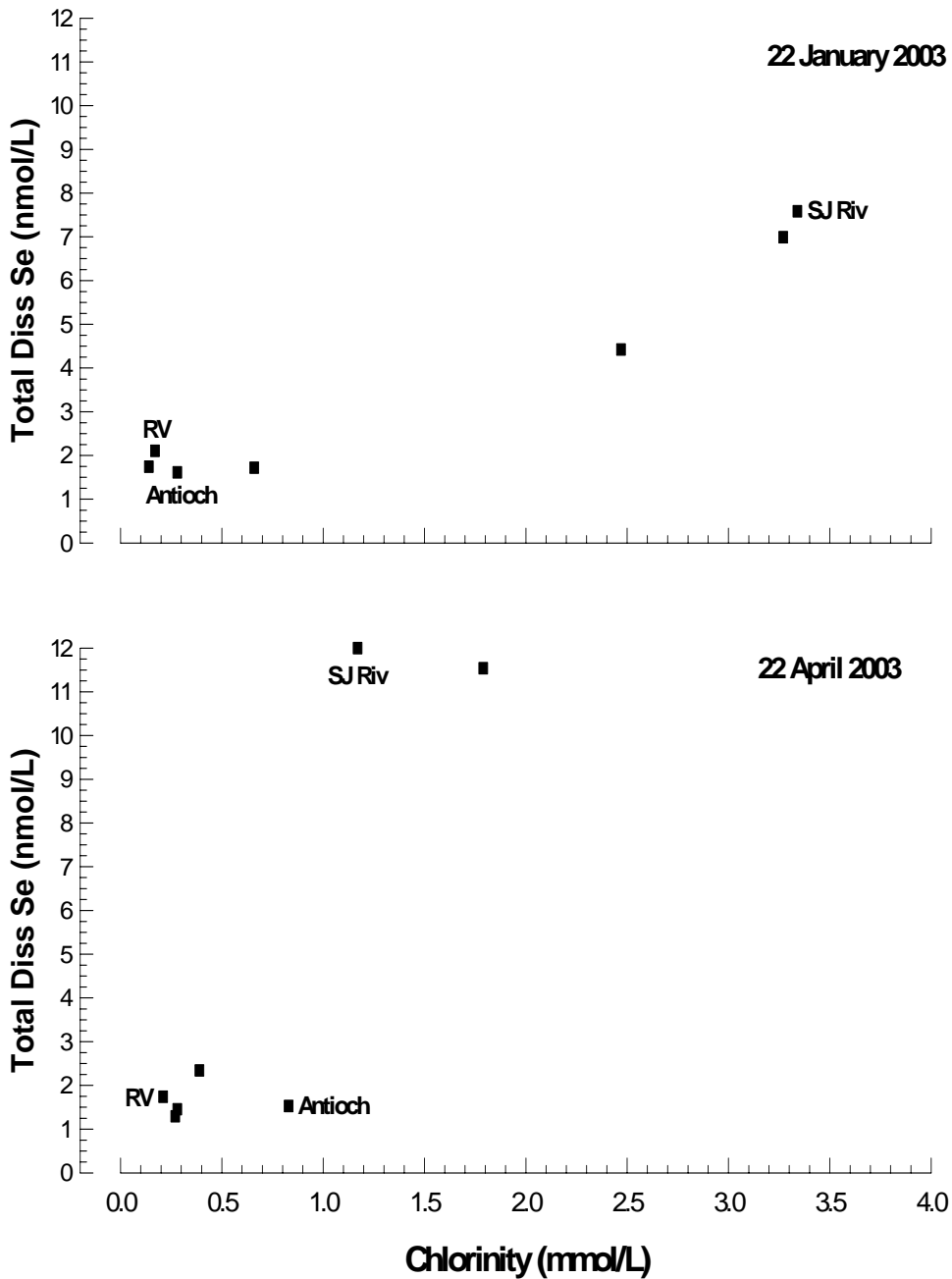


Figure SED2. Total dissolved selenium versus chloride concentration in two Delta transects. Relevant endmembers are identified, including Rio Vista on the Sacramento River (RV), the San Joaquin River (SJ Riv), and Antioch at the westernmost point of the Delta.

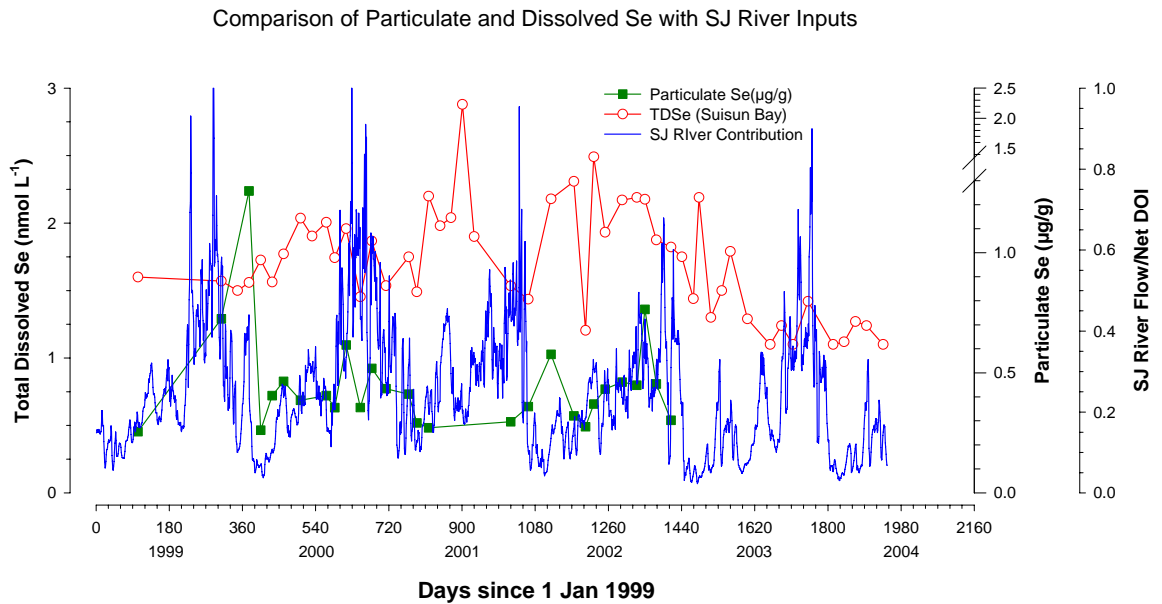
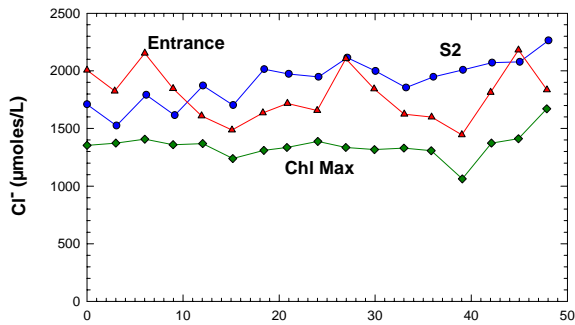
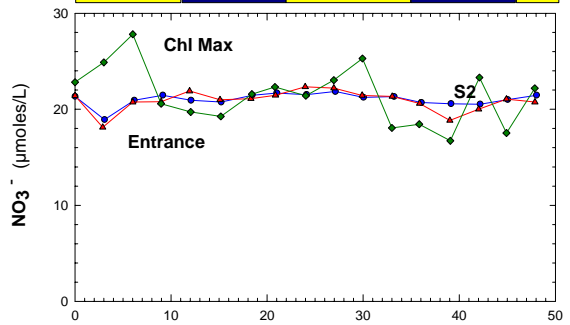


Figure SED3. Dissolved and particulate total selenium at USGS Station 8.1 in the Suisun Bay from 1999 to 2004. Also shown is an estimate of the San Joaquin River input to this region expressed as the ratio of SJ River flow to the Net Delta Outflow Index (DOI).



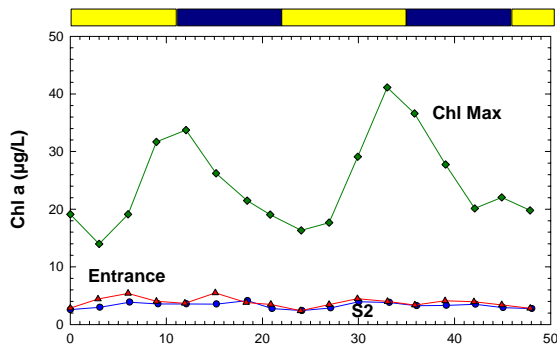
Local Time (from 0740 PDT 09/05/01)

Figure SED4



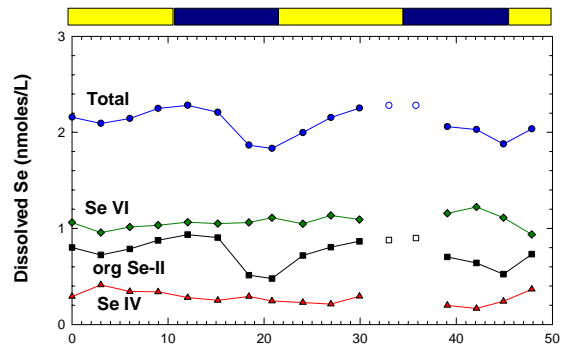
Local Time (from 0740 PDT 09/05/01)

Figure SED5



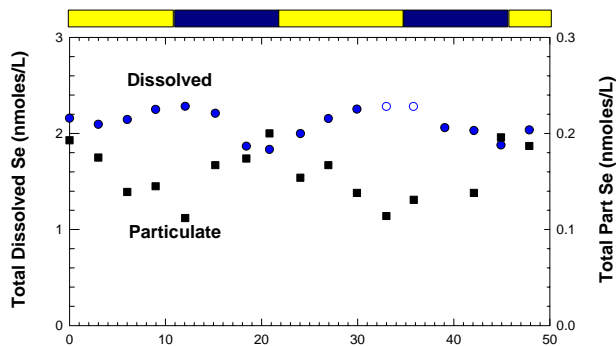
Local Time (from 0740 PDT 09/05/01)

Figure SED6



Local Time (from 0740 PDT 09/05/01)

Figure SED7



Local Time (from 0740 PDT 09/05/01)

Figure SED8

Figures SED4-8. Data from the 2001 Mildred Island experiment. **SED4** shows chloride at the 3 stations as a function of time; **SED5** is nitrate at the 3 stations; **SED6** displays chlorophyll *a* at the 3 stations; **SED7** is dissolved Se at the Chl Max station; and **SED8** is the total dissolved Se and total particulate Se at the Chl Max site. Colored bars represent day and night

Sediments-Mildred Island

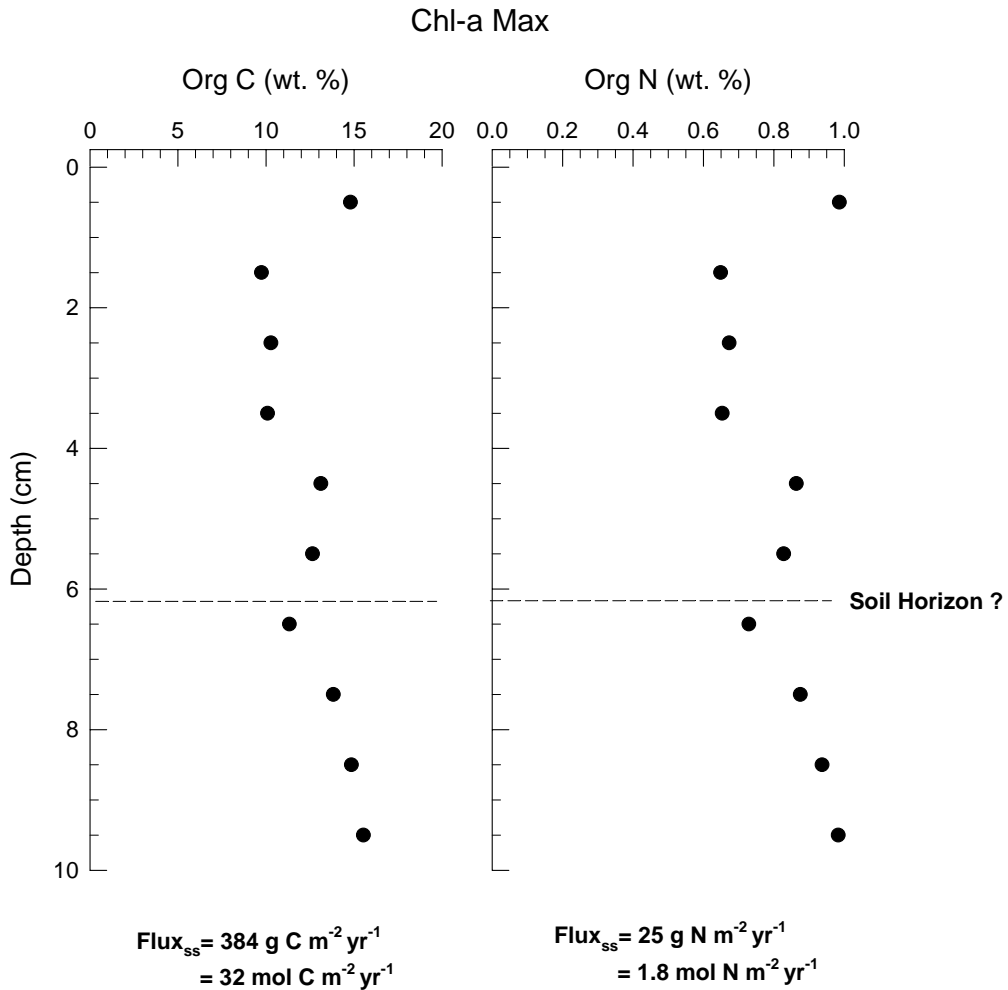


Figure SED9. Sedimentary organic carbon and nitrogen at the Mildred Island Chl Max site in September 2001. Fluxes are calculated by assuming steady state and using the measured sedimentation rate, porosity, and dry sediment density.

Mildred Island Sediment Porewaters

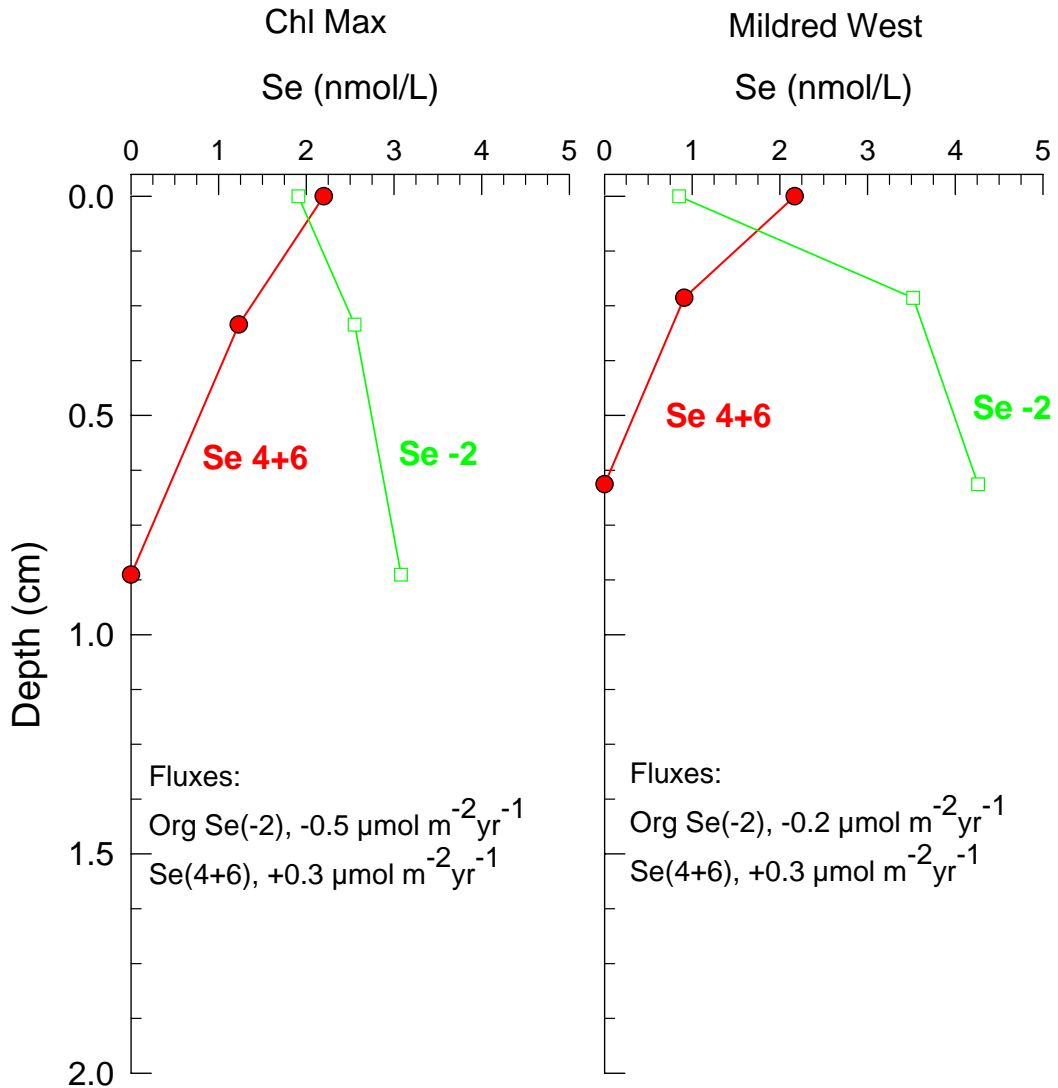


Figure SED10. Fluxes of dissolved selenium into (positive sign) or out of (negative sign) Mildred Island sediments in September 2001 at 2 sites. Calculations are based on observed concentration gradients, porosity, and available diffusion coefficients.

Sediments-Mildred Island

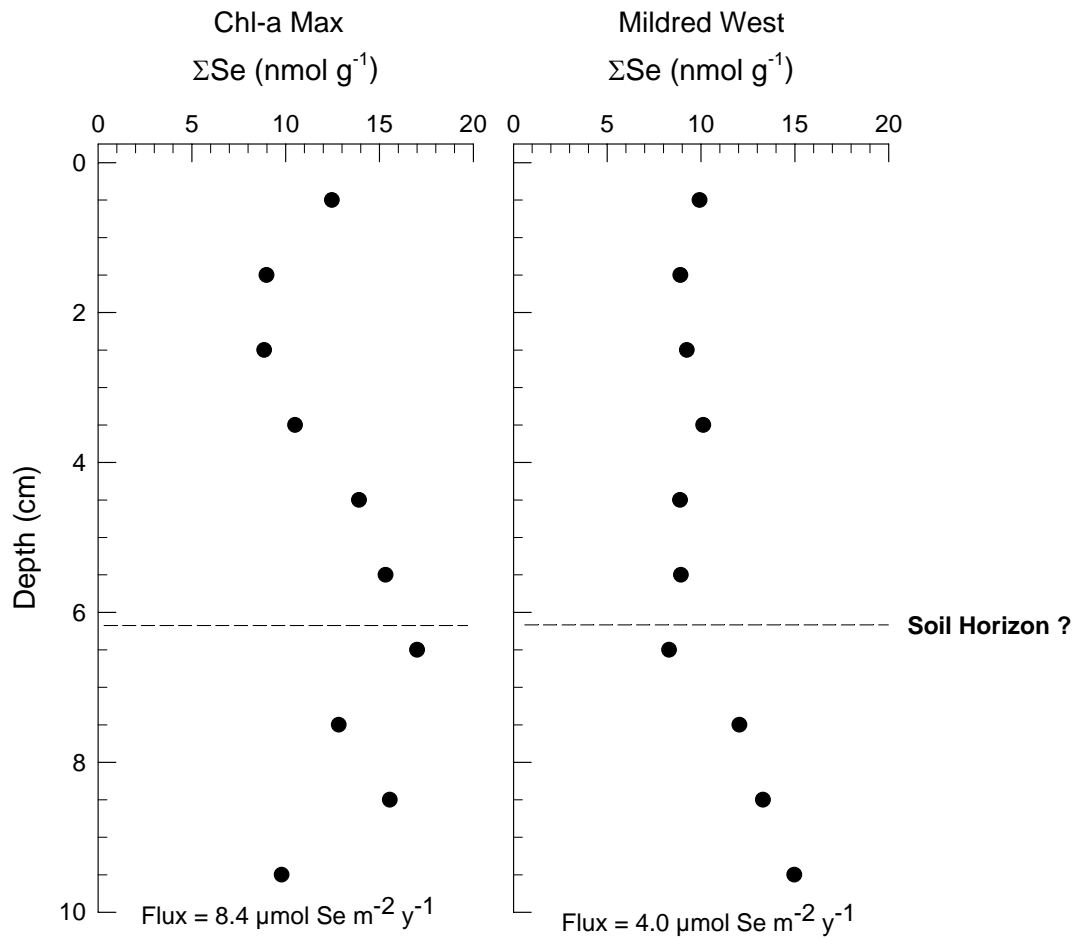


Figure SED11. Sedimentary total selenium at two Mildred Island sites in September 2001. Fluxes are calculated by assuming steady state and using the measured sedimentation rate, porosity, and dry sediment density.

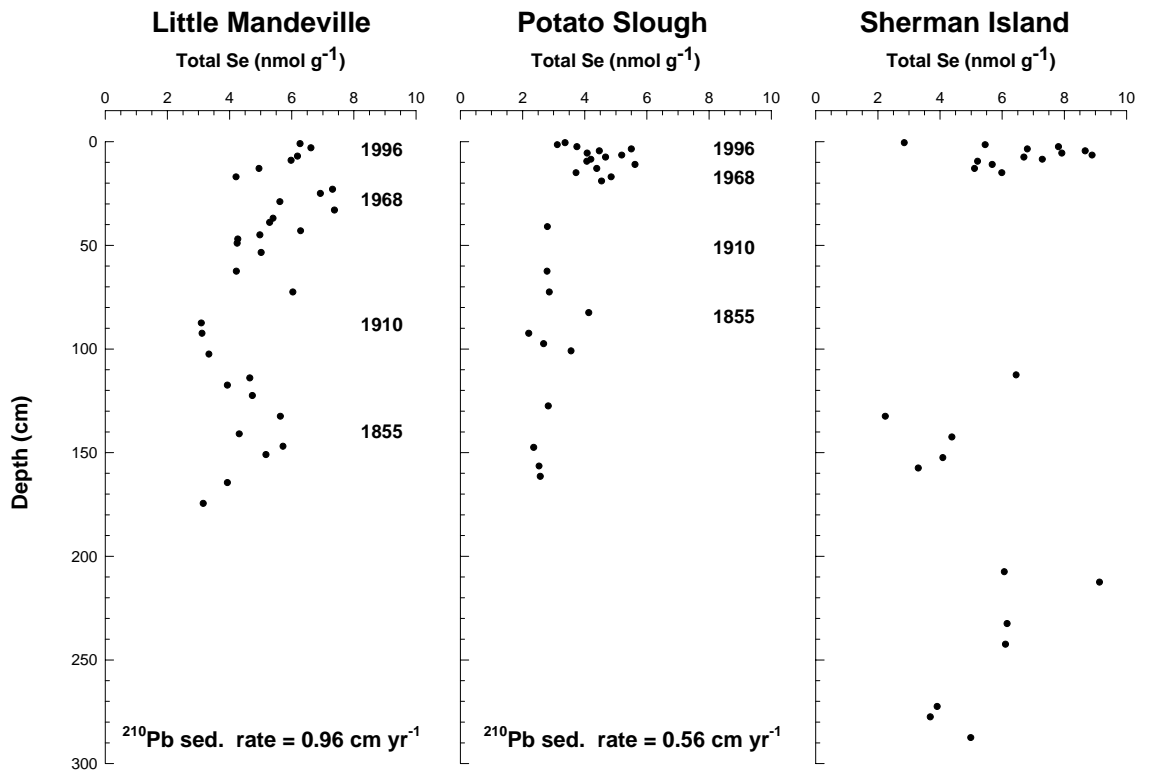


Figure SED12. Solid phase total selenium concentrations at three sites in the Delta. Dates for the Little Mandeville and Potato Slough cores are based on ²¹⁰Pb accumulation rates.

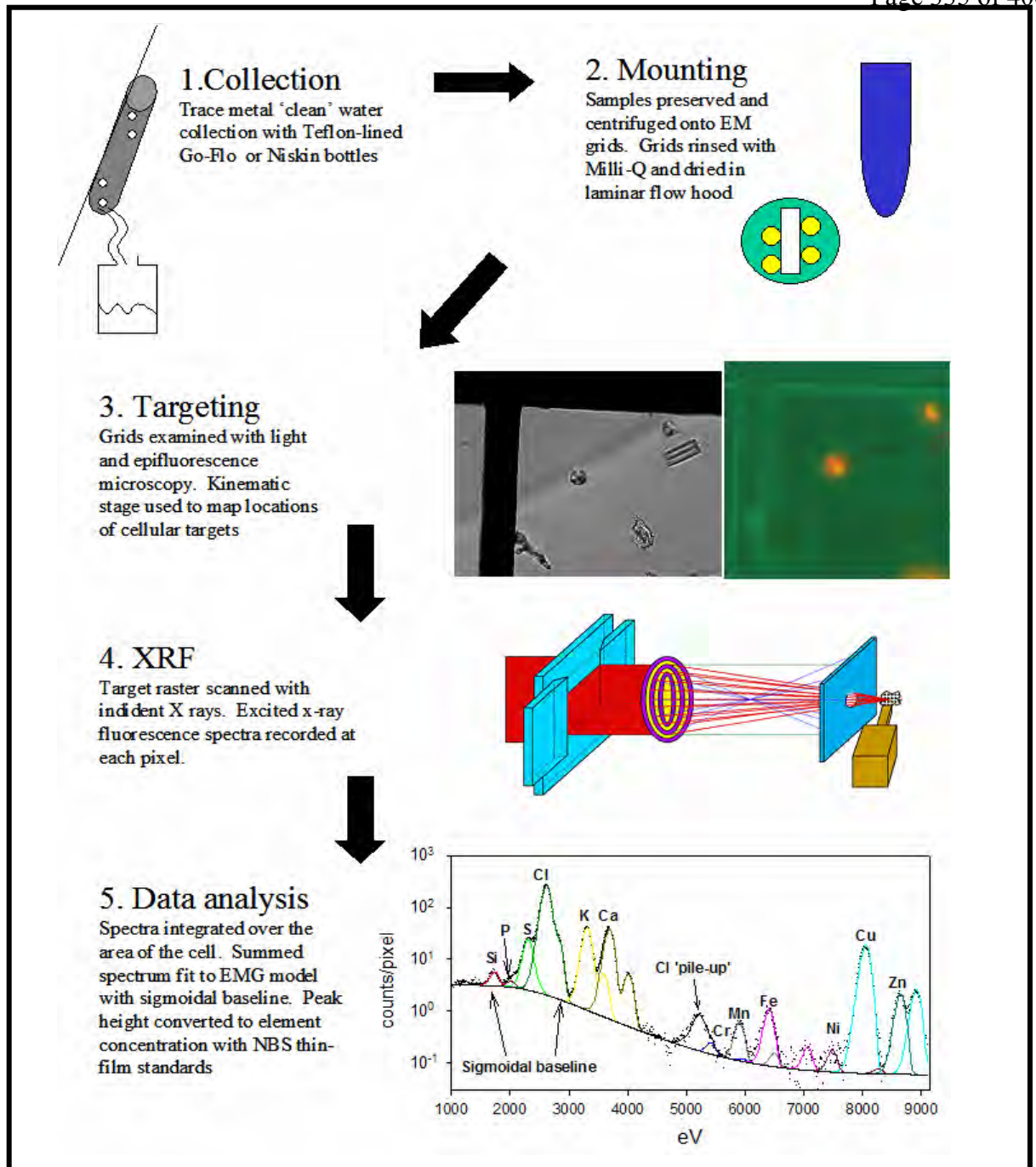


Figure SET1. Procedure for conducting single cell elemental analyses using synchrotron based x-ray fluorescence (SXRF)

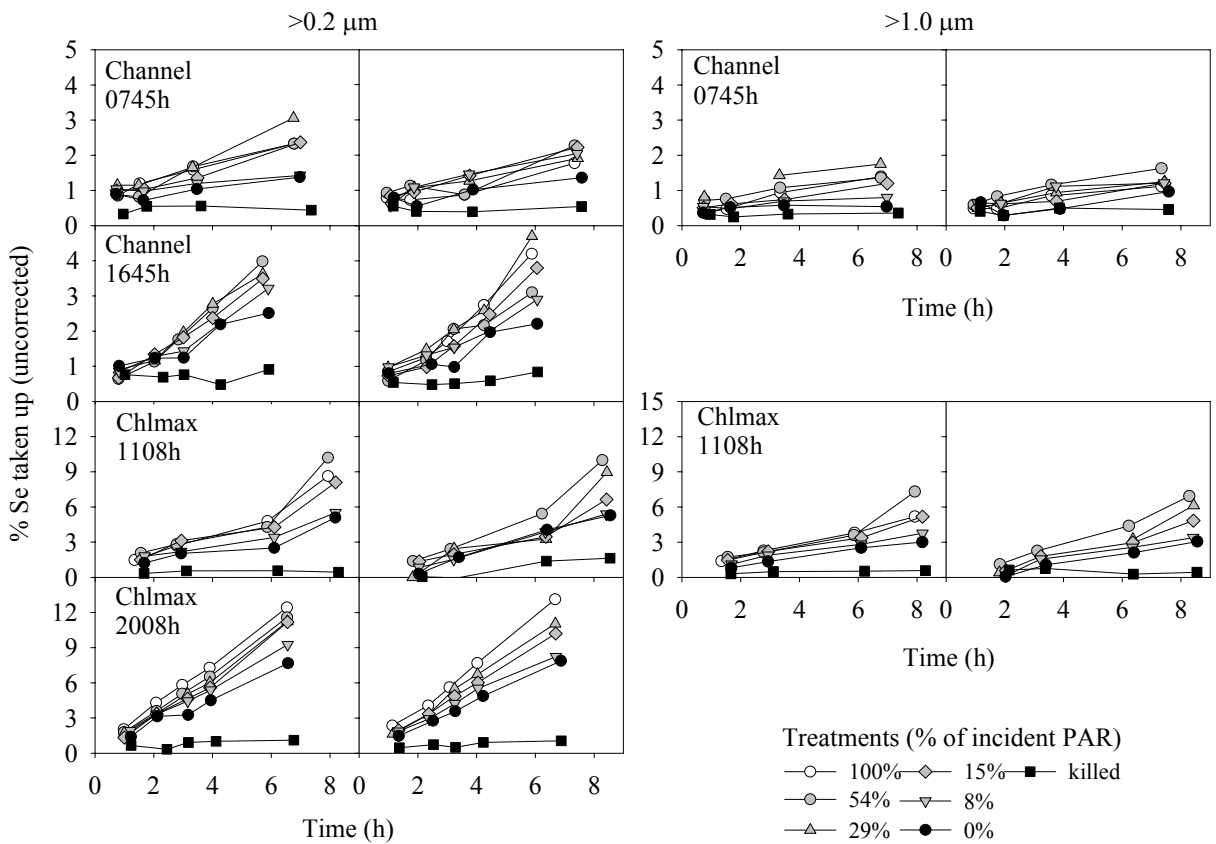


Figure SET2. Time series of selenite uptake by intact communities of plankton during the Mildred Island process experiment.

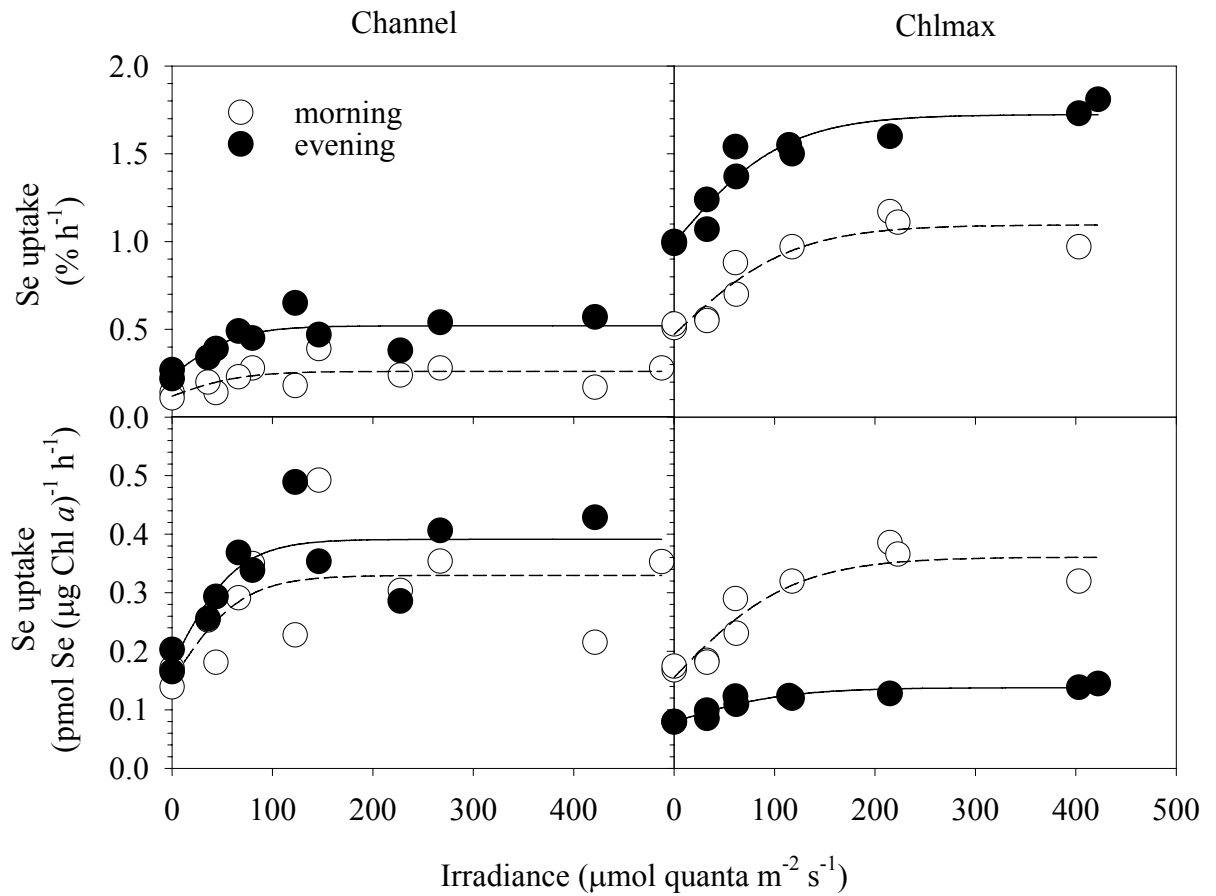


Figure SET3. Effect of light on uptake of selenite by intact plankton communities during the Mildred Island process study.

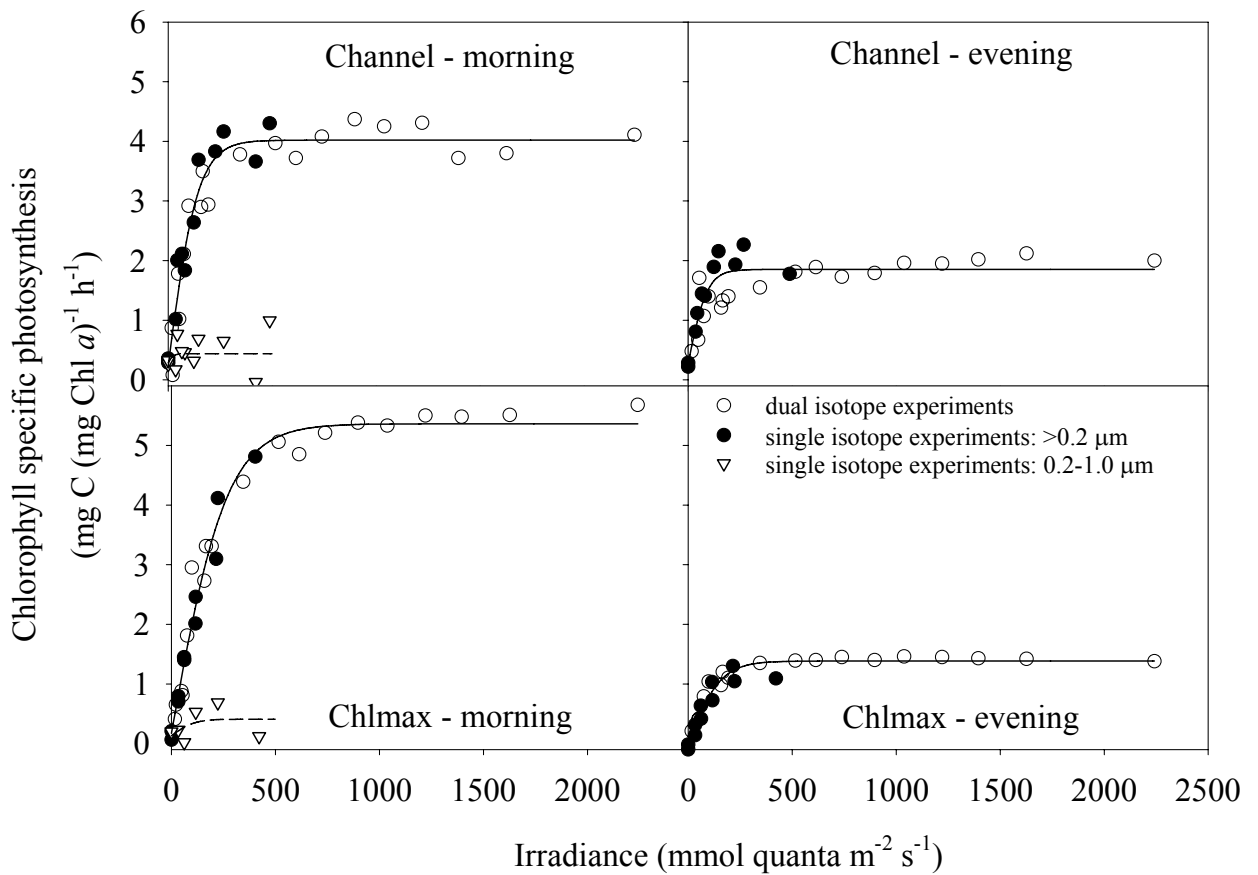


Figure SET4. Photosynthesis vs. light curves during the Mildred Island process study.

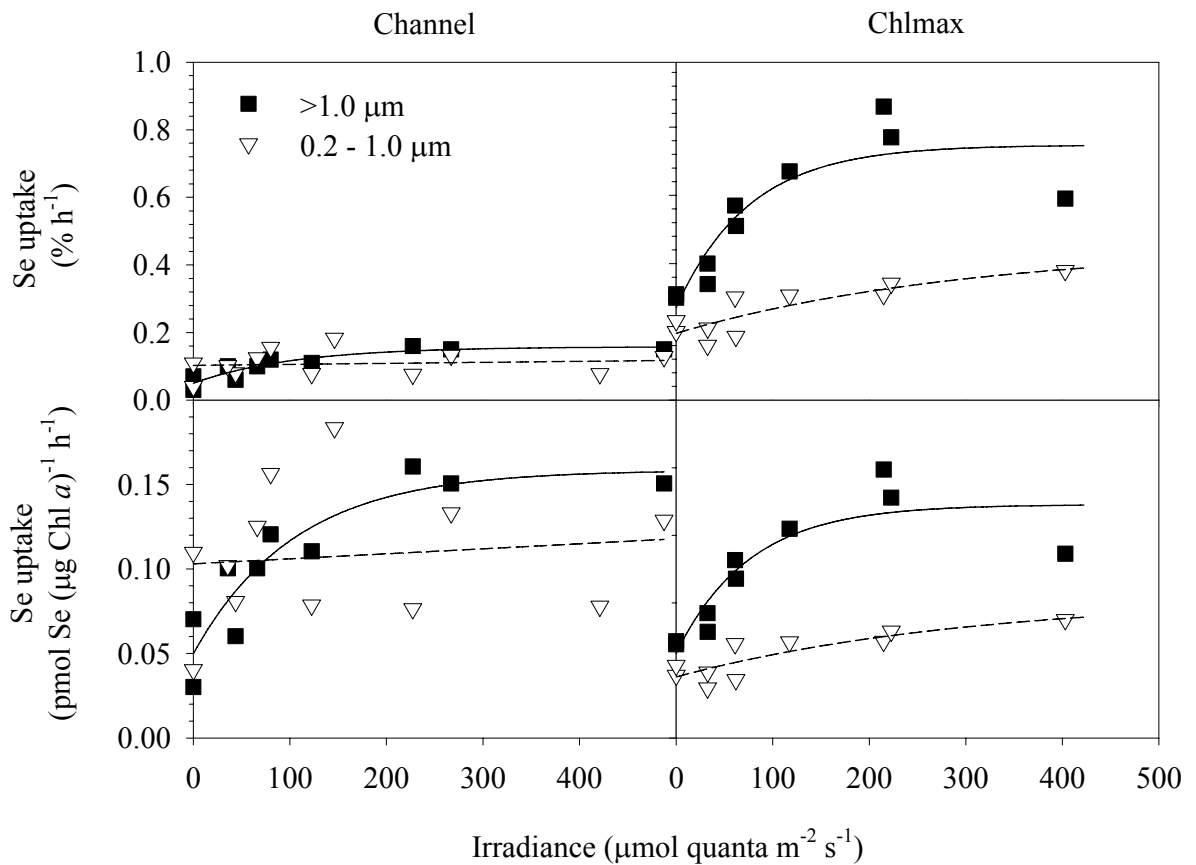


Figure SET5. Amount of selenite taken up into the 0.2-1.0 µm and the >1.0 µm size fractions during the Midred Island process study.

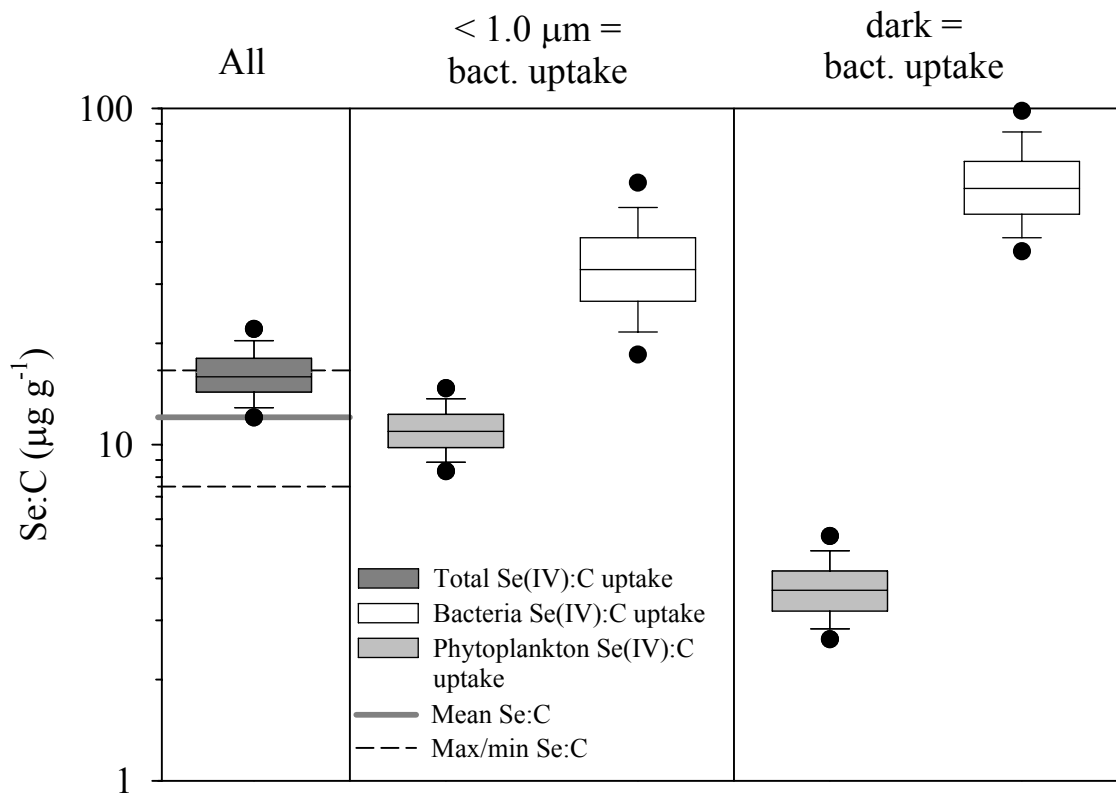


Figure SET6. Estimated Se:C uptake ratios for the intact plankton community, as well as phytoplankton and bacteria during the Mildred Island process study.

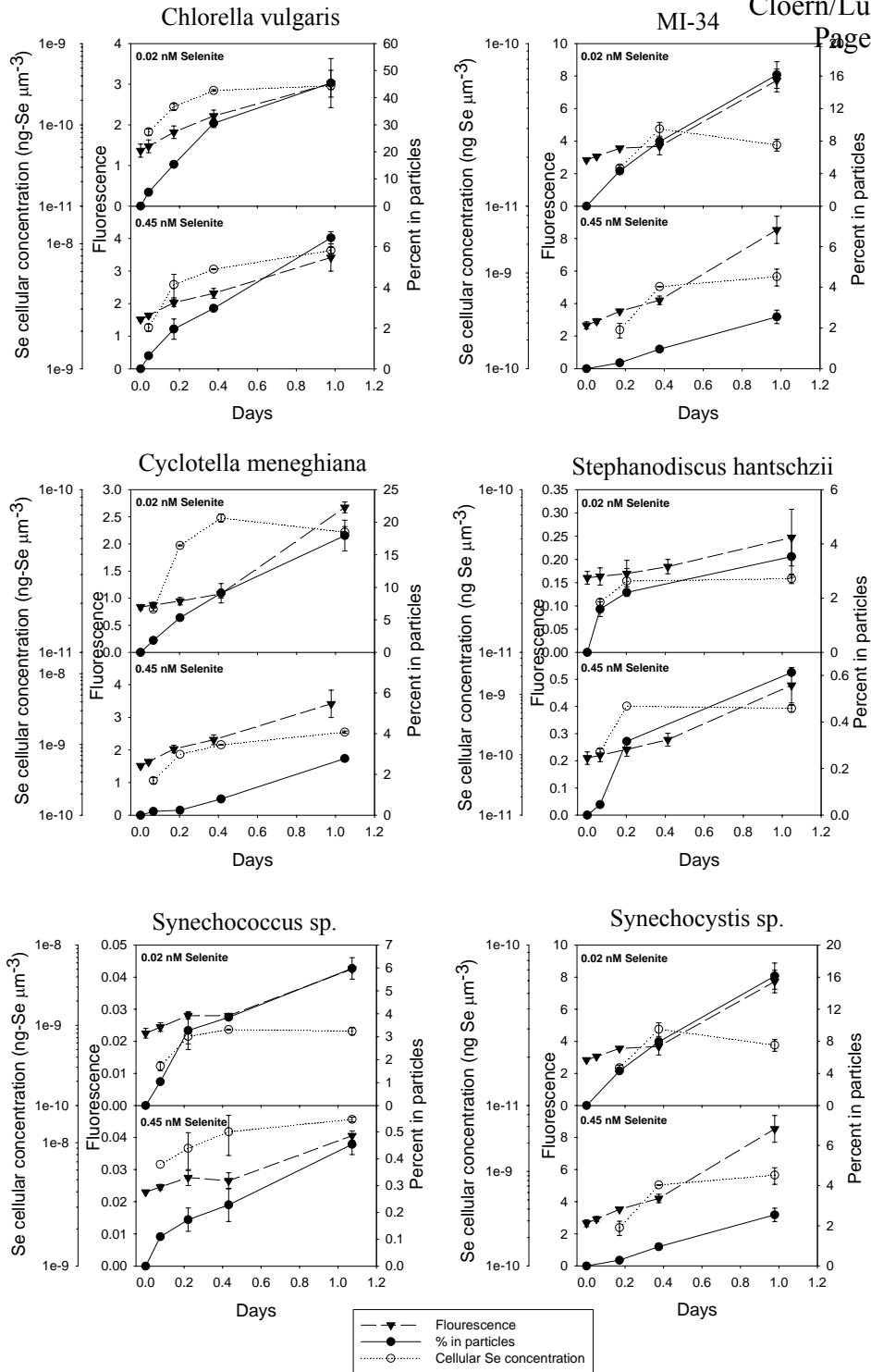


Figure SET7. Uptake of selenite at two concentrations by several freshwater phytoplankters.

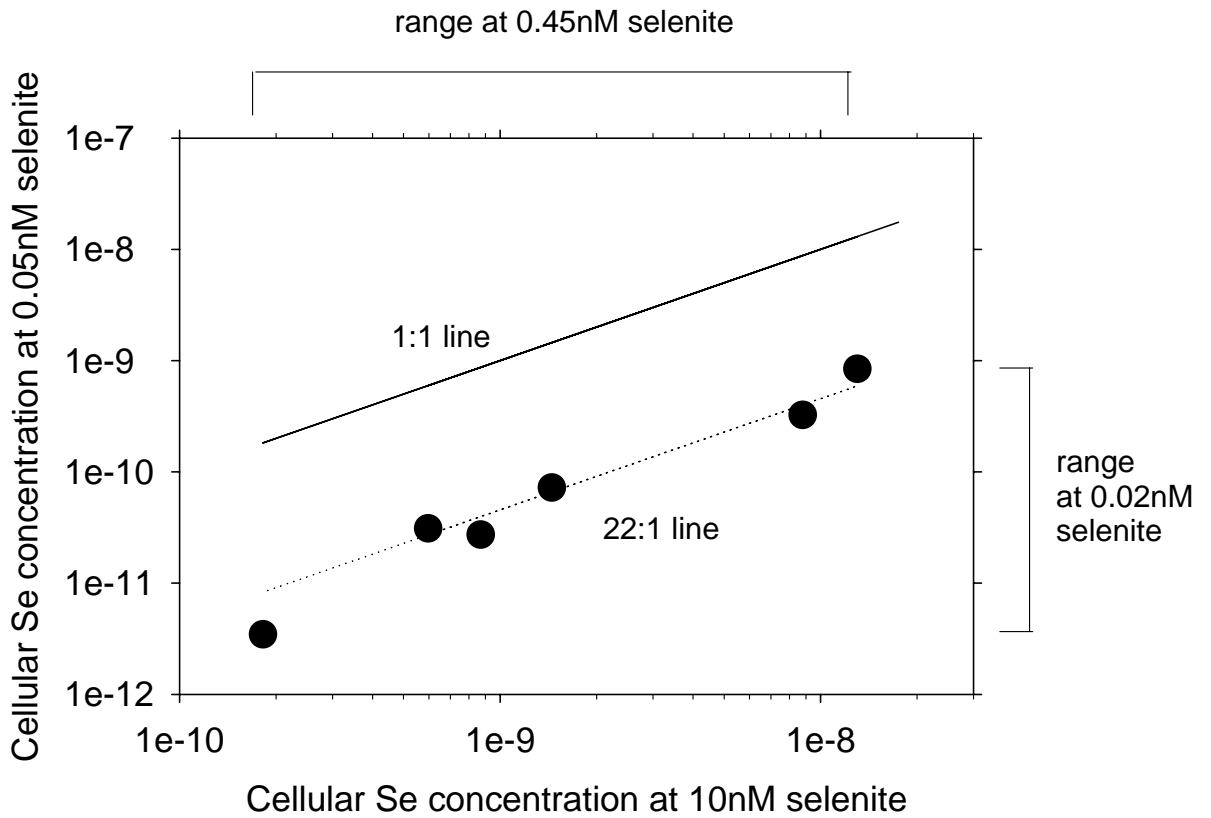


Figure SET8. Comparison of equilibrium cellular Se concentrations by several freshwater phytoplankton species at two concentrations of selenite.

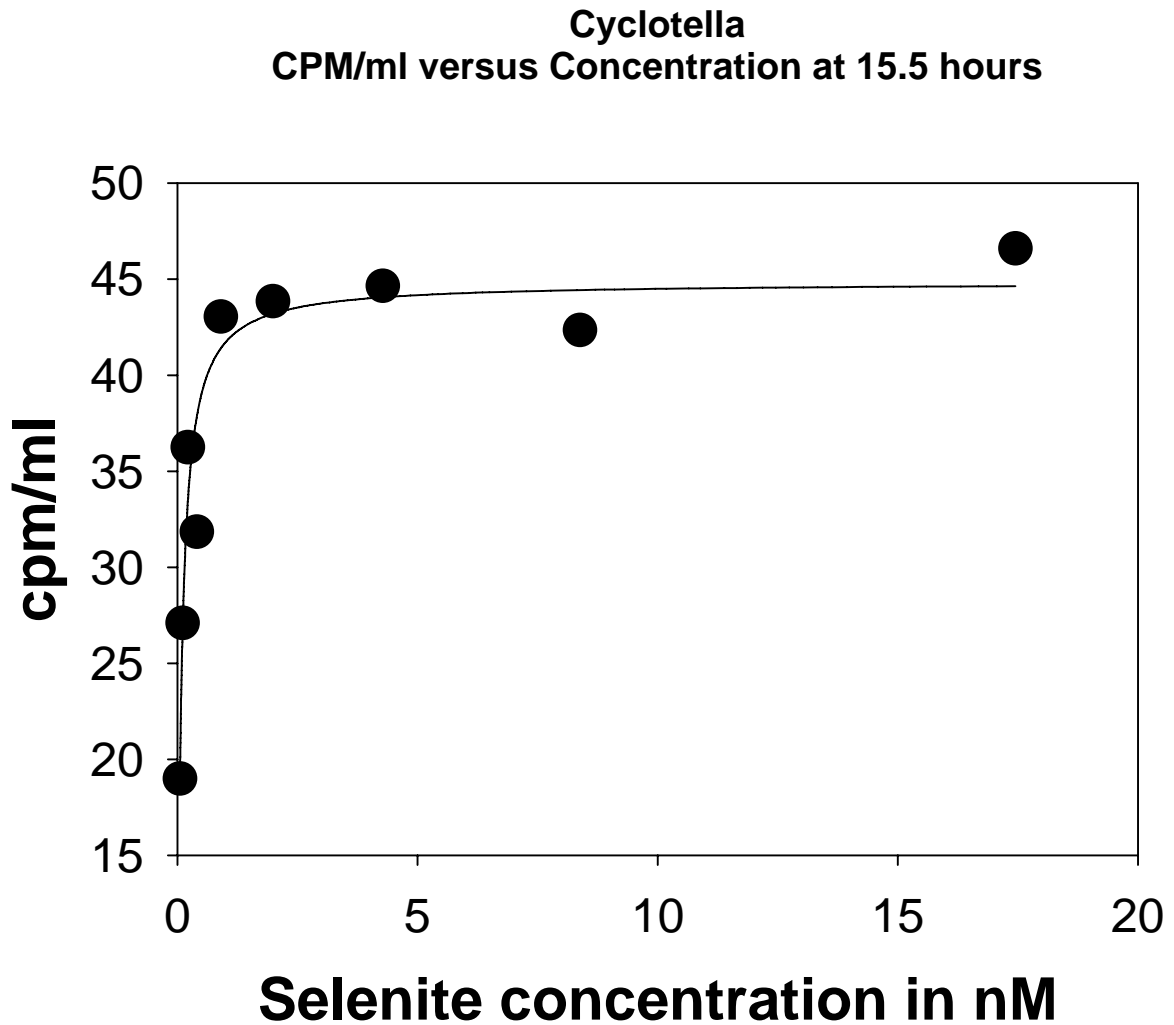


Figure SET9. Change in selenite uptake by the freshwater diatom *Cyclotella meneghiana* as a function of ambient selenite concentration. Units in radioactivity in particles per ml.

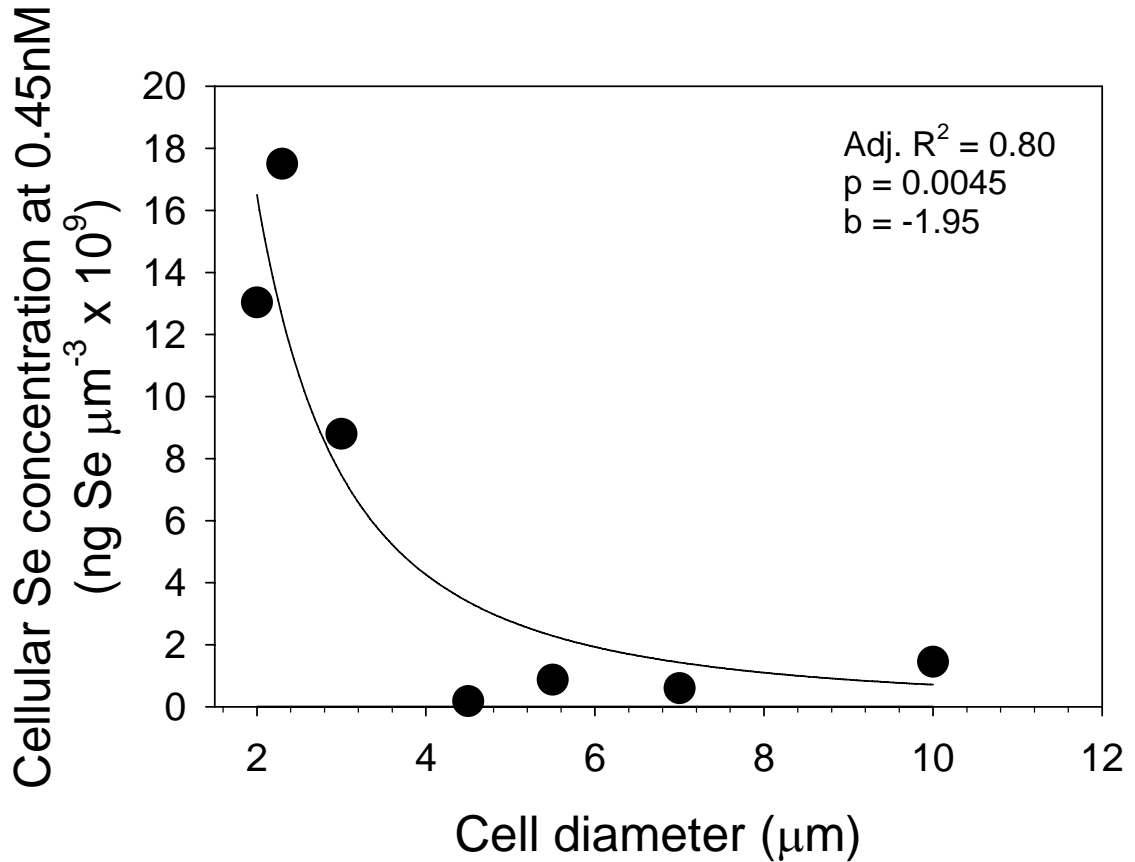


Figure SET10. Relationship between the equivalent spherical diameter of cells of several freshwater phytoplankton species and their equilibrium cellular Se contents at 0.45 nM selenite.

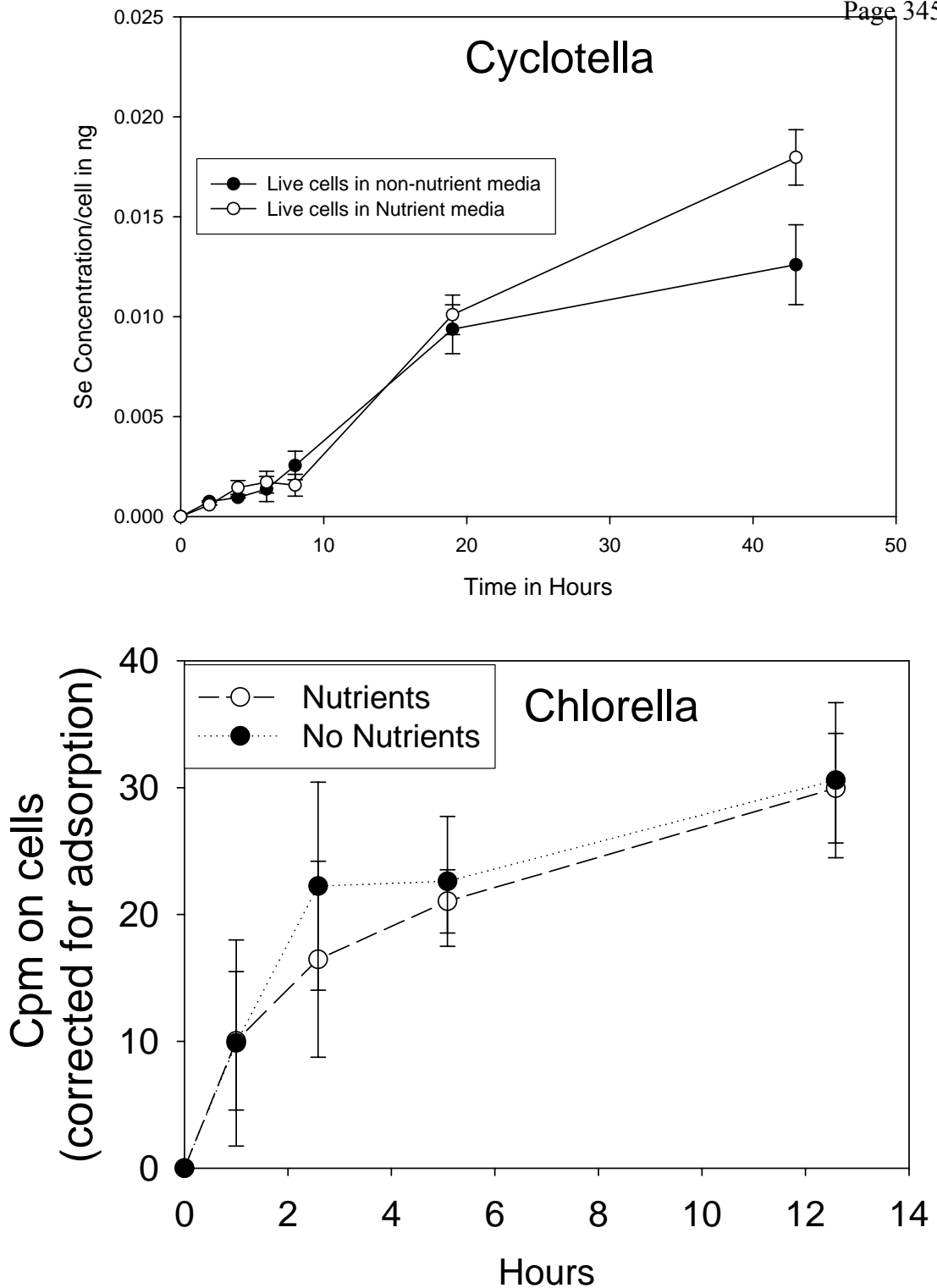


Figure SET11. Comparison of selenite uptake in the presence and absence of f/2 nutrients for two species of freshwater phytoplankton.

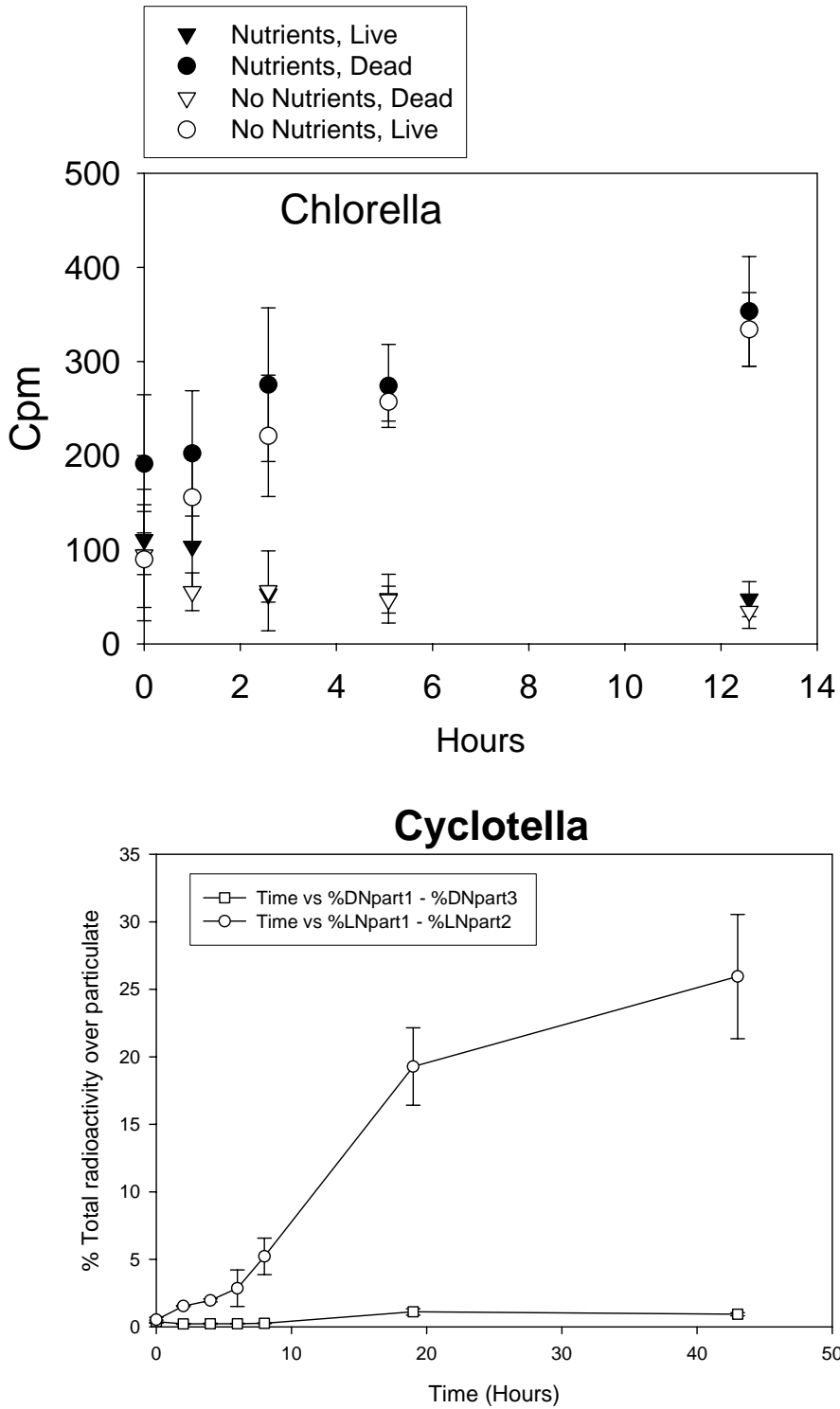


Figure SET12. Comparison of selenite uptake by live and dead cells under different nutrient levels for two freshwater phytoplankton species.

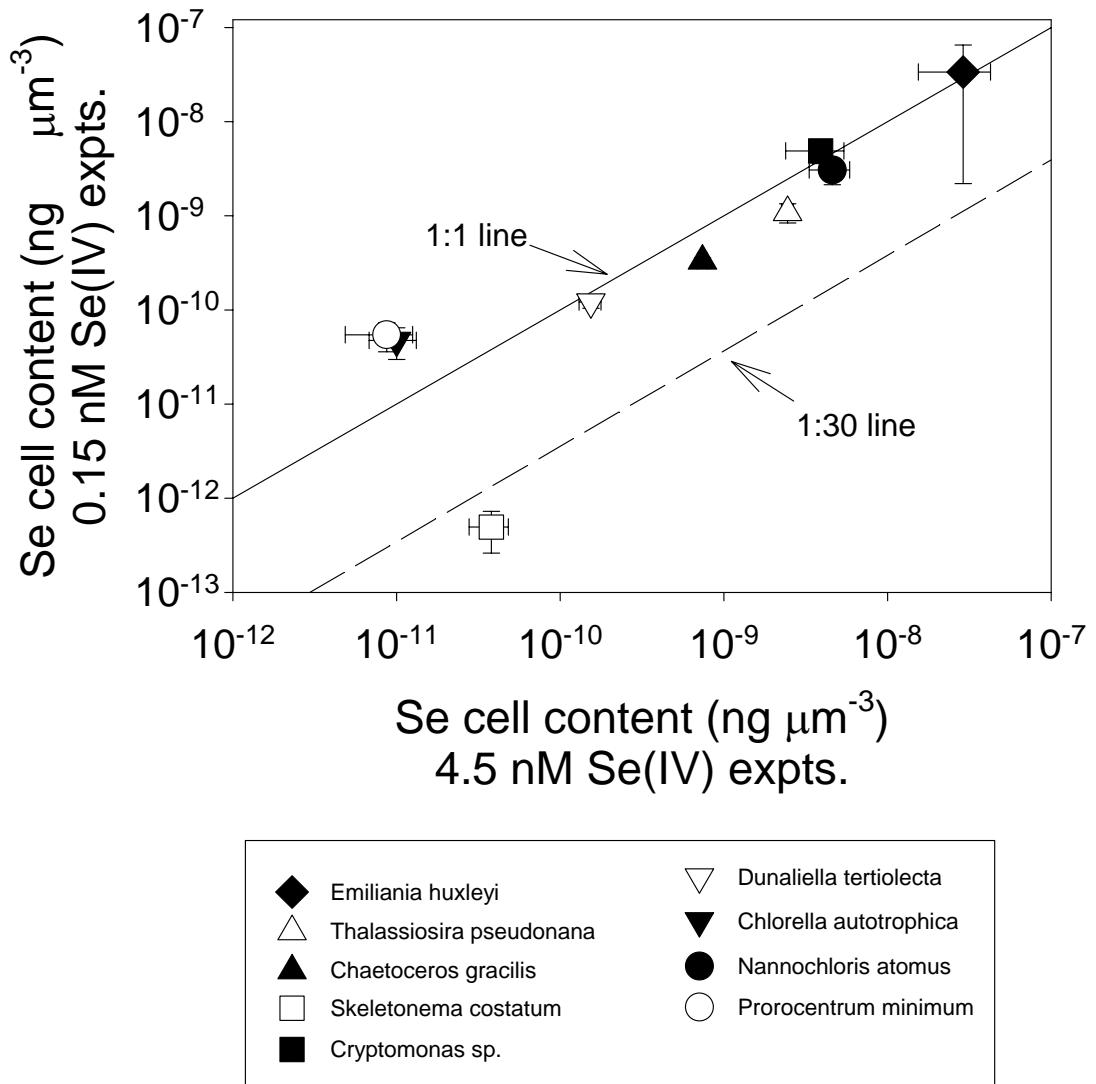


Figure SET13. Correlation between selenite uptake rates exhibited by marine phytoplankton species at 0.15nM and 4.5 nM selenite.

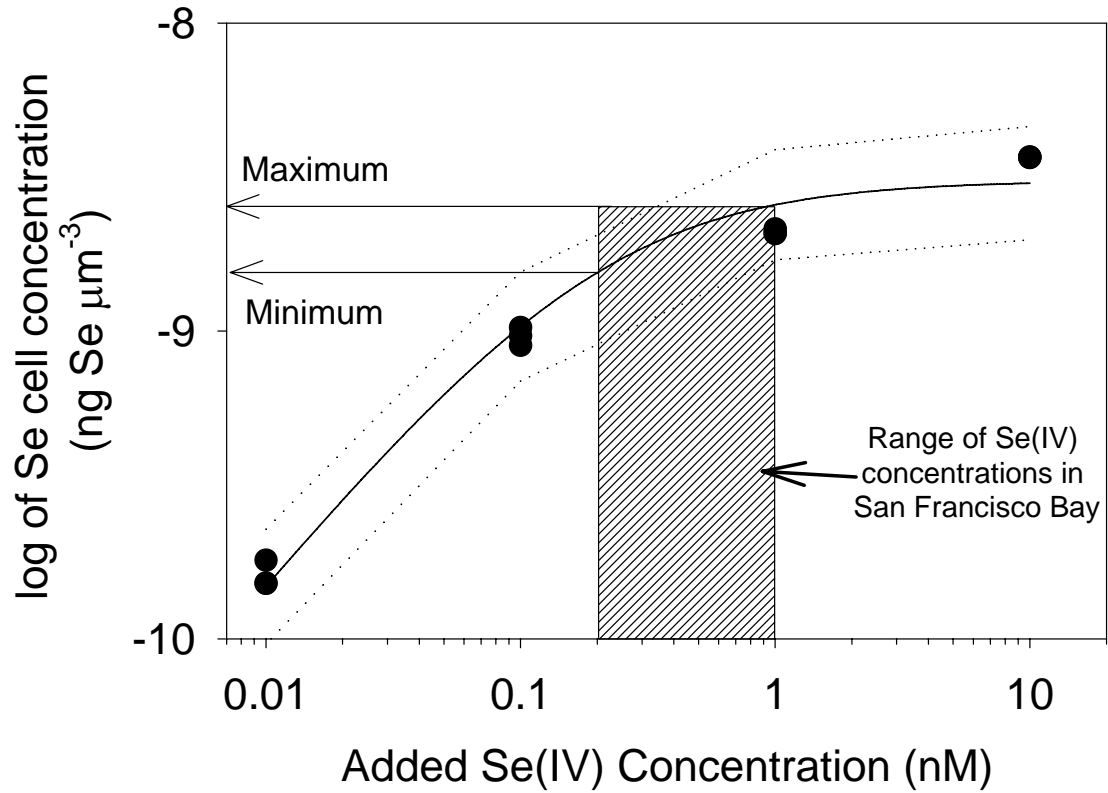


Figure SET14. Non-linear relationship between equilibrium cellular Se concentrations in a marine diatom (*T. pseudonana*) and ambient selenite concentrations.

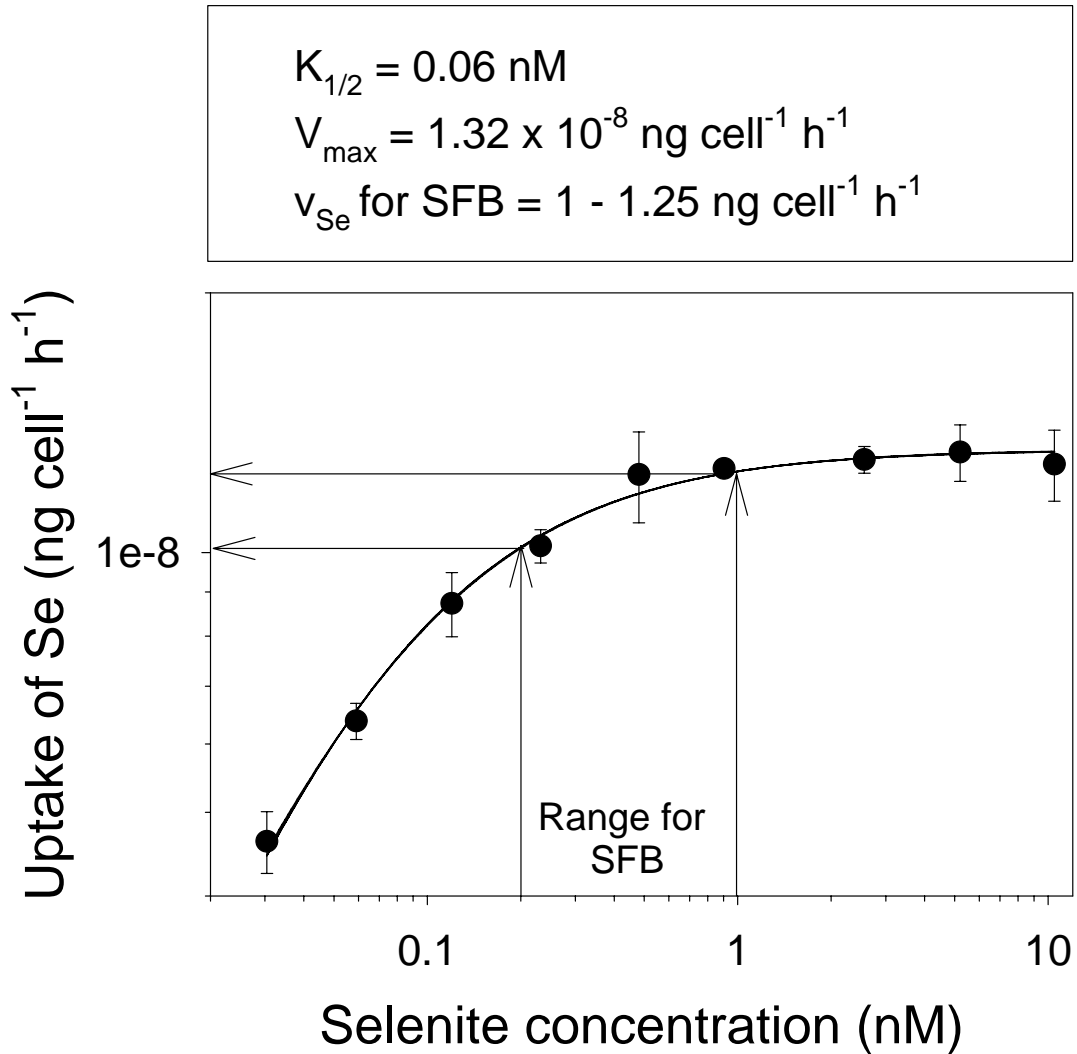


Figure SET15. Michaelis-Menten curve for selenite uptake by a freshwater diatom (*T. pseudonana*).

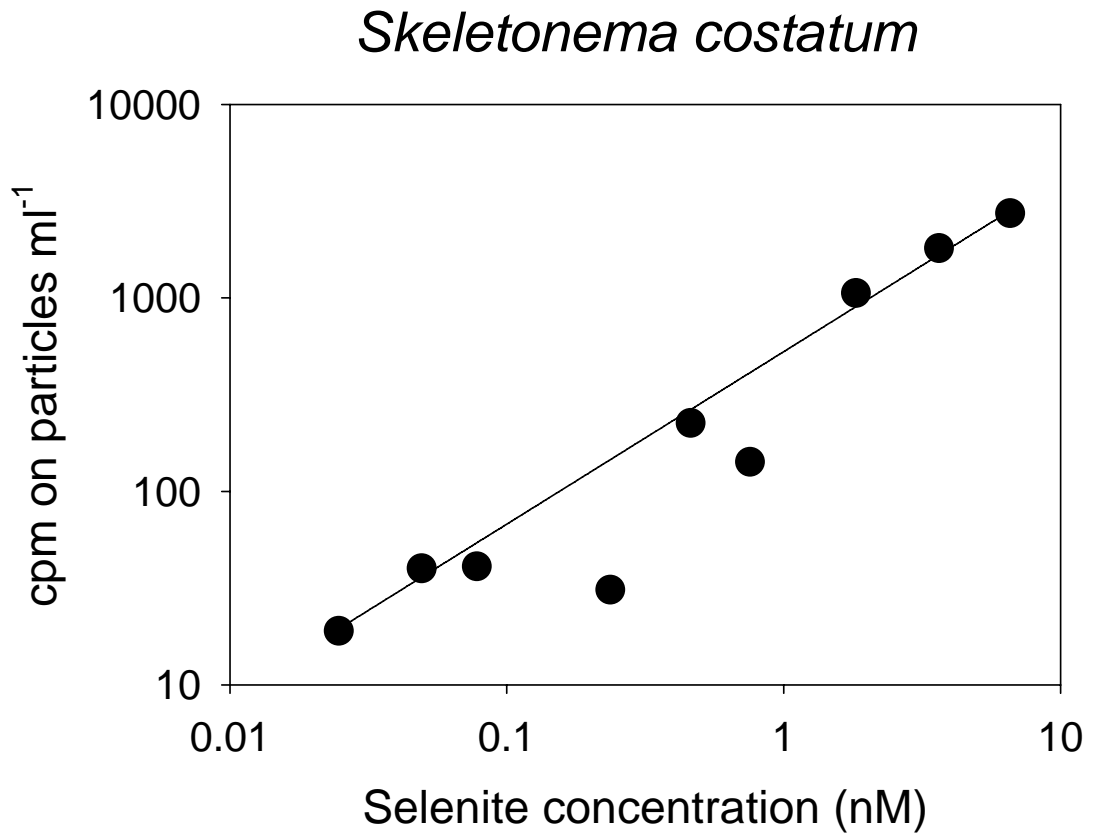


Figure SET16. Linear relationship between ambient selenite concentration and selenite uptake by the non-selenite accumulating freshwater diatom, *Skeletonema costatum*.

Thalassiosira pseudonana

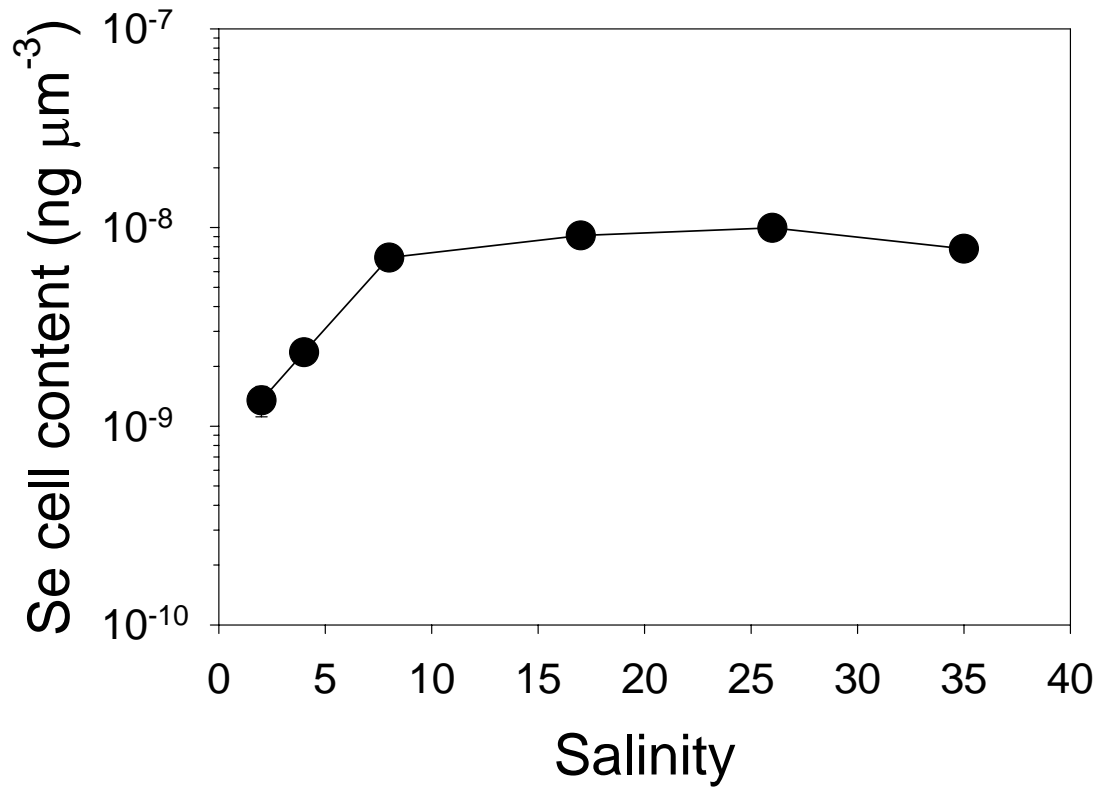


Figure SET17. Effect of ambient salinity on the uptake of selenite by the diatom *T. pseudonana*.

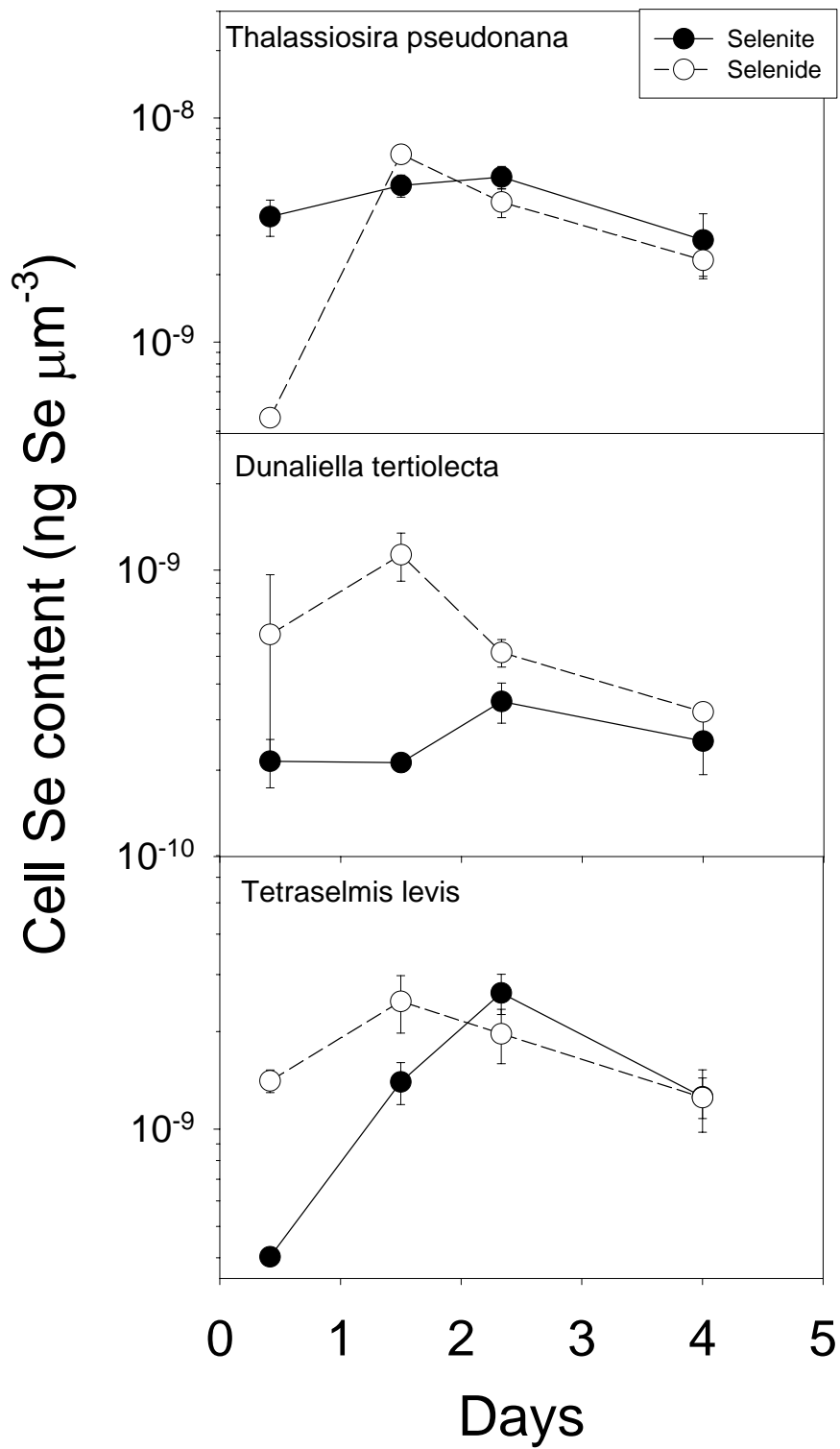


Figure SET18. Accumulation of radiolabeled lysates of *T. pseudonana* in cells of three species of marine phytoplankton.

Effect of Added Selenite on Selenide Uptake

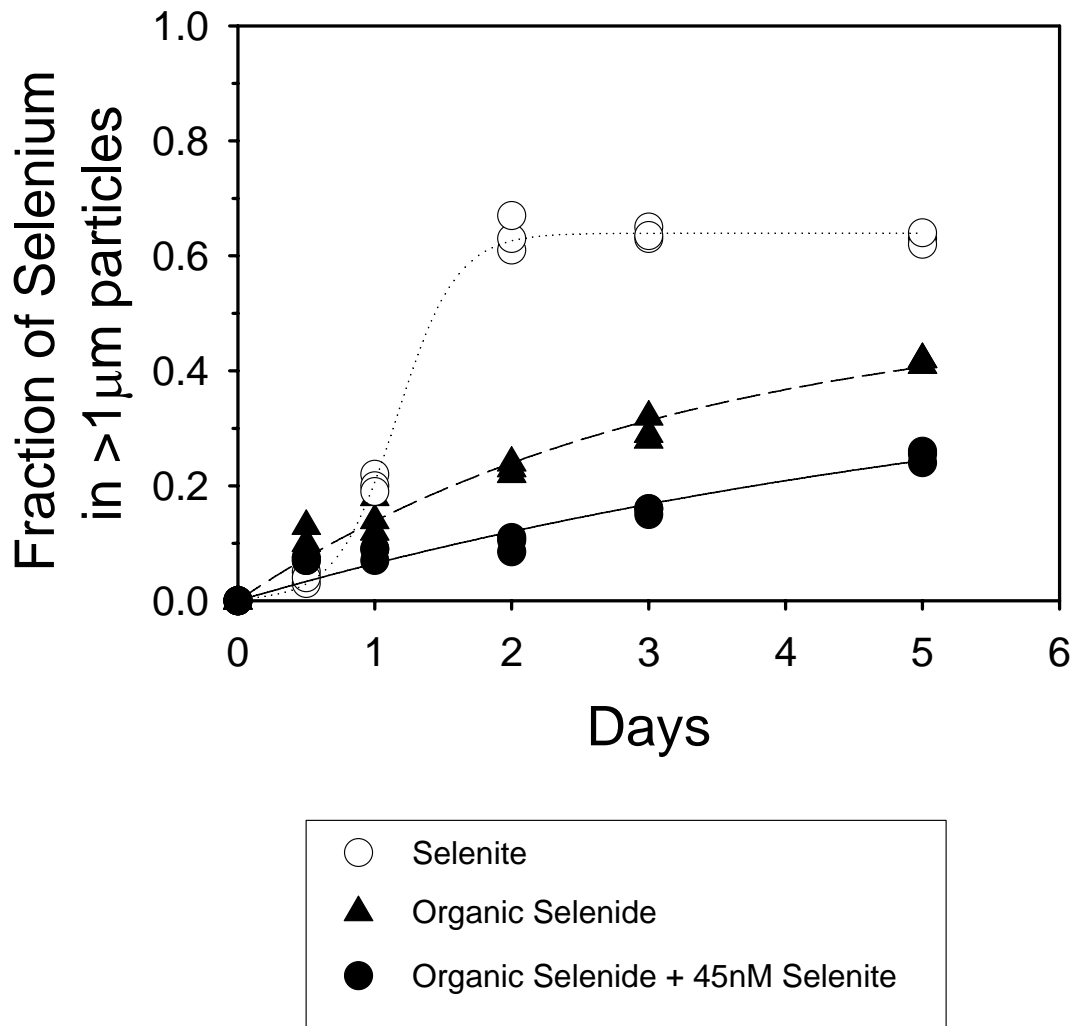


Figure SET19. Time series of radiolabeled lysate uptake by *T. pseudonana*.

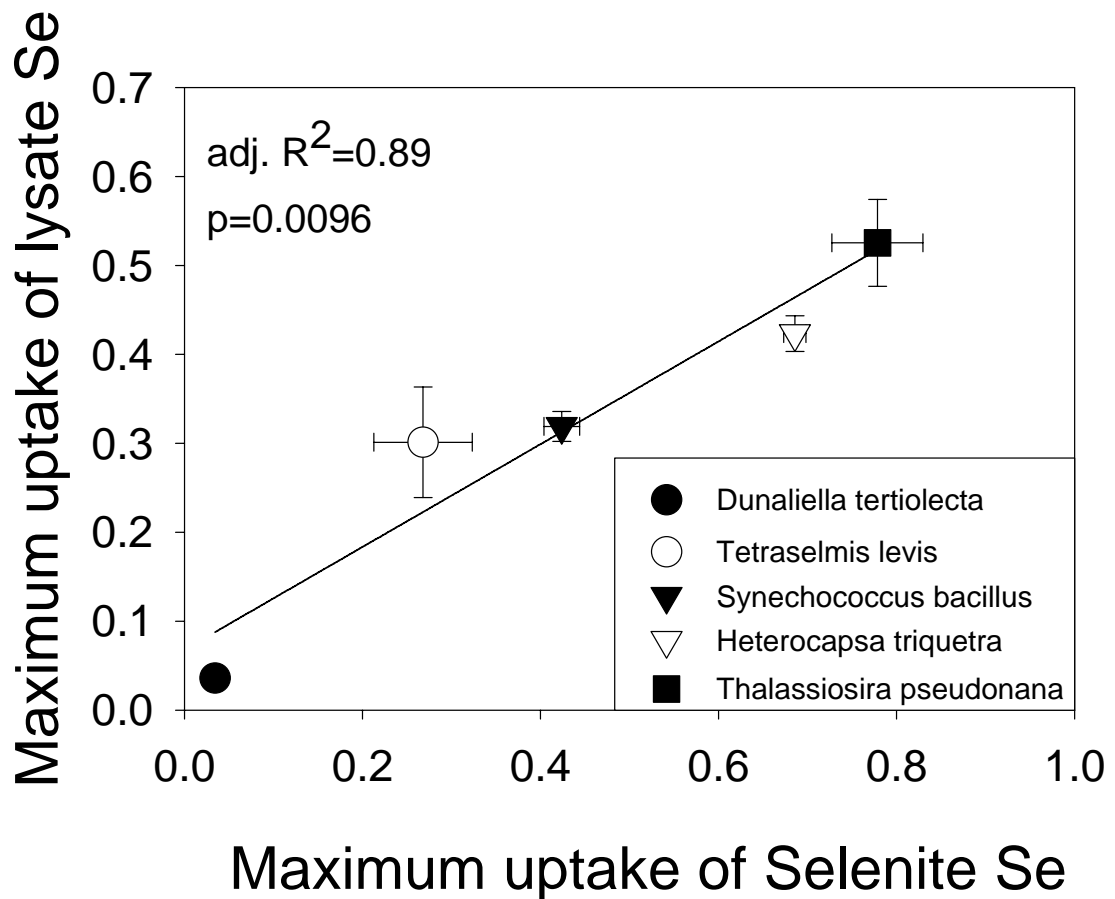


Figure SET20. Correlation between uptake of selenite and selenide by five marine phytoplankton species.

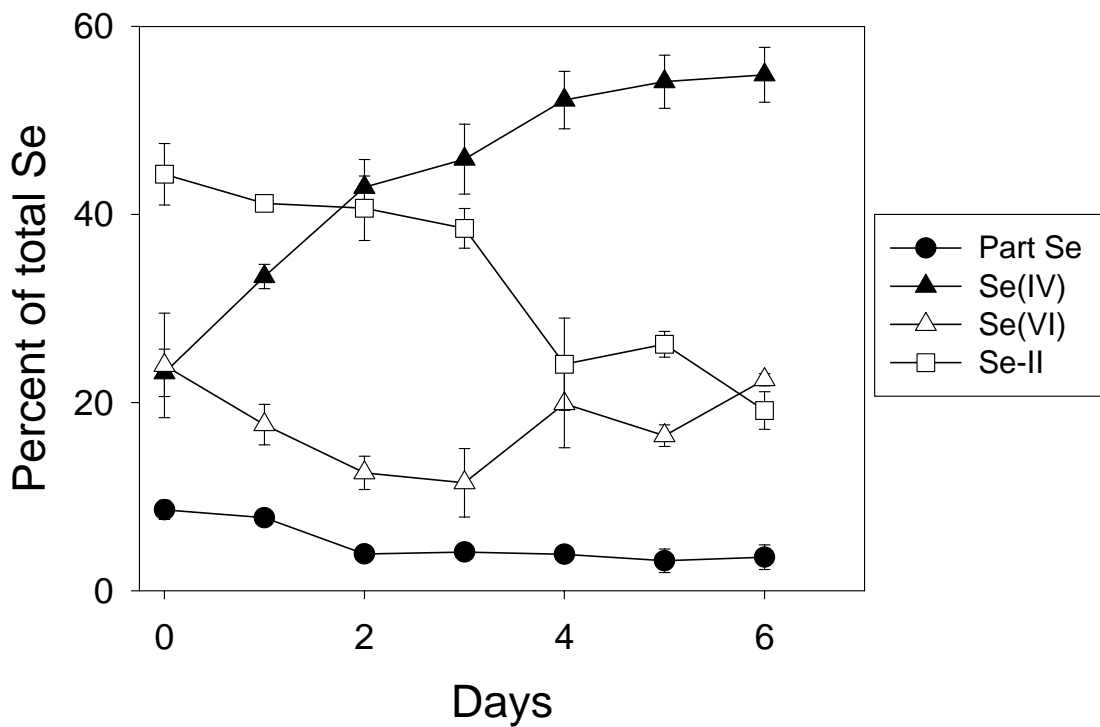


Figure SET21. Mineralization and accumulation of dissolved organic Se (Se-II) by marine bacteria.

Bacterial Uptake of Selenium from Lysates Effect of nutrients

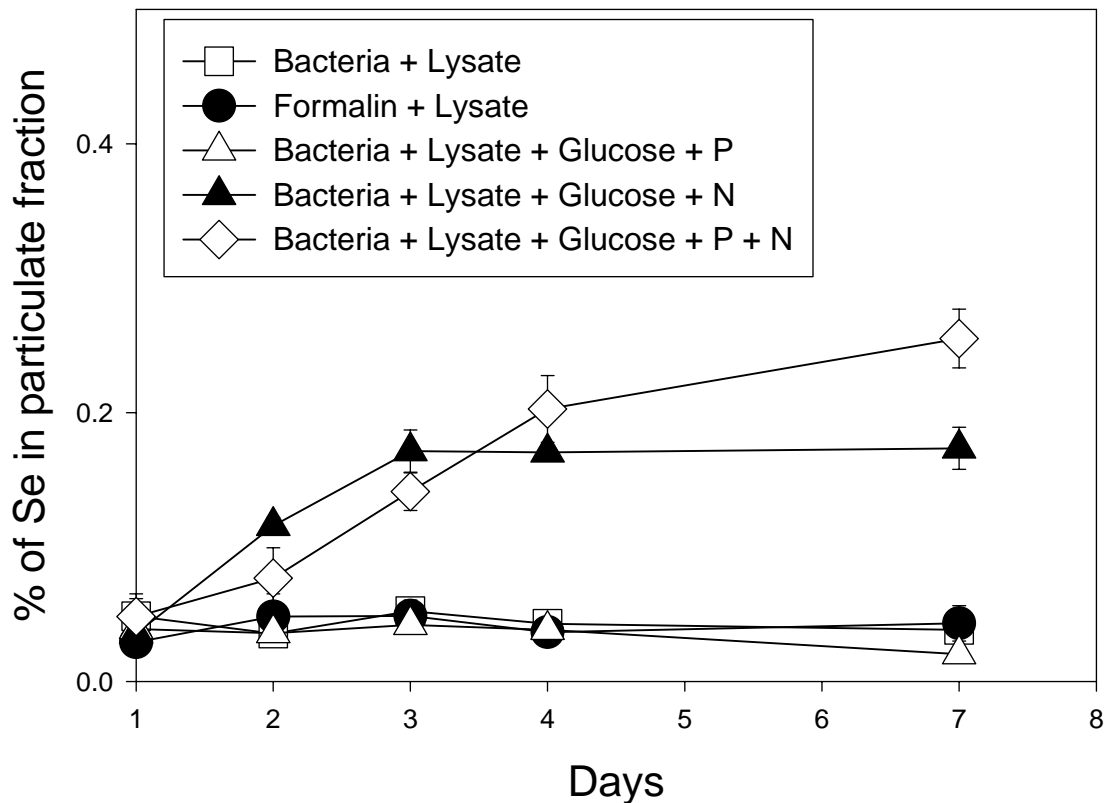


Figure SET22. Effect of ambient nutrients on uptake of radiolabeled lysates of the diatom *T. pseudonana* by marine bacteria.

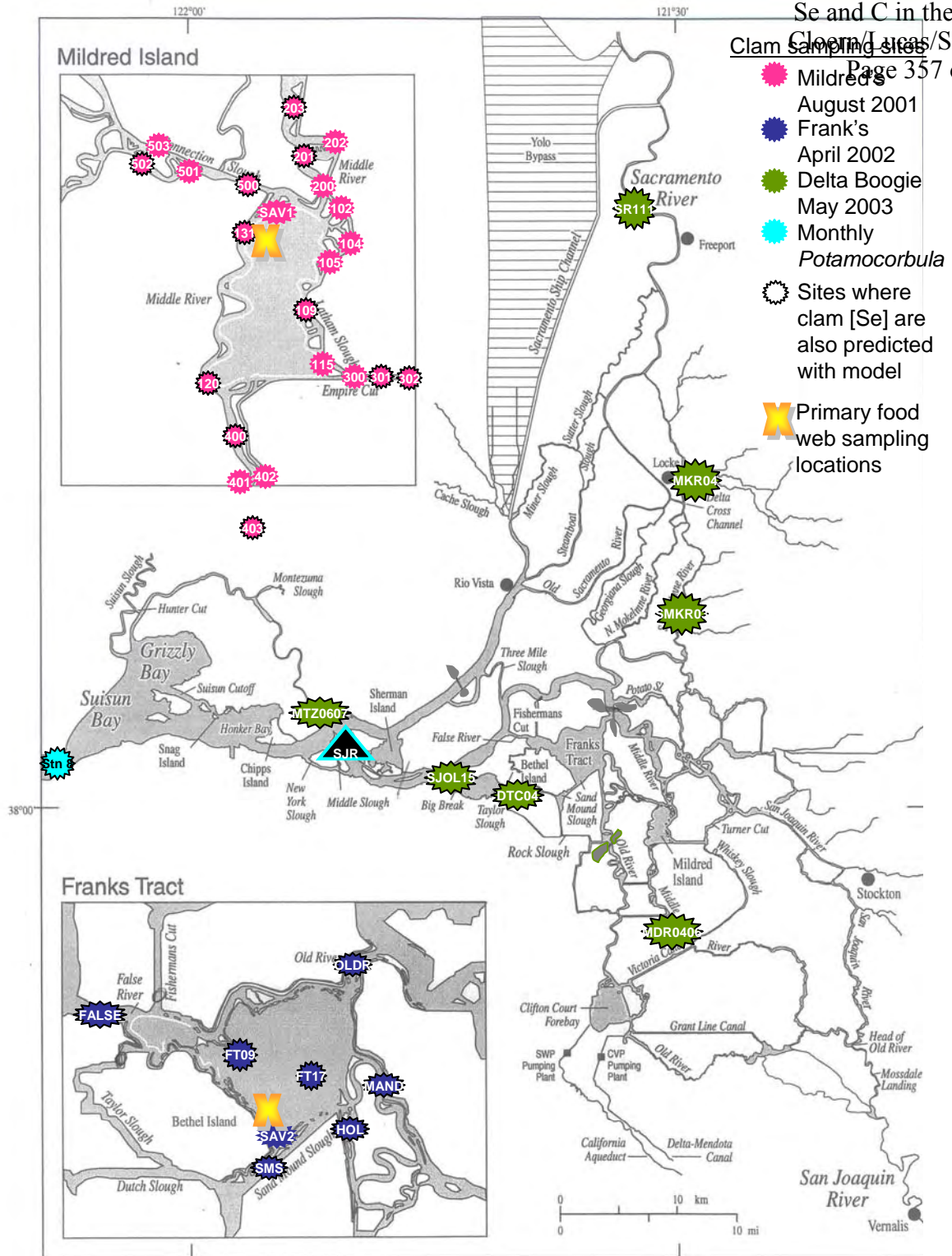


Figure SEF1. Locations and names of clam sampling sites for each of the spatially intensive field studies and primary locations of food web sampling sites in Mildred's Island and Frank's Tract.

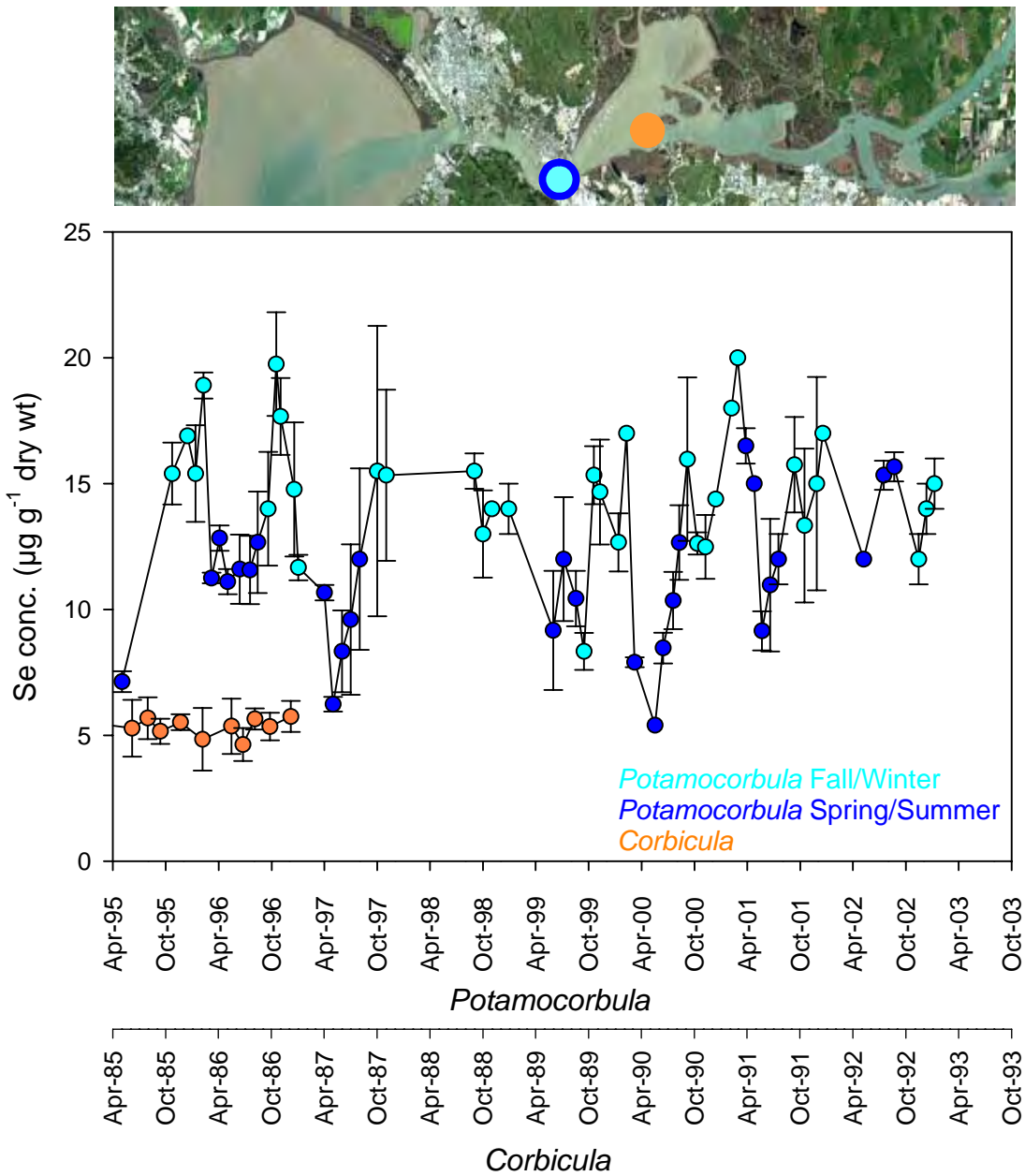


Figure SEF2. Seasonal trends in Se in *Potamocorbula amurensis* (1995 – 2003) and *Corbicula fluminea* (1985 – 1986) at USGS station 8 and Roe Island in Suisun Bay, respectively. Values are means \pm STD.

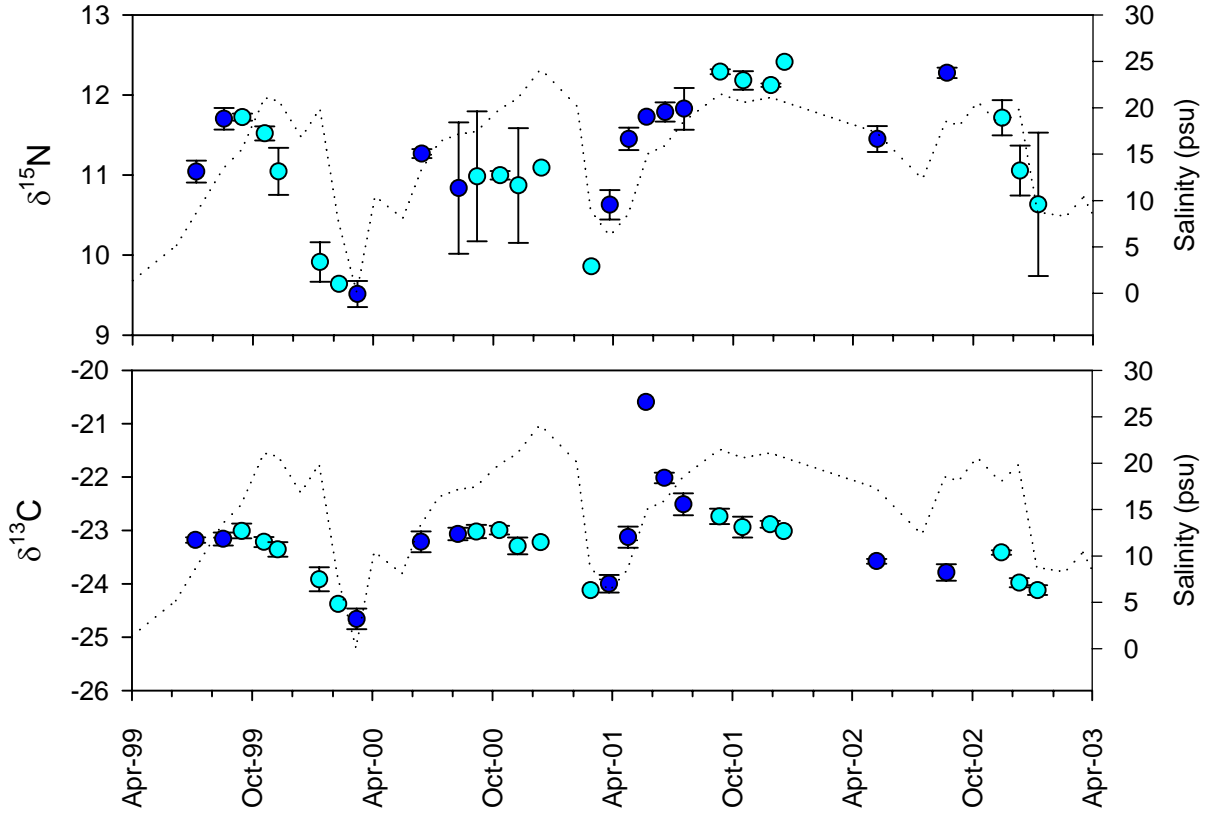


Figure SEF3. Seasonal trends in stable isotopes of carbon ($\delta^{13}\text{C}$) and nitrogen ($\delta^{15}\text{N}$) in the soft tissues of *Potamocorbula amurensis* (1999 – 2003) plotted with bottom salinity (psu) at USGS station 8 in Carquinez St.. Stable isotope values are means \pm STD.

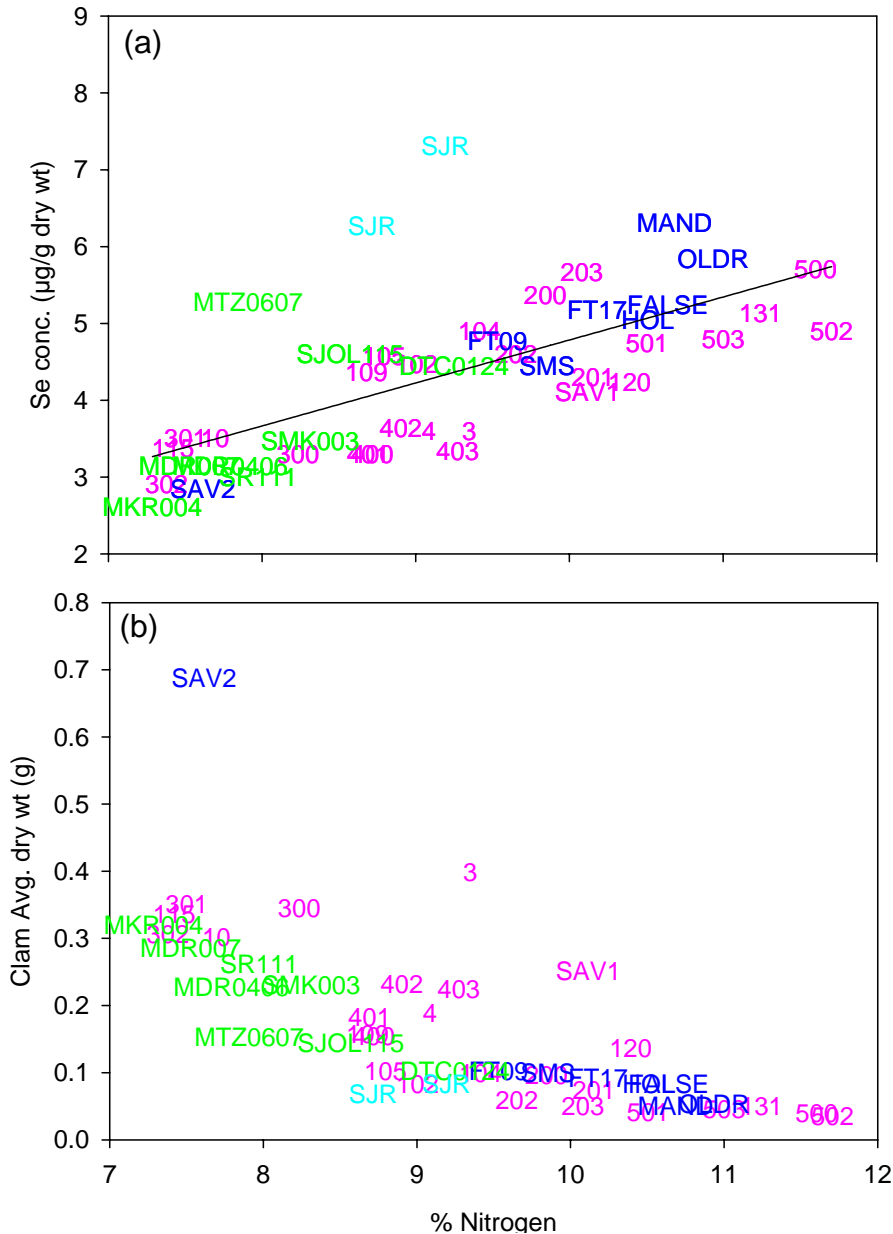


Figure SEF4. Relationship between (a) Se concentration ($\mu\text{g g}^{-1}$) and (b) Clam average dry wt (g) and nitrogen content (% by dry wt) of *Corbicula* collected at sites throughout the Delta between 2001 and 2004 and at overlap sites at the confluence of the San Joaquin and Sacramento Rivers. Values for *Corbicula* collected in September and October 2002 at the overlap site are also shown. Values are means of 3 replicate composites.

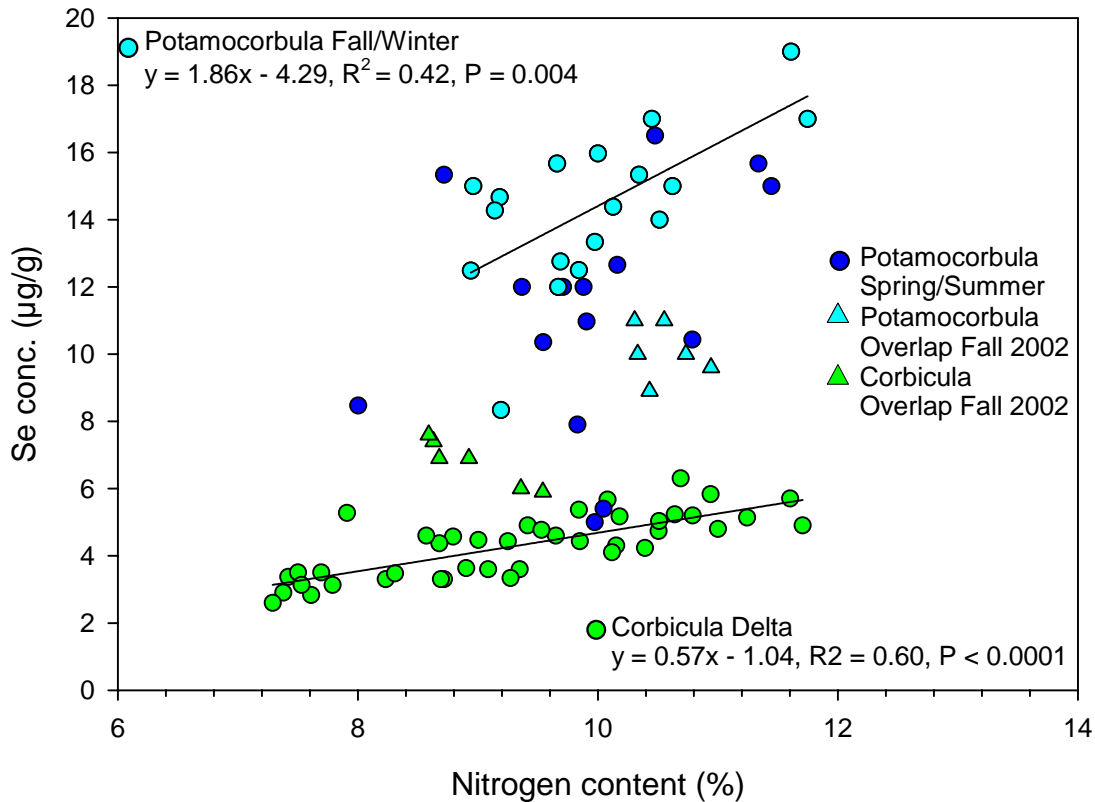


Figure SEF5. Relationship between Se concentration ($\mu\text{g g}^{-1}$) and nitrogen content (% by dry wt) of *Potamocorbula* collected monthly at USGS station 8 and *Corbicula* collected throughout the Delta between 2001 and 2004. Values for *Potamocorbula* and *Corbicula* collected in September and October 2002 at the overlap site are also shown. Values are means of 3 replicate composites.

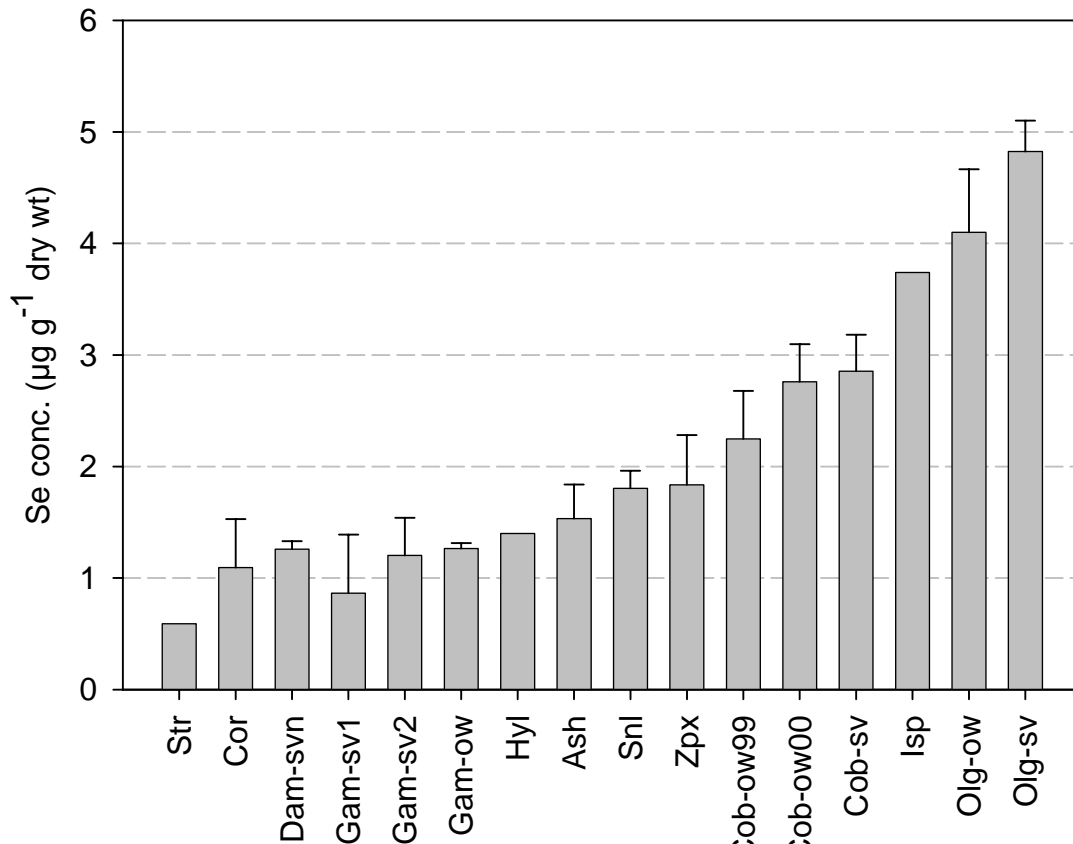


Figure SEF7. Selenium concentrations ($\mu\text{g g}^{-1}$ dry wt) in invertebrates from Mildred's Island. Values are means \pm STD. Str – Stratiomyidae, Cor – Corophium sp., Dam-svn – Damsel fly (collected from SAV in south Mildred's Island), Gam-sv1, Gam-sv2 and Gam-ow – Gammarus sp. (collected from SAV in northern Mildred's Island, southern Mildred's Island and southern opening of Mildred's Island), Hyl – Hyalella sp., Ash – Aeshnidae sp., Snl – planorbidae snail, Zpx – bulk zooplankton, Cob-ow99, Cob-ow00 and Cob-sv – Corbicula (collected at open water sites in 1999 and 2000 and in SAV in Mildred's Island), Isp – Isopod sp. and Olg-ow and Olg-sv – Oligochaete sp. (collected at open water sites and SAV).

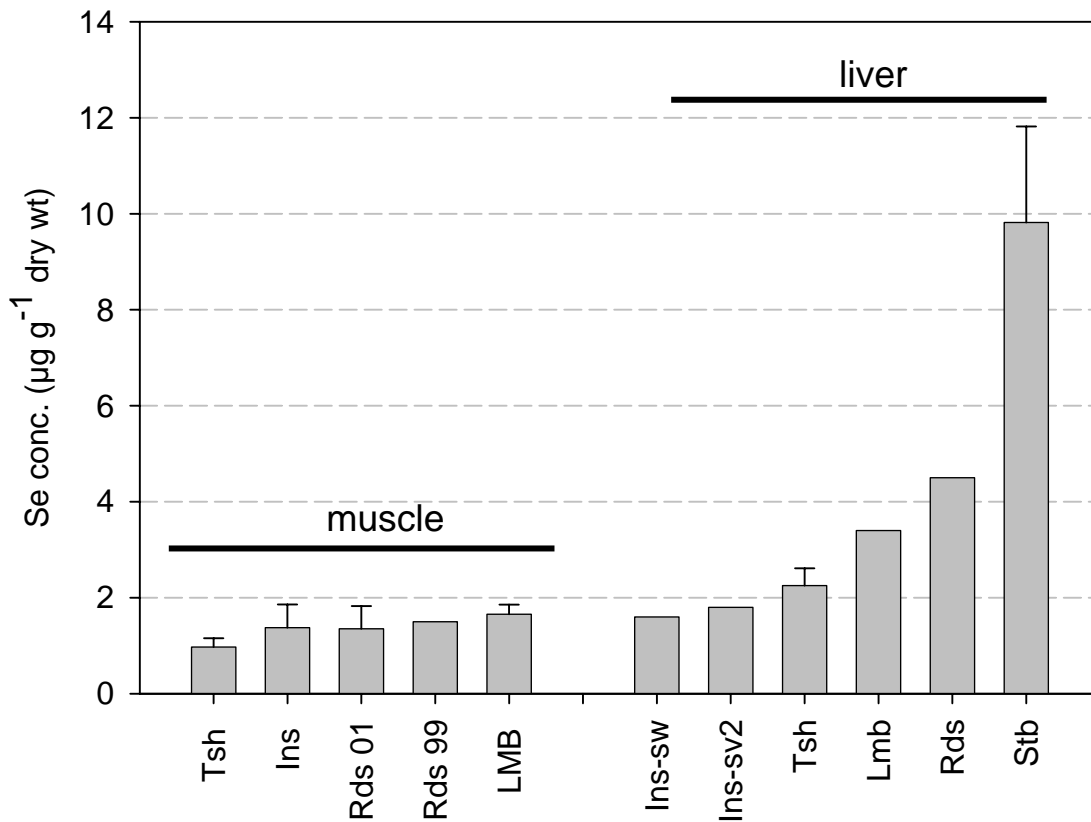


Figure SEF8. Selenium concentrations ($\mu\text{g g}^{-1}$ dry wt) in fish muscle and livers from Mildred's Island. Values are means \pm STD. Tsh – Threadfin shad, Ins – Inland silverside, Rds 01 and Rds 99 – Redear sunfish collected in 1999 and 2000, Lmb – Large mouth bass and Stb – striped bass.

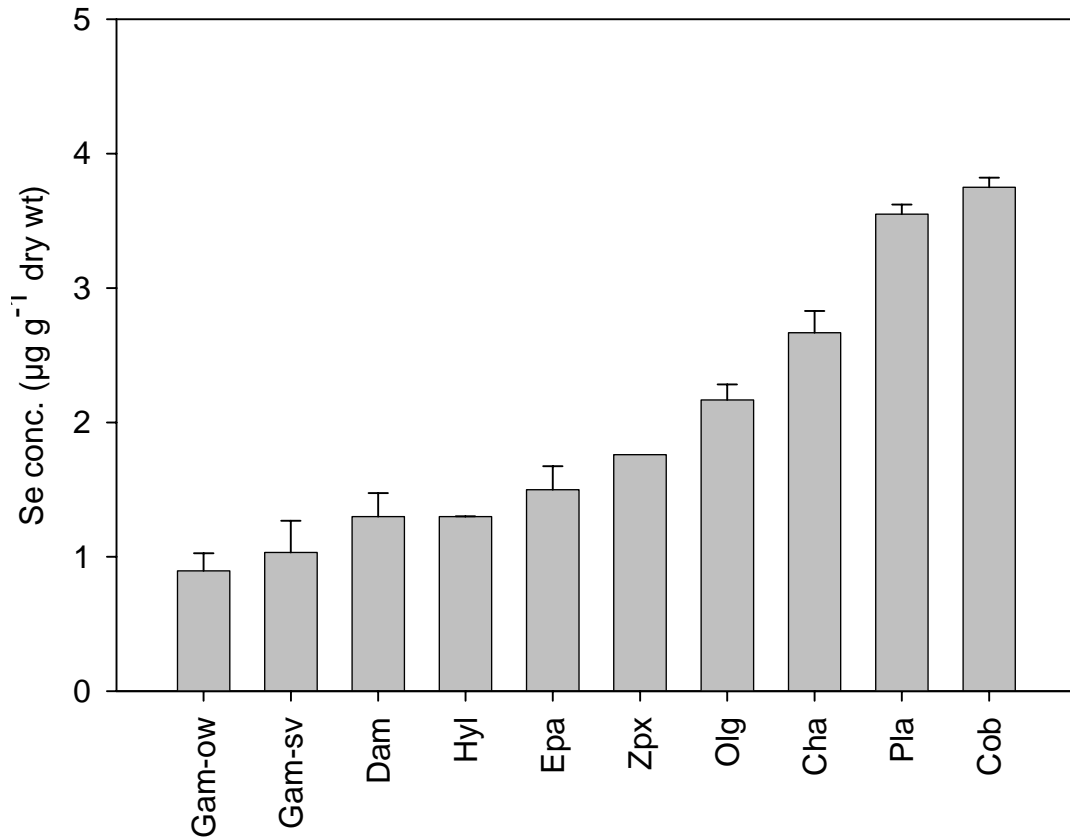


Figure SEF9. Selenium concentrations ($\mu\text{g g}^{-1}$ dry wt) in invertebrates from Frank's Tract. Values are means \pm STD. Gam-ow and Gam-sv (collected from open water and SAV), Dam – Damsel fly, Hyl – *Hyaella* sp., Epa – Epiphytic material (algae, bacteria, protozoans etc), Zpx – bulk zooplankton, Olg – Oligochaete sp., Cha – emerged chironomid larvae, Pla – *Planaria* sp., Cob – *Corbicula*.

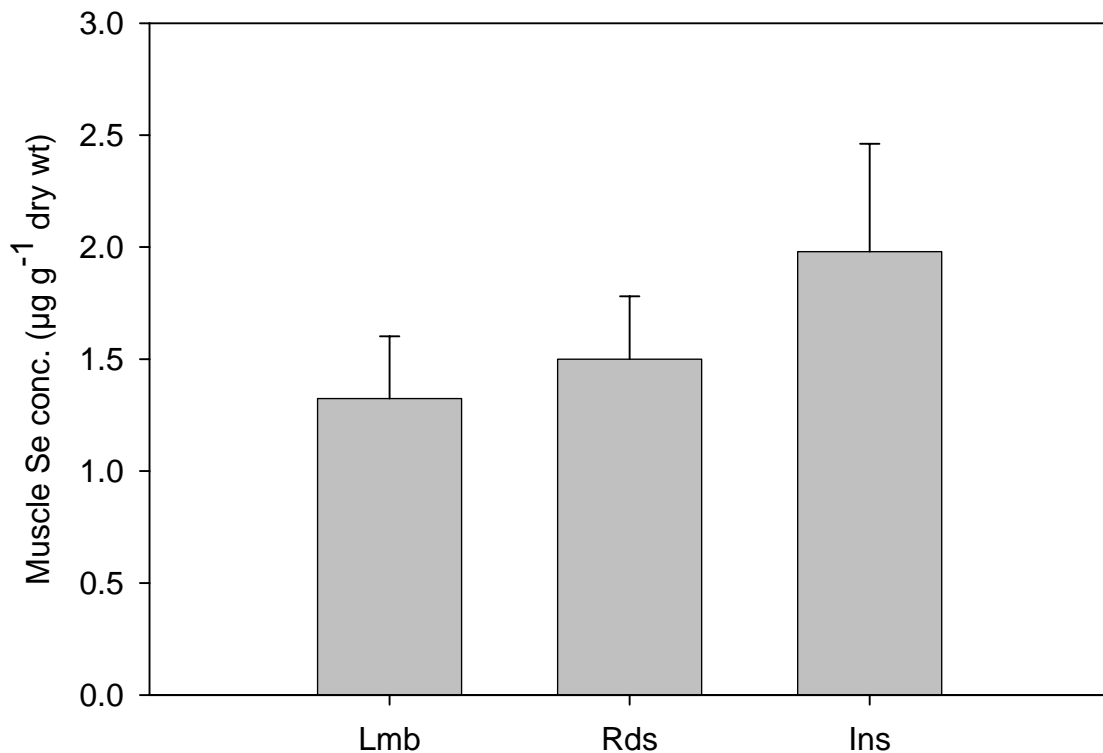


Figure SEF10. Selenium concentrations ($\mu\text{g g}^{-1}$ dry wt) in fish muscle from fish collected from Frank's Tract in April 2002. Values are means \pm STD. Lmb – Large mouth bass, Rds – Redear sunfish and Ins – Inland silverside.

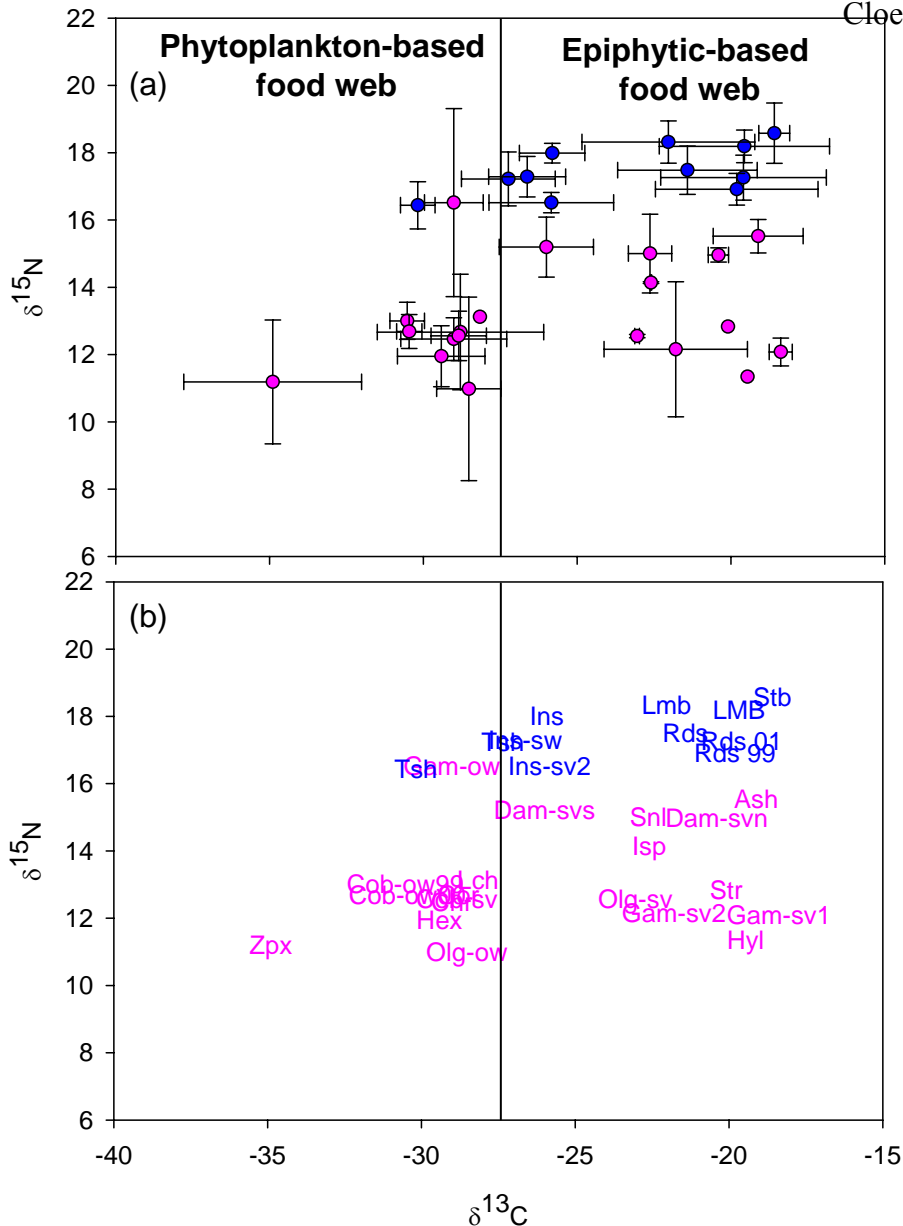


Figure SEF11. Stable isotope plot showing feeding relationships among fish and invertebrates of Mildred's Island. (a) Values are means \pm STD. (b) Species abbreviations represent sample means. Invertebrates shown in pink: Str – Stratiomyidae, Cor – Corophium sp., Dam-svn – Damsel fly (collected from SAV in south Mildred's Island), Gam-sv1, Gam-sv2 and Gam-ow – Gammarus sp. (collected from SAV in northern Mildred's Island, southern Mildred's Island and southern opening of Mildred's Island), Hyl – Hyalella sp., Ash – Aeshnidae sp., Snl – planorbidae snail, Zpx – bulk zooplankton, Cob-ow99, Cob-ow00 and Cob-sv – Corbicula (collected at open water sites in 1999 and 2000 and in SAV in Mildred's Island), Isp – Isopod sp. and Olg-ow and Olg-sv – Oligochaete sp. (collected at open water sites and SAV). Fish sp. shown in blue: Tsh – Threadfin shad, Ins – Inland silverside, Rds 01 and Rds 99 – Redear sunfish collected in 1999 and 2000, Lmb – Large mouth bass and Stb – striped bass.

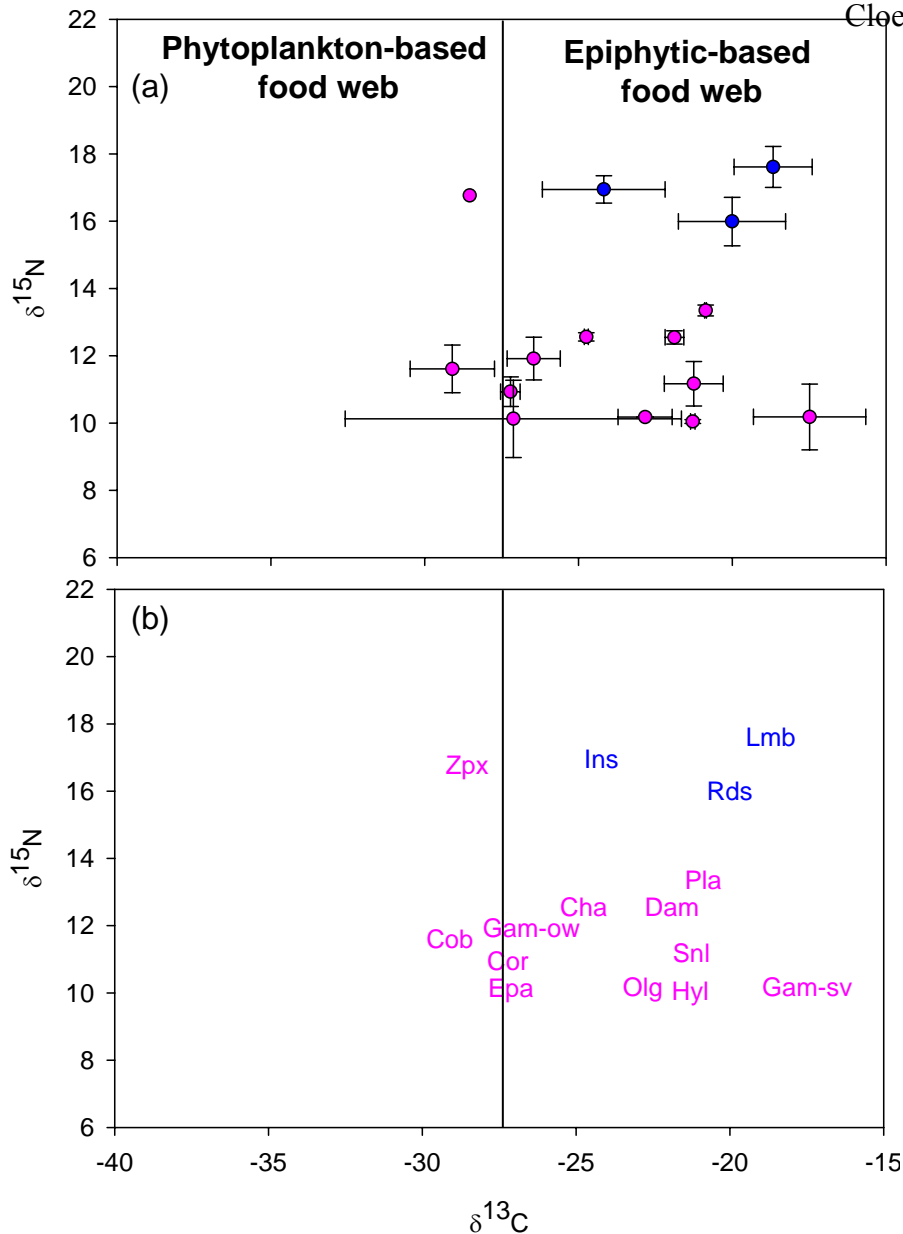


Figure SEF12. Stable isotope plot showing feeding relationships among fish and invertebrates of Frank's Tract. (a) Values are means \pm STD. (b) Species abbreviations represent sample means. Invertebrates shown in pink: Gam-ow and Gam-sv (collected from open water and SAV), Dam – Damsel fly, Hyl – *Hyaella* sp., Epa – Epiphytic material (algae, bacteria, protozoans etc), Zpx – bulk zooplankton, Olg – Oligochaete sp., Cha – emerged chironomid larvae, Pla – *Planaria* sp., Cob – *Corbicula*. Fish sp. shown in blue: Lmb – Large mouth bass, Rds – Redear sunfish and Ins – Inland silverside.

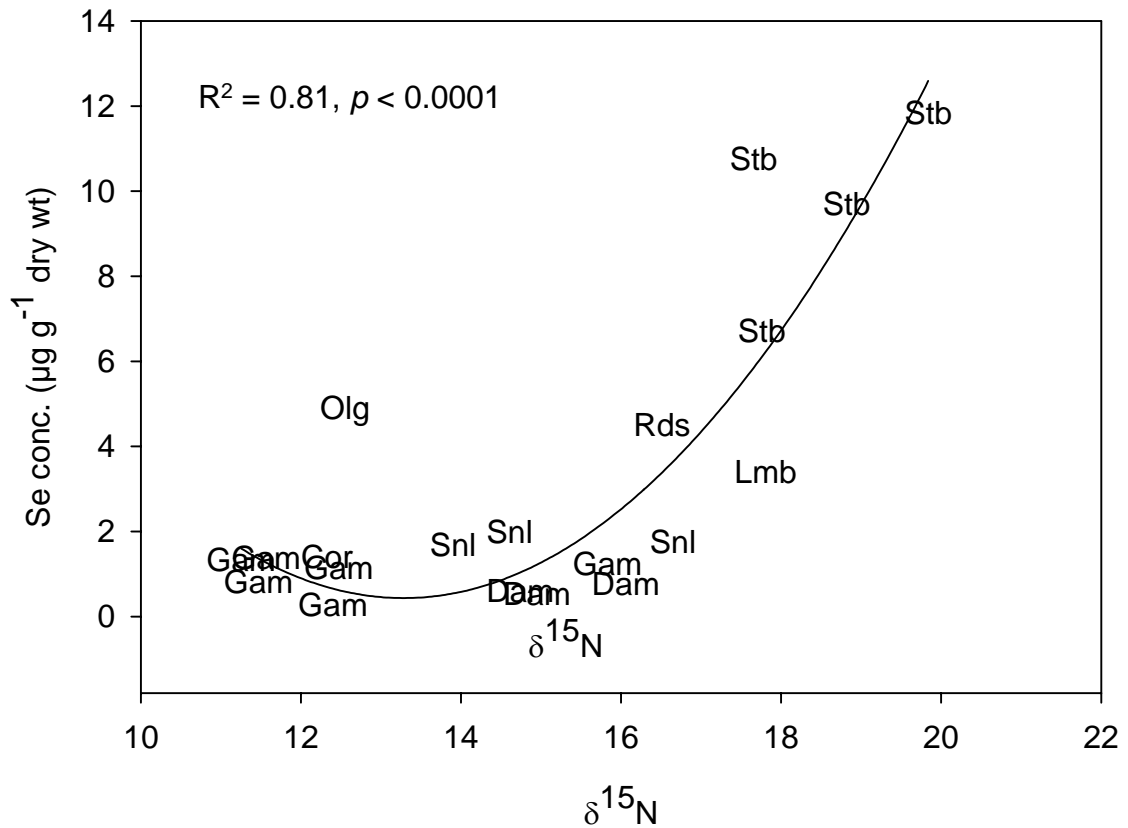


Figure SEF13. Selenium concentrations in the epiphytic-based food web of Mildred's Island (i.e. organisms with $\delta^{13}\text{C}$ values greater than -27‰) Species abbreviations represent sample means. Gam – Gammarus sp., Dam – Damsel fly, Olg – Oligochaete sp., Sni – Planorbidae sp., Lmb – Large mouth bass, Rds – Redear sunfish and Stb – Striped bass. Oligochaete is not included in fitted curve since it is rarely a component of the fish diets.

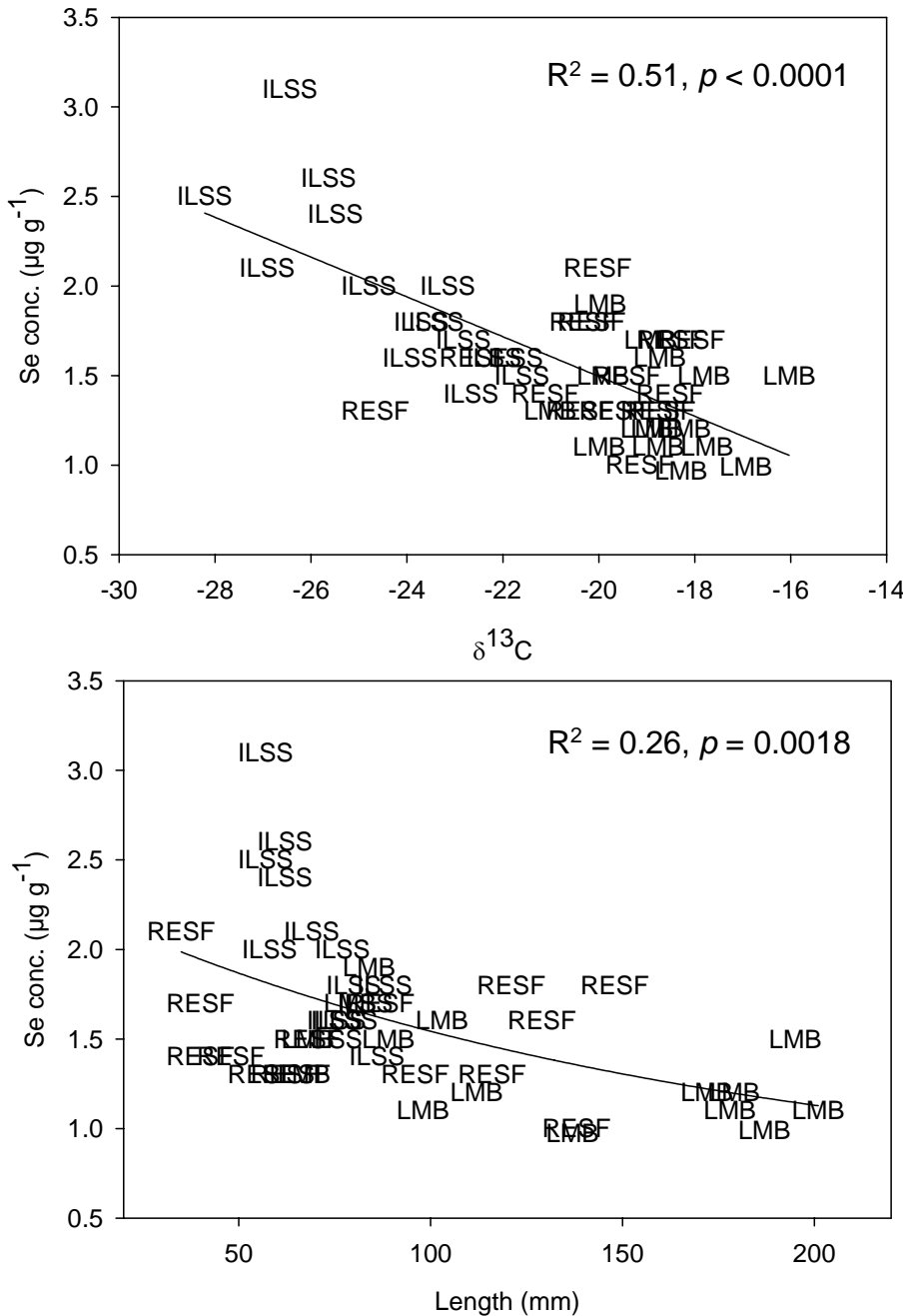


Figure SEF14. Selenium concentrations in Frank's Tract fish as a function of (a) $\delta^{13}\text{C}$ and (b) Length (mm). ILSS – Inland silversides, RESF – Redear sunfish, LMB – Large mouth bass.

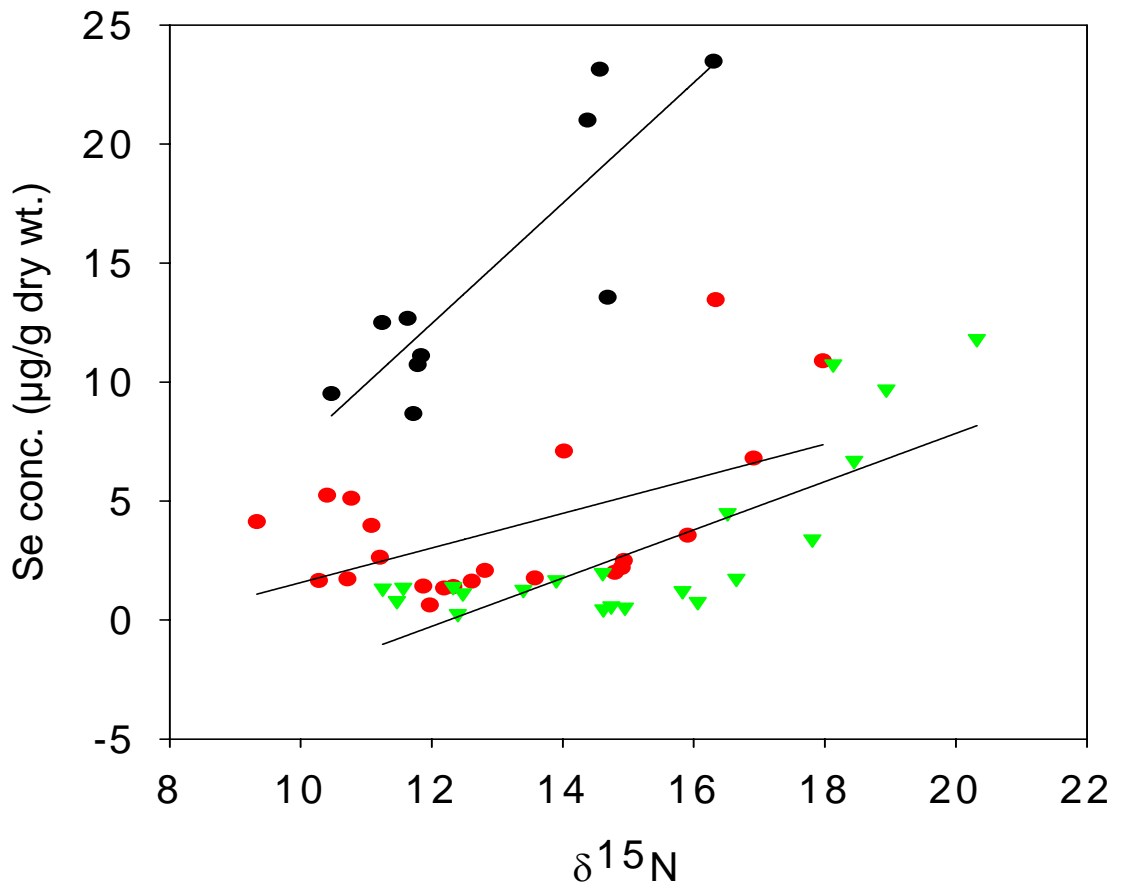


Figure SEF15. Selenium concentrations in organisms in a clam-based food web (black) and crustacean-based food web (red) of San Francisco Bay and in a crustacean-based food web (green) from Mildred's Island in the Delta.

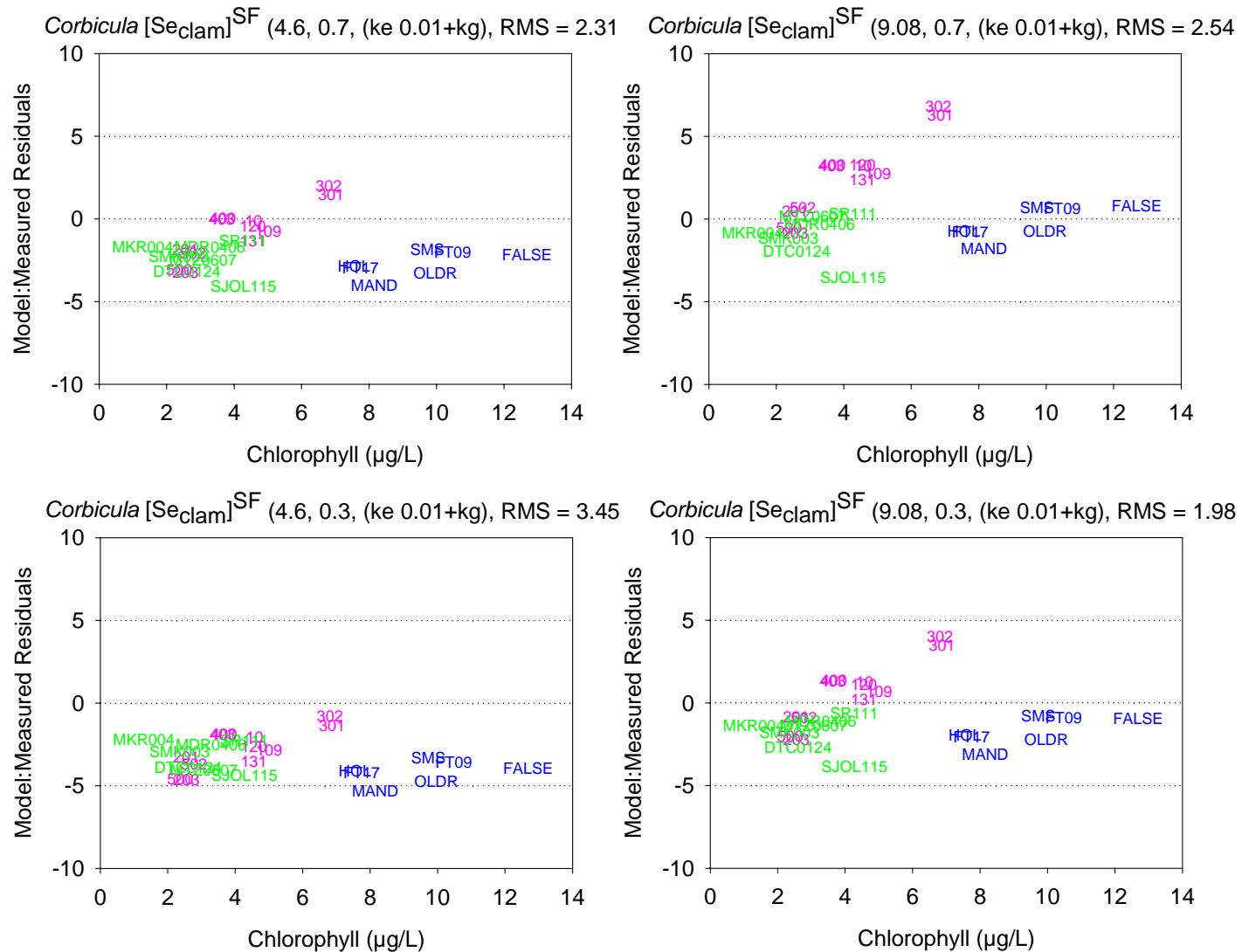


Figure SEF16. *Corbicula* Se model calculated using IR_{PRCOM} plotted against chlorophyll ($\mu\text{g L}^{-1}$). Values are residuals of model – measured Se concentrations in clams ($\mu\text{g g}^{-1}$ dry wt) at individual sites sampled during the Mildred Island Process study (n = 12, August 29, 2001), Frank’s Tract Boogie (n = 7, April 1, 2002) and Delta Boogie (n = 7, May 12, 2003).

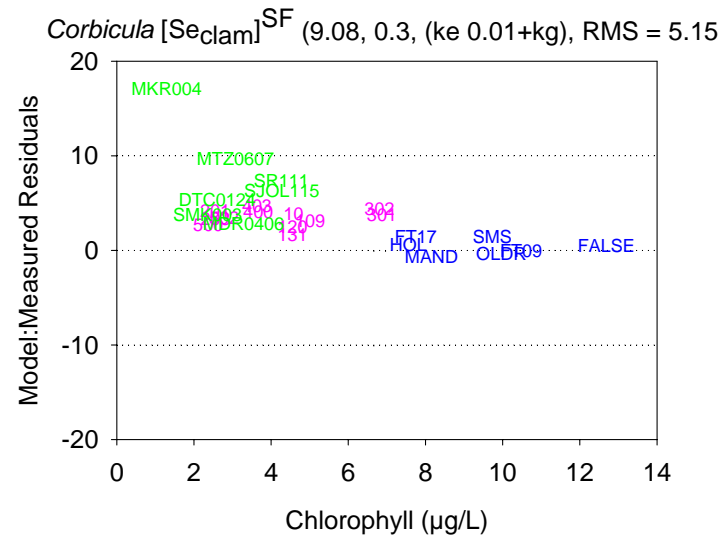
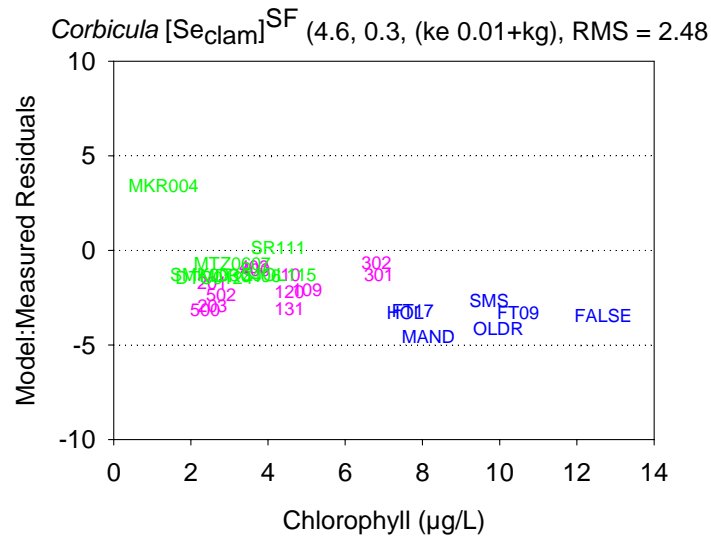
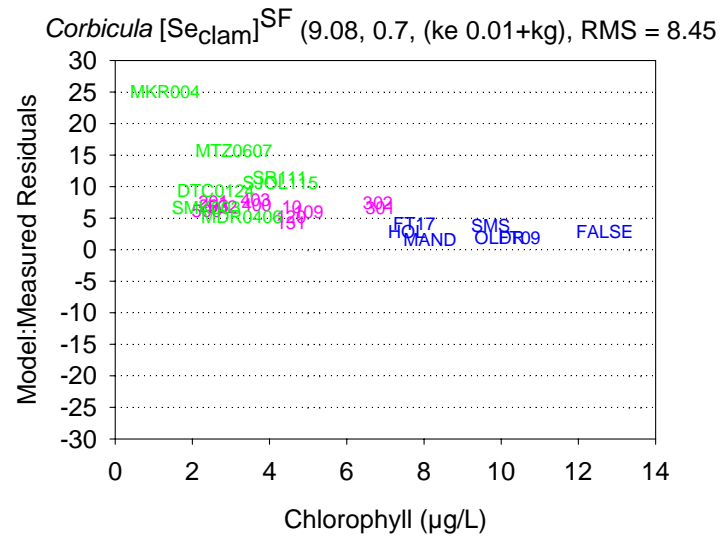
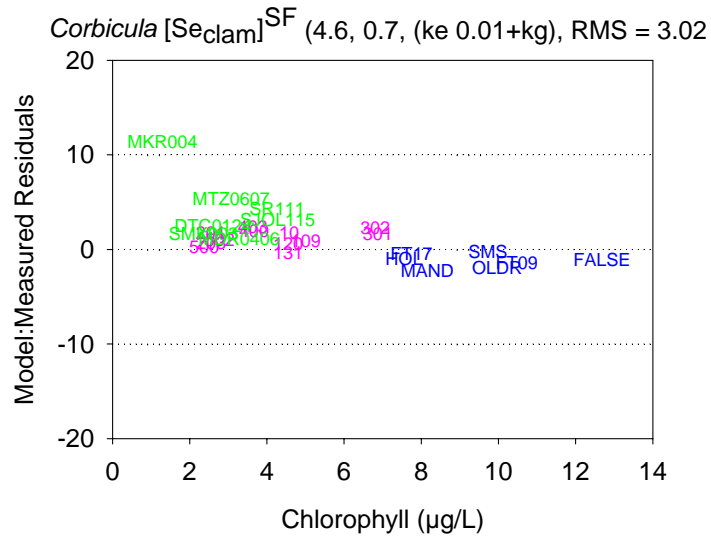


Figure SEF17. *Corbicula* Se model calculated using IR_{SPM} plotted against chlorophyll (µg L⁻¹). Values are residuals of model – measured Se concentrations in clams (µg g⁻¹ dry wt) at individual sites sampled during the Mildred Island Process study (n = 12, August 29, 2001), Frank’s Tract Boogie (n = 7, April 1, 2002) and Delta Boogie (n = 7, May 12, 2003).

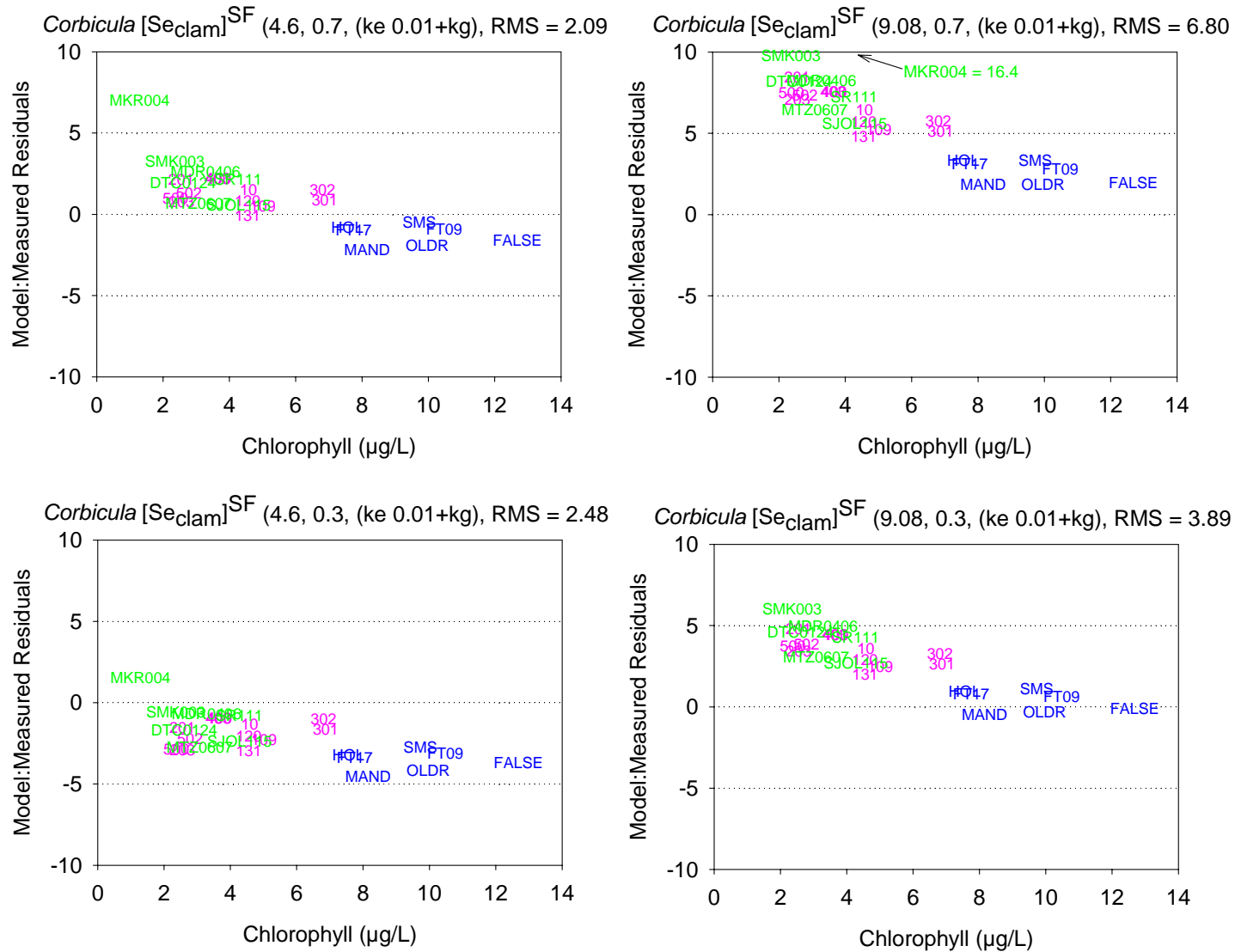
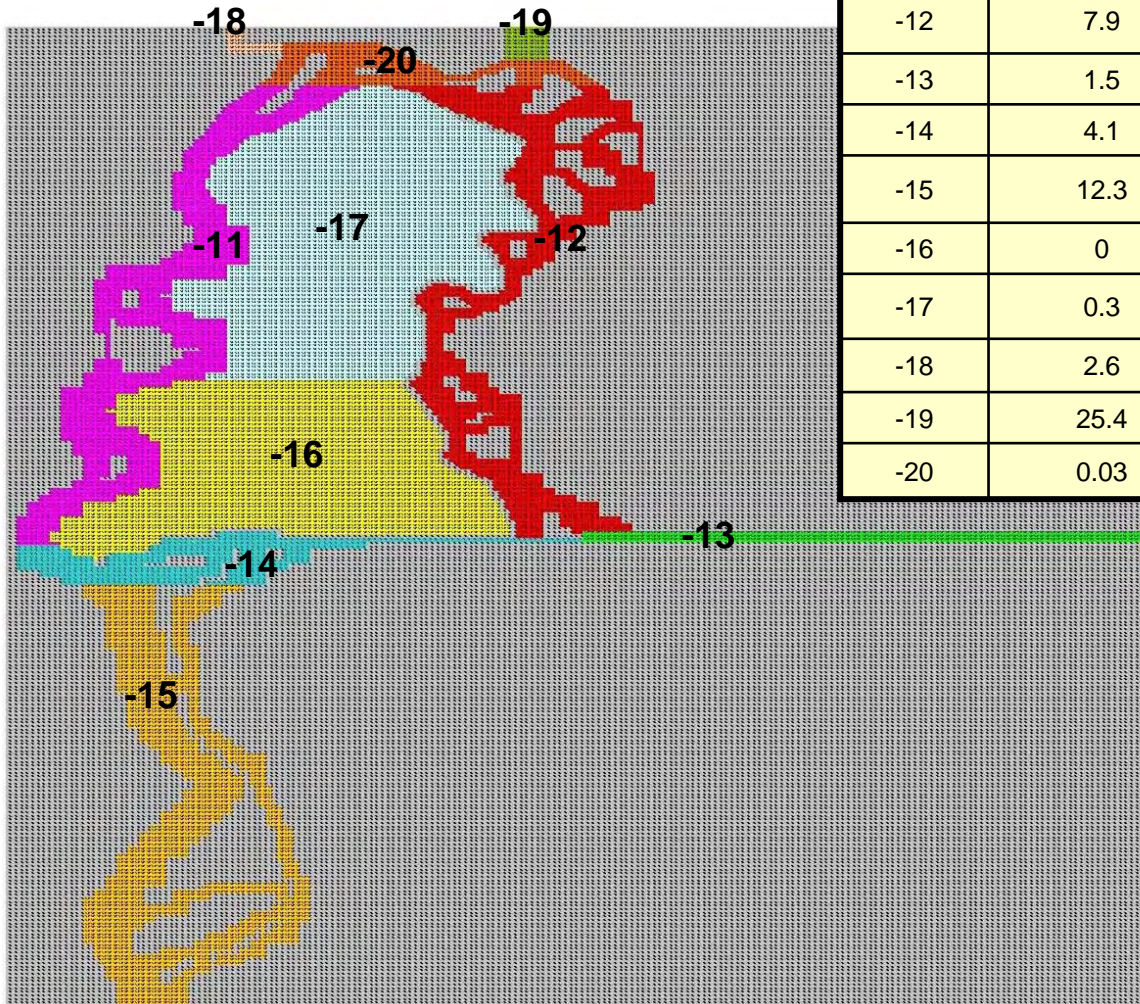


Figure SEF18. *Corbicula* Se model calculated using IR_{SPM} plotted against chlorophyll ($\mu\text{g L}^{-1}$). Values are residuals of model – measured Se concentrations in clams ($\mu\text{g g}^{-1}$ dry wt) at individual sites sampled during the Mildred Island Process study ($n = 12$, August 29, 2001), Frank’s Tract Boogie ($n = 7$, April 1, 2002) and Delta Boogie ($n = 7$, May 12, 2003).



Area #	Benthic Grazing (m3/m2/day)	Light Extinction Coefficient (1/m)	Zooplankton Grazing (1/day)
-11	3.8	1.4	0.2
-12	7.9	1.5	0.2
-13	1.5	2.1	0.1
-14	4.1	1.7	0.2
-15	12.3	1.5	0.3
-16	0	2.3	0.1
-17	0.3	1.5	0.1
-18	2.6	1.4	0.1
-19	25.4	1.3	0.3
-20	0.03	1.4	0.2

Figure ML1. Model domain for TRIM-MILLIE coupled model. Color-coded regions represent areas with distinct combinations of input parameters for the biological model.

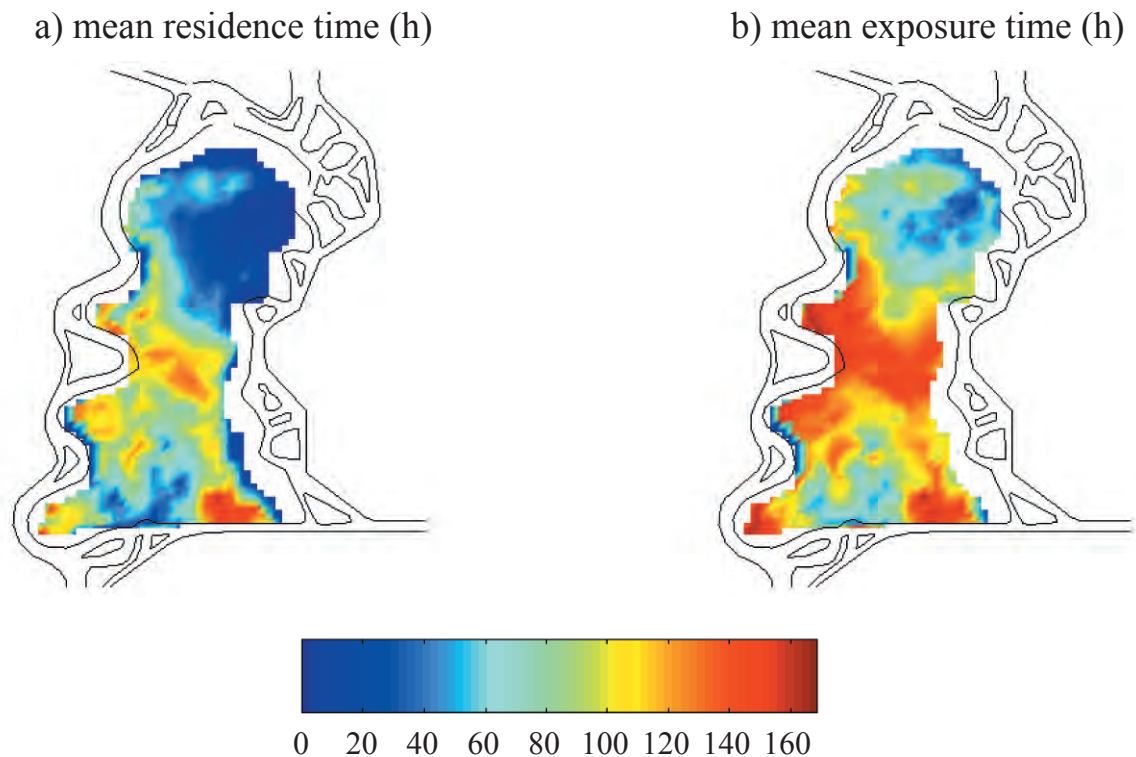


Figure ML2. (a) Mean residence time and (b) mean exposure time for June 1999. The mean reflects the average value at each particle release point for 24 different simulations. The maximum time of 168 h reflects the end of the simulation rather than the maximum residence or exposure time. Exposure is the measure of the total time a particle spends inside the boundaries of MI during the simulation, whereas residence time reflects the time the particle stayed in the domain before exiting once.

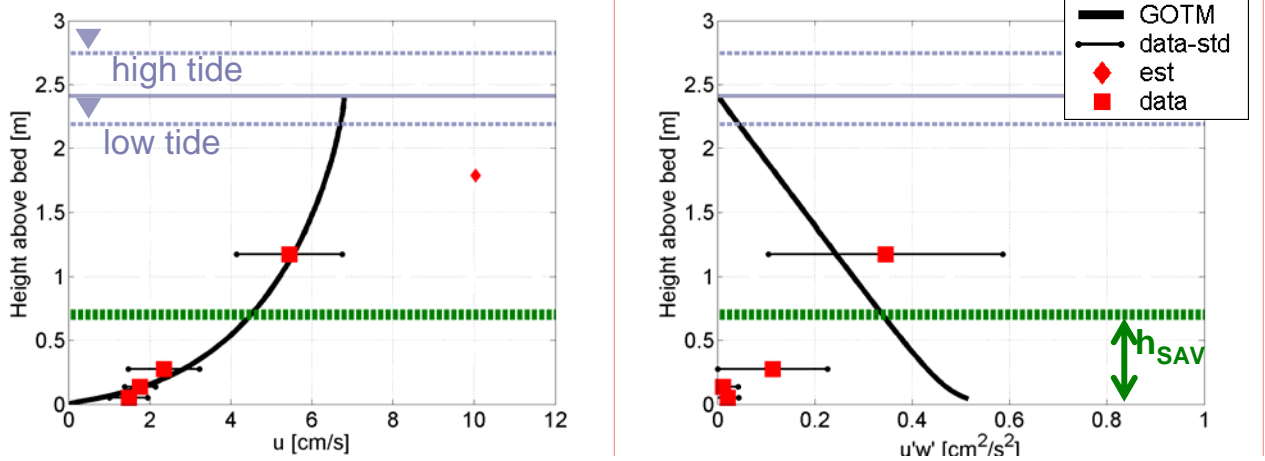


Figure ML3. Comparison of Franks Tract observations and numerical water column model for (a) Mean Velocity; and (b) Turbulent Stresses. The model presented here uses only a bed drag coefficient to represent the frictional effects of vegetation.

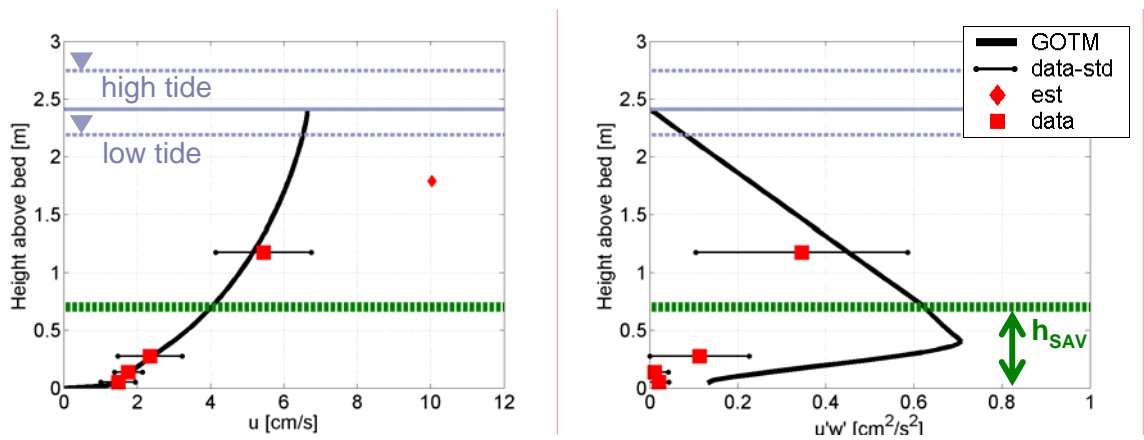


Figure ML4. Modeled velocity and turbulent stress structure using distributed, vegetative drag parameterization. “GOTM” is the model calculations, while the data are represented by the red squares.

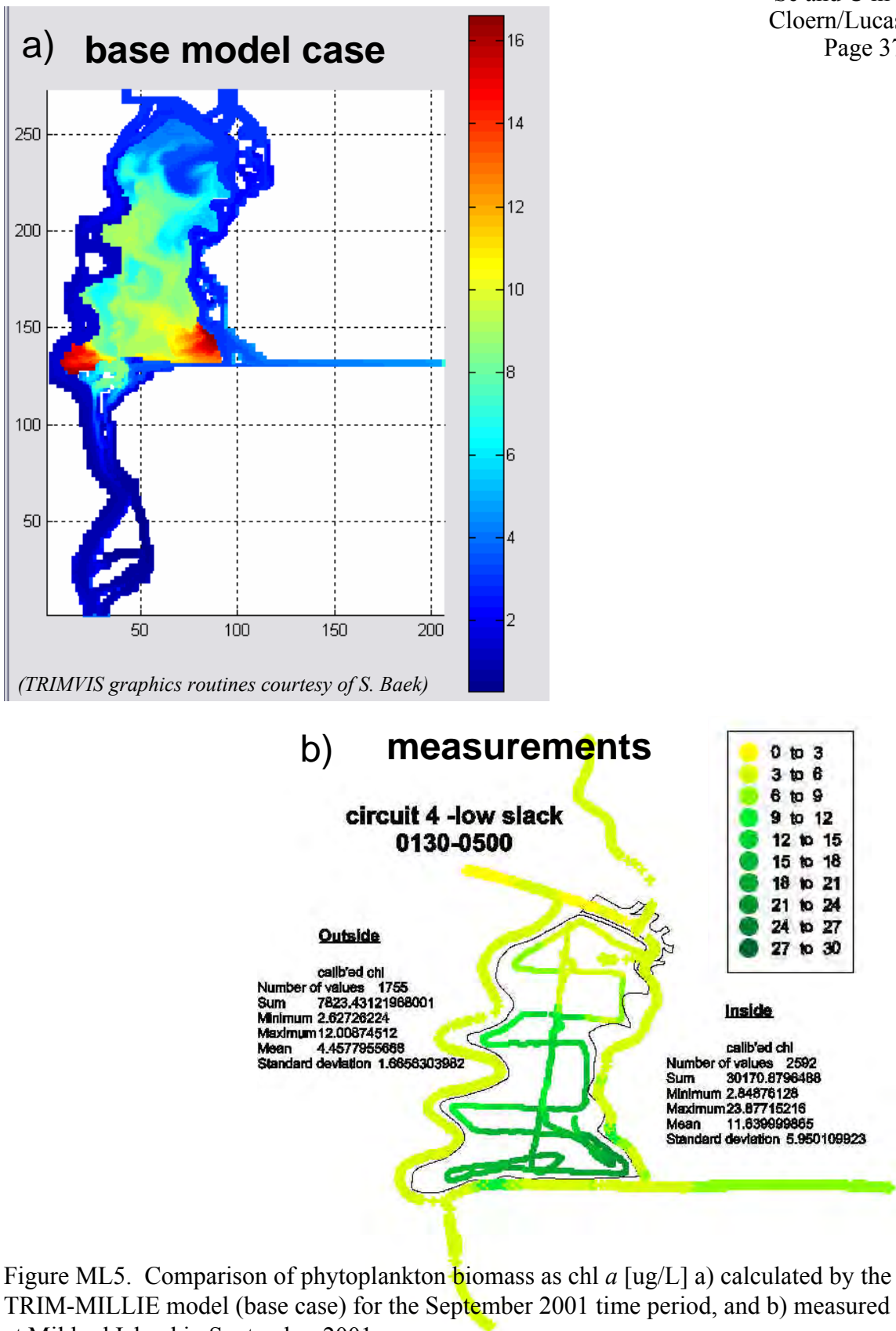


Figure ML5. Comparison of phytoplankton biomass as chl *a* [ug/L] a) calculated by the TRIM-MILLIE model (base case) for the September 2001 time period, and b) measured at Mildred Island in September 2001.

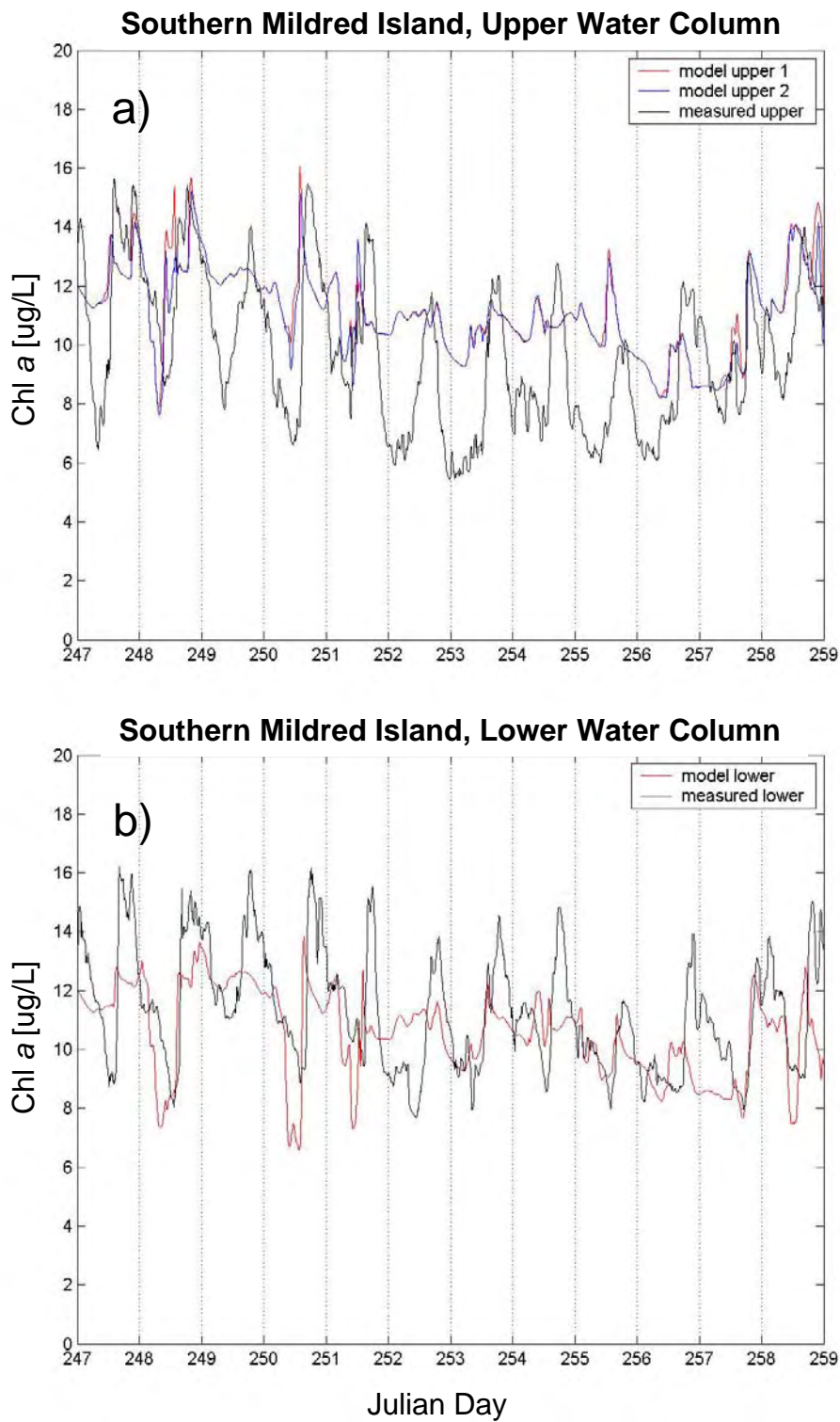


Figure ML6. Comparison of calculated and measured chl *a* time series for southern Mildred Island, September 2001. Calculations are made by TRIM-MILLIE model

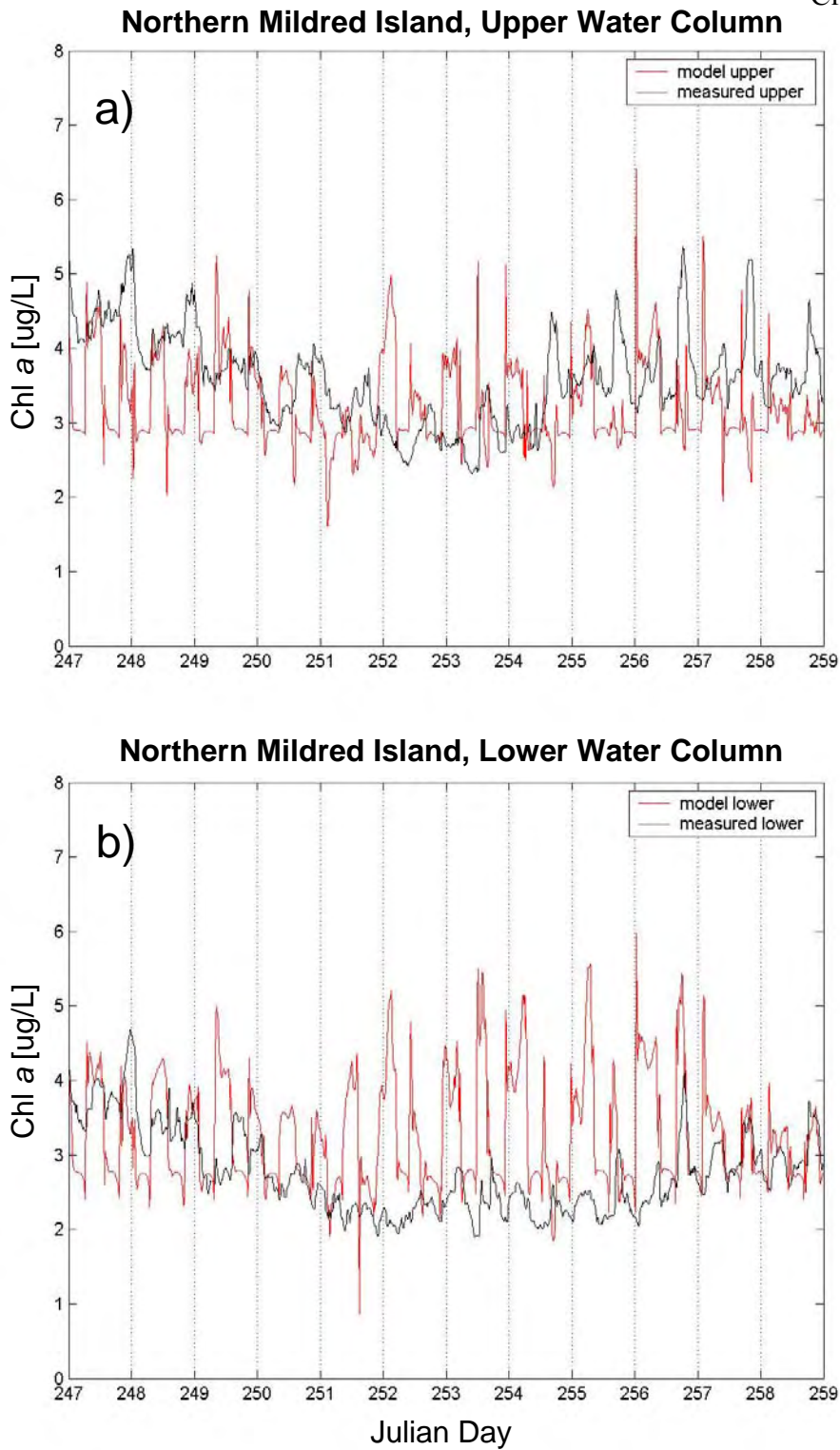


Figure ML7. Comparison of calculated and measured chl *a* time series for northern Mildred Island, September 2001. Calculations are made by TRIM-MILLIE model.

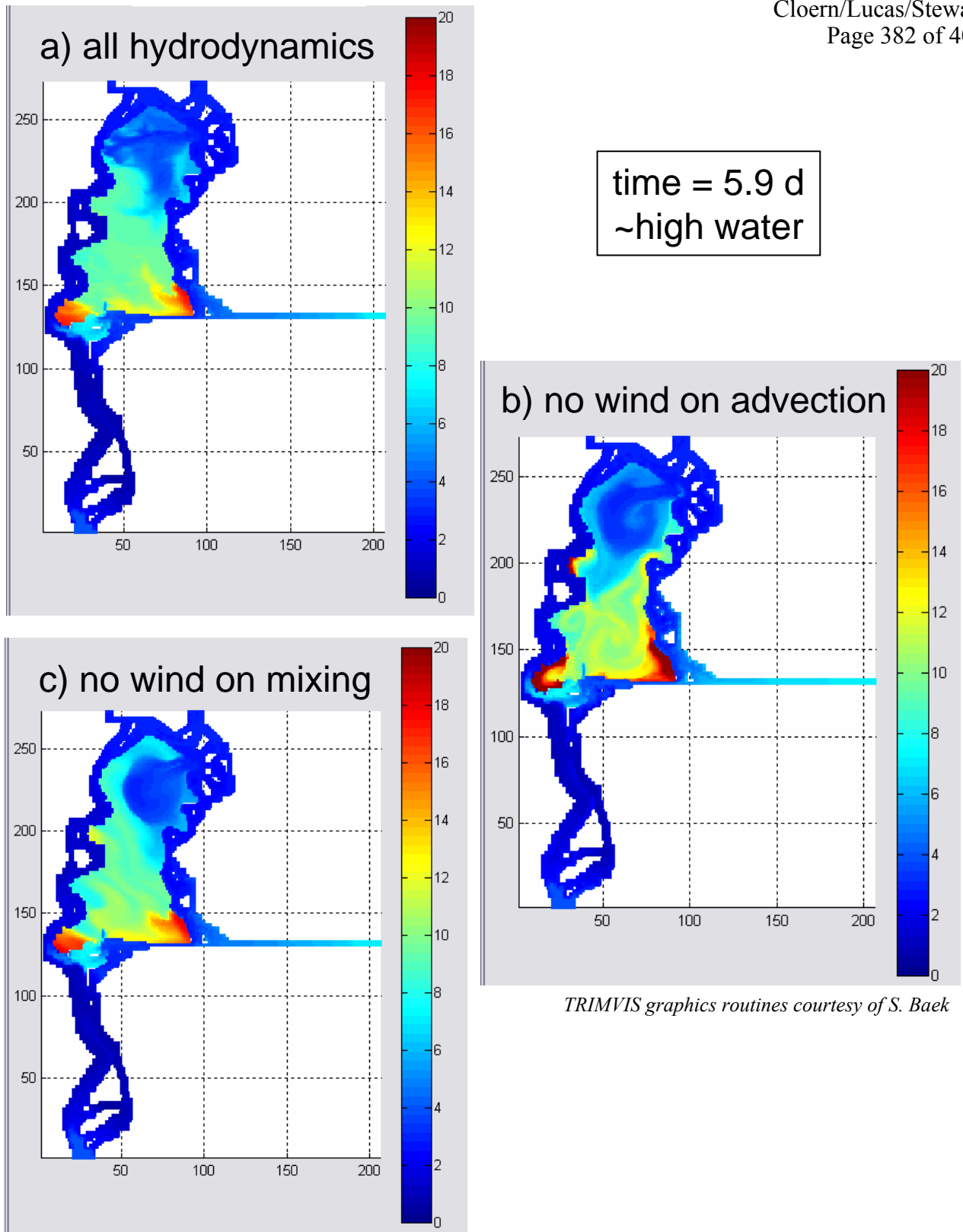


Figure ML8. TRIM-MILLIE model calculations of phytoplankton biomass distributions for three hydrodynamic scenarios at high water: a) all hydrodynamic forcings turned on; b) the wind effect on advection turned off; and c) the wind effect on vertical mixing turned off.

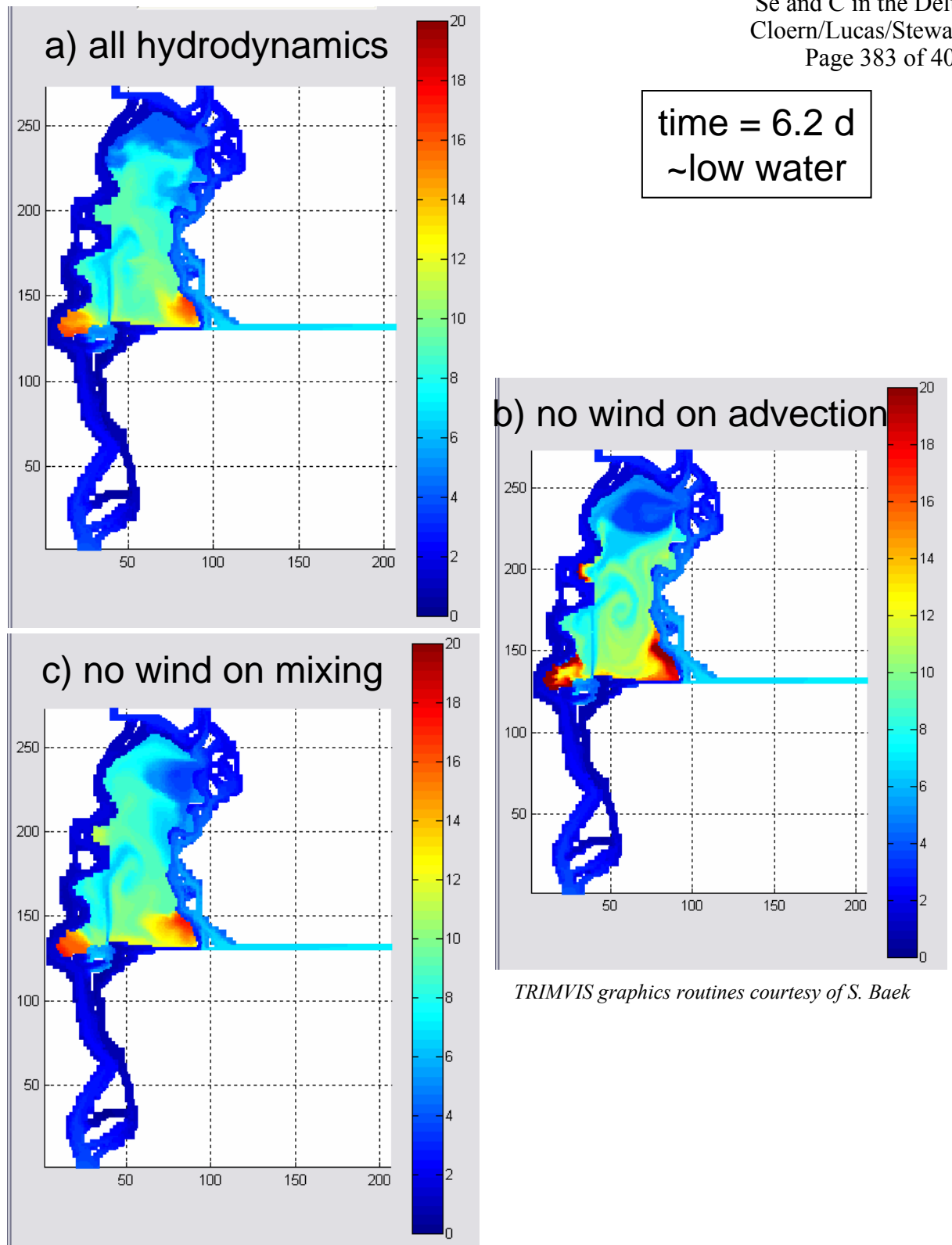


Figure ML9. TRIM-MILLIE model calculations of phytoplankton biomass distributions for three hydrodynamic scenarios at low water: a) all hydrodynamic forcings turned on; b) the wind effect on advection turned off; and c) the wind effect on vertical mixing turned off.

phytoplankton biomass

conservative tracer

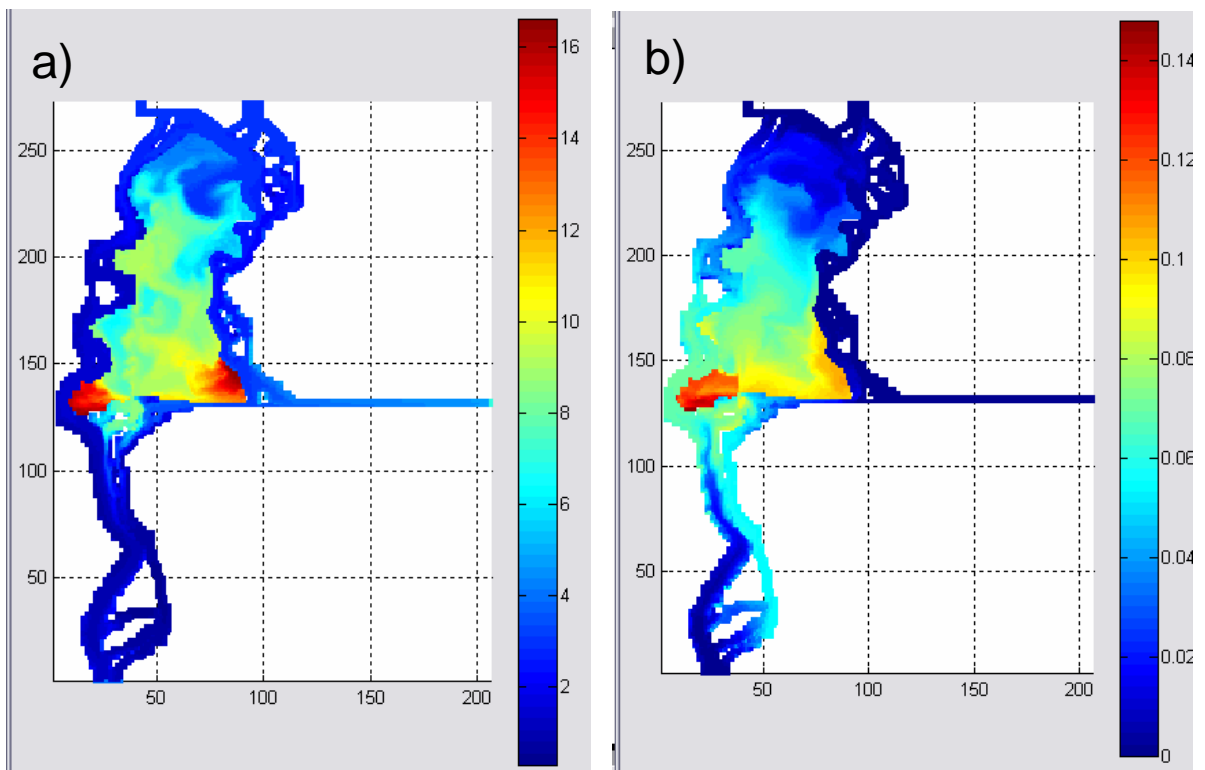


Figure ML10. TRIM-MILLIE calculated distributions of a) phytoplankton biomass [ug chl *a*/L] and b) a conservative tracer for the same hydrodynamic conditions and simulation time.

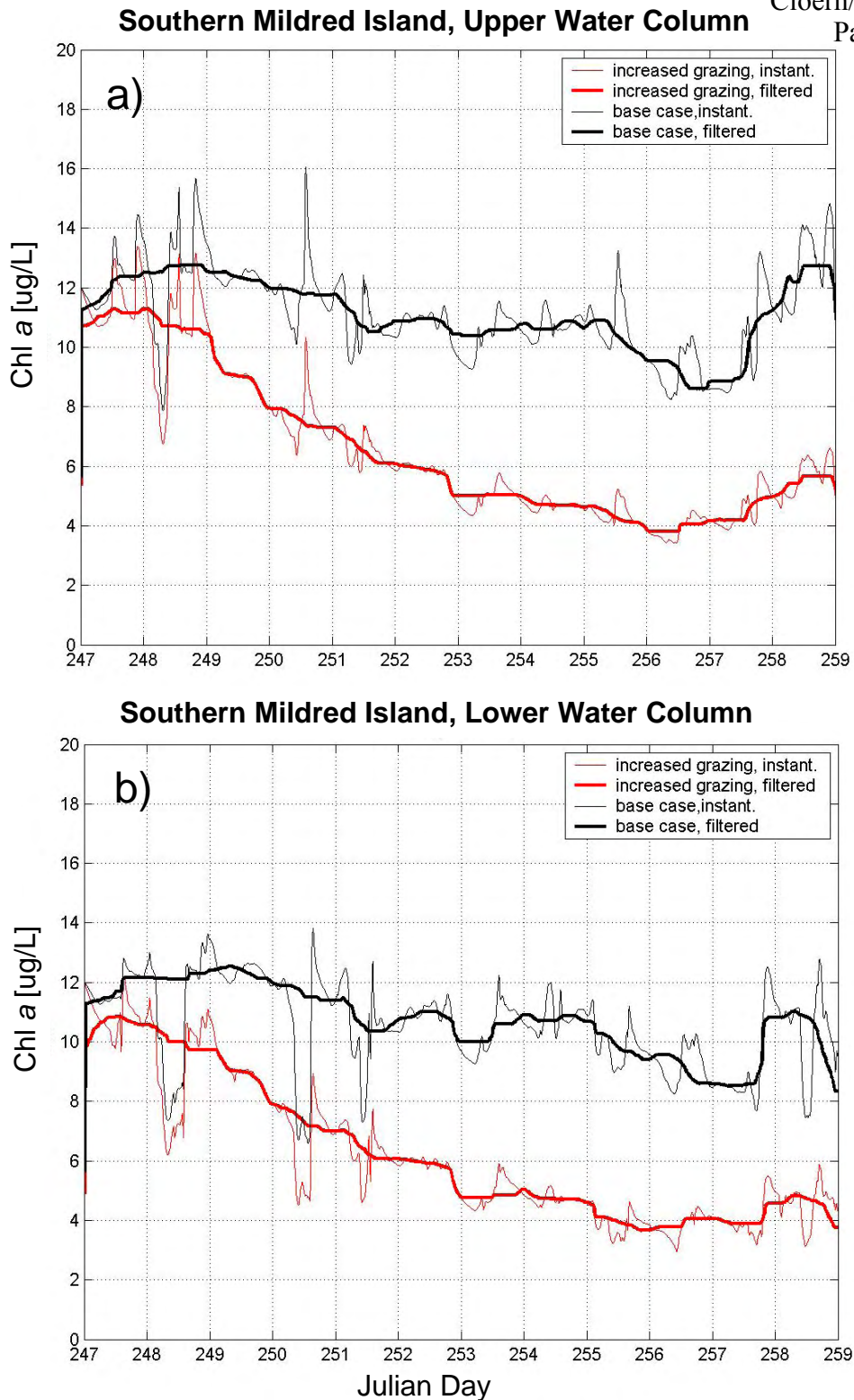


Figure ML12. TRIM-MILLIE calculated time series of southern Mildred Island chl *a* for the base case and increase benthic grazing in the lake interior for a) the upper water column, and b) the lower water column. Instantaneous and 24-h median filtered values are plotted.

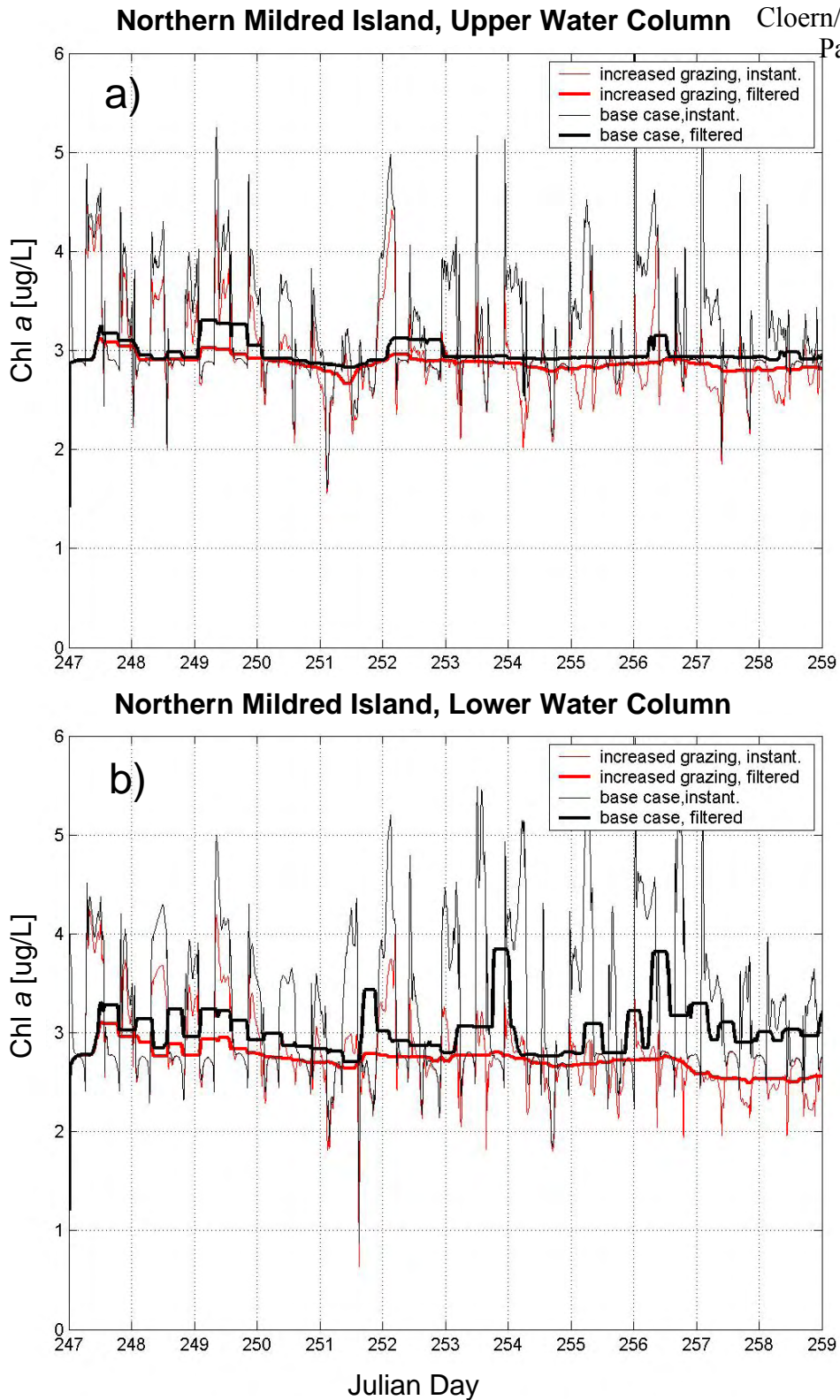


Figure ML13. TRIM-MILLIE calculated time series of northern Mildred Island chl *a* for the base case and increase benthic grazing in the lake interior for a) the upper water column, and b) the lower water column. Instantaneous and 24-h median filtered values are plotted.

Edible Particulate Selenium (based on coupled model) [pg/L]

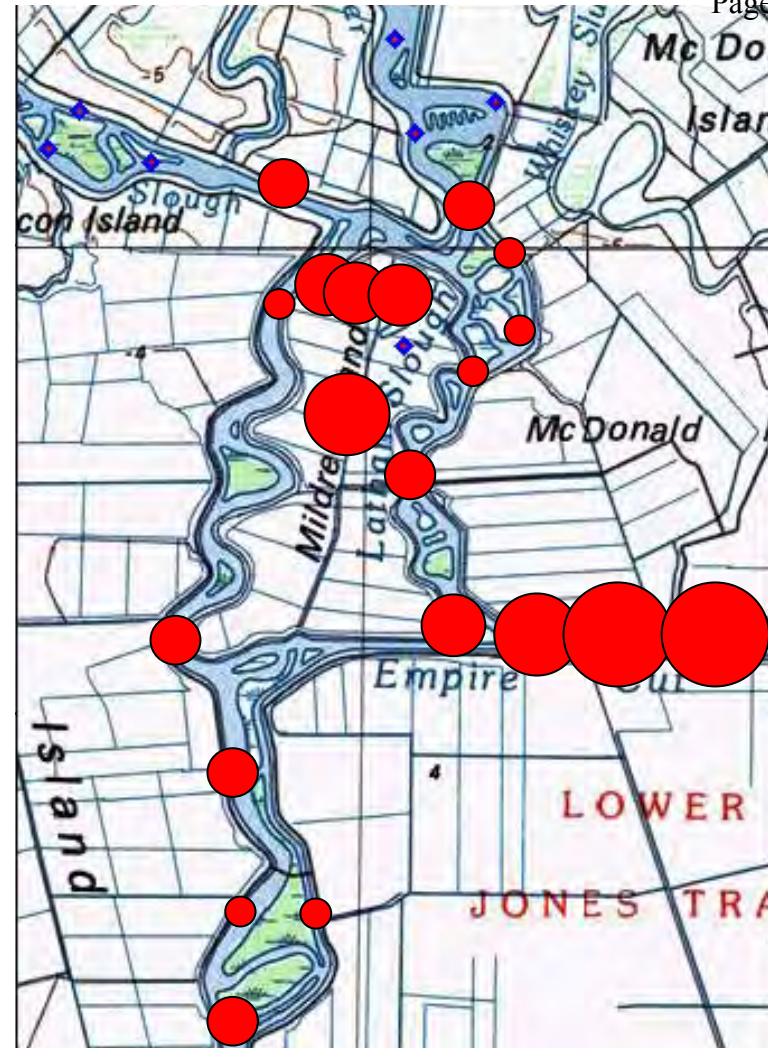


Figure ML14. Edible particulate selenium calculated by coupled TRIM-MILLIE model for September 2001 base case.

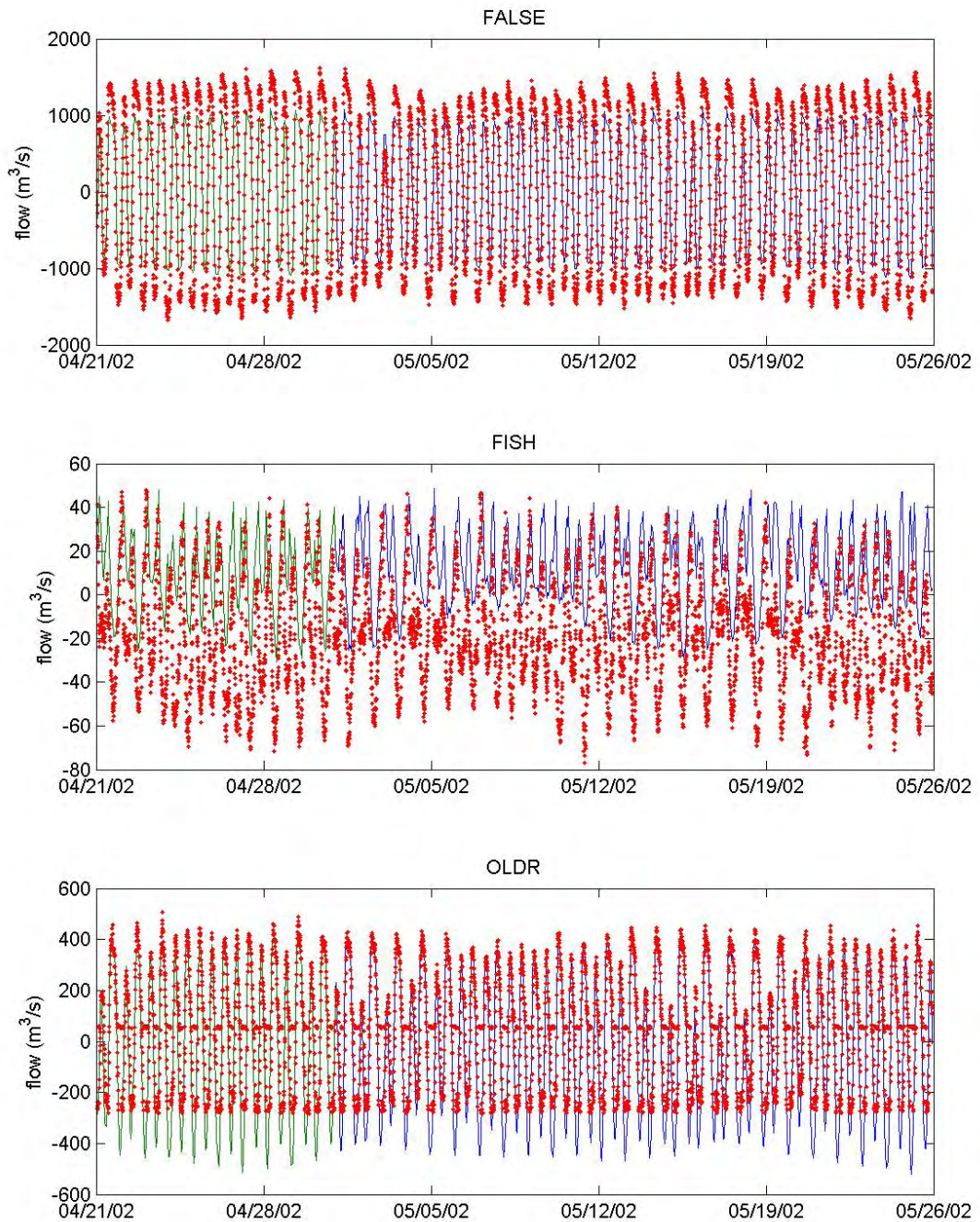


Figure ML15. Comparison of flow in the Franks Tract region calculated by the DELTA-TRIM model (green and blue lines) and measured during Franks Tract 2002 process study (red dots). See Figure C2 for station locations.

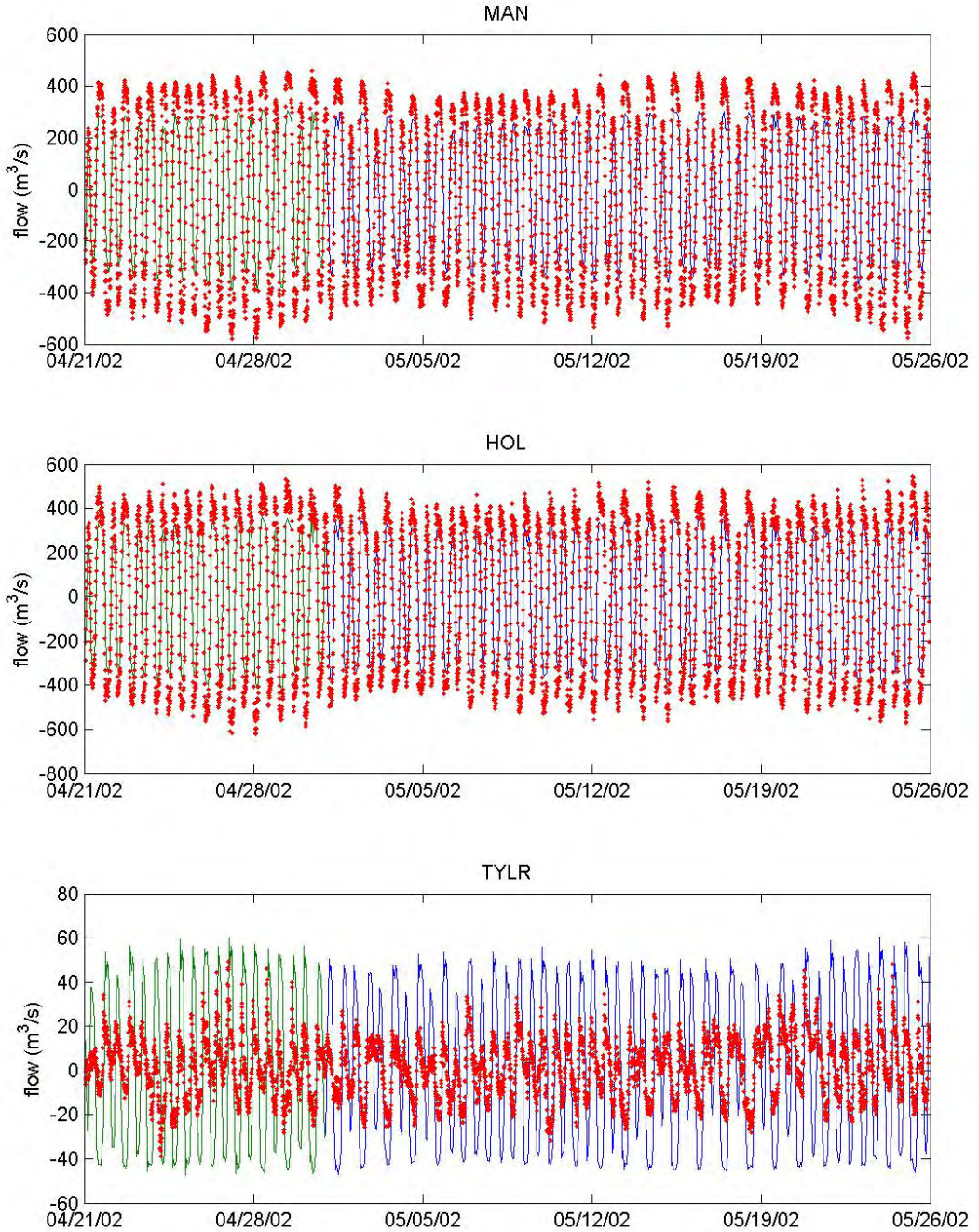


Figure ML16. Comparison of flow in the Franks Tract region calculated by the DELTA-TRIM model (green and blue lines) and measured during Franks Tract 2002 process study (red dots). See Figure C2 for station locations.

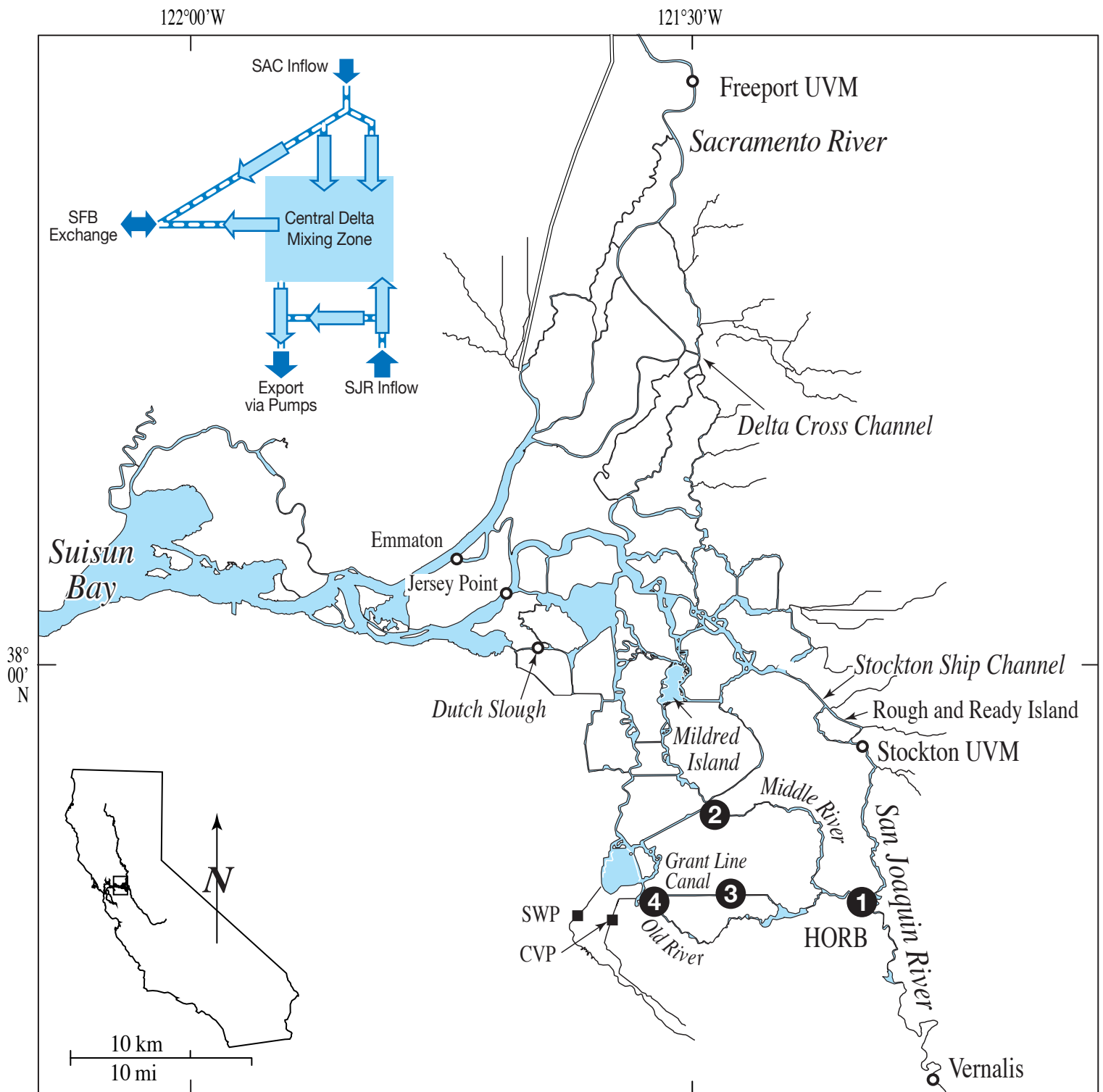


Figure MD1. Map of the Sacramento-San Joaquin Delta. The numbers indicate the location of the four temporary barriers during portions of the year. Inset: Schematic illustrating the base flow routes through the Delta without gate or barrier operations. The dark blue arrows represent the freshwater inputs to the Delta (north: Sacramento @ Freeport; south: San Joaquin @ Vernalis) and export pump operations in the southwest corner of the Delta. The bi-directional arrow represents tidal exchange of Delta water with San Francisco Bay at the junction of the Sacramento and San Joaquin rivers.

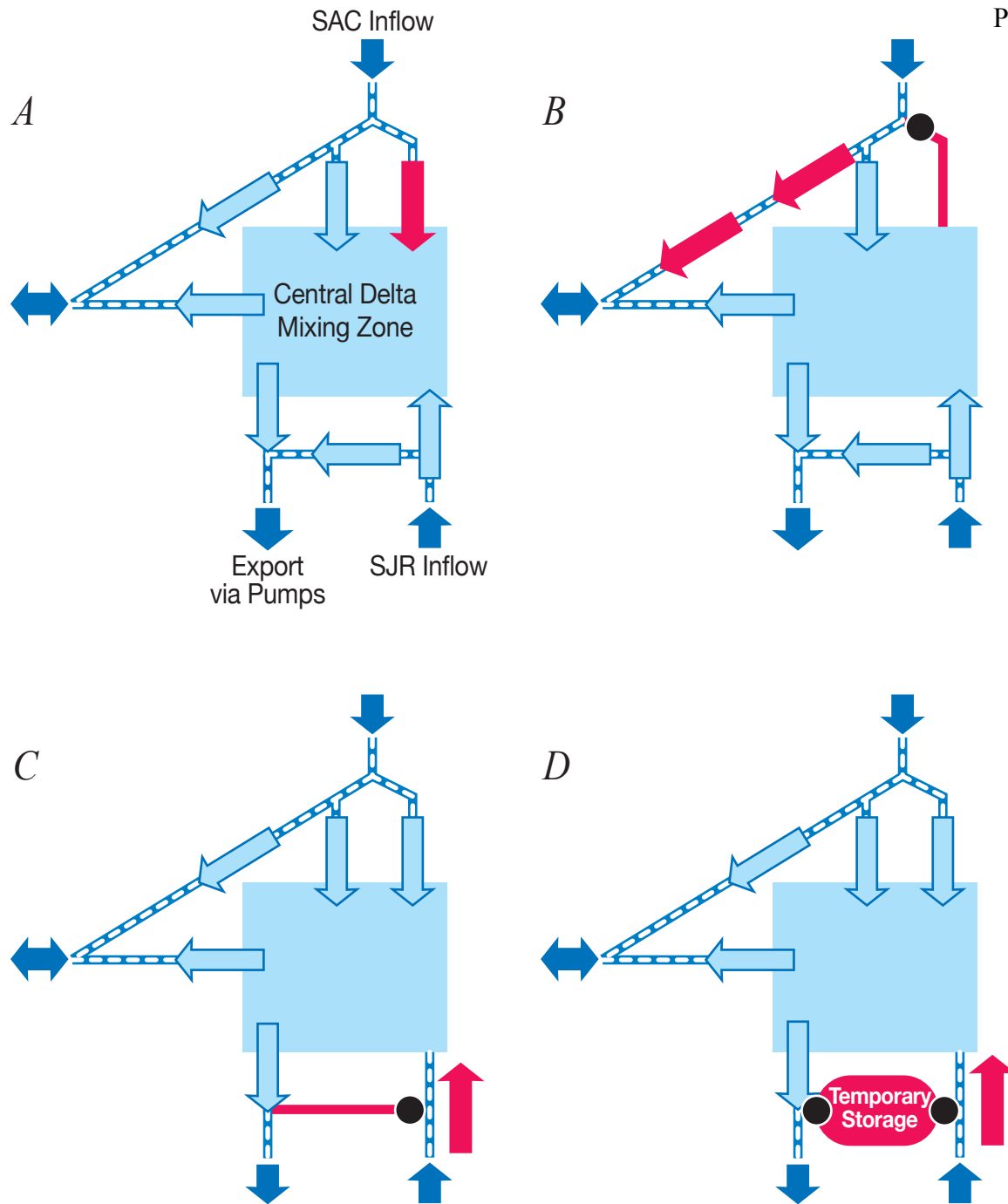
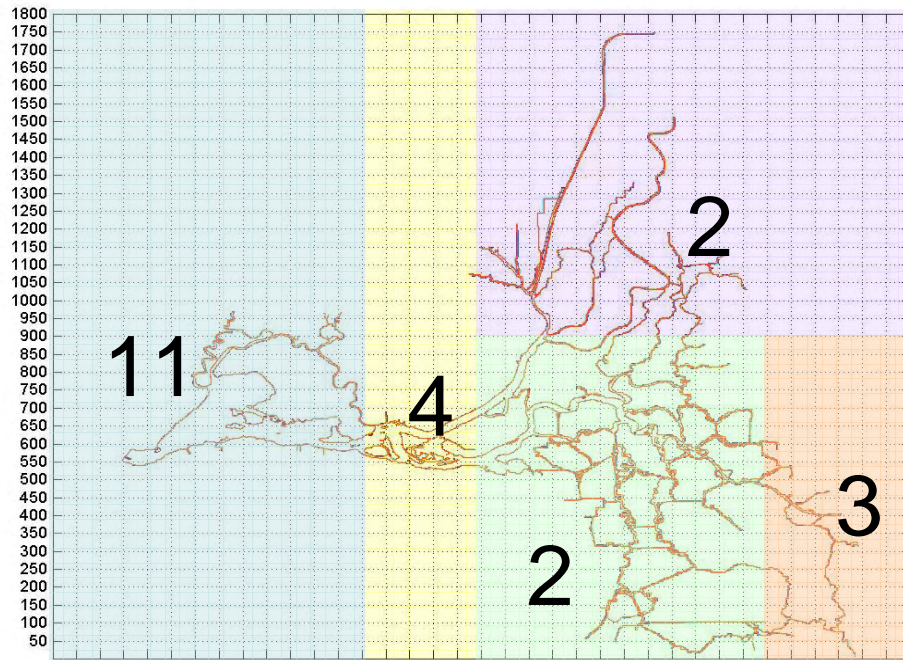


Figure MD2. Schematics illustrating how each diversion in our examples alters flow routing through the Delta. Red denotes the significant flow change caused by each diversion. (a) Keeping the DCC gates open enhances the transfer of SAC water to the central Delta mixing zone. (b) Closing the gates at the DCC redirects flow down the SAC towards SFB rather than flowing into the central Delta mixing zone. (c) Placement of the HORB directs SJR flow towards the central Delta mixing zone rather than flowing through the south Delta towards the export pumps. (d) Placement of all four temporary barriers creates a temporary storage region in the south Delta.

Extinction Coefficient (1/m) Regions



Clam Grazing Rate (m³/m²/day) Regions

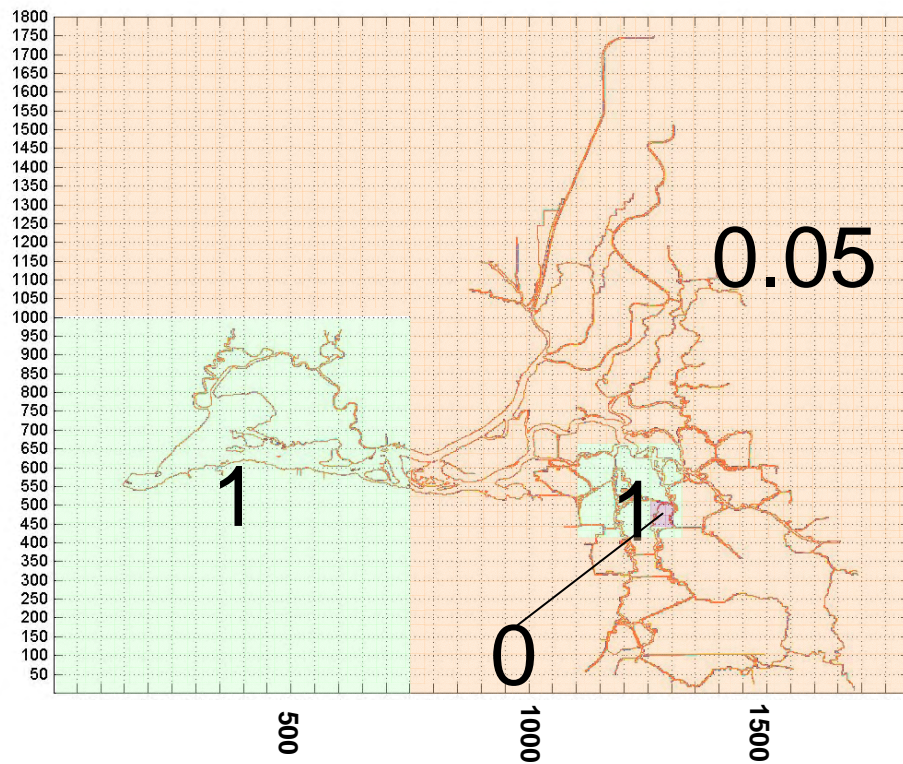


Figure MD3. Areas with assigned light attenuation coefficients and benthic grazing rates for Delta scale coupled model (base case).

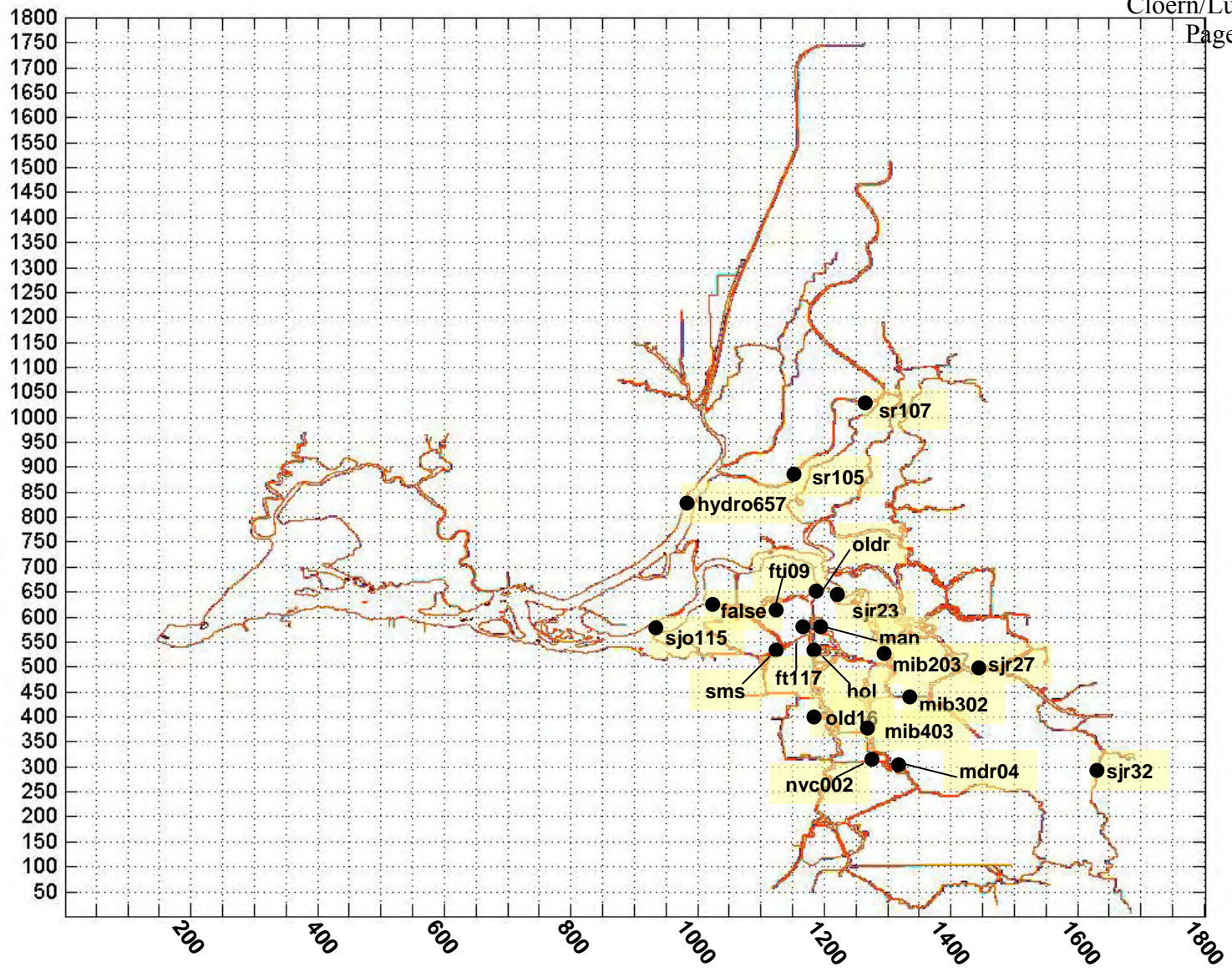
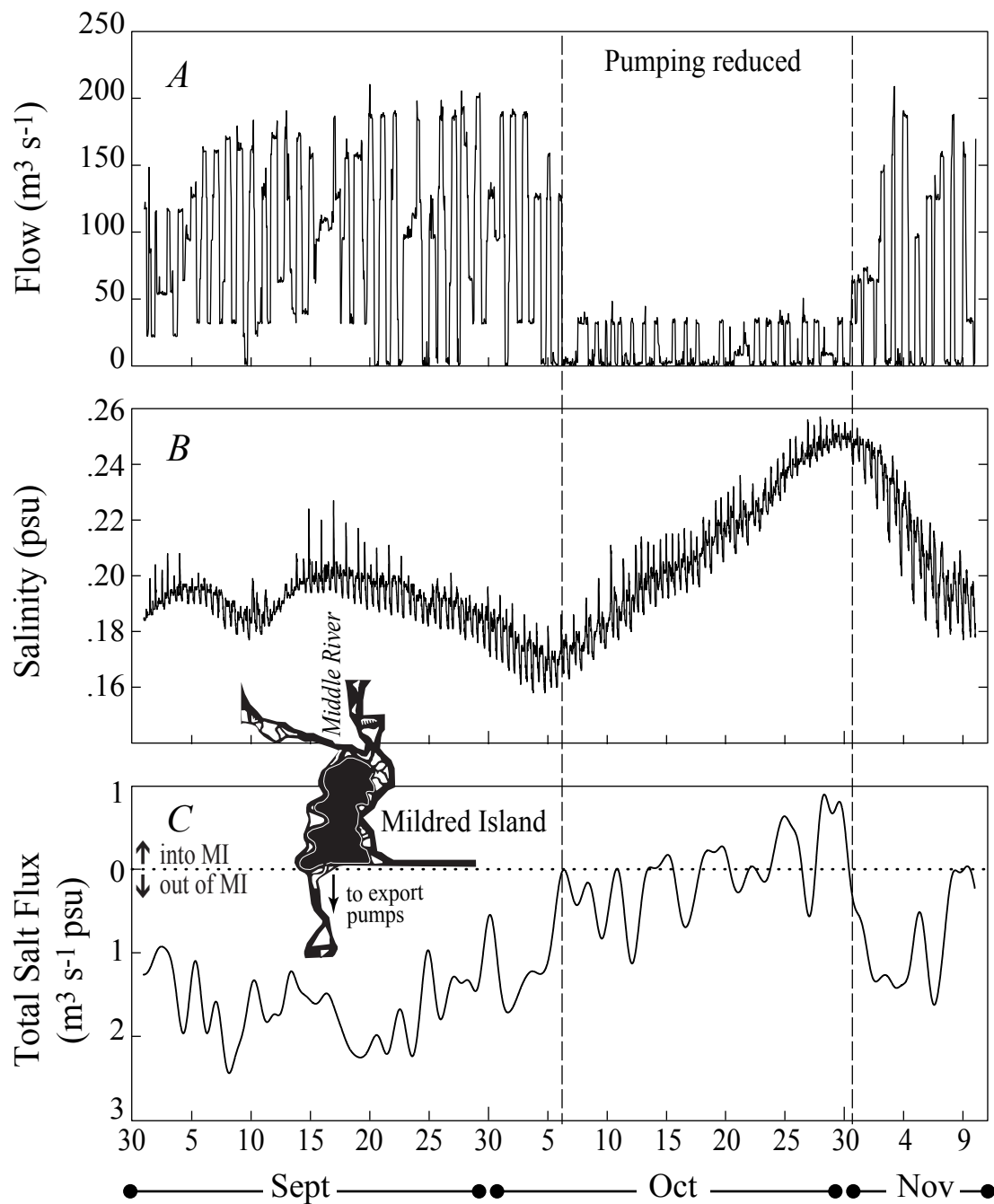


Figure MD4. Time series stations for coupled Delta model.



MD5. The influence of SWP export pump operations on salinity in Mildred Island (central Delta) in autumn 2001. (a) Export rate at the SWP export facilities. (b) Salinity (psu) 1 m above the channel bottom at the northern opening of Mildred Island. (c) Advective salt flux at the southern opening of Mildred Island. Inset: map of Mildred Island and the surrounding channels. Data sources: SWP pump operation data: California Department of Water Resources Interagency Ecological Program database (www.iep.water.ca.gov, Station: CHSWP003). Salinity and flow data calculated from USGS field measurements in Mildred Island (22 Aug 2001-14 Nov 2001).

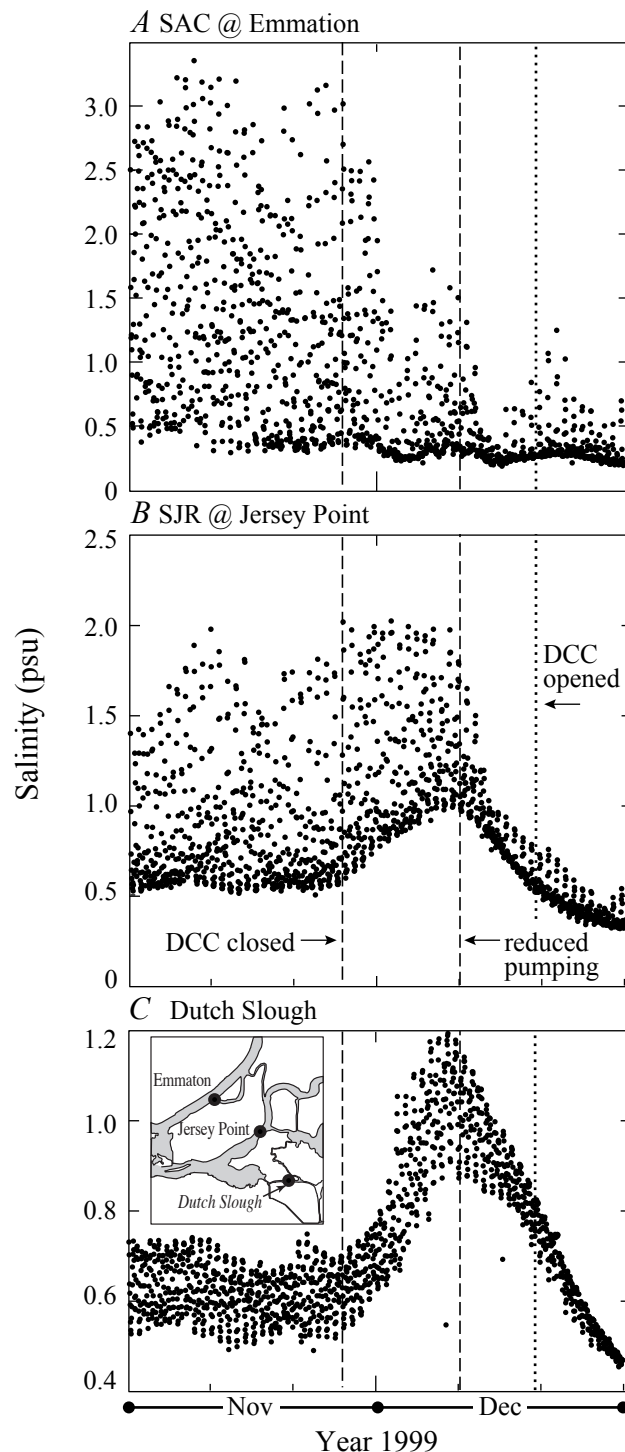


Figure MD6. The influence of DCC gate operations on salinity intrusion in the western Delta during November-December 1999 at (a) SAC at Emmaton, (b) SJR at Jersey Point, and (c) Dutch Slough (inset: map of the region). Datasource: Interagency Ecological Program Database: electrical conductivity (Station: RSAC092, RSAN018, SLDUT007), water temperature (Station: RSAC101, RSAN007), DCC gate operations (Station: RSAC128), and export pump operations (Station: CHSWP003, CHDMC004).

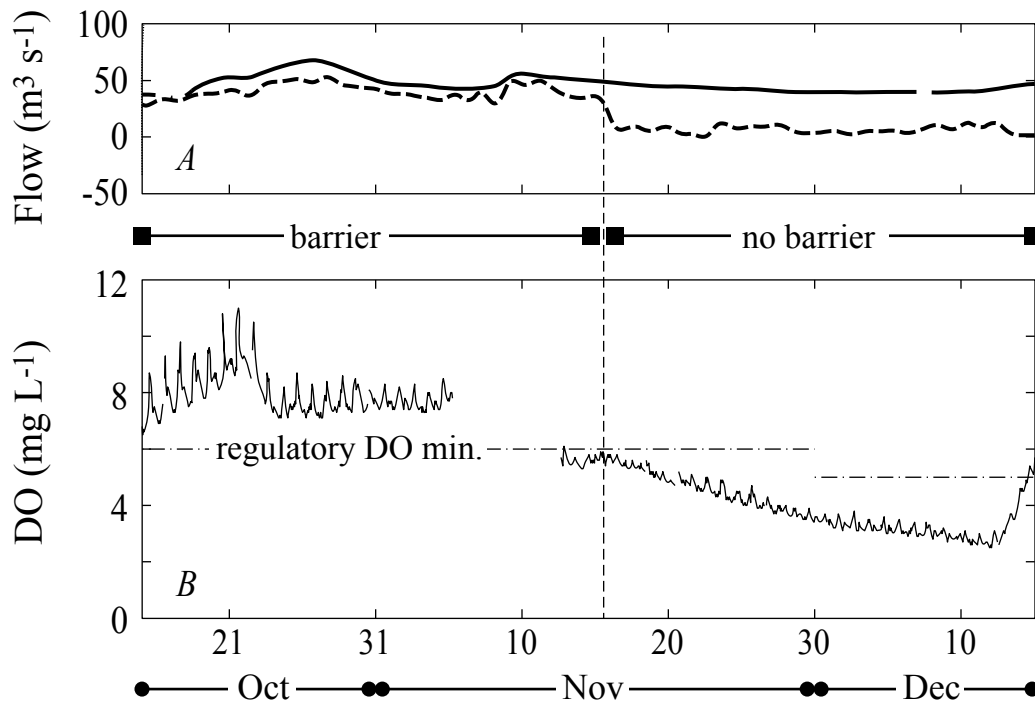


Figure MD7. The influence of HORB removal on SJR flows and DO concentration in the Stockton Ship Channel in autumn 2002. (a) SJR flow ($\text{m}^3 \text{s}^{-1}$) measurements at Vernalis (solid line) and tidally-averaged flow at Stockton (dashed line). The station at Vernalis, upstream of the head of Old River, measures the SJR input flow into the Delta while the second flow station (Stockton) is located directly upstream of the Stockton Ship Channel. (b) Dissolved oxygen 1 m below the surface in the Stockton Ship Channel at Rough and Ready Island (mg L^{-1}). Data sources: Interagency Ecological Program Database: SJR Flow (USGS; Station: RSAN063, RSAN112) and (CDWR; Station: RSAN058), CDWR Bay-Delta Office: Temporary barrier operating schedule (sdelta.water.ca.gov/web_pg/tempmesr.html).

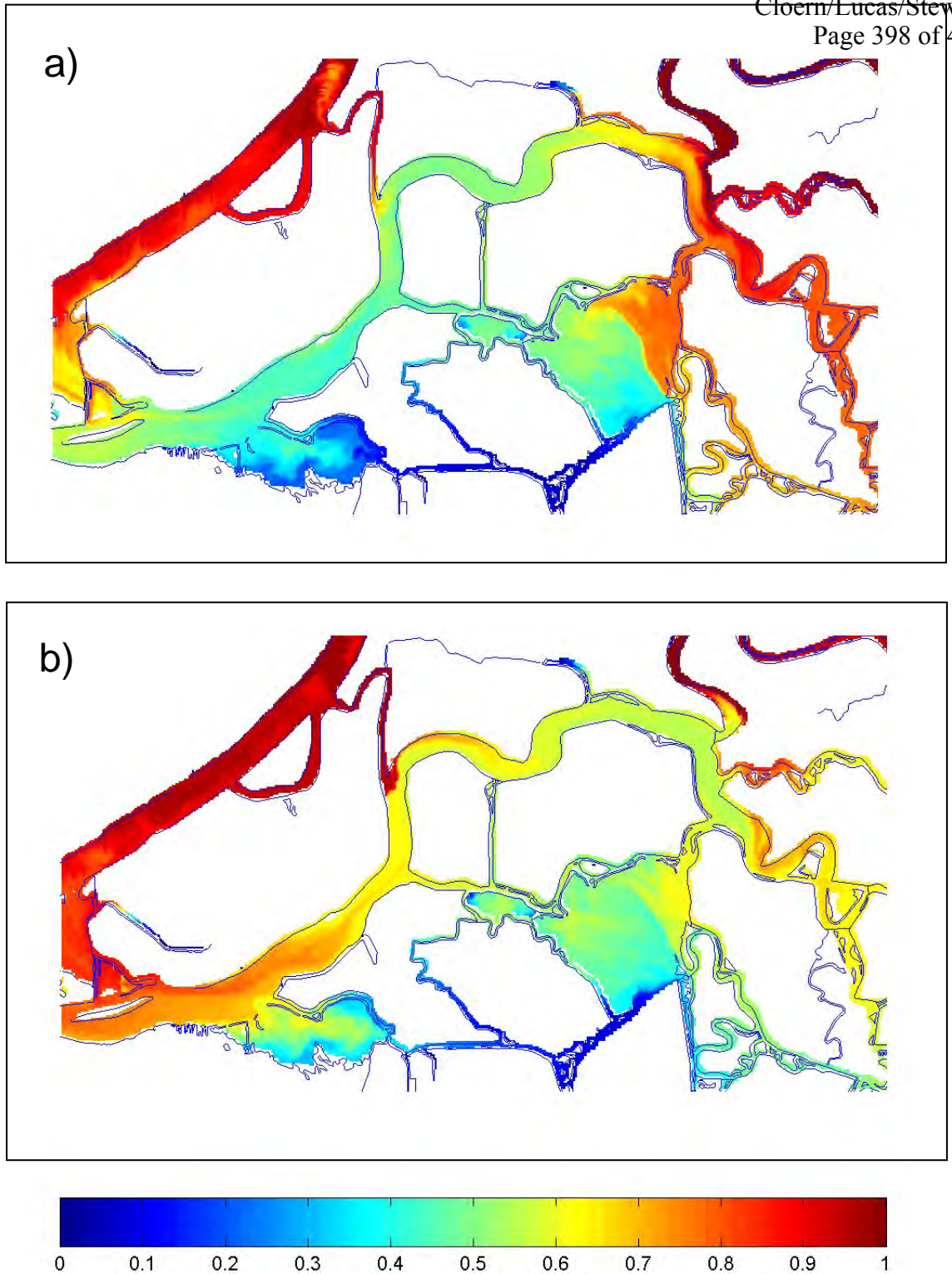


Figure MD8. Distribution of Sacramento source water in the Central Delta for (a) normal Delta Cross Channel operations and (b) Delta Cross Channel closed for the entire simulation. (Range: 0=no Sacramento water and 1=all Sacramento water) The simulation used September 2001 hydrology and the snapshot represents source distribution 35 days into the simulation.

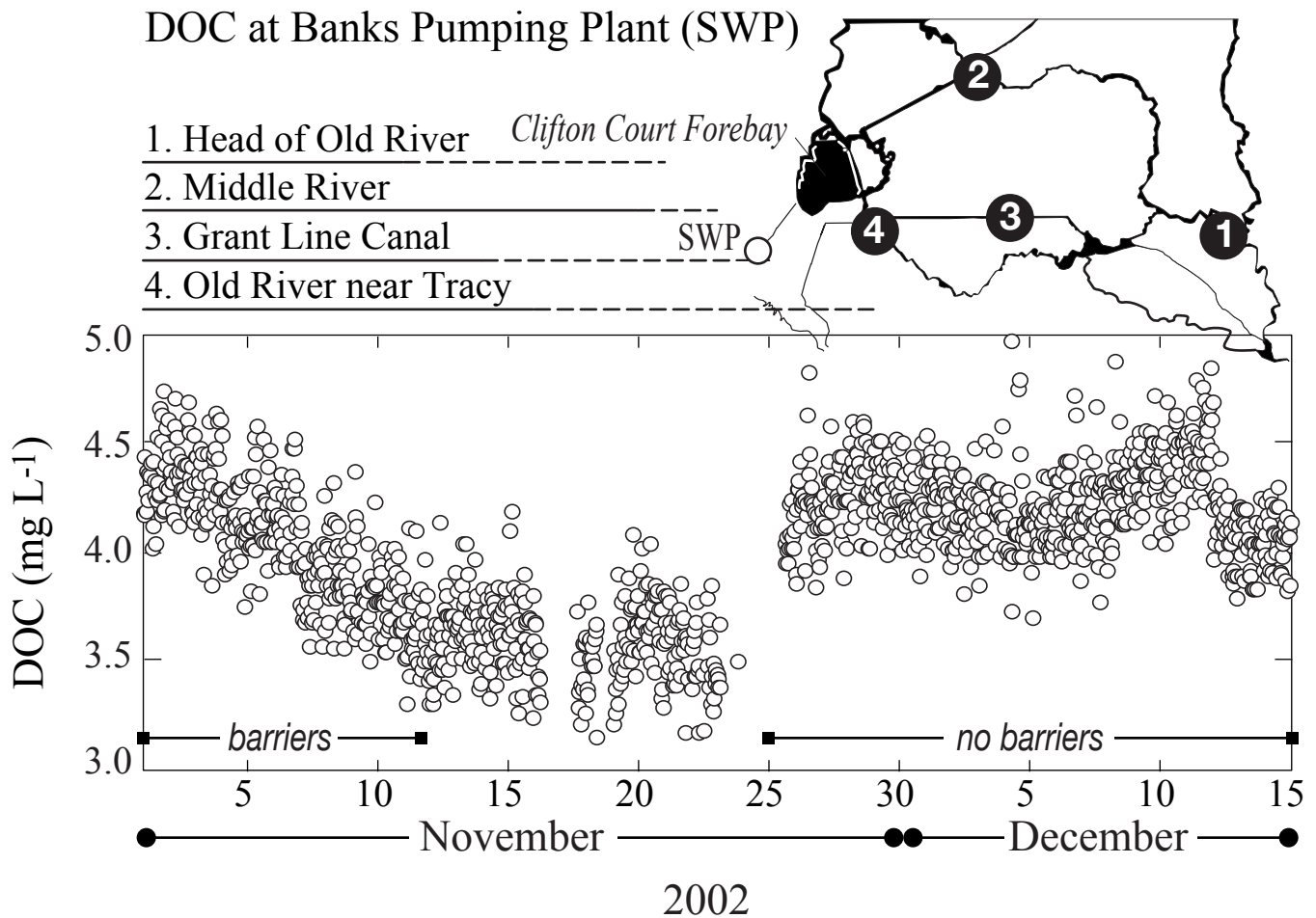
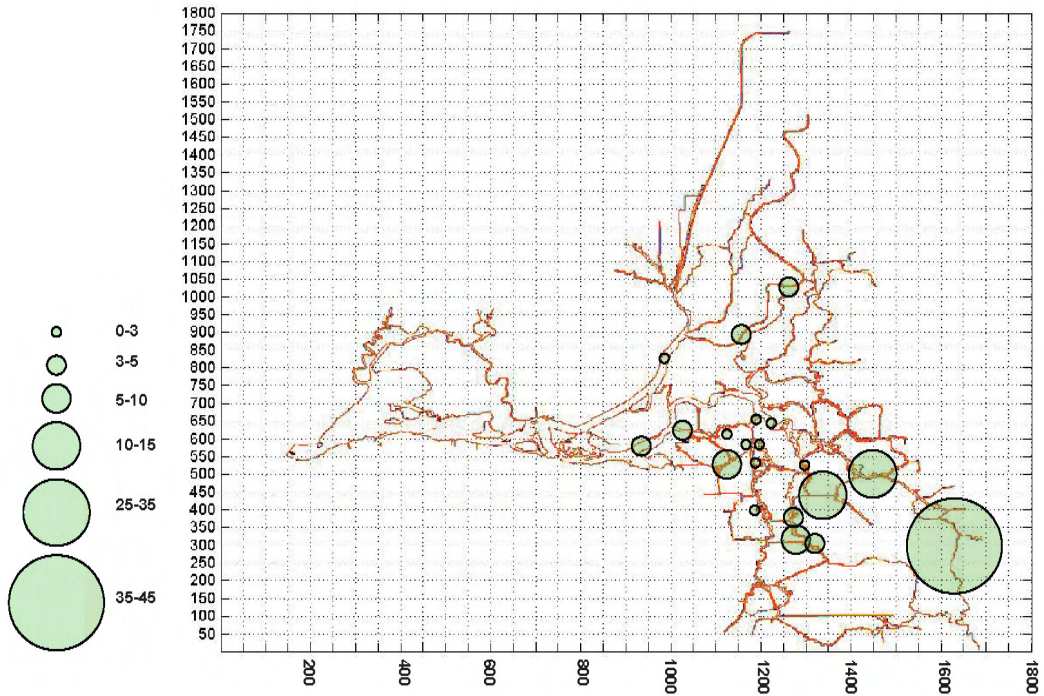


Figure MD9. DOC (mg L⁻¹) at SWP export facilities and temporary barrier operations during autumn 2002. Horizontal lines indicate when each of the temporary barriers are in (solid line) and the barrier demolition periods (dashed line). Inset: Map of the south delta region. The numbers indicate the location of each of the temporary barriers. Data sources: California Data Exchange Center (www.cdec.water.ca.gov): DOC (Station: HRO), CDWR Bay-Delta Office: Temporary barrier operating schedule.

Modeled Chl (ug/L)—Base Case



Measured Discrete Chl (ug/L)—Benthic Boogie 2003

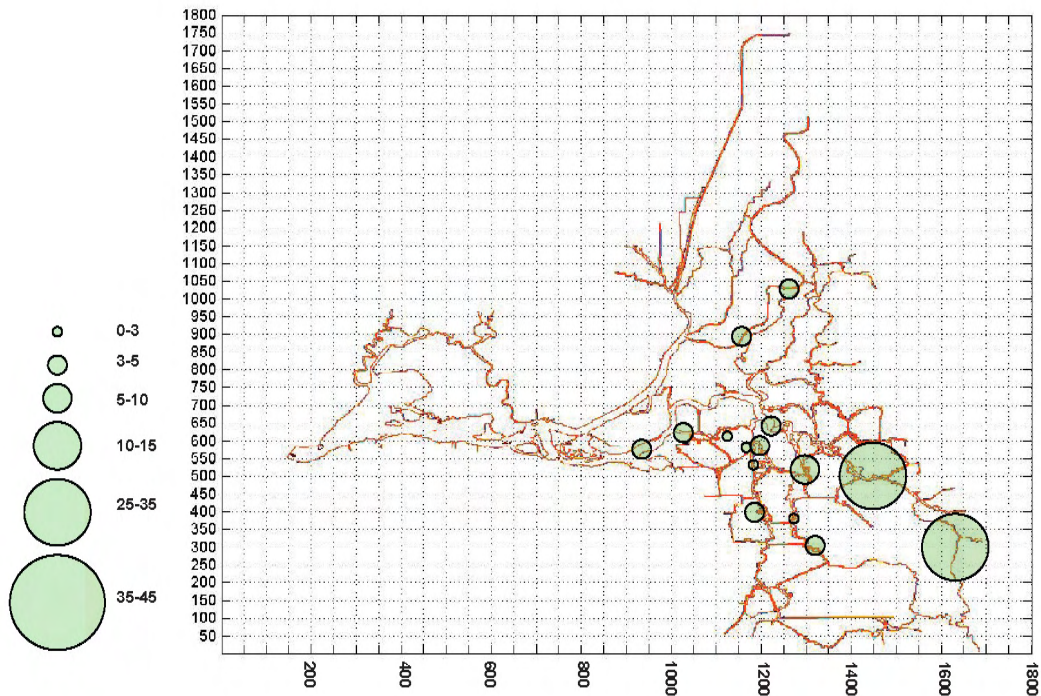


Figure MD10. Comparison of a) modeled chl *a* [ug/L] calculated by Delta scale coupled model, and b) discrete chl *a* measurements during Spring 2003.

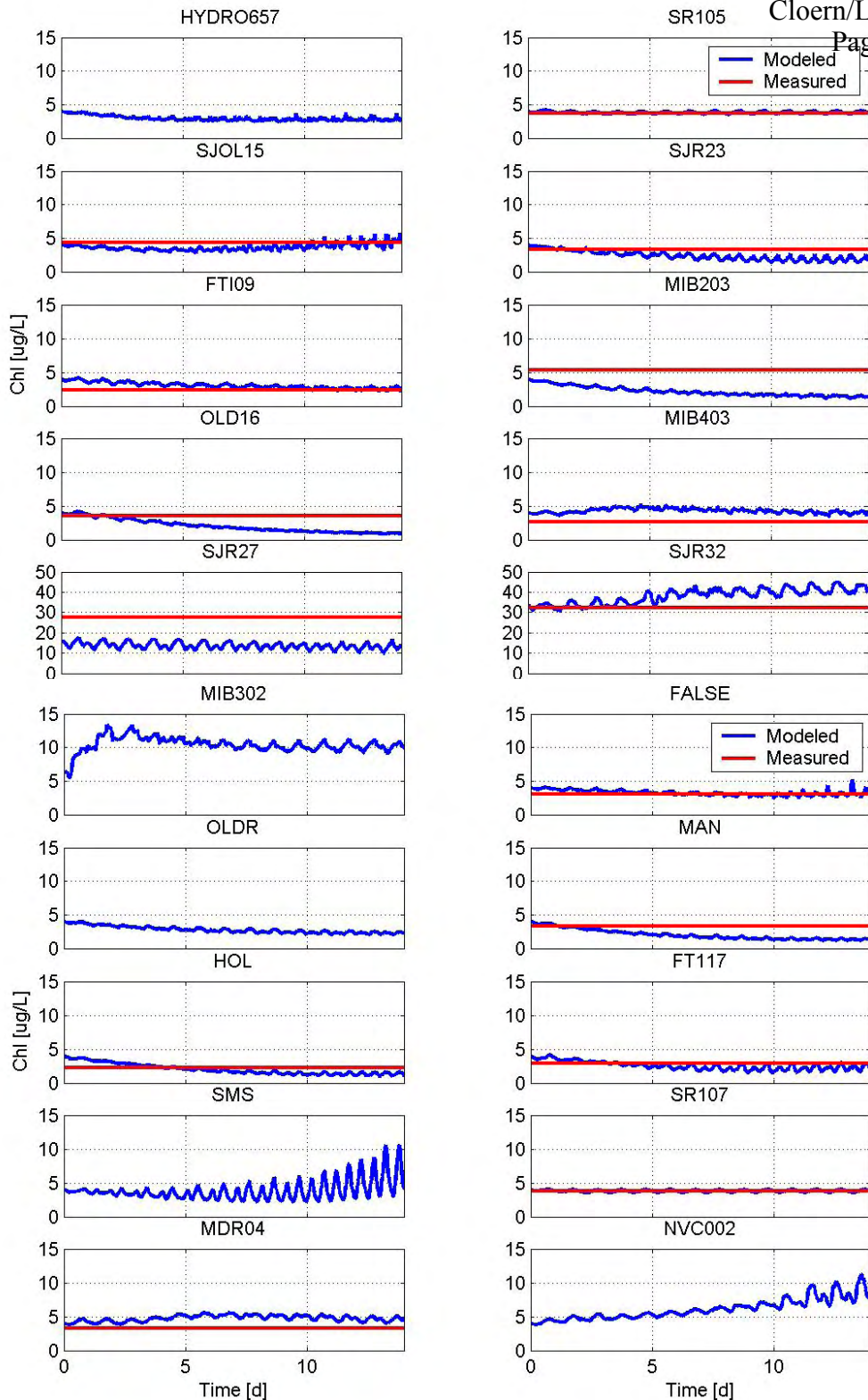


Figure MD11. Time series of chl *a* calculated by coupled Delta scale model for base case (blue lines). Red lines represent a single discrete measurement taken during May 2003. See Figure MD4 for station locations.

Model Predicted Edible Particulate Selenium (pg/L)

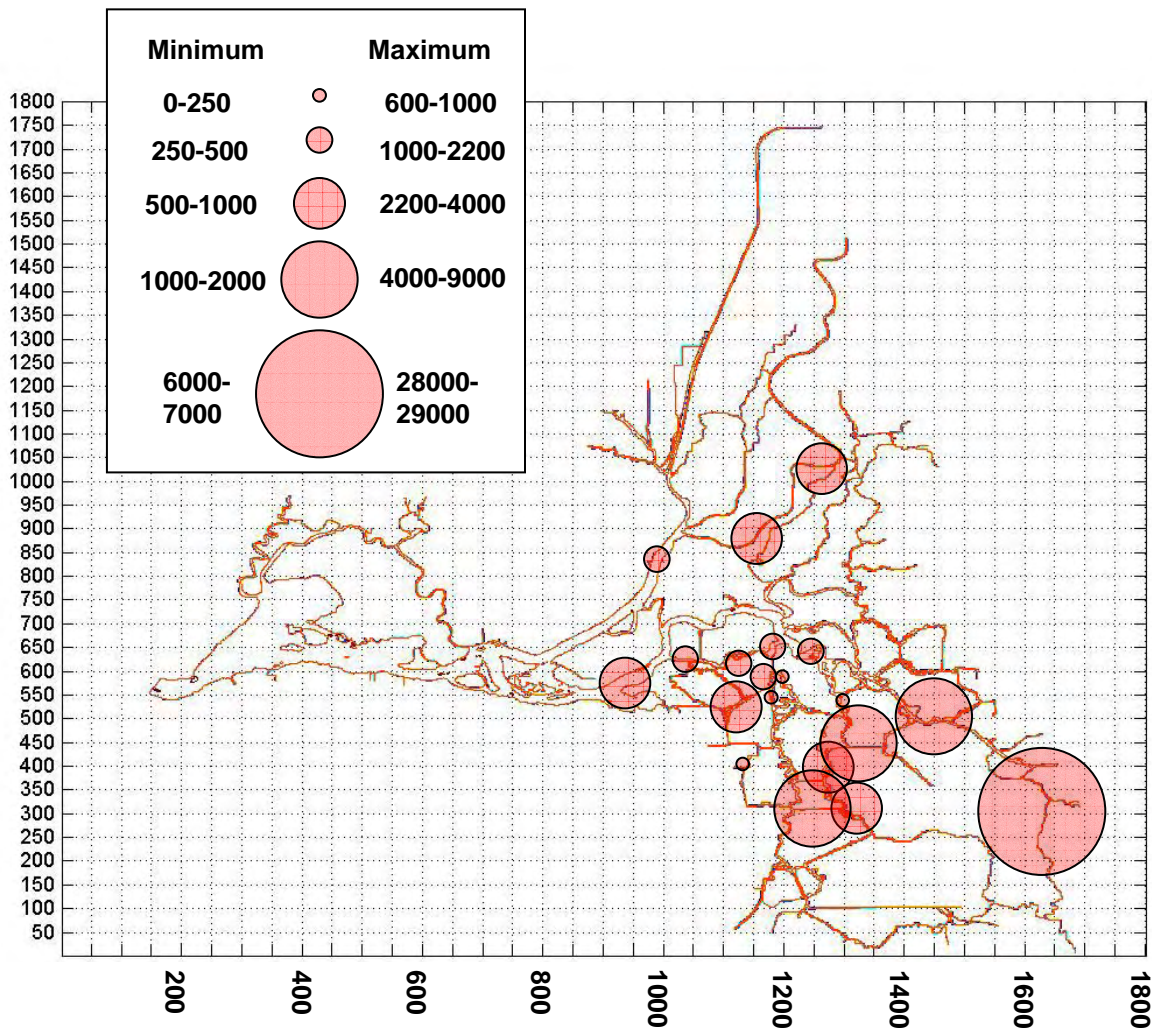
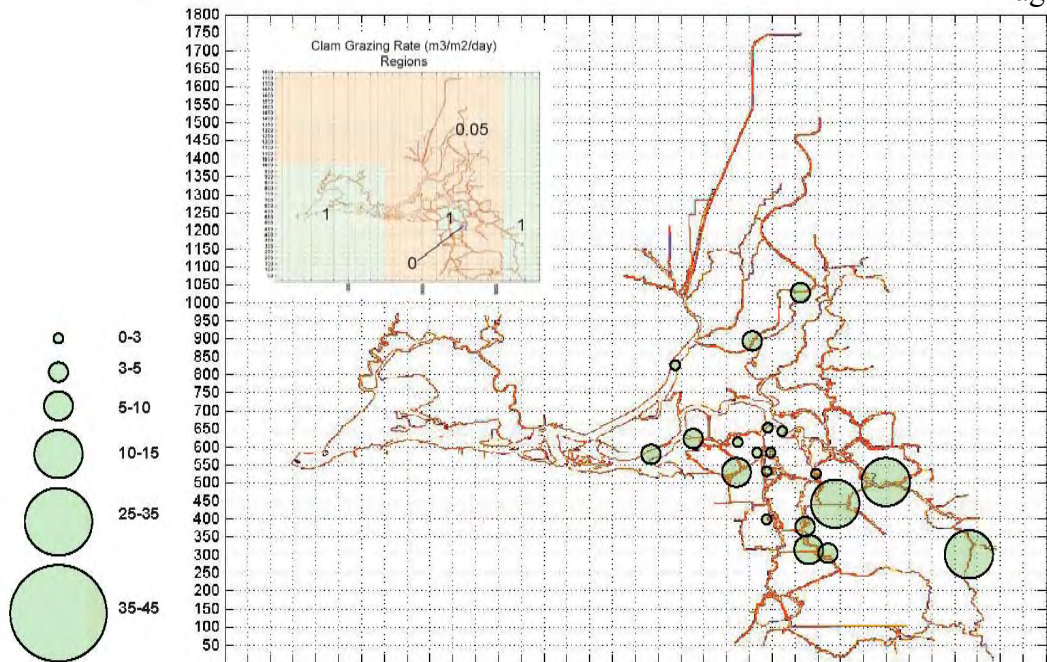


Figure MD12. Edible particulate selenium calculated using coupled Delta scale model for base case. Minimum and maximum values are shown, based on the assumptions that 1) no bacteria is available for ingestion, and 2) bacterial biomass as carbon equals 30% of the phytoplankton standing stock as carbon.



Modeled Chl (ug/L)—Base Case

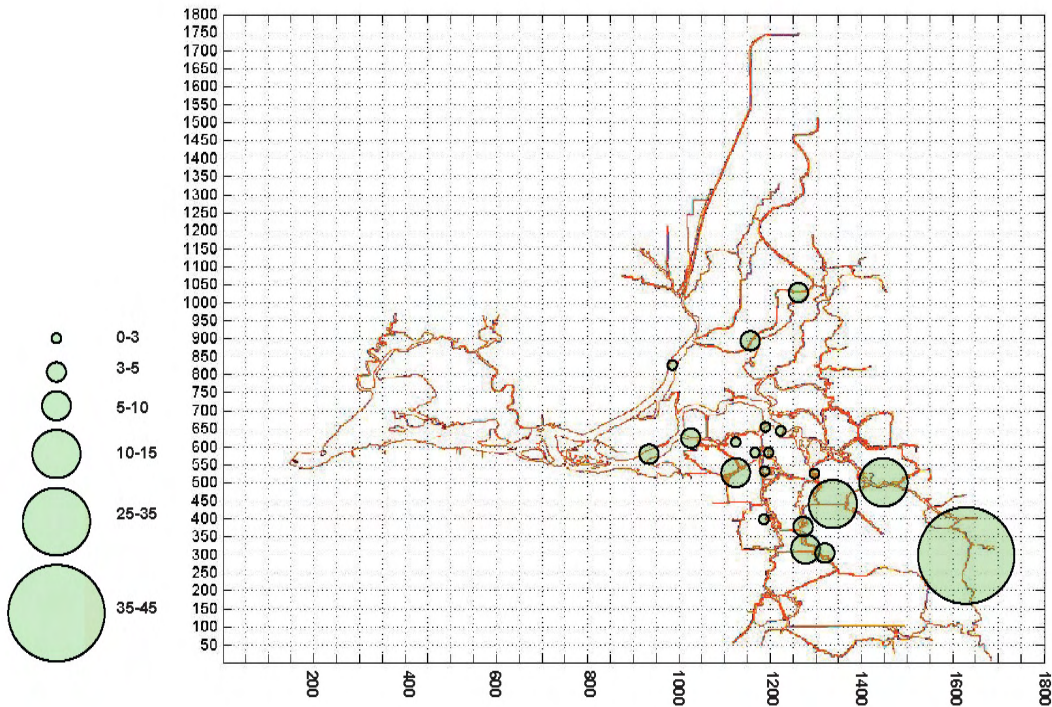


Figure MD13. Calculated chl *a* distributions for the case of increased benthic grazing in the upper San Joaquin River (upper panel; see inset for benthic grazing rate assignments). Bottom panel shows chl *a* for base case, for comparison.

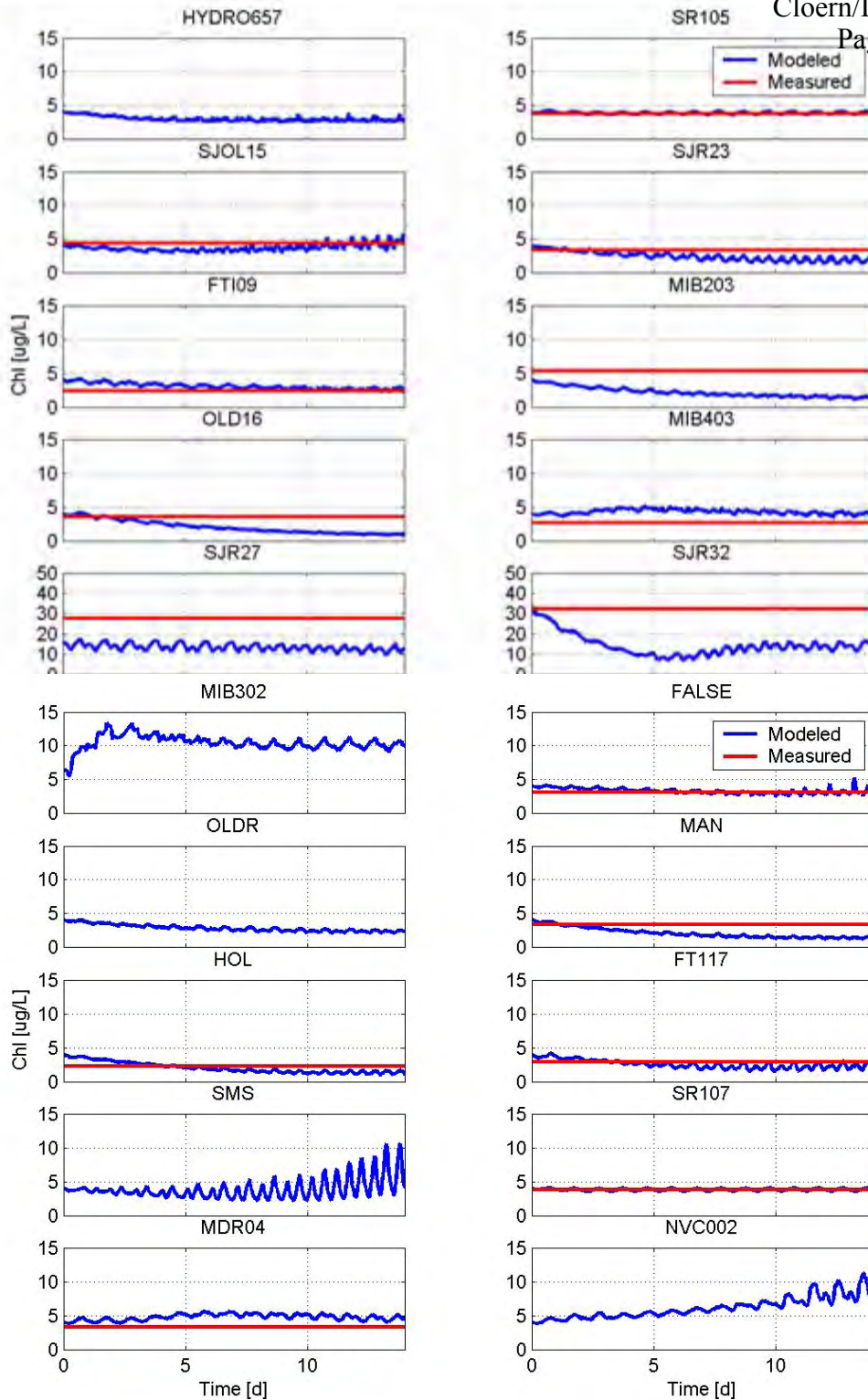
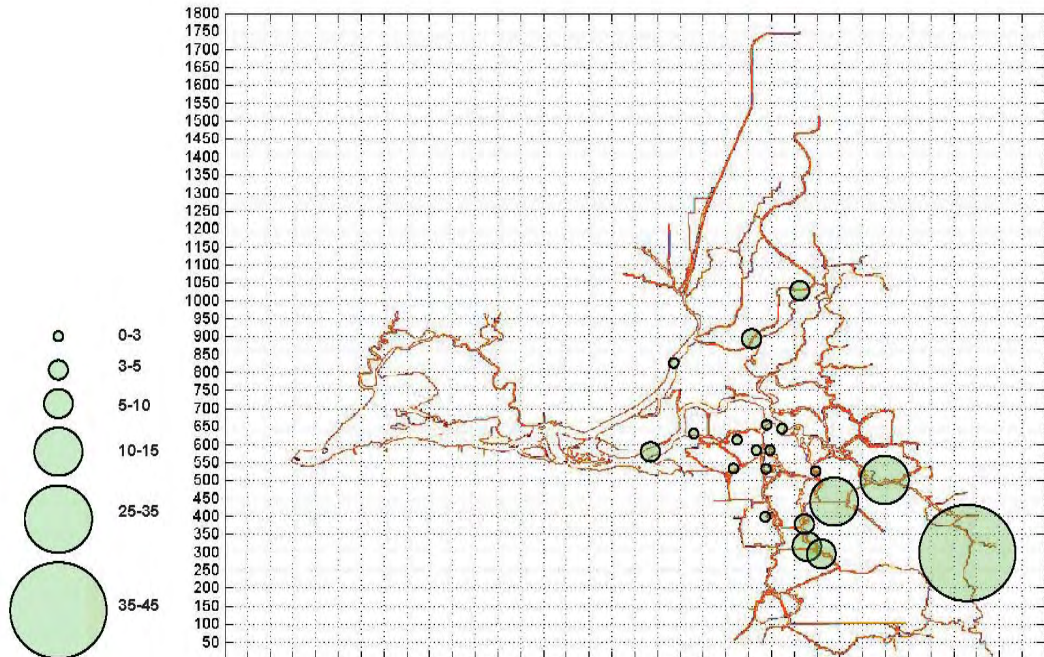


Figure MD14. Time series of chl *a* calculated by coupled Delta scale model for the case of increased benthic grazing in the upper San Joaquin River (blue lines). Red lines represent a single discrete measurement taken during May 2003. See Figure MD4 for station locations.

Modeled Chl with Pumps Turned Off (ug/L)



Modeled Chl (ug/L)—Base Case

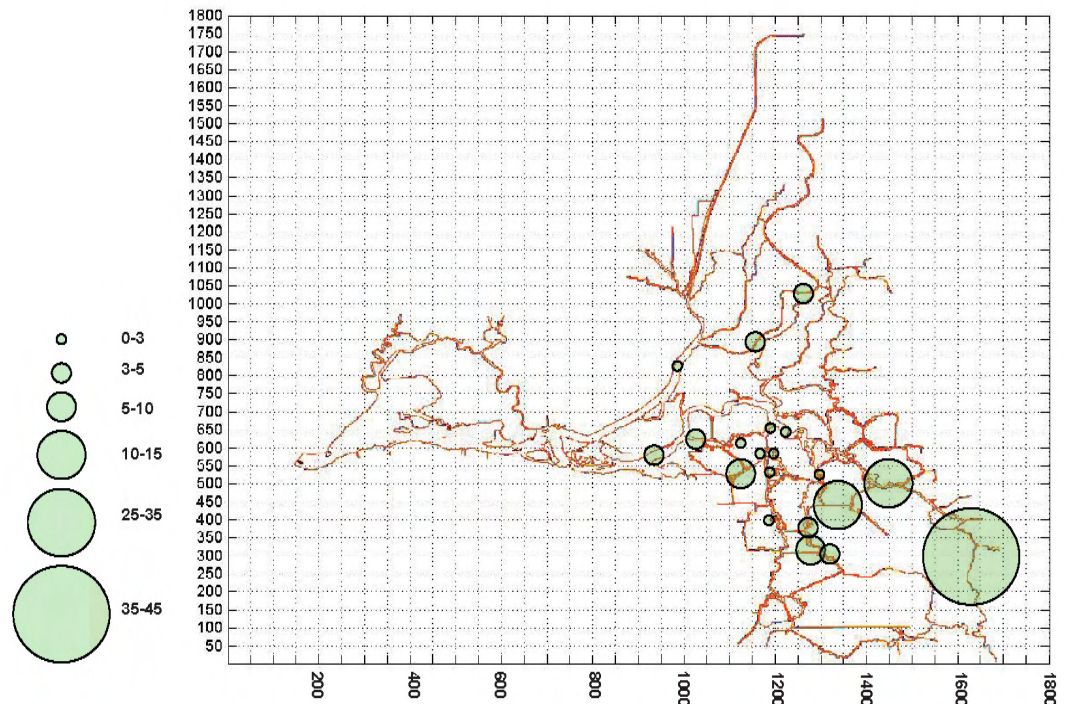


Figure MD15. Calculated chl *a* distributions for the case of zero pumping (upper panel). Bottom panel shows chl *a* for base case, for comparison.

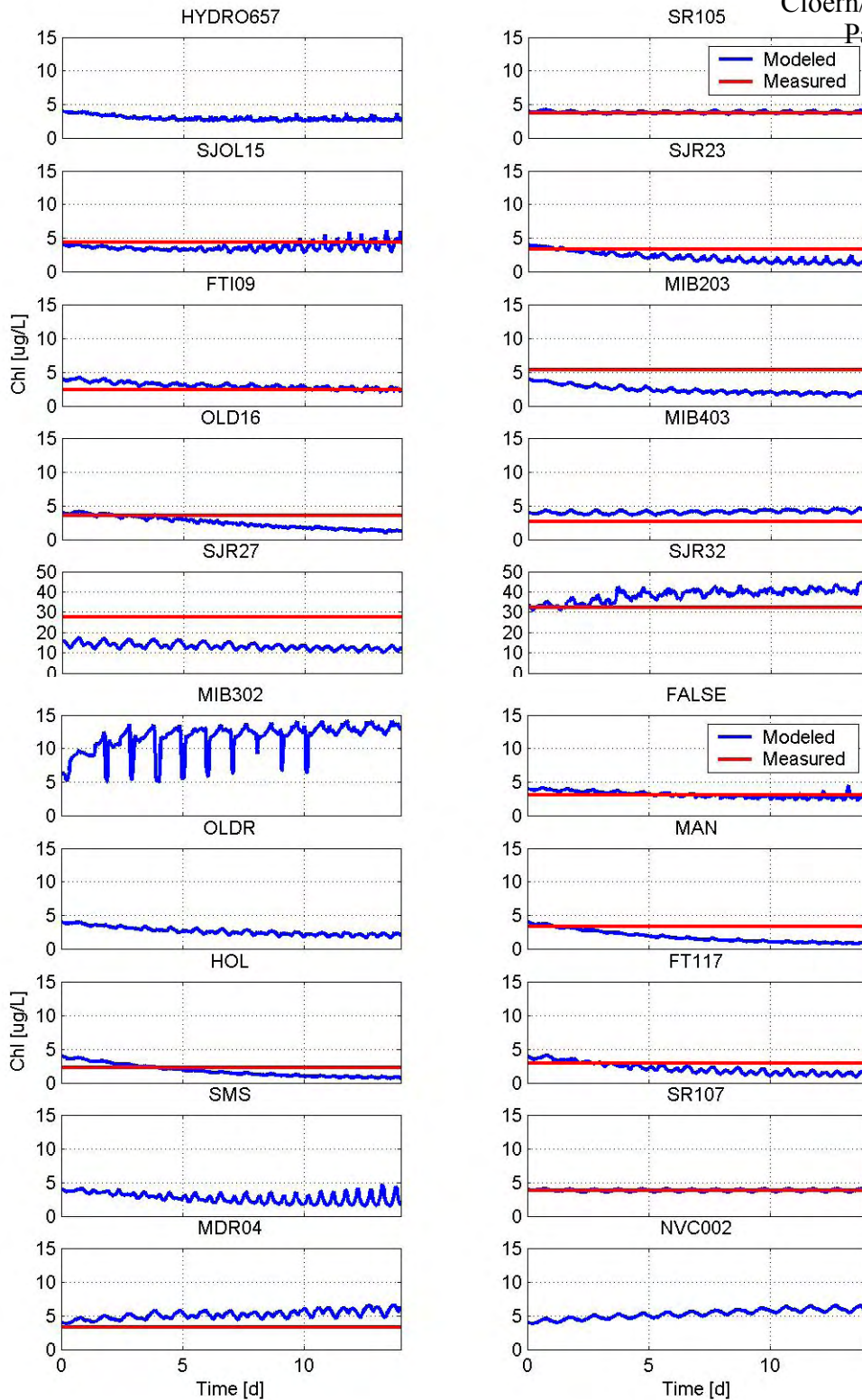


Figure MD16. Time series of chl *a* calculated by coupled Delta scale model for the case of no pumping (blue lines). Red lines represent a single discrete measurement taken during May 2003. See Figure MD4 for station locations.

Monitoring Changes In Selenium Contamination Of The San Francisco Bay-Delta In Response To Restoration And Changing Water Management

prepared by Fisher, Nick

submitted to Ecosystem Restoration Program 2004 Monitoring and Evaluation

compiled 2004-11-19 15:20:34 PST

Project Information

This proposal is for the Ecosystem Restoration Program 2004 Monitoring and Evaluation solicitation as prepared by Fisher, Nick .

3:00PM PST, November 19, 2004: The deadline for submissions has passed. Changes to proposals are no longer allowed.

Proposal Title *Monitoring changes in selenium contamination of the San Francisco Bay-Delta in response to restoration and changing water management*

Project Duration *36 months*

Lead Organization *USGS*

Name *Enter the name of the agency or institution to whom funds would be awarded.*

Lead Organization

Type *federal agency*

Organization Contact

Please provide information for the primary person responsible for oversight of grant operation, management, and reporting requirements at the lead institution.

Social Title *Mr.*

First Name *Russell*

Last Name *Graham*

345 Middlefield Rd. MS470

Street Address

City *Menlo Park*

State Or Province *CA*

ZIP Code Or Mailing Code *94025*

Telephone *650-329-4453 Include area code.*

E-Mail *rgraham@usgs.gov*

Lead Investigator

Is the lead investigator the same as the main contact person?

No.
If not, provide the lead investigator's information below.

Social Title *Dr.*

First Name *Samuel*

Last Name *Luoma*

Institution *USGS*

Institution Type *federal agency*

345 Middlefield Rd. MS465

Street Address

City *Menlo Park*

State Or Province *CA*

ZIP Code Or Mailing Code 94025

Telephone 650-329-4481 Include area code.

E-Mail snuoma@usgs.gov

Provide information about additional investigators below.

Last Name	First Name	Organization
<i>Stewart</i>	<i>Robin</i>	<i>USGS</i>
<i>Fisher</i>	<i>Nicholas</i>	<i>State University of New York, Stony Brook</i>
<i>Baines</i>	<i>Stephen</i>	<i>State University of New York, Stony Brook</i>
<i>Cutter</i>	<i>Gregory</i>	<i>Old Dominion University</i>

Select one topic area that best applies to this proposal.

- at-risk species assessment
- river channel restoration
- estuary foodweb productivity
- ecosystem water and sediment quality
- environmental education
- environmental water management
- fish passage
- fish screens
- harvestable species assessment
- lowland floodplains and bypasses
- local watershed stewardship
- mine remediation
- hydrodynamics, sediment transport, and flow regimes
- non-native invasive species
- riparian habitat
- shallow water and marsh habitat
- upland habitat and wildlife friendly agriculture
- X2 relationships (freshwater - seawater interface)

Select a minimum of three keywords to describe the project.

X adaptive management

- *aquatic plants*

X benthic invertebrates

X biological indicators

- *birds*

- neotropical migratory birds

- shorebirds

- upland birds

- wading birds

- waterfowl

- *climate*

- climate change

- precipitation

- sea level rise

- snowmelt

X contaminants / toxicants / pollutants

- contaminants and toxicity of unknown origin

- emerging contaminants

- mercury

- nutrients and oxygen depleting substances

- organic carbon and disinfection byproduct precursors

- persistent organic contaminants

- pesticides

- salinity

- sediment and turbidity

X selenium

- trace metals

- *database management*

- *economics*
- *engineering*
- civil
- environmental
- hydraulic
- *environmental education*
- *environmental impact analysis*
- *environmental laws and regulations*
- *environmental risk assessment*
- *fish biology*
- bass and other centrarchids
- delta smelt
- longfin smelt
- other species
- salmon and steelhead
- splittail
- striped bass
- sturgeon
- *fish management and facilities*
- hatcheries
- ladders and passage
- screens
- *forestry*
- *genetics*
- *geochemistry*
- *geographic information systems (GIS)*
- *geology*
- *geomorphology*
- *groundwater*
- *habitat*
- benthos
- channels and sloughs
- flooded islands
- floodplains and bypasses
- oceanic
- reservoirs
- riparian
- rivers and streams
- shallow water
- upland habitat
- vernal pools
- water column
- wetlands, freshwater
- wetlands, seasonal
- wetlands, tidal
- *human health*
- *hydrodynamics*
- *hydrology*
- *insects*
- X* *invasive species / non–native species / exotic species*
- *land use management, planning, and zoning*
- *limnology*
- *mammals*
- large
- small
- *microbiology / bacteriology*
- X* *modeling*
- X* conceptual
- X* quantitative
- X* *monitoring*
- *natural resource management*
- *performance measures*
- X* *phytoplankton*
- *plants*
- X* *primary productivity*

- *reptiles*
- *restoration ecology*
- *riparian ecology*
- X sediment*
- *soil science*
- *statistics*
- *subsidence*
- X trophic dynamics and food webs*
- X water operations*
- barriers
- X diversions / pumps / intakes / exports*
- gates
- levees
- reservoirs
- X water quality management*
- X ag runoff*
- mine waste assessment and remediation
- X remediation*
- temperature
- urban runoff
- X water quality assessment and monitoring*
- *water resource management*
- X water supply*
- X demand*
- environmental water account
- water level
- water storage
- X watershed management*
- *weed science*
- *wildlife*
- ecology
- management
- wildlife–friendly agriculture
- *zooplankton*

Does this project have multiple sites?

Yes.

If this project has only one site, provide geographic coordinates of the center point of the restoration action your project will monitor. Enter decimal degrees to the nearest 0.001 without directional characters (N, S, E, W).

Latitude: *example: 38.575; must be between 30 and 45*

Longitude: *example: –121.488; must be between –120 and –130*

Describe the project location using information such as water bodies, river miles, and road intersections.

Suisun Bay – Carquinez Strait through the confluence of the Sacramento and San Joaquin Rivers. Modeling of selenium inputs include hydrology of the Sacramento River (Freeport) and San Joaquin Rivers (Vernalis).

1.3 South Delta Select all ecological management units containing a restoration site you will monitor, or another monitoring site included in your proposal.

1.4 Central and West Delta

2.1 Suisun Bay and Marsh ERP Regions, Ecological Management Zones ("Ecozones") and Ecological Management Units ("Ecountits")

Select each county containing a restoration site you will monitor or a monitoring site included in your proposal.

- Alameda County
- Amador County
- Butte County
- Calaveras County
- X Contra Costa County*
- Colusa County
- El Dorado County
- Fresno County

- Glenn County
- Madera County
- X** Marin County
- Mariposa County
- Merced County
- Napa County
- Nevada County
- Placer County
- Plumas County
- X** Sacramento County
- X** San Joaquin County
- Shasta County
- Solano County
- Stanislaus County
- Sonoma County
- Sutter County
- Tehama County
- Tuolumne County
- Yolo County
- Yuba County

Select each Indian reservation or rancheria containing or adjacent to a restoration site you will monitor or a monitoring site included in your proposal. Use the [California tribal lands](#) as a guide.

Amador County

- Buena Vista Rancheria
- Ione Band of Miwok
- Jackson Rancheria

Butte County

- Berry Creek Rancheria
- Chico Rancheria (Mechoopda)
- Enterprise Rancheria
- Mooretown Rancheria

Calaveras County

- California Valley Miwok Tribe (Sheep Ranch)

Colusa County

- Colusa Rancheria (Cachil Dehe Band of Wintun Indians)
- Cortina Rancheria

El Dorado County

- Shingle Springs Rancheria
- Washoe Tribe Reservations of California and Nevada

Fresno County

- Big Sandy Rancheria
- Cold Springs Rancheria
- Table Mountain Rancheria

Glenn County

- Grindstone Rancheria

Madera County

- North Fork Rancheria
- Picayune Rancheria (Chukchansi)

Placer County

- United Auburn Rancheria

Plumas County

- Greenville Rancheria

Shasta County

- Big Bend Rancheria (Pit River Tribe)
- Montgomery Creek Rancheria (Pit River Tribe)
- Pit River Tribe of California
- Redding Rancheria
- Roaring Creek Rancheria (Pit River Tribe)

Sonoma County

- Cloverdale Rancheria
- Dry Creek Rancheria
- Graton Rancheria
- Lytton Rancheria
- Stewarts Point Rancheria

Tehama County

– Paskenta Band of Nomelaki Indians

Tuolumne County

– Chicken Ranch Rancheria

– Tuolumne Rancheria

Yolo County

– Rumsey Rancheria

List each city (one per line) containing a restoration site you will monitor or a monitoring site included in your proposal.

None

Select all California Congressional districts which contain the applicant organization, a restoration site you will monitor, or another monitoring site included in your proposal.

Select all California Senate districts which contain the applicant organization, a restoration site you will monitor, or another monitoring site included in your proposal.

Select all California Assembly districts which contain the applicant organization, a restoration site you will monitor, or another monitoring site included in your proposal.

Is this proposal for next phase funding of an ongoing project funded by the CALFED ERP or the CVPIA?

Yes.

If it is, identify the ongoing project.

Project Title *Transport, Transformation, and Effects of Se and Carbon in the Delta of the Sacramento–San Joaquin Rivers: Implications for ecosystem restoration*

CALFED Contract Management Agency *Dept. of Water Resources*

Amount Funded *2,600,000*

Date Awarded *2001–01–01*

Lead Institution *USGS*

Project Number *2001–F200*

Have you received funding from CALFED for a project *not* listed above?

Yes.

If you have, list the project(s) below.

Project Title *Assessment of the Impact of Se on Restoration of San Francisco Bay*

CALFED Program *ERP*

CALFED Contract Management Agency *USGS*

Amount Funded *1,600,000*

Date Awarded *1998–01–01*

Project Number *98–2015000–00096*

Project Title *EVALUATION OF MERCURY TRANSFORMATIONS AND TROPHIC TRANSFER IN THE SAN FRANCISCO BAY/DELTA: IDENTIFYING CRITICAL PROCESSES FOR THE ECOSYSTEM RESTORATION PROGRAM (ERP)*

CALFED Program *ERP*

CALFED Contract Management Agency *GCAP*

Amount Funded *2,262,566*

Date Awarded *2003–01–01*

Project Number *ERP –02–P40*

Project Title

CALFED Program

CALFED Contract Management Agency

Amount Funded

Date Awarded

Project Number

Project Title

CALFED Program

CALFED Contract Management Agency

Amount Funded

Date Awarded

Project Number

Project Title

CALFED Program

CALFED Contract Management Agency

Amount Funded

Date Awarded

Project Number

Have you ever submitted a similar proposal to any CALFED PSP?

No.

If you have, describe the submission below.

Project Title

CALFED Program

Date Of PSP

List people you feel are qualified to act as scientific reviewers for this proposal and are not associated with CALFED.

Full Name	Organization	Telephone	E-Mail	Expertise
------------------	---------------------	------------------	---------------	------------------

*adaptive
management*

*adaptive
management*

*adaptive
management*

*adaptive
management*

Give additional comments, information, etc. here.

Executive Summary

This proposal is for the Ecosystem Restoration Program 2004 Monitoring and Evaluation solicitation as prepared by Fisher, Nick .

3:00PM PST, November 19, 2004: The deadline for submissions has passed. Changes to proposals are no longer allowed.

Provide a summary of your project including the following:

- a brief description of your proposed project, including location
- objective
- the restoration action(s) it will monitor, and the approach to implement the proposal
- expected outcomes
- relationship to CBDA ERP or CVPIA goals

This information will be made public on our website shortly after the closing date of this PSP.

Executive summary: We propose to conduct studies that will allow development of a long-term, cost-effective plan to monitor the bioavailability of selenium in San Francisco Bay. Selenium monitoring is essential because of changes in hydrography and restoration of wetlands (Dutch Slough and Suisun Marsh) could either accentuate Se contamination in the Bay or lead to fears that Se contamination is worsening. In the late 1980s and early 1990s, elevated levels of Se were found within tissues of native bottom-feeding fish and diving ducks within Suisun Bay. Reductions in discharge of selenite by refineries near Carquinez Strait were mandated beginning in 1995 in an effort to reduce this contamination. While dissolved Se concentrations declined markedly, Se levels in sturgeon and diving ducks remain high. Adverse effects on white sturgeon and Sacramento splittail have recently been demonstrated. Se toxicity thus remains a threat that may compromise CALFED's water management and restoration efforts in this region. The persistence of Se contamination at the highest trophic levels can be traced to the behavior of a single prey species, the invasive clam *Potamocorbula amurensis*, which now dominates the benthic biomass in the region. Tissue concentrations of Se in *P. amurensis* in Suisun Bay exceed those in other prey organisms, including other bivalves, and cycle annually across the threshold for toxic effects in predators. We have posed several hypotheses that may explain the observed patterns of Se accumulation in *P. amurensis* and enable us to exploit this species as a valuable bioindicator species. Discriminating among these hypotheses will allow us to develop an effective monitoring plan. It will also allow us to understand how Se in *P. amurensis* will respond if increased Se inputs occur into the Bay/Delta from the San Joaquin River due to planned alterations of San Joaquin River discharge. Specifically, we propose to monitor Se in *P. amurensis* and relate concentrations to those in water and discrete particles within Suisun Bay to assess changes in the bioavailable levels that might be coming from SJR inputs at present. These data will extend already existing data sets, greatly increasing the power to detect longer term changes in Se concentrations within key biota and their environment, and establish baselines against which to assess effects of future management actions. Three sites will be sampled representing different levels of influence from the San Joaquin River. We will focus on relating the Se content in the clams with that in their food, since diet constitutes essentially the sole source of Se for these animals. Stable isotopic composition of the clams ($\delta^{34}\text{S}$, $\delta^{13}\text{C}$ and $\delta^{15}\text{N}$) will be monitored to determine if clams are feeding on organic matter produced locally or on material transported from other regions of the ecosystem. These measurements will be coupled with novel measurements of Se concentrations in the phytoplankton and protozoan food of *P. amurensis*. Dual-label radioisotope methods will be used to assess seasonal changes in the average Se content of newly produced phytoplankton. Synchrotron based x-ray fluorescence microscopy (SXRF) will provide estimates of Se content of individual planktonic cells that, coupled with analyses of plankton species composition, will allow us to explain seasonal changes in the Se content of the phytoplankton and relate Se levels in *P. amurensis* to the composition of plankton communities. To aid interpretation of patterns in the clam tissue data, we will also conduct experiments on assimilation and retention of Se in *P. amurensis* from various food items and on the response of Se in plankton to changes in ambient dissolved Se. Based on changes in dissolved Se concentrations predicted from models that account for riverine inputs, estuarine mixing and biogeochemical processes, we will use our results to assess the influence of proposed water and Se management options on Se incorporation into the Suisun Bay food-web. We will suggest monitoring designs for Se in Suisun Bay that will be feasible for USGS and collaborators to perpetuate into the future.

Environmental Compliance

This proposal is for the Ecosystem Restoration Program 2004 Monitoring and Evaluation solicitation as prepared by Fisher, Nick .

3:00PM PST, November 19, 2004: The deadline for submissions has passed. Changes to proposals are no longer allowed.

Successful applicants are responsible for complying with all applicable laws and regulations for their projects, including the National Environmental Policy Act (NEPA) and the California Environmental Quality Act (CEQA).

Any necessary NEPA or CEQA documents for an approved project must tier from the CALFED Programmatic Record of Decision and CALFED Programmatic EIS/EIR to avoid or minimize the projects adverse environmental impacts. Applicants are encouraged to review the Programmatic EIS/EIR and incorporate the applicable mitigation strategies from Appendix A of the Programmatic Record of Decision in developing their projects and the NEPA/CEQA documents for their projects.

CEQA Compliance

Which type of CEQA documentation do you anticipate?

none *Skip the remaining questions in this section.*

negative declaration or mitigated negative declaration

EIR

categorical exemption *A categorical exemption may not be used for a project which may which may cause a substantial adverse change in the significance of a historical resource or result in damage to scenic resources within an officially designated state scenic highway.*

If you are using a categorical exemption, choose all of the applicable classes below.

Class 1. Operation, repair, maintenance, permitting, leasing, licensing, or minor alteration of existing public or private structures, facilities, mechanical equipment, or topographical features, involving negligible or no expansion of use beyond that existing at the time of the lead agency's determination. The types of "existing facilities" itemized above are not intended to be all-inclusive of the types of projects which might fall within Class 1. The key consideration is whether the project involves negligible or no expansion of an existing use.

Class 2. Replacement or reconstruction of existing structures and facilities where the new structure will be located on the same site as the structure replaced and will have substantially the same purpose and capacity as the structure replaced.

Class 3. Construction and location of limited numbers of new, small facilities or structures; installation of small new equipment and facilities in small structures; and the conversion of existing small structures from one use to another where only minor modifications are made in the exterior of the structure. The numbers of structures described in this section are the maximum allowable on any legal parcel, except where the project may impact on an environmental resource of hazardous or critical concern where designated, precisely mapped, and officially adopted pursuant to law by federal, state, or local agencies.

Class 4. Minor public or private alterations in the condition of land, water, and/or vegetation which do not involve removal of healthy, mature, scenic trees except for forestry or agricultural purposes, except where the project may impact on an environmental resource of hazardous or critical concern where designated, precisely mapped, and officially adopted pursuant to law by federal, state, or local agencies.

Class 6. Basic data collection, research, experimental management, and resource evaluation activities which do not result in a serious or major disturbance to an environmental resource, except where the project may impact on an environmental resource of hazardous or critical concern where designated, precisely mapped, and officially adopted pursuant to law by federal, state, or local agencies. These may be strictly for information gathering purposes, or as part of a study leading to an action which a public agency has not yet approved, adopted, or funded.

Class 11. Construction, or placement of minor structures accessory to (appurtenant to) existing commercial, industrial, or institutional facilities, except where the project may impact on an environmental resource of hazardous or critical concern where designated, precisely mapped, and officially adopted pursuant to law by federal, state, or local agencies.

Identify the lead agency.

Please write out all words in the agency title other than United States (Use the abbreviation "US".) and California (Use the abbreviation "CA").

Is the CEQA environmental impact assessment complete?

If the CEQA environmental impact assessment process is complete, provide the following information about the resulting document.

Document Name

State Clearinghouse Number

If the CEQA environmental impact assessment process is not complete, describe the plan for completing draft and/or final CEQA documents.

NEPA Compliance

Which type of NEPA documentation do you anticipate?

none *Skip the remaining questions in this section.*

environmental assessment/FONSI

EIS

categorical exclusion

Identify the lead agency or agencies.

Please write out all words in the agency title other than United States (Use the abbreviation "US".) and California (Use the abbreviation "CA").

If the NEPA environmental impact assessment process is complete, provide the name of the resulting document.

If the NEPA environmental impact assessment process is not complete, describe the plan for completing draft and/or final NEPA documents.

Successful applicants must tier their project's permitting from the CALFED Record of Decision and attachments providing programmatic guidance on complying with the state and federal endangered species acts, the Coastal Zone Management Act, and sections 404 and 401 of the Clean Water Act.

Please indicate what permits or other approvals may be required for the activities contained in your proposal and also which have already been obtained. Please check all that apply. If a permit is *not* required, leave both Required? and Obtained? check boxes blank.

Local Permits And Approvals	Required?	Obtained?	Permit Number (If Applicable)
Conditional Use Permit	-	-	
Variance	-	-	
Subdivision Map Act	-	-	
Grading Permit	-	-	
General Plan Amendment	-	-	
Specific Plan Approval	-	-	
Rezone	-	-	
Williamson Act Contract Cancellation	-	-	
Other	-	-	

State Permits And Approvals	Required?	Obtained?	Permit Number (If Applicable)
Scientific Collecting Permit	-	X	
CESA Compliance: 2081	-	-	
CESA Compliance: NCCP	-	-	
1602	-	-	
CWA 401 Certification	-	-	
Bay Conservation And Development Commission Permit	-	-	
Reclamation Board Approval	-	-	
Delta Protection Commission Notification	-	-	
State Lands Commission Lease Or Permit	-	-	
Action Specific Implementation Plan	-	-	
Other	-	-	

Federal Permits And Approvals	Required?	Obtained?	Permit Number (If Applicable)
ESA Compliance Section 7 Consultation	-	-	
ESA Compliance Section 10 Permit	-	-	
Rivers And Harbors Act	-	-	
CWA 404	-	-	

Other	-	X	
-------	---	---	--

Permission To Access Property	Required?	Obtained?	Permit Number (If Applicable)
Permission To Access City, County Or Other Local Agency Land Agency Name	-	-	
Permission To Access State Land Agency Name	-	-	
Permission To Access Federal Land Agency Name	-	-	
Permission To Access Private Land Landowner Name	-	-	

If you have comments about any of these questions, enter them here.

Land Use

This proposal is for the Ecosystem Restoration Program 2004 Monitoring and Evaluation solicitation as prepared by Fisher, Nick .

3:00PM PST, November 19, 2004: The deadline for submissions has passed. Changes to proposals are no longer allowed.

Does the project involve land acquisition, either in fee or through easements, to secure sites for monitoring?
 No. *Skip to the next set of questions.*
 Yes. *Answer the following questions.*

How many acres will be acquired by fee?

How many acres will be acquired by easement?

Describe the entity or organization that will manage the property and provide operations and maintenance services.

Is there an existing plan describing how the land and water will be managed?
 No.
 Yes. *Cite the title and author or describe briefly.*

Will the applicant require access across public or private property that the applicant does not own to accomplish the activities in the proposal?
 No. *Skip to the next set of questions.*
 Yes. *Answer the following question.*

Describe briefly the provisions made to secure this access.

Do the actions in the proposal involve physical changes in the current land use?
 No. *Skip to the next set of questions.*
 Yes. *Answer the following questions.*

Describe the current zoning, including the zoning designation and the principal permitted uses permitted in the zone.

Describe the general plan land use element designation, including the purpose and uses allowed in the designation.

Describe relevant provisions in other general plan elements affecting the site, if any.

Is the land mapped as Prime Farmland, Farmland of Statewide Importance, Unique Farmland, or Farmland of Local Importance under the California Department of Conservation's Farmland Mapping and Monitoring Program?
 No. *Skip to the next set of questions.*
 Yes. *Answer the following questions.*

Land Designation	Acres	Currently In Production?
Prime Farmland		–
Farmland Of Statewide Importance		–
Unique Farmland		–
Farmland Of Local Importance		–

Is the land affected by the project currently in an agricultural preserve established under the Williamson Act?
 No. *Skip to the next set of questions.*
 Yes. *Answer the following question.*

Is the land affected by the project currently under a Williamson Act contract?
 No. *Skip to the next set of questions.*
 Yes. *Answer the following question.*

Why is the land use proposed consistent with the contract's terms?

Describe any additional comments you have about the projects land use.

Conflict Of Interest

This proposal is for the Ecosystem Restoration Program 2004 Monitoring and Evaluation solicitation as prepared by Fisher, Nick .

3:00PM PST, November 19, 2004: The deadline for submissions has passed. Changes to proposals are no longer allowed.

Complete the following table in order to provide the full names and organizations of all individuals in the following categories.

- Applicant and investigators listed in the proposal who wrote the proposal, will be performing the tasks listed in the proposal or who will benefit financially if the proposal is fund.
- Subcontractors listed in the proposal who will perform some tasks listed in the proposal and will benefit financially if the proposal is funded.
- Individuals not listed in the proposal who helped with proposal development, for example by reviewing drafts, or by providing critical suggestions or ideas contained within the proposal.

Parts of this table are generated from responses given in the project information form.

Role	Full Name	Institution
submitter	Fisher, Nick	<i>State University of New York, Stony Brook</i>
applicant	Graham, Russell	USGS
lead investigator	Luoma, Samuel	USGS
investigator	Stewart, Robin	USGS
investigator	Fisher, Nicholas	State University of New York, Stony Brook
investigator	Baines, Stephen	State University of New York, Stony Brook
investigator	Cutter, Gregory	Old Dominion University
<i>subcontractor</i>	<i>Benjamin Twining</i>	<i>Yale University</i>
<i>subcontractor</i>	<i>Kent Elrick</i>	<i>USGS, Atlanta Georgia</i>
<i>subcontractor</i>	<i>Dick Dufford</i>	<i>Fort Collins, CO</i>
<i>subcontractor</i>	<i>David Harris</i>	<i>UC Davis</i>

Tasks And Deliverables

This proposal is for the Ecosystem Restoration Program 2004 Monitoring and Evaluation solicitation as prepared by Fisher, Nick .

3:00PM PST, November 19, 2004: The deadline for submissions has passed. Changes to proposals are no longer allowed.

For each task in the project's scope of work, please list major deliverables and an estimate of the start and end time (in months from the date the project's contract is executed).

Task ID	Task Name	Start Month	End Month	Deliverables
1	Project Management	1	36	Semiannual and final reports. Periodic invoices
2	<i>Chemistry of dissolved and particulate matter</i>	1	36	DATA: 2 yrs of monthly analyses at two stations in Suisun Bay: dissolved selenite, selenate and organic selenide; suspended particulate total Se, organic selenide, selenite, and elemental Se; Total suspended particulate matter; C and N content of suspended matter; chlorophyll concentrations. OTHER DELIVERABLES: Manuscripts.
3	<i>Determinants of Se concentrations in the plankton</i>	1	36	DATA: up to 1000 SXRF determinations of Se in cells of phytoplankton and protozoa. 2 yrs of monthly analyses at two stations in Suisun Bay: Se:C uptake ratios of phytoplankton; phytoplankton species composition and biomass, protozoan species composition and biomass, free and attached bacterial abundance and biomass; modeled estimates of Se bioaccumulation from plankton by Potamocorbula. OTHER DELIVERABLES: Manuscripts.
4	<i>Unique characteristics of invasive clam – growth, condition, reproduction, uptake kinetics, and/or selective feeding</i>	1	36	DATA: 2 yrs of monthly analyses at three stations in Suisun Bay: Se in Potamocorbula; stable isotopic composition of C, S and N in Potamocorbula; estimates of ingestion, assimilation, and regeneration of Se from detritus. OTHER DELIVERABLES: Manuscripts.

Comments

If you have comments about budget justification that do not fit elsewhere, enter them here.

Budget

This proposal is for the Ecosystem Restoration Program 2004 Monitoring and Evaluation solicitation as prepared by Fisher, Nick .

3:00PM PST, November 19, 2004: The deadline for submissions has passed. Changes to proposals are no longer allowed.

Provide a detailed budget showing how requested funds will be used to carry out the project's scope of work for each year of the project. Costs for each major task described in the "Approach and scope of work" section of your proposal must be presented. The first task in each year should be project management, including the specific costs associated with insuring accomplishment of a specific project, such as inspection of work in progress, validation of costs, report preparation, response to project specific questions and necessary costs directly associated with specific project oversight. Applicants should also include costs associated with managing project funds, including preparation of quarterly and final reports to the funding agency. Tasks for environmental compliance, monitoring, data handling, storage, and dissemination, and public outreach should also be included as appropriate for your project. In calculating indirect costs, assume funds will be awarded by State of California.

The sections in this budget form are derived from the tasks you have defined in the "Tasks and Deliverables" form.

Year 1 (Months 1 To 12)

Task	Labor	Benefits	Travel	Supplies And Expendables	Services And Consultants	Equipment	Lands And Rights Of Way	Other Direct Costs	Direct Total	Indirect Costs	Total
1: project management (12 months)	0	0	0	0	0	0	0	0	\$0	15162	\$15,162
2: Chemistry of dissolved and particulate matter (12 months)	40058	10075	7000	14000	1600	0	0	4500	\$77,233	32438	\$109,671
3: Determinants of Se concentrations in the plankton (12 months)	89099	20755	9500	12500	4000	6000	0	3456	\$145,310	44669	\$189,979
4: Unique characteristics of invasive clam – growth, condition, reproduction, uptake kinetics, and/or selective feeding (12 months)	92736	18387	2000	14780	6624	0	0	0	\$134,527	72908	\$207,435
Totals	\$221,893	\$49,217	\$18,500	\$41,280	\$12,224	\$6,000	\$0	\$7,956	\$357,070	\$165,177	\$522,247

Year 2 (Months 13 To 24)

Task	Labor	Benefits	Travel	Supplies And Expendables	Services And Consultants	Equipment	Lands And Rights Of Way	Other Direct Costs	Direct Total	Indirect Costs	Total
1: project management (12 months)	0	0	0	0	0	0	0	0	\$0	15029	\$15,029
2: Chemistry of dissolved and particulate matter (12 months)	41941	10567	7000	8000	1600	0	0	4500	\$73,608	30915	\$104,523
3: Determinants of Se concentrations in the plankton (12 months)	92504	22859	9500	12500	4000	0	0	3956	\$145,319	47169	\$192,488
4: Unique characteristics of invasive clam – growth, condition, reproduction, uptake	97844	19898	2000	13080	5964	0	0	0	\$138,786	75258	\$214,044

kinetics, and/or selective feeding (12 months)												
Totals	\$232,289	\$53,324	\$18,500	\$33,580	\$11,564	\$0	\$0	\$8,456	\$357,713	\$168,371	\$526,084	

Year 3 (Months 25 To 36)

Task	Labor	Benefits	Travel	Supplies And Expendables	Services And Consultants	Equipment	Lands And Rights Of Way	Other Direct Costs	Direct Total	Indirect Costs	Total
1: project management (12 months)	0	0	0	0	0	0	0	0	\$0	16611	\$16,611
2: Chemistry of dissolved and particulate matter (12 months)	53958	13690	7000	8000	1600	0	0	6000	\$90,248	37904	\$128,152
3: Determinants of Se concentrations in the plankton (12 months)	96029	25075	9500	12500	4000	0	0	3956	\$151,060	49078	\$200,138
4: Unique characteristics of invasive clam – growth, condition, reproduction, uptake kinetics, and/or selective feeding (12 months)	103276	21506	2000	13080	3564	0	0	0	\$143,426	79143	\$222,569
Totals	\$253,263	\$60,271	\$18,500	\$33,580	\$9,164	\$0	\$0	\$9,956	\$384,734	\$182,736	\$567,470

Project Totals

Labor	Benefits	Travel	Supplies And Expendables	Services And Consultants	Equipment	Lands And Rights Of Way	Other Direct Costs	Direct Total	Indirect Costs	Total
\$707,445	\$162,812	\$55,500	\$108,440	\$32,952	\$6,000	\$0	\$26,368	\$1,099,517	\$516,284	\$1,615,801

Do you have cost share partners already identified?

Yes.

If yes, list partners and amount contributed by each:

USGS – \$450,000 SUNY – \$171,571 ODU – 69,415

Do you have potential cost share partners?

No.

If yes, list partners and amount contributed by each:

Are you specifically seeking non-federal cost share funds through this solicitation?

No.

Budget Justification

This proposal is for the Ecosystem Restoration Program 2004 Monitoring and Evaluation solicitation as prepared by Fisher, Nick .

3:00PM PST, November 19, 2004: The deadline for submissions has passed. Changes to proposals are no longer allowed.

Labor

For each task in the scope of work, please provide the estimated hours or days and compensation rate proposed for each position for each year of the project.

Task 1: None Task 2 (ODU): Year 1. Cutter, 1 month, \$9118; Senior Technician, 6 months, \$23740; Undergraduate Lab Assistant, 20 h/week, \$7200 Year 2. Cutter, 1 month, \$9574; Senior Technician, 6 months, \$24927; Undergraduate Lab Assistant, 20 h/week, \$7440 Year 3. Cutter, 2 month, \$20105; Senior Technician, 6 months, \$26173; Undergraduate Lab Assistant, 20 h/week, \$7680

TASK 3 (Stony Brook): Fisher: 2 months per year: \$27099 for Year 1; \$28454 for Year 2; \$29877 for Year 3 Baines: 4 months per year: \$20000 for Year 1; \$21000 for Year 2; \$22000 for Year 3 Palma: 6 months per year: \$21000 for Year 1; \$22050 for Year 2; \$23153 for Year 3 student: 12 months per year: \$21000 per year for each of Years 1, 2 and 3 Task 4: USGS The USGS budget is mainly for salaries not obligated by USGS. Dr. Stewart will spend one-third of her time on this project, or more. Although she is a permanent USGS employee we are obliged to pay her salary with non-USGS funds. The GS-5 technician is essential to the field and lab aspects of the biological studies that are required for modeling to determine if inherent characteristics of Potamocorbula's life cycle determine the high concentrations and seasonal variability. The GS-7 technician is to support the collection and sample preparation for Potamocorbula and for the bottom water and particulate matter (the samples will be collected by USGS and analyzed by ODU). Partial time is requested for a postdoctoral associate to run kinetic studies essential to verifying Potamocorbula bioaccumulation characteristics. We expect to pay only living expenses for the person we have in mind (she has a grant to come to our lab from Hong Kong should the work be funded). USGS has obliged all employees to charge one week of time to projects like this, to pay for administrative activities; so Dr. Luoma is charging one week.

Benefits

Provide the overall benefit rate applicable to each category of employee proposed in the project (e.g., if you budget for three biologists, you only need to provide the benefit rate of a biologist once on the form).

Task 1: None Task 2 (ODU): Cutter: 26% Senior Technician: 29.71% Undergraduate Lab Assistant: 9.04%

Task 3 (Stony Brook): Fisher: 15.5%; Baines and Palma: 35% for Year 1; 37% for Year 2; 39% for Year 3; student: 10.5% for Year 1; 12% for Year 2; 13.5% for Year 3.

Task 4: Post-doc – no benefits GS employees – 30%, 10% (ST-3104)

Travel

Estimate costs for all travel for each task for each year of the project. Travel will only be reimbursed at rates approved by the State of California (with a hotlink to the travel reimbursement rules). Provide purpose all non-local travel. Estimate travel costs for each task for each year of the project. Travel will only be reimbursed at rates approved by the State of California, as provided in DPA Short-Term Travel Reimbursement for All Excluded and Represented Employees . Provide purpose for all non-local travel.

Task 1: None Task 2 (ODU): \$7000 per year for Years 1–3; travel (Virginia–California) for field sampling and training in Year 1; PI group meetings; attend and present results at scientific conferences

Task 3 (Stony Brook): \$9500 per year for each of Years 1, 2 and 3. The travel expenses will cover trips between Stony Brook and Menlo Park, CA, travel associated with field trips for collections of water and organisms, travel to the Advanced Photon Source at Argonne National Lab for SXRF analyses, as well as participation in a national meeting each year to present the results of our work.

Task 4: \$6,000 is requested to cover costs for field technicians while on the RV Polaris monthly cruises and for travel for PIs to attend conferences (SETAC, ASLO, etc.) to present results.

Supplies And Expendables

List general categories of supplies, like office supplies or computer supplies, and the amount needed for each. Indicate the amounts proposed for each category of supplies for each task for each year of the project.

Task 1: None Task 2 (ODU): Year 1. \$14000; includes: purchase and construction of equipment for water column sampling (\$6000), compressed gases and liquid nitrogen (\$4000), reagents and acids (\$2000), filters (\$1000), and miscellaneous laboratory expendables (\$1000) Year 2. \$8000; includes: compressed gases and liquid nitrogen (\$4000), reagents and acids (\$2000), filters (\$1000), and miscellaneous laboratory expendables (\$1000) Year 3.

\$8000; includes: compressed gases and liquid nitrogen (\$4000), reagents and acids (\$2000), filters (\$1000), and miscellaneous laboratory expendables (\$1000)

Task 3 (Stony Brook): Total = \$12500 per year. radioisotopes: \$7000 per year; filters: \$750 per year; gold EM grids: \$500 per year; filtration apparatuses: \$750 per year; acids: \$500 per year; radioactive counting tubes: \$750 per year; biochemicals: \$1000 per year; glassware: \$750 per year; office and computer supplies: \$500 per year

Task 4: Major costs include those for Se analyses (\$85/sample) done by the USGS lab in Atlanta. \$5,700 is required to do the reproduction work on clams (sectioning). The USGS requires all projects utilizing boats for their research to request funds for boat maintenance (\$2000 per year).

Services And Consultants

Identify the specific tasks for which these services would be used. This should include partners, other than the project applicant, in collaborative projects, whether or not the collaboration will be managed through a contractor–subcontractor relationship or through separate contracts between the funding agency and key project partners. Estimate amount of time required and compensation rate. Specify the services which these consultants, subcontractors, or partners will provide. These could include monitoring, laboratory analysis, or other services. List name(s) of partners or other consultants, if they have already been selected, their principal staff assigned to the project and the aspects of their work to be charged to the grant (e.g., salary, travel, supplies, etc.).

Task 1: None Task 2 (ODU): \$1600 per year in Years 1–3 for ICP–MS analyses at the ODU LITER facility.

Task 3 (Stony Brook): Contract with Dr. Benjamin Twining, Yale University to assist with analysis of Se content of individual plankton cells. These analyses will be accomplished at the Argonne National Laboratory using the SXRF microprobe. This work includes spectra fitting, data processing and all other SXRF tasks. It involves three weeks per year of Dr. Twining's time.

Task 4: We will pay UC Davis stable isotope facility to do our stable isotope analyses (they have been doing them for the past 6 years) at a cost of \$8 for C and \$25 for S analyses. We will have Dick Dufford do our phytoplankton taxonomy (\$100 per sample).

Equipment

Identify specific each item of equipment to be purchased and its cost. Equipment is defined as a piece of property costing \$1,000 or more per unit with an expected use of three or more years.

Task 3 (Stony Brook): photosynthetron and associated water bath: \$6000 for Year 1.

Lands And Rights Of Way

List costs of any lands, easements, or rights of way needed for monitoring activities, explaining whether cost are based on completed appraisals of properties to be acquired or are estimates derived by other methods Explain how these costs were estimated (prior experience, recent sales, appraisal of parcels to be acquired, etc). State whether any appraisals used meet applicable state and federal standards, and include support or a rationale for this statement. Reasonable costs for appraisals, title reports, environmental site assessment, and other closing expenses may be included.

None

Other Direct Costs

Provide any other direct costs not already covered for each task for each year of the project.

Task 1: None Task 2 (ODU): Year 1. \$3000 for sample shipping (California–Virginia); \$1500 for publication/presentation charges Year 2. \$3000 for sample shipping (California–Virginia); \$1500 for publication/presentation charges Year 3. \$3000 for sample shipping (California–Virginia); \$3000 for publication/presentation charges

Task 3 (Stony Brook): \$3456 per year for student tuition; \$500 for each of Years 2 and 3 for publication expenses

Indirect Costs/Overhead

Overhead usually includes general office costs such as rent, phones, furniture, general office staff, etc., and is distributed by a predetermined "indirect rate" applied to other specific costs. This is usually an amount or pro rate share of existing salaries and benefits, rent, equipment, materials, and utilities attributable to a function or activity, but not necessarily generated by the function or activity. Where available, use indirect rates approved through state or federal budgetary procedures, such as [Office of Management and Budget Circular A–87 \(Cost Principles for State, Local, and Indian Tribal Governments\)](#), [Office of Management and Budget Circular A–21 \(Cost Principles for Educational Institutions\)](#) or [Office of Management and Budget Circular A–122 \(Cost Principles for Non–Profit Organizations\)](#). Explain what direct costs this rate is applied to when budgeting indirect costs (e.g., labor, benefits, etc.). Where an approved indirect rate is not available, explain what is encompassed in the budget for indirect costs. This could include costs associated with

general office requirements such as rent, phones, furniture, general office staff, etc., generally distributed by a predetermined percentage (or surcharge) of specific costs.

Task 1: The USGS charges a project management rate of (5.06%) that is applied to each collaborating institution based on their yearly total project cost.

Task 2 (ODU): 42% of total direct costs in Years 1–3

Task 3 (Stony Brook): Year 1: 32.88% of total direct costs (minus tuition and equipment); Year 2: 33.25% of total direct costs (minus tuition and equipment); Year 3: 33.25% of total direct costs (minus tuition and equipment).

Task 4: The USGS has an overhead rate of %55.18 of net.

Comments

If you have comments about budget justification that do not fit elsewhere, enter them here.

Task 2 (ODU): Funding for one month per year in Years 1 and 2 of Dr. Cutter's salary is requested. He will oversee the ODU efforts, interface with the investigators at USGS and SUNY SB, interpret the field results, and prepare reports and publications. In Year 3, 2 months salary are requested for Dr. Cutter to additionally work on the interfacing of the ODU, SUNY SB, and USGS data sets using several modeling approaches. Six months of salary in each of Years 1–3 are requested for the Senior Technician who will participate in some of the field sampling, and perform all of the selenium and ancillary parameter determinations from the monthly water column sampling. The Senior Technician will also supervise the Undergraduate Lab Assistant. This Lab Assistant (up to 20 hours per week in Years 1–3) will assist the Senior Technician in cleaning sample bottles and filters, preparing reagents, and processing samples.

Task 3 (Stony Brook): Funds are requested for the support of Prof. Nicholas Fisher (2 months/year) who will coordinate and participate in the Stony Brook effort and be responsible for the overall success of the Stony Brook portion of this project, and for Dr. Stephen Baines, an Assistant Research Professor (4 months/year) who will be involved in all aspects of the research conducted by the Stony Brook team. In addition we request funds for a graduate (PhD) student's stipend; the student will be involved in all aspects of the sampling and SXRF analyses and will use these data as the centerpiece of his/her dissertation. Funds are also requested for 6 months support per year of a technician, Ms. Shelagh Palma, who will maintain algal cultures and radioactive inventories, prepare media, assist with the preparation of SXRF samples, and participate in some of the experiments.

Monitoring changes in selenium contamination of the San Francisco Bay-Delta in response to restoration and changing water management.

Samuel Luoma and Robin Stewart, USGS, Menlo Park; Nicholas S. Fisher and Stephen B. Baines, Stony Brook University; Gregory Cutter, Old Dominion University

1. Problem, Goals, Objectives

A. Problem. Selenium contamination is a serious, imminent threat to CALFED's proposals to restore important populations of species of concern. That threat could grow under some of the scenarios for both restoration and water management. Selenium is hazardous because it is biomagnified through food webs [1] and it is strongly toxic to reproduction in upper trophic level organisms. Important sources presently exist, including irrigation drainage from the western San Joaquin Valley and inputs from industry. Many CALFED restoration and management alternatives would have the net effect of increasing inflows from the San Joaquin River (SJR) to the Delta and Bay, especially relative to the Sacramento River. Water quality is impaired in the SJR because of inputs from irrigation drainage that include (sometimes highly) elevated selenium concentrations. Greater SJR inflows could mean greater selenium inputs to the Bay. The focus of CALFED's ecosystem restoration efforts is, properly, on the creation of suitable habitat for native species in the Bay-Delta. But such habitat will not be adequate to meet CALFED's goals if other actions (or the habitat itself) create conditions that prevent native species from reproducing. Major restoration is planned for shallow water habitats and wetlands in the Delta and upper Bay (e.g. Suisun Marsh, North Delta and Dutch Slough). Studies clearly demonstrate that Delta and Central Valley wetlands, and some kinds of shallow water habitats, can trap and recycle selenium (Cutter et al, in preparation; [2]), ultimately releasing it in forms that can threaten food webs. Recent work conclusively shows that existing levels of selenium contamination already threaten some native fishes that spend time in or near such habitats, notably Green and White Sturgeon, and Sacramento splittail [1,3,4]. Greater recycling of Se in restored wetlands could accentuate effects of greater inputs. If so, the gains made by creation of restored habitat and reduction of refinery inputs would be reversed. The location of these cumulative impacts is likely to be Suisun Bay, a key habitat for many native species at the head of the estuary [5].

B. Purpose Adaptive, integrated management requires that CALFED monitor selenium contamination into the future. If the integrated effect of CALFED actions is greater Se inputs, its implications can be identified and modified. The purpose of this project is to develop a selenium monitoring strategy for the San Francisco Bay-Delta, taking advantage of what has been learned from six years of CALFED funded study of the element and ten years of study before that. An effective early-warning monitoring system must be able to detect increasing threats, but it also must be cost-effective to be sustainable. While it is possible to periodically monitor native fishes, crabs or migratory birds, it is difficult and expensive. The best approach is to monitor a few key variables that affect the supply of bioavailable Se to these species, and determine the response of the system. These could, perhaps, be supplemented by infrequent (e.g. every five years) monitoring of the larger animals. To be useful, this monitoring system must be able to separate influences of water projects from management of selenium sources that are internal to the Bay (like refineries). It must also help to explain the pathways and mechanisms controlling Se contamination so that CALFED can scientifically evaluate management options. Finally, the monitoring should be focused where the threat is most serious and where the cumulative impacts from the element are likely to be greatest.

C. Objectives. Here we propose to bring together more than 20 years of data that exist on Se in the Bay to develop the monitoring strategy. Studies to date characterize occurrence and distribution of selenium, the major mechanisms that control its fate and effects, and severity of specific threats. But the studies also raise an important dilemma. Several alternative explanations are possible for the existing level of selenium contamination in the Bay food web. But it is not clear which is the most important. A second objective of the work is to evaluate these alternatives, so as to identify the most influential factors governing the contamination. The answers will determine if the threat from selenium is growing (and could grow further); or whether forces internal to the Bay are the cause of the existing problems. From knowledge of the important influences on food web bioaccumulation of Se, we can define the most cost-effective measures for on-going monitoring and assessment of cumulative impacts from future restoration/water management changes. To develop the monitoring and assessment strategy, we will address three inter-related questions: 1) How have selenium concentrations in the most vulnerable organisms in the Bay food web changed in response to changing conditions over the last 20 years? 2) What factors drive the response of the Bay food web? 3) Among those factors, which are the best metrics for tracking performance of combined CALFED actions in releasing selenium to the Bay?

We believe we are poised to resolve the above dilemma in three years. A third goal is to use the answers to explicitly develop a Se monitoring plan for the Bay, using a limited number of measures. The products will include a baseline of interpreted data, from which future efficacy of management strategies with regard to selenium can be continuously evaluated; as well as a plan that is sufficiently efficient that it might be feasible for USGS and collaborators to continue to monitor key variables in the years ahead.

Below we lay out the rationale for focusing on selenium, and for emphasizing the invasive clam, *Potamocorbula amurensis*, as a biomonitor. We also explain why it is important to understand the processes that determine Se bioaccumulation by that clam before long-term monitoring moves ahead.

2. Justification

A. Conceptual understanding of Selenium biogeochemistry. Selenium is a well-studied metalloid that exists in natural waters in several valence states. The most prominent dissolved inorganic forms are selenite (SeO_3^{2-}) and selenate (SeO_4^{2-}) while elemental selenium is exclusively associated with particles. In addition, there are organic forms of selenium (organic selenides) that are produced by organisms that have accumulated inorganic selenium out of water [6,7]. Chemically, the behavior of selenium is most similar to that of sulfur, another Group VI element. Although selenium is an essential element for many organisms, elevated concentrations can exert toxic effects. This can occur when selenium substitutes for sulfur in organic compounds, notably sulfur-containing amino acids to produce selenomethionine and selenocysteine, leading to breakdowns in metabolic function (e.g., [8,9]). The tolerance range of most organisms to this element is rather narrow, so increasing selenium concentrations in an organism's tissues from background levels by as little as an order of magnitude and as little as a factor of about 4 can be lethal. In addition to acute toxic effects, sublethal concentrations of selenium in animals can lead to reproductive abnormalities including congenital malformations, growth retardation, impaired swimming, coordination and behavior, chromosomal aberrations, and intestinal lesions [10].

In saline waters, selenium enters the food web primarily through the active uptake of dissolved selenite and organic selenides by phytoplankton and bacteria. Selenite and selenate

tend not to adsorb to particulate matter in saline water, although some adsorption of selenite can occur in freshwaters [11]. Selenate can be taken up by phytoplankton in freshwater [12], but the active biological uptake of selenate in estuarine or marine waters is usually believed to be minimal because it is taken up via the same pathways used for sulfate [13-15], and in seawater sulfate is about 10^7 times more abundant than selenate. Selenite, however, is readily accumulated in phytoplankton and is generally the most available form of inorganic Se to marine phytoplankton [16-19]. Organic selenides, often present at concentrations that can exceed inorganic forms [20], may be rapidly taken up out of seawater by phytoplankton, at rates almost comparable to those for selenite; typically those algal species which bioconcentrate selenite most also are most active in accumulating organic selenides [21]. Se in algal cells, primarily in the form of reduced Se contained in selenoaminoacids in free or combined form in algal cytoplasm [22-26], is readily assimilated from algae by herbivores [25,27-29]; it may even be biomagnified 2-4 times with trophic transfer although such biomagnification is not always observed [30,31].

B. Conceptual understanding of selenium in San Francisco Bay. Much has been learned about the transport and transformations of the different forms of selenium in the Bay-Delta in the past 20 years, in large part due to studies funded by CALFED since 1997. Important potential sources of dissolved selenium were refineries, with inputs as selenite, and irrigation drainage from the San Joaquin Valley (SJV) via the San Joaquin River (SJR), usually with selenate the dominant form [6,32]. Selenium from the SJR historically was recycled back to the SJV by export pumps in the Delta, or was trapped in the Delta. Extreme concentrations of Se ($> 1 \text{ ug g}^{-1}$) are not found in Delta waters or sediments (Table 1). However, Se is recycled within Delta habitats. A gradual conversion of the least dangerous form, selenate, to particulate Se and organic selenide occurs in shallow water habitats where waters have long residence times [33]. Thus the Delta is a net trap for Se, and it may be a source of dangerous forms of selenium under the right conditions. Models indicate that if SJR inflows to the Bay increase, particulate Se concentrations in the Bay could double, even with no increase in irrigation drainage inputs to the SJR (Fig. 1; [34]). Dissolved Se concentrations in Bay waters currently do not exceed proposed water quality criteria, but suspended particulate selenium, particularly the reduced organic form, is the most important source of selenium for the food web [35].

Although hotspots of very high particulate selenium concentrations are not found in the Bay, elevated concentrations in indicator organisms (bivalves, zooplankton, benthic crustaceans) suggest the Bay has long been contaminated compared to surrounding systems. The focal point for that contamination is Suisun Bay (Fig. 2). Early studies suggested that concentrations of Se in waters (including its chemical speciation), suspended particulates and bivalves were the best metrics for evaluating the status of Se contamination in the Bay and Delta [6,36,37]. These parameters were routinely assessed between 1984 and 1989; and from 1995 until the present [4]. Spatial distributions of Se, mass balance models and speciation identified the refineries near Suisun Bay as major sources of Se (especially of selenite) in 1986 [20]. Regulatory action caused the refineries to lower their discharges since ~1996.

Studies show that Se biomagnifies through San Francisco Bay food webs, making these ecosystem especially sensitive to contamination. Se contamination is especially problematic for upper trophic level animals in Suisun Bay that ingest bivalves near the base of their food web. In the mid-late 1980's *Potamocorbula amurensis* began to replace *Corbicula fluminea* as the dominant benthic organism in the bay. After that, Se concentrations in organisms known to feed on benthic organisms increased markedly ([1]; Fig. 4). This suggested that the food web

particulate->*Potamocorbula* -> predators is key to mediating Se contamination in Suisun Bay. There is strong evidence for reproductive inhibition and deformities occurring in two native fishes for which Suisun Bay is an important habitat: white sturgeon and Sacramento splittail [1]. Because these effects are occurring at the existing level of contamination, any increase could be especially problematic. Elevated levels of Se in other native species (Dungeness crab, lesser scaup, greater scaup, canvasback, surf scoter) raise the possibility that they are threatened as well (refs). Understanding the effect of past management actions on Se content of *Potamocorbula* is thus critical to understanding how those actions affect Se contamination of the entire food web.

The reduction in refinery inputs in 1996 resulted in pronounced declines in selenite concentrations around Carquinez Straits [32]. However, the responses of the particulate material, bivalves, and upper trophic level species to this change are complex. Trends in particulate Se concentrations remain unclear with a fair degree of variability and no detectable trend (Fig. 3). However, the record of these difficult measurements is relatively sparse and irregularly spaced in time (Fig. 3). It is difficult to determine from existing data how reduced selenite inputs have affected selenium in particulates.

The trend of Se concentrations in biota is similarly unclear. Because bivalves accumulate virtually all their Se from their diet and not the dissolved phase [37-39], one would expect a correlation between the concentration of selenium in *Potamocorbula* and that in suspended particulate matter, yet no simple linear relationship is evident. Se in *Potamocorbula* exhibits a remarkably regular seasonal cycle that roughly conforms to the relative contribution of the SJR to freshwater inflows, and closely parallels the seasonal cycle of salinity and total S content within clam tissues (Fig. 5). This cycle results in concentrations of Se in clam tissues that are significantly above threshold concentration of $10 \mu\text{g Se g}^{-1}$ dry weight during fall, and significantly below this threshold in spring. In contrast the Se concentration of particulate matter is less regular in its seasonality and exhibits a poor correlation with Se in clam tissues (Fig. 3). The lack of a correlation may reflect the fact that the clams and suspended particles have been sampled at different times. Alternatively, the phytoplankton and protozoa upon which the clams selectively feed constitute <5% of the suspended matter. Thus variability in the Se content of *Potamocorbula* food may be obscured by the total Se content of detrital material. Recent laboratory studies suggest that the Se content of phytoplankton species, including genera represented in Suisun Bay such as *Skeletonema* and *Cryptomonas*, can vary by several orders of magnitude ([19], Fig. 6). Field studies in the Delta suggest that bacteria and their grazers may contain more Se than phytoplankton [12]. Thus, seasonal variability in the composition of the plankton could well contribute to the observed seasonal cycle in Se content of *Potamocorbula*.

As with Se in suspended particulate matter, the annual mean Se concentrations in *Potamocorbula* did not decline after the reductions in selenite loading from the oil refineries at Carquinez Strait; although the seasonal cycle that was evident in 1995 was quite different than that observed in the 1985-89. Se concentrations in the liver of white sturgeon declined modestly since the initial phase of the *Potamocorbula* invasion (after refinery inputs declined). The strong seasonal cycle in *Potamocorbula* Se content requires more analysis before drawing conclusions about long term trends. Studies of cultured phytoplankton raise the possibility the Se content of the phytoplankton and protozoan (the best food for *Potamocorbula*) may not have responded to the management action [19]. Algal species that concentrate Se most effectively appear to do so actively using specific enzymes with high affinity. Se uptake via this pathway is non-linearly related to the ambient concentration of selenite and nearly saturated at the concentrations that now typify the entire North Bay after reductions in selenite loading ([19]; Fig. 7). Thus,

applying the culture uptake kinetics data to field conditions, it can be surmised that the 10-fold reductions in selenite concentration could have caused Se concentrations in algal cells to decline by < 80%. This change is small compared to variations in particulate Se loads and the Se content of phytoplankton that may result from changes in community composition. Questions remain, however, about the applicability of the algal culture studies to communities *in situ*.

Another explanation for the complex response to reductions in selenite discharge is that Se contents of the clams and, to a more variable degree, the suspended particulate matter, is now influenced by inputs from the SJR. Such an effect could result from two mechanisms. Contaminated particles produced near the San Joaquin River could be advected into the regions on Suisun Bay when flow from the SJR was relatively high, then trapped and recycled when residence time increases in Fall [4]. Extended residence of high dissolved selenate and organic selenide concentrations during such periods may influence the Se content of particles produced within Suisun Bay. Patterns in selenate depletion indicate that this form of selenium may be taken up by phytoplankton in lieu of selenite, despite contrary evidence from past studies [32]. Tidal advection of particulates from the SJR is also possible, along bottom waters (unsampled in earlier studies). The contribution of the SJR to total inflows is highest in fall and winter, and this is when Se concentrations increase in *Potamocorbula*. Either of these would mask local changes in the Se content of autochthonous material.

Selenate is the main form of dissolved Se entering the Bay from the SJV and is most likely to increase as a result of planned changes to water management and diversions of central valley water into the Bay/Delta ecosystem [34]. Uptake of dissolved organic selenides by phytoplankton may also contribute to Se contamination at the bottom of the food web [40], since it can constitute a significant fraction of the dissolved Se pool in the Bay and in the incoming rivers [32,41]. Unfortunately, current observations on Se in clams, particles and water are not sufficient to differentiate among the physical alternatives. The dynamic nature of Se in these pools and discrepancies and gaps in the temporal resolution of the various data sets make interpretation problematic. Moreover, chemical approaches employed in the past cannot separately determine the Se contents of the detritus, which dominates the suspended particulate organic matter, and the much less abundant phytoplankton, which probably constitutes the primary food source for *Potamocorbula*.

Recent methodological developments now allow us to discriminate between Se in detrital material and Se in phytoplankton, thus providing us with a means to assess the relative contribution of these two pools to Se accumulation by *Potamocorbula*. First, dual label radioisotopic methods have been developed for estimating the Se:C uptake ratios in newly produced organic matter [12]. This method compares well with bulk chemical measurements when phytoplankton cells dominate the suspended particulate matter. It also lends itself to use in experiments on the effect of ambient selenite and selenate concentrations on Se content of the living plankton. Second, we have recently begun using a technology called synchrotron-based x-ray fluorescence microscopy (SXRF) to measure trace element concentrations in individual natural phytoplankton and protozoan cells [42-44]. In SXRF, high energy monochromatic x-rays are focused on a cell, inducing characteristic x-ray fluorescence spectra that indicate the elemental concentration and composition of the cell. Recent advances in x-ray optics and quantification techniques allow us to detect, accurately and precisely, concentrations of important bioactive elements including Se at subattomole cell⁻¹ concentrations in *individual* cells as small as 2 μm in diameter [42]. These unique measurements, when coupled with analyses of plankton species composition and dissolved Se concentration, will vastly improve our ability to

interpret the cause of change in the Se:C ratio of *Potamocorbula* food and can therefore be used to interpret spatial and temporal trends in the Se concentrations within *Potamocorbula* tissues. In addition, C, S and N stable isotopes can be used to determine if suspended particulate organic material or clam biomass is derived primarily from material produced under marine or freshwater conditions. In this way, they can indicate whether clams in fall are assimilating material imported from the freshwater SJR and Delta, or produced locally in the more saline waters of Suisun Bay.

C. Conceptual Model. From our basic knowledge about the biogeochemistry of Se, and our knowledge of Se fate, distributions and effect in Suisun Bay, the conceptual model in Figure 9 was developed to guide our research. The key organism is *Potamocorbula* because of its ability to concentrate Se effectively from its food and pass it on to benthivorous native fish (Sacramento splittail, white sturgeon) and bird species (diving ducks). Controls on Se in *Potamocorbula* are of two sorts. First, there is the bioenergetic and biokinetic behavior of *Potamocorbula* which affects accumulation of biomass as well as assimilation and retention of Se. Second, there is the variability in the composition of *Potamocorbula*'s food. Suspended particles consist of living phyto- and protozooplankton which almost always constitute < 5% of the suspended particulate organic matter in the Bay, and abiotic particles, including suspended sediment. The living particles almost certainly provide much of the Se for *Potamocorbula* because they are selectively ingested by bivalves [45] and the percentage of ingested Se assimilated from them can be as high as 80 % [46]. Se concentrations within phytoplankton equilibrates quickly (<1 d) with ambient concentrations of dissolved Se [47] and can be measured using radioisotopic techniques or SXRF [12,42]. Detrital particulate organic matter along with its associated bacteria is either imported from the Delta under high flow or resuspended from local sediments due to tidal action and constitutes as much as >95% of the total particulate organic mass (Hypothesis 4). However, the material within these particles is not readily assimilated by clams [35]. Only the organic Se within these particles is potentially available, but its bioavailability is uncertain. Finally, the long lifespan of these particles also means that the detrital pool changes slowly over time. Because decaying phytoplankton probably are the ultimate source of much of the bioavailable detrital matter in the Bay, the detrital organic Se content probably reflects the long-term average Se content of the phytoplankton remains (not necessarily equal to that in living cells). Thus, if clams incorporate appreciable amounts of Se from the detrital organic pool, short-term variations in phytoplankton Se content will have less impact on the Se content of clam tissues.

D. Hypotheses. In summary, careful study of processes that affect Se fate and bioavailability over the past 20 years led to conceptual model in Figure 9. The model identifies four explicit hypotheses about what could be controlling Se concentrations in *Potamocorbula*. Deciding among these possibilities is critical to evaluating the effects of past management actions and to the development of future monitoring activities in the Bay.

1. Se inputs from the SJR to the Bay primarily control the Se content of *Potamocorbula*, so Se remains elevated because of continued inputs from this source. The seasonal increase in Se in bivalves roughly follows the ratio of SJR/total inflows to the Bay (Fig. 3). However, comparisons between suspended particulate selenium and SJR inflow ratios are inconclusive, although the data are sparse (Fig. 3). In Fall, the phytoplankton which are a large component of *Potamocorbula*'s diet could increase their Se contents in response to seasonal inputs of waters containing high selenate and organic selenide concentrations from the SJR.

The implications are that fall Se concentrations within clam food, tissues and predators will not reflect the ambient conditions in Suisun Bay. **Management/Monitoring implications:** Effects of reductions in changes made to selenium inputs to the Bay would have to be assessed during times of the year when SJR inputs are low. Looking forward, the Se in *Potamocorbula* and its predators likely will increase dramatically in response to diversions of Central Valley water into the Bay/Delta. Efficient monitoring of future changes in Se content of biota must take into account resulting changes in SJR seasonal hydrology.

2. **The Se content of *P. amurensis* is determined primarily by the composition of the plankton community, not dissolved concentrations of Se.** Recent studies show that Se uptake by phytoplankton (the plants in the water column preferably selected by many bivalves) differs widely among species and may be relatively insensitive to variation in ambient concentrations of dissolved selenite. The seasonal variation in Se concentrations in clams might reflect higher Se levels in the marine species that predominate in fall, when salinity is high, than in the freshwater algae that predominate in spring, when salinity is low. **Management/Monitoring implications:** Se in clams are unlikely to have changed much, if at all, in response to changes in Se inputs to the Bay. Sampling of phytoplankton and protozooplankton are needed to understand and predict variations in Se content of clams and their predators. Moreover, changes in hydrology or other aspects of the environment that systematically affect the composition of the plankton may effect levels or spatial distribution of Se concentrations in biota.
3. **The Se content of *P. amurensis* is determined by Se:C content of organic detritus which changes very slowly.** Phytoplankton have reduced their Se content in response to selenite reductions. However, because of the size of the pool of organic detritus contained in sediments, changes in the Se:C ratio have been too slow to perceive. Seasonal variability reflects changes in reproduction (e.g., spawning), ingestion rate, retention or assimilation of Se from particulate food by *Potamocorbula*. **Management/Monitoring implications:** Se in clams will eventually decline over time, but slowly, perhaps over decadal time periods. Monitoring efforts must be adjusted with that time-frame in mind. Observable effects of diversions of Central Valley water to the Bay/Delta on Se in biota may also be delayed and difficult to detect, requiring the development of early warning indicators of contamination.
4. **The predominant species of bivalve in Suisun Bay is an especially effective bioaccumulator of Se.** Between 1985 and 1990 the predominant species of bivalve in Suisun Bay changed. *Corbicula fluminea* largely disappeared from Suisun Bay and was replaced by invasion by the exotic clam *Potamocorbula amurensis*. No pre-1995 data exists for *P. amurensis*. So it is possible that concentrations were much higher pre-1995 than at present. It is also possible that this species accumulates this much Se under almost any Se input regime. Se uptake comparisons between *C. fluminea* and *P. amurensis* do not show strong differences in kinetics. But the choice of food or feeding rate differences between the two could be crucial. Better understanding Se uptake and retention in *P. amurensis* compared to *Corbicula* is critical to interpreting how this species will respond to change. **Management/Monitoring implications:** Monitoring of Se contamination of native species essentially requires monitoring of *Potamocorbula* abundances, Se content and dietary contribution. Future inputs are unlikely to affect Se entering the food-web, or the effects are currently impossible to predict.

3. Previously Funded Monitoring

Our conceptual knowledge of selenium in San Francisco Bay was greatly expanded by CALFED supported studies. Publications that stem from that work are indicated by asterisks in the reference list of this proposal. Previously funded monitoring of selenium also was extended by that support. In response to elevated Se concentrations identified by the California Department of Fish & Game's Se verification studies (1987 – 1990), the USGS monitor Se in the clam *Corbicula fluminea* from 1986-1989. Biomonitoring started again in 1995, with support from the Regional Water Quality Control Board, and the USGS Toxic Substance Hydrology Program. Only by this time the exotic Asian Clam, *Potamocorbula amurensis* had replace *C. fluminea* in Suisun Bay. *P. amurensis* were collected at USGS station 8.1 in Carquinez Strait (Fig. 2) periodically during monthly cruises of the R.V. Polaris (website). More regular collection and analysis began with CALFED funding in 1998. In 1998 and in 2001, the USGS in collaboration with Stony Brook and Old Dominion Universities received funds from the CALFED Ecosystem Restoration Program to continue the monitoring program under the following projects:

CALFED #98-2015000-00096 - Assessment of the Impact of Se on Restoration of SF Bay

CALFED #2001-F200 - Transport, Transformation, and Effects of Se and Carbon in the Delta of the Sacramento-San Joaquin Rivers: Implications for ecosystem restoration

Through this period *P. amurensis* were collected at several sites in Suisun Bay, with some breaks in the data because clams occasionally disappeared (often the result of high riverine inflows). Additional USGS monitoring included the collection of water column and benthic samples to assess water quality (e.g. chlorophyll, salinity, turbidity, conductivity) and the benthic community (e.g. diversity, biomass). The USGS has a long history of using benthic clams, including *Potamocorbula amurensis*, to monitor responses of the system to changes in water pollution inputs, water management and restoration.

Since the USGS began monitoring the clams in 1995 a consistent seasonal pattern of Se concentrations in the clams has emerged (Figs. 3,4 ;[4]). Elevated concentrations of Se that exceed toxicity thresholds identified for predator food [48] were observed in the fall (September through November) and would slowly decline to low concentrations in the spring (March through May). Initial analysis of the temporal pattern suggested an obvious link to hydrologic cycles within the estuary (in particular the ratio of SJR/total river inflows), but no single mechanism could unambiguously identified. Furthermore, it was expected that when the refineries changed the speciation of the Se in their effluents and reduced overall concentrations that the clams would respond in time. But, as noted above the response of the bivalves is not a simple one.

To supplement the clam monitoring program at station 8.1 animals from throughout the Suisun Bay food web were collected in one intense study, and the number of sites for *P. amurensis* monitoring was expanded. *P. amurensis* were collected at a total of 20 sites in Northern San Francisco Bay to determine the spatial extent of Se contamination in the estuary. The results indicated that the highest Se exposures were located nearest the confluence of Carquinez Strait and Suisun Bay (Fig. 2). In the spring and fall of 1999, additional clams were collected from sites within Suisun Bay to determine the spatial extent of the seasonal pattern. The highest concentrations were again observed closest to the Carquinez/Suisun Bay point, but all stations showed increases in Se concentrations in the fall.

Dissolved and particulate selenium have been examined in the SF Bay estuary and the Sacramento and San Joaquin Rivers for over 16 years (Cutter and Cutter 2004). Monitoring of Se in *Potamocorbula* was closely integrated with monitoring of suspended particulate and dissolved selenium monitoring in Suisun Bay and Carquinez Straits over 2.5 years of this period (2000-2003). These data and those from other samplings are displayed in Fig. 8. Total dissolved Se ranged from 1.4 – 2.7 nM, consistent with the long term record in the estuary (Cutter and Cutter 2004), while suspended particulate Se (SPSe) ranged from 0.25-2.4 $\mu\text{g g}^{-1}$, also consistent with literature values [6,33]. The first observation from these data is that the concentration of Se on suspended particles bears no resemblance to total dissolved Se, likely due to the multiple sources of suspended particulate Se (in situ production, riverine transport, sediment resuspension). Second, the Se concentrations in *Potamocorbula* show a rough positive correlation with suspended particulate Se, but this relationship is non-linear, likely due to the composition of the particles and the speciation of the Se. Finally, the concentration of SPSe appears to respond to higher SJ River flows (as a ratio of the total inflow), consistent with simulation model predictions ([34]; Meseck and Cutter in prep.) that predict increasing concentrations of SPSe in Suisun Bay and Carquinez Strait with mandated increases in SJ River flow to the estuary.

Upper trophic level animals also were studied as a part of the above work (Stewart et al, 2004). The Selenium Verification study provided a baseline of data on selenium in fish and birds in the 1980's (published by Linville et al. 2002). High concentrations were observed in some species but not others. Stewart et al (2004) re-sampled the upper trophic levels in 1999 and 2000. They showed that predators were the most contaminated with selenium, and that animals that used bivalves as prey were the most contaminated of those. Selenium was biomagnified in all food webs, but the high selenium content of the bivalves compared to other prey, was propagated up that food web. The work of Stewart et al (2004) also showed that it was follow selenium in large predators (e.g. sturgeon) but only at long intervals.

Water, particulates, biomonitors and food webs have also been studied in the Delta, although this work is still in progress. For the purposes of this proposal, the important findings were that the Delta does not seem to have food webs as badly contaminated with selenium as does Suisun Bay. Whatever the cause of the selenium contamination in *P. amurensis* and its predators, it seem to be related to external and/or internal processes specific to Suisun Bay.

4. Approach and scope of work.

A. Conceptual framework for controls of Se in *Potamocorbula* within Suisun Bay.

B. Approach & Scope of work

We will address the four major hypotheses using a combination of standard and novel monitoring measurements, and targeted experiments. We will achieve the above objectives and assess the four hypotheses listed above by completing the following tasks. These tasks and their associated hypotheses are also summarized in Table 2.

Task 1. Project Management. We will produce quarterly reports and a final report to CALFED, summarizing the data collected and the findings based on that data. See Expected Outcomes and Products.

Task 2. Chemistry of dissolved and particulate matter. Since a major hypothesis for the proposed work concerns the nature of the particles themselves that are being filtered by

Potamocorbula, we will characterize (a) the suspended matter during the monthly sampling at two of the three stations by measuring the total suspended solids, organic carbon and nitrogen and their stable isotopes (to characterize the organic matter and sources), chlorophyll and phaeophytin *a* (phytoplankton biomass), biogenic silica (siliceous phytoplankton), and total aluminum (clay mineral contribution); and (b) total Se and its speciation (Se 0, Se IV+VI, organic Se-II). In addition to the above, our simulation model of Se biogeochemistry in the Bay [34] indicates the importance of SJR inputs on the concentrations of dissolved and particulate Se in Suisun Bay and Carquinez Strait, and therefore we proposed determining the concentration and speciation of dissolved Se (total, SeIV, SeVI, org. Se-II) during the monthly sampling. This work will be in conjunction with the selenate uptake measurements.

Sampling will largely follow the methods described in Cutter and Cutter (2004) where a 5 L Go Flo bottle deployed on a non metallic cable obtains the sample, and the water is directly (by nitrogen pressure applied to the bottle) filtered through 0.4 μm membrane filters (pre-weighed to measure total suspended matter) in triplicate for Se (one for total and two for speciation); the filtrate is placed in 1 L borosilicate bottles and acidified to pH 1.5 for dissolved Se determinations. Two additional 0.4 μm filters will be collected, one for aluminum (and other metals) and another for biogenic silica. All of the membrane filters are immediately frozen for storage. Unfiltered water is also passed through solvent cleaned glass fiber filters for the determinations of organic carbon, nitrogen, and sulfur [49], while the chlorophyll and phaeophytin sample is collected on a glass fiber filter and subjected to solvent extraction and fluorometric analysis [50].

The speciation of dissolved Se will be determined using the selective hydride generation/atomic absorption detection method described by Cutter [51-53]. Briefly, within a glass stripping vessel selenite is quantitatively converted to hydrogen selenide using sodium borohydride addition to a sample containing sulfanilamide to eliminate interference due to nitrite and acidified to 4 M HCl. The evolved hydrogen selenide is stripped from solution using He and trapped in a borosilicate U-tube packed with silanized glass wool and immersed in liquid nitrogen. After the trap is removed from the LN₂, an atomic absorption spectrometer fitted with an open quartz tube furnace burning an air-hydrogen flame detects the hydride; instrument response (as peak area) is recorded on a chromatographic integrator. To determine selenate+selenite, another acidified sample is boiled for 15 min, cooled, and then subjected to the selenite determination; selenate is the difference between this determination and that of selenite. Total dissolved Se is determined by boiling a 4 M HCl acidified sample, with the addition of potassium persulfate, and then following the selenite procedure. The difference between total dissolved selenium and selenite+selenate yields the concentration of dissolved organic selenide + elemental Se (this may be colloidal and pass through the 0.4 μm filter). However, many studies have shown that this fraction is primarily organic selenide in the form of dissolved peptides [7,52,54], and hereafter it is referred to as Adissolved organic selenide.” To ensure accuracy, all determinations utilize the standard additions method of calibration, and all samples are analyzed in triplicate to quantify precision (typically < 4% for concentrations above 0.4 nM). The detection limit for all three Se forms is 0.02 nM.

The total Se content of suspended particles and phytoplankton cultures will be determined using wet oxidative digestion followed by selective hydride generation atomic absorption spectroscopy [51,53]. Filters are dried at 40°C, weighed (for TSM concentration), and subsequently digested using a three-step nitric-perchloric acid reflux procedure [55]. After evaporation of most of the nitric acid, the residue is then redissolved in 4M HCl, passed through

a column filled with Bio-Rad AG1 x 8 anion exchange resin (chloride form, 100-200 mesh) to remove iron and stored until final Se analysis. Selective leaches were conducted for determination of particulate Se speciation (elemental Se: [56]; SeIV + SeVI: [55]). Aliquots of the digestion or selective leach solutions are then analyzed using the total dissolved Se procedure as above. The standard additions method of calibration is used to ensure accuracy, and all determinations will be made in triplicate. Accuracy will also be evaluated using the digestion and analysis of standard reference material (NIST 1566 or 1566b oyster tissue). The detection limit for particulate Se is 0.005 nM, with precision (relative standard deviation) of <5%. The filter weights will be corrected for salt content by analyzing the digest solution for Na⁺ using flame AAS.

Filters for organic C and N analyses are dried at 40°C and processed using a Carlo Erba 1500 Elemental Analyzer [49]. The determination of biogenic Si on the membrane filters will utilize the sequential alkaline (1% sodium carbonate) extraction method of [57] to correct for effects by the solubilization of clay minerals. Silicate concentrations in the resulting leach solutions are then determined using standard colorimetric procedures modified for use on an Alpkem Rapid Flow Analyzer. Particulate aluminum concentrations (and other metals) will be determined using a hydrofluoric-nitric acid digestion of the membrane filter in a sealed Teflon “bomb”, followed by analysis of the solution using magnetic sector, ICP/Mass Spectrometry.

Task 3. Determinants of Se concentrations in the plankton

The potential impact of plankton community composition on clam Se will be estimated (Hypothesis 2). First we will track seasonal changes in phytoplankton Se:C uptake ratios measured by dual label isotope procedures. These measurements will be correlated to variations in clam Se. The effect of changing community composition on variability in the Se content of the phytoplankton will be assessed by combining SXRF measurements of Se concentrations in individual plankton cells with information on composition of the phytoplankton community. We will experimentally determine if the Se content of the plankton changes in response to dissolved selenite and selenate concentrations, the latter experiments being relevant to the effects of SJR inflows on Se in clams (Hypothesis 3).

Task 3a. SXRF measurements of Se content of phytoplankton and protozoans. To interpret the changes in Se:C uptake ratios (Task 3b) and the consequences of seasonal variations in plankton composition (Task 3c) to Se incorporation by the clams, we will measure Se within single phytoplankton and protozoan cells using SXRF [42]. In SXRF, individual particles or cells are probed with X rays that induce atoms of heavier elements within the cell to emit fluorescent x-rays. Because the energy of the fluorescence photons are determined by the electron orbitals of the atom emitting them, the fluorescent x-ray spectrum can be analyzed to determine the concentrations of a range of elements within the cells, including Se. Spatial distributions of elements in samples can be determined by scanning a sample in raster fashion relative to a highly focused beam, collecting x-ray emission spectra at each point, and then analyzing these spectra relative to standards (see Fig. 11 for a description of the entire procedure). Along with our colleagues at Argonne National Laboratory, Stefan Vogt and Jörg Maser, we have pioneered spectral modeling software that can accurately quantify concentrations of multiple trace elements within a variable matrix in cells from such fluorescence spectra.

We use an X-ray microprobe because they are significantly more sensitive to trace elements than electron or proton microprobes. Moreover, lower absorption cross-sections allow

deeper penetration of x-rays than electrons, permitting synoptic analyses of entire cells without sectioning or otherwise altering cells. Finally, XRF imparts significantly less radiation damage than charged particles to specimens thicker than a few 100 nm [58]; this is important for preserving elements bound to volatile organic groups, such as Se, and for accurately estimating elemental concentration relative to carbon mass. Several recent technological advances have made it possible for the first time to apply XRF using hard x-rays (x-rays >1000 eV) to aquatic plankton, including (1) the introduction of Fresnel zone plates for submicrometer focusing of the incident beam [59,60] and (2) high-brightness, third generation synchrotron sources such as the Advanced Photon Source (APS) at Argonne National Laboratory in Argonne, IL. We will conduct the SXRF analyses of Se at the 2-ID-E microprobe, which operates at a side-branch of the 2-ID-D/E beamline at the APS, the brightest U.S. facility for hard x-ray experiments. We have conducted quarterly experiments at 2-ID-E since June 2000 and our General User Proposals have always been approved with high marks (see attached letter). This instrument is uniquely suited to this endeavor [61]. The 2-ID-E microprobe uses monochromatized undulator radiation as the x-ray source, and Fresnel zone plate optics to produce a 500-1000 nm focus (when Se is being analyzed). The incident beam energy can be tuned between 7.2–14 keV; we will use an incident beam energy of 13-13.5 keV for analysis of Se.

The sensitivity of the microprobe to Se concentrations is sufficient for the purpose of this proposal. Se fluorescence is clearly evident in spectra obtained from cultured phytoplankton (Fig. 12). Minimum detection limits (MDLs) in SXRF are determined by several variables: the total time over which the sample is exposed to incident x-rays and fluorescence photons are collected, the ambient background of fluorescence at the emission energy for Se, the thickness of the cell being analyzed, the frequency by which incident x-rays induce Se atoms to produce a fluorescent photon and the brightness of the incident x-ray beam. We have determined MDLs for Se and other trace elements under standard analysis conditions in cells with diameters of 5 μm and 20 μm , a range typical of the primary plankton cells ingested by *P. amurensis* and present in Suisun Bay (Table 3). As expected, based on its higher fluorescent yield and lower fluorescence background, Se MDLs are lower than those calculated for other important trace elements. The Se MDL's are ~10-50-fold lower than mean Se:C molar ratios measured in suspended and sediment particles within the Bay/Delta ecosystem (Table 1). Moreover, the MDL's are significantly below the average concentrations of Se in cultured phytoplankton (Table 1) and >1000-fold less than those species that accumulate Se most effectively [47]. We have successfully measured Se concentrations as low as 0.4 ppm in cells grown in media containing limiting amounts of selenite. These concentrations are well below those needed for Se tissue concentrations to exceed toxicity thresholds in bivalves that feed on these cells (Baines et al. 2001).

Samples (0.5 L) for SXRF analyses will be taken at the same time and station as those for standard chemical analyses, stored cold in the dark and brought back to the laboratory for preparation. Once in the laboratory the plankton cells are sedimented onto Ni or nylon carbon/Formvar-coated transmission electron microscopy (TEM) grids with gentle centrifugation. The grids are gently rinsed with very cold Milli-Q deionized water and dried in a darkened laminar flow hood. Once dried, the TEM grids are examined and targets photographed with both transmitted light and epifluorescence microscopy (dry objectives) soon after mounting. Once the targets have been logged, the dried grids are stored in a darkened dessicator under N_2 until SXRF analysis. Se concentrations are normalized to C based on C:biovolume relationships [62]. Several lines of evidence suggest that this approach is accurate [44]. We also anticipate taking advantage of recent hardware upgrades at the beamline to test a new method of estimating

C in cells directly by measuring the phase shift in x-rays passing through the cells. Based on three five day trips to the microprobe every year we anticipate analyzing and mapping a 300-500 cell samples per year for the first two years or 600-1000 cells total (at ≥ 1 cell h^{-1}) at the APS. Since we have found 15 cells are adequate to determine the mean elemental concentration to within 20% for any one cell type, this number should allow us to determine the concentrations of up to 40 different species. Where possible we will analyze concentrations in particular species collected at different ambient concentrations of dissolved Se to determine if there are differences.

Task 3b. Se:C uptake measurements. In addition to the SXRF measurements we will measure Se:C uptake ratios using a dual radiotracer technique [12]. This method takes advantage of the linkage between photosynthesis and Se incorporation and provides a relatively rapid and accurate estimate of the Se content of the phytoplankton. Unlike SXRF, it is also readily adapted for use in experiments on the impact of dissolved selenite, selenate and organic selenide concentrations on Se content of plankton. However, the dual isotope method will not accurately estimate the Se:C uptake ratios in heterotrophic and mixotrophic plankters that feed on particles, and cannot separately determine the Se content of different co-occurring species. We propose to use the dual labeling approach to measure the community averaged phytoplankton Se:C uptake ratios as they vary through time. These data can then be used in biokinetic models estimating the contribution of phytoplankton Se to clams, and in models predicting variability of clam Se over time. Moreover, we will conduct experiments in which selenite, selenate and organic selenide are elevated to values observed in the past (i.e., before reductions in refinery selenite discharge) or in the future (i.e., after water management strategies affect dissolved selenate and selenide concentrations).

Water collected in conjunction with the bulk chemical measurements and the *Potamocorbula* sampling will be stored cold in a completely darkened bottle and transported to the laboratory. Alkalinity, pH, dissolved inorganic C and salinity will be measured on this water sample using standard techniques. We will then add the radiotracer ^{75}Se in the form of NaSeO_3 and ^{14}C in the form of NaHCO_3 at tracer levels. Aliquots will be placed in 20-ml quartz scintillation vial containers within a photosynthetron – a device that produces a temperature controlled environment and exposes each sample to a different amount of light, with the amount of light varying from near surface levels to near dark. Darkened vials will be used to assess uptake in the absence of light, and samples killed using microwaves will be used as controls for abiotic uptake. After 4 h, the samples will be filtered onto 2 μm pore size polycarbonate filters. This size removes most free-living bacteria from the experiment which may not be labeled effectively. It is also near the size that is effectively removed by *Potamocorbula* filtration. The 4-h time frame has yielded significant uptake in previous experiments at sites with similar algal concentrations to those in Suisun and using similar sample volumes [12]. ^{75}Se and ^{14}C on the filters is measured by gamma- and beta scintillation counting, respectively, and converted to total Se and C uptake based on concentrations of selenite and DIC in solution. Uptake rates are determined assuming linear uptake after subtracting blanks and the Se and C data are separately related to light to produce a P:I curve. The Se:C uptake ratios of phytoplankton averaged over a day are then estimated using this P:I curve, the daily insolation pattern and the in situ light profile.

The effect of selenite and selenate concentrations on the Se:C uptake ratio will be assessed in separate set of experiments conducted at saturating, but not inhibiting, light intensities as well as in the dark. For both light levels, one triplicate set of bottles will have only

tracer levels of ^{75}Se added, whereas the other set of triplicates will have enough radioactive selenite and selenate added to the concentrations of these species to produce 2 nM and 10 nM, respectively. The proportional change in Se uptake that results from the increase in concentration will be used to adjust the P:I curves and recalculate the Se:C uptake under the new scenario.

Task 3c. Plankton characterization. To make the best use of the species specific cellular Se concentrations, and to interpret variations in the Se:C uptake ratio, we will characterize the algal and protozoan plankton community at each sampling. Samples for enumeration of phytoplankton will be preserved in buffered Lugol's solution, whereas samples for analysis of protozoans will be preserved with borate buffered 2% glutaraldehyde. Phytoplankton and ciliates will be enumerated using an inverted microscope and the settling method for concentration [63]. Flagellated and ciliated protozoa will be enumerated and sized at 600x using a UV emitting epifluorescence microscope fitted with a low light camera and particle analysis system after staining with DAPI and filtering the sample onto black 1 μm pore size polycarbonate filters [64]. Both free-living and attached bacteria will be also enumerated and sized using epifluorescence microscopy after DAPI staining using the same general methodology, except that a 0.2 μm polycarbonate filter will be used. Biovolumes of protozoa and bacteria will be converted to C based on established relationships [62,65]. These data will be used in conjunction with data on assimilation of Se from bacteria and protozoa (**Task 4c**) to evaluate this source of Se to clams. In addition, we will accumulate as much past data on phytoplankton composition within the Bay as possible. These data will be used to assess the robustness of the patterns observed over the monitoring period, to better address possible causes for observed patterns, and to assess past variability in the exposure of clams to dietary Se.

Task 3d. Modeling contribution of Se from detritus and phytoplankton. To understand how tissue concentrations of Se in clams have responded to reductions in selenite discharge or detrital Se inputs from the SJR, we need to determine how much of the Se in clams is derived from detrital matter, and how much from living plankton. If almost all the Se in clams is derived from the living plankton, then the ability of phytoplankton to accumulate selenate and selenite will determine how Se in the clams responds to management actions. Moreover, because algal biomass responds very quickly (within hours to days) to the ambient chemical environment, such a finding would imply that the response to management actions will be almost immediate. In contrast, to the degree that detrital Se contributes to Se in the clam, the response to management actions will be slow (< 1 year) and possibly complex. This is because detrital Se is a much larger and less dynamic pool of Se that is influenced by the long term average of Se concentrations in dying phytoplankton, and by inputs from transport of exogenous particles from the delta and SJR. Monitoring of the response to the reductions in selenite discharge would have to be long-term and would need to account for the effects of countervailing trends in the delta.

To do this we will use our monitoring measurements and bioaccumulation parameters measured in our experiments as coefficients in a bioenergetic based kinetic model predicting Se concentrations in herbivores under steady state. This can be described by:

$$(1) \quad C_{ss} = [(AE \times IR \times C_f) + (K_u \times C_w)] / (k_e + g)$$

where, C_{ss} is the Se concentration ($\mu\text{g g}^{-1}$) in organism under steady state, K_u is the Se dissolved uptake rate constant ($1 \text{ g}^{-1} \text{ d}^{-1}$) for the consumer in question, C_w is the Se concentration in

the dissolved phase ($\mu\text{g l}^{-1}$), AE is the Se assimilation efficiency from ingested food, IR is the ingestion rate ($\text{g g}^{-1} \text{d}^{-1}$), C_f is the Se concentration in the food ($\mu\text{g mg}^{-1}$), k_e is the Se efflux rate constant (d^{-1}), and g is the growth rate constant (d^{-1}). Since studies have shown accumulation of Se in bivalves via the dissolved pathway is negligible [28,37], Eq. (1) can be simplified to:

$$(2) \quad C_{ss} = AE \times IR \times C_f / (k_e + g).$$

C_{ss} can be calculated for two or more distinct sources of dietary Se as long as the ingestion rates, Se concentrations in food and Se AEs for each source are known (k_e and g are assumed to be the same in both calculations). These values can be compared directly to determine the relative importance of different sources of particulate Se. The concentration of Se in algae and protozoa will be measured using both SXRF and the dual isotope labeling procedure. The biomass of algae in terms of C and dry wt of algae will be determined from chlorophyll measurements using standard ratios between chlorophyll-*a*, C and dry wt. The biomass of protozoa will be determined from biovolume using published regressions [62]. The biomass and Se content of the algae and protozoa will be subtracted from the concentrations of suspended particulate matter and organic Se to determine the Se concentration in detritus. The month to month variation in the contribution of detrital and plankton to the dietary Se for clams will be correlated to changing Se content. We will also attempt to develop statistical relationships based on regression analysis that predicts Se in clams based on suspended particulate organic Se and Se in the phytoplankton and protozooplankton.

Task 4. Unique characteristics of invasive clam – growth, condition, reproduction, uptake kinetics, and/or selective feeding. The work outlined in this task is a combination of field monitoring, laboratory studies, modeling of laboratory and field data and analysis of pre-existing data. Knowledge and understanding of the mechanisms controlling Se accumulation in *P. amurensis* gained from these new measurements will be used to re-examine monitoring data collected since 1995 and to test our models.

Task 4a. Monthly monitoring of Se in *P. amurensis*. Se concentrations will be determined monthly in soft tissues of clams ($n = 3$ composite samples of 20 plus clams) at USGS stations 8.1 (Carquinez St.), Confluence of the Sacramento and San Joaquin rivers and 415 (Montezuma Sl.) using established biomonitoring protocols (Fig. 10). This approach extends the clam Se monitoring dataset began in 1995 at station 8.1 and in 2001 at stations 415 and 4.1 (Chippis Island, near the confluence). Selenium concentrations will be determined by the same laboratory (Kent Elrick, USGS Atlanta, Georgia) and methodology used for previous clam Se monitoring samples. Trends in Se concentrations in clams will be examined in relation to monthly trends in clam biology (food selection – stable isotope composition; physiology – reproduction, condition, growth), suspended particle composition and Se content (Task 3) and bulk suspended particulate Se concentrations (Tasks 2 & 3). Se concentrations in clams will also be used in the biokinetic model to evaluate uptake kinetics (Task 4c).

Se in *P. amurensis* predators – Se will also be determined in the livers of white sturgeon ($n=20$) at one point in time (January 2006 or 2007) using established sampling procedures for this species in San Francisco Bay [1]. Se concentrations in sturgeon have been determined in 1986, 1990, 2000 and 2001. We propose to sample Se in sturgeon to determine if there have been changes in Se liver concentrations relative to changes observed in clams, their primary food

source. We propose only doing this once since Se concentrations in adult sturgeon are expected to change more slowly compared to the clams. These data will contribute to the long-term dataset on Se in sturgeon in Suisun Bay and could be used to assist us in identifying the best Se monitoring protocol for the system.

Task 4b. Physiological controls of Se accumulation in *P. amurensis*. Measurements of clam growth (secondary production), changes in condition (ash-free dry wt) and reproductive status (spawning state) will be used to assess the influence of clam physiology on the seasonal dynamics of Se concentrations in the clam. Because metal concentrations can be sensitive to rapid changes in body mass or condition (resulting from stress, reproduction, etc.), the biokinetic model includes declines in tissue Se through growth. We will measure clam growth by estimating changes over time in soft tissue dry weight. Reproduction in *P. amurensis* may also influence Se concentrations; reproductive status has been measured in *P. amurensis* at USGS stations 8.1 and 4.1 from 1986 through 1997. We will extend this dataset for an additional 3 years (2005-2007) and 1 year between 1998-2004, as indicated by the clam Se data) to determine if changes in reproductive status influence the seasonal trends in tissue concentrations. Specific changes in physiological status of the clams (i.e. body size, growth) analyzed in Task 4a will be known and therefore can be used in running the models in Task 3b to determine their relative contribution to shifts in Se content of *P. amurensis* over the seasons.

Task 4c. Comparisons of uptake kinetics of the invasive clams *P. amurensis* and *Corbicula fluminea*.

Field measurements – Prior to the arrival of *P. amurensis* in 1986, *C. fluminea* was found throughout Suisun Bay. Recent samples of *C. fluminea* collected in the Delta suggest that this species accumulates Se to a much lower degree than *P. amurensis*, despite similar uptake kinetics. It is unclear if the elevated Se concentrations observed in *P. amurensis* is unique to this clam or if the conditions of Suisun Bay provide highly bioavailable Se to all clams. To test this hypothesis the USGS will collect both clams at stations within Suisun Bay where they overlap. Past benthic grabs suggest that these clams do co-occur for a short period in the fall (August – November) near the confluence of the Sacramento and San Joaquin Rivers. Replicate samples (n=3 composites of 20 plus clams) will be collected, analyzed for Se content, stable isotopes (indicates source of food consumed) and compared. These data will be compared to results from biodynamic modeling to determine if *P. amurensis* is a unique bioaccumulator.

Laboratory studies of Se uptake from protozoans and bacteria – We will use established laboratory protocols for gamma-emitting radiotracers (e.g., [28,66]) to carefully examine the uptake of Se by *P. amurensis* and *C. fluminea* from protozoans and bacteria. These experiments, conducted with low, environmentally realistic Se concentrations, are used to determine assimilation efficiencies (AEs). *P. amurensis* does assimilate C from bacteria accounting for approximately 13% of their C uptake [67], but it is unknown if they also assimilate Se from this food source and to what degree. Bacteria in the estuary vary seasonally and thus could be responsible for the seasonal Se pattern in the clams. Assimilation efficiencies determined in these experiments will be used to evaluate implications of bacterial counts in Task 3.

Laboratory studies of Se uptake from detritus. Assimilation by *Potamocorbula* of Se associated with resuspended sediment particles has been measured after incubating the sediments with radiolabeled selenite [35]. It is possible that such measurements may either underestimate or overestimate the availability of depending on which fractions of the sediments were best labeled.

To determine if there is a serious bias we will compare the past measurements to measurements of assimilation from natural particles using stable Se measurements. These experiments will compare the ratio of Se to the ash weight in ingested and fecal material for a set of 20 clams exposed to water collected from Suisun Bay. Se assimilation will be calculated from this comparison in the same way that C assimilation from natural particles is calculated [68]. We will estimate C assimilation at the same time for comparison.

Task 4d. Source tracking of *P. amurensis* food using stable isotopes. Stable isotopes ($\delta^{13}\text{C}$, $\delta^{15}\text{N}$ and $\delta^{34}\text{S}$) will be measured in an aliquot of clam sample (n=3 composite samples of 20 plus clams) prior to Se analysis (Task 4a) to evaluate changes in the composition and source of food particles consumed by the clams. Stable isotopes have been extremely informative in evaluating broad differences in food source (estuarine plankton vs riverine organic matter) in the northern reach of San Francisco Bay [69]. In general, clams that possess a more depleted carbon (-28) or sulfur (8) are expected to be consuming food produced in the freshwater regions of the Delta and not in the Bay (Fig. 11). Furthermore, because stable isotopes of C and S are closely tied to hydrological patterns in the estuary (i.e. salinity cycle, Fig. 3), stable isotopes may provide a means by which to monitor shifts in food source over longer periods of time (allochthonous vs autochthonous) depending on water management practices. Stable isotopes have been analyzed in clams as part of the Se monitoring program since 1999 and thus a history of isotopic signatures is available. The USGS has developed a carbon stable isotope model that can be used to evaluate clam diets and its reliance on autochthonous production [70]. The model makes some basic assumptions about carbon isotopic fractionation by marine phytoplankton and by clams. Using a well-established correlation between salinity and $\delta^{13}\text{C}$ of dissolved inorganic carbon (DIC) the model uses salinity to estimate the carbon isotopic composition of the clams if they were consuming phytoplankton produced at the salinity where the clams were collected (Fig. 11). The model will use stable isotope data collected at station 8.1 and 4.1 and salinity data collected by the Department of Water Resources at Martinez and near the confluence of the Sacramento and San Joaquin Rivers to identify times of year when the clams might be consuming food other than estuarine phytoplankton produced within Suisun Bay. Knowing if the clams are consuming a different type of food from a potentially a different source would be very helpful in understanding changes in Se concentrations in the clams relative to changes in Se concentrations of bulk suspended material.

Task 4e. Modeling of Past, Present and Future Se accumulation in *P. amurensis* This work will utilize data from all Tasks 1-3 to model Se accumulation in *P. amurensis* under varying exposure and physiological conditions. The biokinetic model described above will be utilized [37]. Exposures will be identified in Tasks 2&3. Task 3 will identify actual Se concentrations in specific phytoplankton species. Assimilation efficiencies of different phytoplankton species by *P. amurensis* are known [35] and so if the Se concentrations for these species are known then uptake into the clams can be modeled. Data from Task 4b will be used to model implications of biological changes and processes.

We will test the model against previously collected Se clam data. The model will assist in identifying critical data driving the changes in Se content of the clam and help focus future monitoring efforts for Se in the Bay.

The parameterized biokinetic model will also be used to forecast the response of clam Se to past future scenarios of water management and inputs of selenium contaminated water into the

Bay/Delta ecosystem. A coupled hydrographic-biogeochemical model which accurately predicts historical concentrations of dissolved Se species will be used in this effort. Changes in the inflows from the San Joaquin River will be used to determine impacts under different conditions. The effect of predicted changes in dissolved Se on the Se content of the organisms which are fed upon by *Potamocorbula* will be determined based on results from the experiments conducted as part of task 2b. The implications of these changes for clams will be determined, taking into consideration the contribution of detrital Se to the diet of *Potamocorbula* as well as scenarios about different plant composition. Ultimately, such results will help us plan whether it is necessary only to monitor clams or whether we must also choose among variables such as clam biology, suspended particulates, speciation, phytoplankton species or bacteria.

5. Feasibility. Much of what is known about selenium in San Francisco Bay has come from the studies of these PI's, in collaboration. Each of the co-PI's has extensive experience in the relevant disciplines of biomonitoring, food-web studies, Se chemistry and bioaccumulation, use of radioisotopes, x-ray fluorescence microscopy and phytoplankton ecology. Laboratory space that is appropriately licensed and equipped for use of radioisotopes is available at both USGS in Menlo Park and at MSRC as are facilities and expertise for determination of trace Se concentrations at ODU. Specific measurements (Se in clams, phytoplankton and stable isotopes) will be conducted under contract with laboratories which the PI's have found previously to be reliable and efficient. Outside of the experiments, we will be following sampling and study protocols that we have successfully employed before. Although previous studies have led us to some uncertainties about what causes the present status of selenium in Suisun Bay, the specific hypotheses that are proposed hold promise those uncertainties can be resolved. Where new methodologies and where models are proposed, their feasibility has already been demonstrated (e.g. [34,43]). These groups have a long history of collaborating successfully and productively. A major goal of this proposal is to synthesize the outcomes of that collaboration and other studies into a monitoring plan that can be continued indefinitely.

6. Expected outcomes and products. We will produce quarterly reports and a final report to CALFED, summarizing the data collected and the findings based on that data. We will also produce high quality publications (peer-reviewed and white papers, e.g. IEP newsletter) and presentations (oral and poster) that are relevant, accessible, influential and understandable to the scientific community, managers, and public. In particular, we will create a white paper with recommendations for cost-effectively monitoring Se into the longer term. Our goal is a plan that can be perpetuated by USGS and collaborators. By refining what aspect of monitoring (e.g. bivalves and which related parameters) to perpetuate, we anticipated that plan will be effective at assessing the impacts of future water and Se management actions, as well as natural changes in hydrography. The spatially and temporally referenced monitoring data will be made available for distribution on the Internet via a searchable database that can be easily adapted for use in future monitoring. The co-PIs are committed to communicating their results at a variety of academic and public settings, and will participate in yearly CALFED Science or State of the Estuary conferences. As noted below we intend to organize a public meeting on the issue and the monitoring toward the end of this project.

7. Data handling storage and dissemination. Vital project information will be initially documented in field and laboratory notebooks and data collection sheets. Entries will be legible, complete, written in black ink, dated, signed by the individual making the entry, and accurate enough to permit reconstruction of activities. The accurate and complete transfer of data to electronic media (e.g. Excel spreadsheets) will be verified by a designated QA manager at each research facility. All PI's will use a common electronic data platform (e.g., Microsoft Excel), to facilitate data sharing. Data bases generated by each PI will be primarily maintained by that individual, and will be routinely backed-up on electronic media for security assurance. All notebooks, files, and electronic media related to this project will be securely maintained for a minimum of seven years from the time of project completion. All data will eventually be available to the public on the USGS Trace Element website (<http://www.rcamnl.wr.usgs.gov/trace/>) to facilitate its use under CALFED's data management strategy.

8. Public involvement and outreach. Every year the PI's regularly involve up to three high school students and other interested individuals directly in research. The work done is often submitted to local, regional and national science competitions. We will develop a web page for this specific study. It will describe the research in simple lay terms for general access, and present existing data on selenium. It will be developed through the exiting USGS web structure describing work in the Bay, and can be linked into the ERP site if interest exists. This project will be represented at the USGS Open House in Menlo Park in two years (about 25,000 people attend). As the monitoring plan takes shape we will ask for ERP approval to hold public meeting to discuss the state of knowledge with regard to selenium, and the monitoring plans for the future. We have not discussed this with USEPA, but expect they would be interested in linking this in with their efforts to establish California-wide site-specific Se guidelines. Luoma is on the Board of Directors for a new Bay Center in San Francisco; a center for the public to better understand the Bay. Selenium will be suggested as a topic for presentation to illustrate the challenges and tradeoffs of modern restoration issues.

9. Work schedule. The work schedule is presented in Table 4. Much of the work represents repetitive sampling and analysis and so will continue throughout the period of the grant.

B. Applicability to CALFED Bay-Delta Program ERP Goals, the ERP Draft Stage 1 Implementation Plan, and CVPIA Priorities.

1. ERP and CVPIA Priorities

The goals of the ERP involve reducing stressors and restoring ecosystems and populations of native species. Environmental water quality and selenium are specific areas of concern. Studies supported by earlier CALFED grants [3,4] [1] directly demonstrated that current selenium contamination in the system is affecting reproduction in two native species that are of concern (others, including dungeness crab are possibly threatened, judging from their tissue contamination and surrogate toxicity data). Sacramento splittail was not listed under ESA by USFWS because of USFWS confidence that CALFED's restoration plans would prevent its extinction. Green sturgeon are listed as endangered, and white sturgeon are in decline. Suisun Bay is critical habitat for all these species. More needs to be known about the specific threats to these species. But, monitoring is essential. If selenium contamination in Suisun Bay should

increase, it is critical to recognize that increase is occurring and why, before it causes serious harm. If contamination should stay the same or decline, it is critical to recognize that, so that CALFED actions are not threatened by public outcry about problems that are not under their control (or are not significant).

2. Relationship to Other Ecosystem Restoration Actions, Monitoring Programs, or System-wide Ecosystem Benefits

ERP is also concerned about conflicts among goals for restoration, and conflicts with other CALFED goals. Important water management goals of CALFED involve increasing flows in the SJR, using barriers to circulate more SJR water to Suisun Bay, and improving the quality of exported water by substituting Sacramento water for SJR water. Meanwhile there is great pressure in the western San Joaquin Valley to remove salts and selenium from soils to preserve agriculture. All these changes make it possible that more selenium will enter Suisun Bay in the future. Two of the areas in the Bay-Delta with the greatest potential for habitat restoration are Dutch Slough and Suisun Marsh. Both (are) could be habitats that might trap and recycle selenium, similar to Kesterson National Wildlife Refuge. Suisun Marsh is the habitat where deformed splittail are already found (Stewart et al 2004). While it is important to study these areas directly, it will take time for such studies to yield conclusive results. Monitoring the outcome of the net effect of all these actions, with specific reference to a known issue of concern, is the best way to demonstrate that CALFED is aware of the potential problem and willing to employ a “learn-as-you-go” philosophy to manage them. A cost-effective monitoring program is the way to do that. Cost effective, sustainable, monitoring and assessment requires some knowledge of critical processes and questions in its design. Our proposal is to design, publish and attempt to sustain a program that would cost-effectively feedback reliable information to CALFED about the selenium issue.

C. Qualifications.

Dr. Samuel Luomais a Senior Research Hydrologist with the US Geological Survey, since 1974. He served as the first Lead Scientist for the CALFED Bay-Delta program between August 2000 and November 2003. His research interests include the effects of pollutants in aquatic environments, with special emphasis on metals and metalloids, including several long-term contamination assessment studies (all exceeding 15 years in duration) in the Bay-Delta and the Clark Fork River MT. His work influences fields such as metal bioavailability, dietary exposure of aquatic organisms to metals, tolerance, and determination of metal effects at the individual, population and community level in field studies. He has worked in San Francisco Bay since 1974 and has authored more than 180 peer-reviewed publications, many of them about Bay issues. He and his colleagues began working on the selenium issue in the Bay in the mid-1980's and have been actively involved since then (e.g. see publications [4,5,36,37,37,71-74]). He was editor of *Marine Environmental Research* from 1996 – 2003 and is an editorial advisor for *Marine Ecology Progress Series*. He has participated nationally and internationally as an expert or advisor and is a recipient of several prestigious awards or appointments (most recently a WJ Fulbright Distinguished Scholar award). He served on three USEPA's Science Advisory Board committees. Present studies include modeling potential outcomes from various proposed selenium criteria for USEPA. His experience with monitoring and assessment is extensive. He was one of four people who originally designed USGS' successful National Water Quality Monitoring Assessment. He was invited to form the first Science Advisory group for IEP; and he has

designed a number of monitoring efforts for the Bay-Delta. He will be lead PI for this project and be involved in clam biomonitoring and modeling.

Dr. Robin Stewart is a biologist with the U.S. Geological Survey since 1999 and has over 10 years of experience evaluating the fate and effects of trace element and organic contaminants in aquatic food webs. She received her PhD in ecotoxicology from the University of Manitoba, Winnipeg, Canada in 1998 and has extensive field research experience. She has been a co-Principal Investigator on >\$1million study in Lake Winnipeg following the 1997 Red River flood. She co-manages a multidisciplinary research effort on Se in San Francisco Bay/Delta (granting agencies include: International Joint Commission and CALFED, respectively) and a Calfed proposal to evaluate processes controlling mercury cycling in the San Francisco Bay Delta. Relevant reports and publications include: [1,1,31,70,75,76,76,77,77,78,78]. For the current project, Dr. Stewart will be primarily responsible for monitoring Se in *Potamocorbula* and white sturgeon, stable isotope work and modeling of clam Se.

Dr. Nicholas S. Fisher is a full professor (since 1991) at the Marine Sciences Research Center (MSRC) at the State Univ. of NY (Stony Brook, NY). His Ph.D. is in Biology from SUNY, Stony Brook, 1974 with previous positions Brookhaven Natl. Lab 1986-87; the Marine Environment Lab, Intl Atomic Energy Agency, Monaco, 1980-85; and Ministry for Conservation, Melbourne, Australia, 1977-80. He was recently appointed a Fellow of the John Simon Guggenheim Foundation (2004-) and was elected President of the Biogeochemistry Committee of CIESM in 2001 and 2004. He is on the Editorial Board member of the journals *Marine Ecology Progress Series* and *Marine Environmental Research*; an Invited Member of the Ecology Institute, Oldendorf-Luhe, Germany, 1984-present. His experience with long-term monitoring include Chair, Toxic Substances Working Groups for NOAA Review on Natl. Ocean Pollution Plan, USEPA's EMAP Review Team, and the GESAMP Working Group on Interchange of Pollutants between Atmosphere and Oceans. His research interests include: physiological ecology of plankton; biogeochemical cycling of metals in marine systems; trophic transfer of elements in marine food webs; pollutant cycling and impacts on marine ecosystems. He is author of about 180 peer-reviewed publications, of which over 40 involve the bioaccumulation of selenium in aquatic organisms; these include: [12,19,21,21,25,27-29,31,38,40,66,79-86,86-88]. For the current project, Dr. Fisher will lead the Stony Brook team and be responsible for evaluating the selenium concentrations of plankton and relating this to selenium levels in *Potamocorbula*.

Dr. Stephen B. Baines is a Research Assistant Professor (since 1998) at the Marine Sciences Research Center (MSRC) at the State Univ. of NY (Stony Brook, NY). His education includes a Ph.D. in Biology, Yale, 1993. Previous positions were at McGill University, 1993-95; and University Wisconsin, 1995-98. His research interests include plankton ecology, elemental stoichiometries of plankton, and contaminant-biota interactions. Author of over 20 peer-reviewed publications, of which several involve the bioaccumulation of selenium in aquatic organisms; these include: [12,21,21,31,47,89]. A leader in applying SXRF for analyzing aquatic plankton composition. For the current project, Dr. Baines will conduct the SXRF analyses and the selenium uptake studies by phytoplankton.

Dr. Gregory Cutter is a professor (since 1994) in the Department of Ocean, Earth and Atmospheric Sciences at Old Dominion University in Norfolk, Virginia where he has been on the faculty since 1982. Dr. Cutter received his Ph.D. in Chemistry from UC Santa Cruz in 1982. He is the Editor of the American Society of Limnology and Oceanography's L&O Bulletin, and an Associate Editor for Marine Chemistry and Limnology & Oceanography: Methods. His experience with monitoring is as the Chair of the Biogeosciences Working Group for the US National Science Foundation and Associate Member of the Scientific Committee on Ocean Research's Geotraces Planning Group. His other professional activities include serving on review panels for NSF, NOAA's Sea Grant Program, and various state agencies, and advisory panels for EPA, NOAA, and state agencies. His research interests include: biogeochemical processes affecting trace element speciation and distributions in natural waters and sediments; air-sea transport and exchange of gases and trace elements; paleoceanographic tracers; analytical methods for aquatic chemistry; and computer modeling of biogeochemical processes. He has published more than 60 peer-reviewed publications, including 26 on the analytical chemistry or biogeochemistry of selenium in the aquatic environment [6,7,7,32,41,49,52,55,90-92]. Notably, these include the first published reports on selenium cycling in the San Francisco Bay and the roles of refinery and riverine inputs in this estuary [6,90], and the most recent update on dissolved selenium in the Bay [32]. In addition, Dr. Cutter's latest Ph.D. student created a complete biogeochemical simulation model of selenium in SF Bay [34] that allows the synthesis of findings from various dissolved, suspended particle, sediment, and phytoplankton data sets. For the project described here, he will be in charge of the ODU effort at measuring dissolved and particulate selenium concentrations and speciation (and bulk particulate matter characterization) at the clam monitoring stations, as well as interfacing these data with those from the SUNYSB and USGS groups using various modeling approaches.

D. Cost.

1. Budget (Since funding may be awarded for only parts of a project, your proposal's text should explain which tasks could be funded separately.) None.

2. Cost sharing

USGS: One week of Luoma's salary is included in the grant (by USGS request), but it is expected he will spend one-third of his time on this grant (~18 weeks per year). Some boat costs are included in the grant, but these are only marginal expenses. The facilities of the Luoma project in Menlo Park include existing instrumentation, lab space and people who can participate in field crews, sample preparation, analyses and data management. It is expected that the postdoctoral associate working with Luoma will be partly supported by a grant from elsewhere (Hong Kong), and only her living expenses (which USGS can subsidize) are included here. This amounts to matching funds of about \$150,000 per year net.

SUNY: The full annual salary of Dr. Fisher is covered 75% by his institution. The expected annual effort of Dr. Fisher towards the current project is estimated to be 33%. The requested funding for his salary is 16.7%. This represents an estimated annual cost sharing on the part of his institution (SUNY Stony Brook) of 16.3% for salaries plus benefits which equals \$30,610 for Year 1 and \$96,501 for all years. The costly disposal of all radioactive waste generated in the radioisotope experiments will be covered by SUNY Stony Brook (estimated at \$20,000/yr) as will instrument service contracts for gamma counters (about \$5,000/yr). In addition, due to our "independent investigator status" the SUNY team (Fisher, Baines, Twining) will be given

privileged access at no expense to this grant to the SRI-CAT 2-ID-E microprobe (a side branch of the 2-ID-D/E beam line) at the Advanced Photon Source at the Argonne National Laboratory to conduct the SXRF analyses. The hard x-rays needed for the analyses described in this proposal currently are only available at this site in the US. Further, we have ongoing collaborations with Drs. Jorg Maser and Stefan Vogt at APS, who provide considerable expertise in the daily operations of the beam line and assistance in data interpretation, also at no cost to this project. **ODU:** Dr. Cutter will devote 2 months per year in Years 1 and 2 to this project, and 3 months in Year 3, but Old Dominion University will contribute one month per year of this effort, equivalent to \$69,415 (salary, benefits, overhead).

3. Long-term funding strategy

USGS has been assessing, with biomonitors and supporting variables, the status of metal and metalloid contamination in the Bay-Delta since 1975. The USGS selenium assessment program (biomonitoring) for selenium has continued since 1985, with a hiatus between 1989 and 1995. These programs are possible because of our presence and our permanent infrastructure (boats, permanent employees, laboratories and analytical facilities/capabilities); and we expect that to continue. Given the importance of the selenium issue we expect to continue assessment of this issue at some level. The deeper success of the collaborative studies of selenium have resulted from supplemental support by other sources (DWR, RWQCB, CALFED). USGS intends to continue to seek such support to enrich basic observations with process knowledge. It is expected that between permanent, long-term commitments from our existing programs and continued success in competitive endeavors we can extend a monitoring program for selenium into the foreseeable future.

E. Compliance with Standard Terms and Conditions.

We will comply with all standard terms and conditions. We have no conflicts. Luoma was Lead Scientist at CALFED, but had nothing to do with the present PSP. His participation in the competition was approved by CALFED lawyers.

G. Literature Cited.

1. Stewart AR, Luoma SN, Schlekat CE, Doblin MA, Hieb KA. 2004. Food Web Pathway Determines How Selenium Affects Aquatic Ecosystems: A San Francisco Bay Case Study. *Environ Sci Tech* .
2. Presser, T. S. and Ohlendorf, H. M. Biogeochemical cycling of selenium in the San Joaquin Valley, California, USA. *Environ.Manag.* 11, 805-821. 1987.
3. Teh, S. Effects of dietary selenium on early life stages of Sacramento splittail. *Environ.Sci.Tech.* 2004.
4. Linville RG, Luoma SN, Cutter L, Cutter GA. 2002. Increased selenium threat as a result of invasion of the exotic bivalve *Potamocorbula amurensis* into the San Francisco Bay-Delta. *Aquat Toxicol* 57:51-64.
5. Luoma SN, Presser T. Forecasting Selenium Discharges to the San Francisco Bay-Delta Estuary: Ecological Effects of a Proposed San Luis Drain Extension. US Geological Survey Open-File report 00-416, <http://pubs.water.usgs.gov/ofr00-416/>.
6. Cutter, G. A. The estuarine behaviour of selenium in San Francisco Bay. *Estuar.Coast.Shelf Sci.* 28, 13-34. 1989.
7. Cutter, G. A. and Bruland, K. W. The marine biogeochemistry of selenium: A re-evaluation. *Limnol.Oceanogr.* 29[6], 1179-1192. 1984.
8. Eustice DC, Kull FJ, Shrift A. 1981. Selenium toxicity: aminoacylation and peptide bond formation with selenomethionine. *Plant Physiology* 67:1054-1058.
9. Daniels LA. 1996. Selenium metabolism and bioavailability. *Biological Trace Element Research* 54:185-199.
10. Eisler R. Selenium hazards to fish, wildlife, and invertebrates: a synoptic review. 85 (1.5). US Fish Wildl. Serv. Biol..
11. Riedel, G. F., Sanders, J. G., and Gilmour, C. C. Uptake, transformation, and impact of selenium in freshwater phytoplankton and bacterioplankton communities. *Aquat.Microb.Ecol.* 11, 43-51. 1996.
12. Baines SB, Fisher NS, Doblin MA, Cutter GA, Cutter L, Cole BE. 2004. Light dependence of selenium uptake by phytoplankton and implications for predicting selenium incorporation into food-webs. *Limnology and Oceanography* 49:566-578.
13. Shrift A. 1954. Sulfur-Selenium Antagonism .1. Antimetabolite Action of Selenate on the Growth of *Chlorella-Vulgaris*. *American Journal of Botany* 41:223-230.
14. Brown TA, Shrift A. 1980. Assimilation of selenate and selenite by *Salmonella typhimurium*. *Can J Micrbiol* 26:671-675.

15. Williams MJ, Ogle RS, Knight AW, Burau RG. 1994. Effects of Sulfate on Selenate Uptake and Toxicity in the Green-Alga *Selenastrum-Capricornutum*. *Archives of Environmental Contamination and Toxicology* 27:449-453.
16. Wrench, J. J. and Measures, C. I. Temporal variability in dissolved selenium in a coastal ecosystem. *Nature* 299, 431-433. 1982.
17. Vandermeulen J, Foda A. 1988. Cycling Of Selenite and Selenate In Marine-Phytoplankton. *Marine Biology* 98:115-123.
18. Riedel G, Ferrier D, Sanders J. 1991. Uptake Of Selenium By Fresh-Water Phytoplankton. *Water Air and Soil Pollution* 57:23-30.
19. Baines SB, Fisher NS. 2001. Interspecific differences in the bioconcentration of selenite by phytoplankton and their ecological implications. *Marine Ecology Progress Series* 213:1-12.
20. Cutter GA. 1989. The Estuarine Behavior Of Selenium In San-Francisco Bay. *Estuarine Coastal and Shelf Science* 28:13-34.
21. Baines SB, Doblin MA, Fisher NS, Cutter GA. 2001. Uptake of dissolved organic selenides by marine phytoplankton. *Limnol Oceanogr* 46:1936-1944.
22. Wrench JJ. 1978. Selenium Metabolism In Marine Phytoplankters *Tetraselmis-Tetratele* and *Dunaliella-Minuta*. *Marine Biology* 49:231-236.
23. Foda A, Vandermeulen JH, Wrench JJ. 1983. Uptake and Conversion Of Selenium By a Marine Bacterium. *Canadian Journal Of Fisheries and Aquatic Sciences* 40:215-220.
24. Bottino NR, Banks CH, Irgolic KJ, Micks P, Wheeler AE, Zingaro RA. 1984. Selenium Containing Amino-Acids and Proteins In Marine-Algae. *Phytochemistry* 23:2445-2452.
25. Fisher NS, Reinfelder JR. 1991. Assimilation Of Selenium In the Marine Copepod *Acartia tonsa* Studied With a Radiotracer Ratio Method. *Marine Ecology-Progress Series* 70:157-164.
26. Besser JM, Huckins JN, Clark RC. 1994. Separation Of Selenium Species Released From Se-Exposed Algae. *Chemosphere* 29:771-780.
27. Reinfelder JR, Fisher NS. 1991. The assimilation of elements ingested by marine copepods. *Science* 215:794-796.
28. Wang W-X, Fisher NS, Luoma SN. 1996. Kinetic determinations of trace element bioaccumulation in the mussel *Mytilus edulis*. *Mar Ecol Prog Ser* 140:91-113.

29. Wang W-X, Fisher NS. 1999. Assimilation efficiencies of chemical contaminants in aquatic invertebrates: a synthesis. *Environ Toxicol Chem* 18:2034-2045.
30. Reinfelder, J. R., Fisher, N. S., Luoma, S. N., Nichols, J. W., and Wang, W-X. Trace element trophic transfer in aquatic organisms: A critique of the kinetic model approach. *Sci.Tot.Environ.* 219, 117-135. 1998.
31. Baines SB, Fisher NS, Stewart R. 2002. Assimilation and retention of selenium and other trace elements from crustacean food by juvenile striped bass (*Morone saxatilis*). *Limnology and Oceanography* 47:646-655.
32. Cutter GA, Cutter LS. 2004. The biogeochemistry of selenium in the San Francisco Bay estuary: changes in water column behavior. *Est Coast Shelf Sci* 61:463-476.
33. Doblin, M. A., Baines, S. B., Cutter, L. S., and Cutter, G. A. The biogeochemistry of selenium in San Francisco Bay: seston and phytoplankton. *Est.Coast.Shelf Sci.* 2003.
34. Meseck SL. 2002. Modeling the biogeochemical cycle of selenium in the San Francisco Bay. Old Dominion University.
35. Schlekot CE, Dowdle PR, Lee B-G, Luoma SN, Oremland RS. 2000. Bioavailability of particle-associated Se to the bivalve *Potamocorbula amurensis*. *Environ Sci Technol* 34:4504-4510.
36. Johns, C., Luoma, S. N., and Elrod, V. Selenium accumulation in benthic bivalves and fine sediments of San Francisco Bay, the Sacramento-San Joaquin Delta, and selected tributaries. *Estuar.Coast.Shelf Sci.* 27, 381-396. 1988.
37. Luoma SN, Johns C, Fisher NS, Steinberg NA, Oremland RS, Reinfelder JR. 1992. Determination of selenium bioavailability to a benthic bivalve from particulate and solute pathways. *Environ Sci Tech* 26:485-491.
38. Wang W-X, Fisher NS, Luoma SN. 1996. Kinetic determinations of trace element bioaccumulation in the mussel *Mytilus edulis*. *Mar Ecol Prog Ser* 140:91-113.
39. Roditi HA, Fisher NS. 1999. Rates and routes of trace element uptake in zebra mussels. *Limnology and Oceanography* 44:1730-1749.
40. Baines SB, Fisher NS, Doblin MA, Cutter GA. 2001. Uptake of dissolved organic selenides by marine phytoplankton. *Limnology and Oceanography* 46:1936-1944.
41. Cutter GA, Oatts TJ. 1987. Determination of dissolved sulfide and sedimentary sulfur speciation using gas chromatography-photoionization detection. *Analytical Chemistry* 59:717-721.
42. Twining BS, Baines SB, Fisher NS, Maser J, Vogt S, Jacobsen C, Tovar-Sanchez A, Sanudo-Wilhelmy SA. 2003. Quantifying trace elements in individual aquatic protist

cells with a synchrotron X-ray fluorescence microprobe. *Analytical Chemistry* 75:3806-3816.

43. Twining BS, Baines SB, Fisher NS, Landry ML. 2004. Cellular iron contents of plankton during the Southern Ocean Iron Experiment (SOFeX). *Deep-Sea Research I* 51:1827-1850.
44. Twining BS, Baines SB, Fisher NS. 2004. Element stoichiometries of individual plankton cells collected during the Southern Ocean Iron Experiment (SOFeX). *Limnology and Oceanography* 49:2115-2128.
45. Jorgensen CB. 1990. *Bivalve filter feeding: hydrodynamics, bioenergetics, physiology and ecology*. Olsen and Olsen, Fredensborg.
46. Schlekot CE, Lee B-G, Luoma SN. 2002. Assimilation of selenium from phytoplankton by three benthic invertebrates: effect of phytoplankton species. *Mar Ecol Prog Ser* 237:79-85.
47. Baines SB, Fisher NS. 2001. Interspecific differences in the bioconcentration of selenite by phytoplankton and their ecological implications. *Mar Ecol Progr Ser* 213:1-12.
48. Lemly AD. 2002. *Selenium assessment in aquatic ecosystems*. Springer-Verlag, New York.
49. Cutter GA, Radford-Knoery J. 1991. Determination of carbon, nitrogen, sulfur, and inorganic sulfur species in marine particles. In Hurd D, Spencer D, eds, *Marine particles: Analysis and characterization*, American Geophysical Union, Washington, D.C., pp 57-63.
50. Strickland JDH, Parsons TR. 1972. *A practical handbook of seawater analysis*. Bulletin of the Fisheries Research Board of Canada, Ottawa.
51. Cutter GA. 1978. Species determination of selenium in natural waters. *Anal Chim Acta* 98:59-66.
52. Cutter, G. A. Selenium in reducing waters. *Science* 217[27], 829-831. 1982.
53. Cutter GA. 1983. Elimination of nitrite interference in the determination of selenium by hydride generation. *Anal Chim Acta* 149:391-394.
54. Cutter GA, Cutter LS. 1995. Behavior of dissolved antimony, arsenic, and selenium in the Atlantic Ocean. *Mar Chem* 49:295-306.
55. Cutter GA. 1985. Determination of selenium speciation in biogenic particles and sediments. *Anal Chem* 57:2951-2955.

56. Velinsky DJ, Cutter GA. 1990. Determination of elemental and pyrite-selenium in sediments. *Anal Chim Acta* 235:419-425.
57. DeMaster DJ. 1991. Measuring biogenic silica in marine sediments and suspended matter. In Hurd D, Spencer D, eds, *Marine particles: Analysis and characterization*, American Geophysical Union, Washington, D.C., pp 363-367.
58. Kirz J. 1980. Specimen damage considerations in biological microprobe analysis. *Scanning Electron Microscopy*, pp 239-249.
59. Di Fabrizio E, Romanato F, Gentili M, Cabrini S, Kaulich B, Susini J, Barrett R. 1999. High-efficiency multilevel zone plates for keV X-rays. *Nature* 401:895-898.
60. Yun W, Lai B, Cai Z, Maser J, Legnini D, Gluskin E, Chen Z, Krasnoperova AA, Vladimirovsky Y, Cerrina F, Di Fabrizio E, Gentili M. 1999. Nanometer focusing of hard x rays by phase zone plates. *Review of Scientific Instruments* 70:2238-2241.
61. Maser J. Technical Progress Report. ANL/APS/TB-38. Experimental Facilities Division/User Program Division.
62. Menden-Deuer S, Lessard EJ. 2000. Carbon to volume relationships for dinoflagellates, diatoms, and other protist plankton. *Limnology and Oceanography* 45:569-579.
63. Uttermohl H. 1958. Improvements in the quantitative methods of phytoplankton study. *Mitt Int Ver Limnol* 9:1-25.
64. Vaque D, Pace ML, Findlay S, Lints D. 1992. Fate Of Bacterial Production In a Heterotrophic Ecosystem - Grazing By Protists and Metazoans In the Hudson Estuary. *Marine Ecology-Progress Series* 89:155-163.
65. Bratbak G. 1985. Bacterial Biovolume and Biomass Estimations. *Applied and Environmental Microbiology* 49:1488-1493.
66. Fisher NS, Teyssie J-L, Fowler SW, Wang W-X. 1996. Accumulation and retention of metals in mussels from food and water: a comparison under field and laboratory conditions. *Environ Sci Tech* 30:3232-3242.
67. Werner, I and Hollibaugh, J. T. *Potamocorbula amurensis*: Comparison of clearance rates and assimilation efficiencies for phytoplankton and bacterioplankton. *Limnol.Oceanogr.* 38[5], 949-964. 1993.
68. Conover RJ. 1966. Assimilation Of Organic Matter By Zooplankton. *Limnology and Oceanography* 11:338-345.
69. Canuel, E. A., Cloern, J. E., Rinelberg, D. B., and Guckert, J. B. Molecular and isotopic tracers used to examine sources of organic matter and its incorporation into the food webs of San Francisco Bay. *Limnol.Oceanogr.* 40[1], 67-81. 1995.

70. Thompson J, Stewart AR, Parchaso F, Burau J, Schoellhammer D. 2004. Benthic grazer food sources as defined by bivalve growth, stable isotopes and physical processes. *Limnol Oceanogr* . In prep.
71. Luoma SN, Linville R. A comparison of selenium and mercury concentrations in transplanted and resident bivalves from north San Francisco Bay. San Francisco Estuary Institute.
72. Luoma, S. N. and Linville, R. Selenium trends in North San Francisco Bay. Interagency Ecological Program for the Sacramento-San Joaquin Estuary 10[2], 25-26. 1997.
73. Luoma SN, Decho AW. 1991. Time-courses in the retention of food material in the bivalves *Potamocorbula amurensis* and *Macoma balthica* : significance to the absorption of carbon and chromium. *Mar Ecol Prog Ser* 78:303-314.
74. Luoma, S. N. Bioavailability of trace metals to aquatic organisms - A review. *Sci. Tot. Environ.* 28, 1-22. 1983.
75. Malley, D. F., Stewart, A. R., and Hall, B. D. Uptake of methyl mercury by the floater mussel, *Pyganodon grandis* (Bivalvia, Unionidae), caged in a flooded wetland. *Environ.Toxicol.Chem.* 15[6], 928-936. 1996.
76. Stewart, A. R. Accumulation of Cd by a freshwater mussel (*Pyganodon grandis*) is reduced in the presence of Cu, Zn, Pb, and Ni. *Can.J.Fish.Aquat.Sci.* 56[3], 467-478. 1999.
77. Stewart, A. R. and Malley, D. F. Effect of metal mixture (Cu, Zn, Pb and Ni) on cadmium partitioning in littoral sediments and its accumulation by the freshwater macrophyte *Eriocaulon septangulare*. *Environ.Toxicol.Chem.* 18[3], 436-447. 1999.
78. Stewart AR, Stern GA, Salki A, Stainton MP, Lockhart WL, Billeck BN, Danell R, Delaronde J, Grift NP, Halldorson T, Koczanski K, MacHutcheon A, Rosenberg GB, Savoie DA, Tenkula D, Tomy G, Yarchewski A. Influence of the 1997 Red River flood on contaminant transport and fate in southern Lake Winnipeg.
79. Anastasia JR, Morgan SG, Fisher NS. 1998. Tagging crustacean larvae: assimilation and retention of trace elements. *Limnol Oceanogr* 43:362-368.
80. Fisher NS, Wang W-X. 1996. Assimilation of trace elements by the mussel *Mytilus edulis* : effects of diatom chemical composition. *Marine Biol* 125:715-724.
81. Fisher NS, Reinfelder JR. 1995. The trophic transfer of metals in marine systems. In Tessier A, Turner DR, eds, *Metal speciation and bioavailability in aquatic systems*, John Wiley & Sons, Chichester, pp 363-406.

82. Roditi, H. A., Fisher, N. S., and Sanudo-Willhelmy, S. A. Uptake of dissolved organic carbon and trace elements by zebra mussels. *Environ.Sci.Technol.* 34[13], 2817-2825. 2000.
83. Roditi HA, Fisher NS, Sañudo-Willhelmy SA. 2000. Field testing a metal bioaccumulation model for zebra mussels. *Environ Sci Technol* 34:2817-2825.
84. Wang, W-X. and Fisher, N. S. Accumulation of trace elements in a marine copepod. *Limnol.Oceanogr.* 43[2], 273-283. 1998.
85. Wang W-X, Fisher NS. 1996. Assimilation of trace elements by the mussel *Mytilus edulis* : effects of diatom chemical composition. *Mar Biol* 125:715-724.
86. Wang W-X, Fisher NS. 1997. Modeling metal bioavailability for marine mussels. *Rev Environ Contam Toxicol* 151:39-65.
87. Wang W-X, Reinfelder JR, Lee B-G, Fisher NS. 1996. Assimilation and regeation of trace elements by marine copepods. *Limnol Oceanogr* 41:70-81.
88. Wang WX, Fisher NS. 1999. Assimilation efficiencies of chemical contaminants in aquatic invertebrates: A synthesis. *Environmental Toxicology and Chemistry* 18:2034-2045.
89. Baines, S. B., Fisher, N. S., and Kinney, E. L. The influence of temperature on dietary metal uptake in Arctic and temperate mussels. *Mar.Ecol.Prog.Ser.* 2004.
90. Cutter, G. A. and San Diego-McGlone, M. L. C. Temporal variability of selenium fluxes in San Francisco Bay. *Sci.Tot.Environ.* 97/98, 235-250. 1990.
91. Cutter GA, Krahfors CF. 1988. Sulfide in surface waters of the Western Atlantic Ocean. *Geophysical Research Letters* 15:1393-1396.
92. Cutter GA, Cutter LS. 2001. Sources and cycling of selenium in the western and equatorial Atlantic Ocean. *Deep Sea Research Part II Topical Studies in Oceanography* 48:2917-2931.

ARGONNE NATIONAL LABORATORY

9700 SOUTH CASS AVENUE, ARGONNE, ILLINOIS 60439

Advanced Photon Source

Argonne, 11/16/2004

Drs. Stephen Baines and Nicholas Fisher
Marine Sciences Research Center
Stony Brook University
Stony Brook, NY 11794

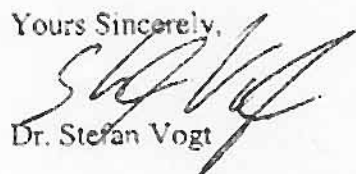
Dear Drs. Baines and Fisher,

We are writing in strong support of your proposal to the CALFED Bay/Delta Estuarine Restoration Program to use the hard x-ray microprobe to study selenium concentrations in the planktonic food of the invasive clam, *Potamocorbula amurensis*, in San Francisco Bay. As you know, beamtime at the Advanced Photon Source is allocated using a competitive review process through the general user access program. You have been very successful obtaining beamtime at APS via this process, and we would expect you to be in an excellent position to compete successfully for beamtime with this proposal as well. We have been collaborating with you in related research for nearly four years now, and our team at the 2-ID-E microprobe continues to be very interested in your projects. In that spirit, our staff will continue to provide you with the same enthusiastic support which we have provided in the past to insure your continued success.

The work you propose is within the capability of the instrument and will fully utilize our new capabilities for combining other microscopic tools, in particular epifluorescence microscopy with X-ray fluorescence microscopy. We hope also to use the opportunity to further standardize methodologies of sample preparation and to improve the usability of the quantification software so that this powerful technique can be more widely available to other environmental scientists. We are particularly excited about quantifying the mass and C content of biological samples using X-ray phase contrast. We currently employ X-ray phase contrast to provide images of cells for targeting purposes. Thus, quantification seems like a feasible goal that will find wide-ranging applications in biology, chemistry and environmental science.

We look forward to continuing our exciting collaboration.

Yours Sincerely,


Dr. Stefan Vogt


Dr. Jörg Maier

Table 1. Comparison of selenium concentrations and Se:C ratios in different selenium pools; ND = not determined; numbers in brackets = range.

Location	n	Se conc. nmol g ⁻¹ dry wt.	Total Se:C (x10 ⁻⁶)	%Elemental Se %
Cultured phytoplankton	11	76.7 ± 46.6	3.2 ± 6.2 0	0
Seston: high flow				
Historic (April 1986)	19	4.9 ± 2.1	ND	ND
Current (June 1998, April 1999)	39	4.8 ± 3.5	3.6 ± 1.7	43 ± 33
Seston: low flow				
Historic (Sept. 986)	22	8.8 ± 2.9	ND	ND
Current (Nov. 1997, Oct. 1998, Nov. 1999)	67	9.2 ± 3.7	5.7 ± 2.9	36 ± 22
Seston: Delta (all seasons)				
Sacramento River	5	7.8 ± 2.6	4.9 ± 2.5	48 ± 37
San Joaquin River	5	8.3 ± 5.2	5.4 ± 3.4	26 ± 35
Sediments: Estuary (0-2cm)a	11	2.00 ± 0.66	3.0 ± 0.8	57 ± 18
Sediments: Delta (0-2 cm)a	11	3.60 ± 2.45	2.8 ± 1.2	53 ± 22

Table 2. List of the variables being measured, the hypotheses they will be used to address and the relationship to past and future monitoring efforts. We also list, in broad terms, the methods to be used and the groups responsible for completing the analyses				
Measurement	Relevant hypotheses: rationale	Relevance to monitoring	Interval	Responsibility
Dissolved and suspended particulate analyses (Task 2)				
Total suspended particulate matter (SPM)	1: Can affect the ability of clams to filter food and selectively ingest high quality organic matter.	Extends 20 years of past data, providing more power to detect changes and relationships.	Monthly	ODU
Total suspended particulate Se	1,2,3,4: Represents the total pool of Se on the particles available for ingestion by the clams. An important normalizing variable.	Same	Monthly	ODU
Elemental suspended particulate Se	3,4: Non-bioavailable but common in sediments that have undergone diagenesis under aerobic conditions. A tracer for older resuspended sediment particles.	Same	Monthly	ODU
Organic suspended particulate Se	3,4: The fraction of particulate Se which is most available to clams. By subtraction from suspended particulate Se will be used to assess detrital Se.	Same	Monthly	ODU
Dissolved selenite, selenate and organic selenide	2,3,4: The forms of selenium that are most clearly under direct management control. Measurements are needed to put measurement of particulate Se and plankton Se content experiments in context.	Same	Monthly	ODU
Organic C and N content of SPM	3,4: Potentially indicates the quality of suspended sediments as food. Also may be helpful in determining source.	Same	Monthly	ODU
Chlorophyll concentrations	2: Reflects the contribution of phytoplankton biomass to the suspended	Same	Monthly	ODU

	particulate matter. Important for assessing			
Plankton (Task 3)				
Se:C uptake ratios of phyto- and bacterio-plankton at natural concentrations of dissolved Se	2: Seasonal changes in Se:C ratios will be related to seasonal variability in clam Se content.	Indicates whether phytoplankton should be target of future monitoring.	Monthly	SBU
Se:C uptake ratios of phyto- and bacterioplankton at elevated concentrations of dissolved Se	2,3,4: Will be compared with uptake at current low levels to determine if Se content of phytoplankton has decreased in response to reduced selenite concentrations or will increase in response to higher selenate concentrations.	Se:C in food of <i>Potamorbula</i> can be related to management actions and past data on dissolved Se concentrations.	Biannually	SBU
Se concentrations in individual phytoplankton and protozoa	2: Species specific information will allow us to evaluate the influence of changing species composition on clam food.	Can use past phytoplankton data to reconstruct Se in <i>Potamocorbula</i> diet. Suggests that species with high Se should be monitored.	Monthly (in combination with species counts)	SBU
Free and attached bacterial counts and biomass	3,4: Bacteria constitute an large and bioavailable fraction of the Se in suspended detritus and free-living bacteria can transform dissolved organic Se into particulate form that is available to clams.	May provide a means of assessing quality of detrital material.	Monthly	SBU

Phytoplankton and protozoan counts and biovolume	2: Will allow us to use SXRF data to predict the average Se content in particulate food and assess ecological mechanisms causing it to change.	Extends past measurements. Will improve ability to determine correlates of plankton composition.	Monthly	SBU
Potamocorbula (Task 4)				
Tissue Se content	1,2,3,4: The central variable to be monitored and explained. Will be collected at two spots to tease out marine and riverine effects.	Extends past data: improves statistical power to detect change.	Monthly	USGS
Growth rate	1: Affects the ability of the clams to concentrate Se and may vary seasonally with temperature, salinity and food abundance.	Interpretation of historic Se measurements in consumers including <i>Potamocorbula</i>	Monthly	USGS
Ingestion rate (in comparison with <i>Corbicula</i>)	1: A major determinant of Se bioaccumulation. May explain difference between <i>Potamocorbula</i> and <i>Corbicula</i> , and could vary seasonally with temperature and food abundance.	Same	Monthly	USGS
Assimilation of Se from phytoplankton, protozoans and bacteria (in comparison with <i>Corbicula</i>)	1: A major determinant of Se bioaccumulation. May explain difference between <i>Potamocorbula</i> and <i>Corbicula</i> , and could vary seasonally with composition of the seston, temperature and ingestion rate.	Same.	Once each during low flow and high flow	USGS
Excretion of assimilated Se (in comparison with <i>Corbicula</i>)	1: A major determinant of Se bioaccumulation. May explain difference between <i>Potamocorbula</i> and <i>Corbicula</i> , and could vary seasonally with in response to changes in environmental variables such as salinity.	Same; also may allow reconstruction of past Se in clams from river flow and salinity.	Once each during low flow and high flow	USGS
Assimilation of detrital Se	4: Utilization of this pool may explain why Se in <i>Potamocorbula</i> has not changed quickly with decreased selenite	Will suggest time scale over which Se in clams must be monitored. Also will indicate	Once each during low flow and high	USGS

	concentrations.	best index of available PSe.	flow	
Stable isotopic composition (³⁴ S, ¹³ C and ¹⁵ N) of clam tissues.	3: In combination with stable isotopic composition of suspended particles will indicate whether clams are assimilating material originating from Suisun Bay or in the SJR and Delta at different times.	Suggests source of Se in clams. Indicates locality and management actions that should be focus of monitoring.	Monthly	USGS

Table 3. Minimum detection limits (MDL) in concentration units for Se and three other metals within phytoplankton cells. Calculations are based on Poisson counting statistics given known fluorescence yields and background fluorescence for the elements in question under standard beam conditions at beamline 2-ID-E at the advanced photon source (Twining et al. 2003). Analysis time was constrained to 40 minutes per cell. Doubling this time lowers the MDL by ~30%.

Element	Minimum Detection Limits					
	5 μm diameter cell			20 μm diameter cell		
	$\mu\text{mol Se mol}^{-1} \text{ C}$	$\mu\text{g Se g}^{-1} \text{ C}$	ppm	$\mu\text{mol Se mol}^{-1} \text{ C}$	$\mu\text{g Se g}^{-1} \text{ C}$	ppm
Se	0.3	1.9	0.6	0.1	0.3	0.1
Fe	1.8	8.6	2.6	0.6	3.0	0.9
Ni	0.7	3.2	1.0	0.2	1.1	0.3
Zn	1.0	5.2	1.6	0.3	1.9	0.6

Figure 1. Predictions of Se concentrations on suspended particles with the Bay/Delta ecosystem at different rates of San Joaquin River flow into the estuary.

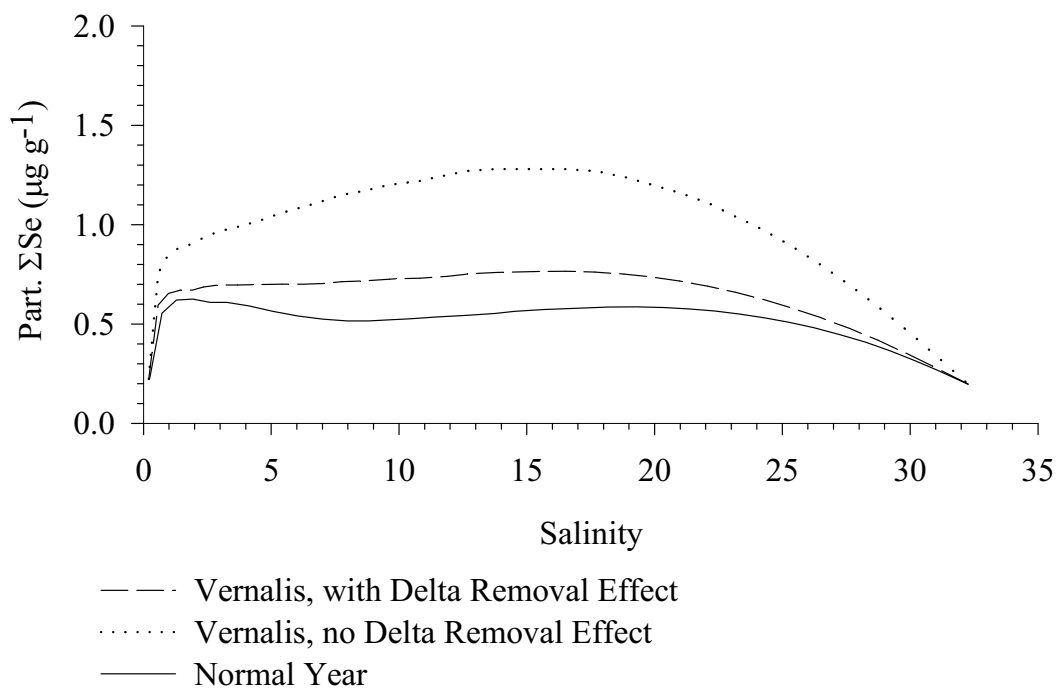


Figure 2. Spatial Distribution of Se ($\mu\text{g/g}$ dry wt.) in *Potamocorbula*.

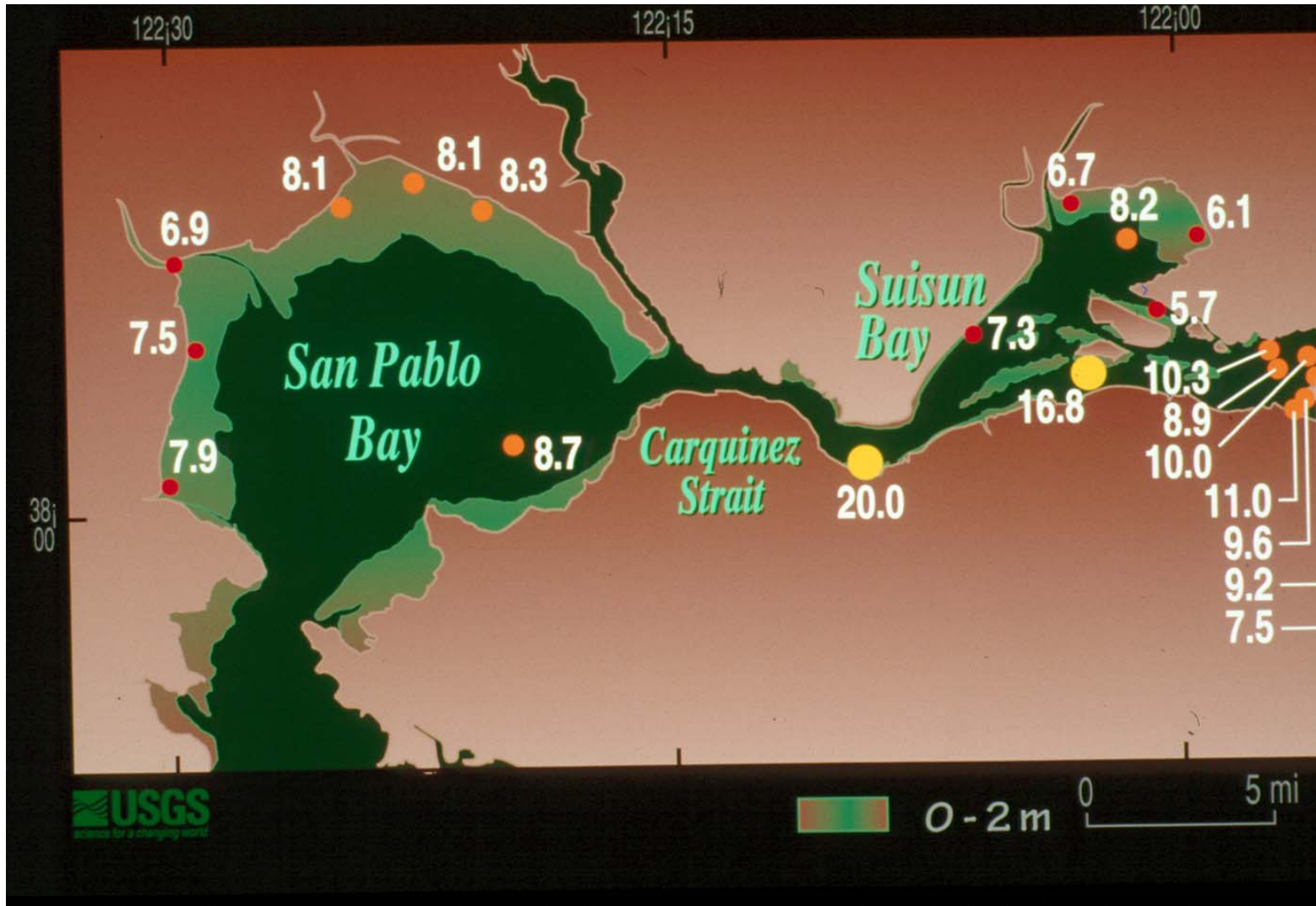


Figure 3. Temporal patterns since 1995 in flow from the San Joaquin River in relation to Se concentrations in clams and suspended particles in Suisun Bay.

Comparison of Particulate and Potamocorbula Se with SJ River Inputs

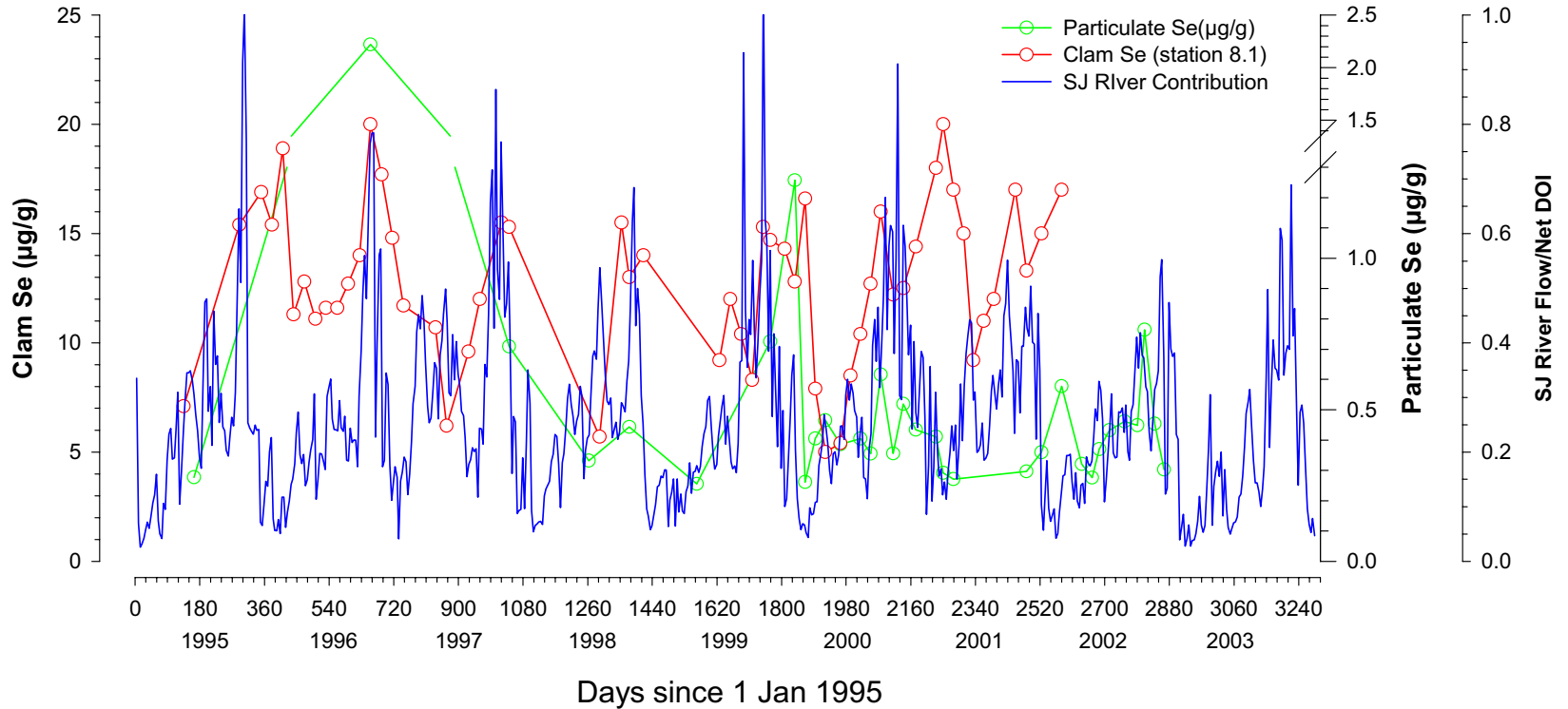


Figure 7. Concentration dependence of selenite uptake by the diatom, *Thalassiosira pseudonana*

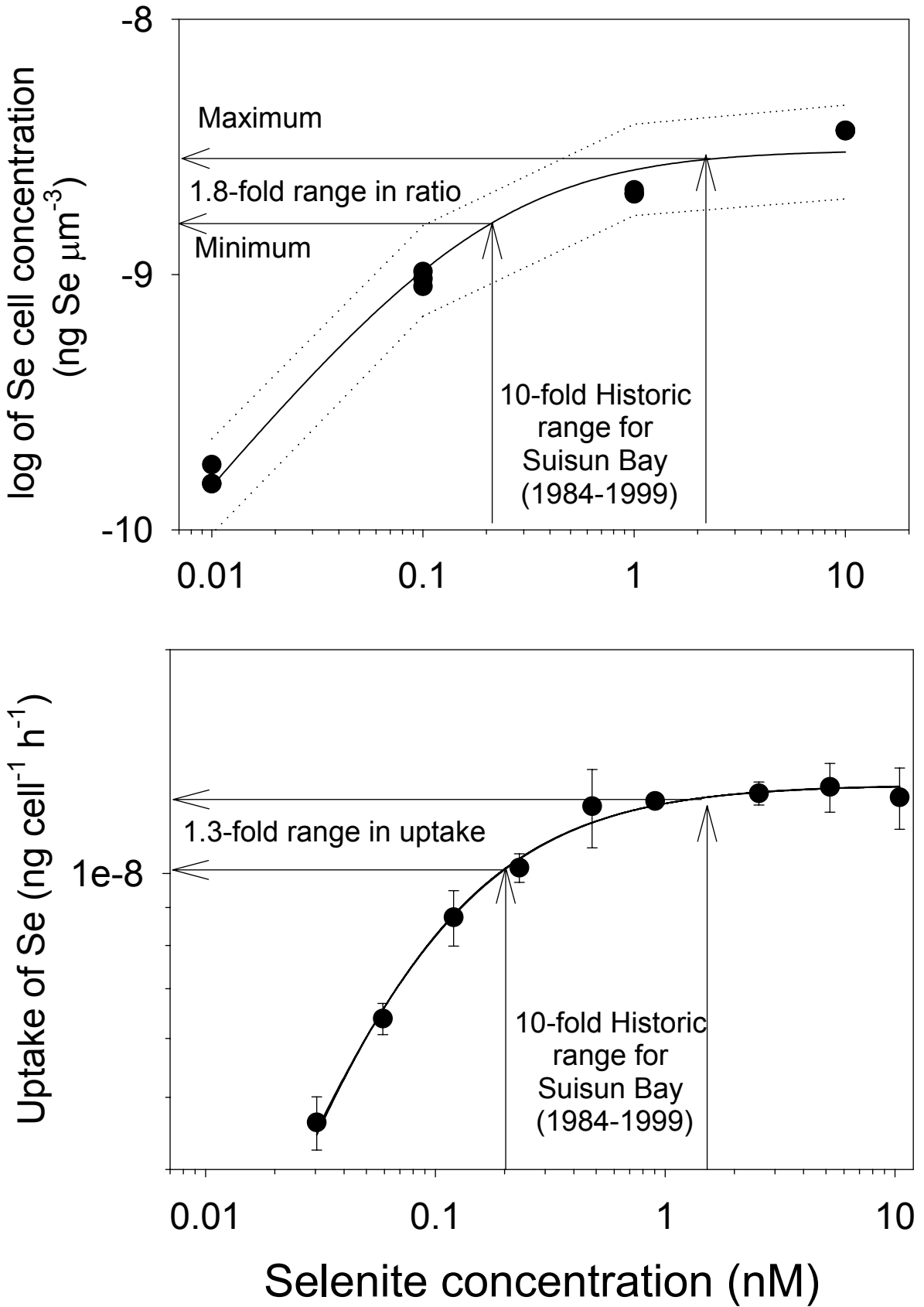


Figure 6. Variability in Se concentration of cultured phytoplankton at two different concentrations of dissolved selenite.

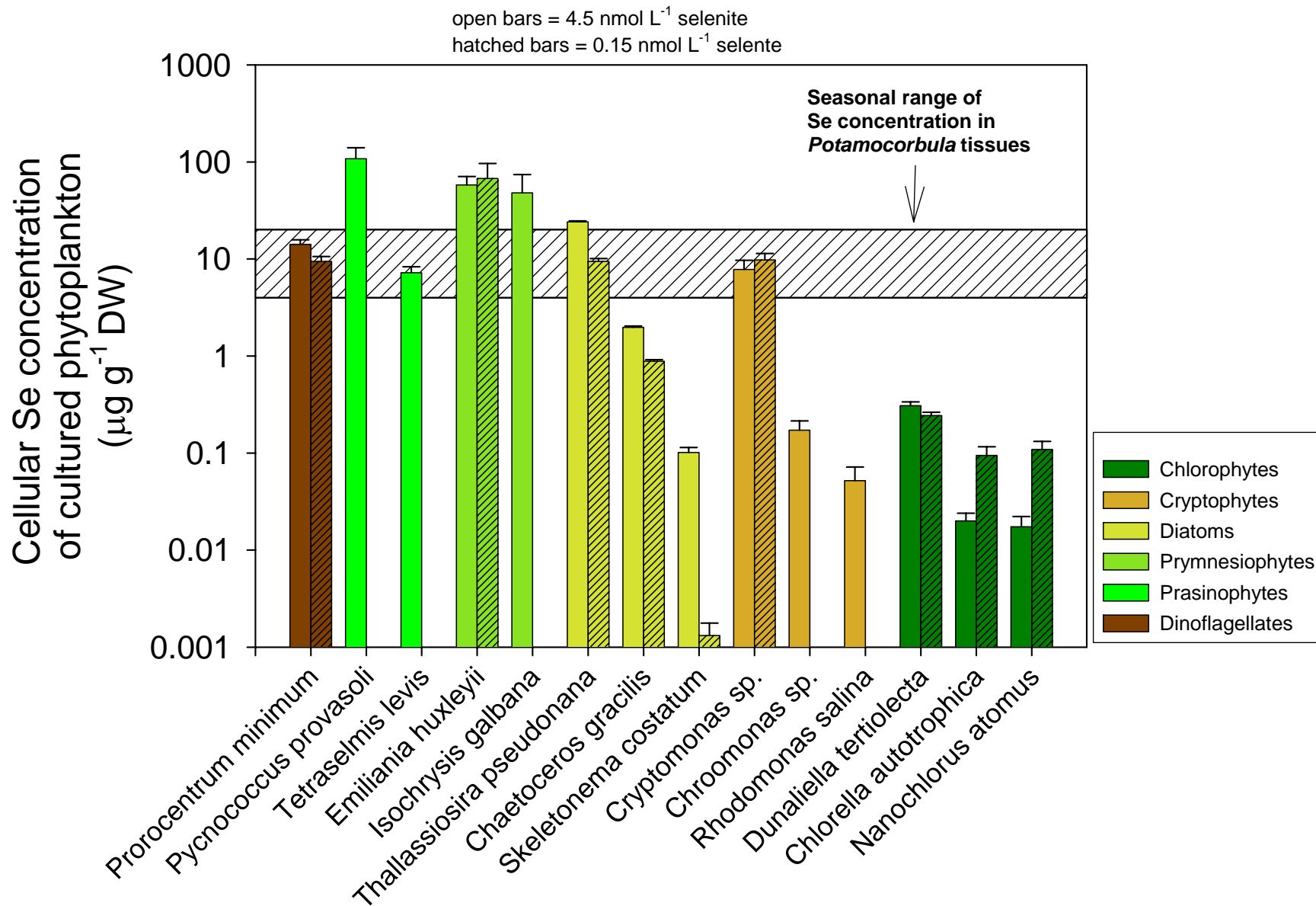
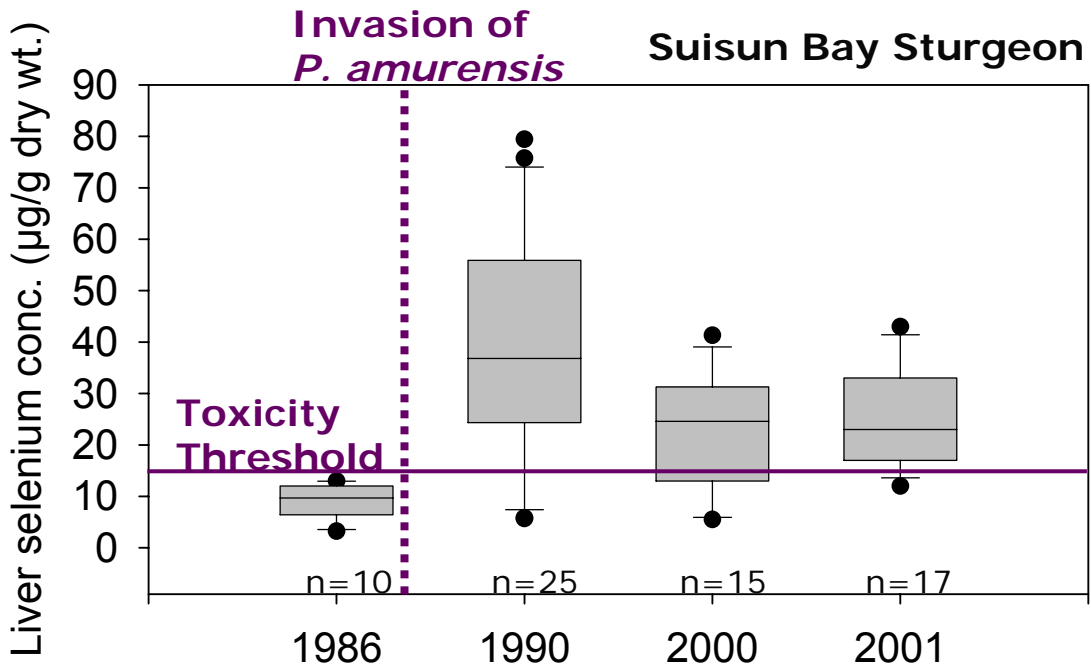
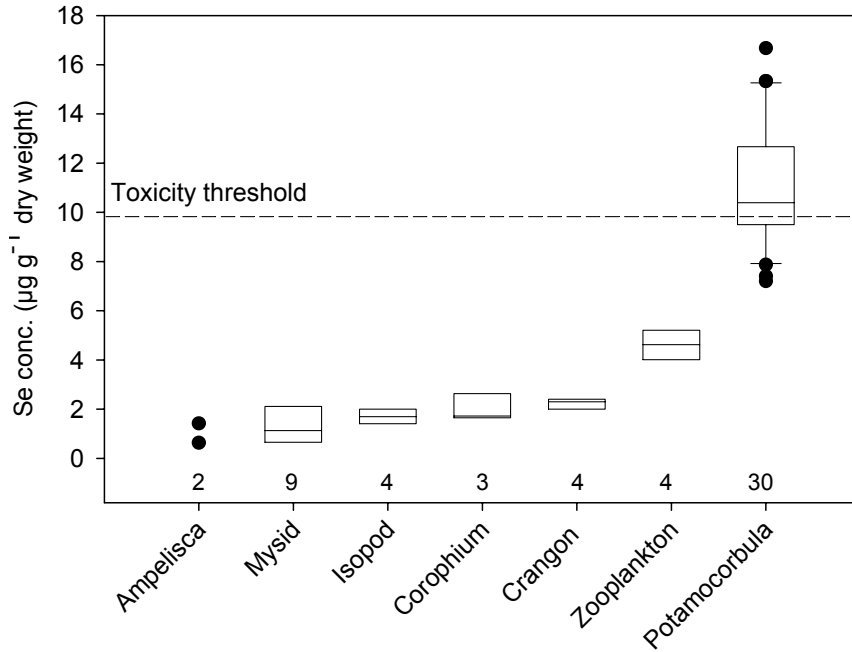


Figure 4. Consumers that have *Potamocorbula* as part of their diet have had Potentially toxic concentrations of Se in tissues since the invasion of *Potamocorbula*.



Data CDFG 1986/1990, Stewart 2000/2001

Figure 5. Relationships among ambient salinity, sulfur content, $\delta^{34}\text{S}$, and Se content of *Potamocorbula* tissues.

Potamocorbula - Carquinez St.

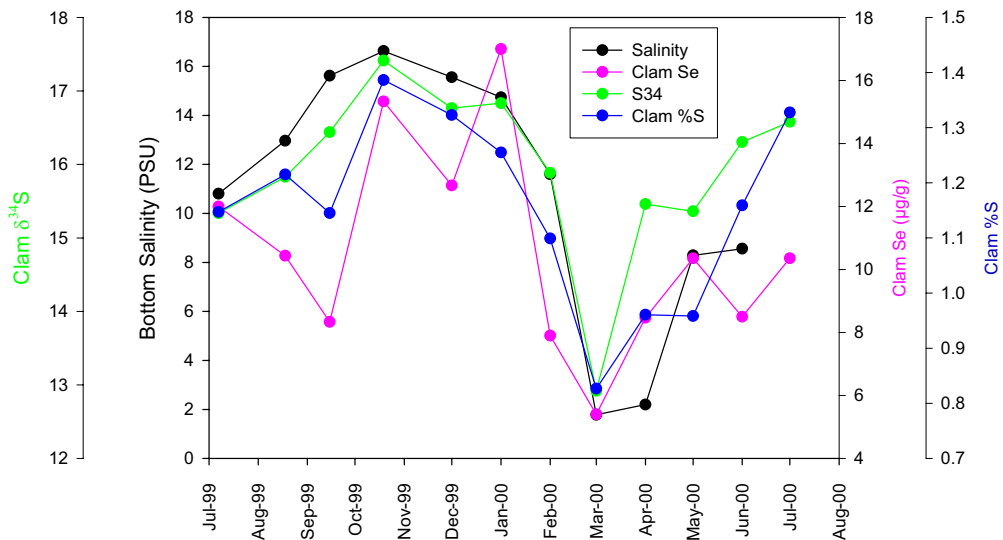
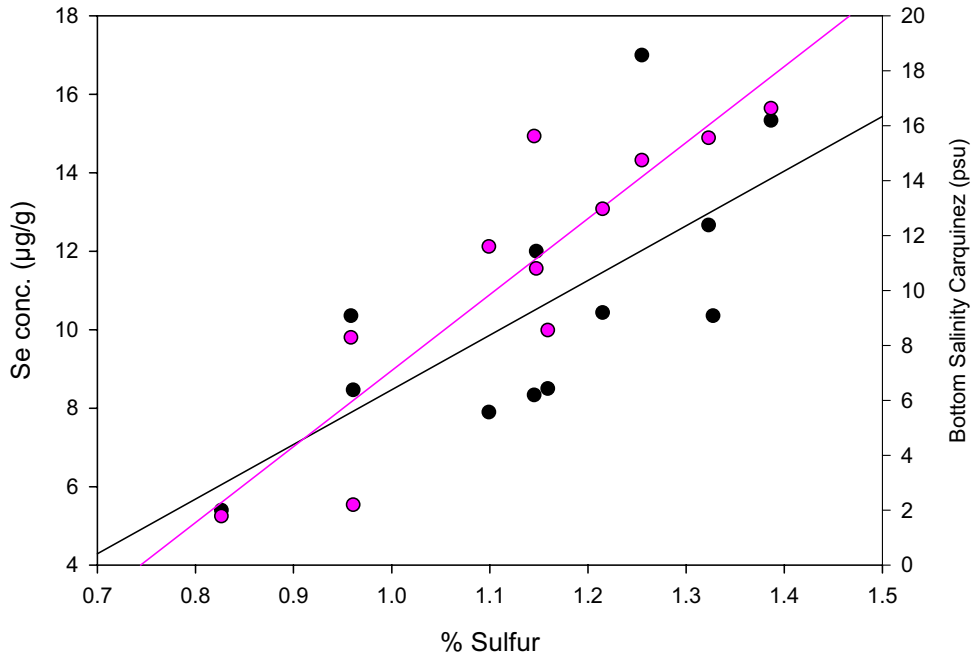


Figure 11. Patterns in stable isotopic composition of dissolved inorganic carbon (DIC) and clams in San Francisco Bay. A. Relationship between isotopic composition of DIC and salinity. B. Seasonal variation in isotopic composition of clams compared to that predicted by salinity and growth variation.

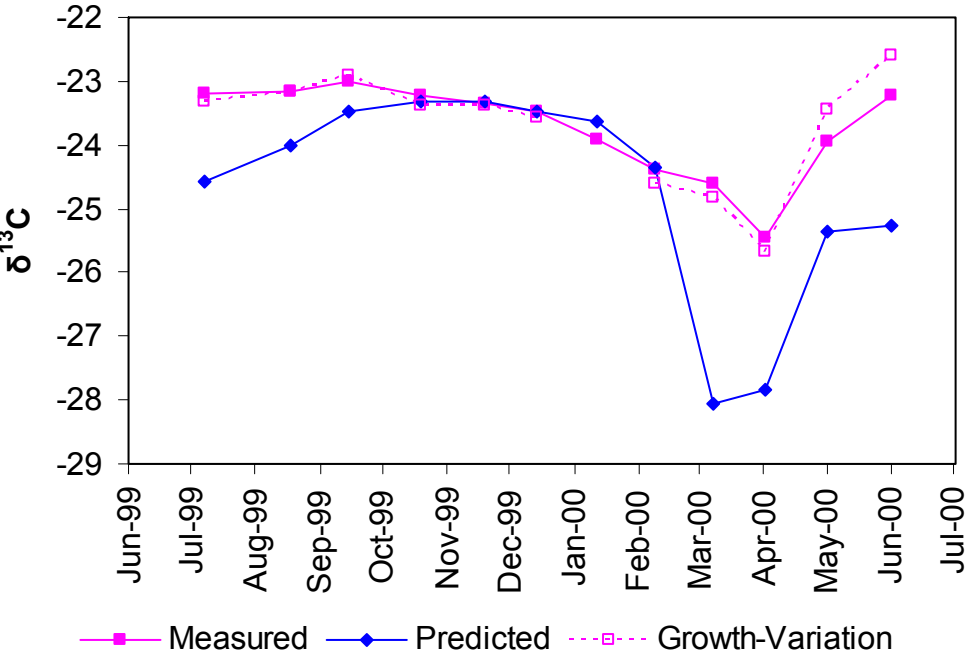
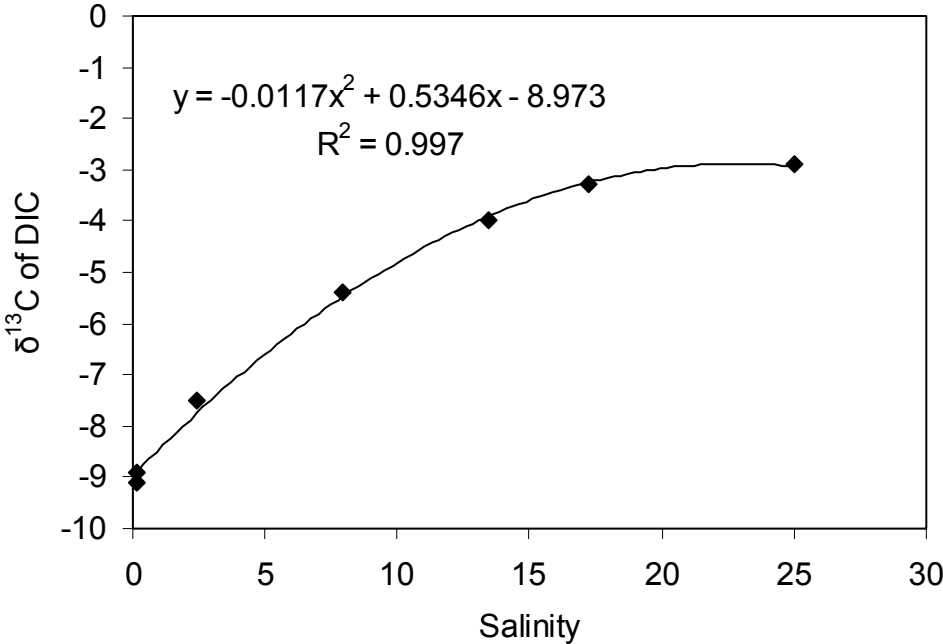


Figure 8. Results of Past monitoring for dissolved and particulate Se in north San Francisco Bay.

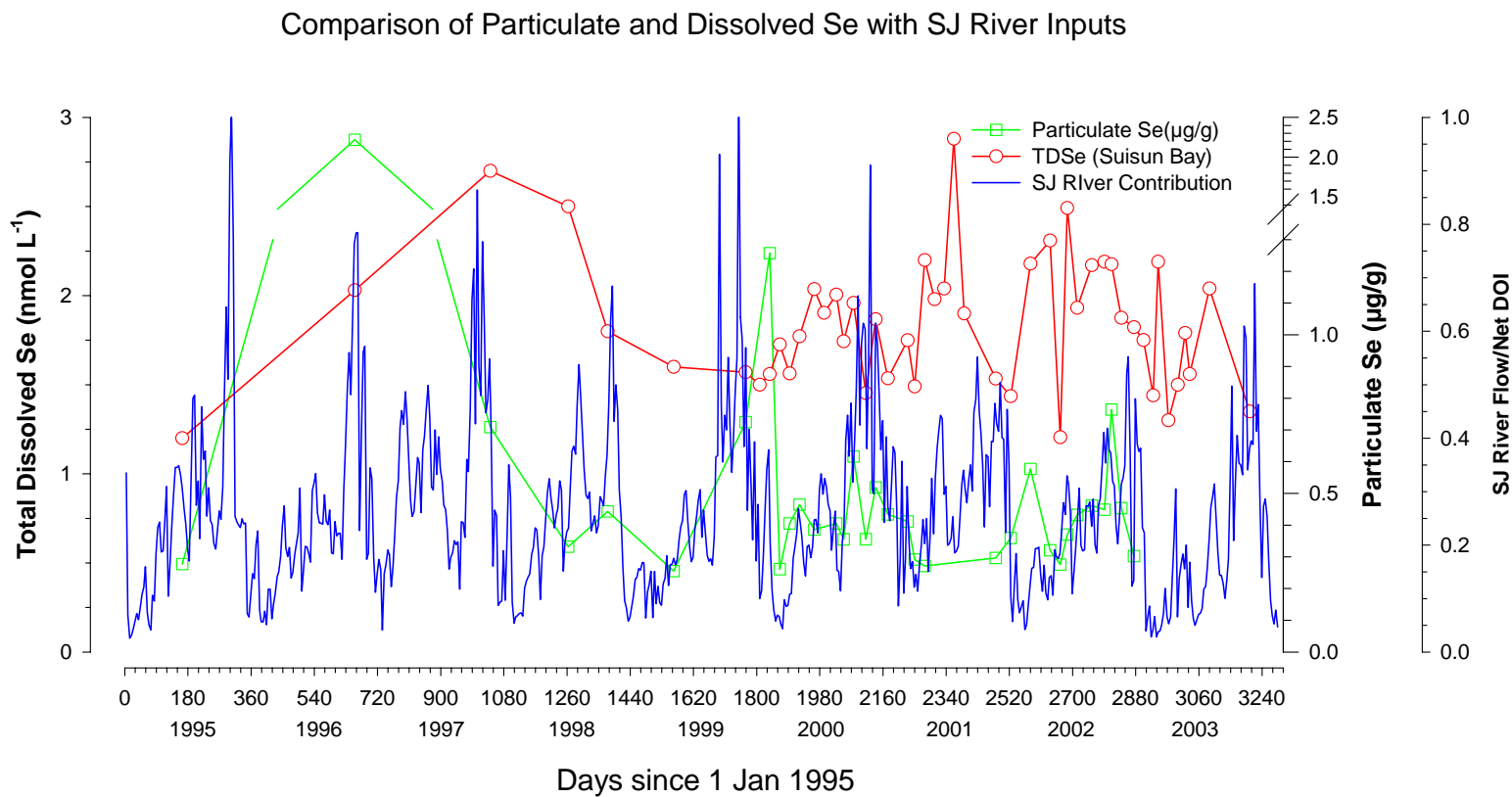


Figure 12. Flow diagram describing the steps involved in preparing and analyzing single cells using SXRF.

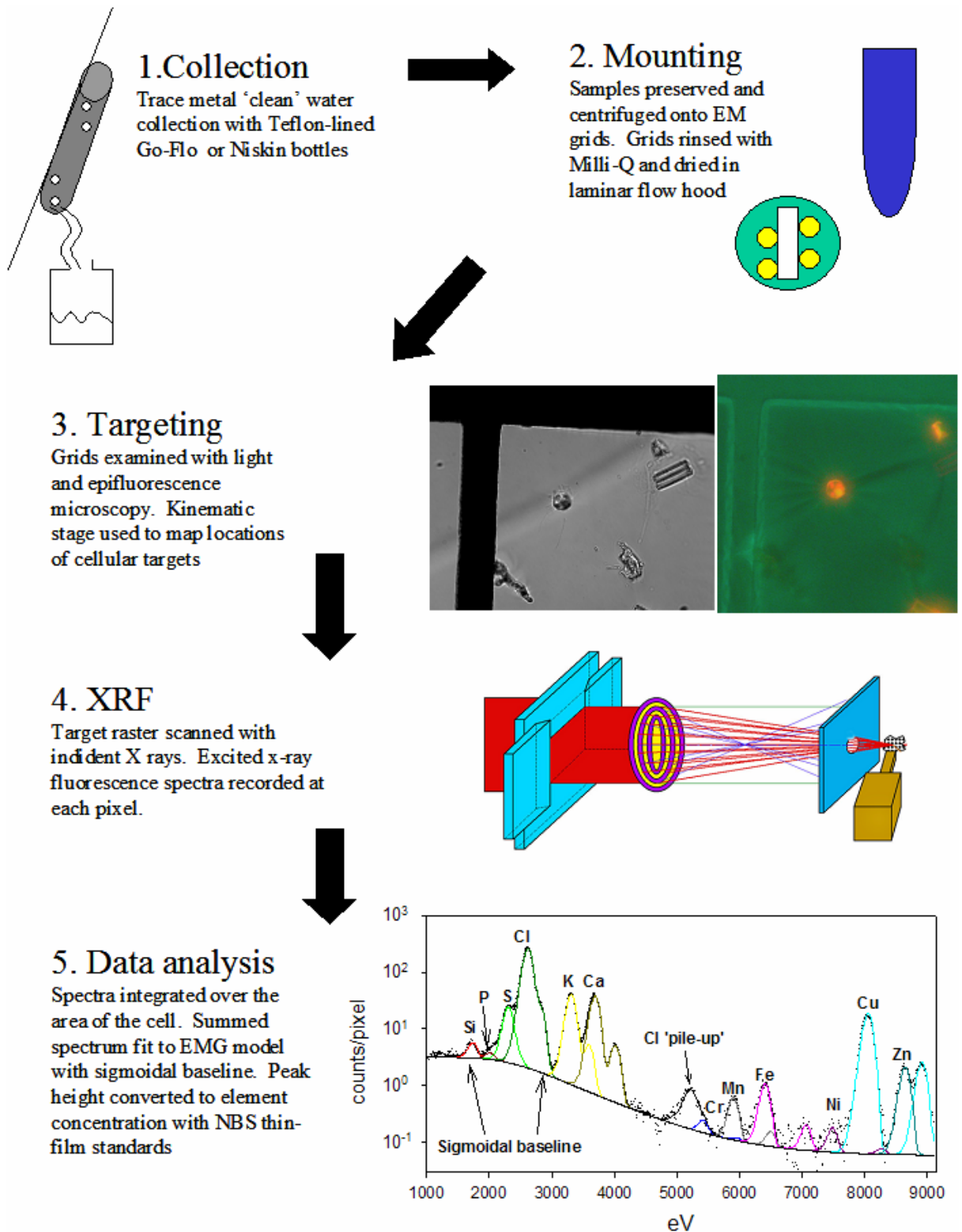


Figure 3. Pictograph describing the steps involved in XRF analysis.

Figure 9. Conceptual Model of Selenium Contamination at Suisun Bay:
Potential monitoring variables

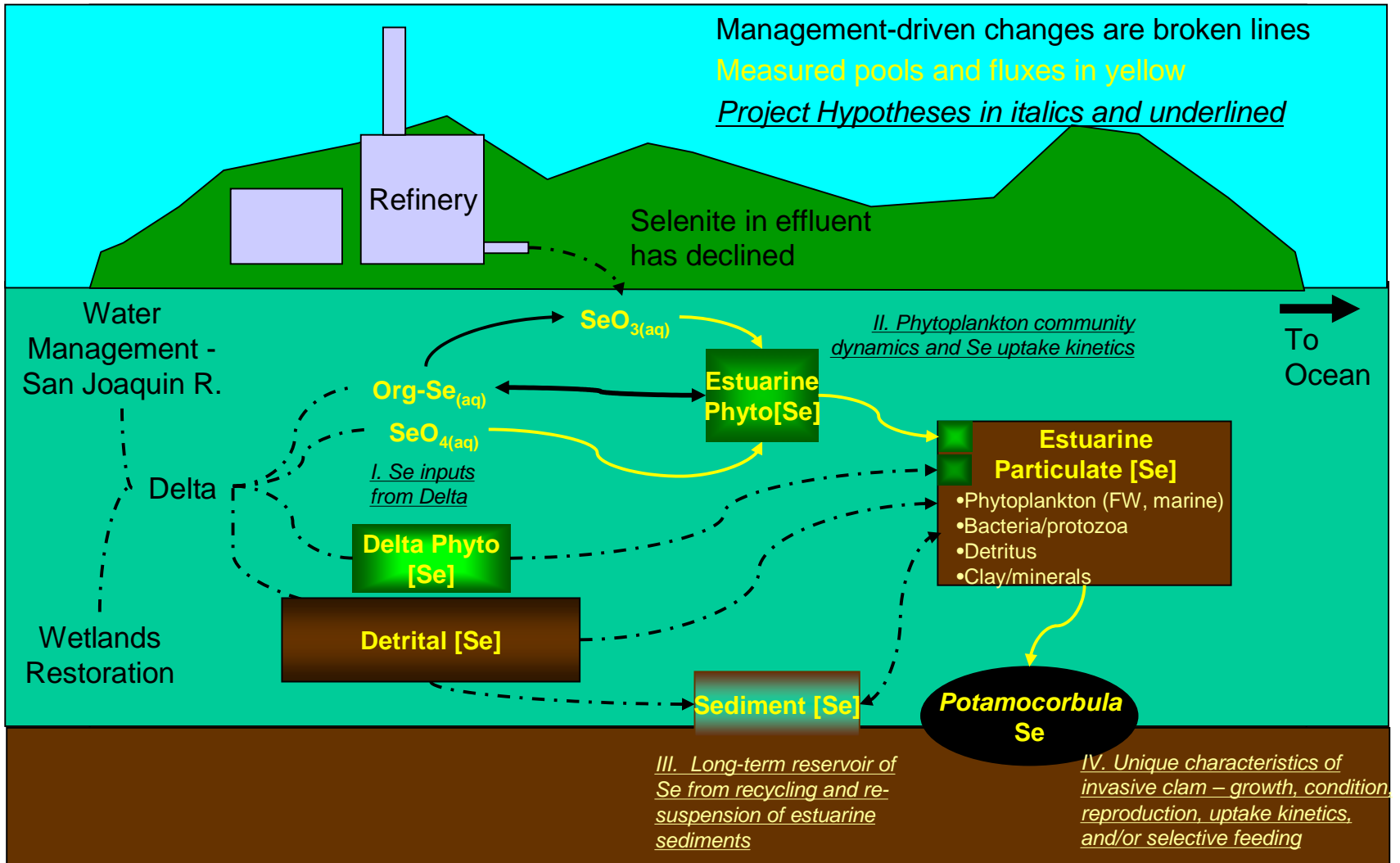
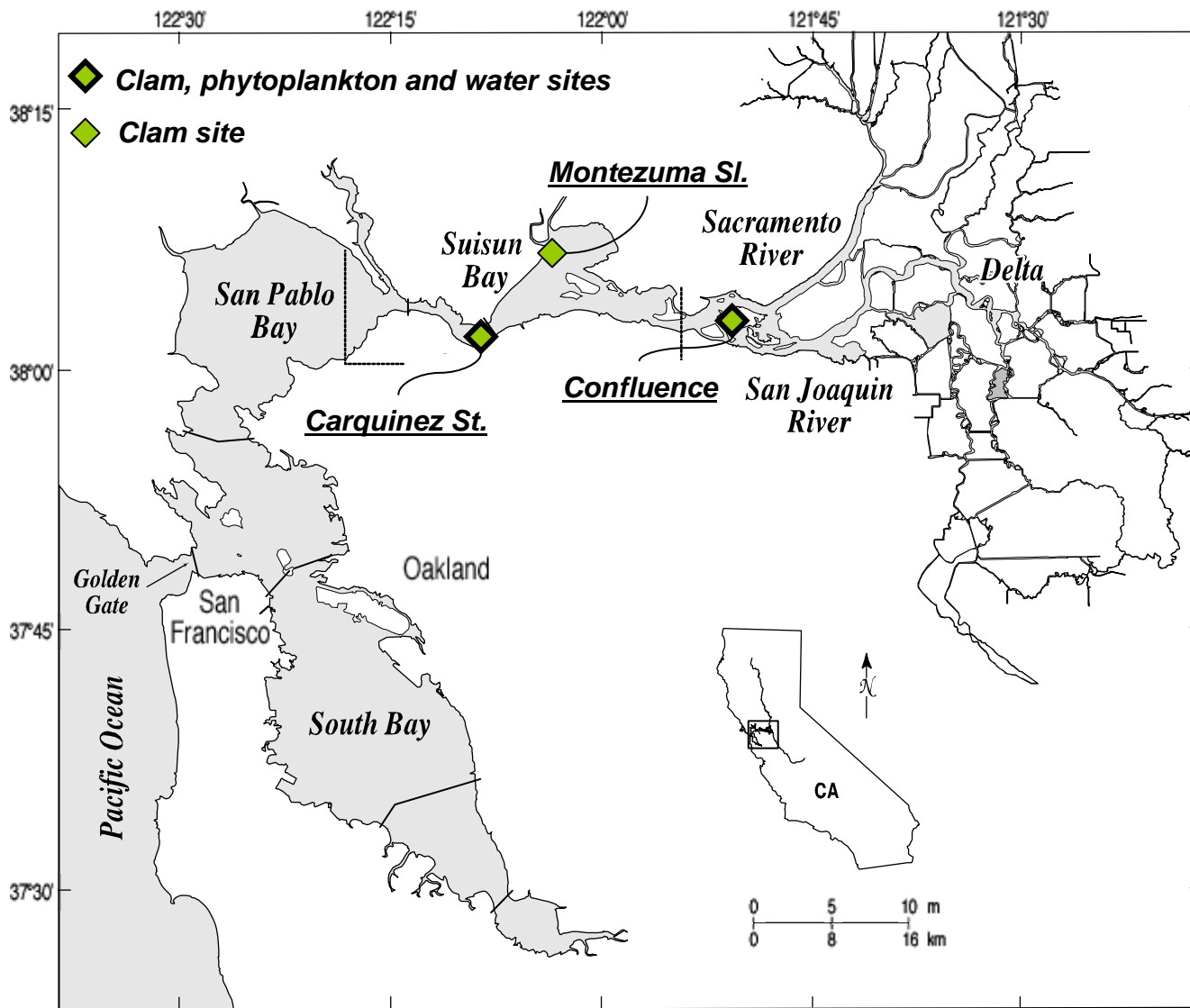


Figure 10. Locations of proposed monitoring locations.



California Home



Monitoring Changes In Selenium Contamination Of The San Francisco Bay-Delta In Response To Restoration And Changing Water Management: Signature

The applicant for this proposal must submit this form by printing it, signing below, and faxing it to +1 877-408-9310.

Failure to sign and submit this form will result in the application not being considered for funding.

The individual signing below declares that:

- all representations in this proposal are truthful;
- the individual signing the form is authorized to submit the application on behalf of the applicant (if applicant is an entity or organization);
- the applicant has read and understood the conflict of interest and confidentiality discussion under the Confidentiality and Conflict of Interest Section in the main body of the PSP and waives any and all rights to privacy and confidentiality¹ of the proposal on behalf of the applicant, to the extent provided in this PSP; and
- the applicant has read and understood all attachments of this PSP.

Proposal Title: Monitoring changes in selenium contamination of the San Francisco Bay-Delta in response to restoration and changing water management

Proposal Number: 2004.02-0096

Submitter: Fisher, Nick (nfisher@notes.cc.sunysb.edu)

N. Fisher

Nov 19/04

Applicant Signature

Date

Nick Fisher

SUNY

Printed Name Of Applicant

Applicant Organization

Help is available: help@solicitation.calwater.ca.gov, +1 877 408-9310

We care about the data we collect. Please read our [privacy policy](#).

URL: https://solicitation.calwater.ca.gov/solicitations/2004.02/proposals/0096/forms/60?form_read_only=1

time: 2004-11-19 14:53:48 PST

user ID: nfisher

client IP: 130.118.33.62

Water Diversion as an Ecosystem Disturbance: Examples from the Sacramento-San Joaquin River Delta (California)

Suggested page heading: Water Diversion as an Ecosystem Disturbance

NANCY E. MONSEN¹

JAMES E. CLOERN¹

JON R. BURAU²

¹*U.S. Geological Survey, 345 Middlefield Road MS/496, Menlo Park, California 94024, USA*

²*U.S. Geological Survey, Placer Hall, 6000 J Street, Sacramento, California 95819-6129, USA*

Corresponding author: Nancy E. Monsen

nemonsen@usgs.gov

phone: (650) 329-4337

fax: (650) 329-4327

Abbreviations: CDWR, California Department of Water Resources; CVP, Central Valley Project; DCC, Delta Cross Channel; DO, Dissolved Oxygen; DOC, Dissolved Organic Carbon; EBFM, Ecosystem-Based Fishery Management; HORB, head of Old River barrier; IEP, Interagency Ecological Program; IWRM, Integrated Water Resources Management; MI, Mildred Island; SAC, Sacramento River; SFB, San Francisco Bay; SJR, San Joaquin River; SWP, State Water Project; THM, trihalomethanes; USGS, United States Geological Survey;

Abstract

Hydrologic manipulations through water-development often come with unanticipated consequences, sometimes conflicting with other goals such as water quality and human health or biological communities and the ecosystem functions supporting them.

Observations from research and monitoring programs in California's Sacramento-San Joaquin River Delta, a highly manipulated hydrologic system, illustrate the concept of flow diversion as an ecosystem disturbance. Hydraulic manipulations directly alter the regional flow paths and indirectly change water quality across the Delta, sometimes creating conflict between different water use priorities. Our examples illustrate how: (1) physically small diversions can have ecosystem-scale effects; (2) regional-scale processes can drive local-scale variability; (3) diversions have multiple benefits and costs; and (4) diversions can reduce the capacity of aquatic ecosystems to assimilate wastes. Our purpose is to encourage a broader framework for water-resource management that explicitly recognizes the interconnections between hydrologic manipulations, water quality, and life-support functions provided by aquatic ecosystems.

Index terms: 1880 Water management, 1803 Anthropogenic effects, 0439 Ecosystems, structure and dynamics, 0442 Estuarine and nearshore processes

Key words: diversion, Sacramento-San Joaquin Delta, ecosystem response, water management

Introduction

Human civilization depends on reliable supplies of water, and our continuing population and economic growth are sustained by control of hydrologic systems on a massive scale. Intense dam construction in the twentieth century produced a reservoir capacity in North America that can store 22% of the continent's annual runoff (Dynesius and Nilson 1994), and now only 2% of the rivers and streams in the United States remain free-flowing (Abramovitz 1996). Water development captures and channelizes surface runoff for land reclamation and flood control, redistributing runoff from wet to dry basins and between wet and dry seasons, expanding habitability of the world's arid zones for human settlement.

Our history of water development has taught that hydrologic manipulations often come with unanticipated consequences, sometimes conflicting with other societal goals. Often the published case studies related to diversions focus on the economic implications of diversions or diversion limits. Some examples of these analyses recently published in *Water Resources Research* include: economic consequences for agricultural production, fishing, and fuelwood collection in the Hadejia-Jama'are floodplain due to upstream diversions in northern Nigeria (Barbier 2003), agricultural economic costs due to lake level restrictions that limit diversions from Upper Klamath Lake (Adams and Cho 1998), and methods to improve water productivity for cotton and rice fields in the Syr Darya Basin, central Asia (Abdullaev and Molden 2004).

The influence of diversions on the ecosystem can be equally important. The Egyptian High Aswan Dam reduced nutrient inputs from the Nile to the Mediterranean Sea,

resulting in the collapse of the sardine and prawn fishing industry (Nixon 2003). The Rhine River, now a fully engineered shipping highway of levees, locks and dams, once supported a salmon run when the river braided and meandered in its natural floodplain (Abramovitz 1996). Diversions from the streams feeding the Aral Sea exposed the seabed resulting in salt and dust storms, causing significant ecological, water supply, health and agricultural damage (Micklin 1988). Road and levee construction around Colombia's Ciénaga Grande de Santa Marta cut off freshwater supplies to the lagoon, killing extensive areas of mangrove forest (Perdomo and others 1998). Diversions along China's Yellow River caused the river to dry up approximately 600 km from the river's mouth with no outflow for 226 days in 1997 causing seawater intrusion and wetland recession in the delta area (Cai and Rosegrant 2004).

California's Sacramento-San Joaquin River Delta is an example of a highly manipulated hydrologic system where diversions significantly alter the ecosystem. In this paper we use observations from research and monitoring programs in the Delta system to illustrate the concept of flow diversion as an ecosystem disturbance. We selected examples to illustrate how: (1) physically small diversions can have ecosystem-scale effects; (2) regional-scale processes can drive local-scale variability; (3) diversions have multiple benefits and costs (e.g. interbasin transfers to meet water-supply demands can degrade water and habitat quality, creating conflict with goals of providing safe drinking water and rehabilitating populations of sensitive or listed species); and (4) diversions can reduce the capacity of aquatic ecosystems to assimilate wastes. Our purpose is to encourage a broader framework for water-resource management that explicitly

recognizes the interconnections between hydrologic manipulations, water quality, and life-support functions provided by aquatic ecosystems. This framework is central to sustainable freshwater development envisioned by Gleick (2000) as: "the use of water that supports the ability of human society to endure and flourish into the indefinite future without undermining the integrity of the hydrological cycle or the ecological systems that depend on it."

California's Delta Ecosystem as a Case Study

California's Delta is the convergence zone of two large rivers (Figure 1), the Sacramento (SAC) and San Joaquin (SJR), draining a 153,000 km² watershed that captures runoff from winter-spring rainfall in the Central Valley and coastal range and spring snowmelt in the Sierra Nevada mountains. The Delta was a 1,400-km² wetland (Atwater and others 1979) that has been transformed into a patchwork of agricultural tracts surrounded by leveed channels, tidal lakes and remnant patches of marsh. As the transition zone between a large river-watershed and the San Francisco Bay estuary (SFB), the Delta is a migration route for anadromous fish such as Chinook salmon, sturgeon, and American shad and permanent habitat for native species such as the endemic delta smelt and Sacramento splittail. The Delta is also the hub of a water-development infrastructure that captures 7.1 km³ of runoff during the wet season and transfers water from the water-rich north to the arid south and coast, for use during the dry summer-autumn (CDWR 1998). Reservoir releases are routed across the Delta to provide drinking water for 22 million people in coastal cities, and supply water to over 18,000 km² of irrigated farmland producing crops valued at over \$13 billion annually (CALFED 2000, CDFA 2002).

These interbasin transfers are made as pumped exports from the south Delta (Figure 1) by the State Water Project (SWP) and the Central Valley Project (CVP) whose combined capacity is $360 \text{ m}^3 \text{ s}^{-1}$. Over 2200 diversions from Delta channels also supply water for local municipalities and irrigation of local farmland (Herren and Kawasaki 2001).

Multiple demands for water transiting the Delta are satisfied through the operation of several man-made structures using a complex suite of flow manipulations and diversions both upstream and within the Delta. We have selected a sub-set of these diversions as examples. A large fraction of the freshwater inflow to the Delta (up to 65% during the dry season in some years) is exported via the SWP and CVP pumps to meet agricultural and municipal demands. The Delta Cross Channel (DCC), a man-made channel and gates, connects the SAC with natural channels east of the SAC (Figure 1) to transfer high-quality fresh water into the central Delta mixing zone for export by the SWP and CVP. A rock barrier is constructed at the head of Old River (Figure 1, barrier 1) during spring and autumn to improve conditions for Chinook salmon migrating through the Delta via the SJR. Three other temporary barriers (Figure 1, barrier 2-4) are constructed each spring and removed each autumn to increase water depth for irrigation intakes within south Delta channels. Each hydraulic manipulation directly alters the regional flow paths or rates and indirectly changes the source mixture and quality of water across the Delta landscape, sometimes creating conflict between different water use priorities.

Diversions Alter Regional Flow Paths, Water and Habitat Quality, and Distributions of Biota

The challenge of satisfying multiple demands on the Delta's water resource is complex because this is a mixing zone of estuarine brackish water and fresh water from three primary sources, each having distinct water quality and chemical signatures (Table 1). For example, inflows from the San Joaquin River, containing a large fraction of irrigation drainage, have high concentrations of salt, nutrients, dissolved organic carbon (DOC), and toxic contaminants such as selenium (Table 1). The Sacramento River, originating from the high Sierra mountains and receiving fewer upstream agricultural inputs than the San Joaquin River, has the highest water quality of the three major fresh water sources to the Delta. Agricultural drainage from peat-rich Delta soils is highly enriched in DOC and other dissolved constituents. In addition to the fresh water sources, landward transport of estuarine water during periods of low river inflow degrades drinking water quality and agricultural supplies because of its high salt content, a major source of bromide to the Bay/Delta system.

Local-scale water diversions are designed to modify the routings of water from the different fresh water sources. In the process, regional-scale flow paths are transformed to an extent that they alter systemwide fluxes of water, salt, nutrients and contaminants, migration routes of anadromous fish, and quality of water delivered to municipalities. We use a simplified schematic of water sources and transport paths linked to the central Delta mixing zone (Figure 1, inset) to illustrate hydraulic alterations of individual diversions and their significance to the Delta ecosystem. The dark blue arrows on the schematic

perimeter represent the outer boundaries of the Delta (north: Sacramento @ Freeport, south: San Joaquin @ Vernalis) and export pump operations in the southwest corner of the Delta. The bi-directional arrow on the left hand side of the diagram represents tidal exchange between the Delta (at the junction of the SAC and SJR) and SFB. Without exports from the system, all freshwater would tidally exchange with SFB at this boundary. The network of channels and open-water regions within the Delta are represented as a central mixing zone with a series of channels that transport water to and from that region.

The magnitude of inflows into the Delta varies widely depending on water year type ranging from wet to critically dry. The SAC contributes the largest volume with daily median flow values ranging from $320 \text{ m}^3 \text{ s}^{-1}$ to $1230 \text{ m}^3 \text{ s}^{-1}$. The SJR, which has several significant diversions upstream of the Delta, is a smaller river by volume with daily flow median ranges from $36 \text{ m}^3 \text{ s}^{-1}$ to $150 \text{ m}^3 \text{ s}^{-1}$. (Median based on data from water years 1956-2001.) In contrast, the tidal exchange at the Delta's western boundary is typically in the range of $\pm 8500 \text{ m}^3 \text{ s}^{-1}$.

Interbasin transfers

The SWP and CVP (Figure 1) pump water from the Delta for export to the San Joaquin Valley, the San Francisco Bay area, the southern coast, and southern California. When the pumps operate, they draw water from both the South Delta and the central mixing zone (Figure 1, inset). The draw of the pumps is large enough to redirect the net flow in nearby channels toward the export facilities, altering regional circulation patterns and water quality. We illustrate these diversion effects with autumn 2001 flow and salinity measurements around Mildred Island (MI), a shallow, 3.8 km^2 tidal lake 25 km north of

the pumps in the central Delta (Figure 1).

A significant reduction in export flow at the SWP occurred between 7 Oct and 6 Nov 2001 (Figure 3a). Flow measurements in the channels surrounding MI and at the major entrances to MI illustrate pump effects on the regional flows and water balance (Figure 4). MI is bounded by a primary north-south channel (Middle River) and two east-west channels separated from these deeper channels by (leaky) levees with discrete openings at the north and south. During the period of high SWP export, the mean net (tidal residual) north to south flow via Middle River was $100 \text{ m}^3 \text{ s}^{-1}$. This mean flow fell to $56 \text{ m}^3 \text{ s}^{-1}$ when exports were curtailed. Because less water was drawn towards the pumps, the net residual flow in the channels surrounding MI and through MI were reduced. In some locations, the direction of net residual flow reversed.

Altering the water balance in the channels around MI, also changes the exchange of salt between this open water region and the surrounding channels. During peak SWP exports in late September, the total salt flux (Fischer and others 1979) through the MI south opening was directed out of MI towards the export pumps (Figure 3c). During the period when the pump operations were curtailed, the salt flux reversed indicating salt from the channels adjacent to the southeast corner of MI entered MI. Based on measurements in September 2001, these channels had higher salt and phytoplankton concentrations than the interior of MI. Therefore, curtailment of pump operations altered local exchange between MI and nearby channels.

Time series of near-bottom salinity in MI near the northern entrance during autumn 2001 revealed small-amplitude tidal oscillations and a larger trend of increasing salinity as

SWP exports were curtailed in October (Figure 3b). This salinity trend, characteristic of all the stations throughout the MI region during this period, is influenced by a variety of factors in addition to pump operations. Salinity measurements downstream of MI indicate estuarine intrusion was not the primary cause of increased salinity around MI during the period. However, the operation of the DCC and placement of a barrier at the head of Old River likely shifted the primary freshwater source into the central Delta from SAC to SJR water with a higher salt content (Table 1). Subsequent sections will discuss in more detail how DCC and barrier operations affect overall water sources and water quality input into the central Delta mixing zone.

Coherent variability of flow around MI, salinity and pump operations illustrates the general principle that diversions can generate system-scale responses. In this example, flows (and salinity) at one geographic location responded almost instantaneously to export diversions occurring 25 km away because those diversions altered regional flows, local exchanges, and source mixture of water in the central Delta. The implications of this diversion effect extend beyond salinity. As SJR-derived salt input increases, so does the input of contaminants including nutrients and selenium that are highly enriched in this river (Table 1). Selenium is a priority pollutant in San Francisco Bay, originating from mobilization of Se-enriched soils by irrigation in the SJR basin and accumulating in food webs downstream leading to potentially toxic levels in consumers (Stewart and others 2004) including the white sturgeon (*Acipenser transmontanus*) and Sacramento splittail (*Pogonichthys macrolepidotus*). Results of our hydrodynamic measurements imply that mass loadings of nutrients and contaminants from the SAC-SJR watersheds to San

Francisco Bay are influenced by diversions as they alter the source mixture of water transported downstream to the estuary from the Delta.

Gate-controlled flow routing

The Delta Cross Channel (DCC) is a 1100 m long, 8 m deep trapezoidal channel built in 1951 to divert water from the Sacramento River to the central Delta (Figure 1). Transfers through the DCC (Figure 2a) establish seaward flows to repel estuarine salinity intrusion into the central Delta and to supply water for exports through the SWP and CVP.

Operation of the DCC has an unintended outcome of opening a conduit for movements of fish, including threatened and endangered races of Chinook salmon, from the Sacramento River into the central Delta and toward the export pumps where predation and entrainment are significant sources of mortality (Bennett and Moyle 1996). Flows through the DCC are controlled through operation of gates. The gates are usually kept open to maintain cross-Delta flows, except during mandated closures from 1 February-20 May of each year and up to 45 days of additional closures from October 1 through January 31 to protect emigrating juvenile Chinook salmon (*Oncorhynchus tshawytscha*) from entrainment into the central Delta. Closure of DCC gates keeps SAC flow in the Sacramento River channel transporting water toward SFB rather than towards the central mixing zone (Figure 2b), creating hydraulic conditions conducive to estuarine salt intrusion into the SJR stem of the system. Regulated closure of DCC gates to facilitate salmon emigration occurs at the end of the dry summer-autumn when river inflows are naturally low and estuarine salinity intrusion is at its peak. These conditions create a conflict between operations to promote recovery of threatened species (DCC closed) and

operations to meet salinity standards for drinking-water and export demands (DCC open).

Records from salinity monitoring and DCC and export pump operations during autumn 1999 illustrate this conflict in SAC routings. The DCC gates were closed on 26 November as the seaward migration of juvenile salmon began, and salinity increased almost immediately on the SJR stem of the western Delta (Figure 5b,c; Jersey Point, Dutch Slough). At the same time, salinity decreased on the SAC stem of the western Delta (Figure 5a; Emmation) due to the additional SAC water routed down this channel as the result of DCC operations (Figure 2b). Salt intrusion on the SJR progressed until salinity exceeded drinking-water standards, mandating curtailment of export pumping (10 December). Even though salmon were still in the DCC region, the DCC gates were re-opened (15 December). These diversions repelled salt intrusion and lowered salinity as intended on the SJR (Figure 5). However, a field study in autumn 2001 demonstrated that opening the DCC gates entrains tagged juvenile salmon away from their natural migration route along the Sacramento River and into the DCC (D. Vogel, personal communication).

Although the DCC diversion channel is a physically small feature of the Delta landscape, it is located in a key hydraulic location. Salinity records (Figure 5) show that discrete diversions at the DCC (Figure 2b) cause rapid downstream changes at the SFB-Delta boundary, especially on the SJR arm of the Delta. Diversion of flow through an artificial channel alters hydraulics to sustain water supply for export and water quality for local municipalities. It also modifies the systemwide salinity distribution, a key attribute of estuarine habitat quality for biota at multiple trophic levels (Jassby and others 1995), and

the spatial distribution and susceptibility of migrating and resident fishes to entrainment mortality. These indirect and direct effects of water diversion on sustainability of native species have motivated adaptive strategies to manage flows to minimize diversion effects on habitat quality and entrainment mortality (see below).

Barrier-controlled flow routing

The San Joaquin River splits into two branches as it enters the Delta: Old River carries flows west toward the export pumps, and the San Joaquin River carries flows north toward the central mixing zone (Figure 1, inset). A temporary rock wall (~ 70 m x 5 m) is constructed at this branch each autumn to improve conditions for adult Chinook salmon migrating up the SJR. The Head of Old River Barrier (HORB) is removed each year during the wet season to protect local levees when SJR discharge is high. Flow measurements above and below the channel branch during autumn 2002 illustrate the effect of a small barrier on the routing of river inflow. The SJR inflow (at Vernalis, Figure 1) was relatively constant ($\sim 45 \text{ m}^3 \text{ s}^{-1}$) from mid-October to mid-December (Figure 6a). Similar-magnitude flows below the river branch (at Stockton, Figure 1) show that most of the SJR inflow was routed along the northerly transit when the HORB was in place. After the barrier was removed on 15 November, most SJR inflow was routed into Old River and, as a result, the net flow at Stockton fell to near zero (Figure 6a).

These flow records reveal barrier-controlled modification of south Delta circulation, dominated by northerly SJR flow (Figure 2c) when the HORB is present and westerly flow (Figure 1, inset) when it is absent. This manipulation of regional-scale circulation can have large effects on local-scale flows and water quality. For example, DO

concentration declined in the downstream Stockton Ship Channel (Figure 6b) immediately after the HORB was removed on 15 November, falling below the 6 mg L^{-1} DO standard (CVRWQCB 1998) to protect biota sensitive to hypoxia. Dissolved oxygen concentrations consistently exceeded the standard from mid-October to mid-November when the HORB was in place. The Stockton Ship Channel is a deep section of the San Joaquin River that receives large loadings of ammonia from local municipal waste and algal biomass produced upstream (Lehman and others 2004). Metabolism of these exogenous inputs consumes oxygen faster than it is replaced by advection and mixing when the HORB is removed and net flows approach zero, so removal of this barrier slows flushing and promotes development of hypoxia in the lower San Joaquin River (Figure 6b). The 6 mg L^{-1} DO standard is based on observations that Chinook salmon adults halt their immigration at lower oxygen concentrations (Hallock and others 1970). As this barrier-controlled diversion directly alters regional flows and hydraulic residence time, it indirectly influences the local-scale balance between oxygen sources and sinks, leading to hypoxia that impedes salmon spawning migration.

Barrier diversions have other unintended effects on water quality, some with implications for human health. Three additional barriers are constructed in the south Delta each spring to prevent the draw of export pumps from depleting water in nearby channels that supply irrigation water to local farm tracts. These four barriers (3 agricultural barriers and the HORB) establish a temporary reservoir as segments of Old and Middle rivers and Grant Line Canal (Figure 1) isolated from the exports and river inflows. The primary inflow source to this temporary storage region is agricultural return water, which is highly

enriched in dissolved organic carbon (Table 1). In this configuration (Figure 2d), the export pumps draw water from central Delta mixing zone of low-DOC SAC and SJR water. When the barriers are removed each autumn, the pumps also draw from the south Delta channels (Figure 1, inset) where DOC has progressively accumulated, leading to pulse increases in the DOC concentration of drinking water supplied primarily to Southern California metropolitan areas.

We illustrate this diversion effect with daily measurements of DOC at the State Water Project during November-December 2002. A step increase in DOC concentration of approximately 0.5 mg L^{-1} occurred between 23 and 26 November, just after the Middle River and head of Old River barriers were removed and during removal of the two barriers closest to the pumps. DOC remained elevated at the SWP for more than two weeks, the approximate flushing time (channel volume/inflow) of the temporary reservoir. The Southern California municipalities (principally Metropolitan Water District) are concerned about elevated DOC levels because carcinogenic trihalomethanes (THM) are formed when high-DOC water is chlorinated for disinfection. Untreated Delta water currently has total THM formation potential 3 to 9 times higher than the THM standard for treated water. As DOC concentrations increase, more disinfection by-products are produced in the treatment process. Therefore, increases in DOC concentrations increases the cost of water treatment (Lam and others 1994). Water management and restoration efforts for the Bay-Delta system have a target level for total organic carbon at the export pumps of 3 mg L^{-1} (CALFED 2000).

These examples illustrate how barrier diversions can cause multiple, regional-scale

changes that potentially conflict with goals of sustaining populations of endangered species and providing safe drinking water.

Discussion/Conclusions

The diversion effects presented above are not unique to the Sacramento-San Joaquin River Delta. However lessons from monitoring and research in this region of highly managed water withdrawals and transfers illustrate four general principles of diversion as an ecosystem disturbance:

Physically small diversions can have ecosystem-scale effects. Examples from California's Delta illustrate how water diversions at key hydrodynamic locations can influence systemwide circulation and water quality, whether the diversions are pumped exports (Figure 1, inset), flow routings into artificial channels (Figure 2a,b), or flow routings with channel barriers (Figures 2c, d). This lesson has been learned elsewhere. For example, a small-scale barrier placed in a hydraulically key location of Columbia's Ciénaga Grande de Santa Marta had devastating, unanticipated consequences on this large lagoon ecosystem. The Barranquilla-Cienaga highway closed off a small break in the barrier island connecting the lagoon to the Caribbean Sea, blocking the lagoon's only drainage outlet. Construction of a second road silted up most of the distributaries and reduced freshwater inflow. The combination of reduced inflow and blocked outflow caused hypersalinity of soils and water and altered water elevation, habitat disturbances that killed 31,000 ha of mangrove forest (Perdomo and others 1998).

Regional-scale processes can drive local-scale variability. Our discovery of salinity

oscillations inside Mildred Island (Figure 3b) occurred during a study to assess ecological functions provided by shallow-water habitats (Lucas and others 2002). The weekly-scale oscillations were a surprise, revealing an unanticipated mode of chemical variability, and they could not be explained with measurements of climate forcing, hydrodynamic processes, and water chemistry inside the lake. We deduced the causal mechanism as a response to pumping operations over 25 km away (Figure 3a), modulated through tidal exchange of salinity variability in the surrounding channel system. This example illustrates how diversions alter regional-scale circulation and water quality, and how variability at this scale is propagated by flow-driven transports to cause variability at the smaller scale of individual habitats. The lesson of displaced effects from basin-scale diversions has been learned elsewhere, sometimes in much larger systems. Construction of the High Aswan dam had significant basin-scale effects hundreds of kilometers downstream at the Nile's outlet to the Mediterranean Sea. The diversion of water and shift in the flood timing through operations of the High Aswan Dam resulted in reduced nutrient influxes to the oligotrophic Mediterranean, altered circulation patterns on the Egyptian shelf, and changes in phytoplankton and fish community structure (Nixon 2003). Ecologists now recognize interconnectedness of habitats as a key attribute of ecosystems (Reiners and Driese 2001); this attribute is highly influenced by diversions of water flows that are the mechanisms that connect aquatic ecosystems.

Diversions have multiple benefits and costs. Seasonal barriers in the South Delta have multiple effects, each with a distinct spatial expression. The HORB barrier is placed to prevent occurrences of hypoxia in the lower San Joaquin River. This same barrier,

however, helps create the isolated reservoir in the south Delta which temporarily raises DOC concentrations delivered to municipal consumers via the export pumps. Diverse responses to flow diversion in the 1960's transformed the Aral Sea, a terminal lake in the former Soviet Union that was the world's 4th largest lake (Micklin 1988). The surrounding desert landscape was converted into a cotton production hub with massive diversions of the Dary'a and Syr Dar'ya (Bedford 1996). In the last 50 years, the Aral Sea has lost four-fifths of its volume, at least half its surface area (Schiermeier 2001), 20 of 24 native fish species, and its commercial fish. The exposed seabed is the source of major salt and dust storms causing ecological and agricultural damage hundreds of kilometers inland.

Diversions can reduce the capacity of aquatic ecosystems to assimilate wastes. As diversions modify the flow paths, flow rates and source mixture of water in open aquatic systems like the Delta, they also modify the ecosystem capacity to assimilate wastes. Consequences include rapid depletions of dissolved oxygen (Figure 6b) in a section of the San Joaquin River receiving inputs of ammonia and organic matter, and pulse inputs of high dissolved organic carbon (Figure 7) from irrigation drainage to exports supplying drinking water to municipalities.

These four principles reflect one core concept: diversions to meet society's demand for reliable water supply have multiple and often unanticipated effects on aquatic ecosystems and the services they provide, including services that sustain biological diversity and promote human health. Fishery scientists now recognize that single-species management has failed to sustain stocks of exploited populations, and international

advisory panels advocate a more holistic framework of Ecosystem-Based Fishery Management (EBFM) that starts "with the ecosystem rather than the target species" (Pikitch and others 2004). This alternative perspective emerged from the realization that fishing has unintended consequences that include habitat destruction, evolutionary shifts in fish populations, and changes in ecosystem structure and function.

Water diversions have analogous consequences, and a hydrologic analog of EBFM is advocated as Integrated Water Resources Management (IWRM) in which development of water, land and related resources are coordinated to maximize economic and social welfare "without compromising the sustainability of vital ecosystems" (World Water Assessment Programme 2003). Ecosystem frameworks for water management consider the full suite of costs and benefits of flow manipulation, and the development of such frameworks becomes more urgent as the world population and scale of water development continue to grow. Water withdrawals for food production are projected to increase 14% in the next 30 years, expanding irrigated land by 450,000 km² in 93 developing countries (World Water Assessment Programme 2003). Allocations for agriculture will increasingly compete with municipal and industrial water demands and allocations for ecosystem sustainability.

Steps toward Integrated Water Resources Management are now being taken around the world. In California's Delta, a new partnership between California and Federal Government agencies called the CALFED Bay-Delta Authority was established in 2000 to "develop a long-term comprehensive plan that will restore ecological health and improve water management for beneficial uses of the Bay-Delta system" (CALFED

2000; calwater.ca.gov). Some of the elements towards this IWRM strategy were built from science-based discoveries of the consequences of diversion in this ecosystem. For example, a dedicated allocation of reservoir storage (Environmental Water Account; CALFED 2000) is used strategically to minimize export mortality when endangered species of fish are detected near the export pumps. In addition, outflow is regulated seasonally to manipulate salinity distributions toward those optimizing habitat quality and biological productivity in the downstream estuary (X2 standard, USEPA 1995). The four general principles illustrated here provide a starting foundation for building complete IWRM strategies in the San Francisco Bay-Delta and other ecosystems disrupted by water diversions.

Acknowledgements

This paper required data from many different people and agencies including Mike Dempsey (CDWR), Fengmao Guo (CDWR), A. Robin Stewart (USGS), and hydrodynamic field measurements made by the USGS/Sacramento Office (Jay Cuetara, Cathy Ruhl). Special thanks to the crew of people involved in the Mildred Island field study that prompted this analysis. We gratefully acknowledge funding by CALFED Grant #ERP-01-C07. We also appreciate the helpful comments by Alan Jassby, Randy Brown, Heather Peterson, and Noah Knowles.

References

Abramovitz, J.N. (1996), Sustaining freshwater ecosystems, in *State of the World, 1996*, edited by L. Starke, pp. 60-77, WW Norton and Company, New York.

Abdullev, I. and D. Molden (2004), Spatial and temporal variability of water productivity in the Syr Darya Basin, central Asia, *Water Resources Research*, 40, W0802, doi:10.1029/2003WR002364.

Adams, R.M. and S.H. Cho (1998), Agriculture and endangered species: An analysis of trade-offs in the Klamath Basin, Oregon, *Water Resources Research*, 34(10): 2741-2749.

Atwater, B.F., S.G. Conard, J.N. Dowden, C.W. Hedel, R.L. MacDonald, and W. Savage (1979), History, landforms, and vegetation of the estuary's tidal marshes, in *San Francisco Bay, The Urbanized Estuary*, edited by T.J. Conomos, pp. 347-385, Pacific Division, American Association for the Advancement of Science, San Francisco.

Barbier, E.B. (2003), Upstream dams and downstream water allocation: The case of the Hadejia-Jama'are Floodplain, northern Nigeria, *Water Resources Research*, 39(11), doi:10.1029/2003WR002249.

Bedford, D.P. (1996), International water management in the Aral Sea Basin, *Water International*, 21, 63-99.

Bennett, W.A., and P.B. Moyle (1996), Where have all the fishes gone? Interactive

factors producing fish declines in the Sacramento-San Joaquin Estuary, in *San Francisco Bay: The Ecosystem*, edited by J.T. Hollibaugh, pp. 519-542, Pacific Division, American Association for the Advancement of Science, San Francisco.

Cai, X., and M.W. Rosegrant (2004), Optional water development strategies for the Yellow River Basin: Balancing agricultural and ecological water demands, *Water Resources Research*, 40, W08S04, doi:10.1029/2003WR002488.

[CALFED] CALFED Bay-Delta Program (2000), Programmatic record of decision, CALFED Bay-Delta Program, Sacramento, California.

[CDFA] California Department of Food and Agriculture (2002), Resource directory, CDFA, Sacramento, California.

[CDWR] California Department of Water Resources (2003), The Municipal Water Quality Investigations Program summary and findings from data collected August 1998 through September 2001, CDWR Division of Environmental Services, Sacramento, California.

[CDWR] California Department of Water Resources (1998), California water plan update, *Bulletin 160-98*, 720 pp., CDWR, Sacramento, California.

[CVRWQCB] Central Valley Regional Water Quality Control Board (1998), The water quality control plan for the Sacramento River Basin and the San Joaquin River Basin, Fourth Edition, CVRWQCB, Sacramento, California.

Cutter, G.A., and L.S. Cutter (2004), Selenium biogeochemistry in the San Francisco Bay

estuary: changes in water column behavior, *Estuarine, Coastal and Shelf Science*, in press.

Dynesius, M., and C. Nilsson (1994), Fragmentation and flow regulation of river systems in the northern third of the world, *Science*, 266, 753-762.

Fischer, H.B., E.J. List, R.C.Y. Koh, J. Imberger, N.H. Brooks (1979), *Mixing in inland and coastal waters*. Academic Press, Inc, San Diego.

Gleick, P.H. (2000), The changing water paradigm a look at twenty-first century water resources development, *Water International*, 25, 127-138.

Hallock, R.J., R.F. Elwell, and D.H. Fry (1970), Migrations of adult king salmon *Oncorhynchus tshawytscha* in the San Joaquin Delta, as demonstrated by the use of sonic tags, *Fish Bulletin 151*, California Department of Fish and Game, Sacramento, California.

Herren, J.R., S.S. Kawasaki (2001), Inventory of water diversions in four geographic areas in California's Central Valley, in *Contributions to the biology of Central Valley Salmonids, Volume 2, Fish Bulletin 179*, edited by R.L. Brown, pp. 343-355, California Department of Fish and Game, Sacramento, California.

Jassby, A.D., W.J. Kimmerer, S.G. Monismith, C. Armor, J.E. Cloern, T.M. Powell, J.R. Schubel, and T.J. Vendlinski (1995), Isohaline position as a habitat indicator for estuarine populations, *Ecological Applications*, 5, 272-289.

Lam, R.H.F., J.P. Brown, A.M. Fan, and A. Milea (1994), Chemicals in California drinking water: source contaminants, risk assessment, risk management, and regulatory

standards, *Journal of Hazardous Materials*, 39, 173-192.

Lehman, P.W., J. Sevier, J. Giulianotti, and M. Johnson (2004), Sources of oxygen demand in the lower San Joaquin River, California, *Estuaries*, 27, 405-418.

Lucas, L.V., J.E. Cloern, J.K. Thompson, and N.E. Monsen (2002), Functional variability of habitats within the Sacramento-San Joaquin Delta: Restoration implications, *Ecological Applications*, 12, 1528-1547.

Micklin, P.P. (1988), Desiccation of the Aral Sea: a water management disaster in the Soviet Union, *Science*, 241, 1170-1176.

Nixon, S.W. (2003), Replacing the Nile: Are anthropogenic nutrients providing the fertility once brought to the Mediterranean by a great river? *Ambio.*, 32, 30-39.

Perdomo, L., I. Ensminger, L.F. Espinosa, C. Elster, M. Wallner-Kersanach, and M. Schnetter (1998), The mangrove ecosystem of the Ciénaga Grande de Santa Marta (Colombia): Observations on regeneration and trace metals in sediment, *Marine Pollution Bulletin*, 37, 393-403.

Pikitch, E.K. and others (2004), Ecosystem-based fishery management, *Science*, 305, 346-347.

Reiners, W.A., and K.L. Driese (2001), The propagation of ecological influences through heterogeneous environmental space, *Bioscience*, 51, 939-950.

Schiermeier, Q. (2001), Ecologists plot to turn the tide for shrinking lake, *Nature*, 412,

756.

Simpson, M.R., and R.N. Oltmann (1993), Discharge measurement using an acoustic Doppler current profiler, *Water-Supply Paper 2395*, 34 pp., U.S. Geological Survey. Reston, Virginia.

Stewart, A.R., S.N. Luoma, C.E. Schlekat, M.A. Doblin and K.A. Hieb (2004), Food web pathway determines how selenium affects aquatic ecosystems: A San Francisco Bay case study, *Environmental Science and Technology*, 38, 4519-4526.

[USEPA] United States Environmental Protection Agency (1995), Water quality standards for surface waters of the Sacramento River, San Joaquin River, and San Francisco Bay and Delta of the State of California, *Federal Register: January 24, 1995* 40 CFR Part 131, 4664-4709.

World Water Assessment Programme, (2003), *United Nations World Water Development Report*. UNESCO Publishing, Paris.

Figure Legends:

Figure 1: Map of the Sacramento-San Joaquin Delta. The numbers indicate the location of the four temporary barriers during portions of the year. Inset: Schematic illustrating the base flow routes through the Delta without gate or barrier operations. The dark blue arrows represent the freshwater inputs to the Delta (north: Sacramento @ Freeport; south: San Joaquin @ Vernalis) and export pump operations in the southwest corner of the Delta. The bi-directional arrow represents tidal exchange of Delta water with San Francisco Bay at the junction of the Sacramento and San Joaquin rivers.

Figure 2: Schematics illustrating how each diversion in our examples alters flow routing through the Delta. Red denotes the significant flow change caused by each diversion. (a) Keeping the DCC gates open enhances the transfer of SAC water to the central Delta mixing zone. (b) Closing the gates at the DCC redirects flow down the SAC towards SFB rather than flowing into the central Delta mixing zone. (c) Placement of the HORB directs SJR flow towards the central Delta mixing zone rather than flowing through the south Delta towards the export pumps. (d) Placement of all four temporary barriers creates a temporary storage region in the south Delta.

Figure 3: The influence of SWP export pump operations on salinity in Mildred Island (central Delta) in autumn 2001. (a) Export rate at the SWP export facilities. (b) Salinity (psu) 1 m above the channel bottom at the northern opening of Mildred Island. (c) Advective salt flux at the southern opening of Mildred Island. Inset: map of Mildred Island and the surrounding channels. Data sources: SWP pump operation data: California Department of Water Resources Interagency Ecological Program database

(www.iep.water.ca.gov, Station: CHSWP003). Salinity and flow data calculated from USGS field measurements in Mildred Island (22 Aug 2001-14 Nov 2001).

Figure 4: Schematic of circulation patterns around Mildred Island during a USGS field experiment during autumn 2001 when (a) the export pumps were operating normally (1 Sep 2001- 6 Oct 2001) and (b) SWP pump operations were curtailed (7 Oct 2001-6 Nov 2001). The dark blue arrows indicate flow measurement locations. The numbers beside the arrows are the average tidally-filtered flow rates (m^3s^{-1}) at each of the field stations. The levee on the east side of MI has several small breaks which connect MI to the outside channel. Because flow was not measured at each levee break, the exchange between MI and this channel cannot be quantified. The light blue arrows at the south MI entrance and in the channel east of MI indicate that the tidally averaged flow reverses directions during portions of the pump reduction period. Velocities through the major entrances to MI and surrounding channels were measured using a suite of instruments including four Sontex Argonaughts, a Sontex ADP, and an RDI Broadband. The velocity measurements were converted into flow measurements using the technique developed by Simpson and Oltmann (1993).

Figure 5: The influence of DCC gate operations on salinity intrusion in the western Delta during November-December 1999 at (a) SAC at Emmaton, (b) SJR at Jersey Point, and (c) Dutch Slough (inset: map of the region). Datasource: Interagency Ecological Program Database: electrical conductivity (Station: RSAC092, RSAN018, SLDUT007), water temperature (Station: RSAC101, RSAN007), DCC gate operations (Station: RSAC128), and export pump operations (Station: CHSWP003, CHDMC004).

Figure 6: The influence of HORB removal on SJR flows and DO concentration in the Stockton Ship Channel in autumn 2002. (a) SJR flow ($\text{m}^3 \text{s}^{-1}$) measurements at Vernalis (solid line) and tidally-averaged flow at Stockton (dashed line). The station at Vernalis, upstream of the head of Old River, measures the SJR input flow into the Delta while the second flow station (Stockton) is located directly upstream of the Stockton Ship Channel. (b) Dissolved oxygen 1 m below the surface in the Stockton Ship Channel at Rough and Ready Island (mg L^{-1}). Data sources: Interagency Ecological Program Database: SJR Flow (USGS; Station: RSAN063, RSAN112) and (CDWR; Station: RSAN058), CDWR Bay-Delta Office: Temporary barrier operating schedule (sdelta.water.ca.gov/web_pg/tempmesr.html).

Figure 7: DOC (mg L^{-1}) at SWP export facilities and temporary barrier operations during autumn 2002. Horizontal lines indicate when each of the temporary barriers are in (solid line) and the barrier demolition periods (dashed line). Inset: Map of the south delta region. The numbers indicate the location of each of the temporary barriers. Data sources: California Data Exchange Center (www.cdec.water.ca.gov): DOC (Station: HRO), CDWR Bay-Delta Office: Temporary barrier operating schedule.

Table Legend:

Table 1 Water quality comparison between the Sacramento River, San Joaquin River, and In-Delta Agricultural Return water for water years 1999-2001.

Table 1: Water quality of Sacramento, San Joaquin, and Agricultural Return Water

Water Quality Parameter	Sacramento at Freeport^a	San Joaquin at Vernalis	In-Delta Agricultural Return Water^b
Specific Conductance (mmhos cm ⁻¹)	144 ± 28	621 ± 183	562 ± 206
pH	7.8 ± 0.2	8.0 ± 0.4	6.8 ± 0.4
Alkalinity (mg CaCO ₃ L ⁻¹)	55 ± 12	85 ± 24	83 ± 18
Dissolved Oxygen (mg L ⁻¹)	9.8 ± 1.4	9.6 ± 1.4	5.5 ± 2.1
Nitrite+Nitrate (mg N L ⁻¹)	0.12 ± 0.05	1.62 ± 0.59	
Orthophosphate (mg P L ⁻¹)	0.024 ± 0.007	0.107 ± 0.054	
Dissolved Organic Carbon (mg C L ⁻¹)	1.84 ± 0.53	2.83 ± 0.47	14.1 ± 7.7
Total Dissolved Selenium (nmol L ⁻¹) ^c	0.91 ± 0.27	8.6 ± 2.5	Negligible ^d

^a USGS Water Quality Database (WY1999-WY2001) for Sacramento (USGS 11447650) and San Joaquin (USGS 11303500) rivers unless otherwise noted.

^b California Department of Water Resources Municipal Water Quality Investigations Program (WY1999-WY2001) for Bacon Island Pumping Plant (DWR B9V75881342), and Twitchell Island. Pumping Plant 1 (DWR B9V80661391) (CDWR 2003); DOC data only from Bacon Island. Different crops produce varying levels of DOC, agricultural return water DOC is expected to vary significantly throughout the Delta.

^c Sacramento river average from two field studies (1984-2000). San Joaquin average from 1997-2000 sampling period. (Cutter and Cutter 2004)

^d Personal communication AR Stewart, 14 May 2003

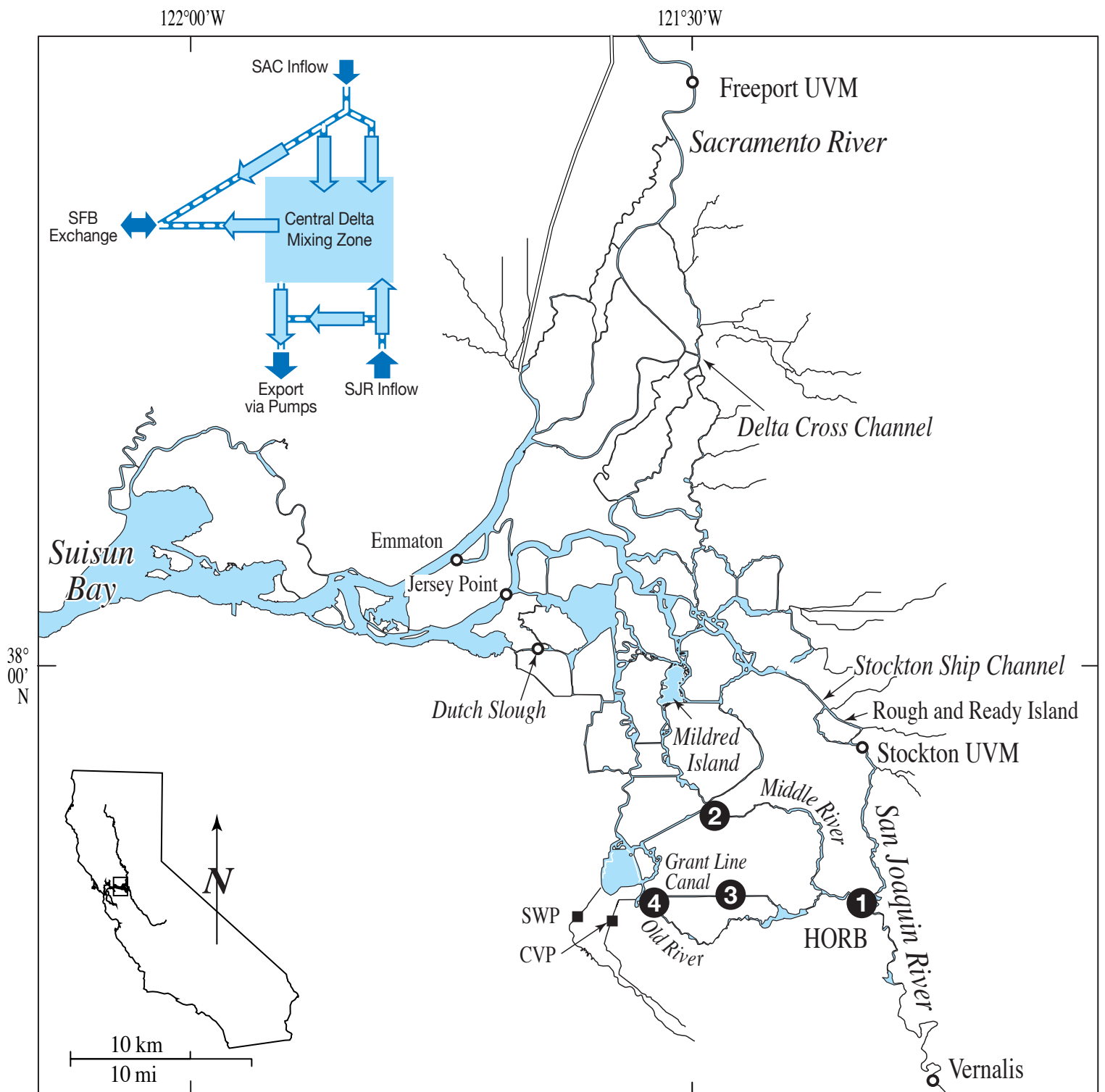


Figure 1 (color): Map of the Sacramento-San Joaquin Delta. The numbers indicate the location of the four temporary barriers during portions of the year. Inset: Schematic illustrating the base flow routes through the Delta without gate or barrier operations. The dark blue arrows represent the freshwater inputs to the Delta (north: Sacramento @ Freeport; south: San Joaquin @ Vernalis) and export pump operations in the southwest corner of the Delta. The bi-directional arrow represents tidal exchange of Delta water with San Francisco Bay at the junction of the Sacramento and San Joaquin rivers.

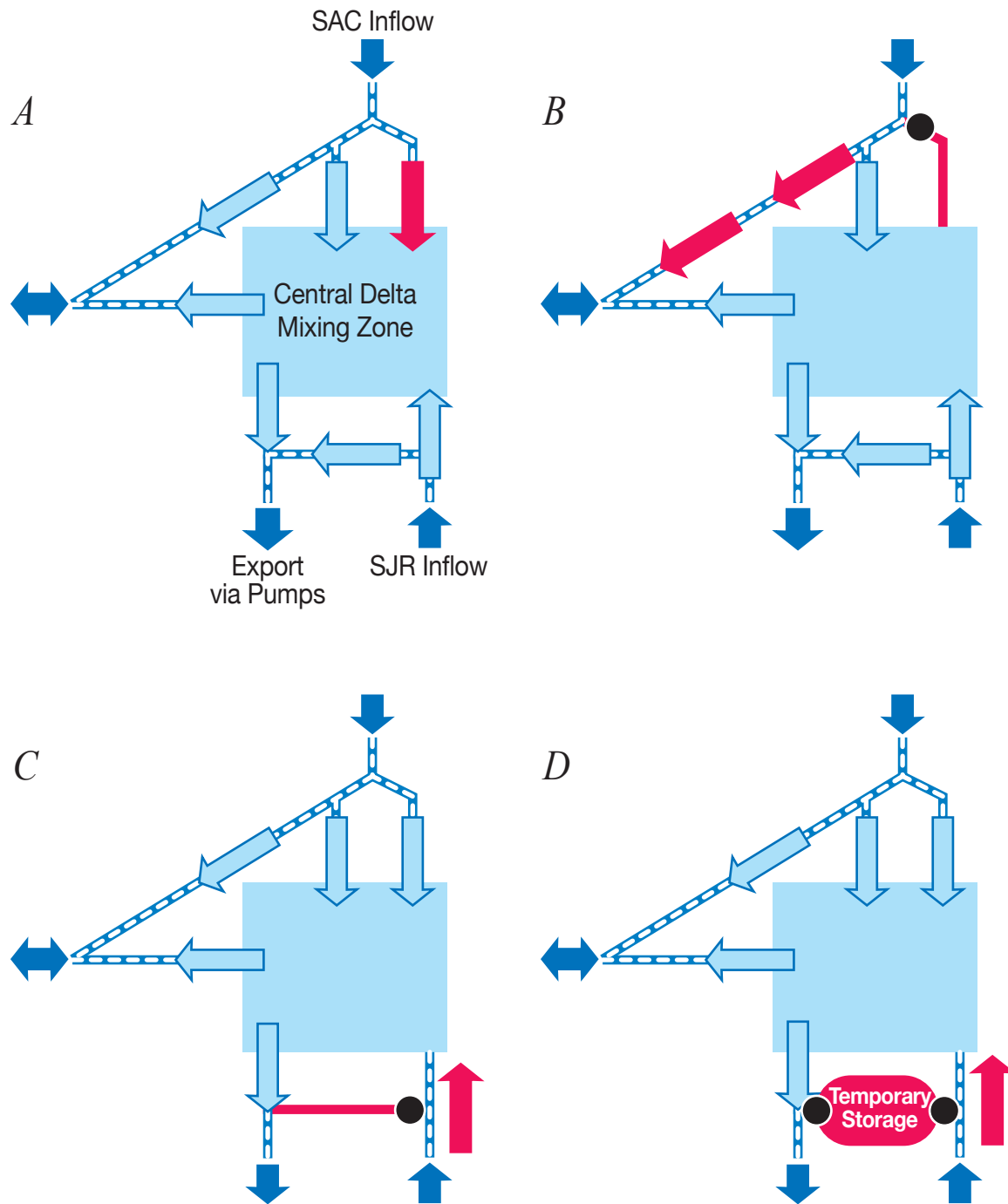


Figure 2 (color): Schematics illustrating how each diversion in our examples alters flow routing through the Delta. Red denotes the significant flow change caused by each diversion. (a) Keeping the DCC gates open enhances the transfer of SAC water to the central Delta mixing zone. (b) Closing the gates at the DCC redirects flow down the SAC towards SFB rather than flowing into the central Delta mixing zone. (c) Placement of the HORB directs SJR flow towards the central Delta mixing zone rather than flowing through the south Delta towards the export pumps. (d) Placement of all four temporary barriers creates a temporary storage region in the south Delta.

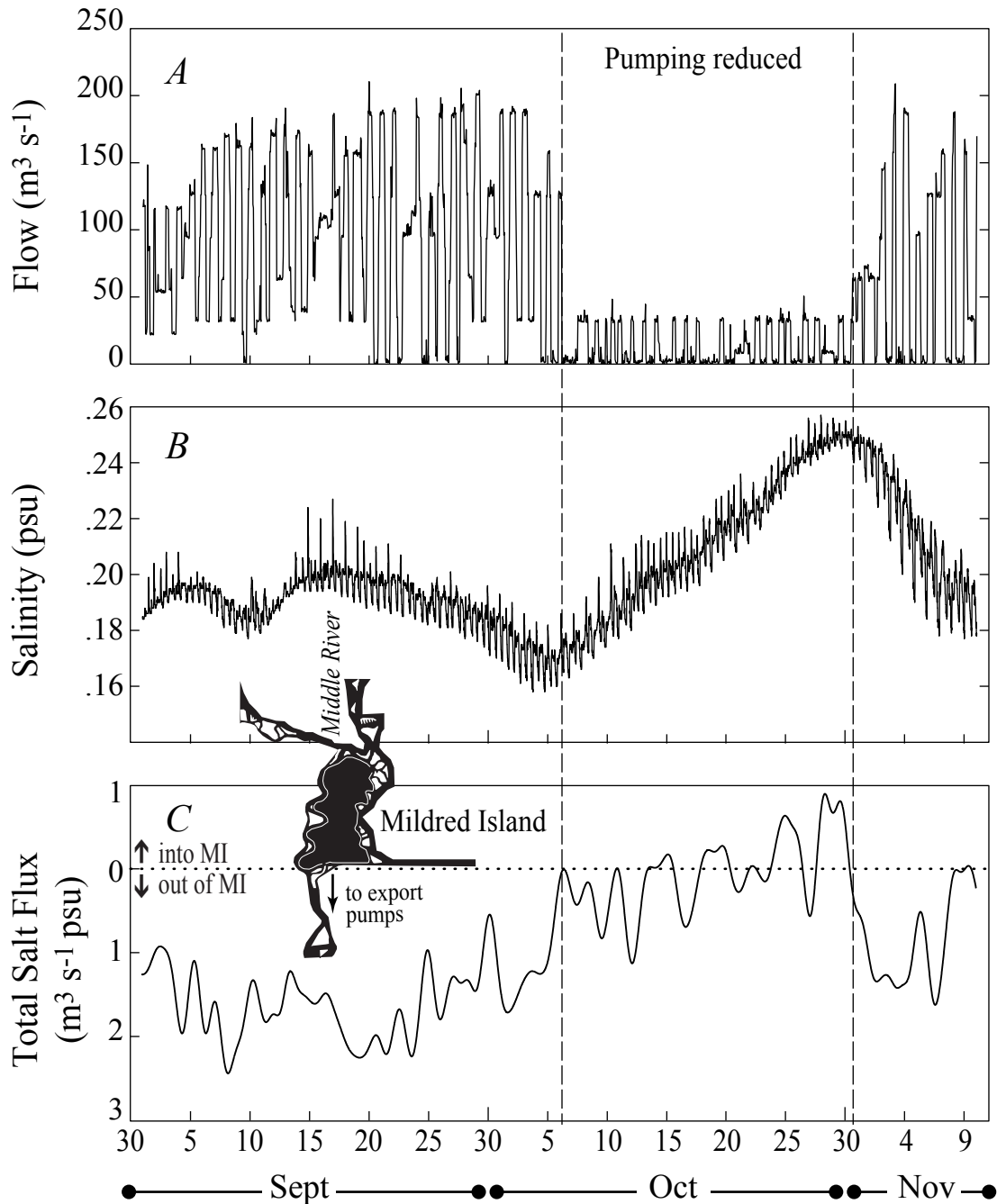


Figure 3 (black and white): The influence of SWP export pump operations on salinity in Mildred Island (central Delta) in autumn 2001. (a) Export rate at the SWP export facilities. (b) Salinity (psu) 1 m above the channel bottom at the northern opening of Mildred Island. (c) Advective salt flux at the southern opening of Mildred Island. Inset: map of Mildred Island and the surrounding channels. Data sources: SWP pump operation data: California Department of Water Resources Interagency Ecological Program database (www.iep.water.ca.gov, Station: CHSWP003). Salinity and flow data calculated from USGS field measurements in Mildred Island (22 Aug 2001-14 Nov 2001).

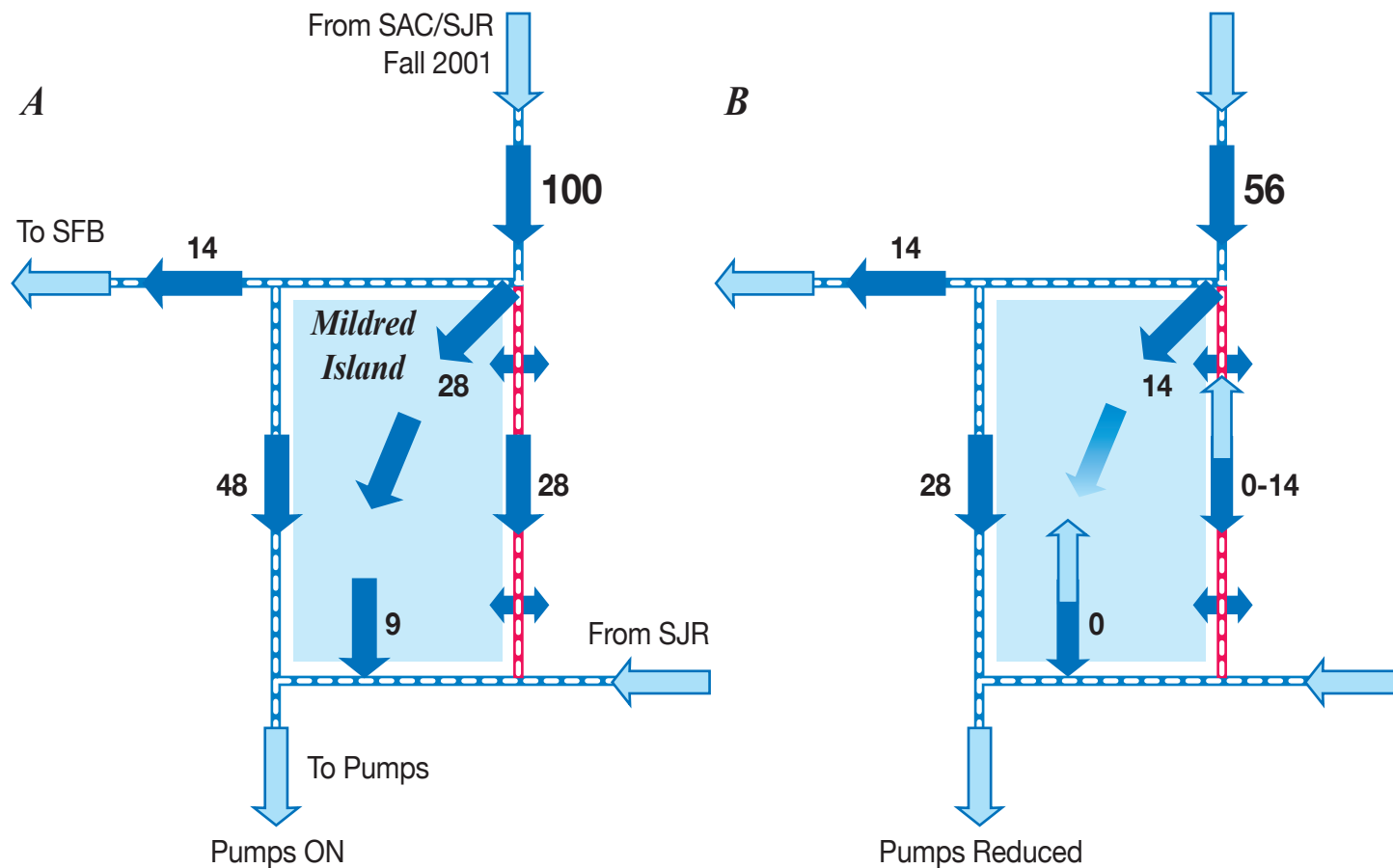


Figure 4 (color): Schematic of circulation patterns around Mildred Island during a USGS field experiment during autumn 2001 when (a) the export pumps were operating normally (1 Sep 2001- 6 Oct 2001) and (b) SWP pump operations were curtailed (7 Oct 2001-6 Nov 2001). The dark blue arrows indicate flow measurement locations. The numbers beside the arrows are the average tidally-filtered flow rates (m^3s^{-1}) at each of the field stations. The levee on the east side of MI has several small breaks which connect MI to the outside channel. Because flow was not measured at each levee break, the exchange between MI and this channel cannot be quantified. The light blue arrows at the south MI entrance and in the channel east of MI indicate that the tidally averaged flow reverses directions during portions of the pump reduction period. Velocities through the major entrances to MI and surrounding channels were measured using a suite of instruments including four Sontex Argonauts, a Sontex ADP, and an RDI Broadband. The velocity measurements were converted into flow measurements using the technique developed by Simpson and Oltmann (1993).

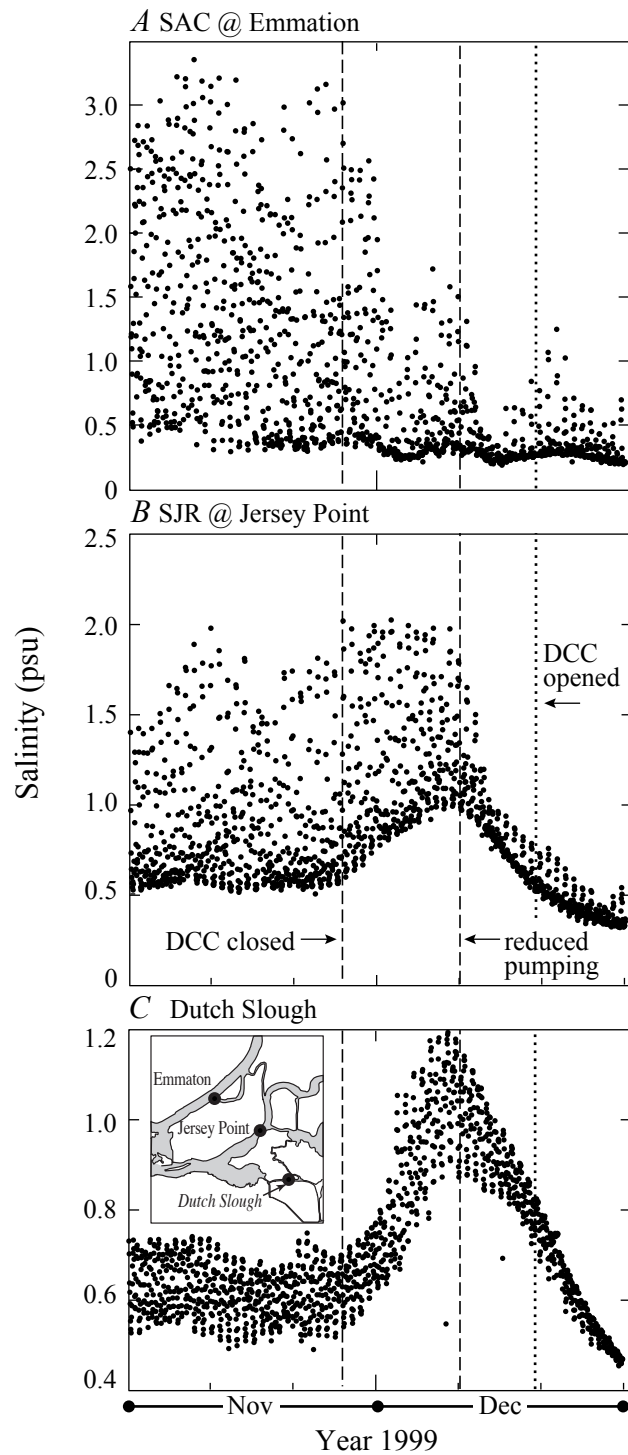


Figure 5 (black and white): The influence of DCC gate operations on salinity intrusion in the western Delta during [November-December 1999 at (a) SAC at Emmaton, (b) SJR at Jersey Point, and (c) Dutch Slough (inset: map of [the region). Datasource: Interagency Ecological Program Database: electrical conductivity (Station: RSAC092, [RSAN018, SLDUT007), water temperature (Station: RSAC101, RSAN007), DCC gate operations (Station: [RSAC128), and export pump operations (Station: CHSWP003, CHDMC004).

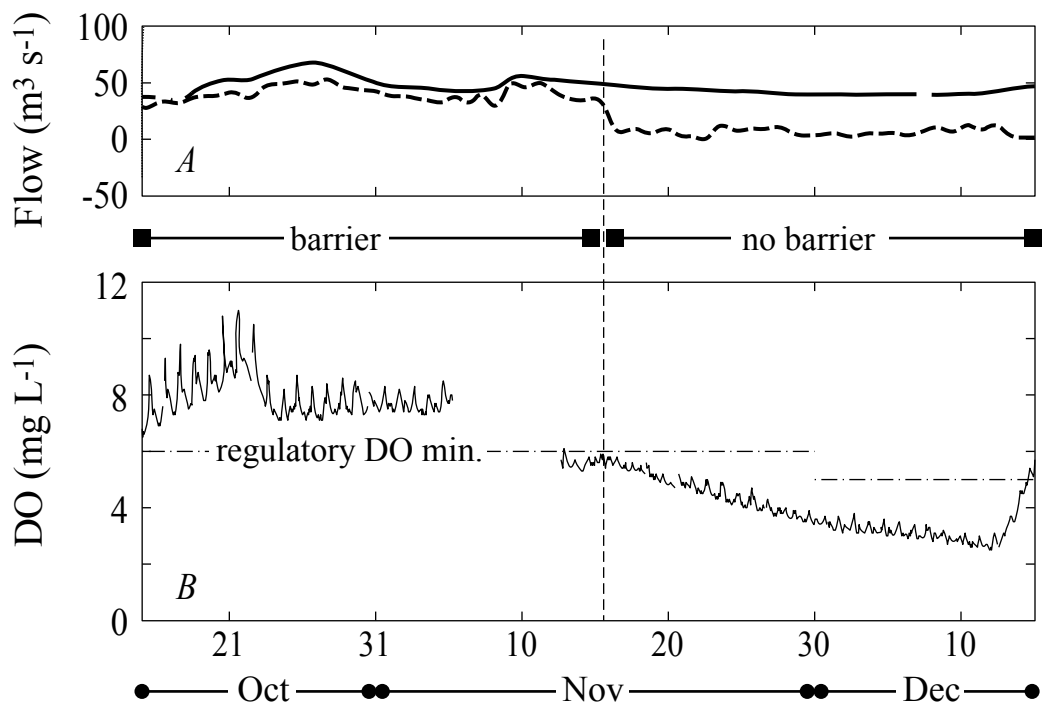


Figure 6 (black and white): The influence of HORB removal on SJR flows and DO concentration in the Stockton Ship Channel in autumn 2002. (a) SJR flow ($\text{m}^3 \text{s}^{-1}$) measurements at Vernalis (solid line) and tidally-averaged flow at Stockton (dashed line). The station at Vernalis, upstream of the head of Old River, measures the SJR input flow into the Delta while the second flow station (Stockton) is located directly upstream of the Stockton Ship Channel. (b) Dissolved oxygen 1 m below the surface in the Stockton Ship Channel at Rough and Ready Island (mg L^{-1}). Data sources: Interagency Ecological Program Database: SJR Flow (USGS; Station: RSAN063, RSAN112) and (CDWR; Station: RSAN058), CDWR Bay-Delta Office: Temporary barrier operating schedule (sdelta.water.ca.gov/web_pg/tempmesr.html).

DOC at Banks Pumping Plant (SWP)

- 1. Head of Old River *Clifton Court Forebay*
- 2. Middle River
- 3. Grant Line Canal
- 4. Old River near Tracy

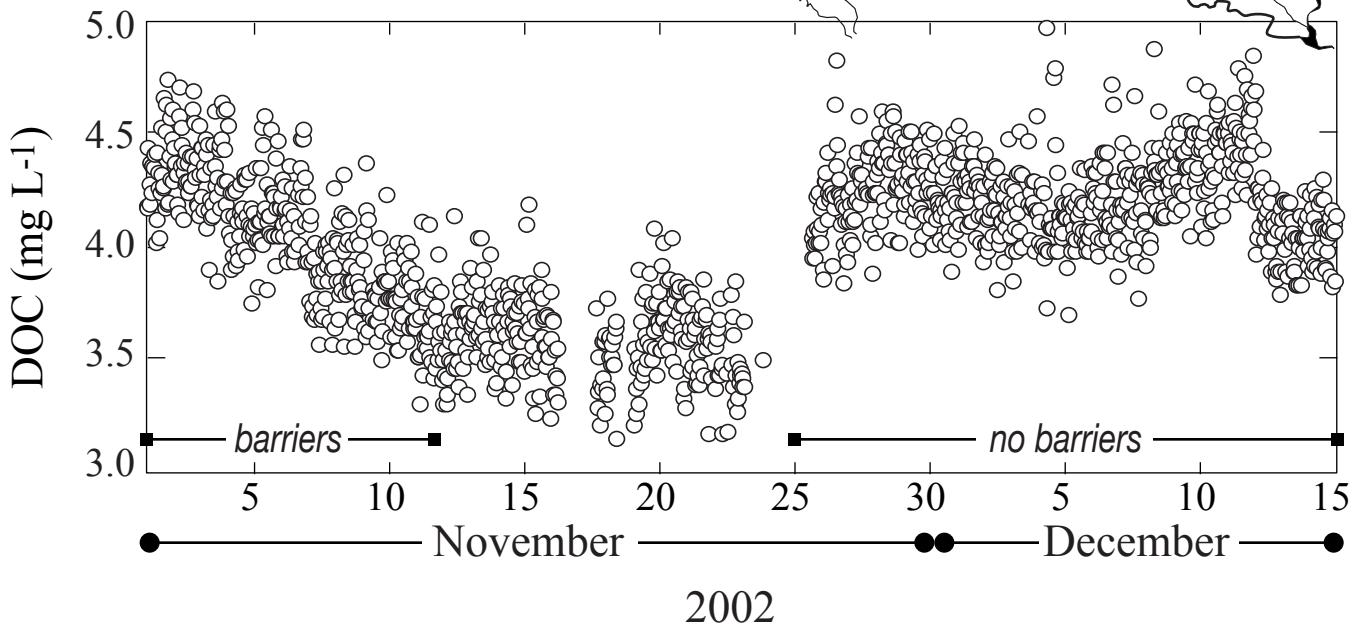
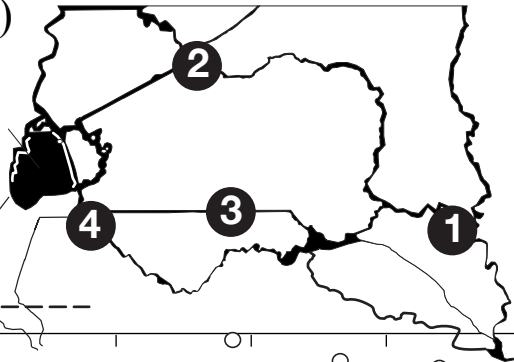


Figure 7 (black and white): DOC (mg L⁻¹) at SWP export facilities and temporary barrier operations during autumn 2002. Horizontal lines indicate when each of the temporary barriers are in (solid line) and the barrier demolition periods (dashed line). Inset: Map of the south delta region. The numbers indicate the location of each of the temporary barriers. Data sources: California Data Exchange Center (www.cdec.water.ca.gov); DOC (Station: HRO), CDWR Bay-Delta Office: Temporary barrier operating schedule.